PALLADACYCLES WITH PALLADIUM-BONDED STEREOGENIC CARBONS: TOOLS FOR EXPLORING REACTION PATHWAYS IN ORGANOMETALLIC CHEMISTRY

By

C2009
John Charles Hershberger

B.S., Missouri University of Science and Technology, 2003

Submitted to the graduate degree program in Chemistry and the Graduate Faculty of the University of Kansas in partial fulfillment of the requirements for the degree of Doctor of Philosophy.

Helena C. Malinakova, Chairperson

Mikhail V. Barybin

Richard S. Givens

Jon A. Tunge

Thomas E. Prisinzano

Date Defended: April 17, 2009

The Dissertation Committee for John Charles Hershberger certifies that this is the approved version of the following dissertation:

PALLADACYCLES WITH PALLADIUM-BONDED STEREOGENIC CARBONS: TOOLS FOR EXPLORING REACTION PATHWAYS IN ORGANOMETALLIC CHEMISTRY

Committee:

Helena C. Malinakova, Chairperson

Mikhail V. Barybin

Richard S. Givens

Jon A. Tunge

Thomas E. Prisinzano

Date Approved: April 27, 2009

Abstract

John Charles Hershberger, Ph.D.

Department of Chemistry, April 2009

University of Kansas

Organometallic chemistry has undoubtedly changed the way synthetic chemists construct molecules as well as the way synthetic chemists *think* about constructing molecules. Three well-known and most widely used transition metal-catalyzed reactions are the cross-coupling reactions, the Heck reaction, and olefin metathesis. Reactions stoichiometric in the transition-metal played an important role in their development, providing insight that could have remained uncovered otherwise.

The first goal of this dissertation is to expand our understanding of how changing the ligand sphere around the palladium center (by utilizing a triphenylphosphine moiety attached to an insoluble polymer support) affects the reactivity of the palladacycles on solid-phase. More specifically, we compared the reactivity of polymer-bound palladacycles to their soluble triphenylphosphine analogs. The second goal of this dissertation is to elucidate how a carbon stereocenter bound to palladium transfers its asymmetry to a second newly formed stereocenter that is also bound to palladium, and the role played by the auxiliary ligand in this process.

The first project detailed in this dissertation describes a basic study of the interactions between a solid-phase support and well-defined palladacycles. The

effects of phosphorus loading, palladium loading, P : Pd ratio, and polymer swelling on the reactivity of the polymer-bound palladacycles were explored. The results of these studies as well as the facile syntheses of 2*H*-1-benzopyrans are presented. We also attempted the synthesis of a library of highly substituted 1,2-dihydroquinolines utilizing this solid-phase technology. Although we were unable to successfully complete the library synthesis, future studies in this area are expected to further elucidate the difference in the reactivities of solid-phase oxa-palladacycles and solid-phase aza-palladacycles.

The second project describes the successful development of an expeditious route to palladapyrrolidinones, a new organometallic scaffold featuring two Csp^3-hybridized stereogenic carbons attached to a palladium center. These are rare examples of palladium complexes bearing two stereogenic carbons bound to a palladium center. It is also the first system in which the effect of an existing carbon stereocenter bound directly to a palladium center upon the formation of a second stereocenter also directly bound to palladium can be studied in detail. Up to 20 : 1 diastereoselectivity was observed during the formation of the second stereocenter and the diastereoselectivity is shown to be ligand-dependent, indicating that the auxiliary ligand sphere plays a significant role in diastereoinduction. Rather unexpectedly, utilizing a chiral non-racemic ligand in the synthesis of palladapyrrolidinones had little effect on the diastereoselectivity of the reaction. A model to explain the diastereoselectivity and the surprising lack of influence of the chiral non-racemic ligand on the diastereoselectivity is proposed based on X-ray structural studies.

To the universe—

May the flame of knowledge burn always

Acknowledgements

First, I would like to acknowledge my parents, Charles and Judith Hershberger for always encouraging me and accepting whatever decision I would make regarding my future. Next, I would like to acknowledge my stepmother and my more extended family: Sharon Hershberger, Amber Downey, and Dana King. Thank you for all your help and encouragement, even though you might think I'm a bit *weird*.

I would next like to thank my high school chemistry teacher, Dr. Lario Yerino. Without having the luck of having you in class, I may have ended up something other than a chemist. I'd also like to thank my undergraduate research advisor, Dr. Harvest Collier, for always being excited about chemistry and asking for my opinions on non-chemistry matters.

The past five and a half years have been a time of incredible personal and professional growth. Two people in particular have been with me the whole way: Ken Stensrud and Tiffany Maher. Ken, it was a wild ride. Graduate school was a roller coaster for both of us. Have fun in Prague and don't forget the snickers. Tiffany, what is there to write here? Your wit and wisdom have been invaluable to me. Thank you.

Dave McGinnis, your optimism and East Coast Attitude have been something I admire. I wish the best of luck to you and Carrie in your future endeavors. Of course, I can't forget Alex Grenning. Even though sometimes he does! Your sunny disposition is always refreshing. Jimmie Weaver, it was always fun sparring with

you about chemistry. Kevin Godber, I hope we can remain cohesive in the future. You constantly remind me there is more to life than chemistry. Atsushi Shiota, while you've been at KU a bit longer than myself, you still have a ways to go. You and Kevin have fun taking the Malinakova Group into the future! I'd also like to acknowledge the current and past members of the Malinakova research group, particularly Chad Hopkins. Some of the ridiculous conversations we had I'll never be able to forget.

I would like to thank my committee for taking time out of their schedules. A thanks is also in order for Jeff Aubé. It hardly seems like almost seven years ago when I worked in your laboratories over the summer as an undergraduate. You showed me what synthetic chemistry could be like. Misha Barybin, thanks for always having the time to answer my questions about inorganic and organometallic chemistry. I'm still trying to wrap my head around those subjects. Dr. Givens, thank you for helping me with my long talk and letting teach your class for a day. Jon Tunge, your wit and extremely deep knowledge of chemistry are something I aspire to.

Finally, I would like to thank my colleague, mentor, and friend Helena Malinakova. Thanks for allowing me to make mistakes. Your patience in dealing with me is something I hope to achieve with others in the future. I've also learned much over the myriad conversations we've had about chemistry and life. I never felt I was working for you, but along with you on the endeavors described here.

PALLADACYCLES WITH PALLADIUM-BONDED STEREOGENIC CARBONS: TOOLS FOR EXPLORING REACTION PATHWAYS IN ORGANOMETALLIC CHEMISTRY

TABLE OF CONTENTS Page #

Abbreviations

Å angstrom

Ac acetyl

acac acetylacetonate

ACMP *o*-anisylcyclohexylmethylphosphine

AgOTf silver trifluoromethanesulfonate

Ar aryl

BDPP 2,4-bis(dipbenylphosphino)pentane

BINAP 2,2'-bis(diphenylphosphino)-1,1'-binaphthyl

Bn benzyl

bipy 2,2'-bipyridyl

Bu butyl

t-Bu tert-butyl

t-BuOK potassium *tert*-butoxide

Bz benzoyl

cat. catalyst/catalytic

$(CD_3)_2CO$ acetone (*deuterated*)

CH_3CN acetonitrile

CH_3COCl acetyl chloride

CHIRAPHOS (2*S*,3*S*)-(–)-bis(diphenylphosphino)butane

cm centimeter

COD 1,5-cyclooctadiene

COE cyclooctene

Cy cyclohexyl

d day(s)

dba dibenzylideneacetone

DCE 1,2-dichloroethane

DCM dichloromethane

DIC diisopropylcarbodiimide

DIOP *trans* 1,2-bis(diphenylphosphinomethyl)-3,5-dioxa-4,4-dimethylcyclopentane

DMAD dimethylacetylenedicarboxylate

DMAP 4-(dimethylamino)pyridine

DMF *N*,*N*-dimethylformamide

DMIP dimenthylisopropylphosphine

DMSO dimethyl sulfoxide

dppe 1,2-bis(diphenylphosphino)ethane

dr diastereomeric ratio

E electrophile

EDCI - 1-ethyl-3-(3'-dimethylaminopropyl)carbodiimide

ee enantiomeric excess

EI electron impact ionization

equiv. equivalent(s)

ESI electrospray ionization

Et ethyl

EtOH ethanol

EWG electron-withdrawing group

FAB fast atom bombardment

GC gas chromatography

h hour(s)

HCl hydrochloric acid

HOAc acetic acid

HOBt 1-hydroxybenzotriazole

HRMS high resolution mass spectrometry

Hz hertz

ICP inductively coupled plasma

IR infrared spectrometry

kcal kilocalorie(s)

KHMDS potassium hexamethyldisilazide

KTp potassium tris(pyrazolyl)borate

LDA lithium diisopropylamide

LiCp lithium cyclopentadienide

Ln ligand

M moles per liter

Me methyl

MeI iodomethane

MeOH methanol

MHz megahertz

mL milliliter

mm millimeter

mmol millimole(s)

mol mole(s)

mp melting point

MS mass spectrometry

N equivalents per liter (Normality)

n-BuLi *n*-butyl lithium

NEt_3 triethylamine

nm nanometer(s)

NMR nuclear magnetic resonance

NOE nuclear Overhauser effect

NR no reaction

Nu nucleophile

OMe methoxy

Ph phenyl

phen 1,10-phenanthroline

PG protecting group

PMP *para*-methoxyphenyl

PPh_3 triphenylphosphine

ppm parts per million

i-Pr iso-propyl

psi pounds per square inch

Pyr. pyridine

R_f retention factor

RCM ring closing metathesis

rt room temperature

TBAF tetra-n-butylammonium fluoride

TBSOTf *tert*-butyldimethylsilyl trifluoromethanesulfonate

Tf trifluoromethanesulfonyl

TFA trifluoroacetic acid

THF tetrahydrofuran

THF-d_8 tetrahydrofuran (*deuterated*)

TLC thin layer chromatography

TMEDA tetramethylethylenediamine

TMS trimethylsilyl

o-Tol *ortho*-tolyl

p-Tol *para*-tolyl

V-65 2,2'-azobis(2.4-dimethyl valeronitrile)

Chapter One

Prologue

Organometallic chemistry has experienced an enormous blossoming over the last 50 years. Compounds with metal-carbon bonds often have different properties than their organic cousins and are widely used from organic synthesis to materials science.[1-4] Synthetic chemists are often intimately acquainted with transition metal chemistry, due to organometallic chemistry's seemingly miraculous ability to mediate transformations that were difficult or impossible to carry out or imagine before the modernization of organometallic chemistry.[5]

Among the most prominent of the transition-metals for the synthetic chemist is palladium. Palladium complexes with a σ-bound carbon are highly versatile reagents and/or intermediates in synthesis.[6-8] Examples of palladium-mediated or palladium-catalyzed reactions with σ-bound carbon intermediates include the Heck reaction,[9] carbonylation,[10] the Tsuji-Trost reaction,[11, 12] the plethora of cross-coupling reactions involving transmetalation (including the Stille, Suzuki, Hiyama, Negishi, and Kumada among others),[13-17] palladium-catalyzed allylations of elctrophiles, C-H activation[7] and decarboxylative coupling chemistry.[18-23]

Due to the high cost of palladium metal, much effort has been invested in developing palladium-catalyzed processes. While many modern palladium-catalyzed transformations do not use reactions stoichiometric in palladium as part of their development, the development of the Heck and Tsuji-Trost reactions both utilized reactions stoichiometric in palladium to gain key mechanistic insights.[9, 24, 25] While not always applicable, stoichiometric reactions and model complexes often give us a

more *direct* view of potential reaction intermediates, helping inspire or guide new reaction types.

However, palladium complexes or intermediates with a σ-bound *alkyl* group remain fairly rare due to the greater probability for σ-bound alkyl groups to have β-hydrogens that are readily accessible for β-hydride elimination. As a result, much less is known about the 'fate' of a sp^3-hybridized carbon bound to a palladium center when a process such as migratory insertion or reductive elimination occurs.[26, 27] In this vein, both projects described in this dissertation have at their heart the use of palladium complexes with a sp^3-hybridized stereocenter directly attached as tools to elucidate reaction pathways.

The following paragraphs describe the layout and content of this dissertation. Chapter Two is a very brief history of some of the examples of transition metal complexes as stoichiometric reagents with a focus on palladium. Section 2.1 is a brief history of organometallic chemistry to the discovery of ferrocene, while sections 2.2 and 2.3 show the reaction types that palladium(II) and palladium(IV) complexes can undergo. Section 2.4 relates the use of transition metal complexes as solid-phase reagents. Section 2.5 describes some of the synthetic uses of complexes with a sp^3-hybridized chiral carbon bound to a metal center. Chapter Two is not meant to be comprehensive but illustrative of the breadth and depth of the types of chemistry transition-metal complexes with a σ-bound carbon ligand can undergo.

The remaining chapters describe the experimental work accomplished in this dissertation. Chapter Three describes our efforts to elucidate some of the factors that

affect the reactivity of palladium complexes attached to a polymer-bound ligand as well as our attempts to apply application of polymer-bound palladacycles to the synthesis of a library of 1,2-dihydroquinolines.

Chapter Four describes the synthesis and characterization of a new organometallic scaffold, the palladapyrrolidinone, a palladacycle featuring two sp^3-hybridized stereogenic carbons bound to palladium. This rare structural feature is only found in few other complexes,[28, 29] and the palladapyrrolidinone scaffold is to the best of our knowledge, the first where the effect of one stereogenic carbon on the stepwise formation of a second stereocenter can be studied. The effects of auxiliary ligands and reaction conditions on the diastereoselectivity are included as well as a study on the effect of a chiral non-racemic ligand on the diastereoselectivity of the reaction. A mechanism for the diastereoselectivity based in part on X-Ray data is also proposed. Chapter Five is a discussion of potential improvements and extensions of the projects described in Chapters Three and Four, as well as a discussion of the potential mechanisms of reductive elimination of the palladapyrrolidinones to give β-lactams.

Chapter Two

Transition Metal Complexes as Reagents in C-C Bond Formation

2.1 Organometallic Chemistry From Inception to the Discovery of Ferrocene

The first widely known organometallic compound was Zeise's salt ($K[PtCl_3(C_2H_4)]\cdot H_2O$), first reported on in 1825.[30] The complex was eventually isolated as beautiful yellow crystals, and Zeise correctly deduced it was a complex of ethylene. In 1901, Grignard reported the action of magnesium on aryl and alkyl chlorides, resulting in the first (relatively) stable organometallic reagents.[31] In 1917, Schlenk described the synthesis of methyl lithium via reaction of ethyl lithium and dimethyl mercury, opening access to alkyl lithium reagents.[32] In 1924, Gilman reported[33] on the reaction of methyl lithium with cupric chloride, eventually leading to modern cuprate chemistry.[34-37] Almost 30 years later, two groups independently discovered ferrocene[38, 39]; this set off a firestorm of experimentation that still resonates today. Wilkinson and coworkers as well as Fischer proposed the iconic structure of ferrocene via reactivity studies[40-42], and Dunitz confirmed it with X-Ray crystallography.[43] With this serendipitous discovery, modern organometallic chemistry began.[44]

2.2 Organopalladium(II) Chemistry From 1960 to Present

A few years after the discovery and elucidation of the structure of ferrocene, Smidt reported work on describing the mechanism of the Wacker process, invoking attack of hydroxide anion on an aqueous solution of an ethylene-palladium(II) complex **2.1** to give intermediate **2.2**, which would undergo β-hydride elimination to generate Pd(0), HCl, and acetaldehyde **2.3**. (Scheme 2.1).[45]

Scheme 2.1

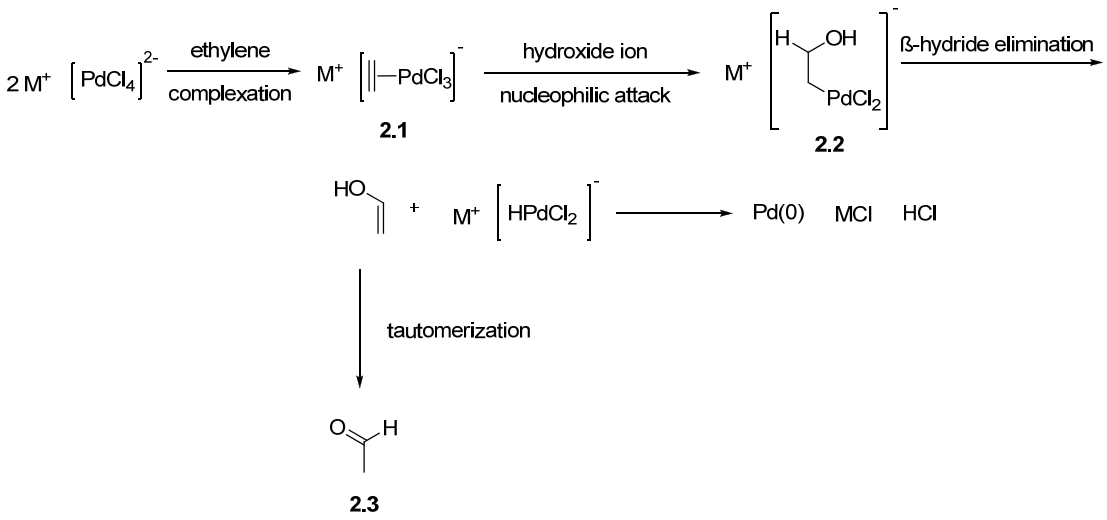

The report of the mechanistic work on the Wacker process helped unveil the potential of palladium complexes to the synthetic chemist. The advantages of the newly discovered Pd(II) reagents included increased stability to water and oxygen in many cases as compared to organomagnesium and organolithium reagents and generally high functional group tolerance.[8] The synthetic versatility of palladium stems from the variety of reactivity modes available to palladium complexes featuring a Pd-C σ-bond (vide infra). Depending on the ligand sphere, Pd-allyl complexes can be made to either transfer a nucleophilic or electrophilic allyl to an external reactant. The relatively non-polarized Pd-C bond also makes carbopalladation reactions of alkenes and alkynes synthetically useful. As with other transition metals, carbonylation is also possible with palladium.[10] In addition, palladium has proved particularly valuable in cross-coupling reactions involving Csp^2-Csp^2 bond formation via transmetalation. The following sections will present a brief, illustrative history of the

utilization of palladium complexes as stoichiometric reagents as springboards for developing new reactions as well as probes for studying mechanisms of interest to synthetic chemists. As palladium chemistry is a very broad area, the rest of the section is divided into subsections detailing the steps and role palladium is playing in mediating C-C bond formation.

2.2.1 C-C Bond-forming Reactions in Which 1,1-Migratory Insertion is a Key Step

Inspired by the work on the Wacker process, as well as reports of amines[46] and acetate[47] as nucleophiles, Tsuji began describing palladium(II)-chloride mediated reactions of alkenes with carbon monoxide to give β-chloro acyl chlorides.[10] Two reasonable mechanisms can be proposed, one involving chloropalladation of the double bond by $PdCl_2$ to generate **2.4**, followed by insertion of carbon monoxide to give **2.5** and reductive elimination to give the acyl chloride **2.6** (Scheme 2.2, mechanism A). The second mechanism (Scheme 2.2, mechanism B) involves insertion of carbon monoxide to $PdCl_2$ to give complex **2.7**, followed by carbopalladation of ethylene to give **2.5** and reductive elimination to give **2.6**.

Scheme 2.2

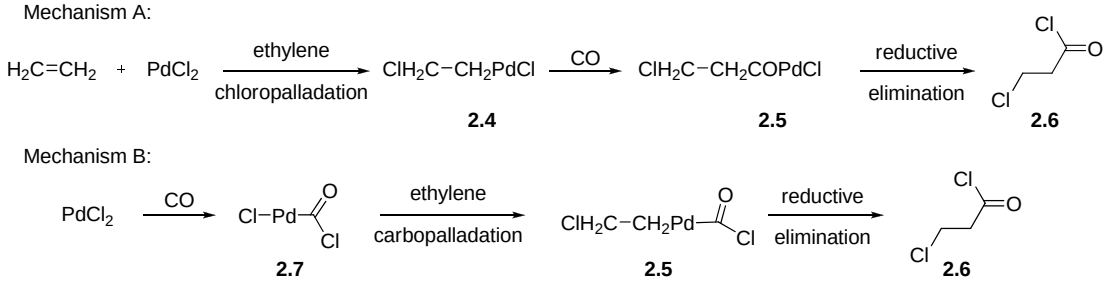

Tsuji also showed that the reaction of π-allyl palladium chloride with carbon monoxide gave acyl chlorides via a similar mechanism for C-C bond formation (Scheme 2.3).[48] In this case, the carbon monoxide breaks the π -allyl palladium dimer complex to give mono-π-allyl complex **2.8**, which then undergoes carbon monoxide insertion to give palladium acyl **2.9**, which undergoes reductive elimination to give the acyl chloride product **2.10**.

Scheme 2.3

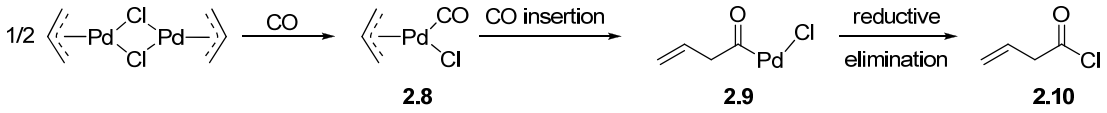

2.8 **2.9** **2.10**

However, when there is more than one site for carbon monoxide attack in an unsymmetrical π-allyl complex, multiple products are seen from both palladium-mediated and non-palladium mediated attack of carbon monoxide.[49] Tsuji disclosed other examples of the reactions of π-complexes derived from higher alkenes (butadiene,[50] allene,[51, 52] cyclooctadienes,[53] and unsaturated esters[54]) with carbon monoxide. Tsuji also communicated the results from the reaction of cyclohexyl isocyanide with π-allyl palladium chloride dimer instead of carbon monoxide (Scheme 2.4).[55]

Scheme 2.4

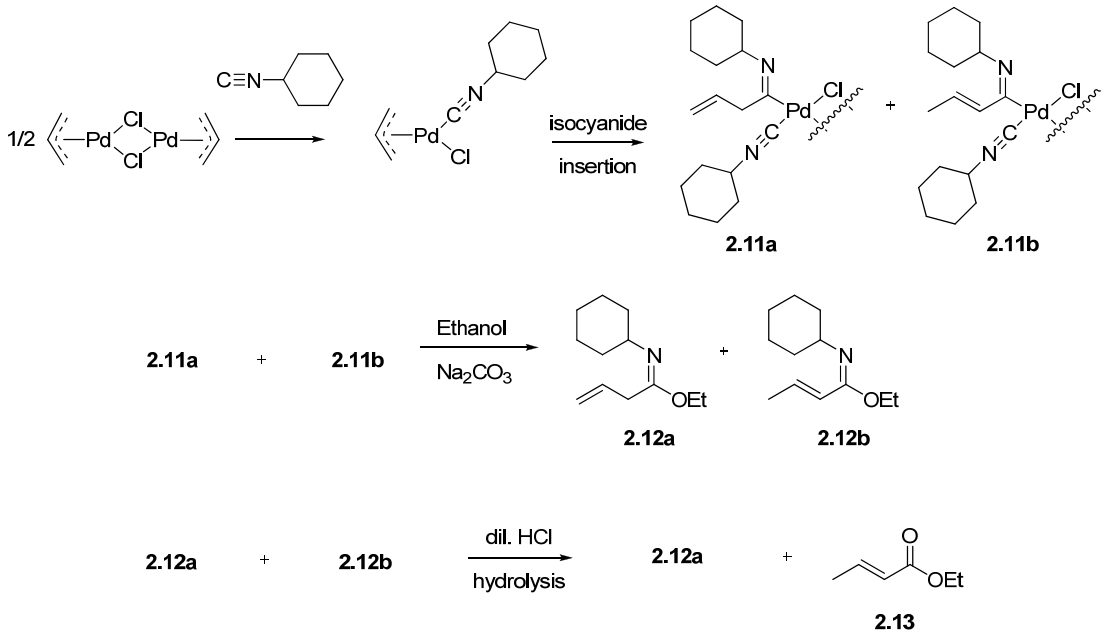

The resulting complexes **2.11a** and **2.11b** were reacted with sodium carbonate and ethanol to afford imidate derivatives **2.12a** and **2.12b** followed by mild acid hydrolysis affording a mixture of products from isocyanide insertion into the Pd-C bond.

In 1976, Yamamoto disclosed a reaction of palladated azobenzene **2.14** with *t*-butyl isocyanide via a similar insertion mechanism as in Scheme 2.4, providing heterocycle **2.15** regiospecifically and in high yield (Scheme 2.5).[56]

Scheme 2.5

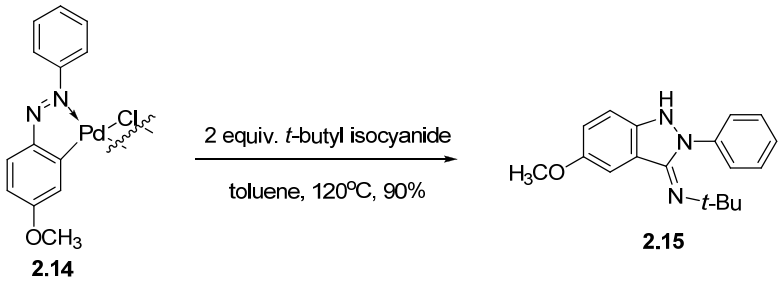

2.14 **2.15**

Heck also reported on the insertions of carbon monoxide[57, 58] into cyclopalladated complexes[59] (**2.16** and **2.18**) derived from azobenzene (Scheme 2.6). In this case, the yield of the carbon monoxide insertion reaction of **2.16** to give **2.17** was low (17%), but structurally interesting lactone **2.19** was formed in 25% yield upon reaction of **2.18** with carbon monoxide.

Scheme 2.6

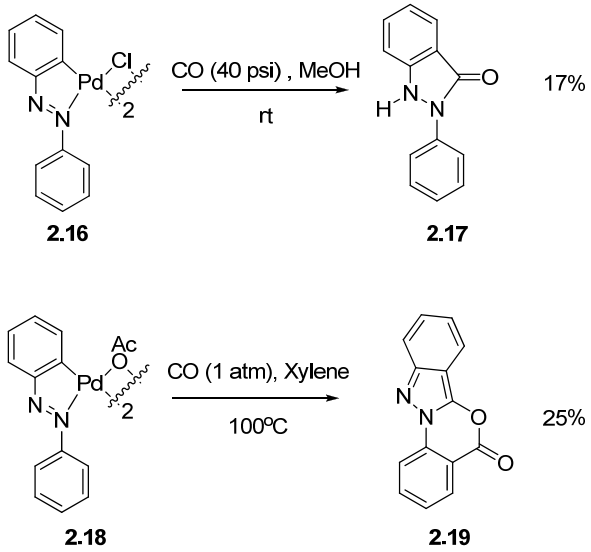

2.16 **2.17**

2.18 **2.19**

Larock reported[60] utilizing *in situ* transmetalation from preformed organomercurials to palladium *en route* to the synthesis of coumarins and butenolides (Scheme 2.7).[61] The presumed alkenyl palladium intermediate forms via transmetalation of **2.20** with

palladium (II). After carbonylation and solvolysis a methyl ester is produced, which ultimately gives the lactone after deprotection of the phenol with HF. Larock reported similar chemistry beginning from the thallation of benzoic acids[62] in the synthesis of isocoumarins.

Scheme 2.7

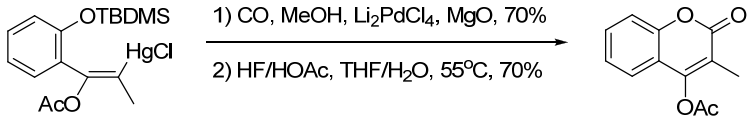

2.20 **2.21**

These examples showcase palladium's ability to allow carbon monoxide or isocyanides to act as a useful phosgene surrogate under mild conditions, often with high regioselectivity.

2.2.2 C-C Bond-forming Reactions Involving External Nucleophilic Attack at Carbon

In 1965, Tsuji[63, 64] disclosed the reaction of the anions derived from ethyl malonate, ethyl acetoacetate, and an enamine with π-allyl palladium chloride dimer (Scheme 2.8).

Scheme 2.8

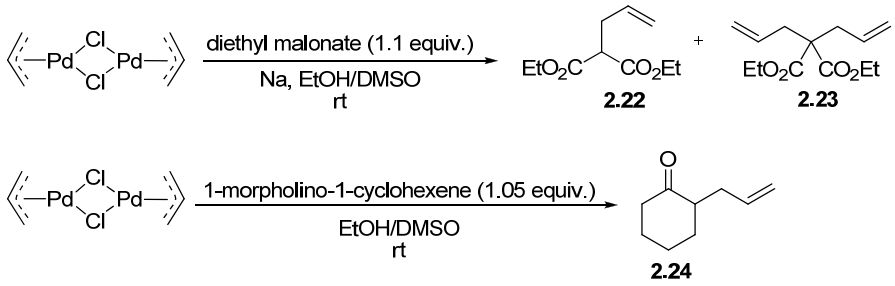

2.22 **2.23**

2.24

Both mono-allylation (to give product **2.22**) and di-allylation (product **2.23**) were reported. The morpholine enamine of cyclohexanone also reacted to give substituted cyclohexanone **2.24**. These were the first examples of what would become known as the Tsuji-Trost reaction, with the terminus of the allyl system acting as the electrophile (vide infra).

Recognizing the potential of this type of reactivity, Trost began describing the scope and limitations of the allylic alkylation reactions, beginning in 1973.[25] A mixture of complexes **2.25** and **2.26** were reacted with diethyl sodiomalonate to give a mixture of alkenes **2.27** and **2.28** in a 63% yield (Scheme 2.9).

Scheme 2.9

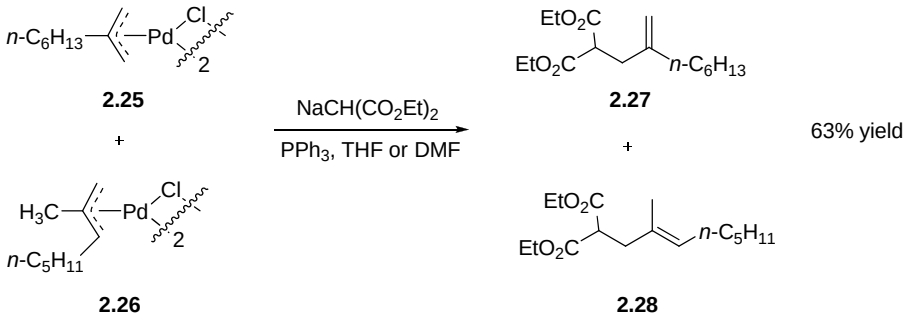

In contrast to Tsuji's report, Trost reported that the π-allyl palladium complexes derived from 2-methyl-1-octene did *not* react with the anion derived from diethyl malonate. Interestingly, Trost's report does not mention the solvent utilized in the failed case. Tsuji's report of a successful reaction had DMSO as a solvent. Trost also reported that the reaction in the presence of triphenylphosphine in THF or DMF allowed for the desired reaction to occur readily. Reaction of the π-allyl complex **2.29** with the anions of diethyl malonate, methyl methylsulfonylacetate, and methyl

methylsulfinylacetate resulted in highly regioselective attack at the less substituted terminus of the π-allyl complex (Scheme 2.10).

Scheme 2.10

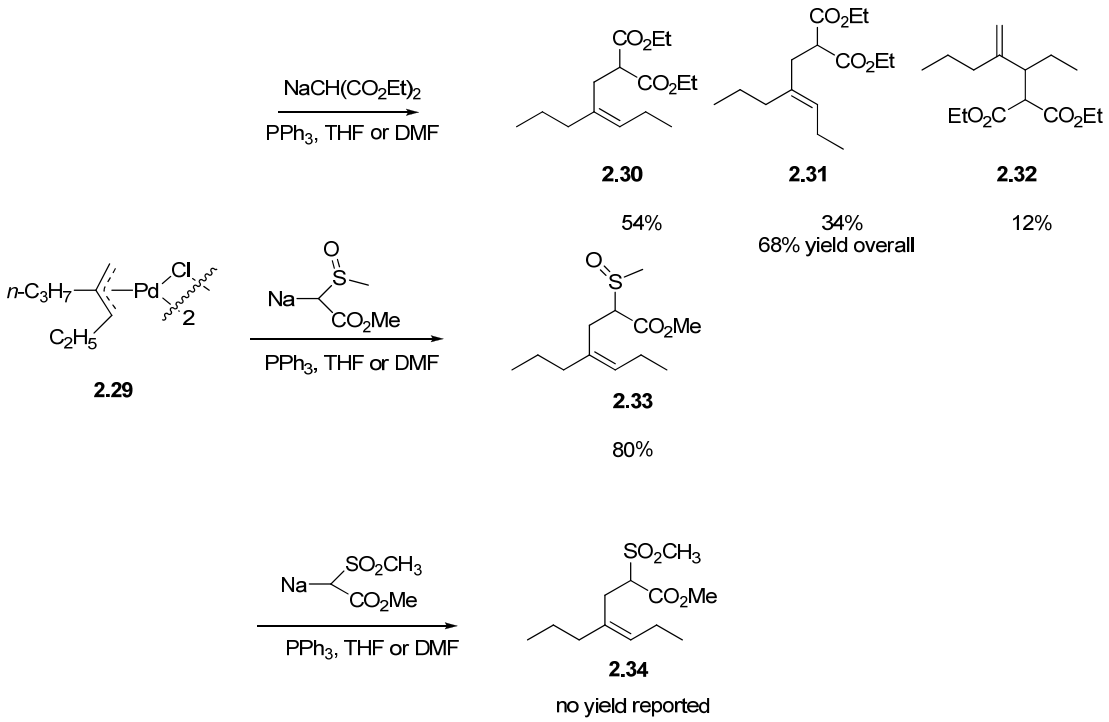

The reaction with the anion of diethyl malonate provided 68% yield, giving 88 : 12 selectivity ((**2.30** + **2.31**) : **2.32**) for attack at the less substituted allyl terminus, while the anions of methyl methylsulfonylacetate and methyl methylsulfinylacetate gave complete regioselectivity for attack at the less substituted end of the allyl system.

Soon after, Trost also disclosed[24] the stereoinduction in the reaction of π-allyl palladium complex **2.35** with diethyl sodiomalonate in the presence of various chiral ligands (Table 1).

Table 2.1 *Effect of P/Pd Ratio, Temperature, and Ligand on the Optical Yield of Product*

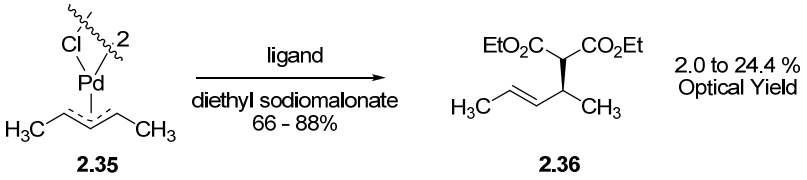

2.35 **2.36**

Ligand	P(N)/Pd	Conditions (°C)	Optical Yield[a] (%)
(+)-DIOP	4/1	0, then 25	12.2 ± 0.8
(+)-DIOP	4/1	-40, 25	22.4 ± 2.2
(+)-DIOP	4/1	-78, 25	17.9 ± 1.8
(+)-ACMP	2/1	25	17.9 ± 1.8
(+)-ACMP	2/1	-40, 25	24.4 ± 1.6
(+)-ACMP	2/1	-78, 25	22.4 ± 2.8
(-)-Sparteine	4/1	25	20.2 ± 2.1
(-)-DMIP	4/1	0, 25	2.0 ± 0.3

[a]defined as the ratio of the optical purity of the product to that of the catalyst

The results indicate that the ligands with the stereocenter closer to palladium were more effective than those where the stereocenter was further away.

Trost also reported[65] on mechanistic aspects of the allylic alkylation reaction. At the time, it was unclear whether the mechanism consisted of nucleophilic attack at the palladium center followed by reductive elimination (Path A, Scheme 2.11) to give

C-C bond formation, or whether the nucleophile directly attacks one of the terminal carbons of the allyl ligand (Path B, Scheme 2.11) to give C-C bond formation.

Scheme 2.11

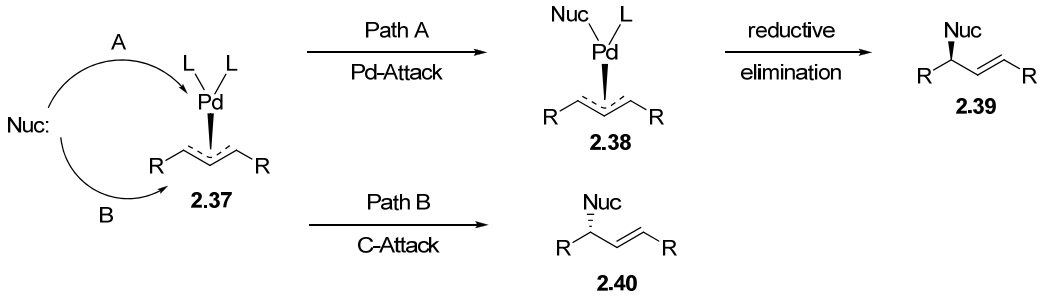

The mechanistic aspect in question has implications for the stereochemical outcome of the C-C bond formation. Path A, involving attack at the palladium center would involve a *retention* of configuration of the Pd-C center via a pathway involving intermediate **2.38** followed by reductive elimination to give **2.39**. Path B would likely involve an *inversion* of configuration of the Pd-C center due to the nature of the π-allyl palladium complex, with the palladium atom and its ligand sphere directing attack at the face opposite due to steric factors. This would generate product **2.40** directly from **2.37**. In order to help answer this question, the π-allyl palladium complex **2.41** was reacted with the anion of diethyl malonate to give **2.42** (Scheme 2.12). Decarbomethoxylation, dihydroxylation and lactonization of carbocycle **2.42** provided **2.43a**, whose stereochemistry as determined by ^{1}H NMR shift analysis showed indirectly that Path B was the likely pathway for the reaction of π-allyl palladium complexes with soft nucleophiles.

Scheme 2.12

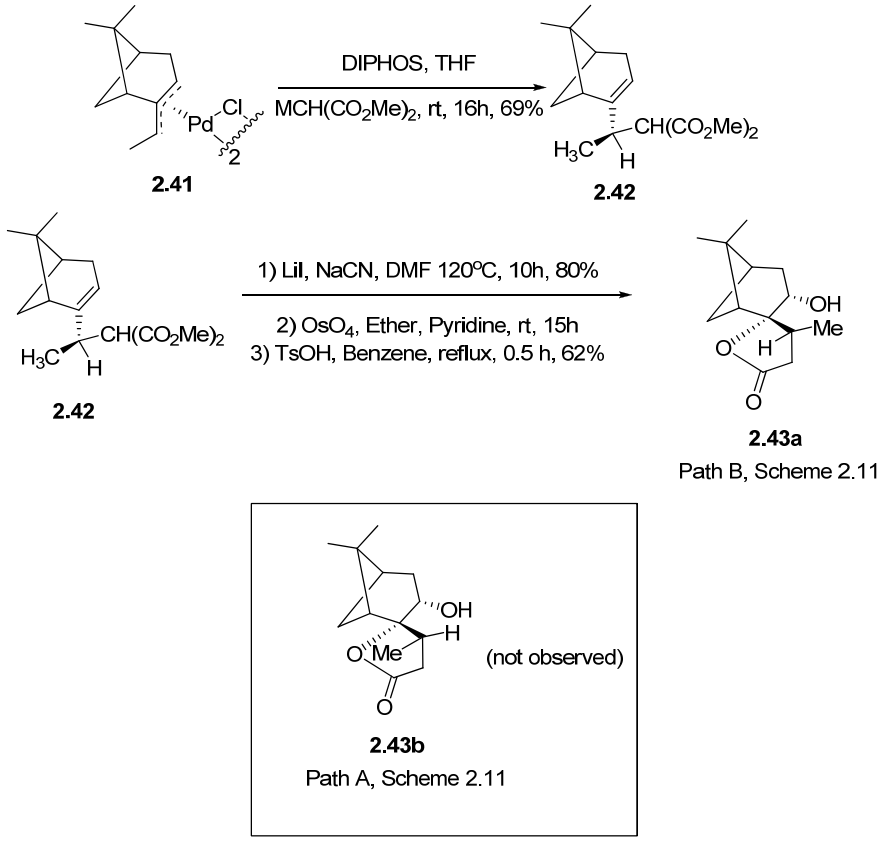

Trost also reported a reaction that established that the stereochemistry of attack on some cyclohexyl systems to be axial in nature.[66] A mixture of π-allyl palladium complexes **2.44a** and **2.44b** with *tert*-butyl substituents on the cyclohexane ring to bias the conformation were reacted with dimethyl sodiomalonate in DMSO to give a 21 : 79 mixture of alkenes **2.45** and **2.46**.

Scheme 2.13

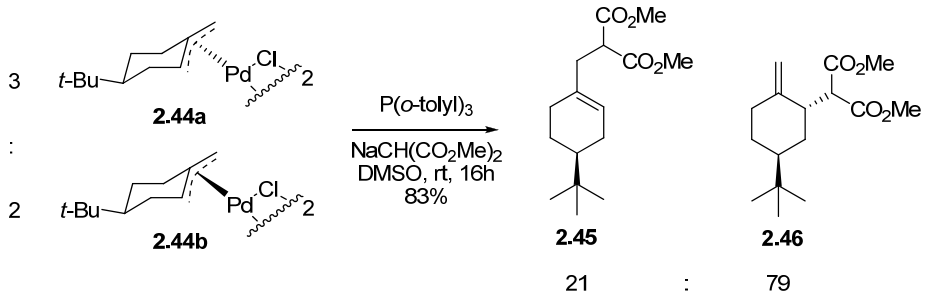

The regiochemical result of this reaction is in contrast to what is generally expected in the reactions of π-allyl complexes with nucleophiles (attack at the more substituted carbon, vide supra). In addition, the mixture of both isomers leads to one diastereomer of the dominant product. This result was attributed to a fast equilibrium between **2.44a** and **2.44b**. As the stereochemistry of the product indicates that the reactive isomer was **2.44b**, the reaction has a very high preference for axial attack due to stereoelectronic effects. Finally, Trost reported the use of this type of chemistry to achieve the unnatural configuration at C-20 in a partial synthesis of 5α-cholestanone[67, 68].

These results indicate that stoichiometric palladium chemistry played a key role in elucidating factors relating to the regiochemistry and mechanism of allylic alkylation reactions, which are now widely used in the catalytic mode[11, 12].

2.2.3 C-C Bond-forming Reactions Involving External Electrophilic Attack at Carbon

There are very few reports of this type of reaction in the *stoichiometric* mode, presumably due to the tendency for palladium(II) allyl complexes to preferentially bind in the η^3 mode, as seen in Section 2.2.2. In 1983, Parra-Hake reported the

reaction of palladium π-allyl dimer **2.47** with aqueous sodium cyanide to give a mixture of bicyclic alkenes **2.49** and **2.50** in a combined 93% yield (Scheme 2.14).[69]

Scheme 2.14

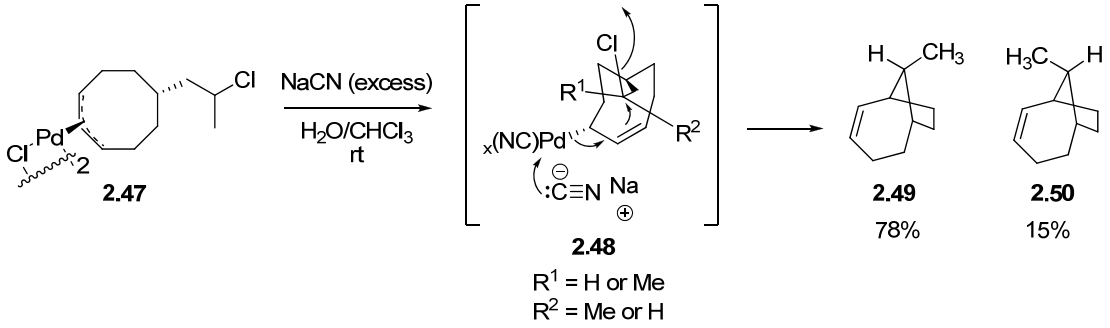

The reaction is proposed to occur via *in situ* formed η^1-allyl species **2.48** formed by the coordination of the cyanide anion. The modest selectivity for **2.49** is presumably due to steric factors.

In 1986, Kurosawa disclosed the reaction of pre-formed η^1-allyl species **2.51** reacting with maleic anhydride to form proposed intermediate **2.52** concomitant with new C-C bond formation (Scheme 2.15).[70]

Scheme 2.15

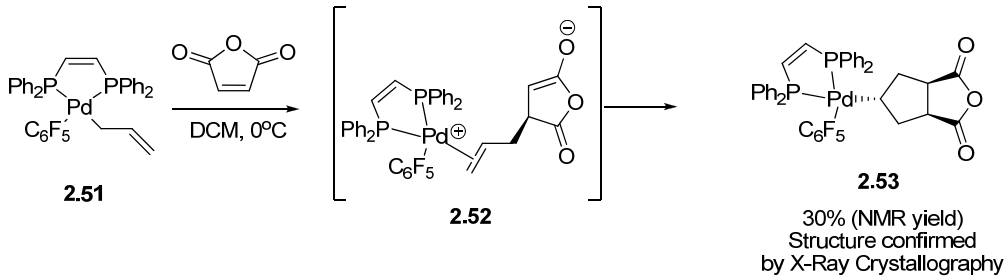

The reaction is put forth as a Sakurai-type addition to the maleic anhydride followed by the palladium center in intermediate cationic complex **2.52** acting as a Lewis acid

to activate the pendant alkene for intramolecular nucleophilic attack to afford complex **2.53** as a product in low yield.

A very recent example of external electrophilic attack at carbon was reported by Jarvo in 2007.[71] Stoichiometric reactions were performed utilizing bidentate NHC-phosphine ligands (such as in complex **2.54**) to find suitable conditions for a catalytic reaction (Scheme 2.16).

Scheme 2.16

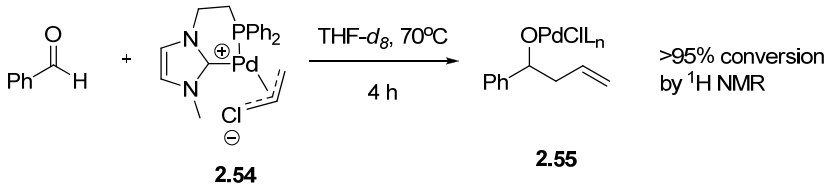

2.54 **2.55**

It was found that coordinating counterions (such as the chloride in **2.54**) and the bidentate ligand made the complex much more nucleophilic as judged by conversion by ^{1}H NMR spectroscopy. Other counterions (OAc, BAr_4^F) resulted in lower conversions to palladium complex **2.55** during the survey.

The results in this section show another facet of the versatility of palladium complexes and intermediates in organic synthesis. Reactions with proposed η^1-allyl palladium intermediates are becoming more widespread.[71, 72]

2.2.4 C-C Bond-forming Reactions Involving 1,2-Migratory Insertion

In 1968, Heck reported one of the first examples of the reaction that would come to bear his name.[9] The requisite palladium aryl or alkyl derivatives were generated *in situ* via transmetalation from the corresponding lead, tin, or mercury compounds to generate "phenylpalladium chloride" (Scheme 2.17).

Scheme 2.17

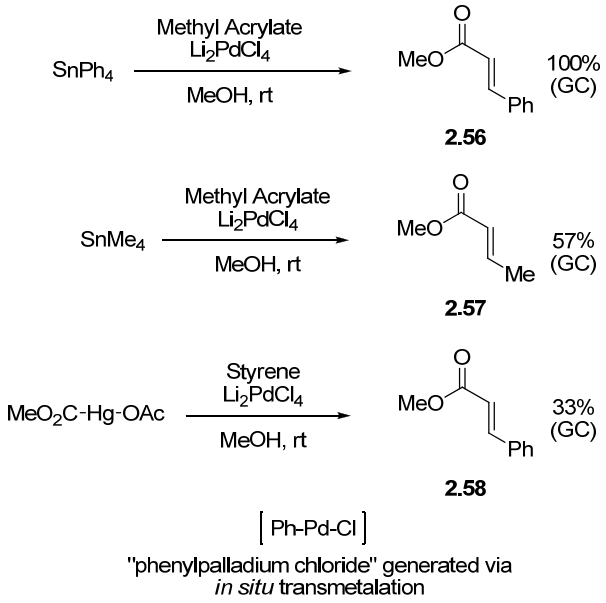

The "phenylpalladium chloride" then reacted with either methyl acrylate or styrene to generate acrylate derivatives **2.56 - 2.58** in 33 – 100% yields by GC analysis. Heck later reported more work, elucidating the likely mechanism of the reaction, utilizing an *in situ* generated "phenylpalladium acetate" complex.[73] The acetate counterion was used because reactions with the chloride counterion resulted in double bond isomerization and/or migration in some substrates. Heck studied the reaction of "phenylpalladium acetate" with propylene to probe the mechanism of the reaction. A variety of products can be expected from the reaction as shown in Scheme 2.18. Reaction via intermediate **2.24** can result in the three products shown from the three different β-hydrogen atoms, while reaction via intermediate **2.25** can result in only one product due to the single β-hydrogen.

Scheme 2.18

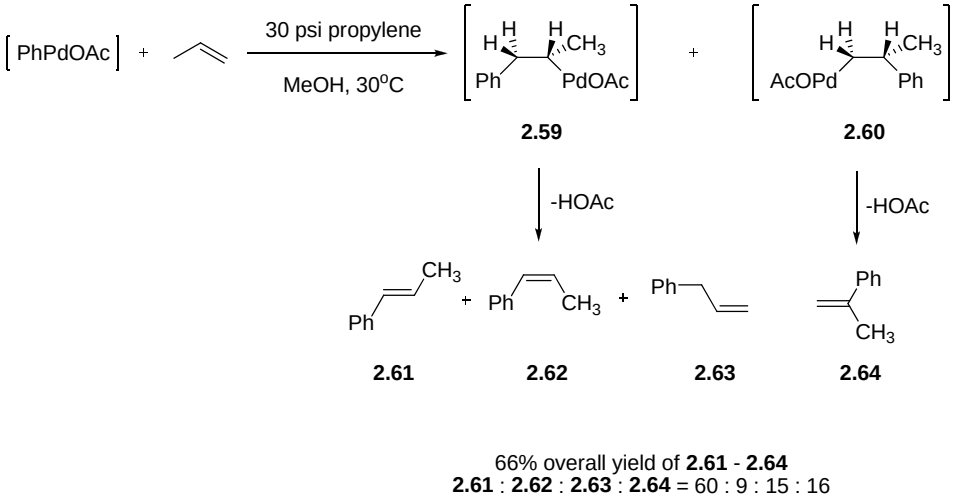

The reaction run in methanol at 30°C and 30 psi propylene resulted in 66% overall yield. The product composition consisted of 60% *trans*-1-phenyl-1-propene **2.61**, 9% *cis*-1-phenyl-1-propene **2.62**, 15% allylbenzene **2.63**, and 16% 2-phenyl-1-propene **2.64**. The product distribution indicates that the majority of products formed are from formal *anti*-Markovnikov addition to propene via intermediate **2.59**. The majority of the *anti*-Markovnikov products resulted from the benzylic β-hydride elimination from the intermediate palladium complex.

Heck also reacted both *trans*-1-phenyl-1-propene **2.65** and *cis*-1-phenyl-1-propene **2.68** with "phenylpalladium acetate" and found the reactions to be stereoselective, with **2.65** giving *trans*-1,2-diphenyl-1-propene **2.67** as the major product, and **2.68** giving *cis*-1,2-diphenyl-1-propene as **2.70** the major product through presumed Pd(II) intermediates **2.66** and **2.69**, respectively (Scheme 2.19).

Scheme 2.19

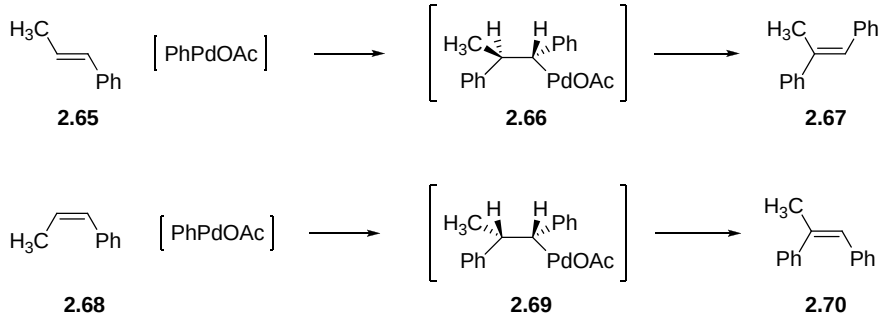

Horino and Inoue reported a regioselective *ortho* vinylation of aromatic amides starting from cyclopalladated complex **2.71** via and intermediate like **2.72** (Scheme 2.20).[74]

Scheme 2.20

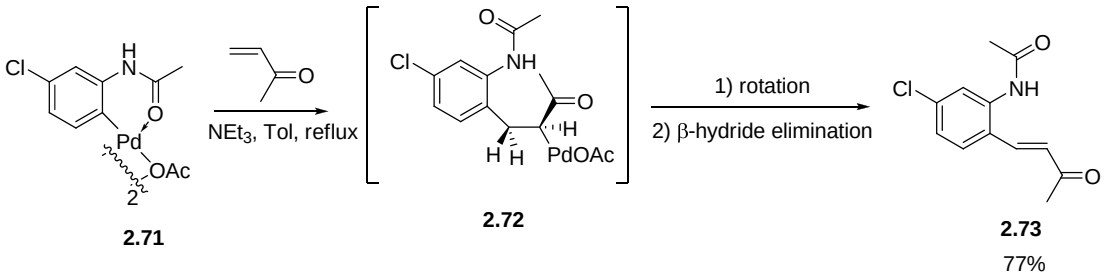

Holton reported a similar reaction to give α,β-unsaturated ketone **2.75** starting from cyclopalladated complex **2.74** as shown in Scheme 2.21.[75] Interestingly, **2.74** has a potentially accessible β-hydrogen in contrast to complex **2.71**.

Scheme 2.21

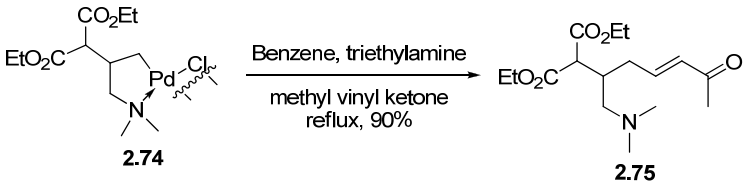

In another interesting use of palladium chemistry, Bergstrom reported the use of *in situ* generated uridine-palladium complexes en route to the formal alkylation of uridines without the use of protecting groups (Scheme 2.22).[76]

Scheme 2.22

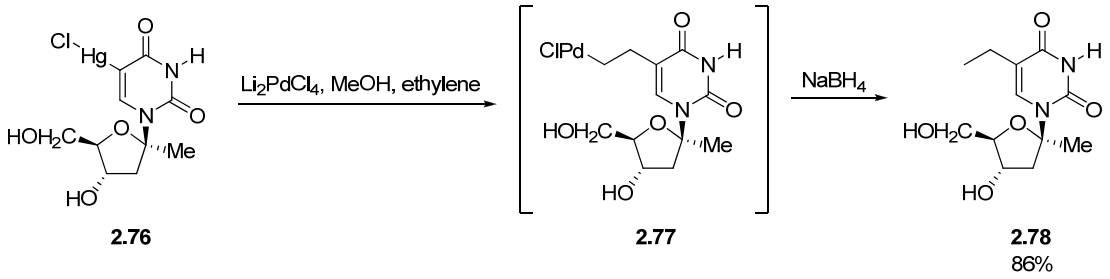

2.76 **2.77** **2.78** 86%

Mercurated uridine **2.76** undergoes transmetalation to generate alkylpalladium intermediate **2.77** with readily accessible β-hydrogens. The intermediate is intercepted by a one-pot reduction with sodium borohydride to give alkylated uridine **2.78**.

As a final example, Heck utilized the 1,2-migratory insertion chemistry to selectively form some rare types of heterocycles, such as multiply substituted naphthalenes and cinnolinium salts (Scheme 2.23).[77, 78] The generation of cationic palladium complexes **2.79** and **2.82** is necessary to activate the complex for migratory insertion of the alkynes to generate intermediates **2.80** and **2.83** which subsequently undergo reductive eliminations to give napthalene **2.81** and cinnolinium salt **2.84**.

Scheme 2.23

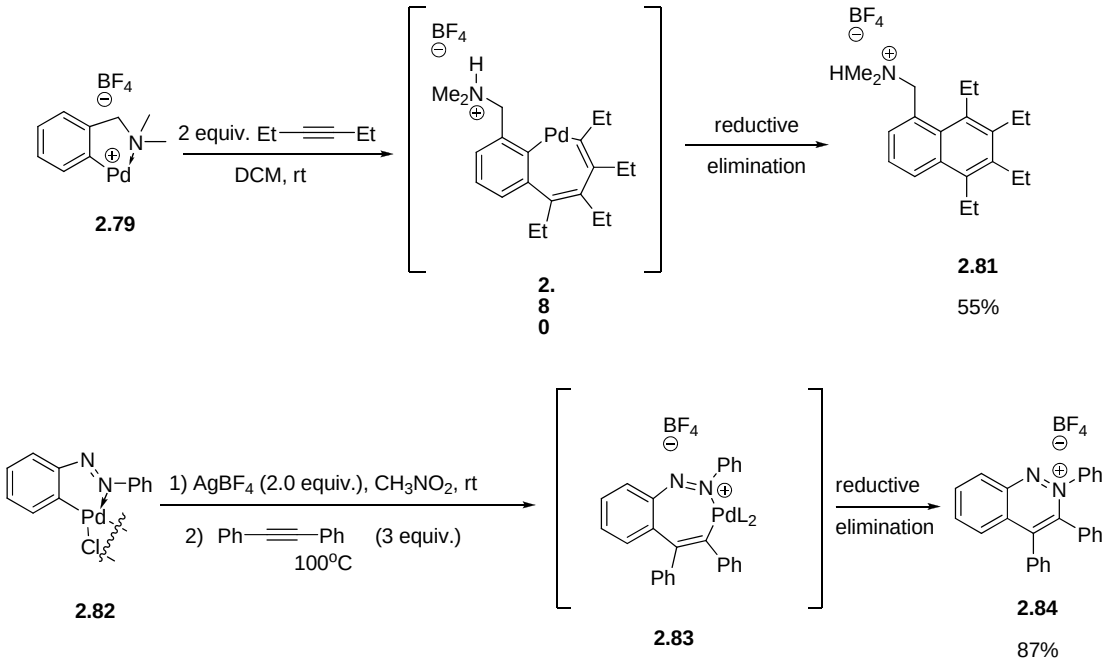

The selected reactions shown in this section showcase the utilization of stoichiometric palladium reactions to partially elucidate the mechanism of the Heck reaction as well as to provide access to a range of products that would be difficult to synthesize using other methods.

2.3 Chemistry of Organopalladium(IV) Complexes

Much synthetic chemistry, both involving C-C and C-Heteroatom bond formation involves proposed organopalladium(IV) intermediates.[79-83] This section will be divided into three parts, each according to how the Pd(IV) intermediate is generated.

2.3.1 Reactions Involving Generation of Pd(IV) Complexes via Reaction With Alkyl or Acyl Halides

In 1986, Canty reported the first example of an isolated triorganopalladium(IV) complex via reaction of palladium(II) bipy complex **2.85** with excess methyl iodide in acetone to give complex **2.86** as colorless crystals in 90% yield. **2.86** was also characterized by X-Ray crystallography.[84]

Scheme 2.24

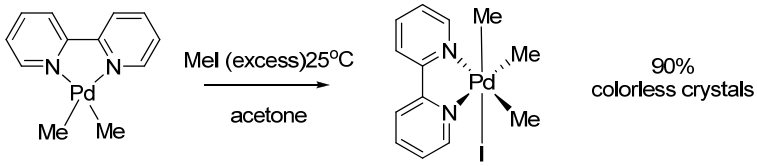

2.85 **2.86**

Holton disclosed the reaction of cyclometalated palladium complex **2.87** with acetyl chloride to give an acetophenone derivative (Scheme 2.25).[85] It is proposed that the reaction goes through Pd(IV) intermediate **2.88** to give acetophenone derivative **2.89** in 81% yield.

Scheme 2.25

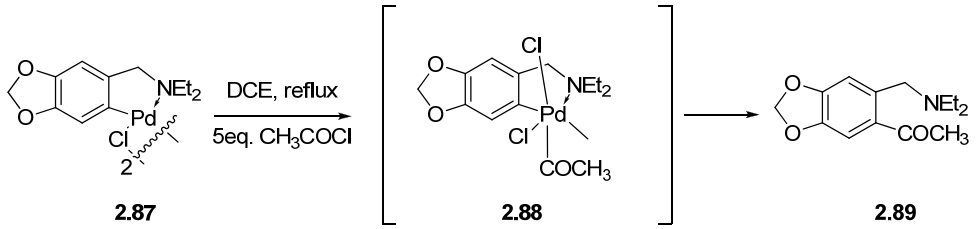

2.87 **2.88** **2.89**

81%

A common way of generating Pd(IV) intermediates is a simple S_N2 reaction of the palladium(II) complexes with alkyl halides (i.e., methyl iodide, benzyl or allyl bromides) to generate Pd(IV) complexes. Some of the complexes are isolable, but

many are metastable and generate organic products along with other Pd(II) complexes. In 1991, Markies et al. reported[86] the reactions of (bipy)PdPhMe **2.90** and (TMEDA)PdPhMe **2.93** with methyl iodide and benzyl bromide (Scheme 2.26). The reactions were monitored by NMR spectroscopy.

Scheme 2.26

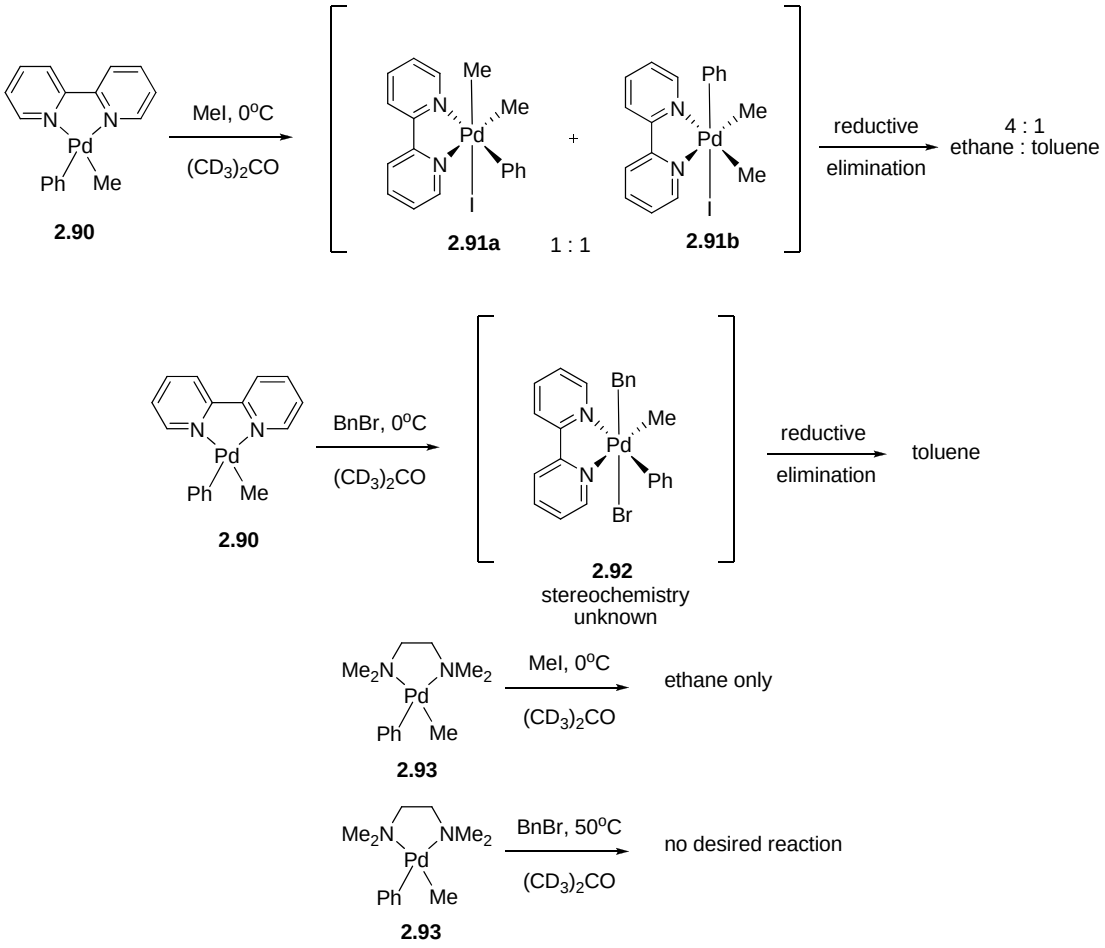

In the reactions with methyl iodide, bipyridyl complex **2.90** was seen to react readily and give a 1 : 1 ratio of isomers of the Pd(IV) complexes **2.91a** and **2.91b** after oxidative addition. Upon reductive elimination, the product mixture consisted of a 4 : 1 ratio of ethane to toluene, indicating that methyl-methyl coupling was more facile

than methyl-phenyl coupling. In the case of TMEDA complex **2.93**, a discrete Pd(IV) complex was not detected and the reaction afforded exclusively ethane. In the case of reactions with benzyl bromide, **2.90** reacted readily to give a Pd(IV) intermediate of unknown stereochemistry and upon reductive elimination only toluene. **2.93** did not react up to the decomposition point of the complex (ca. 50°C). This indicates that reactions with Pd(II) complexes acting as nucleophiles are very sensitive to steric factors.

Canty et al. also provided results on the selectivity of reductive elimination from a series of isolable Pd(IV) complexes[87] via NMR signals of the resulting Pd(II) complexes (some signals of the organic compounds were obscured in the NMR) (Scheme 2.27).

Scheme 2.27

$$Me_2RPd(L_2)Br \xrightarrow[\text{Acetone}]{40^oC} [RPd(L_2)Br + MeMe \ : \ MePd(L_2)Br + RMe]$$

R = Bn, L_2 = bipy	1 : 0
R = Bn, L_2 = phen	3 : 1
R = p-BrC_6H_4, L_2 = bipy	5 : 1
R = p-BrC_6H_4, L_2 = phen	2 : 1
R = $C_6H_5COCH_2$, L_2 = bipy	3 : 1
R = $C_6H_5COCH_2$, L_2 = phen	ca. 1 : 1

As can be seen from Scheme 2.27, the elimination of ethane is highly favored in all these cases. A random elimination of Me-Me and R-Me would result in a 1 : 2 ratio in all cases. Canty also reported on the selectivity of reductive elimination with respect to the anion of the triorganopalladium(IV) complex.[88] The complexes were generated

by abstraction of the bromide counterion with silver nitrate followed by rapid introduction of a different halide salt. Once isolated, the complexes **2.94a - f** were then heated to 30°C in acetone-d_6, where the selectivities of reductive elimination were studied (Scheme 2.28).

Scheme 2.28

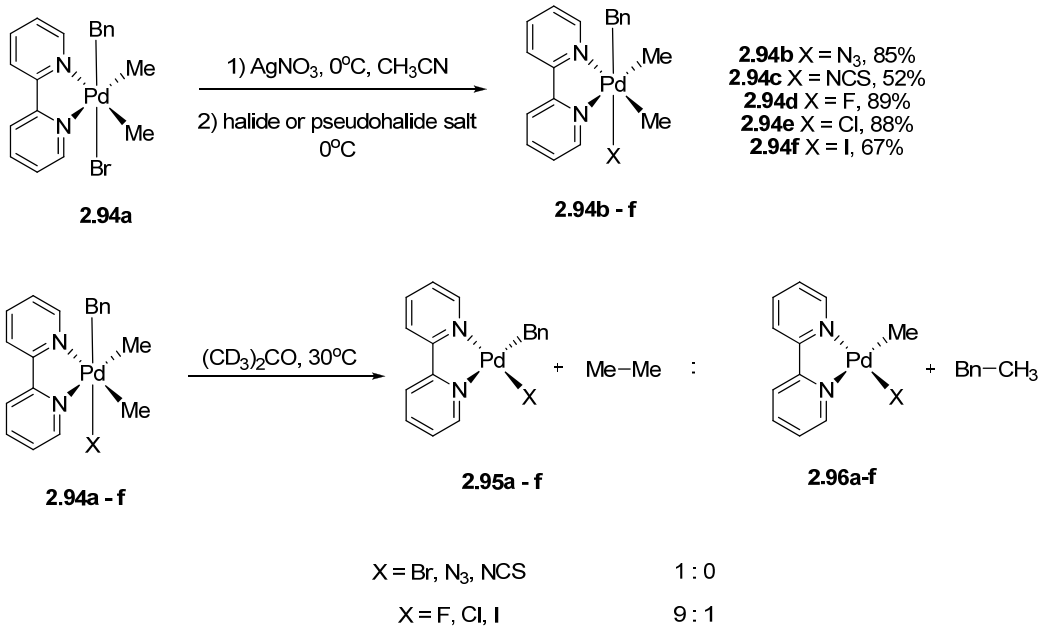

The selectivity of the reductive elimination was not very sensitive to a change in counterion, with ethane elimination predominating in all cases.

Markies et al. studied the selectivity of reductive elimination from triorganopalladium(IV) complexes with three different organic groups (Scheme 2.29).[89]

Scheme 2.29

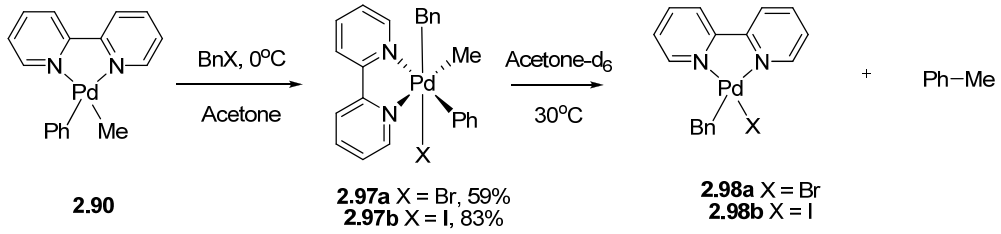

It was found that reductive elimination from Pd(IV) complexes **2.97a** and **2.97b** gave exclusively toluene. The authors concluded this was potentially due to the strength of the benzyl-palladium bond.

2.3.2 Reactions Involving Generation of Pd(IV) Complexes via Hypervalent Iodine Reagents

Oxidative additions of aryl iodides to Pd(II) complexes have not been seen in the stoichiometric mode. However, Canty has shown that by using the much more reactive hypervalent iodine reagents, transfer of alkynyl groups is feasible, generating Pd(IV) complexes **2.99** and **2.100**, observable via ^{1}H NMR spectroscopy (Scheme 2.30).[90]

Scheme 2.30

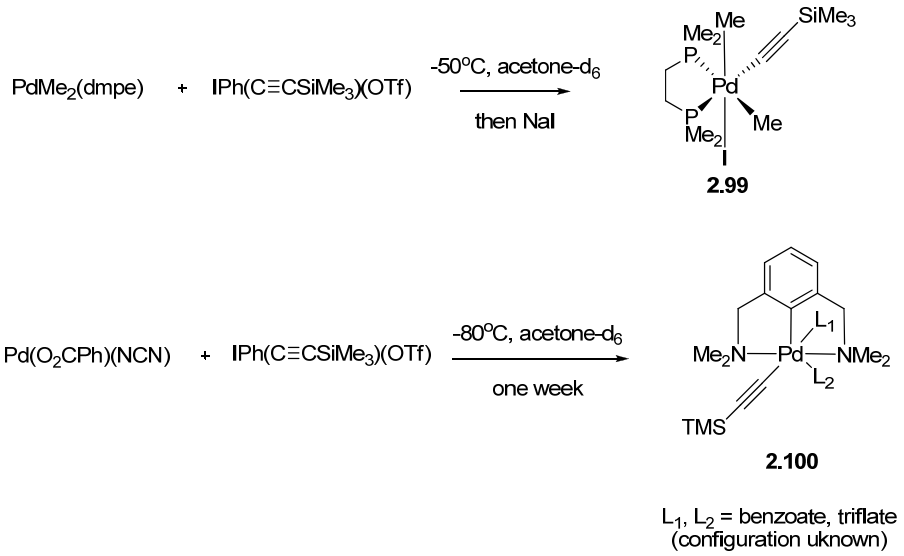

While attempting to elucidate the mechanism of a catalytic arylation reaction,[81] Sanford and co-workers reacted cyclopalladated complex **2.101** with diphenyl iodonium tetrafluoroborate both in the presence and the absence of an external free arylpyridine substrate (**2.102**, Scheme 2.31). In the presence of the additive, a 90% GC yield was observed; in its absence, a 20% yield was observed. The authors speculate this could be due to the free arylpyridine potentially trapping intermediates such as **2.103**.

Scheme 2.31

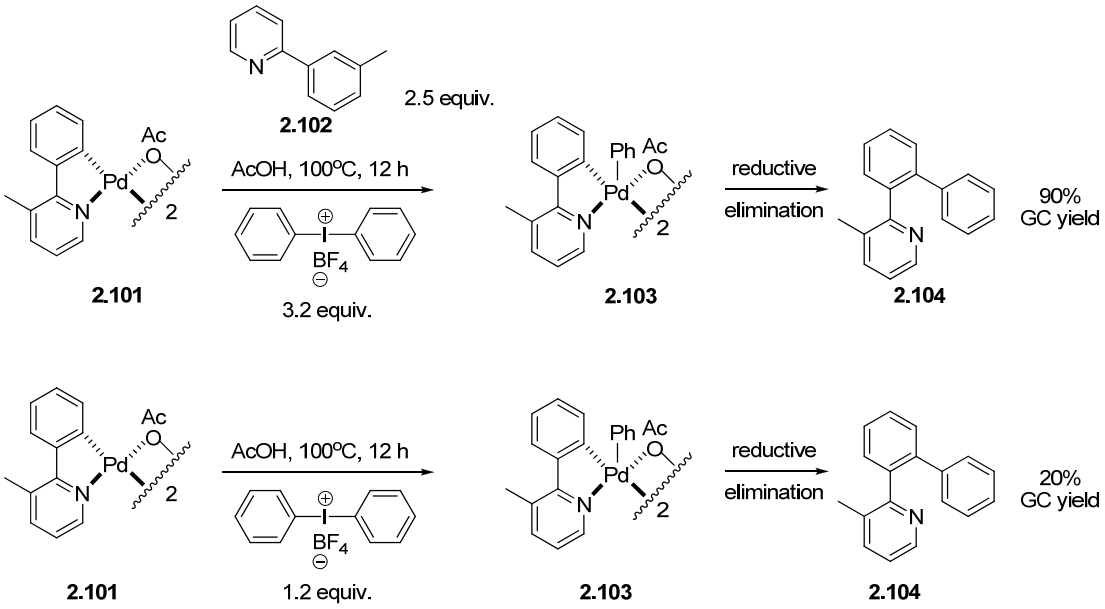

2.3.3 Reactions Involving Generation of Pd(IV) Complexes via Halogens

To the best of our knowledge, the only known example of an isolated organometallic Pd(IV) complex synthesized via oxidation with a halogen is the synthesis of complex **2.106** via oxidation of (bipy)Pd(C_6F_5) **2.105** with chlorine gas (Scheme 2.32) that was reported by Uson, et al.[91]

Scheme 2.32

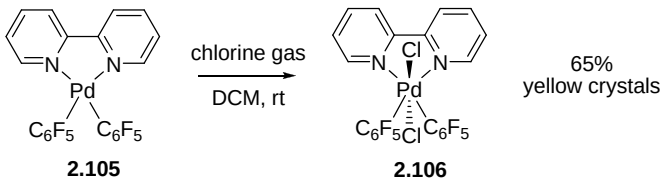

The reactions in this section provide a glimpse into palladium (IV) chemistry, particularly the organometallic compounds of palladium (IV). Much work is

currently being done in this area that will increase the types of palladium catalyzed C-C bond forming reactions, particularly those with Pd(II)/Pd(IV) cycles.

2.4 Organometallic Reagents on Solid Support

The desire for quick, efficient, and reproducible synthesis of long peptide chains, combined with the repetitive nature of the syntheses (protection, activation, coupling, and deprotection) made the synthesis of peptides a good candidate for the development of solid-phase organic synthesis.[92-95]

Solid-Phase Organic Synthesis (SPOS) blossomed in the 1960's. Merrifield helped develop and popularize the technique. Conceptually, the idea of using polymers as a *support* to carry out organic reactions, with the desired organic molecules cleaved when desired was a decided break from traditional polymer chemistry. As polymers can be tailored to have many different properties, the opportunities for this concept to be utilized in organic synthesis were immense. However, the problems to be overcome before the process was to be useful were also quite substantial, since very little was known at the time about the interplay among the conditions in the biphasic reactions. In 1963, Merrifield published the synthesis of a tetrapeptide on a chloromethylated polystyrene/divinylbenzene copolymer.[92] This classic paper, along with other contributions, paved the way for now routine automated peptide synthesis, polymer-supported reagents,[96-101] and the emergence of combinatorial chemistry as a distinct sub-discipline of chemistry.[102]

2.4.1 Combinatorial Chemistry

Combinatorial chemistry was a natural outgrowth from SPOS since there were already established techniques to synthesize many compounds utilizing standard chemistries tailored for use on solid-phase. In addition, the compounds could be isolated in high purity in a very rapid fashion, due to the great reduction in chromatographic separations needed. By the late 1990's, many reviews on solid-phase synthesis had been published. The American Chemical Society Journal *The Journal of Combinatorial Chemistry* was established as well. The creation of the journal helped establish combinatorial chemistry as a sub-discipline of chemistry.

2.4.2 Solid-Phase Organic Synthesis Utilizing Polymer-bound Transition Metal Complexes as Catalysts

Uozumi reported[103] an exploration of the effects of the tether length between the backbone and the phosphine ligand on reactivity as well as the effects of stereogenic centers on the tether and the absolute stereochemistry of the chiral ligand (Scheme 2.33).

Scheme 2.33

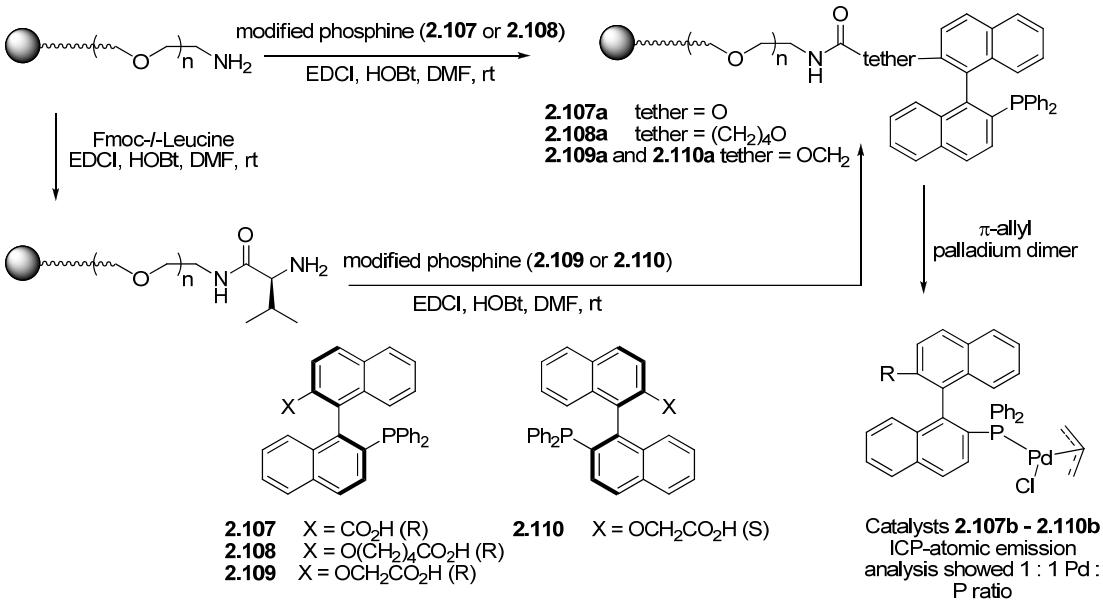

The catalysts **2.37b** – **2.40b** were synthesized via standard peptide coupling chemistry with varying tethers chain lengths. The catalysts **2.107b** – **2.110b** were then used in an asymmetric allylic alkylation to give product **2.111**. The results of the experiments are shown in Table 2.2.

Having a short tether length (catalyst **2.107b**) gave product in very poor yield and ee, while the longer tethers gave much higher yields and improved ee's (catalysts **2.108b** – **2.110b**). In addition, the chirality of the phosphine ligand determined the chirality sense of the product, overwhelming any influence of the chiral sidechain in **2.109b** and **2.110b**.

Table 2.2. *Influence of Tether Length on Yield and % ee of Asymmetric Allylic Alkylation Using Polymer-Bound Phosphine Ligands*

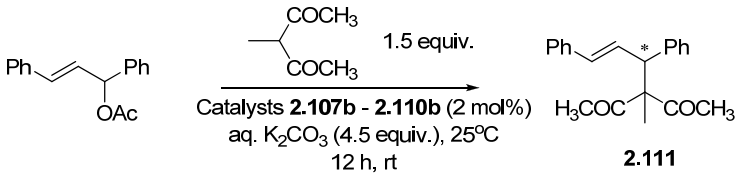

Catalyst	Yield of **2.111**	% ee of **2.111**	Absolute Configuration (R or S)
2.107b	<5%	14	R
2.108b	56%	55	R
2.109b	75%	81	R
2.110b	49%	78	S

Nozaki disclosed an interesting study exploring the relationship between solid-phase catalyst structure and %ee of the *iso* product in a rhodium-catalyzed hydroformylation of styrene (Scheme 2.34).[104] Nozaki explored two avenues of catalyst preparation. The first catalyst preparation (**2.113a**) involved using a trivinyl (R,S)-BINAPHOS (**2.112**) as a monomer followed by complexation by $Rh(acac)(CO)_2$ after polymerization. The second catalyst preparation (**2.113b**) involved the pre-complexation $Rh(acac)(CO)_2$ to the modified (R,S)-BINAPHOS followed by polymerization.[104] In the cases of the analogous solution-phase reaction and cases where the attachment point of the phosphine ligand to the polymer is on only *one* of the binaphthyls, the order of polymerization/complexation does not

greatly affect product yield or ee. However, in the case described here where both binaphthyls are vinylated, the case of pre-complexation (catalyst **2.113b**) gives a significantly higher 85% ee for the *iso* product than the 68% ee for the case where the rhodium is complexed *after* polymerization (Scheme 2.34).

Scheme 2.34

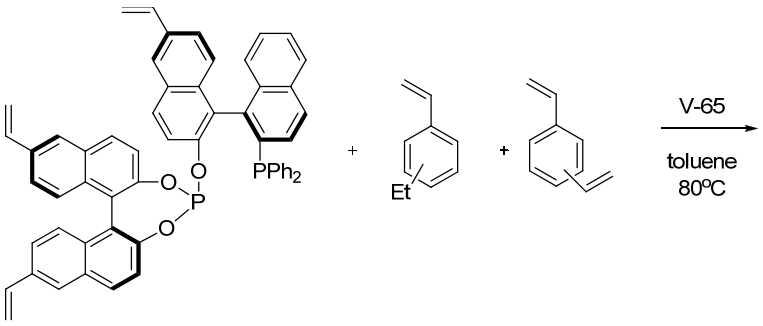

2.112

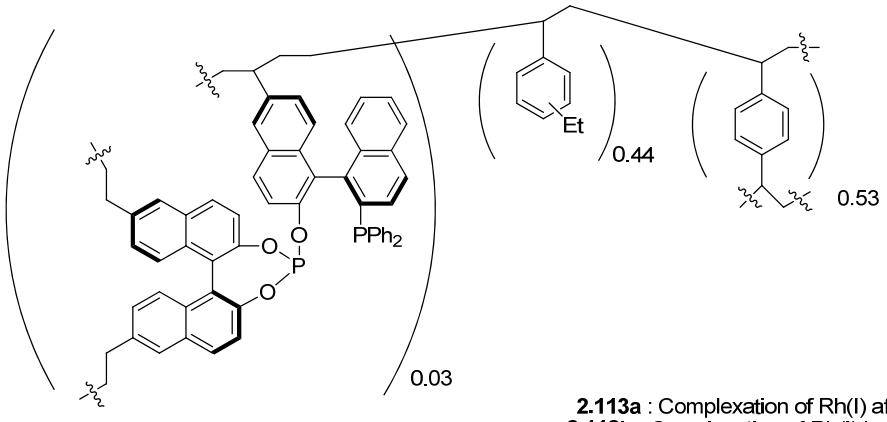

2.113a and **2.113b**

2.113a : Complexation of Rh(I) after polymerization
2.113b : Complexation of Rh(**I**) before polymerization

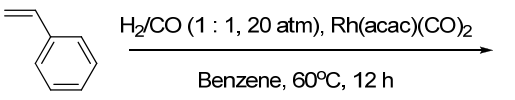

	iso 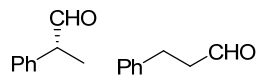 normal
2.113a	88 : 12 (*iso* ee 68%)
2.113b	87 : 13 (*iso* ee 85%)

In 1994, Gilbertson reported the synthesis of unnatural amino acid **2.114** containing a phosphine sulfide moiety starting from acrylic acid (Scheme 2.35).[105]

The new amino acid was sequenced into peptide **2.115**, having the phosphine sulfide moieties on the same side of the helix. The corresponding free phosphine **2.116** was then unveiled via reduction of **2.115** with Raney Ni, and the free phosphine complexed with cationic rhodium complex **2.117** to generate cationic rhodium phosphine complex **2.118**. ^{31}P NMR of **2.118** showed proof of concept, with the expected two doublets resulting from the inequivalent phosphorus atoms splitting each other. It should also be noted that some splitting can also be attributed to ^{31}P-^{103}Rh coupling.

Scheme 2.35

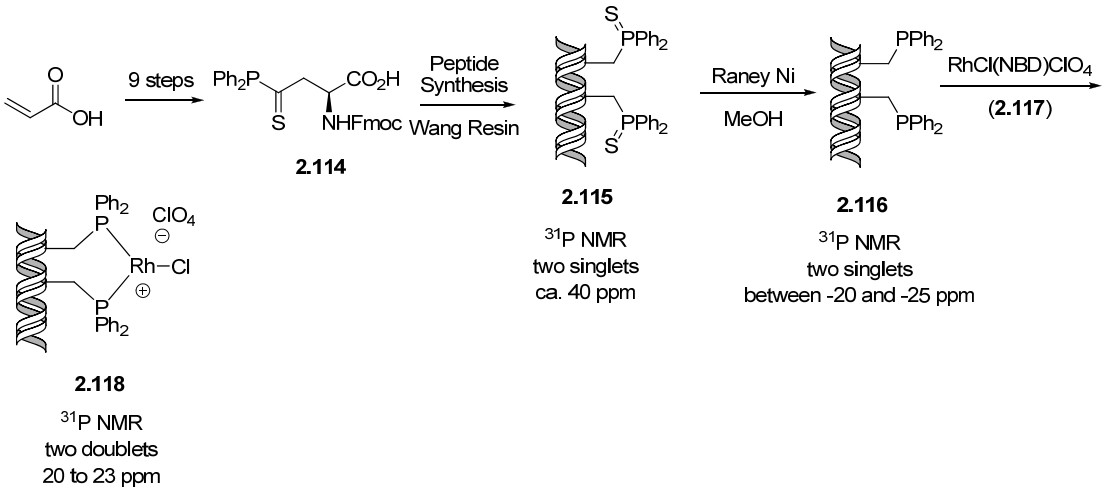

Later, Gilbertson utilized similar chemistry to place the peptide on a PS-bead and explored the effect of the peptide structure on the asymmetric induction during the catalytic hydrogenation of methyl 2-acetamidoacrylate.[106] The ee's were low in this case (4-9%).

2.4.3 Solid-Phase Organic Synthesis utilizing Polymer-bound Transition Metal Complexes as Reagents

Gradén reported the attachment of iron (0) diene complexes **2.119** to a polymer via ester linkages to give polymer-bound complexes **2.120** using peptide coupling chemistry (Scheme 2.36).[107]

Scheme 2.36

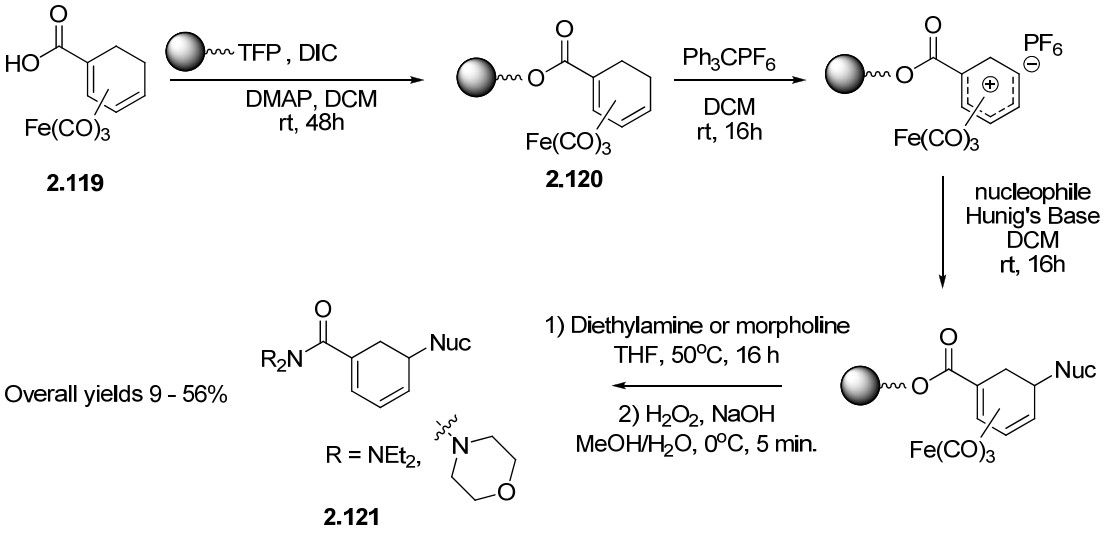

Complexes **2.120** were then converted to amides **2.121** by a sequence of hydride abstraction, nucleophile addition, and cleavage from the resin via aminolysis to give the amides in 9 – 56% overall yields from **2.119** (Scheme 2.36). Nucleophiles included amines, alcohols, phosphines, and amines.

Rigby successfully prepared and utilized phosphine-linked chromium complex **2.124** from soluble precursors **2.122** and **2.123**.[108] The polymer-bound chromium complexes were then reacted with ethyl magnesium bromide followed by decomplexation to afford tertiary alcohol **2.125** (Scheme 2.37).

Scheme 2.37

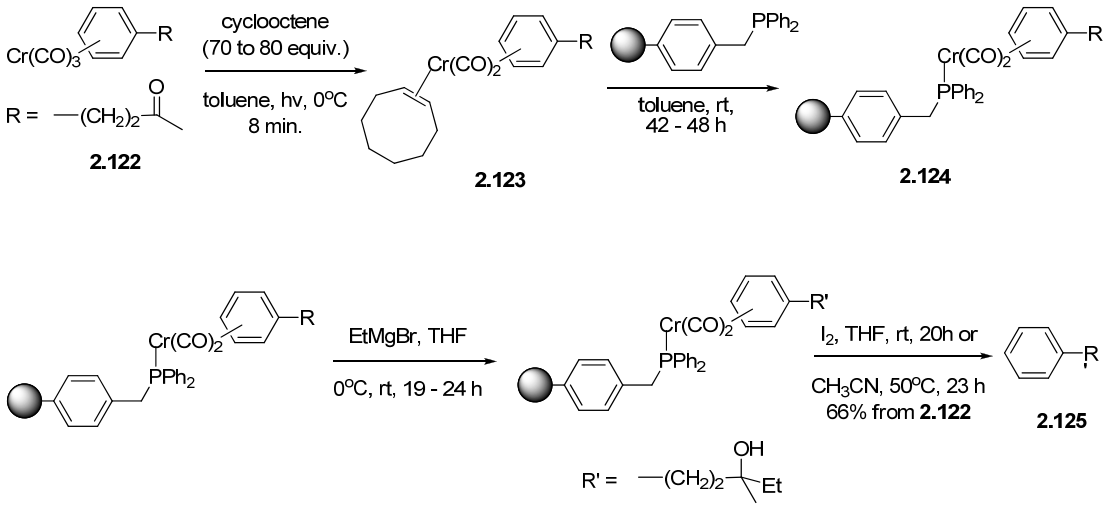

Rigby also reported the ability to perform α-alkylations and Mitsonobu reactions on the solid-phase utilizing the same linker system.[109]

Barluenga reported the synthesis of polymer-bound Fischer carbene complexes attached to solid support with isocyanide ligand **2.126** in 2005.[110] The isocyanide ligand was synthesized from chloromethylated styrene/divinylbenzene co-polymer. $W(CO)_5$(coe) was then loaded onto the polymer via ligand exchange to give polymer-bound tungsten(0) complex **2.127**. **2.127** was then converted into Fischer carbene **2.128** by reaction with phenyl lithium followed by methyl triflate. Barluenga also synthesized complex **2.129** with a longer spacer between the metal complex and the resin. It was noted that complex **2.129** with the longer spacer was more reactive (Scheme 2.38).

Scheme 2.38

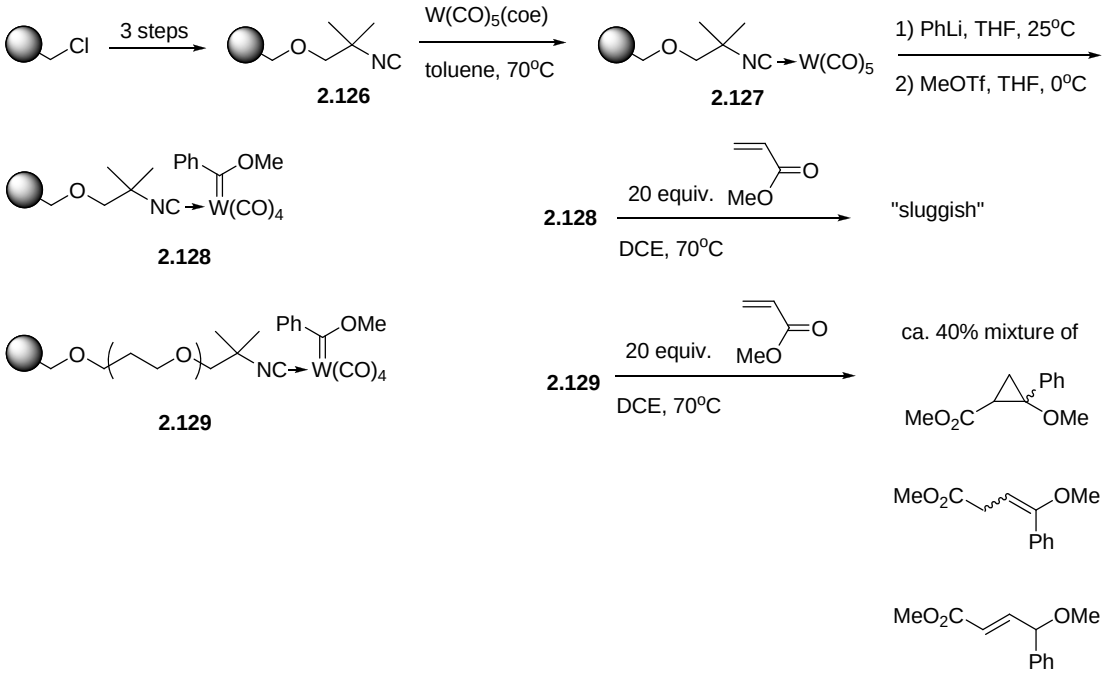

The examples in the preceding sections illustrate how polymer-bound transition-metal complexes can be used both as catalysts and reagents in organic synthesis.

2.5 Organometallic Stereochemistry

The stereochemistry of organometallic complexes is a topic which has importance to a wide range of chemists.[111] The orientation of ligands around or covalently attached to the metal center can have a great impact on the selectivity of the reactions as well as the stereochemistry of the product. While the use of chiral non-racemic ligands is now widespread in catalysis, the focus of this section of the dissertation will be the generation and fate of a stereocenter covalently bound to a metal center.

There are multiple ways to generate M-Csp^3 bonds, including oxidative addition, carbometalation of C-C multiple bonds, and C-H activation. All three mechanisms can have implications for the resulting stereochemistry at the metal center and/or the adjacent carbon. In the case of low-valent transition metal oxidative additions to sp^3-hybridized carbon centers, the mechanism is akin to the classical S_N2 mechanism found in organic chemistry.[112-114] In carbometalation, the regio and stereochemistry is governed by steric and electronic factors and in the case of C-H activation, the precise mechanism is dependent on the substrate and reaction conditions.

2.5.1 Methods and Stereochemical Course of M-C Bond-forming Reactions

In 1986, Liebeskind disclosed a reaction utilizing chiral acyliron complexes **2.130** as chiral acetate equivalents in reactions with prochiral imines.[115] The reactions proceeded with generally good diastereoselectivity and are a rare example of the *metal center* being chiral by virtue of the ligand sphere. The reactions were conducted via deprotonation with LDA followed by the addition of diethylaluminum chloride to give the aluminum enolate **2.131**. Enolate **2.131** was then reacted with the imine to generate two new acyliron complexes, **2.132a** and **2.132b**, in a 75% yield and a ratio of 25 : 1 favoring **2.132a** (Scheme 2.39).

Scheme 2.39

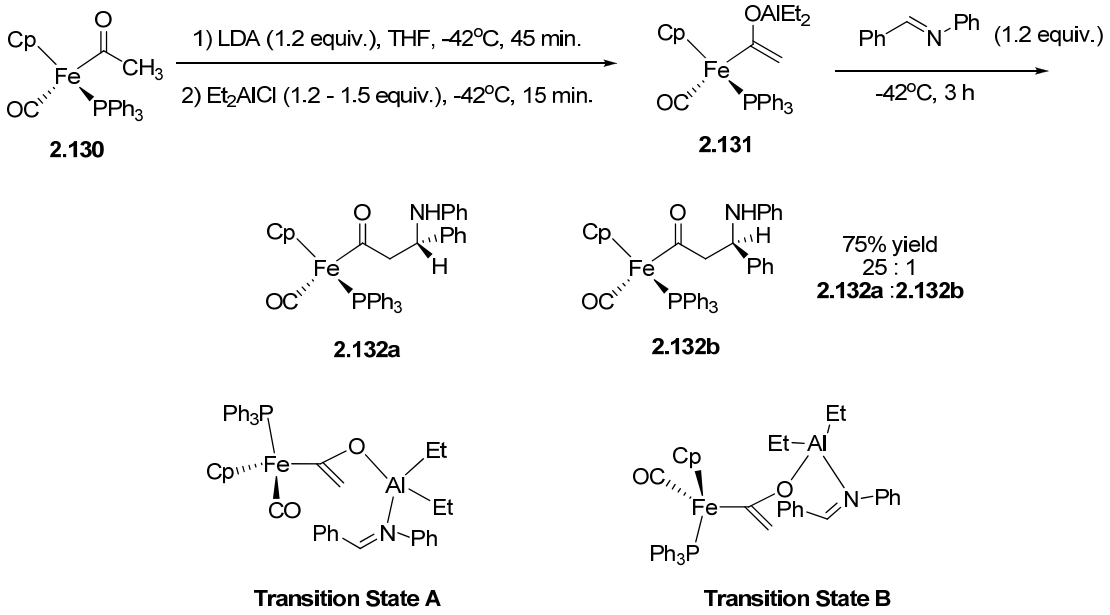

The stereoselectivity is rationalized by a closed transition-state model where the reacting imine will be coordinated to the aluminum center. This would force the C-substituent of the imine toward the chiral iron complex. The authors assume that the PPh_3 ligand is sterically largest and will be ~180° away from the imine substituent. This leads to the prediction that transition state A is more stable than transition state B. The new acyliron complexes **2.132a** and **2.132b** were then oxidized in a non-nucleophilic solvent to give β-lactams.

Liebeskind also reported on the formation of enantiopure η^3 molybdenum complexes derived from D-Arabinose (Scheme 2.40).[116] The oxidative addition of the Mo(0) to enantiopure allylic bromide **2.133** occurs with inversion of configuration to give molybdenum(II) complex **2.134**. This complex was then utilized in a synthesis of tetrahydropyran **2.135**, a scent gland secretion from *Viverra civetta*.

Scheme 2.40

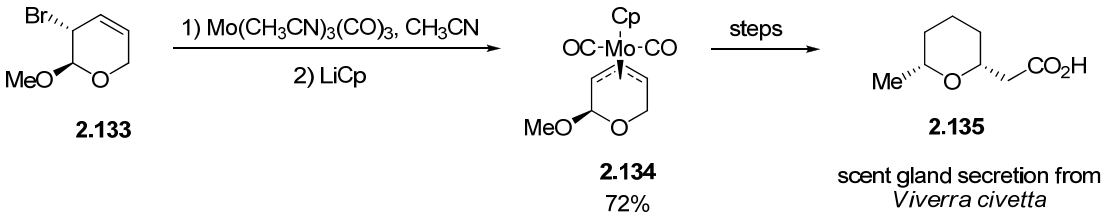

2.133 **2.134** 72% **2.135**

scent gland secretion from *Viverra civetta*

Liebeskind and co-workers also published a study[117] showing how subtle the interplay between conditions and substrate can be in determining the stereochemical course of M-C bond formation (Scheme 2.41).

Scheme 2.41

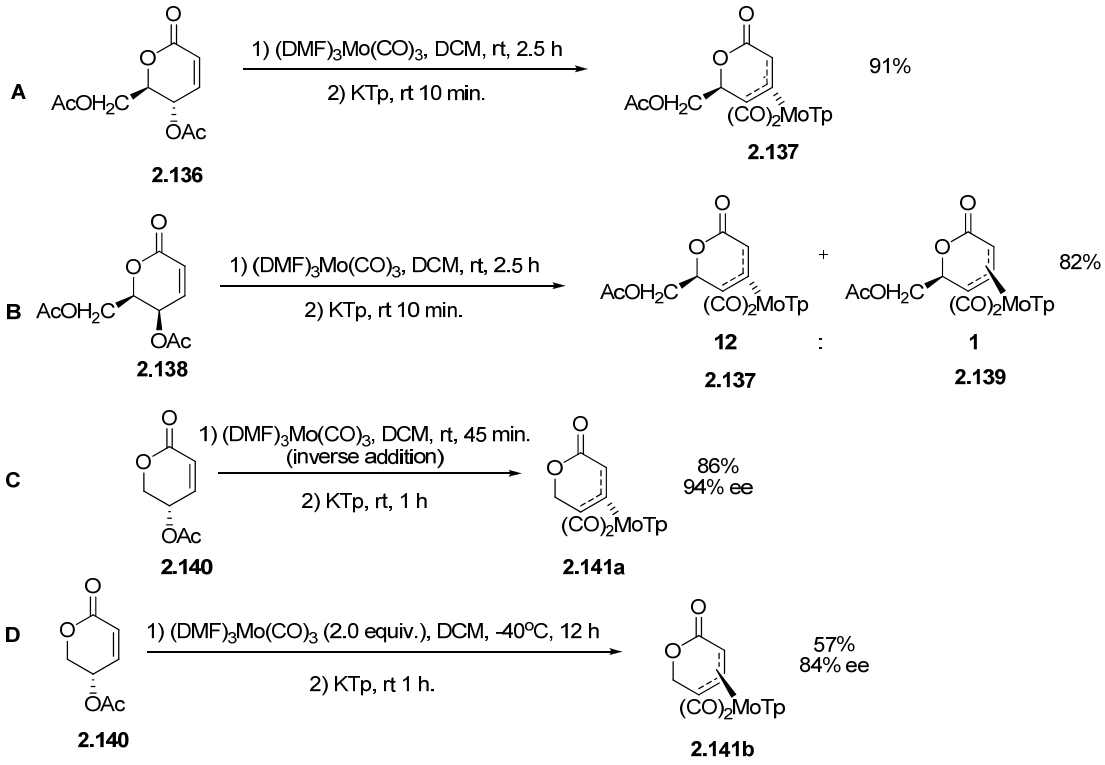

2.136 **2.137** **2.138** **12** : **1** **2.139** **2.137** **2.140** **2.141a** **2.140** **2.141b**

Reactions **A** and **C** result in *retention* of configuration at the chiral center

Reactions **B** and **D** result in *inversion* of configuration at the chiral center

Liebeskind noted that in the cases of reactions A and B depicted in Scheme 2.41, the chiral center on the adjacent carbon had a large impact on the configuration of the product(s). Complex **2.136** gave complex **2.137** as a single diastereomer in reaction A. **2.137** was highly favored (12 : 1) over its diastereomer **2.139** from reaction B. Reactions C and D describe the effects of the concentrations of reactants on the stereochemistry of the oxidative addition of molybdenum(0) complexes to lactone **2.140**. Inverse addition (low concentration of Mo(0) relative to substrate) provided a *retention* of configuration at the chiral center, giving complex **2.141a**, while a higher concentration of Mo(0) relative to the substrate provided an *inversion* of configuration at the chiral center, giving **2.141b**.

Liebeskind proposed the following model to rationalize the concentration effects of Mo(0) on the stereochemical outcome of the reaction (Scheme 2.42).

Scheme 2.42

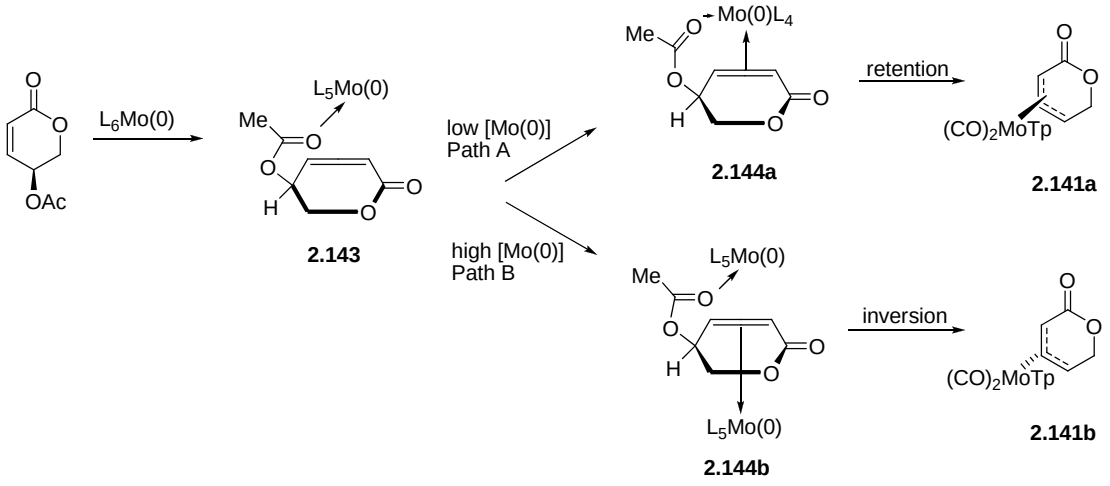

When the Mo(0) concentration is high, the Mo is proposed to bind to both the acetate *and* the face of the alkene opposite of the acetate group (Path B). This results in an

inversion of configuration giving **2.141b** due to the Mo(0) species attack from the opposite face. However, when the Mo(0) concentration is low, the Mo(0) binds only to the acetate group, leading to a retention of configuration giving **2.141a** due to the directing effect of the acetyl group (Path A). This stereochemical divergence in relation to concentration is a rare example of how the concentration and order of addition during reactions can give differing stereochemistry in products when transition metals are used.

The studies in this section suggest that while oxidative addition is usually a straightforward process, more subtle effects can also have an impact on the stereochemical outcome of the oxidative addition reaction.

2.5.2 Mechanism of Asymmetry Transfer

In many of the cases where asymmetric induction is caused by a metal center, the metal blocks a face of a molecule, forcing the reactant to enter on the side opposite the metal. Liebeskind and coworkers have quite extensively utilized this methodology with molybdenum to both explore the basic chemistry of the complexation, as well as subsequent reactions. In the late 1990's and early part of the 21st century, Liebeskind and co-workers disclosed a series of papers describing the synthesis and utilization of highly enantioenriched Mo(II) allyl complexes of heterocycles in the synthesis of complex natural-product like scaffolds as well as natural products.

As the work is quite extensive,[116-130] selected examples will prove illustrative. In 2000, Liebeskind published work on the synthesis of tropanes via formal [5 + 2]

cycloaddition to η^3-pyridynylmolybdenum π-complexes.[124] After separation via a chiral auxiliary, the enantiopure pyridinyl complex **2.145** was utilized in the [5 + 2] process to generate metalated tropane skeletons **2.146**. The complexes were then oxidatively demetalated to produce tropane skeletons **2.147**, bearing an α,β-unsaturated carbonyl. X-Ray diffraction studies on several products proved the hypothesis that the C - C bond formations occurred on the opposite side of the ring from the molybdenum center (Scheme 2.43).

Scheme 2.43

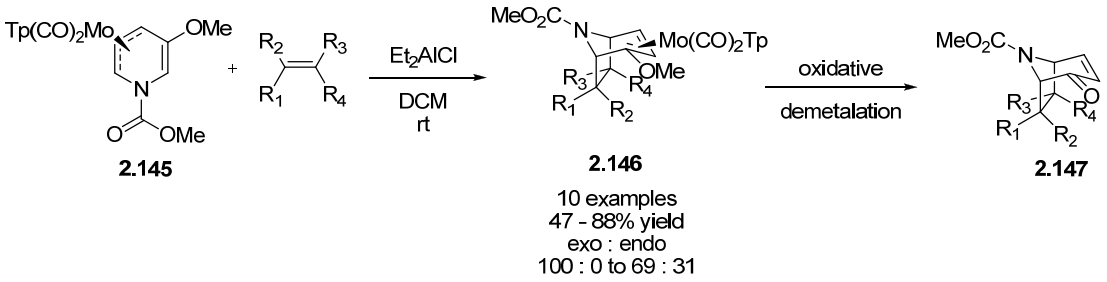

Liebeskind also reported the synthesis of oxa and aza[3.2.1] and [4.3.1] bicyclics with a novel "Michael-type" reaction on scaffold **2.149**.[129] The scaffold is constructed via a Mukaiyama-Michael reaction between the silyl-enol ether of ketone **2.148** and cyclohexenone (Scheme 2.44).

Scheme 2.44

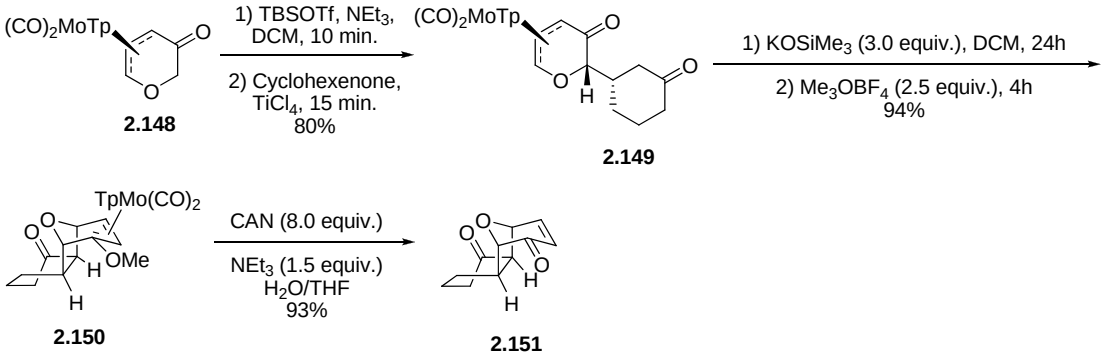

The newly formed ketone **2.149** was then reacted in an intramolecular Michael-type reaction between the enolate of **2.149** and the π-allyl molybdenum species. The resulting bicyclic species **2.150** was generally formed in good yield and with a high preference for the *exo* isomer. As an example, the tricyclodione **2.151** was isolated in >99.9% ee after one recrystallization.

Malinakova and co-workers reported work on the mechanism of stereoinduction from the chiral ligand in a base-induced intramolecular ligand exchange (Scheme 2.45).[131]

Scheme 2.45

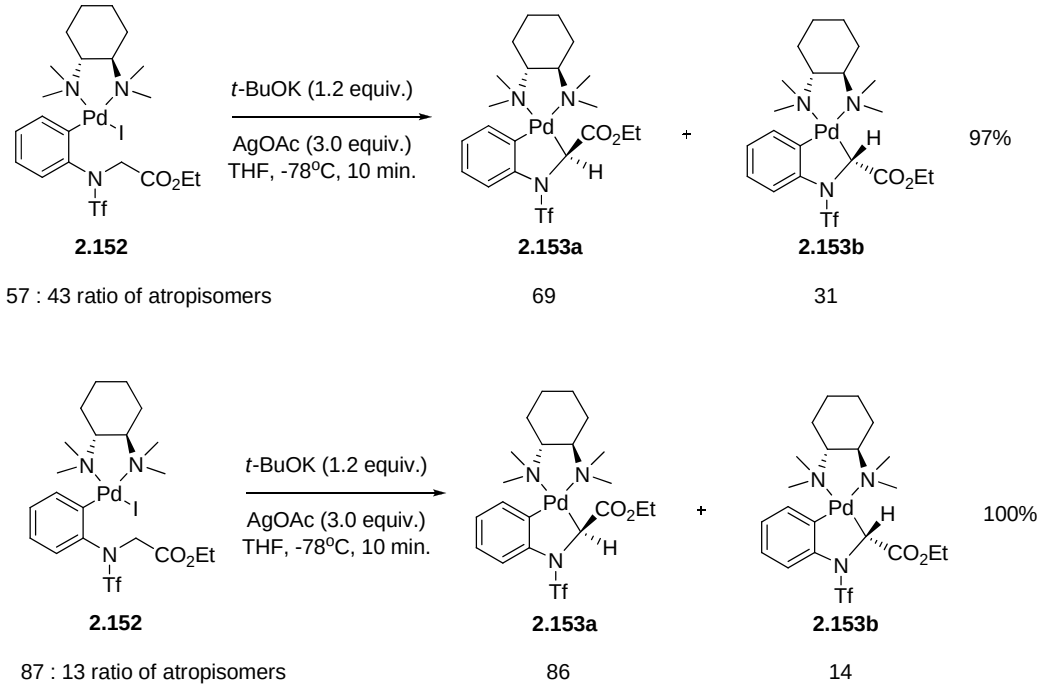

In this case, the diastereoselectivity of the ring closure reaction to give **2.153a** and **2.153b** is correlated to the atropisomer ratio in the palladium(II) iodo complex **2.152**

before ring closure to generate the palladacycle. The atropisomerism arises from hindered rotation around the Pd-aryl bond.

As a final example, Liebeskind recently published a total synthesis of (-)-Adaline, an aza[3.3.1]bicyclic amine featuring a quaternary carbon stereocenter.[132] The enone **2.154** was generated by a Mukaiyama aldol reaction followed by elimination. **2.154** was then reacted with allyl magnesium bromide followed by an acid-promoted semipinacol reaction to give ketone **2.155**. A Wacker oxidation to give **2.156** followed by an intramolecular Michael-type reaction gives intermediate complex **2.157**, which is consequently demetalated to afford **2.158** en route to (-)-Adaline. In this synthesis, the metal center influences the formation of two stereocenters.

Scheme 2.46

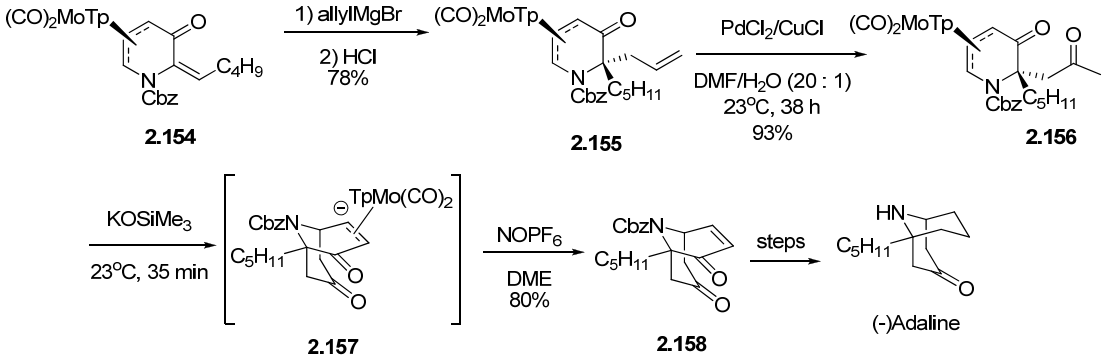

The studies in this section show that many of the same concepts apply to organometallic stereochemistry as do organic stereochemistry (for instance, chiral auxiliaries and atropisomers). However, these studies remain fairly rare, leaving a gap in the literature.

2.5.3 Stereochemistry of C-C Bonds Formed by 1,1-Reductive Elimination From Palladium

Many potential mechanisms exist for elimination of organic fragments from a transition metal.[112, 114, 133-139] However, for palladium-mediated processes forming C-C bonds, by far the most common is 1,1-reductive elimination.[134-137] Stille has published a number of studies on the reductive elimination from palladium(II) complexes and found that a key requirement for reductive elimination is a *cis* arrangement of the carbon fragments to be coupled.[134] In complexes where the ligands are forced to be *trans*, reductive elimination fails to occur from palladium(II). Another factor contributing to reductive elimination is the number of ligands attached to the metal center. Reductive eliminations are generally faster after dissociation of one of the ligands, giving a three-coordinate intermediate.

For this dissertation, the main focus is on the 'fate' of the stereocenter bound to the metal center. Few examples exist that show what happens to the configuration of a chiral non-racemic sp^3-hybridized carbon attached to a metal center that undergoes reductive elimination or its microscopic reverse, oxidative addition. Pfeffer has shown that at least 75% of the stereochemical information is retained when DMAD is inserted into the stereogenic Csp^3-Pd bond of **2.159** followed by reductive elimination to give **2.160**, as judged by ^{1}H NMR analysis of the organic product (Scheme 2.47).[26]

Scheme 2.47

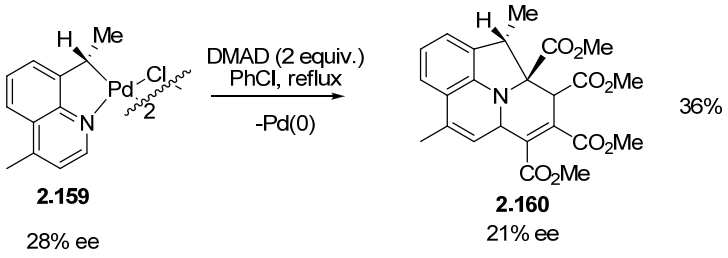

2.159

28% ee

2.160

21% ee

Whitesides and co-workers have shown a similar conservation (ca. 80%) of configuration during an insertion of DMAD into the Csp^3-Fe bond of complex **2.161** to give **2.162** in 60% and >80% retention of stereochemical information, also judged by NMR analysis (Scheme 2.48).[27]

Scheme 2.48

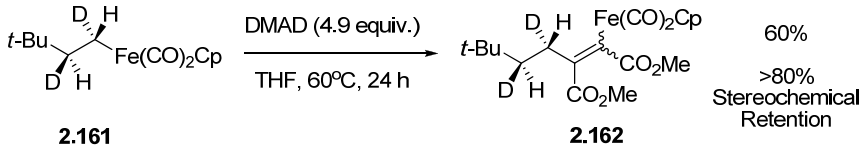

2.161

2.162

These studies suggest a general retention of stereochemical information during migratory insertion and reductive elimination processes. These facts suggest that most C-C bond forming 1,1-reductive eliminations from palladium occur in a concerted manner and generally keep stereochemical information intact.

Chapter Three

Exploration of Polymer-Bound Palladacycles as Reagents for Organic Synthesis

3.1 A Basic Study of the Factors Influencing the Reactivity of Polymer-bound Palladacycles

Since Merrifield's first report of utilizing a resin in the synthesis of a tetra-peptide, solid phase organic synthesis (SPOS) has made large strides,[140, 141] including the development of combinatorial chemistry as a distinct sub-discipline of chemistry. However, the precise effects of the physical properties of the resins on reactivity and kinetics of reactions are difficult to quantify due to the nature of reactions on solid-phase. While swelling of the polymer is generally required for good reactivity[142] on the solid-phase, studies have shown that this is not always the case[143, 144] as the swelled polymer phase *is* the solvent.[145] The swelled polymer phase generally has a much higher viscosity than organic solvents alone, due to the polymer chains moving less freely. In addition, while high loading[146-152] of functional groups on resins is desired for economic purposes, this often has detrimental effects on reactivity due the microenvironments[153] created during synthesis of the resins.

Organometallic reactions on solid-phase are often limited to catalytic reactions, often simply mixing a metal salt with a polymer-bound ligand to generate a catalyst of ill-defined structure.[154-156] One of the complicating factors for organometallic reactions regards the role of the auxiliary ligands often needed for optimal reactivity. As perfect site-isolation is not likely to occur at the low 1-2% cross-link density many polymers used in SPOS have,[157, 158] the attachment of a transition metal complex to solid phase will lead to additional cross-linking, complicating the picture even more.

Few studies have been reported on the tailoring of polymer structure and conditions to optimize reactivity of transition-metal complexes on solid-phase.[158-160] Our group has previously disclosed the regioselective conversion of palladacycles into a variety of 2*H*-1 benzopyrans and 1,2-dihydroquinolines.[131, 161-163] As few studies exist on the effects of polymer structure and ligand to metal ratio on reactivity, we thought our methodology would be a good probe to provide additional insight into organometallic reactions that occur on solid-phase.

In addition, we wished to utilize the polymer-bound palladacycles as reagents for combinatorial chemistry, reasoning that the palladium(0) complex generated would be pre-scavenged by the phosphine resin facilitating isolation of the synthesized heterocycles.

For our initial studies, we chose the commercially available Tentagel S-NH_2 as the base for our polymer-bound phosphine ligand due to its favorable swelling properties in a variety of solvents as well as for its ability to give near solution-quality gel-phase NMR spectra.[164] We anticipated its swelling properties would contribute to making the eventual polymer-bound complex more reactive. We observed that during the initial washing of the Tentagel Resin to make sure all soluble entities were removed that the resin had a marked tendency to adhere to the glassware; this was remedied by capping the hydroxyl groups on the surface of the glassware by washing the glassware used with a 10% v/v solution of dichlorodimethylsilane in chloroform followed by placing in an oven to dry. The washed resin was then used to synthesize the polymer-bound phosphine **3.1** via amide coupling chemistry (Scheme 3.1).[165]

Scheme 3.1

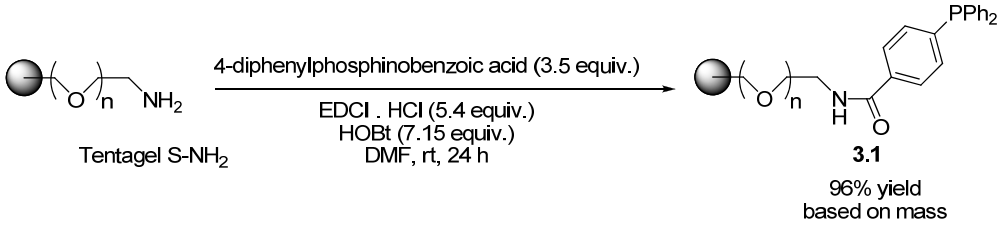

When we attempted to load palladacycle **3.2**[161] onto resin **3.1** via ligand exchange (Scheme 3.2) very little or no loading occurred as observed by gel-phase ^{31}P NMR. In addition, a noticeable peak corresponding to phosphine oxide also appeared in the gel-phase ^{31}P NMR spectrum.

Scheme 3.2

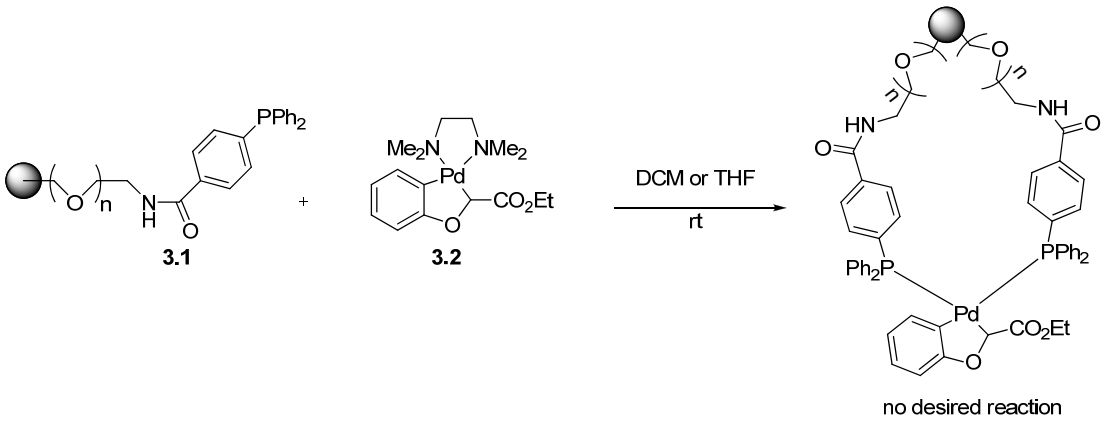

Based on these results, we decided to discontinue using the Tentagel-derived **3.1** as our polymer-bound ligand as it oxidized quite readily under the reaction conditions, causing the color of the resins to rapidly darken, indicating likely metallic palladium formation. We then decided to utilize commercially available polymer-bound triphenylphosphines as our polymer-bound ligands. In these cases, the ligand

exchanges occurred readily to give polymer-bound palladacycles as air-stable yellow solids, as judged by no change in the IR spectrum after sitting on the bench for over two months (vide infra). Polymer-bound phosphine ligands **3.3** – **3.5** were commercially available from Aldrich. We also wished to explore the effects of tether length on the reactivity of the polymer-bound palladacycles. Therefore, we synthesized polymer-bound phosphine **3.6** in one step from a polymer supported benzyl alcohol resin (Wang resin) by an ester coupling with 4-diphenylphosphinobenzoic acid mediated by diisopropylcarbodiimide. The resin had a P loading of 0.9 mmol P/g measured by commercial ICP analysis[159] (Resins **3.3** – **3.6**, Scheme 3.3 and Table 3.1).

Scheme 3.3

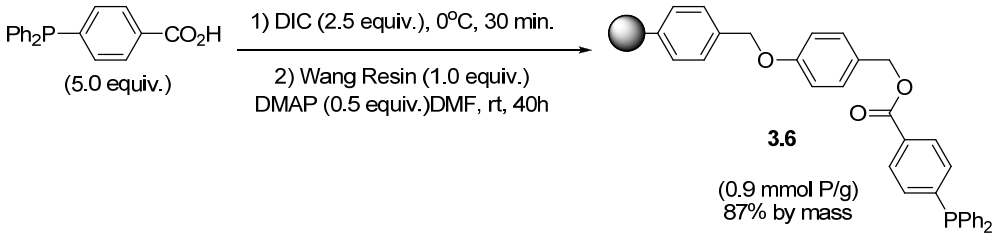

Table 3.1. *Properties of the Resins Used as Polymer-bound Ligands*

	Resin	P loading (mmol P / g)	Price / mmol P ($/mmol) for 5g bottle[a]	Crosslink (%)	Mesh Size	Swelling in DCE (mL/g)[b]
1	**3.3**	3.06	5.03	2	200 – 400	4.5
2	**3.4**	3.01	5.03	2	200 – 400	4.5
3	**3.5**	1.35	9.59	1	100 – 200	5.7
4	**3.6**	0.89[b]	8.47	1	100 - 200	5.3

[a] as of February 2009 from Aldrich. [b] by the volumetric method (see Chapter Six).

Resins **3.3** and **3.4** are the best value ($/mmol P) due to their higher phosphorus loading content, while resins **3.5** and **3.6** have lower cross-link density (1% vs. 2%) and are expected to show higher reactivity than **3.3** and **3.4** due to their higher swelling, as shown in Table 3.1. With resins **3.3** – **3.6** bought or synthesized, we performed the ligand exchange reactions of palladacycle **3.2** with resins **3.3** to **3.6** to give new polymer-bound palladacycles **3.7** – **3.18** (Table 3.2). In order explore the effects of excess phosphine on solid-phase reactions, we chose to vary the Pd : P ratios. Although excess phosphine could cause decreased reactivity, as indicated by studies on solution phase reactions (vide infra), the lower cross-linking and higher swelling of such resins may compensate for this effect. At the time, it was unknown whether the new polymer-bound palladacycles **3.7** – **3.18** would show the decreased reactivity that an excess phosphine ligands relative to palladium had on the analogous solution-phase reactions (vide infra).

Table 3.2 *Properties of Prepared Polymer-bound Palladacycles* ***3.7*** *to* ***3.18***

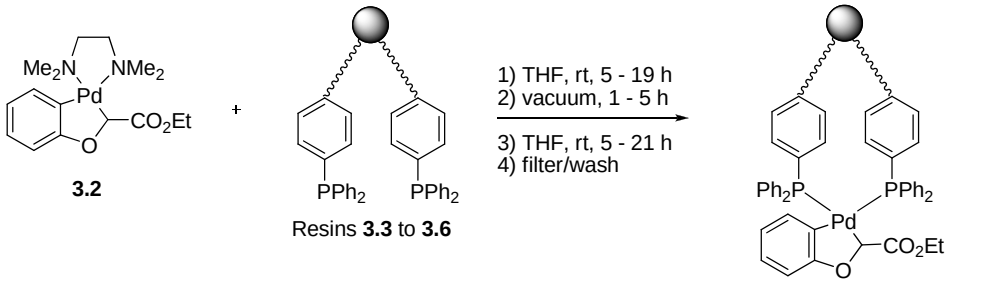

	Resin	Swelling in DCE (mL /g)	Pd : P ratio during loading	Pdt	Pd wt. %[a]	P wt. %[a]	Pd : P in pdt	Swelling in DCE (mL /g)[b]
1	**3.3**	4.5	1 : 2.05	**3.7**	10.03	5.73	1 : 1.9	3.2
2	**3.3**	4.5	1 : 2.05	**3.8**	9.21	6.12	1 : 2.3	2.9
3	**3.4**	4.5	1 : 2.02	**3.9**	9.15	6.78	1 : 2.5	3.6
4	**3.4**	4.5	1 : 3.04	**3.10**	8.41	7.49	1 : 3.0	3.7
5	**3.5**	5.7	1 : 1.69	**3.11**	7.05	3.55	1 : 1.7	--[c]
6	**3.5**	5.7	1 : 1.69	**3.12**	6.30	3.51	1 : 1.9	3.6
7	**3.5**	5.7	1 : 2.53	**3.13**	4.53	2.84	1 : 2.1	4.2
8	**3.5**	5.7	1 : 2.53	**3.14**	5.44	3.84	1 : 2.4	4.1
9	**3.5**	5.7	1 : 5.06	**3.15**	2.72	4.81	1 : 6.0	7.0
10	**3.5**	5.7	1 : 1.69	**3.16**	7.26	3.63	1 : 1.7	--[c]
11	**3.6**	5.3	1 : 1.80	**3.17**	3.34	2.54	1 : 2.6	6.4
12	**3.6**	5.3	1 : 1.80	**3.18**	3.35	2.54	1 : 2.6	6.7

[a] as measured by commercial ICP-MS analysis. [b] by the volumetric method, see Chapter Six [c] not measured

The method of preparation chosen was utilized in an attempt to maximize the loading of palladacycle **3.2** onto the resin. Placing the reaction mixture under vacuum partway through the reaction was carried out to remove any of the volatile TMEDA ligand. The loading experiment was finished by adding fresh THF and letting the mixture stir for an additional period of time before filtration. Methanol, DCM, and ether were chosen as solvents to wash palladacycles **3.7** to **3.18** to force the polymer to undergo swelling and contraction cycles to ensure the removal of soluble materials. For most of the reactions (entries 1 – 10, Table **3.2**) the loading of palladacycle onto the resin was at or above 90% as measured by ^{1}H NMR analysis of the filtrates after the reaction, as well as by a good agreement between the Pd : P ratios at the beginning of the loading and in the final product (compare, columns 3 and 7 in Table 3.2). For entries 11 and 12 describing the synthesis of polymer-bound palladacycles **3.17** and **3.18** from resin **3.6**, it was noticed that nearly 30 mol% of palladacycle **3.2** remained after the reaction. This was likely due to the lower concentration of phosphine groups on resin **3.6**. In addition to the lower concentration of phosphine groups, the phosphine moieties on the resin were also more electron-poor than resins **3.3 – 3.5** due to the ester linkage to the polymer backbone, although a partial oxidation of the phosphine groups on the resin during the synthesis of **3.6** cannot be ruled out.

After commercial ICP-MS analysis for Pd and P content, the reactivity of the new polymer-bound palladacycles **3.7** – **3.18** were tested via reaction with dimethylacetylenedicarboxylate (DMAD) under various conditions. For comparison,

the solution phase reaction consisted of the following conditions: (40°C, DCE, excess DMAD) and gave exclusive formation of **3.19** within one hour. First, we ran experiments using conditions that closely resembled the conditions for the analogous solution phase reactions to give products **3.19** and its unexpected regioisomer **3.20** (vide infra). The results are shown in Table 3.3.

Table 3.3. *Insertion Reactions of DMAD into Immobilized Palladacycles **3.7**, **3.11**, and **3.17** at 40°C in DCE*

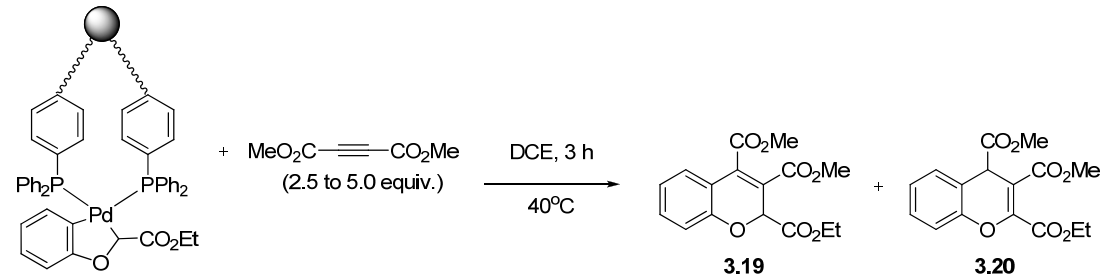

	Pd-cycle	P loading (mmol P/g)	Swelling range (mL /g)	Pd : P ratio range	Yield (**3.19** + **3.20**)	**3.19** : **3.20** ratio	Average yield (%)
1	**3.7**	High (3.0)	3.2	1 : 1.9	17	5 : 1	17
2	**3.11**	Medium (1.4)	--[a]	1 : 1.7	35	22 : 1	35
3	**3.17**	Low (0.9)	6.4	1 : 2.6	87	20 : 1	84
4	**3.17**	Low (0.9)	6.4	1 : 2.6	81	1 : 0	

[a] not measured

Due to the variances in the commercial ICP-MS analyses, we averaged the yields for some reactions in Tables 3.3 and 3.4 in order to generate more useful pieces of data.

The standard deviations in the ICP-MS numbers were ±0.2 to 0.3 %. This translates into a variance of ±0.2 to 0.3 units in the P : Pd ratios.

We observed that the polymer-bound resins with high (3.0 mmol P / g) and medium loading (1.4 mmol P / g) reacted much more sluggishly than the solution-phase counterparts, as shown by the lowered yields relative to the solution phase reaction (>90%, 1 h, 40°C, DCE). The very low yield of the reaction of **3.2** with DMAD (17% yield) is conceivably attributed to the higher local concentration of phosphine slowing down the rate of reaction. The reactions of the low-loading resin gave high yields under these conditions, presumably due to the micro-environment around the palladium center being more solution-like than the higher loading resins. As the higher-loading resin would be the most economical if the yields could be increased, reactions of the polymer-bound palladacycles at elevated temperatures were performed (Table 3.4).

Table 3.4. *Insertion Reactions of DMAD into Immobilized Palladacycles* ***3.7*** *–* ***3.15*** *and* ***3.17*** *at 80°C in DCE*

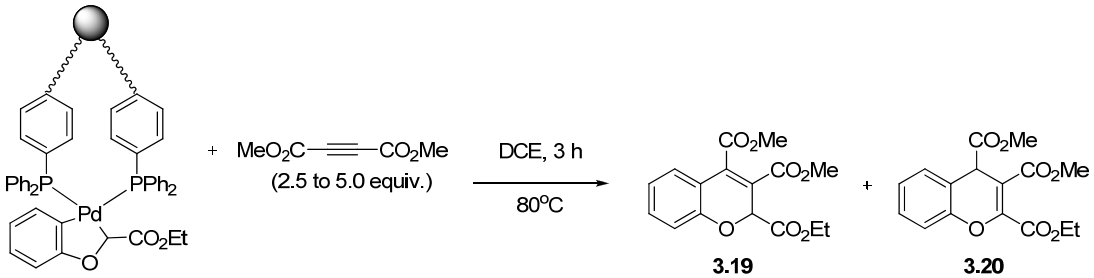

Palladacycles **3.7** - **3.15** and **3.17**

	Pd-cycle	P loading (mmol P/g)	Swelling range (mL /g)[b]	Pd : P ratio	Yield(**3.19** + **3.20**)	**3.19** : **3.20** ratio[a]	Average yield(%)
1	**3.7**	3.0	2.9 – 3.6	1 : 1.9	49	1 : 0	55
2	**3.8**	3.0		1 : 2.3	64	1 : 0	
3	**3.9**	3.0		1 : 2.5	57	2 : 1	
4	**3.9**	3.0		1 : 2.5	50	1 : 0	
5	**3.11**	1.4	3.6 – 4.2	1 : 1.7	86	4 : 1	74
6	**3.12**	1.4		1: 1.9	84	3 : 1	
7	**3.13**	1.4		1 : 2.1	69	3 : 1	
8	**3.13**	1.4		1 : 2.1	72	3 : 1	
9	**3.14**	1.4		1: 2.4	59	2 : 1	
10	**3.17**	0.9	6.4	1 : 2.6	78	12 : 1	79
11	**3.17**	0.9	6.4	1: 2.6	80	12 : 1	
12	**3.10**	3.0	3.7	1 : 3.0	28	1 : 0	34

13	**3.10**	3.0	3.7	1 : 3.0	39	1 : 0	
14	**3.15**	1.4	7.0	1 : 6.0	0	--	0

[a] by ^{1}H NMR analysis of isolated products. [b]range of swelling for samples

At elevated temperatures, yields of **3.19** and **3.20** rose for entries 1 – 11, with high-loading palladacycles **3.7 - 3.9** more than tripling the yield to 55% from the 17% at 40°C. The yields from medium-loading palladacycles **3.11** – **3.14** also slightly more than doubled from 35% at 40°C to 74% at 80°C. The yields from resin **3.17** with the longer tether stayed nearly constant regardless of the reaction temperature. In entries 12 and 13 utilizing the high loading resin with a 1 : 3 P : Pd ratio, the effects of the higher than the desired 1 : 2 Pd : P ratio were seen, with the yield dropping dramatically to 34%. This is the likely result of one extra equivalent of free phosphine during loading. Entry 14 shows that the reaction to form the benzopyrans was completely inhibited when the resin with a 1 : 6 P : Pd ratio was utilized. The results in Table 3.4 indicate that higher swelling leads to greater reactivity for these systems. In addition, lower loading leads to better yields; however, the low loading is not economically desirable. To compare entries 12 – 14 with the analogous solution phase reactions, we performed solution-phase reactions involving an excess of phosphine (Scheme 3.4).

Scheme 3.4

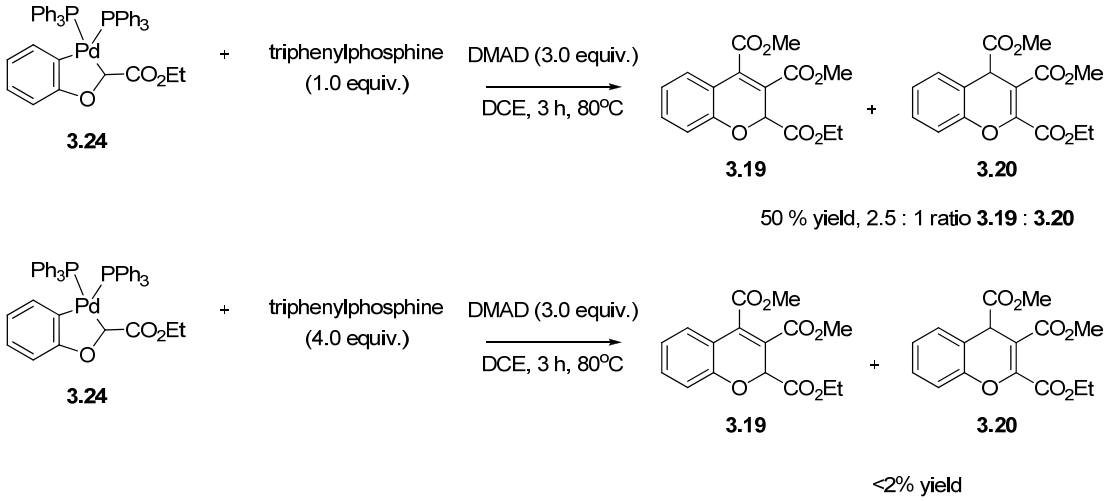

The reaction of palladacycle **3.24** in the presence of one equivalent of free triphenylphosphine lowered the yield to 50%, along with giving significant isomerization to **3.20**. The reaction with four added equivalents of free triphenylphosphine gave < 2% yield. The results for entries 12 – 14 in Table 3.4 are similar to those for the solution-phase experiments. Mechanistically, the solid-phase reaction is likely similar to the analogous solution-phase reaction. A plausible mechanism is shown in Scheme 3.5.

Scheme 3.5

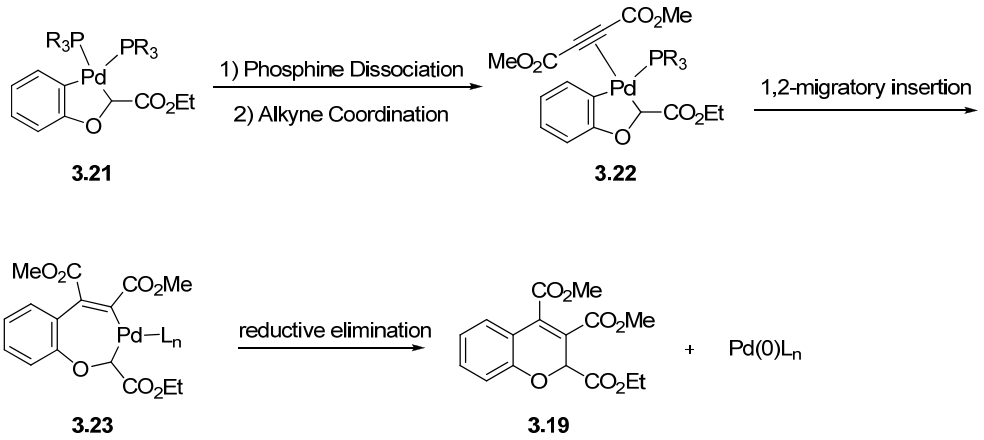

3.21 **3.22** **3.23** **3.19**

Initially, palladacycle **3.21** with two coordinated phosphines undergoes a phosphine dissociation followed by alkyne coordination to produce intermediate palladacycle **3.22** having one phosphine and one alkyne ligand. The mechanism of ligand exchange is likely dissociative, as bidentate ligands (such as dppe) completely inhibit the reaction. 1,2-Migratory insertion of the alkyne then occurs into the Csp^2-Pd bond to afford seven-membered palladacycle **3.23**, which then undergoes reductive elimination to give palladium(0) and product **3.19**. An excess of phosphine slows or completely inhibits the dissociation step, resulting in lower rates or the inhibition of the reaction.

Unexpectedly, in some cases (entries 1 – 3, Table 3.3, and entries 3 and 5 – 11, Table 3.4) we also isolated significant amounts of the chromatographically inseparable isomeric 4*H*-benzopyran **3.20** in addition to the expected 2*H*-benzopyran **3.19**. The structure of **3.20** was supported by nOe studies. Irradiation of the proton at 4.75 ppm in **3.19** in a mixture of **3.19** and **3.20** showed an enhancement of the proton

at 7.41 ppm. In addition, irradiating the singlet at 5.83 ppm in compound **3.19** in a mixture of **3.19** and **3.20** showed no enhancement in the aromatic region.

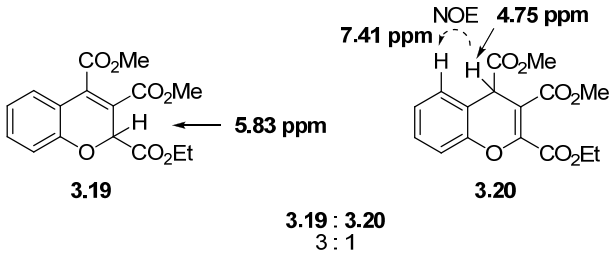

Figure 3.1 *Assignment of Isomer* ***3.20*** *by* ^{1}*H NMR NOE.*

Compound **3.20** was not observed or isolated during the analogous solution-phase reactions.[161] Therefore, the isomerization is likely due to the high local concentration of the palladacycle and/or phosphine groups on the resins (vide infra).

The isomer ratio of **3.19** : **3.20** of the products shown in Tables 3.3 and 3.4 vary significantly with the P loading, P : Pd ratio, and reaction temperature. This suggests that the isomerizations likely depend on the specific micro-environments where the reactions are occurring. In order to elucidate some of the factors responsible for the isomerization, we performed a series of control experiments. In these experiments, we subjected a sample of pure benzopyran **3.19** to DCE, DMAD, triphenylphosphine, a combination of triphenylphosphine and DMAD, and the soluble analog of polymer-bound palladacycles **3.7** – **3.18**, palladacycle **3.24** (Figure 3.2) under conditions similar to the solid-phase reaction conditions (Table 3.5).

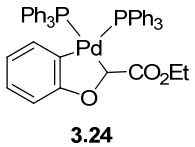

Figure 3.2. *Palladacycle Used in Control Experiments.*

The results of the control experiments are shown in Table 3.5.

Table 3.5. *Control Experiments to Determine Potential Sources of Isomerization of 2H-1 Benzopyran **3.19** to 4H-1 Benzopyran **3.20***

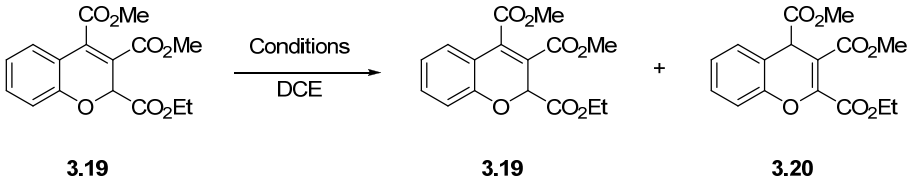

3.19 **3.19** **3.20**

	Compound	Equivalents	Temperature (°C)	Time (h)	**3.19** : **3.20** after reaction
1	DCE only	--	80	3	1 : 0
2	DMAD	2.0	80	3	1 : 0
3	$Pd(OAc)_2$	1.0	80	3	1 : 0
4	Pd_2dba_3/ DMAD	1.0 / 2.0	80	3	1 : 0
5	PPh_3	2.0	80	3	5.5 : 1
6	PPh_3/ DMAD	2.0 each	80	3	7.4 : 1
7	**3.24**	2.0	80	3	1.7 : 1

[a]greater than 95% mass recovery was achieved in all cases.

The results strongly indicate that the high local phosphine concentrations on the polymer in the reaction mixture are a likely cause of the isomerization of **3.19** to **3.20**. Interestingly, the palladacycle **3.24** also caused an even more significant isomerization (entry 7, Table 3.5). To rationalize these results, two plausible

mechanisms for the isomerization of **3.19** to **3.20** are proposed in Scheme 3.6, the first involving only the free phosphine and second involving palladacycle **3.24**.

Scheme 3.6

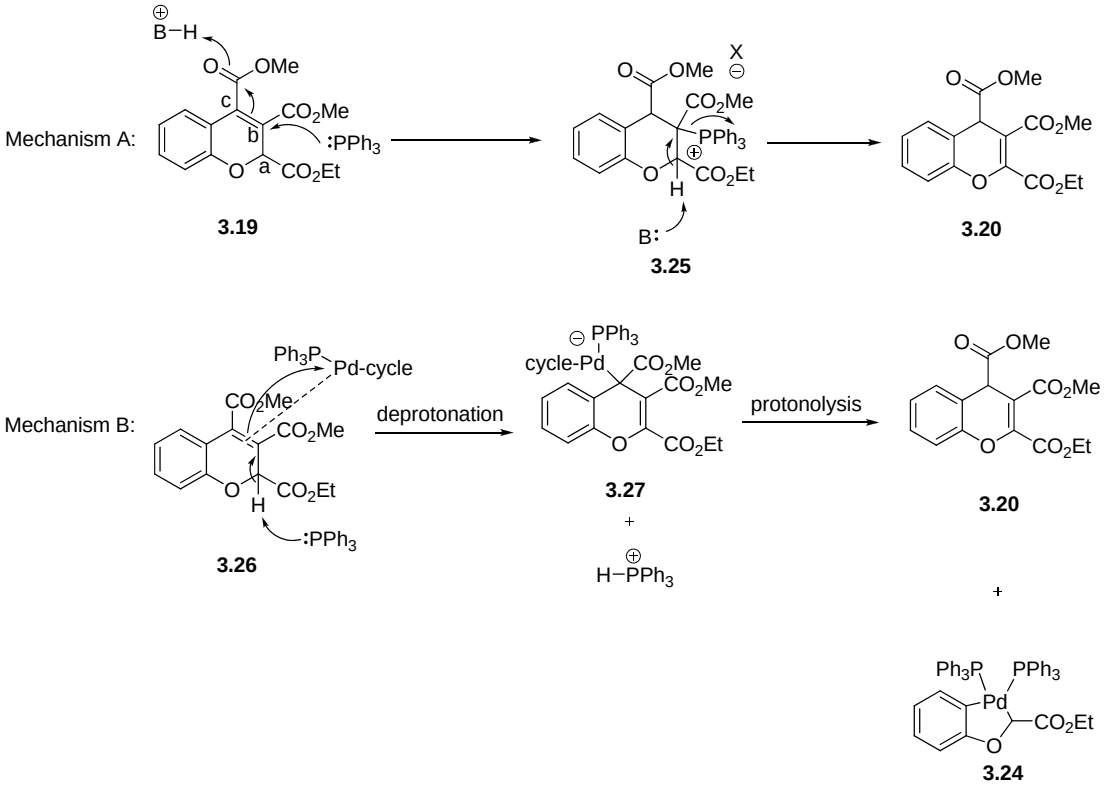

Mechanism A involves the phosphine attacking the carbon labeled *b* in Scheme **3.6**, giving phosphonium intermediate **3.25** after protonation and tautomerization. A base would then deprotonate carbon *a* in **3.25** to give **3.20**. A similar mechanism, involving nucleophilic attack into an α,β-unsaturated system followed by electrophilic attack and deprotonation to regenerate the phosphine, is often proposed for the Baylis-Hillman reaction.[166]

To provide a rationale for the isomerization of **3.19** by palladacycle **3.24**, mechanism B involves palladacycle **3.24** undergoing ligand exchange with **3.19** to

give intermediate π-complex **3.26**, which is now activated for deprotonation by free triphenylphosphine. The deprotonation generates anionic palladium complex **3.27** as a transient intermediate. Protonolysis of **3.27** gives 4*H*-benzopyran **3.20** and regenerates palladacycle **3.24**. As anionic palladium(II) complexes have been isolated, it is reasonable that intermediate such as **3.27** could be long lived enough to be a viable intermediate for the isomerization.[167, 168]

This isomerization proved not to be problematic with mono-activated alkynes in reactions performed by Dr. Lei Zhang with polymer-bound palladacycle **3.16** (Table 3.6).

Table 3.6. *Insertions of Mono-activated Alkynes into Palladacycle* ***3.16***

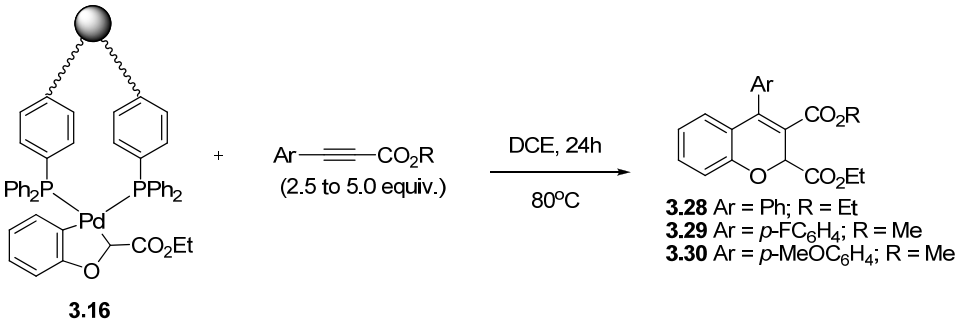

	Product	R	Ar	Yield (%)	Yield of Solution -Phase (%)	% Pd in recovered resin[a]	Recovered Pd (%)
1	**3.28**	Et	Ph	94	76	5.53	78
2	**3.29**	Me	*p*-FC_6H_4	70	62	5.69	72
3	**3.30**	Me	*p*-$OMeC_6H_4$	79	65	6.00	80

[a] by commercial ICP analysis.

In the solid-phase cases with mono-activated alkynes, the yields of benzopyrans were higher than that for the analogous solution-phase reactions, although more time was needed for reaction (24 h vs. 8 h).[161] In addition, the recovered resin from the reaction described in entry 9, Table 3.4 was analyzed by IR spectroscopy (KBr) and gave the following data: 1843 (s br), 1830 (w br), 1718 (s br) cm^{-1}. The analogous soluble complex, $(PPh_3)_2Pd(DMAD)$, shown in Figure 3.3, had the following IR data: IR (KBr, cm^{-1}): 1845 (s),1830 (m) cm^{-1}.[169] These results indicate that the resin had reacted with the DMAD, and that the Pd(0) was likely on the resin as a polymer-bound version of $(PPh_3)_2Pd(DMAD)$.

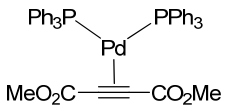

Figure 3.3. *The Complex $(PPh_3)_2Pd(DMAD)$.*

Analysis of the recovered resins also indicated that the palladium could be recovered for potential future use, with up to 80% of the palladium recovered based on ICP analysis of recovered resins. A more immediately practical benefit of the solid-phase work was easier chromatographic purification of the benzopyrans. If the soluble palladacycle is used as a reagent, the complex $(PPh_3)_2Pd(DMAD)$ is difficult to separate from the benzopyran products. The results in Table 3.4 indicate that higher swelling leads to greater reactivity for these systems. In addition, lower loading leads to better yields; however, the low loading is not economically desirable. For future synthetic work (Section 3.2) we chose the medium loading resin for our library synthesis, due to its balance between reactivity and cost.

3.2 Efforts in the Utilization of Polymer-Bound Palladacycles In the Synthesis of a Library of 1,2-Dihydroquinolines

Having shed more light on the effects of phosphorus loading, palladium loading, P : Pd ratio, and swelling on the reactivity of polymer-bound palladacycles, we wanted to utilize the technology to synthesize a library that would both utilize a novel combinatorial methodology as well as generate compounds that have potential drug-like characteristics. The 1,2-dihydroquinoline nucleus is seen in several biologically active compounds,[170-172] and thus are viable targets for library synthesis. The utilization of alkyne insertion into aza-palladacycles in combinatorial chemistry is potentially valuable because the methodology would allow facile access to products with substitution patterns which are difficult to achieve with traditional synthetic methods.[173-175] In addition, suitable amounts (10 – 50 mg) for testing in high-throughput screening assays could be generated rapidly. We decided to apply the knowledge gained from experimental work described in Section 3.1 to synthesize a library of 1,2-dihydroquinolines, the nitrogen analogs of the 2*H*-1 benzopyrans synthesized in the previous section. Preliminary work (Dr. Lei Zhang, Mr. Atsushi Shiota) had indicated that the extension of the work to polymer-bound aza-palladacycles was feasible (Scheme 3.7).

Scheme 3.7

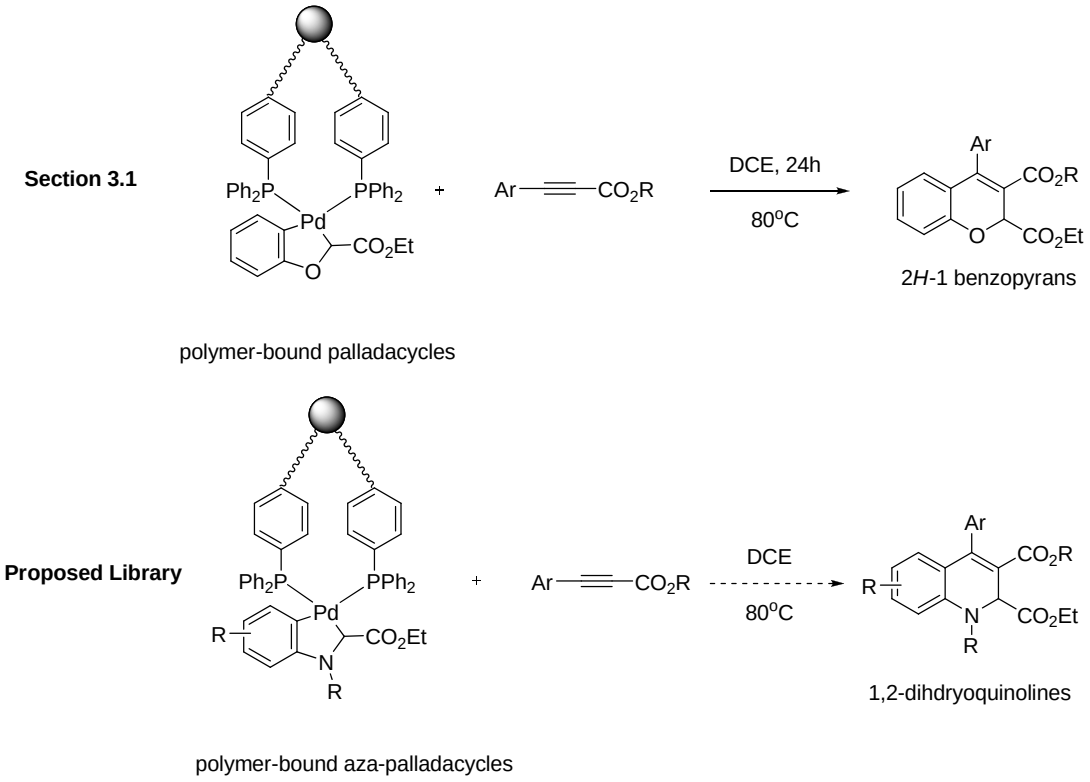

The convergent nature of the reaction between the alkynes and palladacycles to generate the 1,2-dihydroquinolines directed us to vary the substitution pattern on the aromatic ring of the palladacycles as well as vary the aryl groups on the mono-activated alkynes. We chose four polymer-bound aza-palladacycles and six mono-activated alkynes to be the building blocks of the proposed library shown in Figure 3.4.

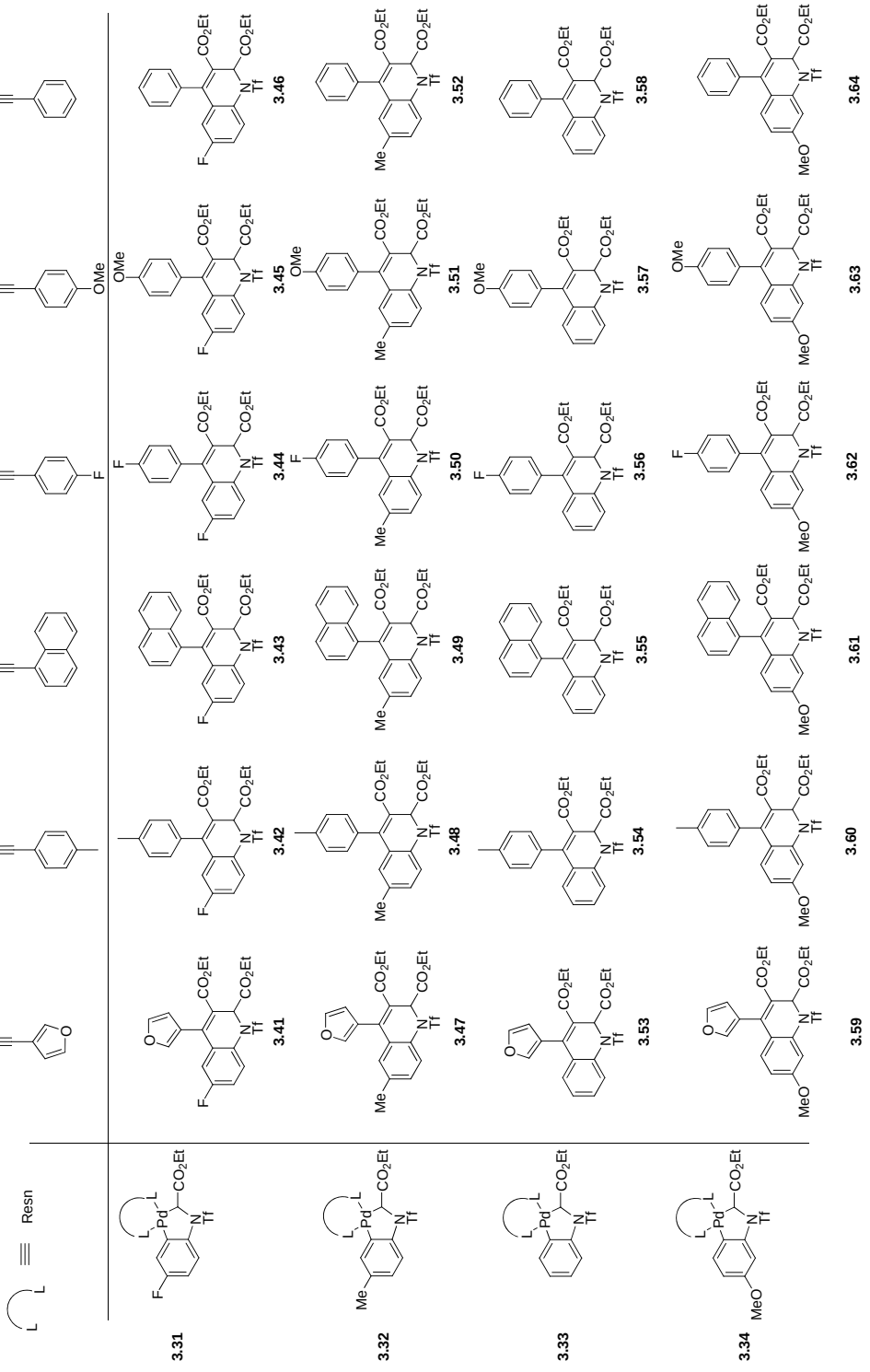

Figure 3.4. *Schematic of Proposed Library.*

Palladacycles **3.31** – **3.34** would be reacted with six alkynes (**3.35** – **3.40**) to give 24 1,2-dihydroquinolines (**3.41 - 3.64).** The retrosynthetic analysis for the palladacycles is shown in Scheme 3.8.

Scheme 3.8

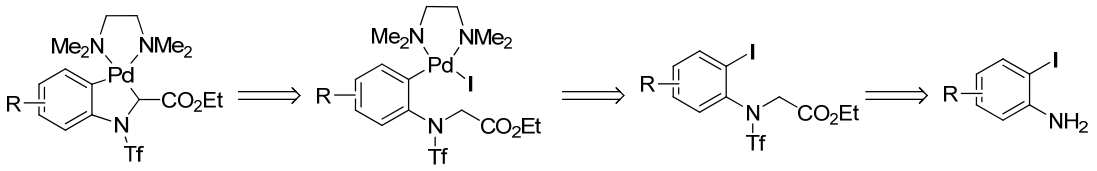

3.65 **3.66** **3.67** **3.68**

Palladacycles **3.65** can be derived from base-mediated intramolecular ligand exchange of Pd(II)-iodo complexes **3.66**. These in turn are derived from iodoesters **3.67** via oxidative addition. The iodoesters can be synthesized from the corresponding iodoanilines **3.68** via triflation and alkylation.

The iodoanilines (except 2-iodoaniline, which is commercially available) were synthesized by either aromatic substitution reactions using $I_2/NaHCO_3$ or by Sandmeyer-type chemistry followed by hydrazine reduction (Scheme 3.9).[176]

Scheme 3.9

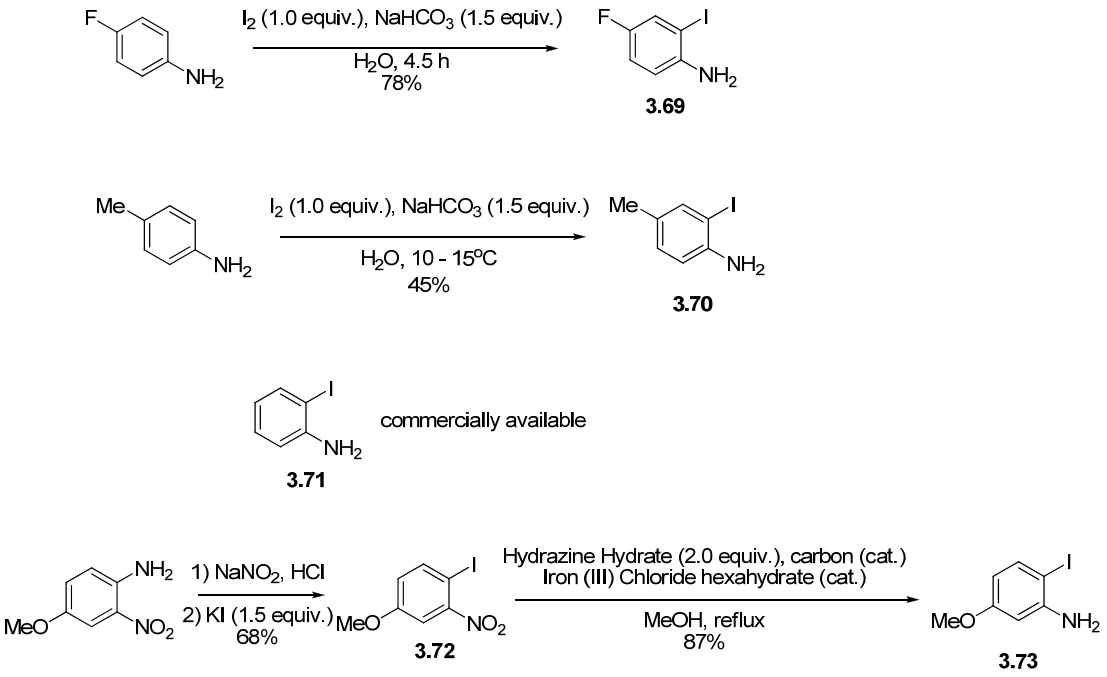

The substituted anilines **3.69** – **3.71** and **3.73** were converted to the triflates **3.74** – **3.77** via reaction with triflic anhydride in the presence of triethylamine in dichloromethane.[177] The results are shown in Table 3.7. For Tables 3.7 – 3.11, the R substituent is numbered for a 2-iodoaniline. The carbon atom attached to nitrogen is numbered 1, and the carbon atom attached to the iodine substituent is numbered 2.

Table 3.7. *Triflation of Iodoanilines* ***3.69*** *–* ***3.71*** *and* ***3.73***

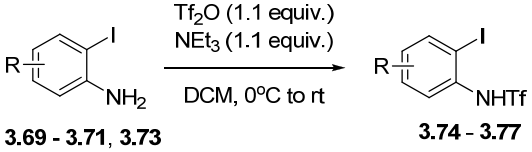

	Substitution Pattern	Product	Yield (%)
1	R = 4-fluoro	**3.74**	54
2	R = 4-methyl	**3.75**	52
3	R = H	**3.76**	38
4	R = 5-methoxy	**3.77**	35

The yields of the N-H triflamides **3.74** – **3.77** were somewhat low, similar to reports by Knochel.[177] The alkylation of the triflamides to give the iodoesters (**3.68**, **3.71**, **3.73**, and **3.78**) proceeded uneventfully by deprotonation by sodium hydride followed by an excess of ethyl bromoacetate.[131] The results are shown in Table 3.8.

Table 3.8. *Alkylation of N-H Triflamides **3.74** – **3.77***

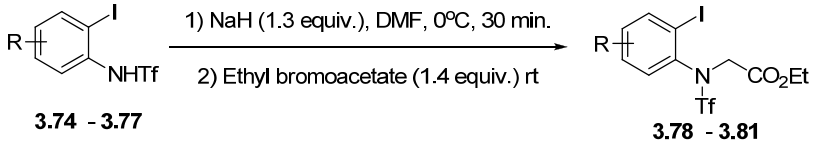

3.74 - 3.77 **3.78 - 3.81**

	Substitution Pattern	Product	Yield (%)
1	R = 4-fluoro	**3.78**	86
2	R = 4-methyl	**3.79**	91
3	R = H	**3.80**	69
4	R = 5-methoxy	**3.81**	78

With the iodoesters synthesized, the synthesis of the palladacycles could commence. First, the palladium(II) iodo complexes **3.82** – **3.85** were synthesized via oxidative

addition of iodoesters **3.78 - 3.81** with Pd_2dba_3 and TMEDA in benzene at 60°C.[131] The results are shown in Table 3.9.

Table 3.9. *Synthesis of Palladium(II) Iodo Complexes* ***3.82*** *–* ***3.85***

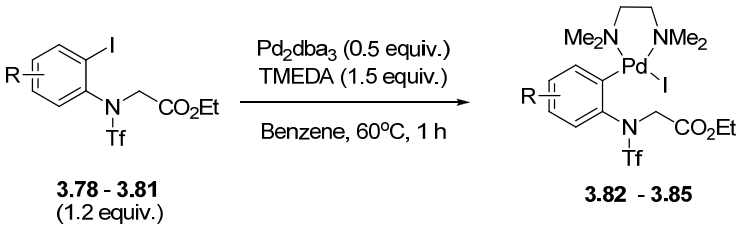

3.78 - 3.81
(1.2 equiv.)

3.82 - 3.85

	Substitution Pattern	Product	Yield (%)
1	R = 4-F	**3.82**	56
2	R = 4-CH_3	**3.83**	67
3	R = H	**3.84**	70
4	R = 5-OMe	**3.85**	58

The reactions afforded the Pd(II) iodo complexes **3.82** – **3.85** as yellow powders in 56 – 70% yield after chromatography on neutral alumina. The TMEDA-palladacycles (±)-**3.86** – (±)-**3.89** were synthesized in 83 – 95% yield via base-mediated ligand exchange followed by filtration through a short plug of basic alumina to afford the palladacycles as white or off-white powders.[131] The results are shown in Table 3.10.

Table 3.10. *Synthesis of Palladacycles (±)-**3.86** – (±)-**3.89***

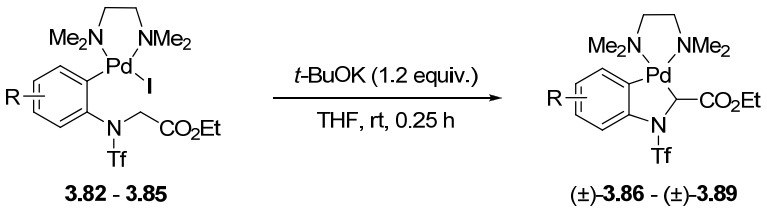

3.82 - 3.85 (±)-**3.86** - (±)-**3.89**

	Substitution Pattern	Product	Yield (%)
1	R = 4-F	(±)-**3.86**	94
2	R = 4-CH_3	(±)-**3.87**	87
3	R = H	(±)-**3.88**	83
4	R = 5-OMe	(±)-**3.89**	95

In order to ensure consistent results for the synthesis of palladacycles (±)-**3.31 –** (±)-**3.34**, we utilized a different batch of the commercially available triphenylphosphine (resin **3.90,** which is similar to **3.5** with a loading of 1.6 mmol P / g, a swelling of 6.7 mL/g, 1 % cross-link density, and 200 – 400 mesh size)**.** The loading of soluble palladacycles (±)-**3.86** – (±)-**3.89** onto resin **3.90** was performed in an analogous fashion to that in Section 3.1 (stirring at room temperature in THF, then removing volatiles, adding fresh THF then stirring again before filtration) to give polymer-bound palladacycles (±)-**3.31** – (±)-**3.34**. The results are shown in Table 3.11.

Table 3.11. *Synthesis of Polymer-Bound Palladacycles (±)-**3.31** – (±)-**3.34***

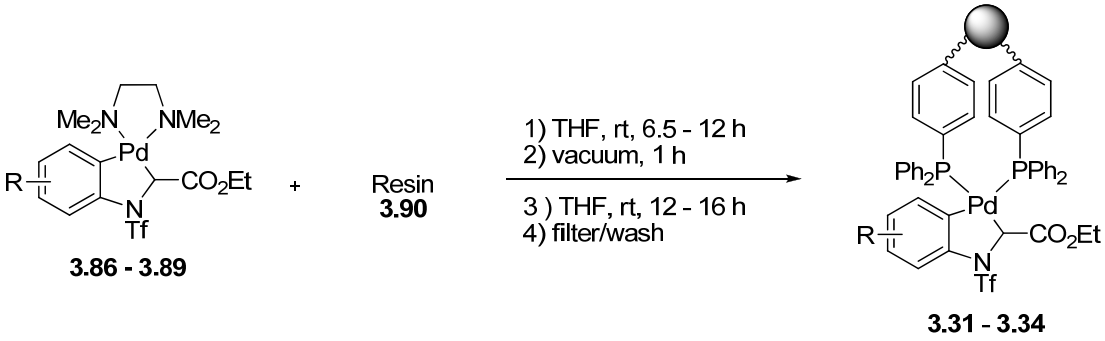

	Substitution Pattern	Pd : P ratio during loading	Pdt	Pd wt. %[a]	P wt. %[a]	Pd : P	Swelling in DCE (mL /g)
1	R = 4-F	1 : 2	**3.31**	5.0	4.1	1 : 2.8	4.7
2	R = 4-CH_3	1 : 2	**3.32**	5.3	4.3	1 : 2.8	--[b]
3	R = H	1 : 2	**3.33**	4.5	4.0	1 : 2.5	3.8
4	R = 5-OMe	1 : 2	**3.34**	5.6	4.2	1 : 2.6	4.6

[a] as measured by commercial ICP-MS analysis. [b] density similar to solvent, unable to obtain accurate reading.

In these cases, incomplete loading occurred, with 14 – 25 mol% of the palladacycles (±)-**3.86** – (±)-**3.89** recovered from the filtrates after reaction, as detected by ^{1}H NMR spectroscopy. As a consequence, the Pd : P ratios were in the range 1 : 2.5 to 1 : 2.8, significantly different from the desired Pd : P ratio of 1 : 2. While discouraged by these results, we forged ahead.

With polymer-bound palladacycles (±)-**3.31** – (±)-**3.34** analyzed, we could now synthesize alkynes **3.35** – **3.40**. The alkyne **3.35** was synthesized by a modified Corey-Fuchs reaction via intermediate dibromoalkene **3.91** (Scheme 3.10).[178, 179]

Scheme 3.10

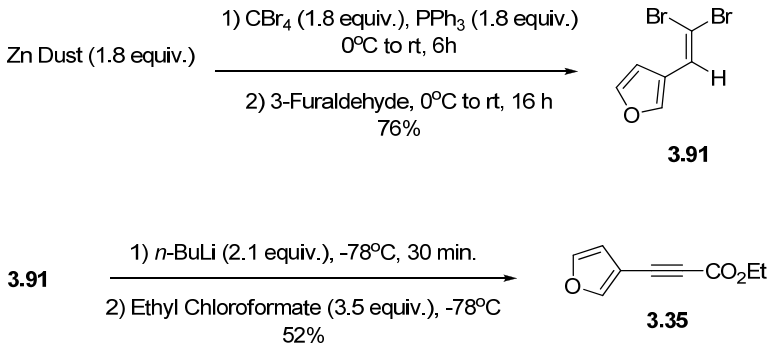

Alkynes **3.36** – **3.40** were synthesized via deprotonation of the corresponding aryl alkynes with *n*-BuLi followed by reaction of the generated anion with an excess of ethyl chloroformate. The results of the syntheses of alkynes **3.36** – **3.40** are shown in Table 3.12.

Table 3.12. *Synthesis of Alkynes **3.36 - 3.40***

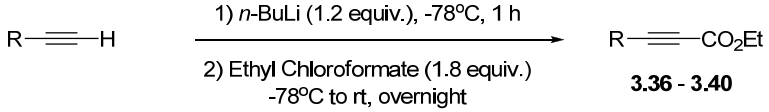

	Substitution Pattern	Product	Yield (%)
1	R = 4-methylphenyl	**3.36**	quant.
2	R = 1-naphthyl	**3.37**	84
3	R = 4-fluorophenyl	**3.38**	82
4	R = 4-methoxyphenyl	**3.39**	quant.
5	R = phenyl	**3.40**	95

Based on the prior work with the oxapalladacycles and preliminary results with the azapalladaycles, we predicted lower yields for the insertion reactions with polymer-

bound palladacycles (±)-**3.31 –** (±)-**3.34**. In order to discover satisfactory conditions to synthesize the library using parallel synthesis methods, a subgroup of compounds needed to be synthesized so that the parameters could be successfully set for the purification process. The purification system utilized by the KU-CMLD featured mass-directed fractionation (MDF). The nature of MDF purification dictates that the compounds to be purified must be ionizable under the electro-spray ionization technique the mass spectrometer utilizes. This has been known in the past to be problematic with some *N*-heterocycles. It was unknown which library members would be detected by the ionization method.

The polymer-bound palladacycle **3.34** bearing the 5-methoxy group on the ring was reacted with alkynes **3.35** to **3.40** produce products **3.59 – 3.64**. The results are shown in Table 3.13.

Table 3.13. *Initial Reactions of Alkynes* ***3.35*** *to* ***3.40*** *with Polymer-Bound Palladacycle* ***3.34*** *in Parallel Format in a Miniblock XT*

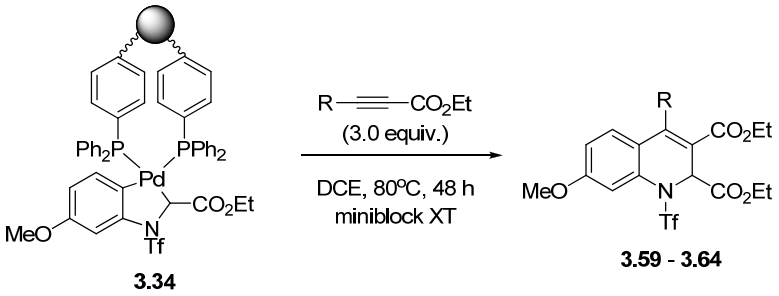

	R	Product	Mass of product (mg)	HPLC purity (%)
1	R = 3-furyl	**3.59**	3.5	73
2	R = 4-methylphenyl	**3.60**	--[a]	--[a]
3	R = 1-naphthyl	**3.61**	1.7	89
4	R = 4-fluorophenyl	**3.62**	2.4	78
5	R = 4-methoxyphenyl	**3.63**	2.1	97
6	R = phenyl	**3.64**	2.0	97

[a]mass ion was not seen by mass spectrometer, no fractions collected

The results from the mass-directed fractionation (MDF) purification were quite disappointing as small amounts of the products were isolated (less than 10% yield in all cases) and the samples showed significant impurities by ^{1}H NMR. We pondered whether it was simply the substitution pattern of palladacycle (±)-**3.34** that was causing the low yields and purities. To probe this possibility, we used similar conditions (3.0 equiv alkyne, 80°C, 48 h) to synthesize the rest of the library

members. For the synthesis of the second sub-library of 18 compounds, we chose to use the Chemspeed SLT-100 due to its ability to automate much of the synthesis and filtration. Due to technical limitations of using the Chemspeed machine, we could not synthesize library members **3.52** and **3.58** (Figure 3.5).

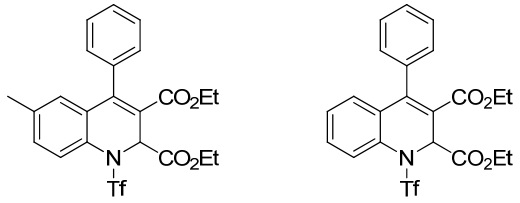

3.52 **3.58**

Figure 3.5. *The Two Library Members Not Attempted.*

The results from the MDF purification of these reactions were quite poor as well. The mass spectrometer did not detect the molecular peak in six of the sixteen samples. As the automated mass-directed fractionation is an integral part of the library synthesis, we postponed the project after receiving these results.

In conclusion, we explored the effect of the microenvironment around the palladium center in the solid phase using a palladium complex that has a well-defined reactivity in solution. We found that even a moderately high loading (3.0 mmol P/g) of phosphine on the resin gave rise to harmful microenvironmental effects, including an isomerization that was not observed in the analogous solution-phase reaction and lowered yields, presumably due to higher local concentrations of phosphines. A relatively lower loading (1.4 mmol P/g) resin gave a polymer-bound palladacycle that was able to approach the yields of the solution-phase reaction without significant isomerization in many cases. The low-loading resin with a longer tether length

reacted quite readily to give high yields at both low and high temperatures. However, the low-loading resin is the least economically viable of the three, with only 0.9 mmol P/g of phosphine on the resin. In addition, the loading of the palladacycle onto this polymer was incomplete, suggesting that either the concentration of the phosphine groups is too low for effective loading of the resin, or that some of the phosphine groups were oxidized during the synthesis of the resin. An excess of the phosphine during loading (> 1 : 2 Pd : P) resulted in drastically lowered yields. The data suggest that concentration effects are likely to be magnified during solid-phase reactions. The variability of the isomerization depending on the individual reaction indicates that conditions at the reaction sites differ even within individual batches of polymer-bound palladacycle. The resins swelling capacity did correlate well with reactivity, with the higher-swelling resins generating higher reactivity.

Although we did not achieve our aim of synthesizing a library of 1,2-dihydroquinolines utilizing the system developed in Section 3.1, we are optimistic that future work will uncover more of the factors involved in modulating the reactivity of metal complexes coordinated to polymer-bound ligands, particularly the factors involved in the reactivity of aza vs. oxa-palladacycles, allowing for a successful library synthesis. In addition, future endeavors would potentially pave the way for the use of other polymer-bound complexes in less of a “black box” manner.

Chapter Four:

Synthesis and Characterization of Pallada(II)pyrrolidinones: Palladacycles with Two Pd-bonded Stereogenic Carbons

4.1 Attempted Alternative Synthesis of Palladacycles by C-H Activation

4.1.1 Rationale

Much of modern palladium chemistry involves intermediates which do not have a carbon stereocenter attached to the palladium atom that is also transferred to the product (vide supra). Consequently, the chemistry of palladium complexes having a carbon stereocenter adjacent to palladium is not well-explored,[111] particularly as it concerns the mechanism of stereoinduction when a chiral non-racemic auxiliary ligand is present during a Pd-C bond forming step. This is likely due to the fact that sp^3-hybridized alkyl palladium species are much more likely to have readily accessible β-hydrogens, which can lead to undesirable β-hydride elimination. Our group has synthesized a variety of complexes with a stereocenter adjacent to the palladium center without accessible β-hydrogens and studied their interactions with chiral ligands (Scheme 4.1). Complexes **4.1** – **4.3**, **4.8**, and **4.9** are readily isolable complexes, while **4.6** and **4.7** must be formed *in situ* due to the increased steric hindrance imposed by the quaternary carbon center.

Scheme 4.1

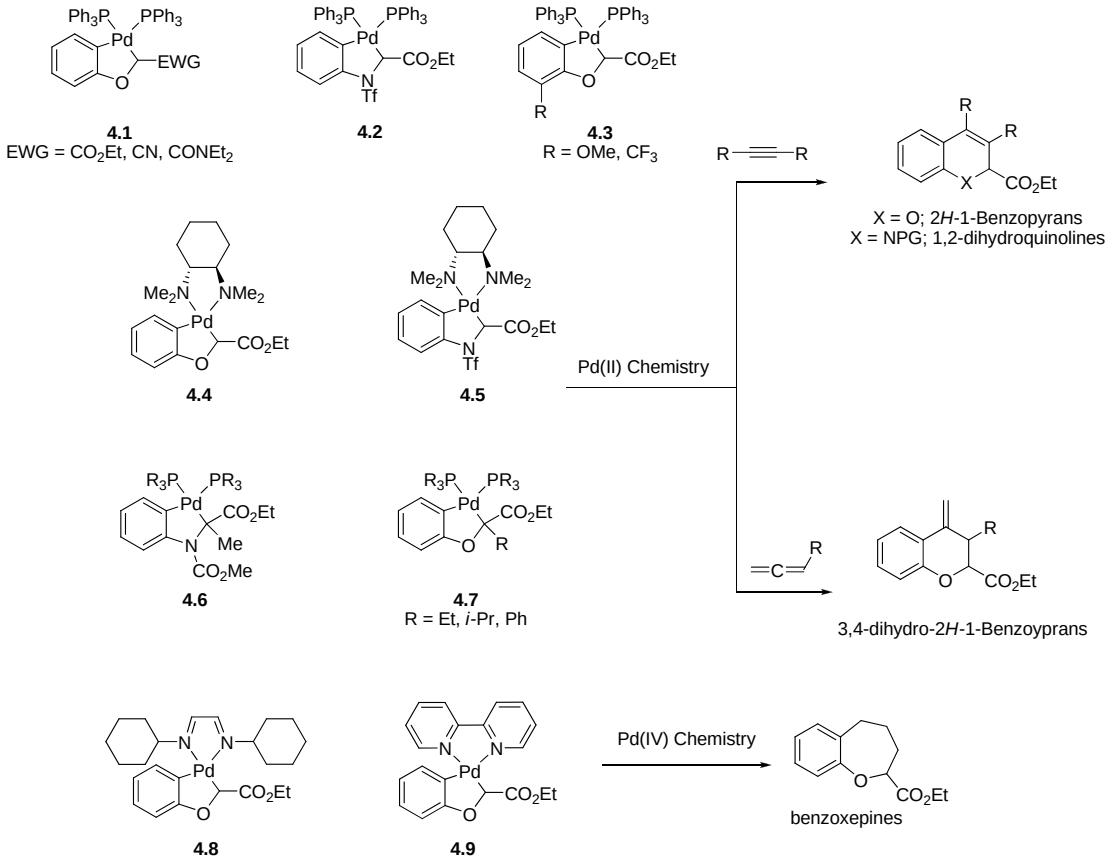

Another advantage of this chemistry is the ability to access heterocyclic systems with rare substitution patterns. 2*H*-1-benzopyrans,[161] 1,2-dihydroquinolines,[163] and benzoxepines[180] can all be readily accessed via palladacycles as intermediates. The monodentate phosphine ligands of complexes **4.1** – **4.7** are necessary as ligand exchange must occur before the desired reactions can proceed. For complexes **4.8** and **4.9**, the flat bidentate nitrogen ligands stabilize the palladium(IV) intermediates (see Chapter Two).

However, for the syntheses of palladacycles **4.1** – **4.9**, the presence of an electron-withdrawing group to activate the C-H bond toward deprotonation is necessary to form the Pd-C bond via an intramolecular ligand exchange. The electron-withdrawing group, such as an ester or an amide, also makes the stereocenter potentially more susceptible to racemization or epimerization. The methodology could be improved if the need for the electron-withdrawing group was eliminated as the stereocenter formed would conceivably be more configurationally stable. A wider variety of organic products could also be synthesized, greatly improving the scope of the reaction as well as allowing for other fundamental studies of complexes generated by forming the stereocenter without the electron-withdrawing group.

4.1.2 Inspiration from Arndtsen

While planning ways to generate palladacycles without the electron withdrawing group, we read the work of Arndtsen and co-workers.[181] In 2001, Arndtsen published a paper detailing the development of a palladium-catalyzed synthesis of imidazolines **4.11** from imines, acyl chlorides, and carbon monoxide while attempting to synthesize peptides. The initial reaction involved the cationic palladium complex **4.10** synthesized from an imine, acyl chloride, and a Pd (0) source (Scheme 4.2).

Scheme 4.2

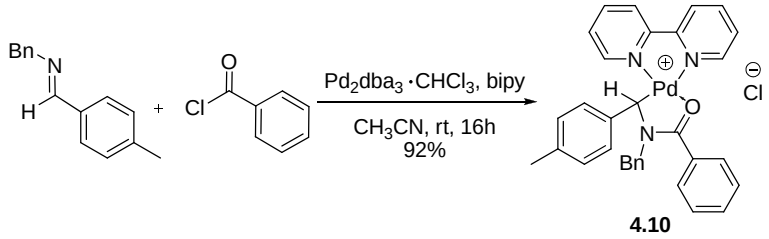

Next, Arndtsen reacted the fully characterized complex **4.10** with carbon monoxide in acetonitrile at 55°C for five days. An unexpected imidazoline product incorporating two imine fragments was formed in 35% yield (Scheme 4.3).

Scheme 4.3

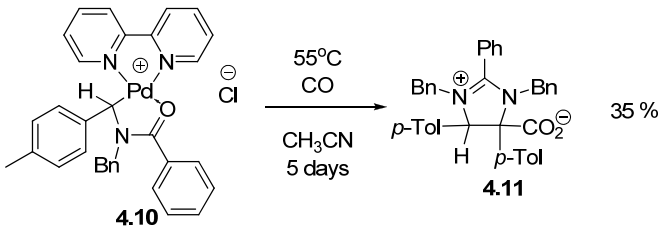

Intrigued by this result, Arndtsen then monitored the reaction by NMR spectroscopy (Scheme 4.4) utilizing ^{13}CO, and found that the source of the imine for the cyclization was generated via a reductive decyclization of complex **4.10** to generate iminium salt **4.13** (which is in equilibrium with the imine and acyl chloride) and Pd(0)-bipy complex (Path B, Scheme 4.4). The imine generated in Path B then reacts with the product from CO insertion into complex **4.10** (Path A, Scheme 4.4) to generate the imidazoline **4.11** as a single diastereomer with a *trans* orientation of *p*-tolyl groups as determined by X-Ray crystallography.

Scheme 4.4

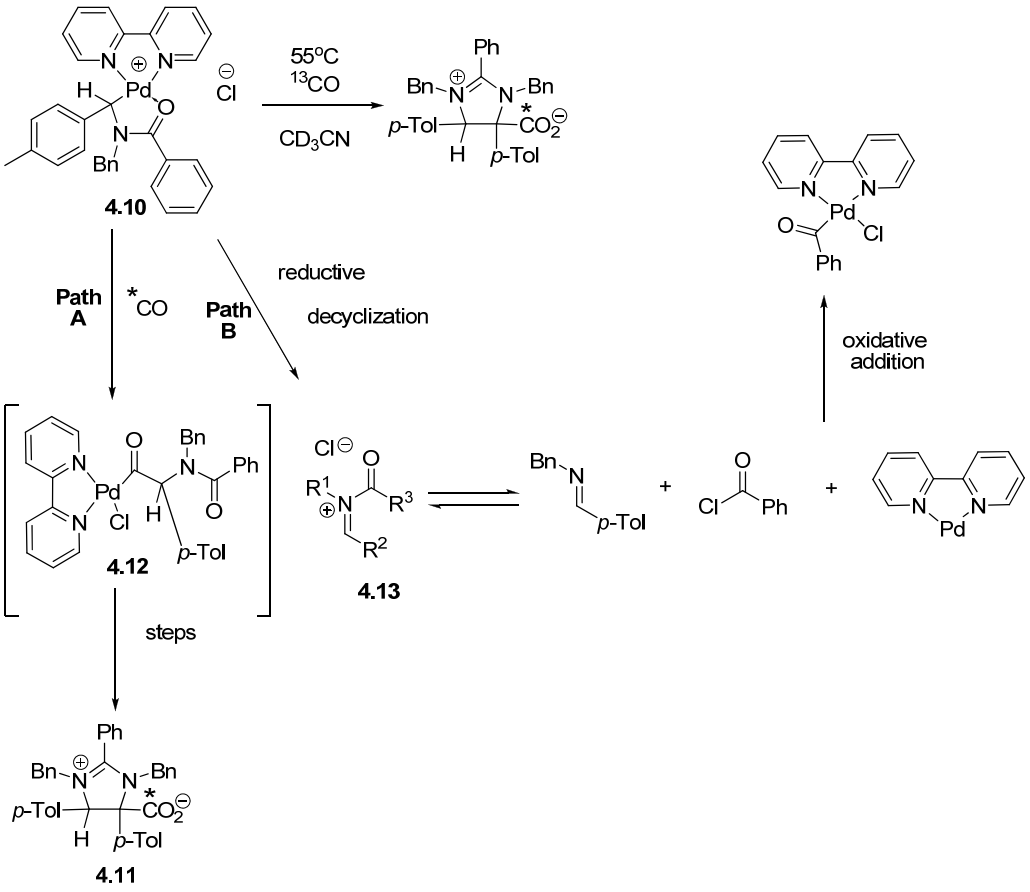

This suggested that the reaction could also occur by simply mixing the imine, acyl chloride, palladium (0) source and ligand together in acetonitrile while heating under a CO atmosphere; a 70% yield was isolated when this process was carried out. While monitoring this reaction by NMR spectroscopy, Arndsten observed that all the substrates added to the system were incorporated in the product as well as the fact that HCl was liberated. This indicated that Pd(0) was potentially being released from the reaction, which led to the hypothesis that it could be made catalytic in palladium. Arndsten was indeed successful in this endeavor; the results are shown in Table 4.1.

Table 4.1. *Effects of Substrates and Ligands in the Synthesis of Imidazolines Reported by Arndtsen*

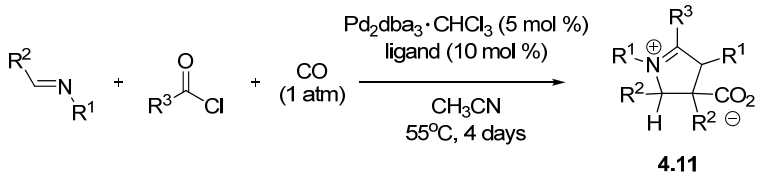

	Ligand	R^1	R^2	R^3	Yield (%)
1	bipy	Bn	*p*-Tol	Ph	82
2	bipy	Me	*p*-Tol	Ph	92
3	bipy	Bn	*p*-$CH_3SC_6H_4$	Ph	73
4[a]	bipy	Bn	*p*-ClC_6H_4	Ph	62
5	bipy	$CH_2CH_2OCH_3$	*p*-ClC_6H_4	Ph	78
6	bipy	Bn	*p*-Tol	CH_3	70
7	bipy	Ph	*p*-Tol	Ph	--
8	bipy	Bn	*p*-$NO_2C_6H_4$	CH_3	--
9	pyridine	Bn	*p*-Tol	Ph	87
10	dppe	Bn	*p*-Tol	Ph	--
11[b]	no ligand	Bn	*p*-Tol	Ph	83

[a] reaction complete in 3 days [b] reaction complete in 24 h

Entries 1 – 8 in Table 4.1 show that bipyridine lowers the rate of the reaction (4 days) when compared to entry 11 using no auxiliary ligand (complete in 24 h). Strong bidentate phosphine ligands (dppe, entry 10) completely inhibit the reaction, as did

imines that were relatively electron-poor (entries 7 and 8). The proposed catalytic cycle with 2,2'-bipyridyl as the ligand is shown in Scheme 4.5.

Scheme 4.5

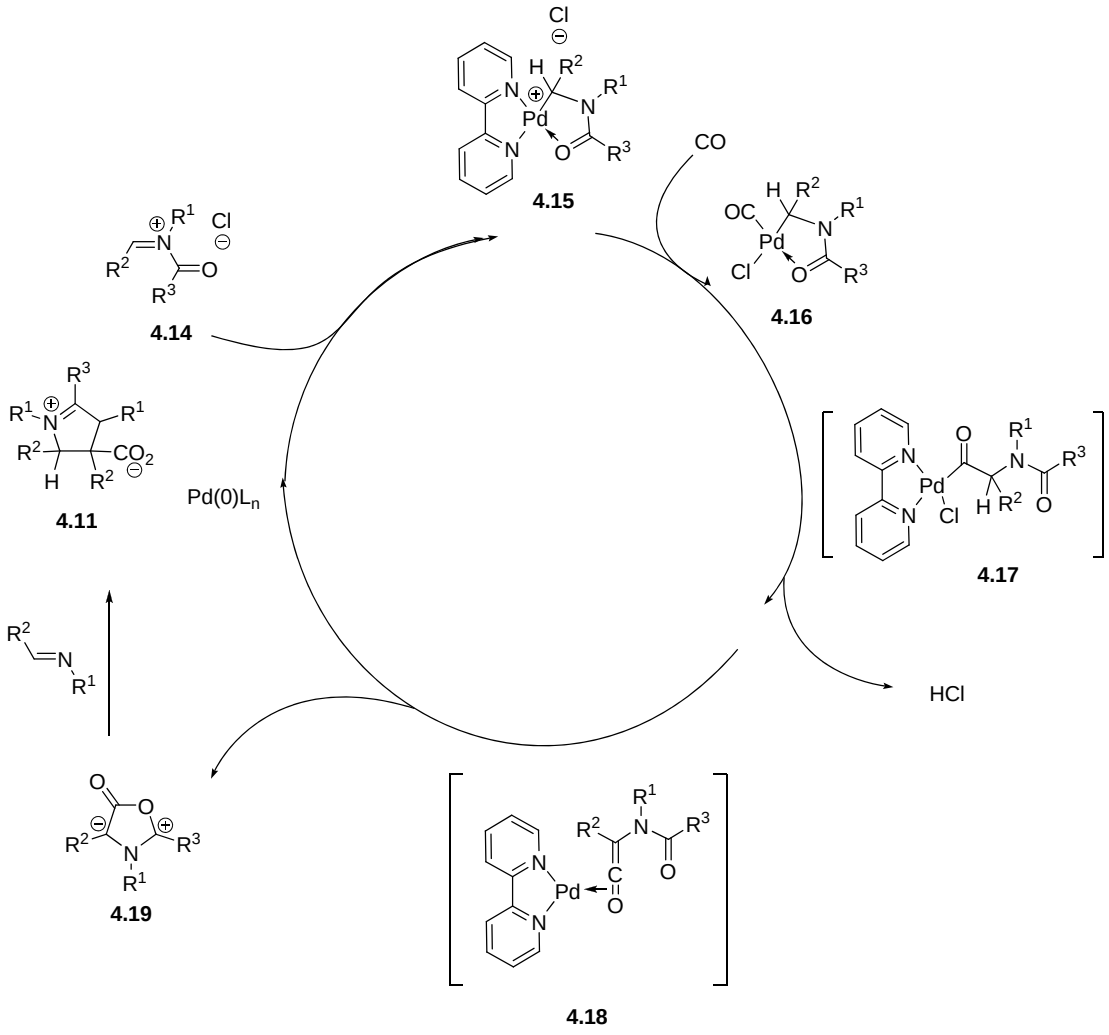

In this reaction, Pd(0) acts as a nucleophile, attacking iminium salt **4.14** to generate chelated cationic complex **4.15** after complexation of bipyridyl.[182] The next step is a displacement of the bipyridyl ligand with carbon monoxide and chloride ion to give intermediate complex **4.16**. Complex **4.16** then undergoes carbon monoxide insertion

to give complex **4.17**, which can then eliminate HCl to give palladium-complexed ketene intermediate **4.18**. After palladium decomplexation, the münchnone **4.19** is formed and reacts with another equivalent of imine in a [3+2] cycloaddition followed by ring-opening to give imidazoline **4.11**.

Inspired by complex **4.10** synthesized by Arndtsen, we proposed to form the stereogenic carbon adjacent to the palladium center via reaction of a suitable Pd(0) species with an acyliminium salt, followed by C-H activation of the PMP substituent on the nitrogen atom to give a new class of palladacycles without an electron-withdrawing group on the stereogenic carbon (Scheme 4.6).

Scheme 4.6

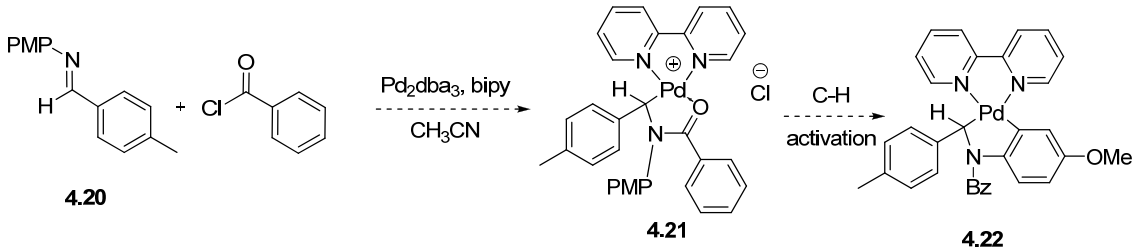

In the proposed synthesis, imine **4.20** bearing an *N*-PMP substituent would react with benzoyl chloride and Pd (0) in an analogous manner to Scheme 4.3 to give complex **4.21** which could then conceivably undergo a C-H activation of the PMP ring to give palladacycle **4.22** without a strong electron-withdrawing group attached to the sp^3-hybridized carbon.

In Arndtsen's original report, the acyliminium salt was added as an isolated species. We also attempted to isolate a pure acyliminium salt, but after much experimentation we were unable to isolate a pure species, as indicated by ^{1}H NMR

spectroscopy. This is not surprising, as these extremely reactive species are almost exclusively generated and used *in situ*.[183]

Therefore, we decided to simply make the iminium species *in situ*. With this in mind, we replaced the imine in Arndtsen's original procedure with *p*-anisidine derived imine **4.20** containing a *N*-PMP group to synthesize the cationic palladium complex precursor **4.21** for C-H activation. Our attempts to utilize Arndtsen's procedure did not produce a pure product via crystallization or trituration with ether. The ^{1}H NMR spectrum of the complex mixture included a new singlet at 5.86 ppm, which is likely the C-H proton on the carbon attached to the palladium center. The shift for the analogous proton in complex **4.10** bearing an N-Bn group is 5.11 ppm.[181] All attempts to chromatograph the material using alumina or silica failed, as the palladium salt was strongly attracted to the solid phase. We also utilized a Soxhlet extraction using ether in another attempt to purify the material, but the ^{1}H NMR consistently had multiple peaks in the region assigned to the *p*-OMe group (ca. δ 3.80 ppm). Upon reviewing Arndtsen's work, we noted that the cationic complexes having triflate instead of chloride as the counterion did not undergo the carbon monoxide insertion desired in their system. We thought this was significant, since this indicates that the cationic complex is made more stable by the anion metathesis.

4.1.3 Attempted C-H Activation

We were finally able to generate cationic complex **4.22** bearing a triflate anion by performing the acyl iminium formation, the oxidative addition, the dimer breaking

reaction, and the anion metathesis reaction in a four-step, one pot procedure (Scheme 4.7). Complex **4.22** was fully characterized.

Scheme 4.7

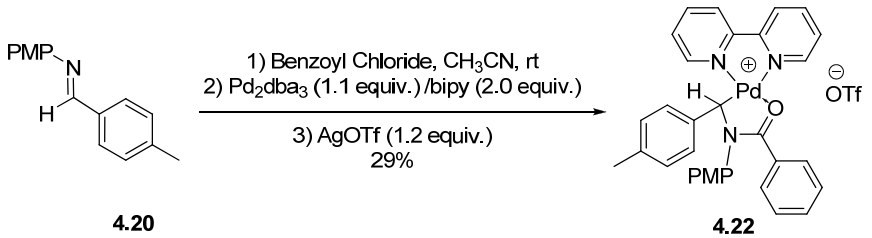

4.20 **4.22**

We then attempted to form product **4.23** via C-H activation of the PMP ring of **4.22** under various conditions (Table 4.2). Unfortunately, none of the conditions employed proved promising. Many of the reactions gave complex mixtures of products via decomposition. Even under conditions with an oxophilic Lewis acid (entry 7, Table 4.2), no reaction was seen. Based on this screening, we wondered why we were not observing C-H activation of this complex. One explanation is that the carbonyl is complexed very strongly to the palladium center, not allowing the amide to rotate. If the rotation is inhibited, then an intramolecular C-H activation is not possible because the reactive portions of the molecule cannot come close enough to one another for the reaction to occur. Indeed, when we dissolved complex **4.22** in CD_3CN and performed a variable temperature ^1H NMR (400 MHz) experiment, we observed that the peaks corresponding to the protons on the 2,2'-bipyridyl ligand (signals marked with circles in Figure 4.1) became significantly broader at 70°C, while the resonances corresponding to the other protons in the molecule did not change significantly (Figure 4.1).

Table 4.2. *Attempted C-H Activation of Complex* ***4.22***

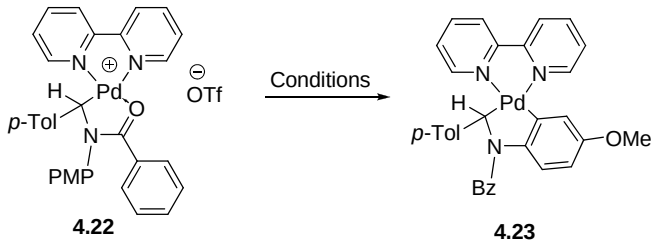

4.22 **4.23**

	Solvent	Base (equiv.)	Additive (equiv.)	Time (h)/ Temperature (^{o}C)	Result
1	CH_3CN	NaOAc (5.0)	--	24 h/ 95^{o}C	NR
2	CH_3CN	Cs_2CO_3 (5.0)	--	24 h/ 95^{o}C	Decomp.[a]
3	CH_3CN	NaOAc (5.0)	NaI (2.0)	24 h/ 95^{o}C	Decomp.[a]
4	CH_3CN	Cs_2CO_3 (5.0)	NaI (2.0)	24 h/ 95^{o}C	Decomp.[a]
5	CH_3CN	Cs_2CO_3 (5.0)	--	24 h/ rt	Decomp.[a]
6	CH_3CN	Cs_2CO_3 (5.0)	--	24 h/ 50^{o}C	Decomp.[a]
7	CH_3CN	Cs_2CO_3 (5.0)	$Sc(OTf)_3$ (3.0)	24 h/ 80^{o}C	NR

[a] ^{1}H NMR of crude reaction mixture showed decomposition of starting material

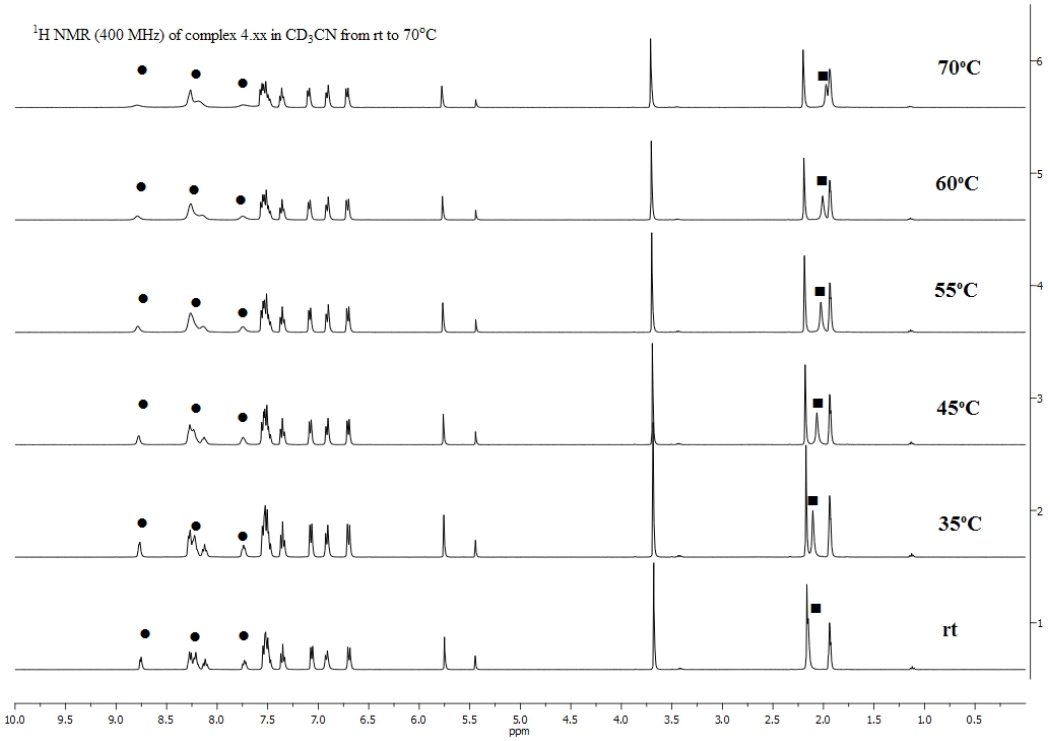

● - protons of bipy ligand ■ - protons of adventitious water

Figure 4.1. *Variable Temperature ^{1}H NMR Spectra of Complex* ***4.22*** *in CD_3CN.*

The spectra in Figure 4.1 indicate that the bipyridyl ligand is more labile than the chelated amide moiety. We realized that our strategy would probably not work with this system, as it is highly unlikely that the C-H activation can occur without the Pd center and the aromatic ring being in close enough proximity to react.

4.2 Synthesis and Characterization of Palladapyrrolidinones

4.2.1 Rationale

Not being able to find conditions to form palladacycle **4.23** without an electron-withdrawing group, we elected to utilize our knowledge of the synthesis and isolation of cationic palladium complexes such as **4.22** to pursue another new type of palladacycle. An earlier member of the research group (Ms. Susmita Gupta) had isolated and partially characterized the palladium complex **4.25** from the reaction of palladium complex **4.24** with *t*-BuOK at room temperature in THF (Scheme 4.8).

Scheme 4.8

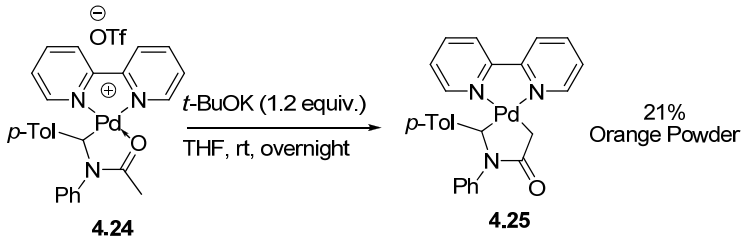

4.24 **4.25**

The complex was characterized by IR, ^{1}H NMR and ^{13}C NMR and is shown as the C-Pd enolate. The ^{1}H NMR signals (2.50 ppm, d, J = 13.9 Hz, 1 H and 3.39 ppm, d, J = 13.9 Hz, 1 H), IR (1615 cm^{-1}), and the ^{13}C NMR (182.9 ppm) are consistent with the C-Pd enolate structure bearing two diastereotopic protons on the carbon adjacent to the palladium center as well as the endocyclic amide functional group.

We pondered whether we could synthesize a complex that has *two* stereogenic centers attached to palladium by utilizing a substituted acetyl chloride to generate cationic complexes **4.26**, which could then be deprotonated with a suitable base to

generate O-palladium enolates **4.27**. The latter would subsequently tautomerize to C-palladium enolates **4.28** (Scheme 4.9).

Scheme 4.9

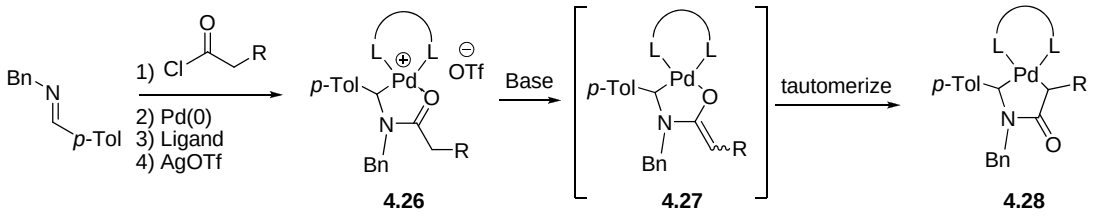

Substantial evidence points toward the likelihood that C-Pd enolates **4.28** would be the dominant and isolable products. Hartwig has reported that in many cases the ester or amide enolates (**4.29 – 4.34**) are more stable in the C-bound tautomer form.[184] A notable exception are those enolates (**4.33** and **4.34**) that would possess a quaternary carbon center if C-bound, due to steric hindrance outweighing the electronic preference for the C-Pd enolate structure in these complexes with bidentate phosphine ligands. Relevant examples are shown in Figure 4.2. Complexes **4.29** and **4.30** are the closest to those detailed in this dissertation; we had good reason to believe that in our case we would be able to isolate the C-Pd enolate. The C-Pd enolate should then react in a similar manner to an alkyl palladium complex due to the relatively non-polar C-Pd bond. If these reactions could be realized, the complexes generated could provide a model for the metal-mediated C-C bond formation between two sp^3-hybridized carbon atoms.

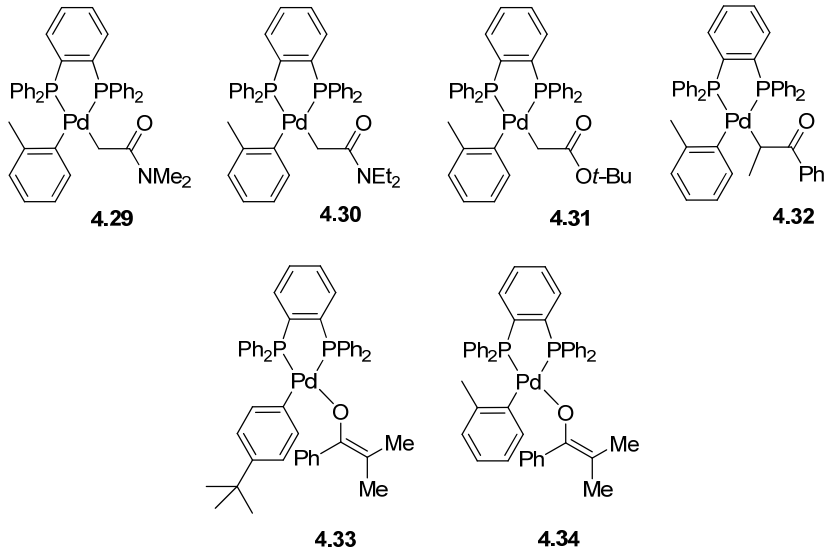

Figure 4.2. *C and O-bound Palladium Enolate Complexes Reported by Culkin and Hartwig.*[184]

The design of palladium-catalyzed reactions utilized to form a bond between two sp^3-hybridized and potentially stereogenic carbons is currently an area of intense research.[111, 185, 186] While strides are being made in the area, methods for the transition-metal mediated formation of a C-C bond between two stereogenic sp^3-hybridized carbons remain rare. However, there is a dearth of studies on stable palladium complexes bearing two carbon stereocenters attached to palladium,[28, 29] presumably due to both the lack of methods to synthesize them as well as the potential for synthetically deleterious β-hydride elimination in some cases. Only a few other systems that feature two stereogenic sp^3-hybridized carbons attached to palladium are known (Figure 4.3).

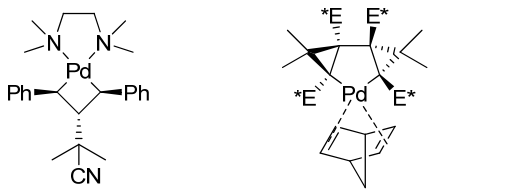

4.35 **4.36**
E* = -CO_2-(*S*)-CH(Me)CO_2Me

Figure 4.3. *Palladium Complexes Bearing Two Stereogenic Carbons Attached to a Palladium Center.*

Complex **4.35** was synthesized by Hoffmann via attack of a nitrile enolate on π-allyl palladium dimer, and complex **4.36** was synthesized via a concerted oxidative cyclization of cyclopropenes with palladium(0). Both **4.35** and **4.36** were studied by X-Ray crystallography. However, neither of the synthetic methods to produce **4.35** and **4.36** provided a way to study the influence of the first carbon-bound stereocenter on the second.

The palladapyrrolidinone system is a potentially powerful model complex to explore the influence of the initially formed stereocenter and the auxiliary ligand sphere on the stereoselectivity of the formation of a second stereocenter. In addition, studies can also be performed on how a chiral non-racemic ligand would affect the diastereoselectivity of the reaction. To our knowledge, no studies of this type have been reported.

4.2.2 Synthesis of Cationic Palladium Complexes as Precursors

Utilizing phenylacetyl chloride as the acyl chloride and TMEDA as the ligand, we were able to isolate complex **4.37** as a yellow solid in 25% yield utilizing the same four-step one-pot reaction used to synthesize complex **4.22** (Scheme 4.10).

Scheme 4.10

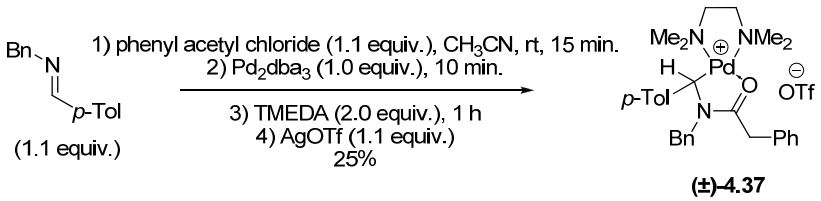

(±)-4.37

While we were able to isolate a pure product, we were unsatisfied with the low yield and wished to improve it. The increase in the equivalents of imine, acyl chloride, ligand, and silver triflate relative to palladium afforded an improved yield of 67% (Scheme 4.11). The likely reason for the increase in the yield is that more of the highly reactive acyliminium species is present when excesses of acyl chloride and imine are used.

Scheme 4.11

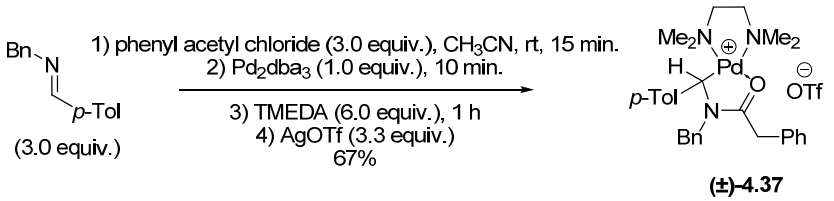

(±)-4.37

We were also able to synthesize the bipy complex (±)-**4.38** in an analogous fashion in 65% yield (Scheme 4.12).

Scheme 4.12

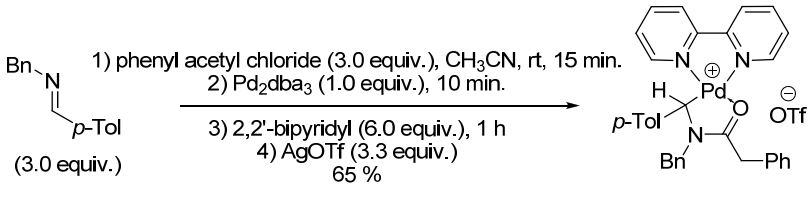

(±)-4.38

When we attempted to synthesize the dppe complex (±)-**4.39** using the same method, we could not completely separate the product from an unknown complex which was apparently formed from the chelation of silver species with the dppe ligand. However, we were able to synthesize (±)-**4.39** in 74% yield via ligand exchange of complex (±)-**4.37** in dichloromethane with excess dppe (Scheme 4.13).

Scheme 4.13

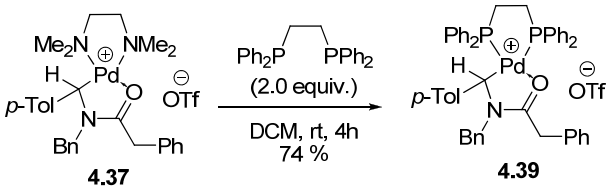

4.2.3 Synthesis of Palladapyrrolidinones via Deprotonation

With complex (±)-**4.37** synthesized, we attempted the deprotonation/tautomerization to form complex (±)-**4.40**, a palladapyrrolidinone bearing a TMEDA ligand. Upon adding 1.1 equiv. of a 1.0 M solution of *t*-BuOK in THF to a solution of (±)-**4.37** in THF at room temperature and letting the reaction stir for 2 h, we obtained a crude mixture of *cis*-(±)-**4.40** and *trans*-(±)-**4.40** (predominantly *cis*-(±)-**4.40**) in 52% yield and dr 91 : 9 *cis* : *trans* by ^{1}H NMR (Scheme 4.14).

Scheme 4.14

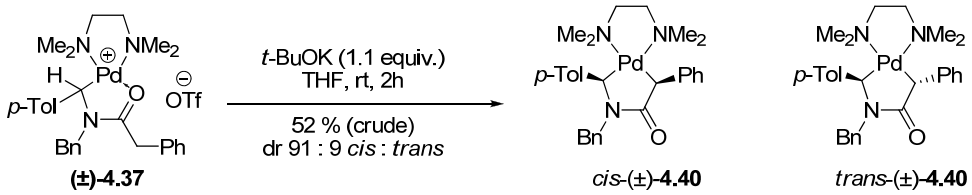

This result confirmed our hypothesis that we could both form and isolate the C-Pd enolate, as the characterization data for the complex were consistent with the proposed C-Pd enolate structure (vide infra). We wished to find conditions that would give us a higher yield as well as a suitable purification method. When we attempted the same reaction at 45°C for 30 minutes in THF with 1.1 equivalents of *t*-BuOK, we found that we achieved a much higher yield of complex (±)-**4.40** (77%) as well as a dr similar to the initial experiment of 89 : 11 *cis* : *trans* by ^{1}H NMR after purification by flash chromatography on silica followed by trituration with pentane. Analogous conditions were used for the reaction of (±)-**4.39** bearing the dppe ligand (1.1 equiv *t*-BuOK, 45°C, THF, 30 min) to give complex (±)-**4.41** in a 72 : 28 dr by ^{1}H NMR still favoring the *cis* isomer (Scheme 4.15).

Scheme 4.15

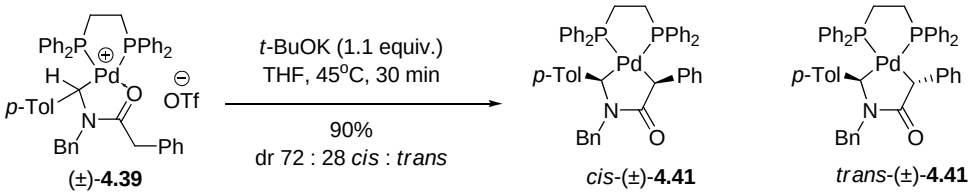

However, when the reaction was run with (±)-**4.38** bearing the bipy ligand, a mixture of *cis* (±)-**4.42** and *trans* (±)-**4.42** was isolated in high yield (86%, Scheme 4.16) and low dr. Interestingly, the bipy ligand gave the *trans* diastereomer in a slight excess in this case.

Scheme 4.16

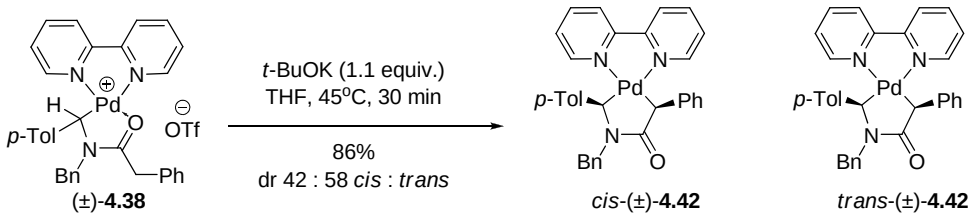

Several pieces of evidence point to the C-Pd enolate structures featuring a lactam ring presented for the three complexes ((±)-**4.40**, (±)-**4.41**, and (±)-**4.42**, bearing TMEDA, dppe, and bipy ligands respectively). The first piece of evidence is the IR frequencies, which are consistent with the proposed structure. The second piece of evidence is from NMR spectra. In the ^{1}H NMR spectrum, the signals for the methine protons on the carbons adjacent to the palladium centers are singlets that are observed upfield from 5 ppm, indicating that it is likely not a proton attached to a sp^2-hybridized carbon.[187] The ^{13}C NMR spectrum shows signals in the proper region for an amide.[187] The information is summarized in Table 4.3. In order to establish the dr for complexes (±)-**4.40**, (±)-**4.41,** and (±)-**4.42**, we utilized the ^{1}H NMR signals of the benzylic protons, as these allowed for the most precise integration. In the spectrum of (±)-**4.40**, we used the signal at 4.89 ppm (d, J = 14.8 Hz) for the *trans* diastereomer, and signal at 4.84 ppm (d, J = 14.8 Hz) for the *cis* diastereomer. For complex (±)-**4.41**, the signals used were found at 5.12 ppm (dd, J = 14.0 Hz, 1.6 Hz) for the *trans* diastereomer, and 4.03 ppm (dd, J = 14.4 Hz, 2.0 Hz) for the *cis* diastereomer. For complex (±)-**4.42**, the signals used were found at 5.09 ppm (d, J = 14.5 Hz) for the *trans* diastereomer, and 5.05 ppm (d, J = 15.0 Hz) for the *cis* diastereomer.

Table 4.3. *Spectral Data Supporting the Structural Assignments of (±)-**4.38** – (±)-**4.40***

Complex	Ligand	^{1}H NMR (ppm)	^{13}C NMR (ppm)	IR (cm^{-1})
(±)-**4.40**	TMEDA	4.12, 3.99 *cis* 4.13, 3.94 *trans*	182.2 *cis* 182.5 *trans* 182.5 (t, J(^{13}C-^{31}P) = 6.4 Hz *cis*	1617
(±)-**4.41**	dppe	4.75 (t, J = 7.6 Hz), 4.40 (dd, J = 8.8 Hz, 6.0 Hz) *cis* 4.78 (t, J = 7.0 Hz, 4.53 (t, J = 7.0 Hz) *trans*	182.2 (t, J(^{13}C-^{31}P) = 6.4 Hz *trans*	1607
(±)-**4.42**	bipy	4.71, 4.66 *cis* 4.65, 4.63 *trans*	181.9 *cis* 182.5 *trans*	1616

Finally, we have been able to obtain X-ray crystal structures for all three *cis* diastereomers of complexes (±)-**4.40**, (±)-**4.41**, and (±)-**4.42**, bearing TMEDA, dppe, and bipy ligands respectively (see section 4.4). A 75 : 25 *cis* : *trans* mixture of (±)-**4.40** bearing the TMEDA resulting from a poor choice of elution system (low gradient of ethyl acetate in hexanes) for column chromatography was crystallized via slow diffusion of pentane into a solution of (±)-**4.40** in benzene. While performing the X-ray analyses, Dr. Victor Day observed that the crystals had crystallized in two

distinct polymorphic shapes. The major *cis* diastereomer crystallized as rectangular parallelepipeds, and the minor *trans* diastereomer crystallized as triangular plates. In this case, the diastereomers manifested their differing physical properties by crystallizing as noticeably different polymorphs, allowing us to assign the signals for the *cis* diastereomers by taking crystals of the major *cis*-(±)-**4.40** and performing ^{1}H NMR spectroscopy upon them. We also attempted to obtain ^{1}H NMR of the minor *trans* diastereomer, but were unable to separate enough crystalline material. In addition, we were eventually able to isolate a highly enriched sample of the *cis* diastereomer of complex (±)-**4.40** by observing that during rotary evaporation of the ethyl acetate eluent from column chromatography, a solid precipitated near the end of solvent removal. This solid was isolated and found to also be a highly enriched sample of the *cis* diastereomer by ^{1}H NMR. A comparison of the signals in the ^{1}H NMR spectrum of the separated *cis* diastereomer from the crystallization, the isolated *cis* diastereomer from chromatography, and a mixture of diastereomers are shown in Figure 4.4.

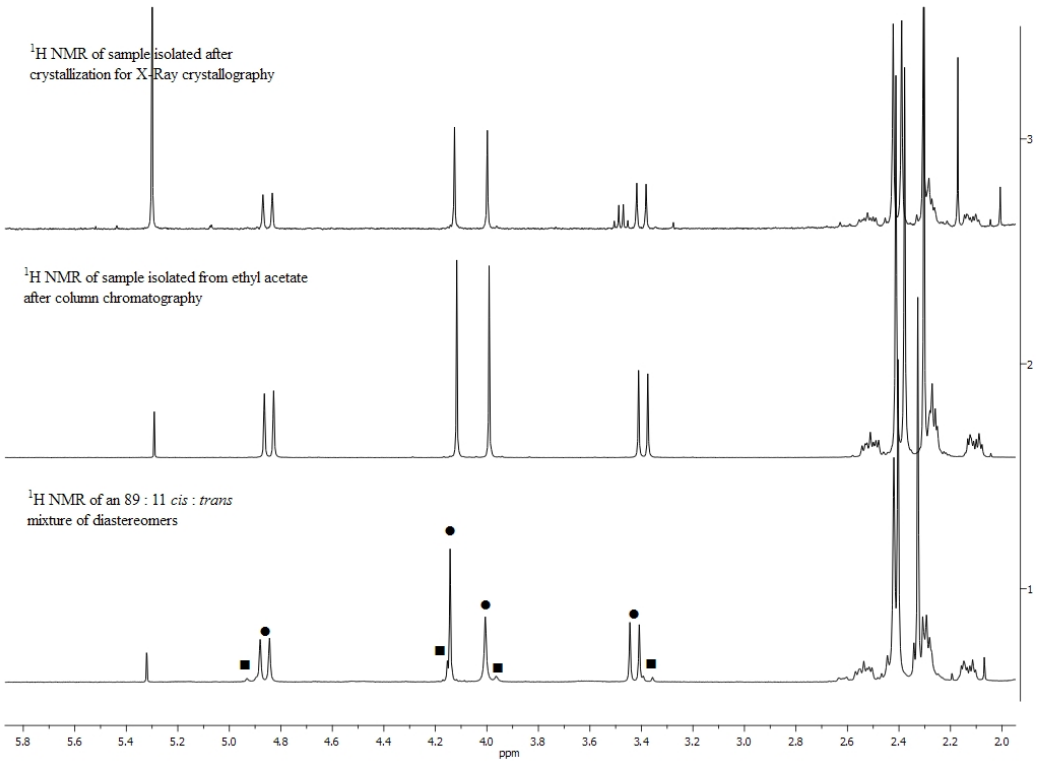

● - signals for *cis* diastereomer ■ - signals for *trans* diastereomer

Figure 4.4. *Comparison of ^{1}H NMR Spectra of Highly Enriched Samples of cis-*(±)-***4.40*** *vs. an Isolated Mixture of cis and trans-*(±)-***4.40.***

Notably, when ^{31}P NMR spectra were obtained at room temperature on complex (±)-**4.41** bearing the dppe ligand, the expected doublet of doublets for each diastereomer due to the *cis* arrangement of inequivalent phosphorus atoms of the dppe ligand was not observed. Instead, two sets of broad signals were observed (34.8 and 32.7 ppm for the *cis* isomer, and 39.5 and 35.9 ppm for the *trans* diastereomer). We also performed a low temperature ^{31}P NMR experiment at -70°C on complex (±)-**4.41** in $CDCl_3$. However, no sharpening of the signals were seen at this temperature (Figure 4.5).

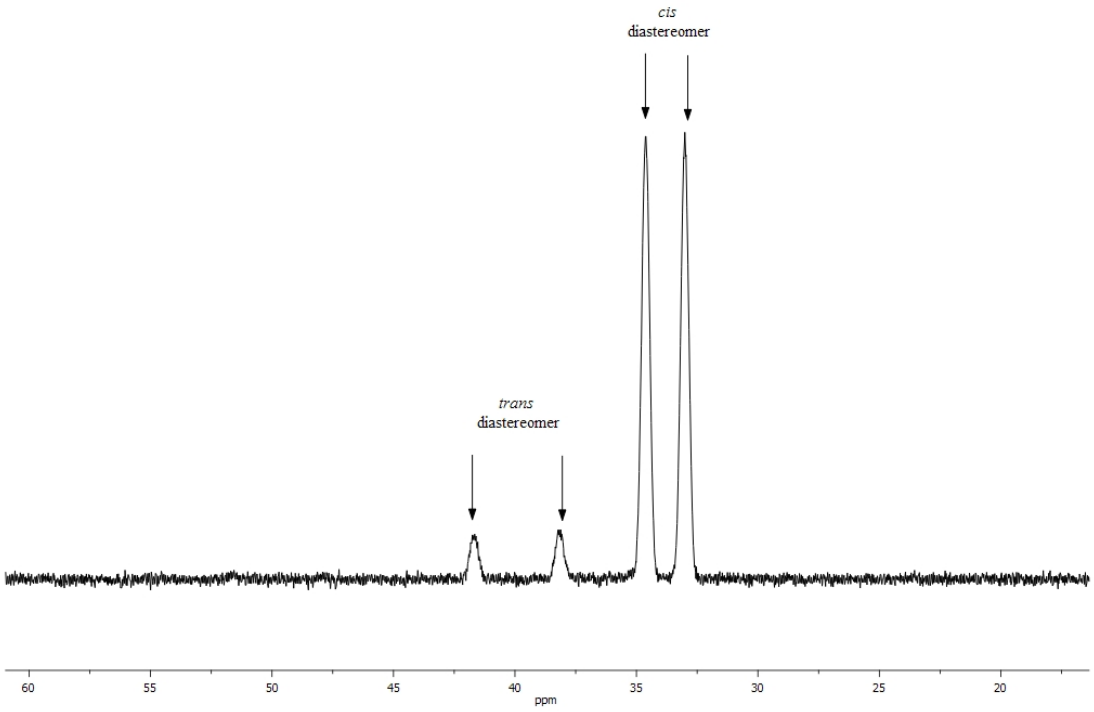

Figure 4.5. *^{31}P NMR (162 MHz, $CDCl_3$, -70°C) Spectrum of an 87 : 13 cis : trans Mixture of Complex (±)-**4.41.***

Previous work from our group has shown that steric hindrance arising from a fully substituted sp^3-hybridized carbon stereocenter also leads to broadened ^{31}P NMR signals.[163] In this work, the combined steric hindrance of two tertiary sp^3-hybridized carbon stereocenters attached to palladium contributes to the observed broadening of signals.

We assigned *cis* and *trans* signals for **4.41** bearing the dppe ligand, and **4.42** bearing the bipy ligand via ligand exchange with an excess of the appropriate ligand

(Scheme 4.17). Our group has reported previously that the Csp^3-Pd centers are configurationally stable under similar conditions.[162]

Scheme 4.17

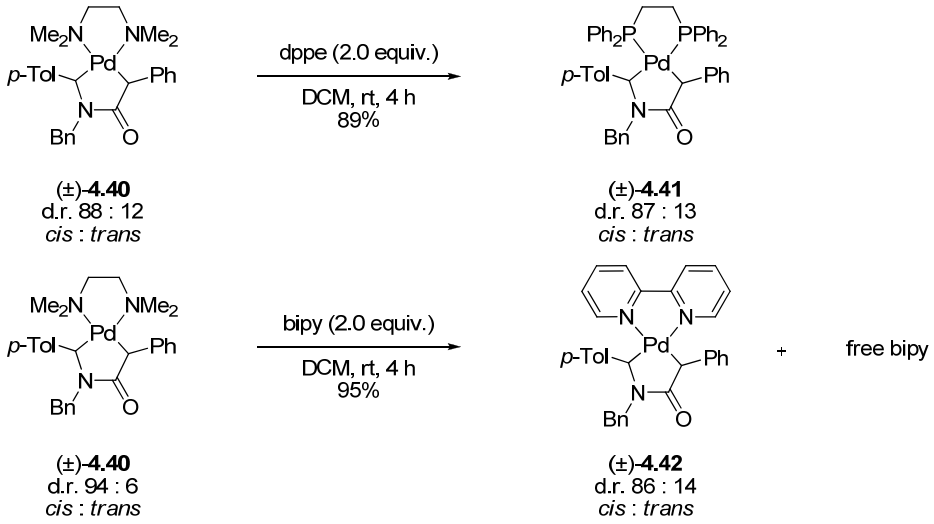

Both reactions occurred in high yield and stereochemical fidelity, with little change in the diastereomeric ratios from the starting materials to products in either case. Keeping in mind that the major signals of complex (±)-**4.40** are the cis diastereomers, and that the centers are configurationally stable, it is logical to conclude that the major signals in the samples of (±)-**4.41** and (±)-**4.42** shown in Scheme 4.17 are also of the *cis* isomer. In the case of the bipyridine ligand, the ligand was difficult to separate from the product, resulting in residual amounts of the bipy in the product. We also explored the effect of the concentration of the enolate on both the reaction yield and the dr. In addition to the aforementioned *t*-BuOK base, we also explored the likely *stoichiometric* generation of the enolates using the stronger bases KHMDS and LDA (Table 4.4).

Table 4.4. *Effect of Base on the dr of Ring Closure Reactions in THF in the Synthesis of Complexes (±)-**4.40** – (±)-**4.42***

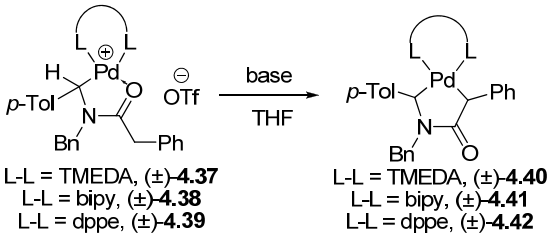

	Cationic Complex	Auxiliary Ligand	Base (equiv.)	Product	Yield	dr (*cis* : *trans*)
1	**4.37**	TMEDA	*t*-BuOK (1.1)	(±)-**4.40**	82 [a]	88 : 12
2	**4.37**	TMEDA	*t*-BuOK (1.1)	(±)-**4.40**	67 [b]	94 : 6
3	**4.37**	TMEDA	KHMDS (1.0)	(±)-**4.40**	35 [b]	95 : 5
4	**4.37**	TMEDA	LDA (1.0)	(±)-**4.40**	25 [c]	88 : 12
5	**4.39**	dppe	*t*-BuOK (1.1)	(±)-**4.41**	90 [a]	72 : 28
6	**4.39**	dppe	*t*-BuOK (1.1)	(±)-**4.41**	89 [b]	74 : 26
7	**4.39**	dppe	KHMDS (1.0)	(±)-**4.41**	86 [b]	76 : 24
8	**4.39**	dppe	LDA (1.0)	(±)-**4.41**	86 [c]	77 : 23
9	**4.38**	bipy	*t*-BuOK (1.1)	(±)-**4.42**	86 [a]	42 : 58
10	**4.38**	bipy	*t*-BuOK (1.1)	(±)-**4.42**	83 [b]	75 : 25
11	**4.38**	bipy	KHMDS (1.0)	(±)-**4.42**	71 [b]	57 : 43
12	**4.38**	bipy	LDA (1.0)	(±)-**4.42**	64 [c]	83 : 17

[a] reaction run at 45°C for 30 min. [b] reaction run at room temperature for 5 h
[c] reaction run at -78°C for 1 h followed by warming to rt and stirring for 4 h

Entries 1 – 4 of Table 4.4 show that the yields of complex (±)-**4.40** bearing the TMEDA ligand decrease dramatically with the increase in the strength of the base. This indicates that the complex or an intermediate is unstable when a strong base is used. Entries 5 – 8 show that the yields and diastereomeric ratios of complex (±)-**4.41** with the dppe ligand are practically invariable with the changes in reaction conditions. Conversely, entries 9 - 12 show that the yields and diastereomeric ratios of complex (±)-**4.42** bearing the bipyridyl ligand vary significantly based on the reaction conditions. This is likely due to the difference in the bipyridine ligand vs. the TMEDA/dppe ligands. The flat bipyridyl ligand removes much steric hindrance, likely lowering the difference in transition state energies.

4.3 Configurational Stability of Palladapyrrolidinones

As control of stereochemistry is quite useful in modern synthetic organic chemistry,[188] a study of the configurational stability of the stereocenter located adjacent to the carbonyl moiety of the amide group was undertaken. Our group has previously shown that the stereocenter adjacent to an *exocyclic* ester could be quite labile when a chiral non-racemic ligand was present on the palladium center, giving rise to moderate to high diastereomeric excess under proper conditions.[131] In our case, it was unknown i) whether the stereocenter could be epimerized and ii) whether the *cis* or the *trans* diastereomers were more stable for each palladapyrrolidinone. We examined two distinct types of stability: stability under thermal conditions and stability under basic conditions.

4.3.1 Configurational Stability under Basic Conditions

As palladium catalyzed reactions such as the Buchwald-Hartwig amination, the Heck reaction, and the Sonogashira reaction often involve the use of a base, we thought it is prudent to explore the stability of the palladapyrrolidinones under basic conditions. Interestingly, 1.1 equivalents of base was needed to achieve epimerization during the selected reaction times for complex (±)-**4.40** bearing the TMEDA ligand, in line with previous reports.[162] We think it is likely that small amounts of complex **4.44** are generated and subsequently reprotonated with the *t*-BuOH produced from the deprotonation. Therefore, we used 1.1 equivalents of base for the experiments with (±)-**4.41** bearing the dppe ligand, and (±)-**4.42** bearing the bipy ligand, as shown in Table 4.5.

Table 4.5. *Results of Base-mediated Epimerization of Complexes* (±)-***4.40****,* (±)-***4.41*** *and* (±)-***4.42*** *at Room Temperature*

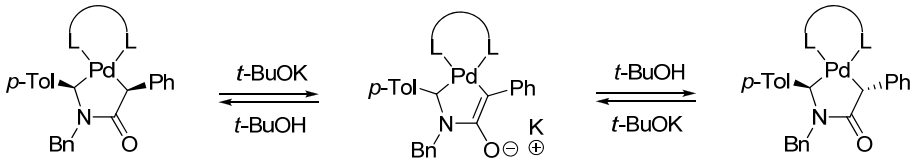

4.44

L-L = TMEDA, bipy, dppe

	Complex	Auxiliary Ligand	Initial dr (*cis* : *trans*)	Solvent, Time (min)	Base (equiv.)[a]	Yield of Recovered Material (%)	dr of recovered material (*cis* : *trans*)
1	(±)-**4.40**	TMEDA	90 : 10	THF, 60	*t*-BuOK, 0.1	83	94 : 6

2	(±)-**4.40**	TMEDA	90 : 10	THF, 60	*t*-BuOK, 0.5	82	93 : 7
3	(±)-**4.40**	TMEDA	90 : 10	THF, 5[b]	*t*-BuOK, 1.1	83	88 : 12
4	(±)-**4.40**	TMEDA	90 : 10	THF, 30[b]	*t*-BuOK, 1.1	82	78 : 22
5	(±)-**4.41**	dppe	87 : 13	THF, 60	*t*-BuOK, 1.1	91	42 : 58
6	(±)-**4.41**	dppe	87 : 13	THF, 180	*t*-BuOK, 1.1	92	42 : 58
7	(±)-**4.42**	bipy	42 : 58	THF, 60	*t*-BuOK, 1.1	96	22 : 78
8	(±)-**4.42**	bipy	42 : 58	THF, 180	*t*-BuOK, 1.1	92	23 : 77

[a] 1.1 equivalents of base was needed to achieve epimerization [b] due to the instability of the complex under the epimerization conditions, shorter times were used

In all cases, a shift toward the *trans* diastereomers was seen under basic conditions, indicating that they are likely more stable than the *cis* diastereomers. While publishing a manuscript based in part on work in this chapter,[189] a reviewer suggested that as the equilibrations required 1.1 equivalents of *t*-BuOK, the generation of intermediates such as **4.44** could occur stoichiometrically, and that protonation could occur upon workup instead of our proposed mechanism involving

low concentrations of the enolate intermediate (see Table 4.5). In order to address this question, we performed an *in situ* NMR experiment (monitoring by both ^{31}P and ^{1}H NMR) in an attempt to observe any significant quantities of intermediates such as **4.44**. The reaction was run at room temperature in THF-d_8 in an NMR tube with 1.1 equivalents of *t*-BuOK (1.0 M in THF) (Scheme 4.18).

Scheme 4.18

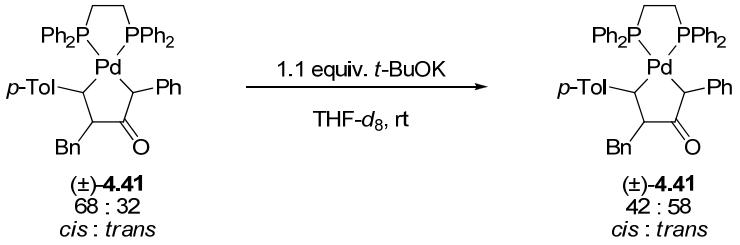

^{31}P NMR (162 MHz) spectra were taken before addition of *t*-BuOK, 30 minutes after addition of base, and 50 minutes after addition of base (Figure 4.6).

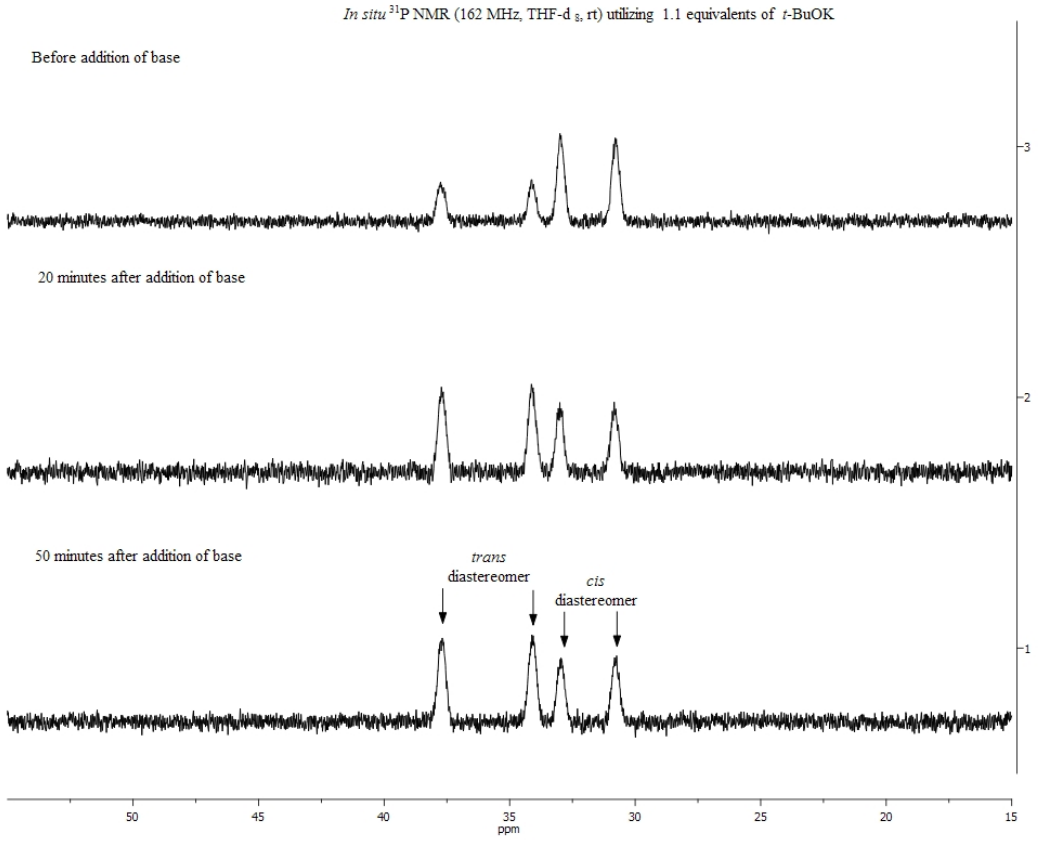

Figure 4.6. *In situ* ^{31}*P NMR (162 MHz) During the Reaction of (±)-**4.41** with 1.1 Equivalents of t-BuOK.*

^{1}H NMR (400 MHz) spectra were taken before addition of *t*-BuOK, 20 minutes after addition of base, and 60 minutes after addition of base (Figure 4.7).

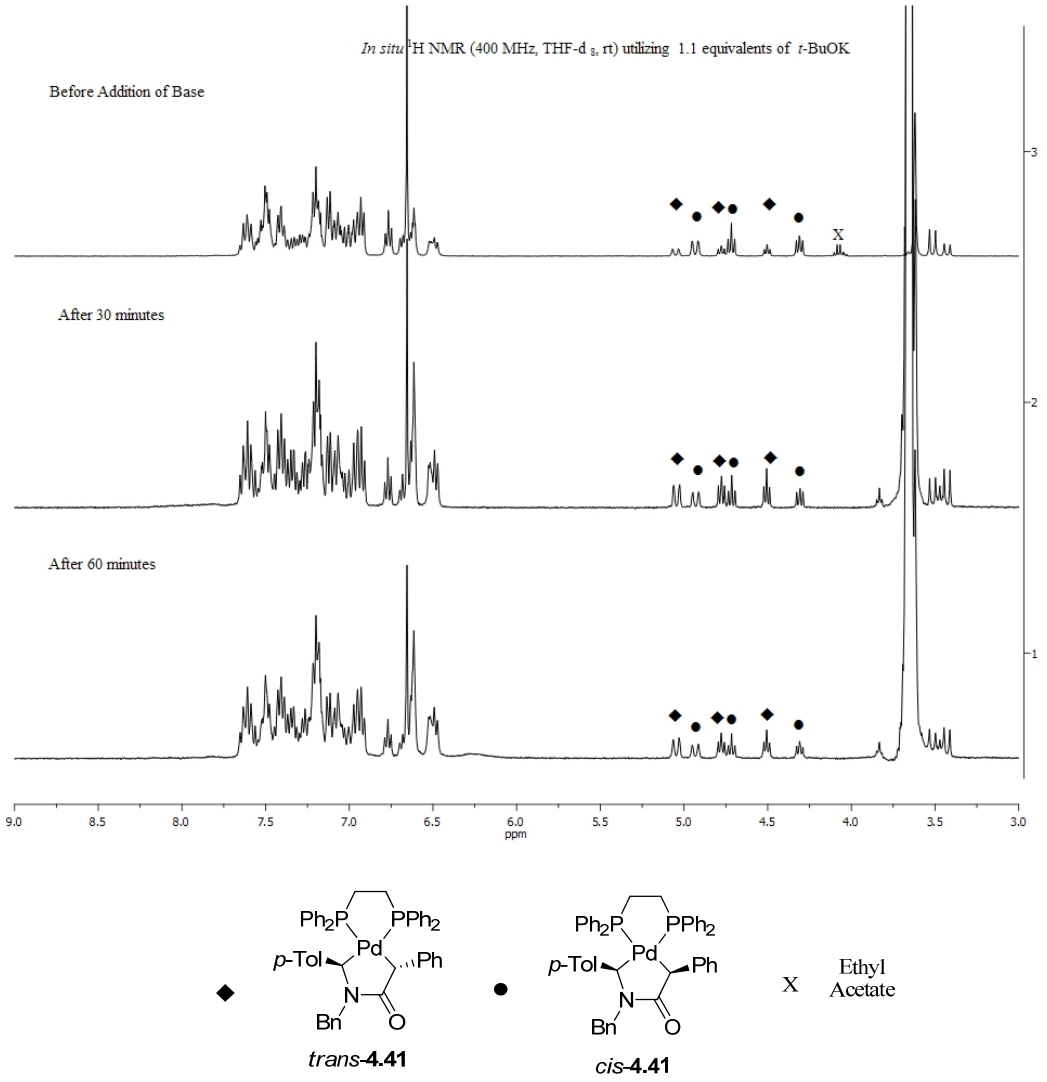

Figure 4.7 *In situ [1]H NMR (400 MHz) During the Reaction of (±)-**4.41** with 1.1 Equivalents of t-BuOK.*

No evidence in the NMR spectra (Figures 4.6 and 4.7) supports the proposal that a stoichiometric amount of the intermediate **4.44** was generated during the reaction before being quenched during workup. The data are consistent with our earlier proposal of the reaction proceeding through low concentrations of intermediate **4.44** when *t*-BuOK is used as the base.

4.3.2 Configurational Stability under Thermal Conditions

We reasoned that heating the diastereomeric mixtures of (±)-**4.40**, (±)-**4.41**, and (±)-**4.42** in a solvent such as THF would generate a small but significant equilibrium may between the O and C-Pd forms of the enolate which would allow for epimerization of the center via sp^2-hybridized intermediate **4.43**. We also wanted to see whether epimerization occurred under conditions similar to those used in the elevated temperature ring closing reactions (entries 1, 5, and 9, Table 4.4). We therefore heated solutions of complexes (±)-**4.40** – (±)-**4.42** in THF at 45°C for 3 hours before recovering the material. Table 4.6 shows the results of the experiments.

Table 4.6. *Thermal Isomerization of Complexes* (±)-***4.40,*** (±)-***4.41, and*** (±)-***4.42***[a]

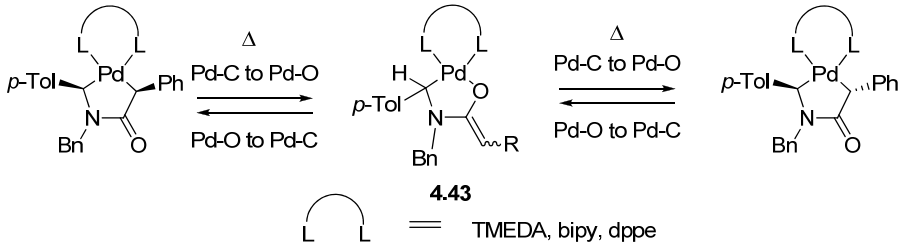

	Palladium Complex	Auxiliary Ligand	dr of starting material (*cis* : *trans*)	Solvent, Temperature (°C)	Recovery Yield (%)	dr of recovered material (*cis* : *trans*)
1	(±)-**4.40**	TMEDA	88 : 12	THF, 45	92	88 : 12
2	(±)-**4.41**	dppe	91 : 9	THF, 45	90	83 : 17
3	(±)-**4.42**	bipy	63 : 37	THF, 45	96	50 : 50

[a] all reactions run for 3 hours.

The TMEDA ligand (entry 1) appears unable to form proposed intermediate **4.43** as the material is returned in an unchanged dr of 88 : 12 *cis* : *trans*. For both the dppe and bipy ligands (entries 2 and 3), there is a noticeable change in the dr as measured by ^{1}H NMR spectroscopy. In these cases, the dppe and bipy ligands are likely better able to accommodate the proposed intermediate (±)-**4.43** with the more ionic Pd-O bond.

4.4 X-Ray Structural Studies

As the synthesized palladapyrrolidinones are the first examples of their class, it is prudent to study the metrical parameters of the complexes in more detail in order to gain more insight into the observed initial preference for the *cis* diastereomers and the slight preference for the *trans* diastereomers when allowed to equilibrate.

4.4.1 X-Ray Crystallographic Studies of (±)-4.40, (±)-4.41, and (±)-4.42

As mentioned previously, we were able to obtain X-Ray structures for complexes *cis*-(±)-**4.40**, *trans*-(±)-**4.40**, *cis*-(±)-**4.41**, and *cis*-(±)-**4.42**. The ORTEP plots are shown in Figures **4.8** – **4.11**.

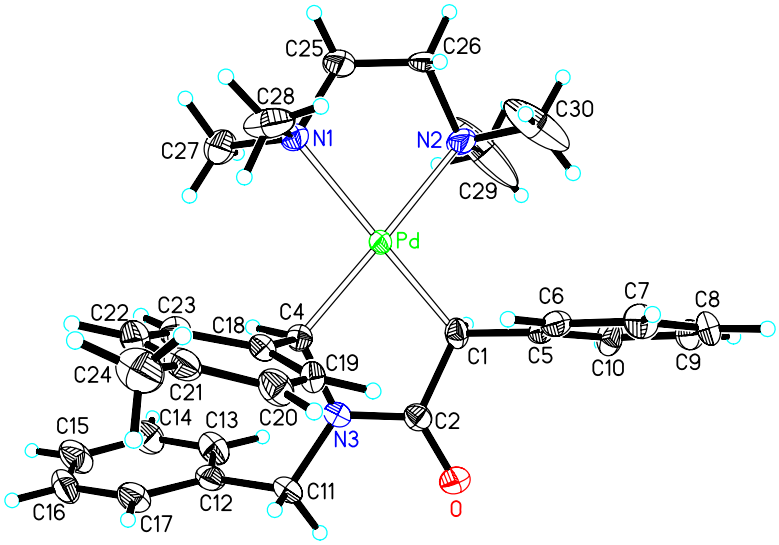

Figure 4.8. *ORTEP plot of cis-(±)-**4.40**. Ellipsoids are Drawn at the 50% Probability Level.*

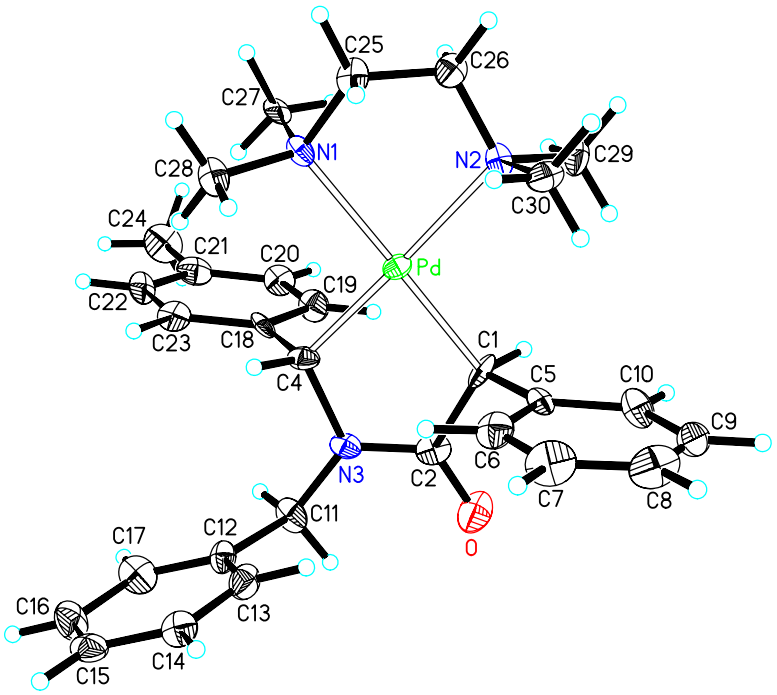

Figure 4.9. *ORTEP plot of trans-(±)-***4.40***. Ellipsoids are Drawn at the 50% Probability Level.*

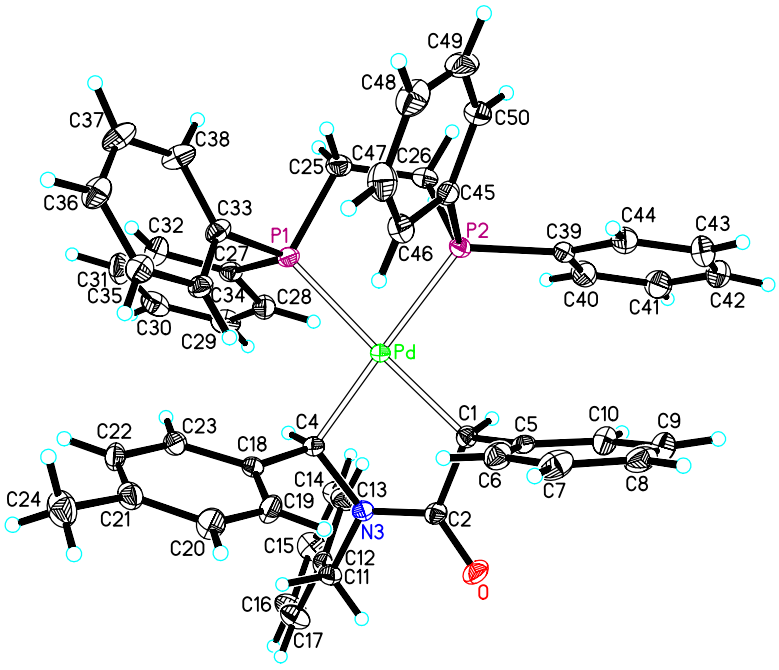

Figure 4.10. *ORTEP plot of cis-(±)-**4.41**. Ellipsoids are Drawn at the 50% Probability Level.*

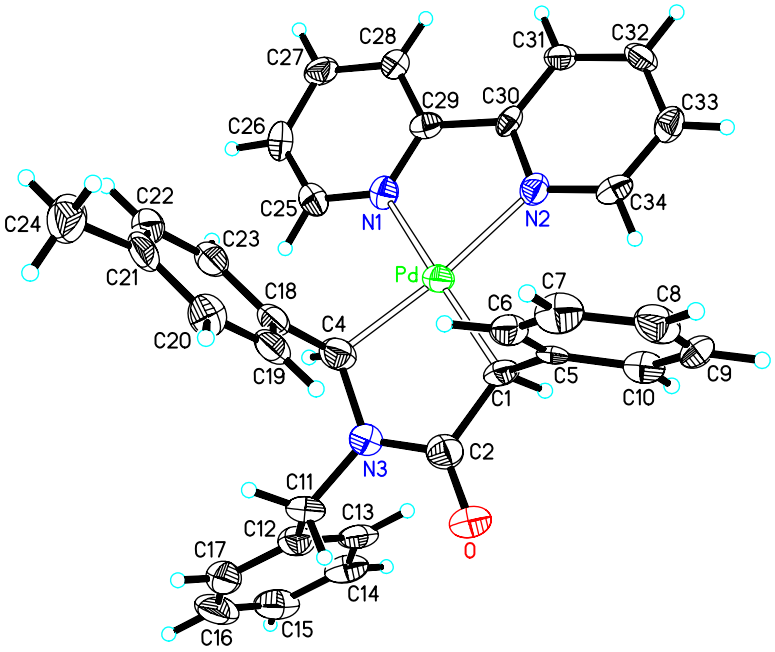

Figure 4.11. *ORTEP plot of cis-(±)-**4.42**. Ellipsoids are Drawn at the 50% Probability Level.*

Study of the metrical parameters revealed the only significant differences in the parameters for the metallacycles of *cis* (±)-**4.40** and *cis* (±)-**4.41** involve the bonds to the metal (vide infra). The Pd−C(1) bond lengths (2.040(4) Å in *cis* (±)-**4.40** and 2.082(2) Å in *cis* (±)-**4.41**) in both complexes are slightly shorter than the Pd−C(4) bond lengths (2.048(3) Å in *cis* (±)-**4.40** and 2.096(2) Å in *cis* (±)-**4.41**). Additionally, both Pd−C bonds in *cis* (±)-**4.40** are shorter than either Pd−C bond in *cis* (±)-**4.41**, presumably due to the greater *trans* influence of phosphines over amines. Notably, the conformations of the five-atom square planar coordination grouping and pyrrolidinone ligands in *cis* (±)-**4.40** and *cis* (±)-**4.41** are remarkably similar, causing

the 21 nonhydrogen atoms of the two complexes to superimpose with a root-mean-square (rms) deviation of 0.17 Å. Each of the five-atom square-planar coordination groupings, as well as each of the five nonhydrogen atom groupings (Pd, O, C(1), C(2), N(3) and C(4)) in both *cis* (±)-**4.40** and *cis* (±)-**4.41** palladacycles, are coplanar to within 0.05 Å.

4.4.2 A Steric Footprint

Interestingly, a distinct folding, defined by the dihedral angle (α) between the normals to the mean planes of the five-atom square planar coordination groupings (plane labeled **a** in Figure 4.12) and the actual six-atom **L···L** mean plane groupings containing the two heteroatoms and their four methyl or phenyl carbons (plane labeled **b** in Figure 4.12), was observed in the solid state structures of complexes *cis* (±)-**4.40** and *cis* (±)-**4.41**.

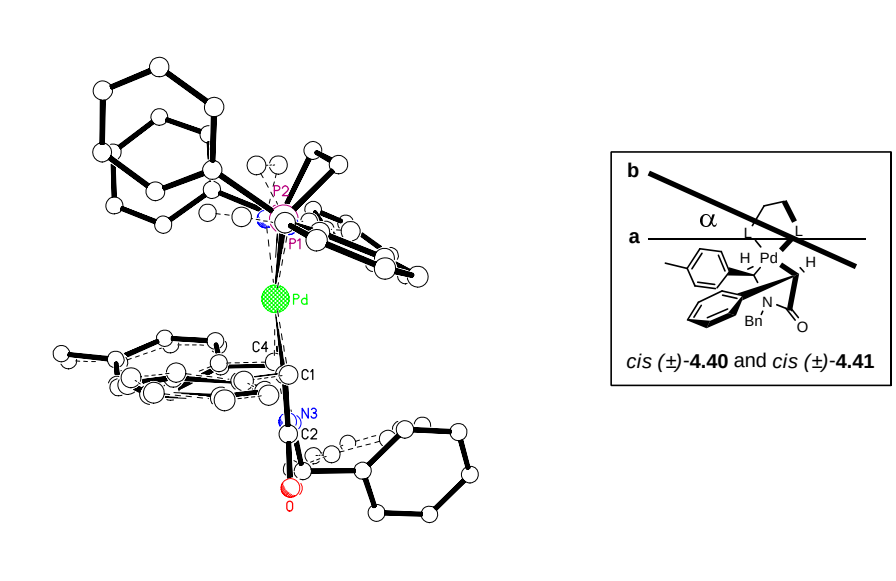

Figure 4.12. *Superimposed Molecular Structures of cis (±)-**4.40** and cis (±)-**4.41** Based on X-ray Crystallographic Data. Hydrogen Atoms are Omitted for Clarity.*

Thus, the pyrrolidinone ligands "fold" by 6° or 9° along the C(1)···C(4) polyhedral edge, and the TMEDA and dppe (**L···L**) ligands "fold" by 13° or 25° along their respective N(1)···N(2) and P(1)···P(2) polyhedral edges away from the pyrrolidinone ligands. As expected, both "fold" angles are larger for the complex *cis* (±)-**4.41**. Experiments reported in Table 4.4 showed that, in the presence of both TMEDA and dppe auxiliary ligands, the formation of the *cis* diastereomer of palladacycles (±)-**4.40** and (±)-**4.41** from palladium-chelated amide complexes (±)-**4.37** bearing the TMEDA ligand and (±)-**4.38** bearing the dppe ligand was favored. Conceivably, this "folding" of the pyrrolidinone and the **L···L** ligands is sterically induced by nonbonding interactions between atoms in the secondary coordination sphere (Table 4.7), and, if preserved in the solution-phase structures, it may play a significant role in inducing the initial preference for the *cis*-isomers as the kinetically favored products (vide infra).

Table 4.7. *Selected Non-bonded Interactions in Palladapyrrolidinones (±)-**4.40** – (±)-**4.42***

Complex	(±)-**4.40**	(±)-**4.40**	(±)-**4.41**	(±)-**4.42**
L-L	TMEDA	TMEDA	dppe	bipy
isomer	*trans*	*cis*	*cis*	*cis*
Contact	Distance (Å)			
H11B···O	2.36	2.39	2.35	2.37
H11A···C18	2.60	2.73	2.71	2.72
H4···C12	2.89	2.66	2.95	3.02
O···C11	2.793	2.787	2.771	2.772
O···C5	2.997	2.926	2.901	2.925
H27B···C18	2.71	2.70[a]		
H27B···C23	2.79	2.62[a]		
H25···H4				2.24
H34···C10				2.66
H6···H19				2.19
H6···C19				2.70

[a]Contact is H28c···C18 and H28c···C23, respectively

The data in Table 4.7 suggest that each of the observed solid-state structures shown in Figures 4.8 – 4.11 contains non-bonded contacts between the **L···L** and pyrrolidinone ligands, defined by distances between the atoms that are significantly

shorter than the van der Waals radii[190] (H···H, 2.40 Å, H···O, 2.60 Å, O···C, 3.10 Å, and H···C, 2.90 Å). These contacts indicate a common conformation for the pyrrolidinone ligand near carbon C(4) when it is coordinated to two adjacent square-planar coordination sites on the palladium center. They are also consistent with a unique 'steric footprint' for the benzyl substituent in these systems. Thus, the benzyl substituent likely has little freedom of rotation about the N(3)-C(11) and/or C(11)-C(12) bonds.

The planar nature of the palladapyrrolidinone ring contributes to the rigidity of the structures and thus the small difference in energies between the *cis* and *trans* diastereomers, as evidenced by equilibration experiments summarized in Tables 4.5 and 4.6. The X-ray structures for the *cis* (±)-**4.42** as well as the *trans* (±)-**4.40** palladacycle (Figures 4.9 and 4.11) do not show the folding phenomenon. For *trans* (±)-**4.40** bearing the TMEDA ligand, this likely reflects a slight decrease in steric interactions. For *cis* (±)-**4.42** bearing the bipy ligand, this lack of folding suggests that a possible reason for the greater sensitivity to the reaction conditions as well as slightly higher energy difference between *cis* and *trans* diastereomers for (±)-**4.42** vs. (±)-**4.41** is due to the steric bulk of the bipy ligand being further away from the stereocenters.

4.5 The Effect of Chiral Non-Racemic Ligands on Diastereoselectivity of Ring Closure in the Synthesis of Palladapyrrolidinones

Having observed that the TMEDA and dppe ligands gave the *cis* isomer preferentially under the reaction conditions (1.1 equiv. *t*-BuOK, THF, 45°C, 30 min.)

we wished to further explore the role of the ligand in the system by utilizing a chiral non-racemic C_2-symmetric ligand to influence formation of the second stereocenter.

We wished to explore the influence of a chiral non-racemic ligand on both the selectivity of the Pd-C bond formation after deprotonation as well as equilibration. We chose (*S*,*S*)-CHIRAPHOS initially because we believed it would likely give a tight 5-member chelate ring with the palladium center and give the greatest chance for us to observe either a significant increase (matched pair) or a significant decrease (mismatched pair) in the diastereoselectivity in the formation of the second stereocenter.[131] We hypothesized that we could synthesize the complexes bearing the (*S*,*S*)-CHIRAPHOS in an analogous fashion to the reactions with dppe to form cationic complex (±)-**4.39** and palladapyrrolidinone (±)-**4.41**. This proved to be the case. Complex (±)-**4.37** was reacted with 2.0 equivalents of (*S*,*S*)-CHIRAPHOS in DCM at room temperature to afford a high yield of complex **4.45** as a yellow solid in 1 : 1 dr (Scheme 4.19).

Scheme 4.19

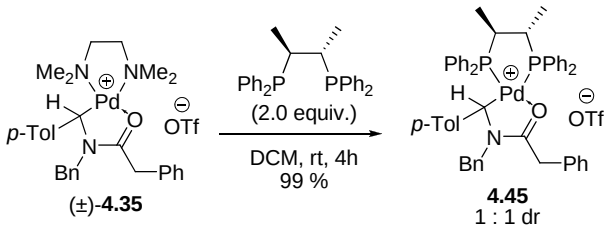

Complex **4.45** was then reacted in the same fashion as cationic complexes **4.37** – **4.39** (45°C, THF, 1.1 equiv. *t*-BuOK, 30 min.) to give a mixture of the four possible diastereomers **4.46a**, **4.46b**, **4.46c,** and **4.46d** in 91% combined yield (Scheme 4.20). Diastereomers **4.46a** and **4.46b** represent the "cis" diastereomers, while **4.46c** and

4.46d represent the "trans" diastereomers. The ratio of **4.46a** : **4.46b** : **4.46c** : **4.46d** was 5.9 : 7.3 : 2.0. 1.0 (spectrum B in Figure 4.13), and the *cis* (**4.46a** + **4.46b**) to *trans* (**4.46c** + **4.46d**) ratio was 81 : 19. Assignments of absolute configurations to particular isomers of **4.46** are completely arbitrary.

Scheme 4.20

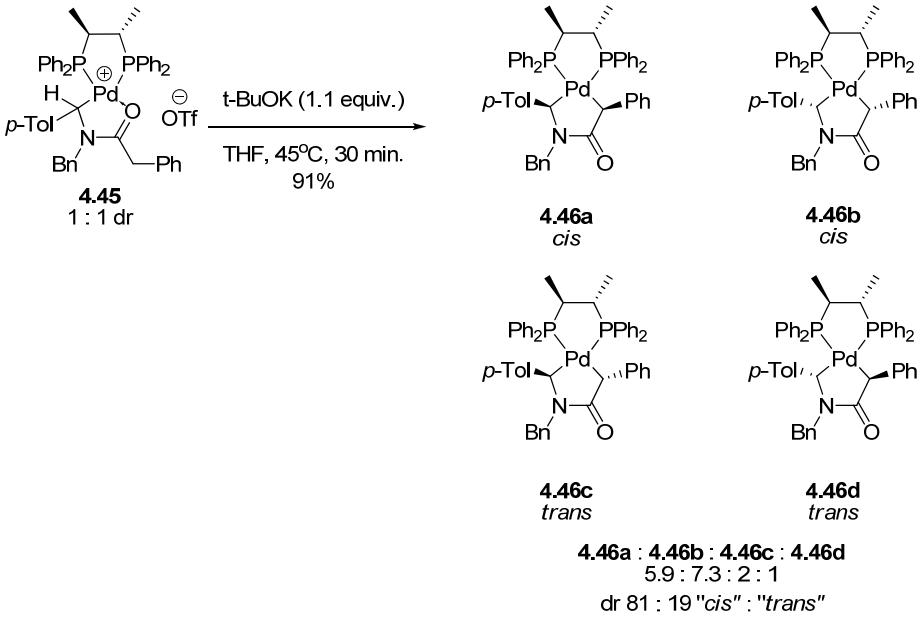

The ^{1}H NMR spectrum for this mixture of diastereomers was too complex to assign signals to the each diastereomer. However, the signals in the ^{31}P NMR spectrum were separated enough to assign signals to each diastereomer. In order to establish the ratios of the diastereomers of **4.46** in the reaction mixture, a standard sample with known ratios of diastereomers had to be prepared. Based on our earlier studies, we hypothesized that if we reacted a sample of (±)-**4.40** bearing the TMEDA ligand with a known diastereomeric ratio with (*S*,*S*)-CHIRAPHOS, we would be able to isolate a known ratio of diastereomers **4.46a** – **4.46d**. This was also successful. When we

reacted a 91 : 9 *cis* : *trans* mixture of (±)-**4.40** bearing the TMEDA ligand with 2.0 equivalents of (*S*,*S*)-CHIRAPHOS in DCM at room temperature we isolated an 83% yield of **4.46a - 4.46d** with a *cis* : *trans* ratio of 91 : 9 (Scheme 4.21). For the reaction described in Scheme 4.21, the major sets of signals in the ^{31}P NMR spectrum were assigned to the *cis* diastereomers of **4.46**, and the minor sets of signals to the *trans* diastereomers of **4.46**.

Scheme 4.21

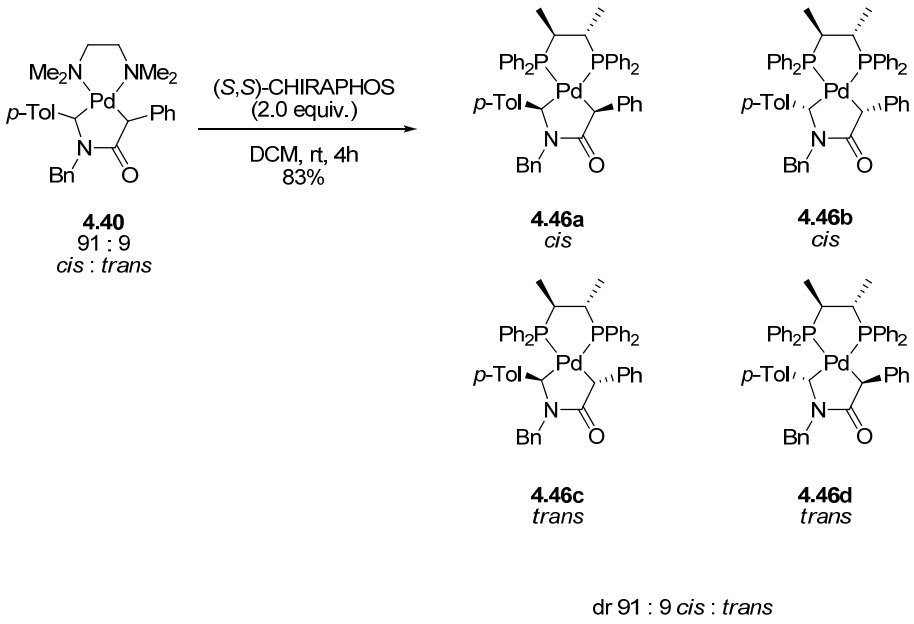

The ^{31}P NMR spectra of **4.46a – 4.46d** from the ring closure reaction (labeled **B** in Figure 4.13) in addition to the known mixture (labeled as **A** in Figure 4.13) are shown in Figure 4.13.

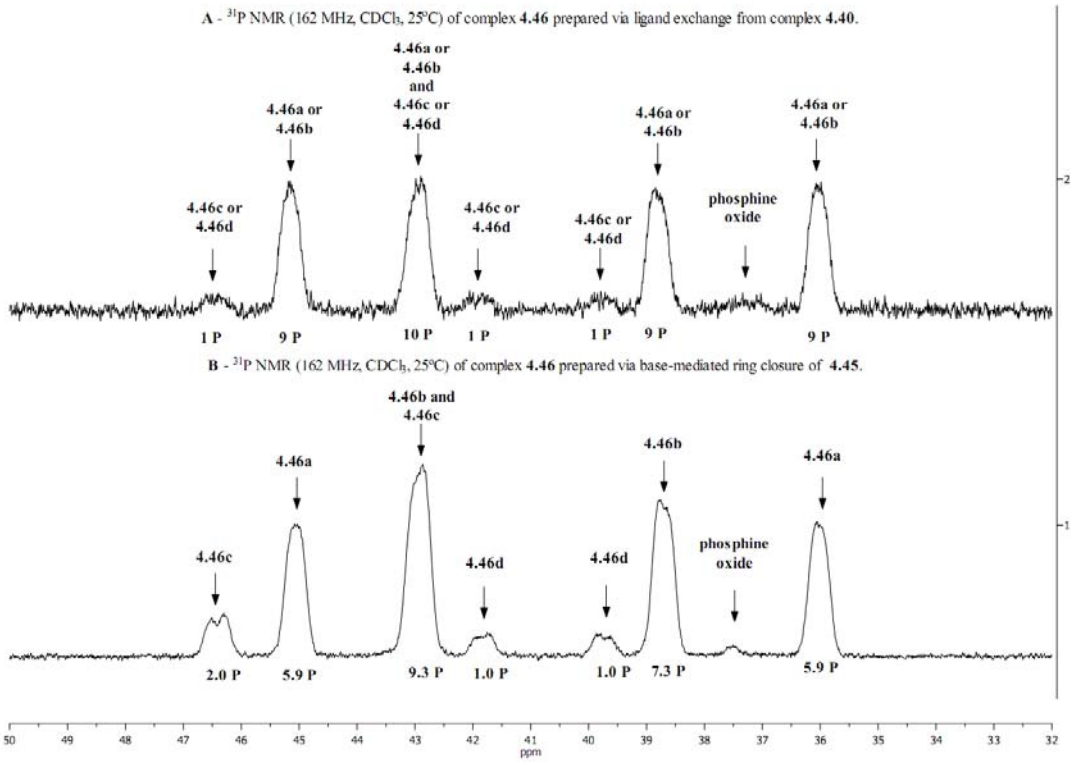

Figure 4.13. *^{31}P NMR (162 MHz) Spectra of* ***4.46a*** *–* ***4.46d*** *Formed via Ligand Exchange from Complex (±)-****4.40*** *(A) and That Formed From Ring Closure of* ***4.45*** *(B).*

As can be seen in Figure 4.13, spectrum B shows that the ring closure reaction generated the four diastereomers in different amounts, allowing for differentiation of signals for **4.46a** – **4.46d**, while spectrum A shows which sets of ^{31}P NMR signals correspond to the "cis" and "trans" diastereomers, **4.46a** and **4.46b** vs. **4.46c** and **4.46d**, respectively. It can also be seen that only two of the eight signals overlap, allowing for a clear differentiation of signals.

Reasoning that the additional stereocenters on the (*S*,*S*)-CHIRAPHOS ligand could rigidify the structure and allow for calculation of the coupling constants for the ^{31}P

signals, we subjected a 91 : 9 mixture of **4.46a** + **4.46b** : **4.46c** + **4.46d** to variable temperature ^{31}P NMR from -70°C to 80°C in toluene-d_8 (Figure 4.14). Unfortunately, no sharpening of the signals was observed at temperatures in this range.

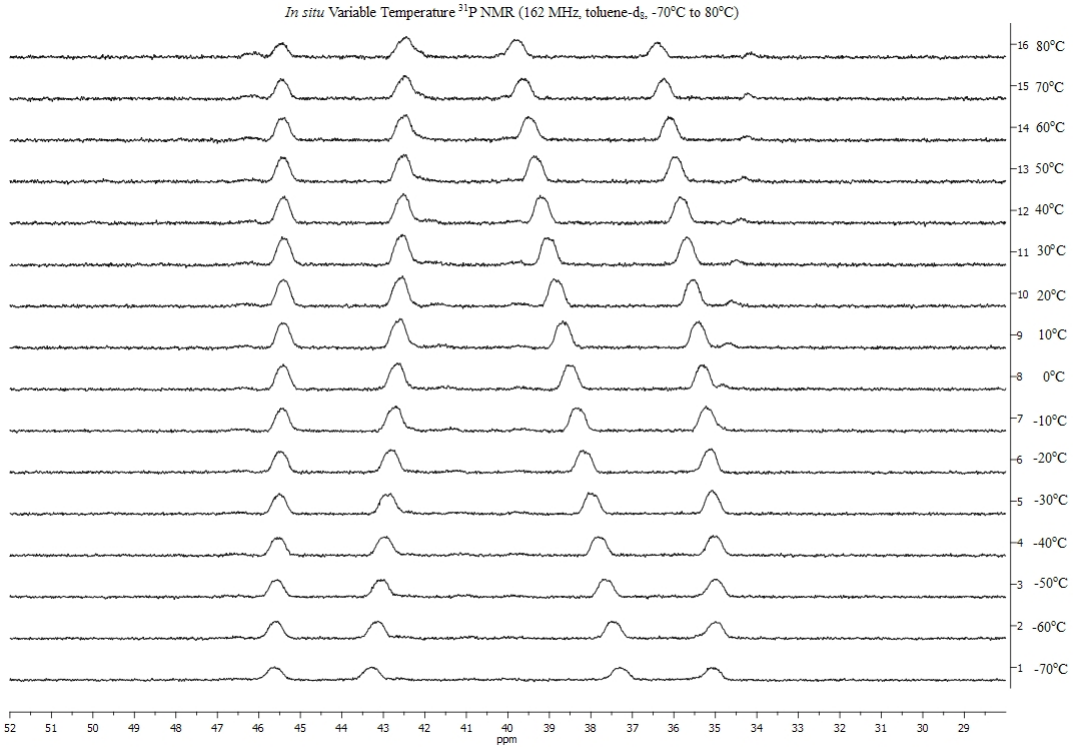

Figure 4.14 *^{31}P NMR (162 MHz) Spectra of Complex* ***4.46a – 4.46d*** *From -70°C to 80°C.*

Unfortunately, we were unable to obtain X-ray quality crystals of complex **4.46** and thus unable to precisely assign particular chemical shifts to absolute configurations. We also tested the stability of the relatively acidic stereocenter by subjecting a sample of **4.46** with dr of 81 : 19 "*cis* : *trans*" to 1.1 equivalents of *t*-BuOK in THF for 3 h at room temperature. A 75% yield of dr 57 : 43 "*cis* : *trans*" was recovered (Scheme 4.22), indicating that the *trans* diastereomers of **4.46** are the more stable products.

Scheme 4.22

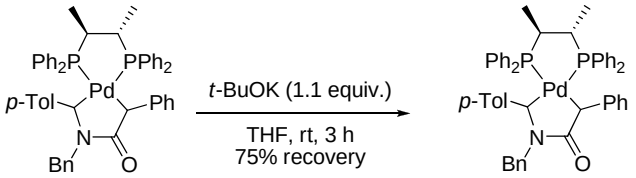

4.46
(*cis* (**4.46a** + **4.46b**)) : *trans* (**4.46c** + **4.46d**))
cis : *trans* 81 : 19

4.46
(*cis* (**4.46a** + **4.46b**)) : *trans* (**4.46c** + **4.46d**))
cis : *trans* 57 : 43

We also wished to isolate cationic complex **4.45** or palladapyrrolidinone **4.46** in an improved diastereomeric ratio to try to assign signals to particular stereoisomers. In order to accomplish this, we attempted kinetic resolutions involving complexes (±)-**4.37** and (±)-**4.40** However, when we reacted both (±)-**4.37** and a highly enriched sample of (±)-*cis*-**4.40** both bearing a TMEDA ligand with substoichiometric amounts of (*S*,*S*)-CHIRAPHOS at room temperature in DCM, we observed little to no selectivity in crude ^{1}H NMR spectra of the mixtures of diastereomers **4.46** and **4.45** (Figures 4.15 and 4.16).

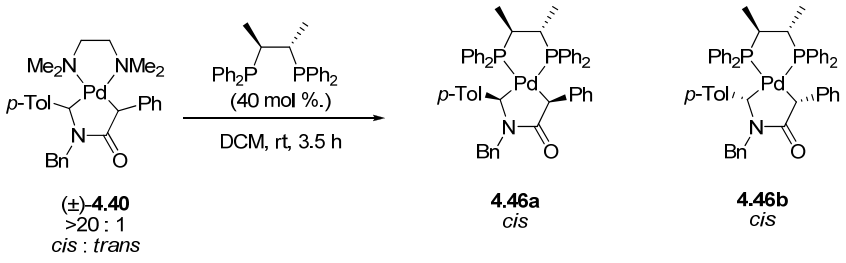

(±)-**4.40**
>20 : 1
cis : *trans*

4.46a
cis

4.46b
cis

(1 : 1 dr by ^{1}H NMR of crude mixture)

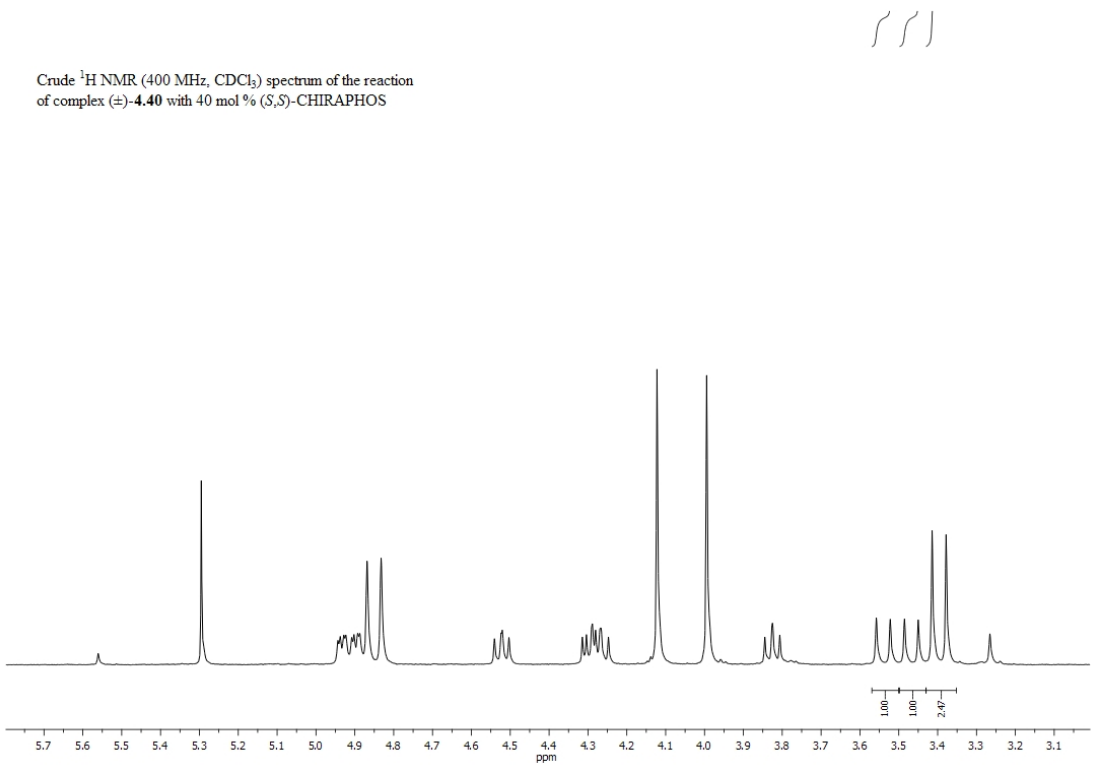

Figure 4.15. *^{1}H NMR Spectrum (400 MHz) of Crude Product After Reaction of Complex* ***4.40*** *with 40 mol % (S,S)-CHIRAPHOS.*

Integration of the signals for one of the benzylic protons in the *N*-benzyl group at 3.40 ppm (d, J = 14.5 Hz, 2 H) for the cis complex (±)-**4.40**, and the two signals for benzylic protons in the *N*-benzyl group at 3.54 ppm (d, J = 14.4 Hz, 1 H) and at 3.47 ppm (d, J = 14.2 Hz, 1 H) for the two diastereomers of the *cis* complexes **4.46a** and **4.46b** in the ^{1}H NMR spectra of the crude product isolated from the described experiment was used to establish the ratios of the unreacted complex (±)-**4.40** to the newly formed complexes **4.46a, 4.46b**, as well as the ratios of the two diastereomers **4.46a** : **4.46b**. The reaction with 40 mol% of (*S,S*)-CHIRAPHOS afforded the ratio **4.40** : **4.46a,b** = 55 : 45 and the ratio **4.46a** : **4.46b** = 1 : 1. The

experimental data (e.g. 55 : 45 ratio of **4.40** : **4.46a, 4.46b**) may reflect the limitation in the precision of the ^{1}H NMR technique.

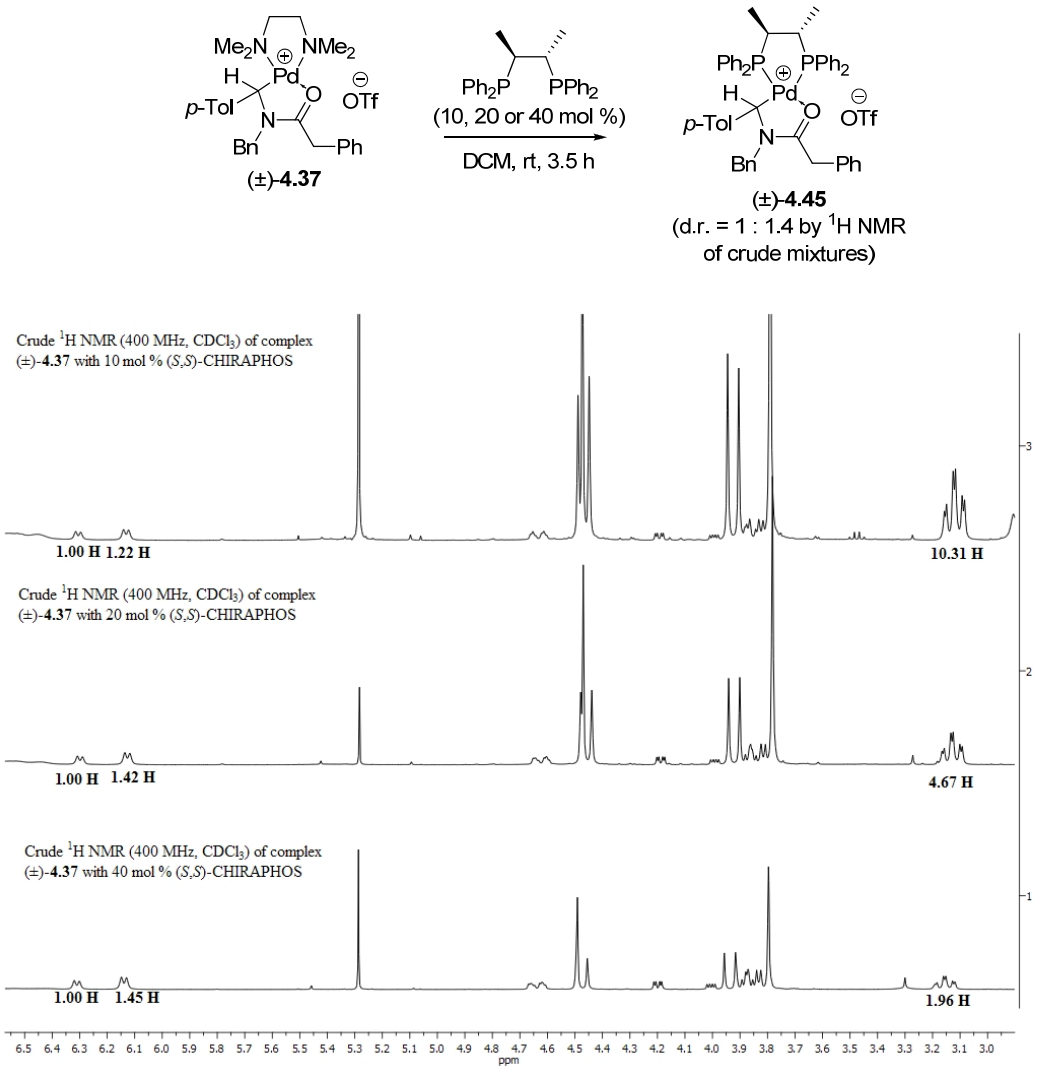

Figure 4.16. *^{1}H NMR (400 MHz) Spectrum of the Crude Product From Reaction of Complex* ***4.37*** *with 10, 20, and 40 mol % (S,S)-CHIRAPHOS.*

Integration of the ^{1}H NMR signals for a proton in the backbone of the TMEDA ligand at 3.16 ppm (td, J = 13.0 Hz, 3.5 Hz, 1.0 Hz, 1 H) of the racemic complex **4.37** and the signals for aromatic protons at 6.31 ppm (d br, J = 6.9 Hz, 2 H)

and 6.14 ppm (d br, J = 6.9 Hz, 2 H) in the two diastereomers of the complexes **4.45a** and **4.45b** respectively in the ^{1}H NMR spectra of the crude products isolated from these experiments was used to establish the ratios of the unreacted complex (±)-**4.37** to the newly formed complexes **4.45a, 4.45b**, as well as the ratios of the two diastereomers **4.45a** : **4.45b**. The ratios of (±)-**4.37** : **4.45a, 4.45b** indicated that a complete conversion of the (*S*,*S*)-CHIRAPHOS ligand to the complexes **4.45a** and **4.45b** occurred. The results are summarized in Table 4.8.

Table 4.8. *Results From ^{1}H NMR Analysis of Crude Products from the Reaction of Complex (±)-**4.37** with 10, 20, and 40 mol% (S,S)-CHIRAPHOS*

	mol% (*S*,*S*)-CHIRAPHOS	Integration of (±)-**4.37** (H)	Integration of **4.45a** (H)	Integration of **4.45b** (H)	(±)-**4.37** : (**4.45a** + **4.45b**)	**4.45a** : **4.45b**
1	10	10.31	1.00	1.22	90 : 10	55 : 45
2	20	4.67	1.00	1.42	79 : 21	58 : 42
3	40	1.96	1.00	1.45	62 : 38	58 : 42

Figures 4.15 and 4.16 indicate that little difference exists in the reaction rates of one enantiomer over the other in reactions of both palladapyrrolidinone (±)-**4.40** and its precursor (±)-**4.37**, both with a TMEDA ligand. We also screened the following ligands to ensure we had the best result with common chiral non-racemic ligands with C_2 symmetry: (*S*,*S*)-DIOP, (*S*)-BINAP, and (*S*,*S*)-BDPP. Before we could utilize a ligand for comparison, we needed to establish that the ligand could

exchange with the cationic complex to give the necessary precursor for ring closure. We also needed to ensure that the signals in the ^{31}P NMR spectra of the corresponding pyrrolidinones could be used for the calculation of the dr of the products as well as ensure a complete conversion of the ligand exchange of (±)-**4.40** bearing the TMEDA ligand with the chiral ligands to be able to assign ^{31}P NMR signals for the "*cis*" and "*trans*" diastereomers as done for **4.46**. Therefore, we ran two different types of experiments in NMR tubes. The first experiment was a ligand exchange reaction of cationic complex (±)-**4.37** bearing the TMEDA ligand with the desired chiral ligand in CD_2Cl_2 at room temperature. The second experiment was a ligand exchange of complex (±)-**4.40** with desired the chiral ligand in CD_2Cl_2 at room temperature. A successful result in the reactions of the chiral ligand with the cationic complex (±)-**4.37** would be a complete exchange of the chiral ligand for the TMEDA ligand, with no starting material present in the crude ^{1}H NMR spectrum. If the ligand does not completely exchange with TMEDA, then the new complex cannot be used as the starting material for cyclization because it would not necessarily be isolated as a 1 : 1 mixture of diastereomers. In the second case, a complete exchange with (±)-**4.40** is also necessary so that we may determine the dr via the ^{31}P NMR spectra in a procedure similar to that of complex **4.46**. Finally, the signals in the ^{31}P NMR spectrum must be separated enough to calculate the dr of the reactions.

Complex (±)-**4.37** and the desired chiral ligand were dissolved in CD_2Cl_2 and transferred to an NMR tube, and ^{1}H NMR spectra were recorded periodically. For the chiral ligands (*S*,*S*)-DIOP and (*S*,*S*)-BDPP, ^{1}H NMR spectra showing complete

conversion of the starting material to the corresponding phosphine complex were recorded after 3 hours. For the chiral ligand (*S*)-BINAP, the reaction was still incomplete after 24 h. The spectra are shown in Figure 4.17.

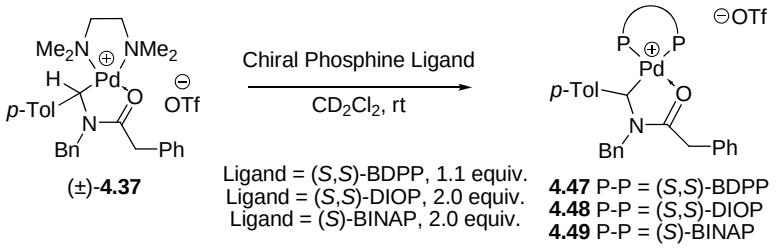

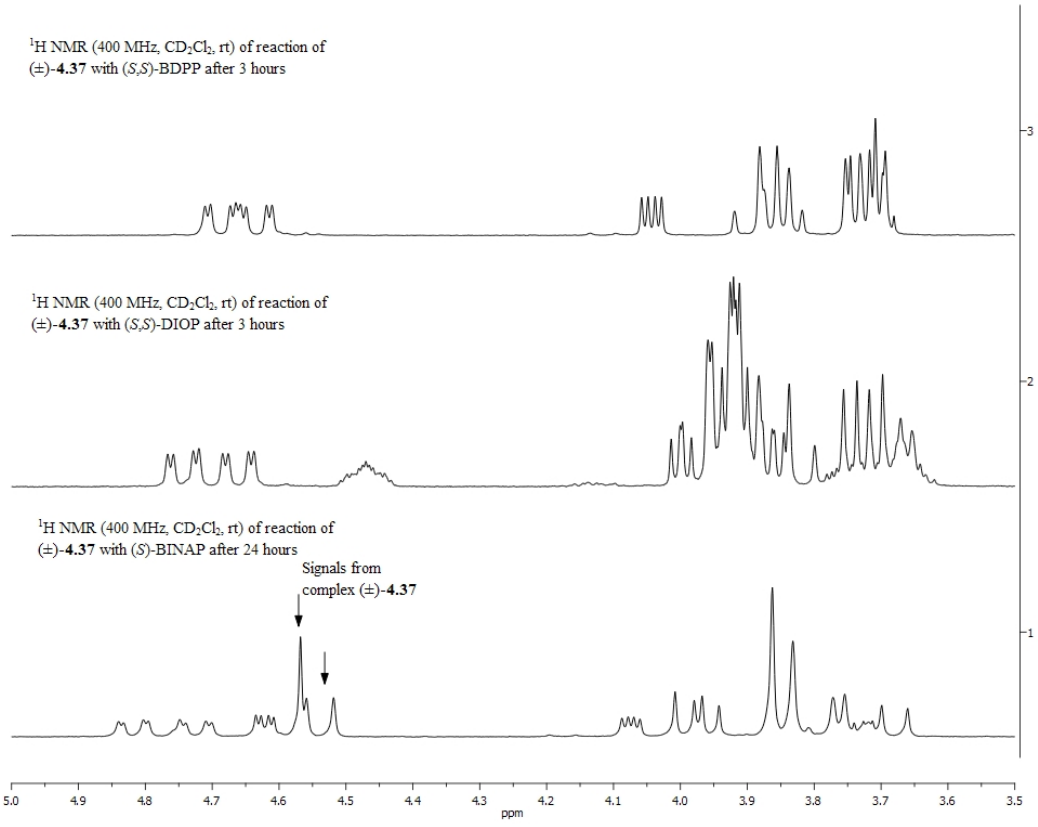

Figure 4.17. *In situ* ^{1}*H NMR (400 MHz) Recorded After Reactions of* ***4.37*** *with (S,S)-BDPP, (S,S)-DIOP, and (S)-BINAP to Generate* ***4.47***, ***4.48***, *and* ***4.49***, *Respectively.*

We also performed ligand exchange experiments with complex **4.40**. Complex **4.40** and the desired chiral ligand (2.0 equiv.) were dissolved in CD_2Cl_2 and transferred into an NMR tube. For **4.50** bearing the (*S*,*S*)-BDPP ligand and **4.51** bearing the (*S*,*S*)-DIOP ligand a ^1H NMR (400 MHz) spectrum indicating complete conversion was recorded after 3 hours. For **4.52** bearing the (*S*)-BINAP ligand, seven hours elapsed before ^1H NMR (400 MHz) showed complete conversion (Figure 4.18).

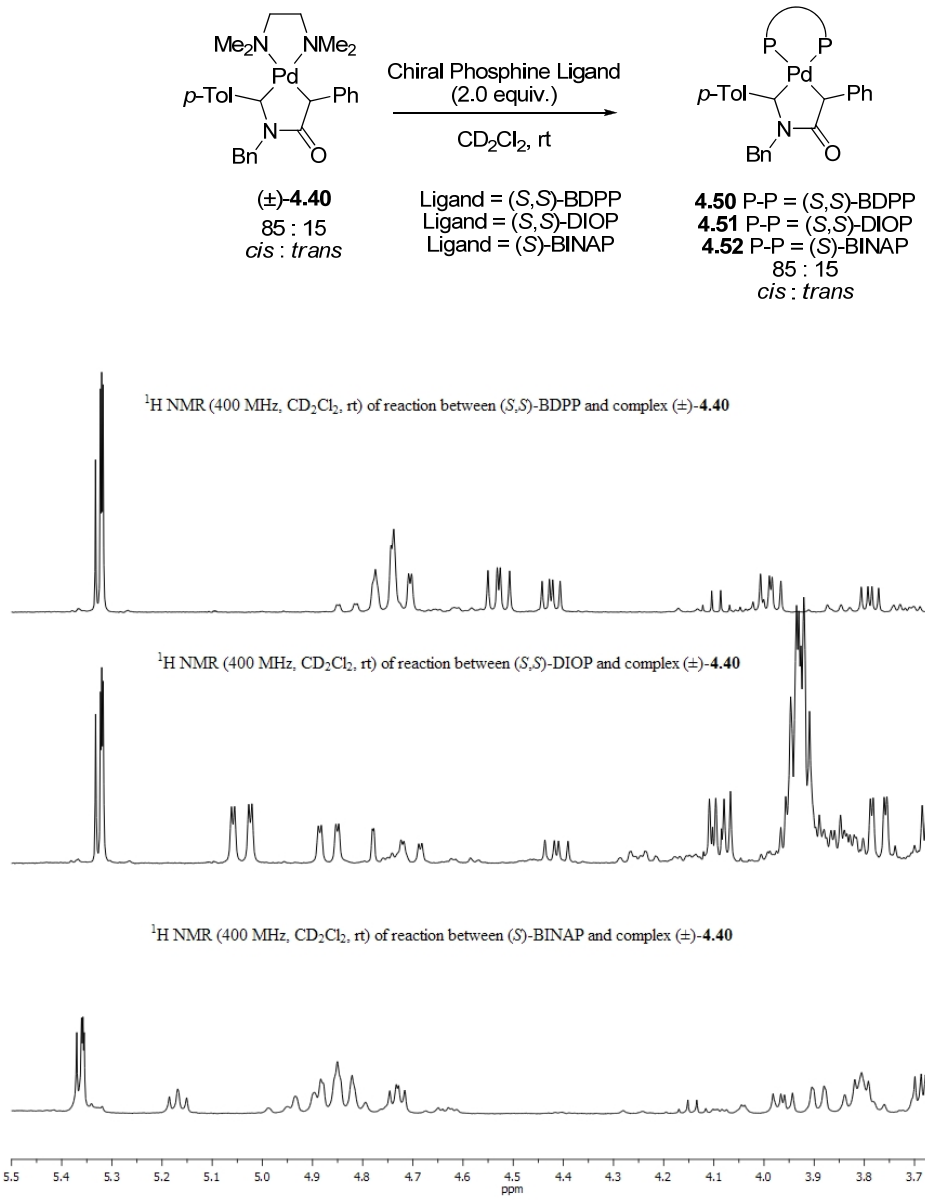

Figure 4.18. *In situ* ^{1}*H NMR (400 MHz) Spectra Recorded After Reaction of* (±)-***4.40*** *with the Chiral Ligands (S,S)-BDPP, (S,S)-DIOP, and (S)-BINAP to Generate* ***4.50***, ***4.51***, *and* ***4.52*** *Respectively.*

As the ^{1}H NMR spectra for the reactions of (±)-**4.40** with the chiral ligands (*S*,*S*)-BDPP, (*S*,*S*)-DIOP, and (*S*)-BINAP showed completion, we also obtained ^{31}P NMR spectra (162 MHz) for the three experiments. The spectra are shown in Figure 4.19.

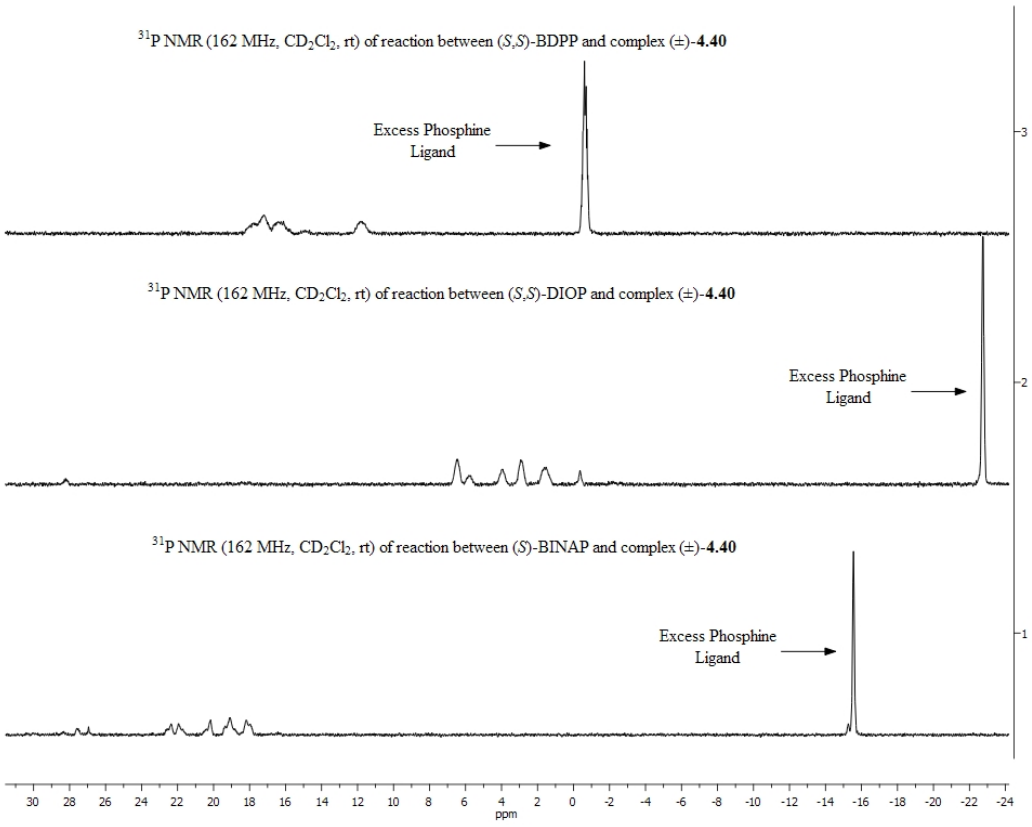

Figure 4.19. *In situ* ^{31}*P NMR Spectrum Recorded After Reaction of* (±)-***4.40*** *With the Chiral Ligands (S,S)-BDPP, (S,S)-DIOP, and (S)-BINAP to Generate Complexes* ***4.50***, ***4.51***, *and* ***4.52***, *Respectively.*

Unfortunately, the spectra were not resolved enough to allow the assignment of *cis* and *trans* diastereomers. The *in situ* NMR data shown above in Figures 4.17 – 4.19 indicate that the (*S*,*S*)-CHIRAPHOS ligand was the only ligand of the four tested that proved useful for measuring the effect of double diastereodifferentiation on the

formation of a second stereocenter when stereocenters are present both on a carbon adjacent to the palladium center as well as in the auxiliary ligand sphere.

4.6 A Model for Diastereoselectivity

The previous sections of Chapter Four have shown that the palladapyrrolidinone synthesis generally favors the *cis* diastereomers under the reaction conditions, while under thermal or basic isomerization conditions, the *trans* diastereomers become predominant. We also observed that the complexes bearing chiral non-racemic ligand (*S*, *S*)-CHIRAPHOS afforded a ratio of *cis* to *trans* diastereomers similar to that of the dppe ligand. This observation intrigued us, as C_2-symmetric chiral non-racemic ligands often lead to high levels of stereoselectivity due to their fewer reactive conformations versus non C_2-symmetric chiral non-racemic ligands.[188, 191] We wished to propose a mechanism that accounts for the discrepancy between the initial expectation of observing either a reinforcement or degradation of the *cis* : *trans* selectivity when (*S*,*S*)-CHIRAPHOS was used as a ligand, the consistent levels of diastereoselectivity for the TMEDA and dppe ligands, and the more variable levels of selectivity in the bipy cases.

When attempting to rationalize these results, two issues arise. The first involves how the Pd-C bond is formed and the second involves which isomers of the *N*,*O*-acetal moiety are generated. For the cases of the TMEDA and dppe ligated species, we observed similar diastereoselectivities in each case, regardless of the choice of the base. For the TMEDA cases, we observed selectivities in the range of 95 : 5 to 88 : 12 *cis* : *trans*, and for the dppe cases, we observed selectivities in the

range of 77 : 23 to 72 : 28 *cis* : *trans*. Based on these observations, we conclude that it is possible that the O-Pd enolate is reacting through only one isomer (i.e., the E or Z isomer), although other possibilities cannot be ruled out.

If we assume that the reactive conformation will be one that has a C-H bond perpendicular to the plane of the chelated amide in order to achieve the greatest overlap and be most acidic,[192] we can draw four plausible conformations (A – D, shown for TMEDA ligand, Scheme 4.23). It should be noted that the chelated amide ring is planar.

Scheme 4.23

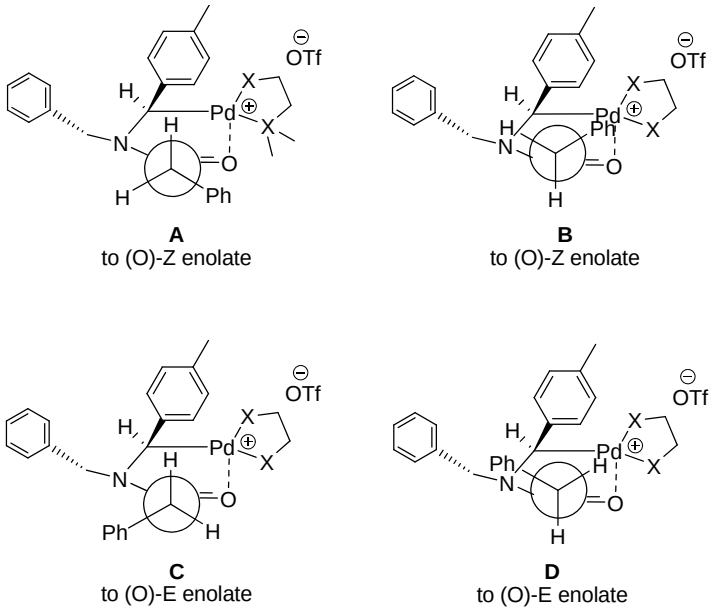

If the secondary ligand sphere (constituting all of the atoms of the auxiliary ligand that are not directly bound to palladium) is the largest steric factor, we can rationalize that the deprotonation is occurring through conformations C or D because conformations A and B are destabilized by steric factors, giving the (O)-E enolate.

Once the enolate is formed, C-Pd bond formation can then occur. The precise nature of the interaction between the palladium and the oxygen is unknown, but we believe it more likely that a structure like **A** in Scheme 4.24 is the intermediate on the way to palladapyrrolidinones (±)-**4.40** – (±)-**4.42**, although ionic intermediate **B** cannot be excluded. Structure **A** exhibits significant allylic strain; however, the other geometric isomer may be less favored due to interactions with the secondary ligand sphere of the auxiliary ligands of the palladium center.

Scheme 4.24

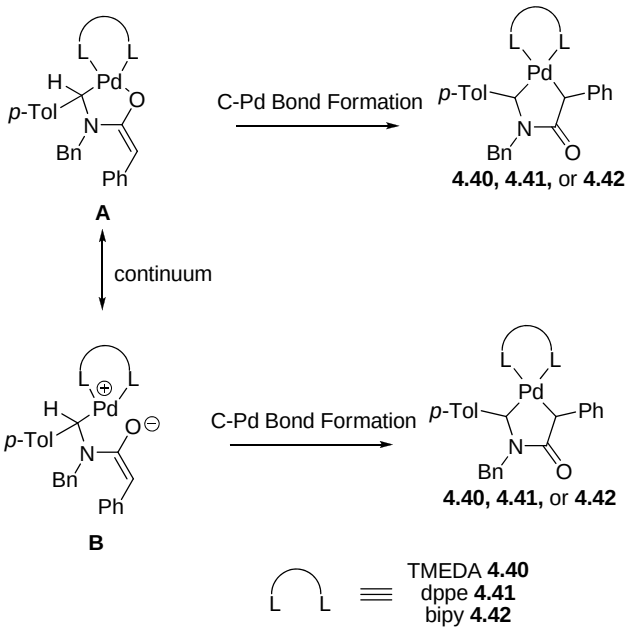

We hypothesize that in the cases of the TMEDA and dppe ligated species, the O(E)-O-Pd enolate, once formed, can then rotate clockwise or counterclockwise to give the *cis* and *trans* diastereomers, respectively. We conclude that the aforementioned 'folding' (section 4.4.2, page 124) of the ligand sphere makes the clockwise rotation during the η^1-η^3-η^1 shift the lower energy pathway to give the *cis*

palladapyrrolidinones *cis* (±)-**4.40**, *cis* (±)-**4.41**, **4.46a**, and **4.46b** as major products due to unfavorable steric interactions with the ligand sphere in the rotation to give the *trans* products (Scheme 4.25). The benzyl group may already be 'locked' into place (see Section 4.4.2) and may not move much during the formation of the Pd-C bond.

Scheme 4.25

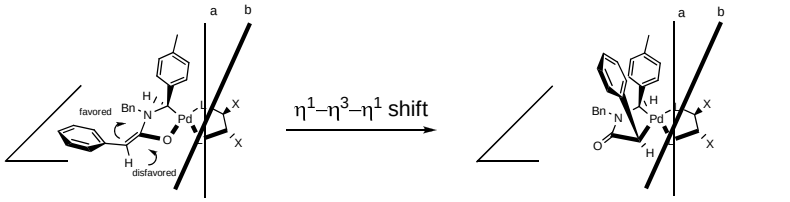

O(E)-O-Pd enolate

cis **4.40**, *cis* **4.41, 4.46a,** and **4.46b**

L = NMe_2 or PPh_2, X = H, Me

However, it should be noted that as we have not directly observed any intermediates along the reaction course, that pathways involving mixtures of enolate isomers or only the O(*Z*)-O-Pd enolate cannot be ruled out. The precise mechanism of stereoinduction awaits further study.

For the bipy cationic complex (±)-**4.42**, there is no 'fold' angle in the bipy ligand as seen from the X-Ray data. This indicates that the secondary ligand sphere is much less involved in the diastereoinduction, and that the initially formed stereocenter can exert little influence through the ligand sphere as in the formation of the palladapyrrolidinones bearing the TMEDA, dppe, and (*S*,*S*)-CHIRAPHOS ligands. It also indicates that both the O(E) and O(Z)-enolates may be viable intermediates in this case since the flat bipyridyl ligand conceivably provides less steric hindrance during the deprotonation step.

In summary, we have successfully synthesized and characterized the first examples of palladapyrrolidinones, endocyclic Pd-amide enolates bearing two Pd-bonded stereogenic carbons. We observed that the diastereoselectivity can vary quite greatly depending on the ligand, from as high as 95 : 5 *cis* : *trans* in the case of TMEDA, to as little as (42 : 58 *cis* : *trans*) in the case of the bipy ligand. We observed a surprising lack of double diastereodifferentiation when utilizing the chiral non-racemic ligand (*S*,*S*)-CHIRAPHOS in the synthesis. Based in part on X-Ray crystallographic data, we proposed a mechanism that we believe accounts for the preference for the *cis* diastereomers in the products when the ligands are TMEDA, dppe, or (*S*,*S*)-CHIRAPHOS as well as for the lack of selectivity in the case where the ligand is 2,2'-bipyridyl. The proposed mechanism also accounts for the surprising lack of double diastereodifferentiation when (*S*,*S*)-CHIRAPHOS was utilized.

Chapter Five

Future Work

5.1 Solid-Phase Synthesis

With the failure of polymer-bound palladacycles **3.1** to give separable products via MDF protocols, one solution would be to improve the protocol for the insertion reaction on solid-phase. The synthesis of polymer-bound palladacycles **3.7** to **3.18** used to explore the synthesis of 2*H*-1 benzopyrans gave reproducible levels of loading vs. the molar P : Pd ratio during loading. In contrast, the loading of palladacycles **3.31** – **3.34** gave consistently lower results (1 : 2.5 – 1 : 2.8) within experimental error. The resin utilized during the initial experiments by Mr. Atsushi Shiota and Dr. Lei Zhang had a loading of 1 : 2.0. While we find it unlikely that the cause of the lower loading is predominantly from oxidation of the polymer-bound triphenylphosphine ligand, this possibility has not been rigorously ruled out.

The electron-withdrawing ability of the triflate group as measured by the acidity of phenol[193] vs. *N*-phenylmethanesulfonamide[194] vs. *N*-phenyl triflamide[194] (Figure 5.1) could also adversely effect the reaction. due to the resulting reduced electron density at the palladium center.

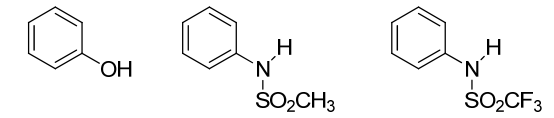

pKa = **10.0** (H_2O) pKa = **8.85** (H_2O) pKa = **4.45** (H_2O)

Figure 5.1. *pKa Values (in H_2O) for Phenol, N-phenylmethanesulfonamide, and N-phenyltriflamide, Respectively*

It can be envisioned that the triflate group on the nitrogen atom would adversely impact the co-ordination of the alkyne, as well as the rates of other steps such as

reductive elimination, multiple insertion, and oligomerization/polymerization processes, potentially leading to lower yields and purities particularly when a significant excess of alkyne is used as a reactant. While the analogous solution-phase reactions with the aza-palladacycles are quite similar to the oxa-palladacycles, steps in the formation of 1,2-dihydroquinolines may be slowed down on solid phase, leading to undesirable side products (Scheme 5.1).

Scheme 5.1

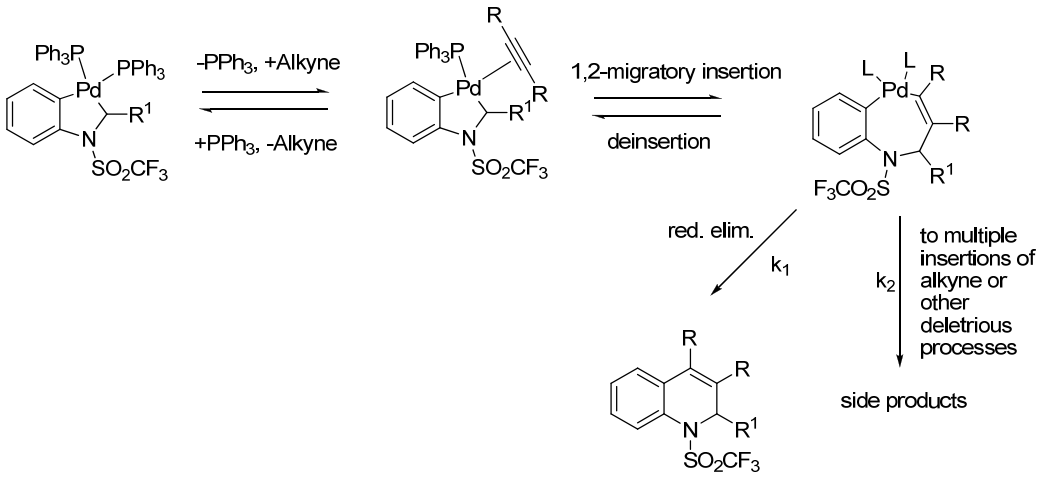

A third obstacle to be overcome is the inability of the mass spectrometer to detect the molecular ion of the 1,2-dihydroquinolines discussed in Chapter Three. Two main routes could give improvement to the library synthesis. First, different reaction conditions could be found for the loading reaction, potentially including a study similar to that performed in Section 3.1 to determine how the structure of the palladacycle effects the reactivity of the polymer-bound aza-palladacycles. Second, the *N*-protecting group could be systematically changed from triflate to a group that would 1) improve the loading of palladium onto the resin, thus improving the purity

and/or yield of the reaction and/or 2) improve the likelihood that the mass spectrometer will detect and separate the desired compound from the crude product.

Experiments to expand the scope of the *N*-protecting group could both lead to fundamental insights about the reaction as well as an improvement in the yields of 1,2-dihydroquinolines both in solid phase and solution phase reactions. Potential *N*-protecting groups would include alkyl and aryl groups, as well as other carbonyl derivatives.

5.2 Palladapyrrolidinones

As noted in Chapter Four, the palladapyrrolidinone system can provide a great model for the formation of a new stereogenic center in relation to a pre-existing stereocenter. Also of interest is what occurs when the complex is induced to undergo reductive elimination. As there are two stereogenic centers in the molecule, the *cis* and *trans* β-lactams formed from 1,1-reductive elimination would be easily distinguishable by the coupling constants of the protons on the stereocenters.[195] Two ways to induce reductive elimination in palladium(II) complexes are generating a three-coordinate T or Y-shaped intermediate[137] by using a mono-dentate ligand and removing electron density from the palladium center, such as through oxidation.[112, 136, 196-198]

We attempted to induce reductive elimination of complexes (±)-**4.40** bearing the TMEDA ligand and (±)-**4.42** bearing the bipy ligand in one of three ways. First, we removed electron-density from the palladium center by reacting the complex with an excess of maleic anhydride. Second, we attempted to generate a Pd(IV)

intermediate by oxidation with molecular iodine. Finally, we generated a potentially more labile Pd(II) phosphine complex *in situ* by reaction of (±)-**4.40** with an excess of triphenylphosphine.

The only product we were able to isolate and identify from the reactions was the known lactam (±)-**5.1**,[199] obtained via reaction of palladacycle (±)-**4.42** with an excess of maleic anhydride in refluxing toluene. The reaction is shown in Scheme 5.2.

Scheme 5.2

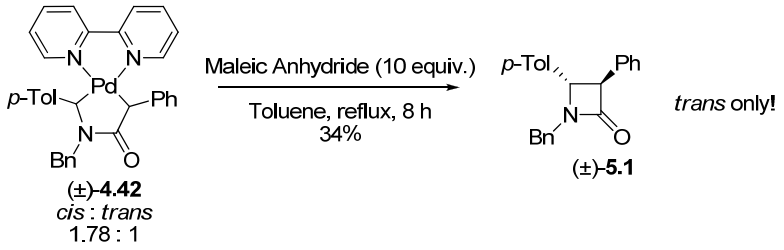

The result from Scheme 5.2 suggests that a simple 1,1-reductive elimination may not be operating due to fact that the diastereomeric ratio in the palladacycles is not faithfully transferred to the product, although this cannot be ruled out. Alternative mechanisms include the following three possibilities. First, a 1,1-reductive elimination followed by an isomerization of the β-lactam products could be occurring. The second possibility involves an isomerization of complex (±)-**4.42** before the reductive elimination process, after which the products may or may not isomerize further. The fourth possibility is that the palladium is not truly mediating the C-C bond formation. A look at the structures of (±)-**4.40** and (±)-**4.42** reveals that they are organometallic analogs of 1,1-dioxo-4-thiazolidinones, which are known to undergo extrusion of SO_2 to give β-lactams.[200, 201]

Due to the steric congestion around the palladium center, reductive elimination could be significantly slowed down. This would allow Pd(0) extrusion to be a competitive process, giving intermediates (such as **A** in Scheme 5.3) similar to those proposed in the classical Staudinger β-lactam synthesis. Alternatively, the extrusion could be stepwise, leading to an intermediate (structure **B** in Scheme 5.3) which could also explain the formation of the *trans* product (Scheme 5.3).

Scheme 5.3

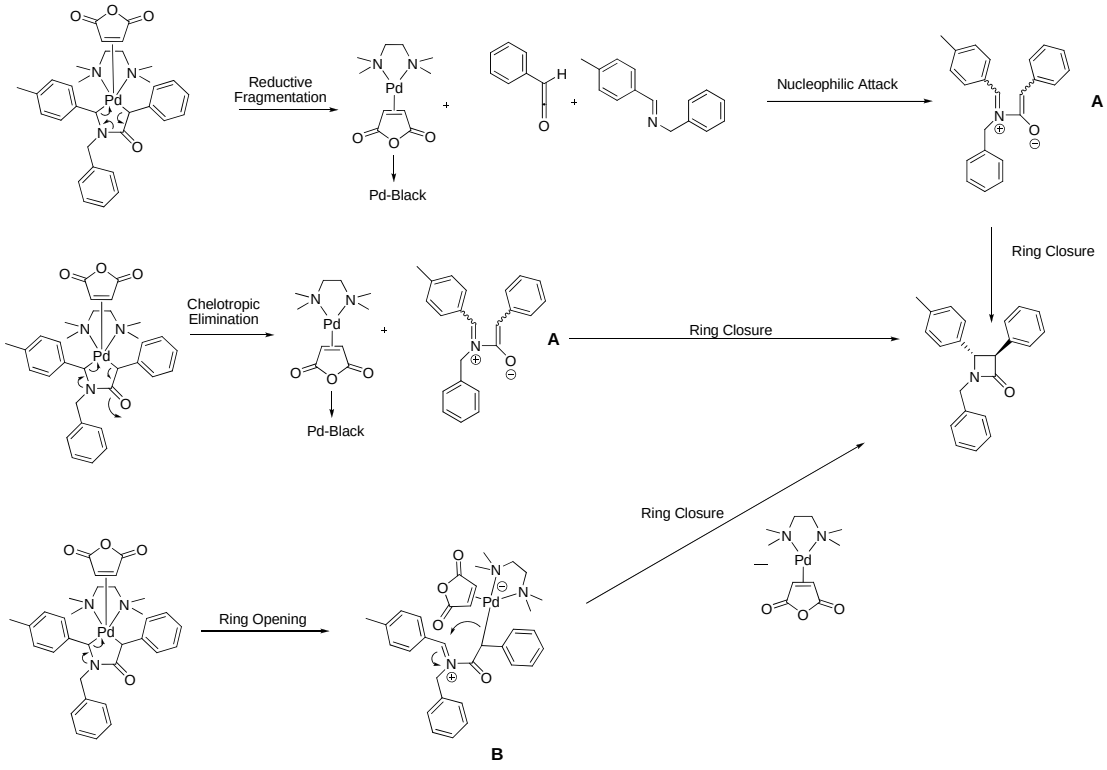

Near the end of the work described in Chapter Four, we were able to isolate a highly enriched sample of *cis*-(±)-**4.40**. The ability to isolate the highly enriched *cis* diastereomer will allow for the synthesis of other diastereoenriched *cis* complexes with other ligands as well as monitor the effect of reaction conditions on the yield and

cis : *trans* ratio of β-lactam (±)-**5.1**, generating additional insights into the mechanism of the reductive elimination process, which is still unclear at this time.

With the ability to independently change the structure of both aryl groups on the stereogenic carbons, opportunities can be seen for potentially monitoring the *cis* : *trans* ratio of the palladapyrrolidinones as a function of aryl substituents on the *para* position of the aromatic rings. The use of imines that are chiral on the *N*-substituent would allow another probe into how a stereogenic center farther away affects the diastereoselectivity of the process. In addition, the relative ease of β-lactam formation as well as other organic products could also be seen in relation to the structure of the aryl groups.

Another interesting change to the structure of the complexes would be to utilize pivaldehyde benzyl imine. The change in sterics and electronics provided by exchanging the *p*-tolyl group for the *t*-butyl group would provide for an interesting comparison study.

A distinctly different approach to utilizing the knowledge from Chapter Four would be to use different metals to generate yet different organometallic analogs for use in organic synthesis. Other metals could be used to generate late transition-metal analogs of palladapyrrolidinones which would have different properties than the known palladapyrrolidinones.

Chapter Six

Experimental Section

General Experimental

Unless otherwise indicated, all NMR data were collected at room temperature in $CDCl_3$ with internal $CHCl_3$, (δ 7.26 ppm for ^{1}H and 77.00 ppm for ^{13}C) for ^{1}H and ^{13}C NMR, external 85% H_3PO_4 (δ 0 ppm for ^{31}P), and neat trifluoroacetic acid as an external reference for F spectra (δ -76.55 ppm for ^{19}F). IR spectra were measured in thin films from DCM on salt (NaCl) plates. Melting points were taken in open capillary tubes and are uncorrected. Mass spectra were measured under electrospray ionization (ES+) conditions. Analytical thin-layer chromatography (TLC) was carried out on commercial Merck silica gel 60 plates, 250 μm thickness, with fluorescent indicator (F-254) or stained with aqueous $KMnO_4$ solution. Column chromatography was performed with 32-63 μm silica gel (Sorbent). Tetrahydrofuran (THF) was freshly distilled from sodium/benzophenone. Acetonitrile and DCM were kept over 3Å (8-12 mesh) molecular sieves under an atmosphere of dry argon; other solvents were used as received. Unless otherwise specified, all reactions were carried out under an atmosphere of dry argon in oven dried (at least 6 h at 140 ^{o}C) glassware. (*E*)-*N*-(4-methylbenzylidene)-1-phenylmethanamine and (E)-4-methoxy-*N*-(4-methylbenzylidene)aniline were made by heating a 1 : 1 mixture of benzylamine or *p*-anisidine and *p*-tolualdehyde with molecular sieves in refluxing benzene overnight, followed by filtration, removal of solvents under reduced pressure and then distillation to afford pure imines. Other materials were used as received from commercial suppliers.

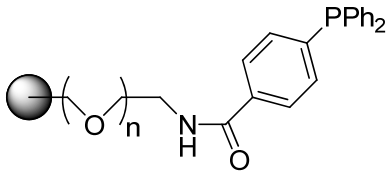

3.1

Compound **3.1** was prepared according to a modified literature procedure.[165] To a suspension of Tentagel S-NH_2 (1.084 g, 0.488 mmol) in DMF (10 mL) was added 4-diphenylphosphinobenzoic acid (0.483 g, 1.575 mmol), 1-ethyl-3-(3'-dimethylaminopropyl)carbodiimide hydrochloride (0.467 g, 2.430 mmol), and N-Hydroxybenzotriazole (0.435 g, 3.21 mmol) and the suspension allowed to stir for 24 h at room temperature. The resin was then filtered and washed with DMF (5 × 20 mL), DCM (8 × 20 mL), and Et_2O (2 × 20 mL) and then dried under reduced pressure to afford the product (1.167 g) as a light yellow spongy solid.

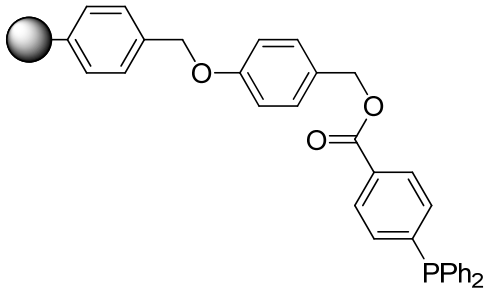

3.6

Compound **3.6** was prepared according to a modified literature procedure.[202] A solution of (*p*-diphenylphosphino)benzoic acid (6.00 g, 19.6 mmol) and diisopropylcarbodiimide (1.24 g, 9.79 mmol) in DCM (70 mL) was stirred at 0°C for 0.5 h under argon. Solvent was removed under reduced pressure, and the crude product was dissolved in DMF (30 mL). The resulting DMF solution was added to a

pre-swelled solution of Wang Resin (3.24 g, 1.21 mmol OH/g, 3.91 mmol OH) in DMF (60 mL) and the reaction mixture was stirred at rt under argon for 1 h. Solid DMAP (0.239 g, 1.96 mmol) was added, and the stirring was continued for additional 39 h at rt. The crude reaction mixture was filtered, and the solid was washed successively with THF, DCM, DMF, THF, DCM (100 mL each) to afford resin **3.6** (4.221 g) as an off-white solid: 2.75% mass P (0.887 mmol P/g of resin). Swelling Capacity in DCE: (swelled volume/dry weight, mL/g): 5.3 mL/g.

General Procedure for the Preparation of Immobilized Palladacycles 3.7 - 3.18

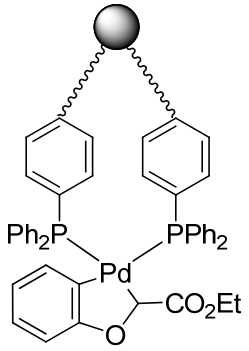

Polymer-bound Palladacycles **3.7** – **3.18**

A suspension of the phosphine resins **3.3 – 3.6** (equivalent to 1.6-3.1 mmol P) in the solution of the palladacycle **3.2** (1 mmol) in THF (10-33 mL /1 mmol Pd) was stirred for the initial time period (5-19 h) at rt under argon. Volatile components were removed under reduced pressure (1 mm Hg, 1-5 h). Fresh THF (10-15 mL/1 mmol Pd) was added, and the resulting suspension was stirred for the second time period (5-21 h). In some cases, the cycle of stirring and evacuation was repeated as indicated. The suspension was filtered, and the resin was washed successively with methanol

(20 mL), DCM (20 mL), methanol (20 mL), DCM (20 mL) and diethyl ether (20 mL), and dried under reduced pressure (1 mmHg) to afford immobilized palladacycles **3.7 – 3.18** as yellow powdery solids. The reaction yields were calculated as mol% of Pd present in the isolated immobilized palladacycle per mmol of palladacycle **3.2** used. The resins were characterized by the analyses (ICP) of P and Pd content, infrared spectroscopy and swelling capacity in 1,2-dichloroethane. The combined filtrates were evaporated, and the resulting crude extracts were analyzed by ^{1}H NMR spectroscopy to establish the content of any unreacted palladacycle **3.2**.

Palladacycle 3.7. Treatment of resin **3.3** (0.670 g, 9.50% P, 3.06 mmol P/g, 2.05 mmol P) and palladacycle **3.2** (0.401 g, 1.0 mmol) according to the described method, repeating the stirring/evacuation cycle 5 times, afforded the immobilized palladacycle **2a** (0.715 g, 68%): ICP analyses: 10.03% mass Pd, 5.73% mass P; IR (KBr, cm^{-1}) 1707 (m); Swelling Capacity in DCE: (swelled volume/dry weight, mL/g): 3.2. The material in the combined filtrates (0.038 g) contained only traces of palladacycle **3.2**.

Palladacycle 3.8. Treatment of resin **3.3** (0.670 g, 9.50% P, 3.06 mmol P/g, 2.05 mmol P) and palladacycle **3.2** (0.400 g, 1.0 mmol) according to the described method, repeating the stirring/evacuation cycle 4 times, afforded the immobilized palladacycle **3.8** (0.806 g, 70%): ICP analyses: 9.21% mass Pd, 6.12% mass P; IR (KBr, cm^{-1}) 1705 (m); Swelling Capacity in DCE: (swelled volume/dry weight, mL/g): 2.9 mL/g. The material in the combined filtrates contained significant quantities of palladacycle **3.2**.

Palladacycle 3.9. Treatment of resin **3.4** (0.670 g, 9.34% P, 3.01 mmol P/g, 2.02 mmol P) and palladacycle **3.2** (0.401 g, 1.0 mmol) according to the described method afforded the immobilized palladacycle **3.9** (0.824 g, 71%): ICP analyses: 9.15% mass Pd, 6.78% mass P; IR (KBr, cm^{-1}) 1705 (m); Swelling Capacity in DCE: (swelled volume/dry weight, mL/g): 3.6 mL/g. The material in the combined filtrates (0.104 g) contained approximately 95% of unreacted palladacycle **3.2** (25% mol of Pd).

Palladacycle 3.10. Treatment of resin **3.4** (1.01 g, 9.34% P, 3.01 mmol P/g, 3.04 mmol P) and palladacycle **3.2** (0.403 g, 1.0 mmol) according to the described method afforded the immobilized palladacycle **3.10** (1.22 g, 96%): ICP analyses: 8.41% mass Pd, 7.49% mass P; IR (KBr, cm^{-1}) 1705 (m); Swelling Capacity in DCE: (swelled volume/dry weight, mL/g): 3.7 mL/g. The material in the combined filtrates (0.023 g) contained only traces of unreacted palladacycle **3.2**.

Palladacycle 3.11. Treatment of resin **3.5** (1.250 g, 4.18% P, 1.35 mmol P/g, 1.69 mmol P) and palladacycle **3.2** (0.3996 g, 1.0 mmol) according to the described method, repeating the stirring/evaporation cycle 5 times, afforded the immobilized palladacycle **3.11** (1.34 g, 88%): ICP analyses: 7.05% mass Pd, 3.55% mass P. The material in the combined filtrates (0.048 g) contained approximately 95% of unreacted palladacycle **3.2** (12% mol of Pd).

Palladacycle 3.12. Treatment of resin **3.5** (1.250 g, 4.18% P, 1.35 mmol P/g, 1.69 mmol P) and palladacycle **3.2** (0.400 g, 1.0 mmol) according to the described method afforded the immobilized palladacycle **3.12** (1.190 g, 71%): ICP analyses: 6.30% mass Pd, 3.51% mass P. Swelling Capacity in DCE: (swelled volume/dry weight,

mL/g): 3.6 mL/g. The material in the combined filtrates (0.042 g) contained approximately 95% of palladacycle **3.2** (11% mol of Pd).

Palladacycle 3.13. Treatment of resin **3.5** (1.878 g, 4.18% P, 1.35 mmol P/g, 2.53 mmol P) and palladacycle **1** (0.400 g, 1.0 mmol) according to the described method afforded the immobilized palladacycle **3.13** (1.98 g, 84%): ICP analyses: 4.53% mass Pd, 2.84% mass P; IR (KBr, cm^{-1}) 1716 (m); Swelling Capacity in DCE: (swelled volume/dry weight, mL/g): 4.2 ml/g. The material in the combined filtrates (0.018 g) contained approximately 85% of palladacycle **3.2** (4.5% mol of Pd).

Palladacycle 3.14. Treatment of resin **3.5** (1.875 g, 4.18% P, 1.35 mmol P/g, 2.53 mmol P) and palladacycle **1** (0.401 g, 1.0 mmol) according to the described method, repeating the stirring/evacuation cycle 5 times, afforded the immobilized palladacycle **3.14** (1.94 g, 100%): ICP analyses: 5.44% mass Pd, 3.84% mass P; IR (KBr, cm^{-1}) 1717 (m); Swelling Capacity in DCE: (swelled volume/dry weight, mL/g): 4.1 ml/g. The material in the combined filtrates (0.018 g) did not contain any remaining palladacycle **3.2**.

Palladacycle 3.15. Treatment of resin **3.5** (1.875 g, 4.18% P, 1.35 mmol P/g, 2.53 mmol P) and palladacycle **3.2** (0.200 g, 0.50 mmol) according to the described method, afforded the immobilized palladacycle **3.15** (2.10 g, 107%): ICP analyses: 2.72% mass Pd, 4.81% mass P; IR (KBr, cm^{-1}) 1715 (m); Swelling Capacity in DCE: (swelled volume/dry weight, mL/g): 6.9 ml/g. The material in the combined filtrates (0.060 g) did not contain any remaining palladacycle **3.2**.

Palladacycle 3.16. Treatment of resin **3.5** (1.25 g, 4.18% P, 1.35 mmol P/g, 1.69 mmol P) and palladacycle **3.2** (0.400 g, 1.00 mmol) according to the described method, afforded the immobilized palladacycle **3.16** (1.43 g, 97%): ICP analyses: 7.26% mass Pd, 3.63% mass P. The material in the combined filtrates (0.044g) contained only traces of the remaining palladacycle **3.2**.

Palladacycle 3.17. Treatment of resin **3.6** (1.833 g, 2.75% P, 0.89 mmol P/g, 1.631 mmol P) and palladacycle **3.2** (0.361 g, 0.900 mmol) according to the described method, afforded the immobilized palladacycle **3.17** (1.87 g, 65%): ICP analyses: 3.34% mass Pd, 2.54% mass P; IR (KBr, cm^{-1}) 1717 (m); Swelling Capacity in DCE: (swelled volume/dry weight, mL/g): 6.4 ml/g. The material in the combined filtrates (0.127 g) contained > 95% palladacycle **3.2** (30% mol of Pd).

Palladacycle 3.18. Treatment of resin **3.6** (1.825 g, 2.75% P, 0.89 mmol P/g, 1.624 mmol P) and palladacycle **3.2** (0.360 g, 0.900 mmol) according to the described method, afforded the immobilized palladacycle **3.18** (1.88 g, 66%): ICP analyses: 3.35% mass Pd, 2.54% mass P; IR (KBr, cm^{-1}) 1717 (m); Swelling Capacity in DCE: (swelled volume/dry weight, mL/g): 6.7 ml/g. The material in the combined filtrates (0.122 g) contained > 95% palladacycle **3.2** (32% mol of Pd).

Measurements of the Swelling Capacities by the Volumetric Method. A plunger, removed from a 1 mL plastic syringe (Henke Sass Wolf), was cut to remove the handle providing a tight plug for the syringe tip. The modified plunger was reinserted into the syringe body. The resulting assembly was attached vertically to a ring stand, and was used as a "micro" graduated cylinder. A sample of the dry polymer

(approximately 50 mg) was inserted into the syringe, appropriate solvent was added (0.5-0.7 mL) and the suspension was allowed to equilibrate for 1 h. Subsequently, the volume occupied by the swelled polymer was established utilizing the calibration of the syringe body. As indicated in Table 6.1, the majority of the resins floated in 1,2-dichloroethane, and only a few of the high loading polymer samples sank to the bottom. The swelling capacities provided in Table 6.1, and Tables 3.1 – 3.4 and 3.11 of Chapter Three correspond to the volume of the swelled polymer per 1 g of the dry resin. For comparison, this method was used to measure the swelling capacity of the Wang Resin (1.21 mmol OH/g, 200-400 mesh, 1% crosslinking) in THF. The measured value (6.10 mL/g, swelled volume per weight of dry resin) is an average of three (3) measurements. This result is in acceptable agreement with values available in the literature (6.0 ml/g for HL-Wang resin 1.16 OH/g).[203]

Table 6.1. Measurement of Swelling Capacities for Wang Resin, resins **3.3** – **3.6**, polymer-bound palladacycles **3.7** – **3.18** and **3.31** – **3.34**, and resin **3.90**.

Resin or Polymer-bound Palladacycle	Solvent	mass of dry resin (g)	volume of swollen resin (mL)	swelling capacity (mL/g)	rounded/average swelling capacity (mL/g)
Wang	THF	0.0584	0.35	5.993	
		0.0555	0.34	6.126	6.1
		0.1049	0.65	6.196	
	DCE	0.0518	0.30	5.791	5.8
3.3	DCE	0.0551	0.25	4.537	4.5
3.4	DCE	0.0530	0.24	4.528	4.5
3.5	DCE	0.0457	0.26	5.689	5.7
3.6	DCE	0.0544	0.29	5.331	
	DCE	0.0524	0.27	5.153	5.3
	DCE	0.0541	0.29	5.360	
3.7	DCE	0.0530	0.17	3.207[a]	3.2
3.8	DCE	0.0549	0.16	2.914[a]	2.9
3.9	DCE	0.0547	0.20	3.656	3.6
3.10	DCE	0.0517	0.19	3.675[a]	3.7
3.12	DCE	0.0550	0.20	3.636[b]	3.6
3.13	DCE	0.0574	0.24	4.181	4.2
3.14	DCE	0.0555	0.23	4.144	4.1
3.15	DCE	0.0531	0.37	6.967	7.0
3.17	DCE	0.0549	0.35	6.375	6.4
	DCE	0.0533	0.34	6.379	
3.18	DCE	0.0528	0.36	6.818	6.7
	DCE	0.0555	0.37	6.667	
3.31	DCE	0.0516	0.24	4.651	4.7
3.32	DCE				--[c]
3.33	DCE	0.0557	0.21	3.770	3.8
3.34	DCE	0.0520	0.24	4.615	4.6
3.90	DCE	0.0506	0.34	6.719	6.7

[a] Resin sank in 1,2-dichloroethane [b] Resin partially sank, partially floated in 1,2-dichloroethane [c] density of resin similar to solvent, unable to obtain reading

Procedure for Experiments in Tables 3.3 and 3.4

General Procedure for the Synthesis of 2*H*-1-Benzopyrans 3.19 and 3.20 from Immobilized Palladacycles 3.7 – 3.15, 3.17, and 3.18.

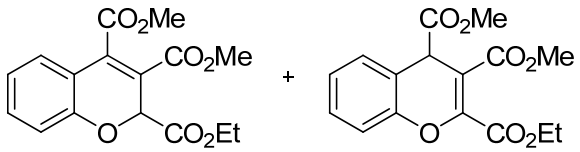

3.19 **3.20**

To a suspension of the immobilized palladacycles **3.7 – 3.15**, **3.17**, and **3.18.** (0.100 – 0.175 mmol of total Pd) in 1,2-dichloroethane (6.0 mL) was added neat dimethyl acetylenedicarboxylate (2.6 – 5.2 mol equiv). The suspension was stirred for 3 h at the indicated temperature (40°C or 80°C) under argon. The reaction mixture was filtered, the resin was washed successively with methanol (20 mL), methylene chloride (20 mL), methanol (20 mL), methylene chloride (20 mL) and diethyl ether (20 mL), and dried under high vacuum to afford the recovered resins as yellow to dark orange powders. The filtrate and resin washes were combined, solvents were removed under reduced pressure, and the crude product was purified by flash chromatography over silica, eluting with ether/hexane (1 : 6) or ethyl acetate/hexane (1 : 4) to afford benzopyran **3.19** accompanied in some cases by smaller amounts of chromatographically inseparable regioisomeric benzopyran **3.20**, as colorless or light yellow oil: ^{1}H NMR ($CDCl_3$, 400 MHz) (**3.19** : **3.20** = 3 : 1 mol ratio) δ 7.41 (d, *J* = 7.5 Hz, 0.25 H), 7.33 (td, *J* = 8.8 Hz, 1.5 Hz, 0.75 H), 7.16 (dd. *J* = 7.8 Hz, 1.4 Hz, 0.75 H), 7.16-7.12 (m, 0.25 H), 7.06 (t, *J* = 8.0 Hz, 1 H), 6.98 (td, *J* = 8.0 Hz, 1.0 Hz, 1 H), 5.82 (s, 0.75 H), 4.74 (s, 0.25 H), 4.41 (q, *J* = 7.1 Hz, 0.5 H), 4.20-4.03 (m, 1.5

H), 3.94 (s, 2.25 H), 3.83 (s, 2.25 H), 3.77 (s, 0.75), 3.71 (s, 0.75 H), 1.40 (t, J = 7.1 Hz, 0.75 H), 1.17 (t, J = 7.1 Hz, 2.25 H); ^{13}C NMR ($CDCl_3$, 100 MHz) (**3.19** : **3.20** = 3 : 1 mol ratio) δ (171.1), 168.4, 166.3, (165.2), 163.6, (162.5), 153.5, (151.6), (148.8), 137.8, (135.9), 133.1, (129.4), (128.8), 126.6, (125.5), 122.6, 117.8, (117.1), (116.7), 117.4, 117.1, 71.1, (62.6), 61.9, (52.9), 52.8, 52.6, (52.3), (40.9), 13.9 (signals for the minor regioisomer **6** are given in parentheses); IR (neat, cm^{-1}) (**3.19** : **3.20** = 3 : 1 mol ratio) 1760 (m), 1736 (m), 1723 (s).

Experiment from entry 1, Table 3.3. Treatment of palladacycle resin **3.7** (0.1007 g, 10.03% Pd, 0.0949 mmol Pd) with DMAD (0.055 mL, 0.064 g, 0.450 mmol, 4.7 equiv) at 40°C according to the general procedure including chromatographic separation with ether/hexane mixtures afforded benzopyrans **3.19** and **3.20** (0.005 g, 17%, **3.19** : **3.20** = 5 : 1 mol ratio) as a colorless oil, and the recovered resin (0.100 g) as a yellow solid.

Experiment from entry 2, Table 3.3. Treatment of palladacycle resin **3.11** (0.2025 g, 7.05% Pd, 0.134 mmol Pd) with DMAD (0.059 mL, 0.068 g, 0.479 mmol, 3.6 equiv) at 40°C according to the general procedure including chromatographic separation with ether/hexane mixtures afforded benzopyrans **3.19** and **3.20** (0.015 g, 35%, **3.19** : **3.20** = 22 : 1 mol ratio) as a yellow oil, and the recovered resin (0.189 g) as a reddish-brown solid.

Experiment from entry 3, Table 3.3. Treatment of palladacycle resin **3.17** (0.4026 g, 3.34% Pd, 0.127 mmol Pd) with DMAD (0.046 mL, 0.053 g, 0.375 mmol, 3.0 equiv) at 40°C according to the general procedure including chromatographic

separation with ether/hexane mixtures afforded benzopyrans **3.19** and **3.20** (0.035 g, 87%, **3.19** : **3.20** = 20 : 1 mol ratio) as a yellow oil, and the recovered resin (0.3755 g) as an orange solid.

Experiment from entry 4, Table 3.3. Treatment of palladacycle resin **3.17** (0.4018 g, 3.34% Pd, 0.126 mmol Pd) with DMAD (0.046 mL, 0.053 g, 0.375 mmol, 3.0 equiv) at 40°C according to the general procedure including chromatographic separation with ether/hexane mixtures afforded a pure benzopyran **3.19** (0.033 g, 81%) as a yellow oil, and the recovered resin (0.3755 g) as an orange solid.

Experiment from entry 1, Table 3.4. Treatment of palladacycle resin **3.7** (0.1007 g, 10.03% Pd, 0.0949 mmol Pd) with DMAD (0.055 mL, 0.064 g, 0.450 mmol, 4.7 equiv) at 80°C according to the general procedure including chromatographic separation with ether/hexane mixtures afforded a pure benzopyran **3.19** (0.015 g, 49%) as a light yellow oil, and the recovered resin (0.046 g) as a reddish brown solid.

Experiment from entry 2, Table 3.4. Treatment of palladacycle resin **3.8** (0.2018 g, 9.21% Pd, 0.175 mmol Pd) with DMAD (0.110 mL, 0.127 g, 0.894 mmol, 5.1 equiv) at 80°C according to the general procedure including chromatographic separation with ether/hexane mixtures afforded a pure benzopyran **3.19** (0.036 g, 64%) as a light yellow oil, and the recovered resin (0.212 g) as a red solid.

Experiment from entry 3, Table 3.4. Treatment of palladacycle resin **3.9** (0.2035 g, 9.15% Pd, 0.175 mmol Pd) with DMAD (0.110 mL, 0.127 g, 0.894 mmol, 5.1 equiv) at 80°C according to the general procedure including chromatographic separation with

ether/hexane mixtures afforded benzopyrans **3.19** and **3.20** (0.032 g, 57%, **3.19** : **3.20** = 2 : 1 mol ratio) as a yellow oil, and the recovered resin (0.228 g) as an orange solid.

Experiment from entry 4, Table 3.4. Treatment of palladacycle resin **3.9** (0.2000 g, 9.15% Pd, 0.172 mmol Pd) with DMAD (0.110 mL, 0.127 g, 0.894 mmol, 5.2 equiv) at 80°C according to the general procedure including chromatographic separation with ether/hexane mixtures afforded a pure benzopyran **3.19** (0.028 g, 50%) as a light yellow oil, and the recovered resin (0.2231 g) as a red solid.

Experiment from entry 5, Table 3.4. Treatment of palladacycle resin **3.11** (0.2029 g, 7.05% Pd, 0.134 mmol Pd) with DMAD (0.059 mL, 0.068 g, 0.479 mmol, 3.6 equiv) at 80°C according to the general procedure including chromatographic separation with ether/hexane mixtures afforded benzopyrans **3.19** and **3.20** (0.037 g, 86%, **3.19** : **3.20** = 4 : 1 mol ratio) as a yellow oil, and the recovered resin (0.144 g) as a reddish-brown solid.

Experiment from entry 6, Table 3.4. Treatment of palladacycle resin **3.12** (0.2400 g, 6.30% Pd, 0.142 mmol Pd) with DMAD (0.046 mL, 0.053 g, 0.375 mmol, 2.6 equiv) at 80°C according to the general procedure including chromatographic separation with ether/hexane mixtures afforded benzopyrans **3.19** and **3.20** (0.038 g, 84%, **3.19** : **3.20** = 3 : 1 mol ratio) as a yellow oil, and the recovered resin (0.208 g) as a reddish solid.

Experiment from entry 7, Table 3.4. Treatment of palladacycle resin **3.13** (0.3050 g, 4.53% Pd, 0.129 mmol Pd) with DMAD (0.059 mL, 0.068 g, 0.479 mmol, 3.7 equiv) at 80°C according to the general procedure including chromatographic

separation with ether/hexane mixtures afforded benzopyrans **3.19** and **3.20** (0.029 g, 69%, **3.19** : **3.20** = 3 : 1 mol ratio) as a yellow oil, and the recovered resin (0.3681 g) as a reddish solid.

Experiment from entry 8, Table 3.4. Treatment of palladacycle resin **3.13** (0.3044 g, 4.53% Pd, 0.129 mmol Pd) with DMAD (0.059 mL, 0.068 g, 0.479 mmol, 3.7 equiv) at 80°C according to the general procedure including chromatographic separation with ether/hexane mixtures afforded benzopyrans **3.19** and **3.20** (0.030 g, 72%, **3.19** : **3.20** = 3 : 1 mol ratio) as a yellow oil, and the recovered resin (0.3036 g) as a reddish solid.

Experiment from entry 9, Table 3.4. Treatment of palladacycle resin **3.14** (0.2990 g, 5.44% Pd, 0.153 mmol Pd) with DMAD (0.059 mL, 0.068 g, 0.479 mmol, 3.1 equiv) at 80°C according to the general procedure including chromatographic separation with ether/hexane mixtures afforded benzopyrans **3.19** and **3.20** (0.029 g, 59%, **3.19** : **3.20** = 2 : 1 mol ratio) as a yellow oil, and the recovered resin (0.2335 g) as a reddish solid. The recovered resin was analyzed by IR (KBr, cm^{-1}): 1843 (s br), 1830 (w br), 1718 (s br).

Experiment from entry 10, Table 3.34. Treatment of palladacycle resin **3.17** (0.4015 g, 3.34% Pd, 0.126 mmol Pd) with DMAD (0.046 mL, 0.053 g, 0.375 mmol, 3.0 equiv) at 80°C according to the general procedure including chromatographic separation with ether/hexane mixtures afforded benzopyrans **3.19** and **3.20** (0.031 g, 78%, **3.19** : **3.20** = 12 : 1 mol ratio) as a yellow oil, and the recovered resin (0.3655 g) as an orange solid.

Experiment from entry 11, Table 3.4. Treatment of palladacycle resin **3.17** (0.4018 g, 3.34% Pd, 0.125 mmol Pd) with DMAD (0.046 mL, 0.053 g, 0.375 mmol, 3.0 equiv) at 80°C according to the general procedure including chromatographic separation with ether/hexane mixtures affordedbenzopyrans **3.19** and **3.20** (0.033 g, 80%, **3.19** : **3.20** = 12 : 1 mol ratio) as a yellow oil, and the recovered resin (0.3831 g) as an orange solid.

Experiment from entry 12, Table 3.4. Treatment of palladacycle resin **3.10** (0.1620 g, 8.41% Pd, 0.128 mmol Pd) with DMAD (0.059 mL, 0.068 g, 0.479 mmol, 3.8 equiv) at 80°C according to the general procedure including chromatographic separation with ether/hexane mixtures afforded a pure benzopyran **3.19** (0.012 g, 28%) as a light yellow oil, and the recovered resin (0.1806 g) as an orange solid.

Experiment from entry 13, Table 3.4. Treatment of palladacycle resin **3.10** (0.1621 g, 8.41% Pd, 0.128 mmol Pd) with DMAD (0.059 mL, 0.068 g, 0.479 mmol, 3.8 equiv) at 80°C according to the general procedure including chromatographic separation with ether/hexane mixtures afforded a pure benzopyran **3.19** (0.016 g, 39%) as a light yellow oil, and the recovered resin (0.1744 g) as a red solid.

Experiment from entry 14, Table 3.4. Treatment of palladacycle resin **3.15** (0.480 g, 2.72% Pd, 0.123 mmol Pd) with DMAD (0.046 mL, 0.053 g, 0.375 mmol, 3.0 equiv) at 80°C according to the general procedure did not afford any detectable quantities of benzopyrans **3.19** and **3.20**. The recovered resin (0.5894 g) was obtained as a reddish solid.

Procedures for the Solution Phase Control Experiments: Isomerization Studies with 2*H*-1-Benzopyran 3.19.

A sample of benzopyran **3.19** was subjected to the conditions indicated in Table 3.5 for the indicated time. Column chromatography with ethyl acetate/ hexanes mixtures then provided the recovered products in >95% in all cases.

Solution Phase Reaction of Palladacycle 3.24 (L = PPh_3) with DMAD in the Presence of Excess PPh_3.

Control experiments involving reactions of palladacycle **3.24** (L = PPh_3) with DMAD (3.0 equiv) and additional free PPh_3 in the amount of 1.0 equiv. and 4.0 equiv (3 h, 80°C) afforded mixtures of benzopyrans **3.19** and **3.20** (2.5 : 1 mol ratio of **3.19** : **3.20**) in combined yields 50% and < 2%, respectively.

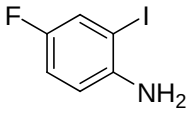

3.69

The known compound 4-fluoro-2-iodoaniline (**3.69**) was prepared according to a modified literature procedure.[176] To a solution of 4-fluoroaniline (2.066 g, 18.595 mmol) and sodium bicarbonate (5.155 g, 61.364 mmol) in water (30 mL) was added solid iodine (4.720 g, 18.595 mmol) in small portions over 15 minutes at room temperature. The solution was allowed to stir for 4.5 hours, after which the reaction was poured into water (60 mL) and extracted with DCM (3 × 60 mL). The DCM layer was then washed with a saturated solution of $Na_2S_2O_3$ (5 mL), dried (Na_2SO_4), and the organic solvents removed under reduced pressure to give a crude product.

The crude product was then chromatographed over silica gel (1 : 9 EtOAc : Hex) to afford the product (3.430 g, 78%) as an orange oil. Analytical data for compound **3.69** was identical to literature reported values.[204]

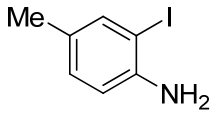

3.70

The known compound 2-iodo-4-methylaniline (**3.70**) was prepared according to a modified literature procedure.[176] To a solution of *p*-toluidine (0.9535 g, 8.897 mmol) and sodium bicarbonate in water (10 mL) was added solid iodine (2.624 g, 10.338 mmol) in small portions over 15 minutes at 10- 15°C. The reaction was stirred for 1 h and allowed to warm to room temperature. The solution was then poured into a separatory funnel and extracted with ether (4 × 30 mL), dried ($MgSO_4$), and then solvents removed under reduced pressure to give a crude product. The crude product was then chromatographed over silica (1 : 9 Hex : EtOAc) to afford the product (1.076 g, 45%) as a pink oil. Analytical data for compound **3.70** was identical to literature reported values.[205]

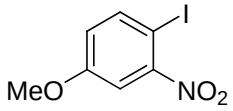

3.72

The known compound 1-iodo-4-methoxy-2-nitrobenzene (**3.72**) was prepared according to a modified literature procedure.[176] To a 0°C solution of 4-methoxy-2-nitroaniline (5.573 g, 33.141 mmol) in 1 : 1 conc. HCl/H_2O (70 mL) was added a cold (0°C) solution of sodium nitrite (2.515 g, 36.455 mmol) in H_2O (10 mL). After 15 minutes, TLC indicated that the diazonium salt formation was complete. The diazonium mixture was poured into a cold (0°C) solution of potassium iodide (8.252 g, 49.712 mmol). The mixture was allowed to stir for 30 minutes and slowly warm to room temperature. The solution was filtered and washed with 1 : 1 conc. HCl/H_2O (100 mL) and H_2O to give a crude product. The crude solid was then chromatographed over silica 1 : 5 EtOAc : Hex and crystallized from hexanes to afford the product (6.285 g, 68% yield) as a yellow-orange solid. Analytical data for compound **3.72** was identical to literature reported values.[176]

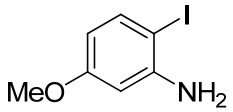

3.73

The known compound 2-iodo-5-methoxyaniline (**3.73**) was prepared according to a modified literature procedure.[176] To a solution of 1-iodo-4-methoxy-2-nitroaniline (4.772 g, 17.100 mmol), Iron (III) chloride hexahydrate (0.071 g, 0.261 mmol), and activated carbon (0.037 g, 3.078 mmol) at reflux in MeOH (70 mL) was added

hydrazine monohydrate (2.634 g, 34.202 mmol) dropwise. After the addition of hydrazine, the solution was allowed to reflux for 6.5 h. The solution was then filtered through celite, and the solvent removed under reduced pressure. The crude oil was then taken in DCM, washed with water and brine, dried, and then the dichloromethane removed under reduced pressure. The crude product was then chromatographed over silica (5 : 95 EtOAc : Hex) to afford the product (3.692 g, 87%) as an unstable light brown solid which needed to be stored in the dark at low temperature. Analytical data for compound **3.73** was identical to literature reported values.[176]

General Experimental Procedure for Triflation of Iodo-anilines:

To a solution of the iodo-aniline (1.0 equiv.) and triethylamine (1.1 equiv.) in dichloromethane was added triflic anhydride (1.1 equiv.) at 0^{o}C. The reaction was stirred for 10 minutes at that temperature and then allowed to warm to room temperature. After the reaction was complete via TLC monitoring, the crude reaction mixture was added to a separatory funnel and extracted thrice with dichlormethane. The dichloromethane extracts were dried over $MgSO_4$ and the solvent removed under reduced pressure to give a crude product. This product was then chromatographed on silica, eluting with hexanes/EA mixtures to give the products.

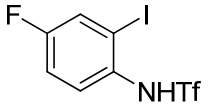

3.74

1,1,1-trifluoro-*N*-(4-fluoro-2-iodophenyl)methanesulfonamide (**3.74**) was prepared according to a modified literature procedure.[177] 2-iodo-4-fluoroaniline (3.284 g, 13.856 mmol), triethylamine (1.541 g, 15.242 mmol), and triflic anhydride (4.300 g, 15.242 mmol) were treated according to the general procedure described above, eluting with 1 : 9 EtOAc : Hex to afford 1,1,1-trifluoro-N-(4-fluoro-2-iodophenyl)methanesulfonamide (2.748 g, 54%) as an orange oil that solidified at room temperature: mp = 59 - 62 °C; R_f = 0.32 (1:1 Hex/EA); ^{1}H NMR (400 MHz, $CDCl_3$) δ 7.58 (dd, *J* = 7.6 Hz, 2.8 Hz, 1 H), 7.54 (dd, *J* = 8.8 Hz, 4.8 Hz, 1 H), 7.13 (m, 1 H), 6.33 (br s, 1 H); ^{13}C NMR (125 MHz, $CDCl_3$) δ 160.7 (d, $J(^{13}C - ^{19}F)$ = 251.3 Hz), 132.0 (d, $J(^{13}C - ^{19}F)$ = 3.5 Hz), 126.7 (d, $J(^{13}C - ^{19}F)$ = 30.5 Hz), 126.1 (d, $J(^{13}C - ^{19}F)$ = 8.6 Hz), 119.7 (q, $J(^{13}C - ^{19}F)$ = 320.5 Hz), 116.7 (d, $J(^{13}C - ^{19}F)$ = 22.4 Hz), 94.3 (d, $J(^{13}C - ^{19}F)$ = 8.6 Hz); ^{19}F NMR (376 MHz, $CDCl_3$) δ -74.3 (s, 3 F), -110.4 (m, 1 F); IR (thin film, cm^{-1}) 1140; HRMS (ES^-) calcd for $C_7H_3F_4INO_2S$ (M – H+), 367.8866; found, 367.8871.

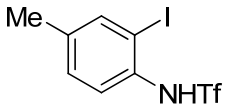

3.75

1,1,1-trifluoro-*N*-(2-iodo-4-methylphenyl)methanesulfonamide (**3.75**) was prepared according to a modified literature procedure.[177] 2-iodo-4-methylanililne (1.039 g, 4.457 mmol), triethylamine (0.496 g, 4.903 mmol), and triflic anhydride (1.383 g, 4.903 mmol) were treated according to the general procedure described above, eluting with 1 : 9 EtOAc : Hex to give 1,1,1-trifluoro-N-(2-iodo-4-methylphenyl)methanesulfonamide (0.784 g, 48%) as a yellow oil that solidified at room temperature to afford a yellow solid: mp = 64 - 65 °C; R_f = 0.60 (1:1 Hex/EA); ^{1}H NMR (500 MHz, $CDCl_3$) δ 7.68 (s, 1 H), 7.45 (d, J = 8.5 Hz, 1 H), 7.17 (d, J = 8.0 Hz, 1 H), 2.32 (s, 3 H); ^{13}C NMR (125 MHz, $CDCl_3$) δ 139.9, 139.3, 132.9, 130.5, 123.9, 119.7 (q, J(^{13}C – ^{19}F) = 321.1 Hz), 93.4, 20.4; ^{19}F NMR (376 MHz, $CDCl_3$) δ -74.2 (s, 3 F); IR (thin film, cm^{-1}) 1140; HRMS (ES$^-$) calcd for $C_8H_6F_3INO_2S$ (M – H+), 363.9116; found, 363.9118.

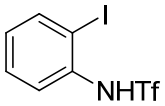

3.76

The known compound 1,1,1-trifluoro-*N*-(2-iodophenyl)methanesulfonamide (**3.76**) was prepared according to a modified literature procedure.[177] 2-iodoaniline (3.328 g, 15.196 mmol), triethylamine (1.690 g, 16.715 mmol), and triflic anhydride (4.716 g,

16.715 mmol) were treated according to the general procedure described above, eluting with 1 : 9 EtOAc : Hex to give the product (2.026 g, 38%) as an orange oil. Analytical data for compound **3.76** was identical to literature reported values.[177]

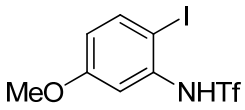

3.77

1,1,1-trifluoro-*N*-(2-iodo-5-methoxyphenyl)methanesulfonamide (**3.77**) was prepared according to a modified literature procedure.[177] 2-iodo-5-methoxyaniline (3.567 g, 14.333 mmol), triethylamine (1.594 g, 15.767 mmol), and triflic anhydride (4.448 g, 15.767 mmol) were treated according to the general procedure described above, eluting with 1 : 19 EtOAc : Hex to give the product (1.929 g, 35%) as a pale orange oil that solidified at room temperature: mp = 61 - 62 $^{\circ}$C; R_f = 0.33 (4:1 Hex/EA); ^{1}H NMR (500 MHz, $CDCl_3$) δ 7.88 (dd, J = 8.5 Hz, 2.5 Hz, 1 H), 6.99 (s, 1 H), 6.84 (dt, J = 9.0 Hz, 3.0 Hz, 1 H), 3.83 (s, 3 H); ^{13}C NMR (125 MHz, $CDCl_3$) δ 160.3, 141.7, 135.9, 119.3 (q, J(^{13}C – ^{19}F) = 320.0 Hz), 119.1, 118.9, 89.7, 55.9; ^{19}F NMR (376 MHz, $CDCl_3$) δ -75.4 (s, 3 F); IR (thin film, cm^{-1}) 1126; HRMS (ES$^-$) calcd for $C_8H_6F_3INO_3S$ (M – H+), 379.9065; found, 363.9077.

General Experimental Procedure for Alkylation of triflamides:

To a solution of the triflamide (1.0 equiv.) in DMF was added 60% NaH (dispersion in mineral oil, 1.3 equiv.) in small portions at 0°C. The solution was then allowed to warm to room temperature, where it was stirred for 0.5 h followed by dropwise

addition of ethyl bromoacetate (1.4 equiv.). The reaction was allowed to stir for 8 h at room temperature. Methanol (3 mL) was added, and the mixture was poured into water (30 mL) extracted with ethyl acetate (3 × 30 mL), and dried (Na_2SO_4) to afford a crude product, which was purified by flash chromatography over silica eluting with EtOAc/Hexanes mixtures to afford the products.

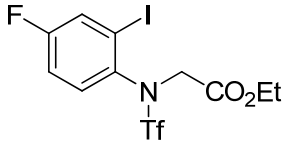

3.78

Ethyl 2-(1,1,1-trifluoro-*N*-(4-fluoro-2-iodophenyl)methylsulfonamido)acetate (**3.78**) was prepared according to a modified literature procedure.[131] 1,1,1-trifluoro-*N*-(2-iodo-4-fluorophenyl)methanesulfonamide (2.209 g, 5.984 mmol), DMF (6 mL), 60% NaH (0.311 g, 7.78 mmol), and ethyl bromoacetate (1.399 g, 8.378 mmol) were treated according to the general procedure described above, eluting with 1 : 9 EtOAc : Hex to give the product (2.334 g, 86%) as a pale orange oil: R_f = 0.56 (4:1 Hex/EA); ^{1}H NMR (500 MHz, $CDCl_3$) δ 7.83 (dd, *J* = 9.0 Hz, 5.5 Hz, 1 H), 7.63 (dd, *J* = 7.5 Hz, 3.0 Hz, 1 H), 7.12 (ddd, *J* = 9.0 Hz, 7.5 Hz, 3.0 Hz, 1 H), 4.77 (d, *J* = 18.5 Hz, 1 H), 4.20 (m, 3 H), 1.27 (t, *J* = 7.0 Hz, 3 H); ^{13}C NMR (125 MHz, $CDCl_3$) δ 167.2, 162.1 (d, $J(^{13}C - ^{19}F)$ = 254.6 Hz), 136.1 (d, $J(^{13}C - ^{19}F)$ = 12.0 Hz), 134.2, 127.2 (d, $J(^{13}C - ^{19}F)$ = 25.0 Hz), 119.6 (q, $J(^{13}C - ^{19}F)$ = 320.4 Hz), 116.3 (d, $J(^{13}C - ^{19}F)$ = 22.1 Hz), 62.1, 53.1, 14.0 (some signals account for more than one carbon); NMR (376 MHz, $CDCl_3$) δ -73.7 (s, 3 F), -107.5 (s, 1 F); IR (thin film, cm^{-1}) 1755, 1146; HRMS (FAB^+) calcd for $C_{11}H_{11}F_4INO_4S$ (M + H+), 455.9389; found, 455.9394.

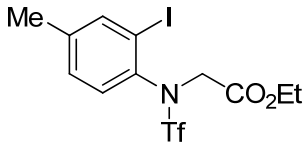

3.79

Ethyl 2-(1,1,1-trifluoro-*N*-(2-iodo-4-methylphenyl)methylsulfonamido)acetate (**3.79**) was prepared according to a modified literature procedure.[131] 1,1,1-trifluoro-*N*-(2-iodo-4-methylphenyl)methanesulfonamide (1.033 g, 2.830 mmol), DMF (3 mL), 60% NaH (0.147 g, 3.679 mmol), and ethyl bromoacetate (0.662 g, 3.962 mmol) were treated according to the general procedure described above, eluting with 1 : 9 EtOAc : Hex to give the product (1.168 g, 91%) as a yellow oil: R_f = 0.56 (4:1 Hex/EA); ^{1}H NMR (500 MHz, $CDCl_3$) δ 7.8 (s, 1 H), 7.69 (d, J = 8.5 Hz), 7.20 (d, J = 8.5 Hz), 4.77 (d, J = 18.5 Hz), 4.26 – 4.15 (m, 3 H), 2.32 (s, 3 H), 1.27 (t, J = 7.0 Hz, 3 H); ^{13}C NMR (125 MHz, $CDCl_3$) δ 167.2, 141.9, 140.7, 137.2, 132.5, 130.0, 119.6 (q, J(^{13}C – ^{19}F) = 320.4 Hz), 99.3, 61.9, 53.1, 20.5, 13.9; ^{19}F NMR (376 MHz, $CDCl_3$) δ -74.9 (s, 1 F); IR (thin film, cm^{-1}) 1757, 1146; HRMS (ES$^+$) calcd for $C_{12}H_{13}F_3INO_4SNa$ (M + Na), 473.9460; found, 473.9462.

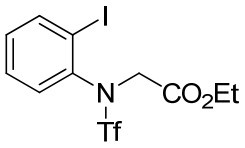

3.80

Ethyl 2-(1,1,1-trifluoro-*N*-(2-iodophenyl)methylsulfonamido)acetate (**3.80**) was prepared according to a modified literature procedure.[131] 1,1,1-trifluoro-N-(2-iodophenyl)methanesulfonamide (1.5026 g, 4.280 mmol), DMF (4 mL), 60% NaH

(0.222 g, 5.564 mmol), and ethyl bromoacetate (1.000 g, 5.992 mmol) were treated according to the general procedure described above, eluting with 1 : 9 EtOAc : Hex to give the product (1.292 g, 69%) as a pale orange oil. Analytical data for compound **3.80** was identical to literature reported values.[131]

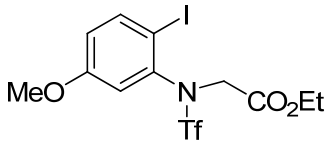

3.81

Ethyl 2-(1,1,1-trifluoro-*N*-(2-iodo-5-methoxyphenyl)methylsulfonamido)acetate (**3.81**) was prepared according to a modified literature procedure.[131] 1,1,1-trifluoro-*N*-(2-iodo-5-methoxyphenyl)methanesulfonamide (1.867 g, 4.897 mmol), DMF (5 mL), 60% NaH (0.255 g, 6.367 mmol), and ethyl bromoacetate (1.145 g, 6.856 mmol) were treated according to the general procedure described above, eluting with 1 : 19 EtOAc : Hex to give the product (1.780 g, 78%) as a pale orange oil: R_f = 0.26 (4:1 Hex/EA); ^{1}H NMR (500 MHz, $CDCl_3$) δ 7.75 (d, J = 9.0 Hz, 1 H), 7.42 (d, J = 2.5 Hz, 1 H), 6.73 (dd, J = 8.5 Hz, 2.5 Hz, 1 H), 4.78 (d, J = 18.5 Hz, 1 H), 4.26 – 4.16 (m, 3 H), 3.81 (s, 3 H), 1.28 (t, J = 7.5 Hz, 3 H); ^{13}C NMR (125 MHz, $CDCl_3$) δ 167.3, 160.3, 140.5, 140.3, 119.7 (q, J(^{13}C – ^{19}F) = 320.4 Hz), 119.0, 117.8, 87.5, 62.0, 55.7, 53.1, 14.0; ^{19}F NMR (376 MHz, $CDCl_3$) δ -73.7 (s, 1 F); IR (thin film, cm^{-1}) 1755, 1146; HRMS ES$^+$) calcd for $C_{12}H_{13}F_3INO_5SNa$ (M + Na), 489.9409; found, 489.9386.

General Experimental Procedure for Oxidative addition of Aryl Iodides with Pd_2dba_3:

To a solution of tris(dibenzylideneacetone)dipalladium(0) (Pd_2dba_3) (0.5 equiv.) and aryl iodide (1.2 equiv.) in benzene (40 mL/mmol Pd) was added tetramethylethylenediamine (TMEDA) (1.5 equiv.). The mixture was stirred at 60°C for 1 h. The suspension was filtered through a plug of Celite, and the solvents removed under reduced pressure to give a crude product. The crude product was purified by flash chromatography over neutral alumina eluting with ether/hexanes (1 : 1) to remove excess dibenzylideneacetone (dba) and subsequently with ether/hexanes (2 : 1) to afford the palladium(II) complexes as yellow solids.

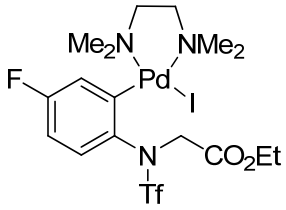

3.82

(*N*-Ethoxycarbonylmethyl)-(*N*-trifluoromethanesulfonyl)-6-amino-3-fluorophenyl]iodo(tetramethylethylenediamine)-palladium (**3.82**) was prepared according to a modified literature procedure.[131] Ethyl 2-(1,1,1-trifluoro-*N*-(2-iodo-4-fluorophenyl)methylsulfonamido)acetate (2.002 g, 4.399 mmol), Pd_2dba_3 (1.678 g, 1.833 mmol), and TMEDA (0.639 g, 5.499 mmol) were treated according to the procedure above affording the product (1.380 g, 56%) as a yellow powder: mp = 150 – 151°C (dec.); R_f = 0.55 (hexanes : EA 1 : 2); ^{1}H NMR (500 MHz, $CDCl_3$) δ 7.40 (dd, *J* = 8.5 Hz, 5.5 Hz, 1 H), 7.12 (dd, *J* = 9.0 Hz, 3.0 Hz, 1 H), 6.56 (td, *J* = 8.5 Hz,

3.0 Hz, 1 H), 5.32 (d, J = 19.0 Hz, 1 H), 4.76 (d, J = 19.0 Hz, 1 H), 4.19 – 4.12 (m, 2 H), 3.10 – 3.04 (m, 1 H), 2.76 (s, 3 H), 2.75 (s, 3 H), 2.74 – 2.68 (m, 1 H), 2.65 (s, 3 H), 2.45 – 2.40 (m, 2 H), 2.14 (s, 3 H), 1.23 (t, J = 7.5 Hz, 3 H); ^{13}C NMR (125 MHz, $CDCl_3$) δ 168.3, 159.6 (d, $J(^{13}C - ^{19}F)$ = 251.3 Hz), 145.5 (d, $J(^{13}C - ^{19}F)$ = 5.0 Hz), 139.3 (d, $J(^{13}C - ^{19}F)$ = 2.5 Hz), 130.8 (d, $J(^{13}C - ^{19}F)$ = 9.0 Hz), 123.1 (q, $J(^{13}C - ^{19}F)$ = 120.0 (q, $J(^{13}C - ^{19}F)$ = 322.5 Hz), 110.8 (d, $J(^{13}C - ^{19}F)$ = 22.5 Hz), 61.9, 61.4, 58.7, 55.0, 51.8, 50.5, 49.3, 48.8, 14.1; ^{19}F NMR (376 MHz, $CDCl_3$) δ -73.1 (s, 3 F), -114.5 (m, 1 F); IR (thin film, cm^{-1}) 1753, 1147; HRMS (ES^+) calcd for $C_{17}H_{27}N_3O_4IF_4SPd$ (M + H), 677.9737; found, 677.9751.

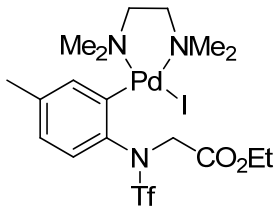

3.83

(*N*-Ethoxycarbonylmethyl)-(*N*-trifluoromethanesulfonyl)-2-amino-5-methylphenyl]iodo(tetramethylethylenediamine)-palladium (**3.83**) was prepared according to a modified literature procedure.[131] Ethyl 2-(1,1,1-trifluoro-*N*-(2-iodo-4-methylphenyl)methylsulfonamido)acetate (1.1509 g, 2.551 mmol), Pd_2dba_3 (0.973 g, 1.063 mmol), and TMEDA (0.371 g, 3.19 mmol) were treated according to the procedure above affording the product (0.962 g, 67%) as a yellow powder: mp = 152 – 154°C (dec.); R_f = 0.58 (hexanes : EA 1 : 2); ^{1}H NMR (500 MHz, $CDCl_3$) δ 7.29 – 7.26 (m, 2 H), 6.67 (dd, J = 8.0 Hz, 1.5 Hz, 1 H), 5.33 (d, J = 19.5 Hz, 1 H), 4.78 (d, J

= 19.0 Hz, 1 H), 4.14 (m, 2 H), 3.07 (td, *J* = 11.0 Hz, 3.0 Hz, 1 H), 2.78 – 2.67 (m, 7 H), 2.63 (s, 3 H), 2.40 (tt, *J* = 13.0 Hz, 3.5 Hz, 2 H), 2.22 (s, 3 H), 2.09 (s, 3 H), 1.23 (t, *J* = 7.0 Hz); ^{13}C NMR (125 MHz, $CDCl_3$) δ 168.4, 141.5, 140.8, 137.7, 136.6, 129.5, 125.2, 120.1 (q, $J(^{13}C - ^{19}F)$ = 322.5 Hz), 61.8, 61.3, 58.5, 55.1, 51.7, 50.4, 49.1, 48.6, 21.0, 14.1; ^{19}F NMR (376 MHz) δ-72.0 (s, 3 F); IR (thin film, cm^{-1}) 1755, 1142; HRMS (ES^+) calcd for $C_{18}H_{30}N_3O_4IF_3SPd$ (M + H), 673.9989; found, 677.9986.

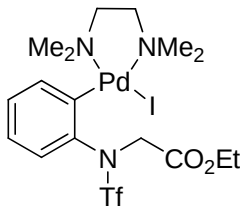

3.84

(*N*-Ethoxycarbonylmethyl)-(*N*-trifluoromethanesulfonyl)-2-aminophenyl]iodo(tetramethylethylenediamine)-palladium (**3.84**) was prepared according to a modified literature procedure.[131] Ethyl 2-(1,1,1-trifluoro-*N*-(2-iodophenyl)methylsulfonamido)acetate (1.265 g, 2.894 mmol), Pd_2dba_3 (1.104 g, 1.206 mmol), and TMEDA (0.4204 g, 3.617 mmol) were treated according to the procedure above affording the product (1.106 g, 70%) as a yellow powder. Analytical data for compound **3.84** was identical to literature reported values.[131]

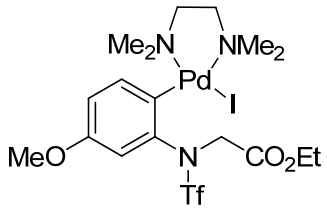

3.85

(*N*-Ethoxycarbonylmethyl)-(*N*-trifluoromethanesulfonyl)-2-amino-4-methoxyphenyl]iodo(tetramethylethylenediamine)-palladium (**3.85**) was prepared according to a modified literature procedure.[131] Ethyl 2-(1,1,1-trifluoro-*N*-(2-iodo-5-methoxyphenyl)methylsulfonamido)acetate (1.539 g, 3.294 mmol), Pd_2dba_3 (1.257 g, 1.372 mmol), and TMEDA (0.479 g, 4.117 mmol) were treated according to the procedure above affording the product (1.103 g, 58%) as a yellow powder: mp = 145 – 148°C (dec.); R_f = 0.52 (hexanes : EA 1 : 2); ^{1}H NMR (500 MHz, $CDCl_3$) δ 7.28 (d, *J* = 8.5 Hz, 1 H), 7.13 (d, *J* = 3.0 Hz, 1 H), 6.67 (dd, *J* = 8.5 Hz, 3.0 Hz, 1 H), 5.37 (d, *J* = 19.0 Hz, 1 H), 4.80 (d, *J* = 19.0 Hz, 1 H), 4.16 (m, 2 H), 3.71 (s, 3 H), 3.05 – 3.03 (m, 1 H), 2.75 (s, 3 H), 2.74 (s, 3 H), 2.72 – 2.67 (m, 1 H), 2.61 (s, 3 H), 2.46 – 2.39 (m, 2 H), 2.13 (s, 3 H), 1.24 (t, *J* = 7.0 Hz); ^{13}C NMR (125 MHz, $CDCl_3$) δ 168.4, 157.0, 143.0, 136.9, 128.4, 120.1 (q, $J(^{13}C - ^{19}F)$ = 325.0 Hz), 115.6, 114.5, 61.8, 61.3, 58.6, 55.2, 55.0, 51.7, 50.5, 49.2, 48.8, 14.1; ^{19}F NMR (376 MHz) δ-73.1 (s, 3 F); IR (thin film, cm^{-1}) 1753, 1144; HRMS (ES^+) calcd for $C_{18}H_{30}N_3O_5IF_3SPd$ (M + H), 689.9938; found, 689.9926.

General Experimental Procedure for Formation of palladacycles via base-induced ring closure:

To a solution of palladium(II) iodo complexes (1.0 equiv.) in THF (36 mL/mmol Pd) was added dropwise *t*-BuOK (1.2 equiv.). The mixture was stirred for 0.25 h at room temperature and then filtered through a plug of basic alumina eluting with EtOAc/hexanes (2 : 1 (240 mL)). The solvent was removed under reduced pressure to afford the palladacycles as white solids after trituration with ether.

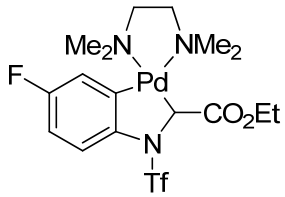

(±)-**3.86**

((±)-[(*N*-Ethoxycarbonylmethine)-(*N*-trifluoromethanesulfonyl)3-fluoro-aza-1,6-phenylene] (tetramethylethylenediamine)palladium ((±)-**3.86)** was prepared according to a modified literature procedure.[131] (*N*-Ethoxycarbonylmethyl)-(*N*-trifluoromethanesulfonyl)-6-amino-3-fluorophenyl]iodo(tetramethylethylenediamine)-palladium (0.751 g, 1.107 mmol) and t-BuOK (1.0 M in THF, 1.33 mL, 1.33 mmol) were treated according to the procedure above affording the product (0.575 g, 94%) as a white powder: mp = 186 – 187°C (dec.); R_f = 0.26 (hexanes : EA 1 : 2); ^{1}H NMR (500 MHz, $CDCl_3$) δ 7.22 (br s, 1 H), 6.71 (dd, *J* = 9.25 Hz, 2.5 Hz, 1 H), 6.65 (td, *J* = 9.0 Hz, 3.0 Hz, 1 H), 5.05 (s, 1 H), 4.00 (q, *J* = 7.0 Hz, 2 H), 2.79 (s, 3 H), 2.78 (s, 3 H), 2.73 – 2.68 (m, 1 H), 2.67 – 2.60 (m, 8 H), 2.56 – 2.49 (m, 1 H), 1.09 (t, *J* = 7.0 Hz); ^{13}C NMR (125 MHz, $CDCl_3$)

δ 175.0, 159.6, 157.6, 149.7, 144.7, 120.3 (q, $J(^{13}C - ^{19}F)$ = 326.3 Hz), 119.4 (d, $J(^{13}C - ^{19}F)$ = 18.8 Hz), 116.9, 111.0 (d, $J(^{13}C - ^{19}F)$ = 23.8 Hz), 61.1, 60.1, 59.7, 50.6, 50.0, 49.5, 48.8, 14.1; ^{19}F NMR (376 MHz) δ-73.0 (br s, 3 F), -119.1 (br s, 1 H); IR (thin film, cm^{-1}) 1710, 1146; HRMS (ES^+) calcd for $C_{17}H_{26}N_3O_4F_4SPd$ (M + H), 550.0615; found, 550.0623.

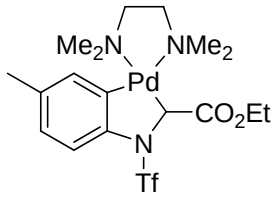

(±)-**3.87**

((±)-[(*N*-Ethoxycarbonylmethine)-(*N*-trifluoromethanesulfonyl)5-methyl-aza-1,2-phenylene] (tetramethylethylenediamine)palladium ((±)-**3.87)** was prepared according to a modified literature procedure.[131] (*N*-Ethoxycarbonylmethyl)-(*N*-trifluoromethanesulfonyl)-2-amino-5-methylphenyl]iodo(tetramethylethylenediamine)-palladium (0.752 g, 1.116 mmol) and *t*-BuOK (1.0 M in THF, 1.34 mL, 1.34 mmol) were treated according to the general procedure above, affording the product (0.529 g, 87%) as a white powder: mp = 183 – 185°C (dec); R_f = 0.55 (hexanes : EA 1 : 2); ^1H NMR (500 MHz, $CDCl_3$) δ 7.18 (br s, 1 H), 6.83 (s, 1 H), 6.78 (dd, *J* = 8.0 Hz, 1.0 Hz, 1 H), 4.02 (m, 2 H), 2.82 (s, 3 H), 2.78 (s, 3 H), 2.69 – 2.59 (m, 9 H), 2.56 – 2.49 (m, 1 H), 2.23 (s, 3 H), 1.11 (t, *J* = 7.0 Hz); ^{13}C NMR (125 MHz, $CDCl_3$) δ 175.4, 151.4, 141.2, 133.9 (2 C), 132.1, 125.6, 120.3 (q, $J(^{13}C - ^{19}F)$ = 323.8 Hz), 116.0, 61.2, 60.0, 59.6, 50.7, 49.9,

49.5, 48.8, 21.3, 14.1; ^{19}F NMR (376 MHz) δ-73.0 (br s, 3 F); IR (thin film, cm^{-1}) 1712, 1134; HRMS (ES^{+}) calcd for $C_{18}H_{29}N_3O_4F_3SPd$ (M + H), 546.0866; found, 550.0825.

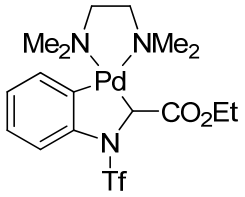

(±)-**3.88**

((±)-[(*N*-Ethoxycarbonylmethine)-(*N*-trifluoromethanesulfonyl)aza-1,2-phenylene] (tetramethylethylenediamine)palladium ((±) **3.88**) was prepared according to a modified literature procedure.[131] (*N*-Ethoxycarbonylmethyl)-(*N*-trifluoromethanesulfonyl)-2-aminophenyl]iodo(tetramethylethylenediamine)-palladium (0.740 g, 1.122 mmol) and *t*-BuOK (1.0 M in THF, 1.35 mL, 1.35 mmol) were treated according to the procedure above affording the product (0.497 g, 83%) as a white solid. Analytical data for compound (±)-**3.88** was identical to literature reported values.[131]

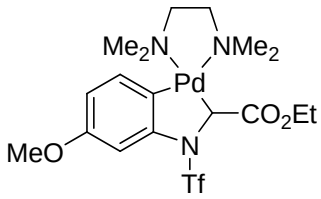

(±)-**3.89**

((±)-[(*N*-Ethoxycarbonylmethine)-(*N*-trifluoromethanesulfonyl)4-methoxy-aza-1,6-phenylene] (tetramethylethylenediamine)palladium ((±)-**3.89)** was prepared according to a modified literature procedure.[131] (*N*-Ethoxycarbonylmethyl)-(*N*-

trifluoromethanesulfonyl)-2-amino-4-methoxyphenyl]iodo(tetramethylethylenediamine)-palladium (0.759 g, 1.100 mmol) and *t*-BuOK (1.0 M in THF, 1.32 mL, 1.32 mmol) were treated according to the procedure above affording the product (0.539 g, 95%) as a white solid: mp = 175 – 177°C (dec); R_f = 0.23 (hexanes : EA 1 : 2); ^{1}H NMR (500 MHz, $CDCl_3$) δ 6.97 (br s, 1 H), 6.91 (d, *J* = 8.5 Hz, 1 H), 6.48 (dd, *J* = 8.3 Hz, 1.5 Hz, 1 H), 4.01 (q, *J* = 7 Hz, 2 H), 3.74 (s, 3 H), 2.78 (s, 3 H), 2.76 (s, 3 H), 2.71 – 2.67 (m, 1 H), 2.65 – 2.58 (m, 8 H), 2.52 – 2.48 (m, 1 H), 1.11 (t, *J* = 7.5 Hz); ^{13}C NMR (125 MHz, $CDCl_3$) δ 175.4, 157.4, 153.9, 133.0, 130.7, 120.3 (q, $J(^{13}C - ^{19}F)$ = 325.0 Hz), 109.1, 103.0, 61.2, 60.0, 59.6, 55.2, 50.6, 49.9, 49.7, 49.0, 48.6, 14.1; ^{19}F NMR (376 MHz) δ-73.7 (br s, 3 F); IR (thin film, cm^{-1}) 1711, 1126; HRMS (ES^+) calcd for $C_{18}H_{29}N_3O_5F_3SPd$ (M + H), 562.0815; found, 562.0807.

General Experimental Procedure for Synthesis of Polymer-Supported Palladacycles 3.31 – 3.34:

A suspension of the phosphine resin and the palladacycle in THF was stirred for an initial time period (6.5 to 8 hours) under argon. Volatile components were removed under reduced pressure (1 mmHg, 1 h). Fresh THF was added, and the resulting suspension was stirred for the second time period (10 – 16 h). The suspension was filtered, and the resin was washed with methanol (20mL), DCM (20 mL), methanol (20 mL), DCM (20mL), and ether (20mL) then dried under reduced pressure to give

the polymer-supported palladacycles as yellow powdery solids. The filtrates were evaporated, and the crude extracts were analyzed by ^{1}H NMR spectroscopy.

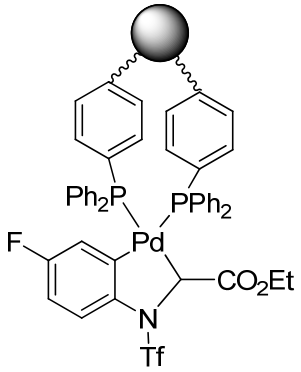

3.31

Treatment of ((±)-[(*N*-Ethoxycarbonylmethine)-(*N*-trifluoromethanesulfonyl)3-fluoro-aza-1,6-phenylene] (tetramethylethylenediamine)palladium ((±)-**3.86**) (0.502 g, 0.912 mmol) and phosphine resin **3.90** (1.6 mmol P/g, 1.140 g, 1.824 mmol P) were treated according to the procedure above, affording the product (1.222 g, 63%) as a yellow powdery solid. ICP analyses: 5.0% mass Pd, 4.1% mass P. The material in the combined filtrates (0.114 g) and contained >95% palladacycle (±)-**3.86** (23% mol Pd).

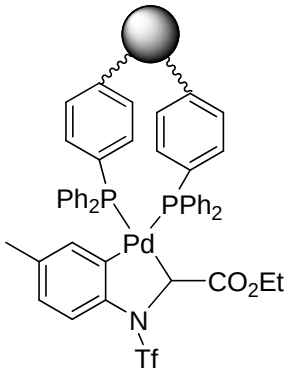

3.32

((±)-[(*N*-Ethoxycarbonylmethine)-(*N*-trifluoromethanesulfonyl)5-methyl-aza-1,2-phenylene] (tetramethylethylenediamine)palladium ((±)-**3.87**) (0.495 g, 0.907 mmol) and phosphine resin **3.90** (1.6 mmol P/g, 1.133 g, 1.813 mmol P) were treated according to the procedure above, affording the product (1.411 g, 77%) as a yellow powdery solid. ICP analyses: 5.3% mass Pd, 4.3% mass P. The material in the combined filtrates (0.122 g) and contained >95% palladacycle (±)-**3.87** (25% mol Pd).

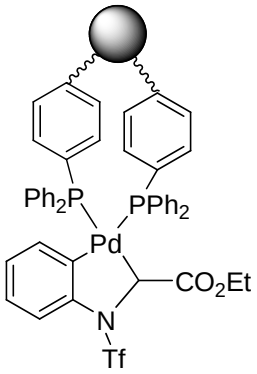

3.33

((±)-[(*N*-Ethoxycarbonylmethine)-(*N*-trifluoromethanesulfonyl)aza-1,2-phenylene] (tetramethylethylenediamine)palladium ((±) **3.88**) (0.456 g, 0.857 mmol), and phosphine resin **3.90** (1.6 mmol P/g, 1.072 g, 1.715 mmol P) were treated according to the procedure above, affording the product (1.323 g, 65%) as a yellow powdery solid. ICP analyses: 4.5% mass Pd, 4.0% mass P. The material in the combined filtrates (0.105 g) and contained >95% palladacycle (±)-**3.88** (23% mol Pd).

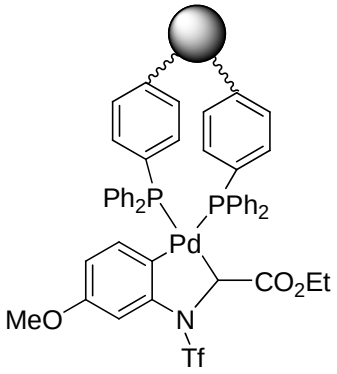

3.34

((±)-[(*N*-Ethoxycarbonylmethine)-(*N*-trifluoromethanesulfonyl)4-methoxy-aza-1,6-phenylene] (tetramethylethylenediamine)palladium ((±)-**3.89)** (0.467 g, 0.831 mmol) and phosphine resin **3.90** (1.6 mmol P/g, 1.038 g, 1.661 mmol P) were treated according to the procedure above, affording the product (1.189 g, 75%) as a yellow powdery solid; ICP analyses: 5.6% mass Pd, 4.2% mass P. The material in the combined filtrates (0.065 g) and contained >95% palladacycle (±)-**3.89** (14% mol Pd).

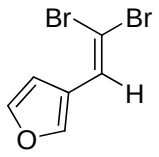

3.91

3-(2,2-dibromovinyl)furan (**3.91**) was prepared according to a modified literature procedure.[179] To a slurry of zinc dust (1.387 g, 21.216 mmol) in DCM (10 mL) at 0°C a solution of carbon tetrabromide (7.036 g, 21.216 mmol) in DCM (10 mL) was added dropwise. After 30 minutes of stirring, a solution of triphenylphosphine (5.567 g, 21.216 mmol) in DCM (7 mL) was added dropwise. The resulting solution was allowed to stir for six hours and allowed to warm to room temperature. The solution was again cooled to 0°C, and a solution of 3-furaldehyde (1.113 g, 11.813 mmol) in DCM (5 mL) was added dropwise. The solution was then stirred for 13 hours, slowly warming to room temperature. To the crude reaction mixture was added 50 mL pentane, which caused a dark substance to precipitate. The liquid was decanted, and the procedure repeated four more times. The pentane solvent was removed under reduced pressure to give an oil, which was then chromatographed over silica eluting with 5 : 95 EtOAc : Hex to afford the product (2.261 g, 76%) as a yellow oil. The compound is known to be metastable and thus was used immediately in the next reaction. Analytical data for compound **3.91** was identical to literature reported values.[179]

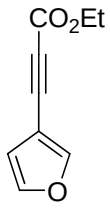

3.35

Known compound ethyl 3-(furan-3-yl)propiolate (**3.35**) was prepared according to a modified literature procedure.[179] To a solution of 3-(2,2-dibromovinyl)furan (2.261 g, 8.976 mmol) in THF (23 mL) was added dropwise *n*-BuLi (1.6 M in hexanes, 11.8 mL, 18.880 mmol) at -78°C. After 30 min stirring at this temperature, ethyl chloroformate (3.410 g, 31.415 mmol) was added in one portion. After 15 min, the cold bath was removed and the solution was stirred for an additional 10 min before the reaction was quenched with saturated NH_4Cl (15 mL), extracted with ether (3 × 50 mL), and dried (Na_2SO_4). The solvents were removed to afford a crude product, which was then chromatographed on silica eluting with 1 : 19 EtOAc : Hex to afford the product (0.766 g, 52%) as a pale yellow oil. Analytical data for compound **3.35** was identical to literature reported values.[206]

General Procedure for Synthesis of alkynes 3.36 to 3.40

To a solution of the terminal alkyne (1.0 equiv.) at -78°C in THF was added *n*-BuLi (1.2 equiv., 1.6 M in hexanes). The resulting solution was allowed to stir for 1 h at this temperature, and then ethyl chloroformate (1.8 equiv.) was added in one portion. The reaction was then poured into water (30 mL), extracted with hexanes (3 × 30 mL), the organic portion dried (Na_2SO_4), and the solvents removed under reduced

pressure to afford a crude product, which was then purified by flash chromatography over silica eluting with ethyl acetate/hexanes mixtures to give the products.

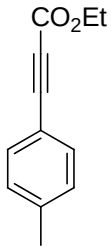

3.36

Known compound ethyl 3-*p*-tolylpropiolate (**3.36**) was prepared according to a modified literature procedure.[207] 4-ethynyltoluene (0.458 g, 3.943 mmol) was treated according to the general procedure described above (using 20 mL THF) with *n*-BuLi (3.0 mL, 4.800 mmol), followed by ethyl chloroformate (0.770 g, 7.097 mmol). The crude product was purified using 3 : 97 EtOAc : Hex as eluent to afford the product (0.763 g, 100%) as an orange oil. Analytical data for compound **3.36** was identical to literature reported values.[208]

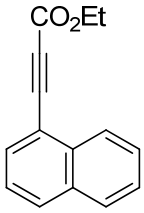

3.37

Ethyl 3-(naphthalen-1-yl)propiolate (**3.37**) was prepared according to a modified literature procedure.[207] 1-ethynylnaphthalene (0.535 g, 3.515 mmol) was treated according to the general procedure described above (using 18 mL THF) with *n*-BuLi (2.6 mL, 4.160 mmol), followed by ethyl chloroformate (0.687 g, 6.328 mmol). The

crude product was purified using 3 : 97 EtOAc : Hex as eluent to afford the product (0.659 g, 84%) as a yellow oil: R_f = 0.30 (hexanes : EA 4 : 1); ^{1}H NMR (500 MHz, $CDCl_3$) δ); ^{1}H NMR (500 MHz, $CDCl_3$) δ 8.34 (d, *J* = 8.0 Hz, 1 H), 7.95 (d, *J* = 8.5 Hz, 1 H), 7.88 (d, *J* = 8.5 Hz, 1 H), 7.85 (d, *J* = 7.0 Hz, 1 H), 4.36 (q, *J* = 7.0 Hz, 2 H), 1.40 (t, *J* = 7.5 Hz, 3 H); ^{13}C NMR (125 MHz, $CDCl_3$) δ 154.2, 133.6, 133.0, 131.3, 128.4, 127.6, 126.9, 125.8, 125.1, 117.2, 85.3, 84.4, 62.1, 14.1; IR (thin film, cm^{-1}) 2208, 1712; HRMS (ES^+) calcd for $C_{15}H_{13}O_2$ (M + H), 225.0916; found, 225.0901.

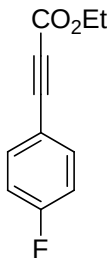

3.38

Known compound ethyl 3-(4-fluorophenyl)propiolate (**3.38**) was prepared according to a modified literature procedure.[207] 1-ethynyl-4-fluoro-benzene (0.524 g, 4.362 mmol) was treated according to the general procedure described above (using 22 mL THF) with *n*-BuLi (3.3 mL, 5.280 mmol), followed by ethyl chloroformate (0.852 g, 7.852 mmol). The crude product was purified using 3 : 97 EtOAc : Hex as eluent to afford the product (0.684 g, 82%) as a beige solid. Analytical data for compound **3.38** was identical to literature reported values.[209]

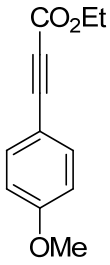

3.39

Known compound ethyl 3-(4-methoxyphenyl)propiolate (**3.39**) was prepared according to a modified literature procedure.[207] 4-ethynylanisole (0.510 g, 3.856 mmol) was treated according to the general procedure described above (using 20 mL THF) with *n*-BuLi (2.9 mL, 4.640 mmol), followed by ethyl chloroformate (0.852 g, 7.85 mmol). The crude product was purified using 5 : 95 EtOAc : Hex as eluent to afford the product (0.832 g, 100%) as a pale yellow oil. Analytical data for compound **3.39** was identical to literature reported values.[210]

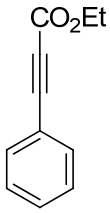

3.40

Known compound ethyl 3-phenylpropiolate **(3.40**) was prepared according to a modified literature procedure.[207] Phenylacetylene (0.465 g, 4.553 mmol) was treated according to the general procedure described above (using 23 mL THF) with *n*-BuLi (3.4 mL, 5.440 mmol), followed by ethyl chloroformate (0.889 g, 8.195 mmol). The crude product was purified using 5 : 95 EtOAc : Hex as eluent to afford the product

(0.755 g, 95%) as a pale yellow oil. Analytical data for compound **3.40** was identical to literature reported values.[211]

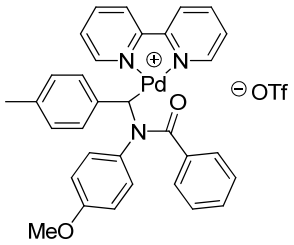

(±)-**4.22**

To a stirred solution of (E)-4-methoxy-N-(4-methylbenzylidene)aniline (0.462 g, 2.049 mmol) in acetonitrile (5 mL) was added neat benzoyl chloride (0.288 g, 2.049 mmol) to afford a bright yellow solution, which was stirred for 15 min at rt under argon. Acetonitrile (35 mL) was added followed by Pd_2dba_3 (1.032 g, 1.127 mmol) and 2,2'-bipyridyl (0.640 g, 4.099 mmol), and the reaction mixture was stirred for one hour. Silver trifluoromethanesulfonate (0.632 g, 2.459 mmol) was added, and the reaction mixture was allowed to stir for an additional 1 h. The acetonitrile was removed *in vacuo*, and then the residue was dissolved in dichloromethane and filtered through celite to give an orange solution. The dichloromethane was removed under reduced pressure, and the residue triturated with ether to give an orange solid as a crude product which was then purified by flash chromatography over silica eluting with dichloromethane/acetonitrile (3 : 1) to afford complex (±)-**4.22** (0.395 g, 26%) as a pale yellow solid: mp = 175 - 180°C (dec.); R_f = 0.33 (4 : 1 DCM/CH_3CN); ^{1}H NMR (500 MHz, CD_3CN) δ 8.68 (d, J = 5.0 Hz, 1 H), 8.62 (d, J = 4.5 Hz, 0.2 H),

8.30 (d, J = 8.0 Hz, 0.2 H), 8.22 (d, J = 5.0 Hz, 1 H), 8.18 (d, J = 8.0 Hz, 1 H), 8.16 – 8.12 (m, 2 H), 8.06 (td, J = 8.0 Hz, 1.5 Hz, 1 H), 7.99 (t, J = 8.0 Hz, 0.2 H), 7.67 (td, J = 6.0 Hz, 1.0 Hz, 1 H), 7.54 – 7.48 (m, 5.4 H), 7.38 (d, J = 8.0 Hz, 2 H), 7.09 (d, J = 8.0 Hz, 2 H), 6.94 (d, J = 8.5 Hz, 2 H), 6.71 (d, J = 9.0 Hz, 2 H), 5.70 (s, 1 H), 3.70 (s, 3 H), 2.15 (s, 3 H); ^{13}C NMR (125 MHz, CD_3CN) δ 180.2, 160.6, 157.6, 154.0, 152.2, 151.7, 149.9, 142.2, 142.1, 140.0, 138.5, 134.3, 133.3, 132.4, 130.9, 130.8, 129.8, 129.7, 128.9, 128.8, 125.0, 124.3, 122.6 (q, J(^{13}C – ^{19}F) = 320.8 Hz), 115.5, 72.8, 56.6, 21.6 several signals account for more than one carbon; ^{19}F NMR (376 MHz) δ −77.2 (s, 3 F); IR (thin film, cm^{-1}) 1585, 1155 ; HRMS (ES$^+$) calcd for $C_{32}H_{28}N_3O_2Pd$ [(M−CF_3SO_3)$^+$], 592.1216; found, 550.1218.

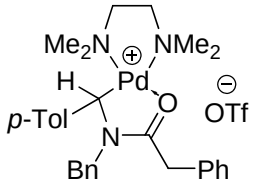

(±)-**4.37**

To a stirred solution of (*E*)-*N*-(4-methylbenzylidene)-1-phenylmethanamine (0.733 g, 3.503 mmol) in acetonitrile (5 mL) was added neat phenyl acetyl chloride (0.541 g, 3.503 mmol) to afford a pale yellow solution, which was stirred for 15 min at rt under argon. Acetonitrile (25 mL) was added, followed by Pd_2dba_3 (0.529 g, 0.578 mmol), and the reaction mixture was allowed to stir for additional 10 min. Neat TMEDA (0.814 g, 7.006 mmol) was added, and the reaction mixture was stirred for 1 h. Silver trifluoromethanesulfonate (0.990 g, 3.854 mmol) was added, and the reaction mixture

was allowed to stir for an additional 1 h. The resulting suspension was filtered through a plug of celite, and the celite was washed with additional acetonitrile until the eluent was colorless. Solvents were removed under reduced pressure, the crude product was triturated with ether and dissolved in dichloromethane, and the dichloromethane solution was filtered through celite. Solvents were removed under reduced pressure to afford a crude product which was purified by flash chromatography over silica eluting with dichloromethane/acetonitrile (3:1) to afford the amide complex (±)-**4.37** (0.544 g, 67%) as a yellow solid: mp = 54−74 °C; R_f = 0.50 (9:1 CH_2Cl_2/MeOH); ^{1}H NMR (500 MHz, $CDCl_3$) δ 7.37−7.27 (m, 6 H), 7.20 (d, J = 6.9 Hz, 2 H), 7.08 (br s, 4 H), 6.92 (d, J = 6.6 Hz, 2 H), 4.46 (s, 1 H), 4.45 (d, J = 16.1 Hz, 1 H), 3.91 (d, J = 16.1 Hz, 1 H), 3.77 (s, 2 H), 3.16 (td, J = 13.0 Hz, 3.5 Hz, 1 H), 2.73 (td, J = 13.9 Hz, 3.15 Hz, 1 H), 2.62 (s, 3 H), 2.61 (s, 3 H), 2.49−2.39 (m, 5 H), 2.25 (s, 3 H), 1.64 (s, 3 H); ^{13}C NMR (125 MHz, $CDCl_3$) δ 180.9, 138.0, 137.3, 133.5, 132.3, 129.9, 129.0 128.9, 128.5, 128.2, 127.7, 127.6, 127.0, 120.7 (q, J(^{13}C − ^{19}F) = 320.8 Hz), 65.1, 64.0, 57.2, 52.3, 51.0, 49.9, 47.3, 46.7, 39.4, 21.1, several signals account for more than one carbon; ^{19}F NMR (376 MHz) δ −76.8 (s, 3 F); IR (thin film, cm^{-1}) 1578 (s), 1153 (s); HRMS (ES$^+$) calcd for $C_{29}H_{38}N_3OPd$ [(M−CF_3SO_3)$^+$], 550.2050; found, 550.2038. Anal. Calcd for $C_{30}H_{38}F_3N_3O_4PdS$: C, 51.47; H, 5.47; N, 6.00. Found: C, 52.34; H, 5.29; N, 5.66.

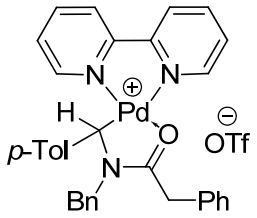

(±)-**4.38**

To a stirred solution of (E)-N-(4-methylbenzylidene)-1-phenylmethanamine (0.419 g, 2.002 mmol) in 3 mL acetonitrile was added neat phenyl acetyl chloride (0.310 g, 2.002 mmol) resulting in a pale yellow solution. After 15 min, 14 mL acetonitrile was added followed by Pd_2dba_3 (0.3025 g, 0.330 mmol). The reaction was allowed to stir for 10 min, after which time 2,2'-bipyridyl (0.626 g, 4.01 mmol) was added and the reaction stirred for 1 h. Silver trifluoromethanesulfonate (0.570 g, 2.203 mmol) was added and the reaction allowed to stir for an additional hour. The resulting suspension was filtered through a plug of celite (the celite was washed with additional acetonitrile until colorless) and solvents removed under reduced pressure. The crude product was then triturated with ether followed by trituration with cold methanol to afford (±)-**4.38** (0.318 g, 65%) as a yellow microcrystalline solid: R_f = 0.40 (9 : 1 CH_2Cl_2 : MeOH); ^{1}H NMR (500 MHz, $CDCl_3$) δ 8.56 (d, *J* = 4.4 Hz, 1 H), 8.52 (d, *J* = 8.2 Hz, 1 H), 8.48 (d, *J* = 8.2 Hz, 1 H), 8.17 (td, *J* = 7.9 Hz, 1.6 Hz, 1 H), 8.07 (td, *J* = 7.9 Hz, 1.6 Hz, 1 H), 7.95 (d, *J* = 4.7 Hz, 1 H), 7.61 (dd, *J* = 7.2 Hz, 5.4 Hz, 1 H), 7.45 – 7.30 (m, 11 H), 7.10 (d, *J* = 7.9 Hz, 2 H), 7.03 (d, *J* = 6.6 Hz, 2 H), 5.00 (s, 1 H), 4.50 (d, *J* = 16.5 Hz, 1 H), 3.94 (d, *J* = 16.5 Hz, 1 H), 3.90 (d, *J* = 15.0 Hz, 1 H), 3.87 (d, *J* = 15.0 Hz, 1 H), 2.24 (s, 3 H); ^{13}C NMR (125 MHz, $CDCl_3$) δ 181.6, 156.3, 152.0, 150.0, 147.9, 141.1, 140.9, 137.9, 137.6, 133.5, 132.2, 130.0, 129.3,

129.2, 128.7, 128.5, 128.2, 128.0, 127.3, 127.1, 127.0, 124.5, 123.7, 120.9 (q, J(^{13}C – ^{19}F) = 320.8 Hz), 66.4, 51.3, 39.7, 21.3, several signals account for more than one carbon; ^{19}F NMR (470.81 MHz) δ -77.0 (s, 3F); IR (thin film from DCM, cm^{-1}) 1578 (s), 1155 (s); HRMS (ES) calcd for $C_{33}H_{30}N_3OPd$ (M+), 590.1423, found 590.1424.

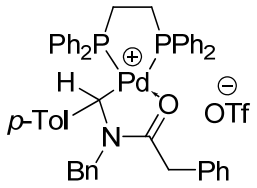

(±)-**4.39**

Amide complex (±)-**4.37** (0.464 g, 0.663 mmol) and 1,2-bis(diphenylphosphino)ethane (0.528 g, 1.325 mmol) were dissolved in dichloromethane (7 mL). The resulting yellow solution was stirred for 5 h at rt under argon. Solvents were removed under reduced pressure, and the crude product was purified by flash chromatography over silica eluting with dichloromethane/acetonitrile (6:1) to afford complex (±)-**4.39** (0.479 g, 74%) as a yellow solid: mp = 75−90 °C; R_f = 0.46 (9:1 CH_2Cl_2/MeOH); ^{1}H NMR (500 MHz, $CDCl_3$) δ 7.70−7.64 (m, 2 H), 7.50−7.16 (m, 22 H), 7.12 (td, J = 7.8 Hz, 2.5 Hz, 2 H), 6.88 (d, J = 12.3 Hz, 1 H), 6.87 (d, J = 11.3 Hz, 1 H), 6.82 (d, J = 6.6 Hz, 2 H), 6.78 (d, J = 7.9 Hz, 2 H), 6.30 (br s, 2 H), 4.74 (dd, J = 15.5 Hz, 2.8 Hz, 1 H), 4.34 (dd, J = 8.2 Hz, 3.5 Hz, 1 H), 4.02 (dd, J = 15 Hz, 2 H), 3.95 (d, J = 15.8 Hz, 1 H), 2.74−2.44 (m, 3 H), 2.21 (s, 3 H), 2.00−1.84 (m, 1 H); ^{13}C NMR (125 MHz, $CDCl_3$) δ 182.0 (dd, J(^{13}C − ^{31}P) = 8.3 Hz, 1.8 Hz), 138.7 (d, J(^{13}C − ^{31}P) = 5.5 Hz), 136.0, 134.0,

133.4 (d, $J(^{13}C - ^{31}P)$ = 11.0 Hz), 132.8, 132.75 (d, $J(^{13}C - ^{31}P)$ = 11.9 Hz), 132.5 (d, $J(^{13}C - ^{31}P)$ = 13.8 Hz), 132.3 (d, $J(^{13}C - ^{31}P)$ = 11.9 Hz), 132.0 (dd, $J(^{13}C - ^{31}P)$ = 31.2, 2.8 Hz), 131.5 (dd, $J(^{13}C - ^{31}P)$ = 14.7, 2.8 Hz), 130.4, 130.1, 129.5, 129.4 (d, $J(^{13}C - ^{31}P)$ = 15.0 Hz), 129.3, 129.2, 129.1, 129.0, 128.92 (d, $J(^{13}C - ^{31}P)$ = 11.0 Hz), 128.2, 127.7, 127.3, 127.2, 126.8, 125.2, 124.0, 123.5, 120.9 (q, $J(^{13}C - ^{19}F)$ = 320.8 Hz), 76.8 (dd, $J(^{13}C - ^{31}P)$ = 99.4 Hz, 5.0 Hz), 52.2 (d, $J(^{13}C - ^{31}P)$ = 4.6 Hz), 40.0, 31.4 (dd, $J(^{13}C - ^{31}P)$ = 37.6 Hz, 20.2 Hz), 21.1 (dd, $J(^{13}C - ^{31}P)$ = 30.0 Hz, 7.3 Hz), 20.9, several signals account for more than one carbon; ^{31}P NMR (162 MHz, $CDCl_3$) δ 51.5 (br s, 1 P), 38.5 (br s, 1 P); ^{19}F NMR (376 MHz) δ −76.8 (s, 3 F); IR (thin film, cm^{-1}) 1554 (s), 1150 (s); HRMS (ES^+) calcd for $C_{49}H_{46}NOP_2Pd$ [$(M-CF_3SO_2)^+$], 832.2089; found, 832.2062. Anal. Calcd for $C_{50}H_{46}F_3NO_4P_2PdS$: C, 61.13; H, 4.72; N, 1.43. Found: C, 61.09; H, 4.39; N, 1.36.

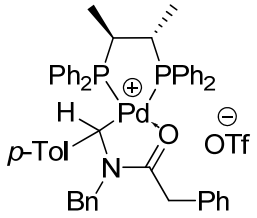

4.45

Amide complex (±)-**4.37** (0.203 g, 0.291 mmol) and (2*S*,3*S*)-bis(diphenylphosphino)butane (0.124 g, 0.291 mmol) were dissolved in dichloromethane (6 mL). The resulting yellow solution was stirred for 3.5 h at rt under argon. Solvents were removed under reduced pressure, and the resulting crude product was purified by flash chromatography over silica, eluting with dichloromethane/MeOH (19:1) to afford complex **4.45** (0.292 g, 99%) (dr 1:1) as a

yellow solid: mp = 77−100 °C; R_f = 0.58 (6.5:1 CH_2Cl_2/MeOH); ^{1}H NMR (500 MHz, $CDCl_3$) δ 7.78−7.72 (m, 1 H), 7.70−7.45 (m, 13.5 H), 7.44−7.38 (m, 0.5 H), 7.33−7.07 (m, 12 H), 7.02−6.95 (m, 1 H), 6.79 (d, *J* = 7.0 Hz, 1 H), 6.74−6.68 (m, 2 H), 6.66 (d, *J* = 7.88 Hz, 1 H), 6.31 (d, *J* = 6.9 Hz, 1 H), 6.14 (d, *J* = 6.9 Hz, 1 H), 4.64 (dd, *J* = 16.8 Hz, 3.2 Hz, 0.5 H), 4.62 (dd, *J* = 15.8 Hz, 2.8 Hz, 0.5 H), 4.20 (dd, *J* = 8.5 Hz, 2.8 Hz, 0.5 H), 4.01 (dd, *J* = 7.6 Hz, 4.0 Hz, 0.5 H), 3.93−3.77 (m, 3 H), 2.67−2.56 (m, 0.5 H), 2.32−2.20 (m, 2 H), 2.18−2.10 (m, 0.5 H), 2.09 (s, 1.5 H), 1.90−1.80 (m, 0.5 H), 1.10−0.94 (m, 6 H); ^{13}C NMR (125 MHz, $CDCl_3$) δ 181.93, 181.87, 139.0 (d, $J(^{13}C - ^{31}P)$ = 6.4 Hz), 137.4 (d, $J(^{13}C - ^{31}P)$ = 4.6 Hz), 136.1 (t, $J(^{13}C - ^{31}P)$ = 12.0 Hz), 135.8 (d, $J(^{13}C - ^{31}P)$ = 1.8 Hz), 135.4 (d, $J(^{13}C - ^{31}P)$ = 13.8 Hz), 135.0 (d, $J(^{13}C - ^{31}P)$ = 12.8 Hz), 133.9 (d, $J(^{13}C - ^{31}P)$ = 16.5 Hz), 133.1 (d, $J(^{13}C - ^{31}P)$ = 2.8 Hz), 132.7, 132.5, 132.3 (d, $J(^{13}C - ^{31}P)$ = 1.8 Hz), 132.16, 132.13, 132.11, 132.08, 131.8 (d, $J(^{13}C - ^{31}P)$ = 11.0 Hz), 131.6 (d, $J(^{13}C - ^{31}P)$ = 10.1 Hz), 131.3, 131.2 (d, $J(^{13}C - ^{31}P)$ = 2.8 Hz), 130.3, 129.5 (d, $J(^{13}C - ^{31}P)$ = 11.0 Hz), 129.47, 129.42, 129.34, 129.32, 129.26, 129.24, 129.21, 129.18, 129.14, 129.07, 128.9 (d, $J(^{13}C - ^{31}P)$ = 4.6 Hz), 128.8 (d, $J(^{13}C - ^{31}P)$ = 12.5 Hz), 128.5 (d, $J(^{13}C - ^{31}P)$ = 11.0 Hz), 128.3, 128.05 (d, $J(^{13}C - ^{31}P)$ = 2.8 Hz), 128.0, 127.7, 127.5 (d, $J(^{13}C - ^{31}P)$ = 2.8 Hz), 127.3, 127.2, 127.1, 127.0, 126.9, 126.84, 126.79, 126.7, 126.63, 126.60, 126.5, 126.2, 125.2 (d, $J(^{13}C - ^{31}P)$ = 54.1 Hz), 124.1 (d, $J(^{13}C - ^{31}P)$ = 51.5 Hz), 123.9 (d, $J(^{13}C - ^{31}P)$ = 48.6 Hz), 121.3 (q, $J(^{13}C - ^{19}F)$ = 319.3 Hz), 120.1 (d, $J(^{13}C - ^{31}P)$ = 49.5 Hz), 76.9 (dd, $J(^{13}C - ^{31}P)$ = 402.3 Hz, 6.0 Hz), 76.8 (d, $J(^{13}C - ^{31}P)$ = 208.0 Hz, 5.8 Hz), 53.4, 52.3 (dd, $J(^{13}C - ^{31}P)$ = 12.0 Hz, 4.3 Hz), 43.9 (dd,

$J(^{13}C - ^{31}P)$ = 35.8 Hz, 23.8 Hz), 42.6 (dd, $J(^{13}C - ^{31}P)$ = 34.8 Hz, 22.9 Hz), 39.9, 31.8, 31.3 (dd, $J(^{13}C - ^{31}P)$ = 44.0 Hz, 10.1 Hz), 31.1 (dd, $J(^{13}C - ^{31}P)$ = 44.0 Hz, 11.0 Hz), 29.6, 21.0, 20.8, 14.1 (m), 14.08 (dd, $J(^{13}C - ^{31}P)$ = 54.6 Hz, 5.5 Hz), 14.01 (d, $J(^{13}C - ^{31}P)$ = 5.5 Hz), 14.0 (dd, $J(^{13}C - ^{31}P)$ = 5.5 Hz), several signals account for more than one carbon; ^{31}P NMR (162 MHz, $CDCl_3$) δ 59.7 (br s, 1 P), 57.6 (br s, 1 P), 47.5 (br s, 1 P), 42.9 (br s, 1 P); ^{19}F NMR (376 MHz) δ −76.7 (s, 3 F); IR (thin film, cm^{-1}) 1562 (s), 1150 (s); HRMS (ES^+) calcd for $C_{51}H_{50}NOP_2Pd$ [$(M-CF_3SO_2)^+$], 860.2402; found, 860.2389. Anal. Calcd for $C_{52}H_{50}F_3NO_4P_2PdS$: C, 61.81; H, 4.99; N, 1.39. Found: C, 62.36; H, 4.65; N, 1.37.

General Procedure for the Synthesis of Palladacycles via Ring Closure

To a solution of cationic palladium complex (0.1 M) in THF at a given temperature was added a solution of base (*t*-BuOK 1.0 M in THF, KHMDS 0.5 M in toluene, LDA 2.0 M in heptane/THF/ethylbenzene), and the reaction mixture was stirred for the designated time(s) under argon. The suspension was diluted with dichloromethane, and the solvents were removed under reduced pressure. The oily residue was dissolved in dichloromethane and filtered through celite to remove any insoluble materials. Solvents were removed under reduced pressure, and the crude product was purified by flash chromatography over silica eluting with ethyl acetate (EtOAc) and hexane mixtures or with EtOAc to afford the corresponding palladacycles as yellow or orange solids.

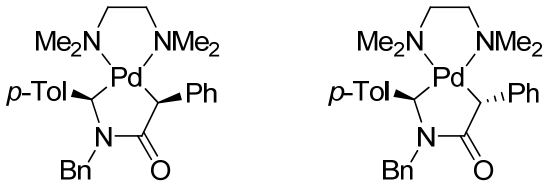

(±)-**4.40**

Amide complex (±)-**4.37** (0.540 g, 0.7710 mmol) was treated with *t*-BuOK (0.85 mL, 0.85 mmol) at 45°C according to the general procedure described above. Elution with EtOAc/Hex (1:1) and EtOAc followed by trituration with pentane afforded complex (±)-**4.40** (0.3471 g, 82%) (dr 88:12, *cis*:*trans*) as a light orange powder: mp = 162−170 (dec.); R_f = 0.36 (100% EtOAc); ^{1}H NMR (500 MHz, $CDCl_3$) δ 7.62 (d, *J* = 7.0 Hz, 1.8 H), 7.38 (d, *J* = 7.5 Hz, 0.3 H), 7.33 (d, *J* = 7.9 Hz, 2 H), 7.30−7.23 (t, *J* = 7.0 Hz, 1 H), 7.24−7.12 (m, 5.5 H), 7.12−6.97 (m, 3.4 H), 4.89 (d, *J* = 14.8 Hz, 0.12 H), 4.84 (d, *J* = 14.5 Hz, 0.88 H), 4.13 (s, 0.12 H), 4.12 (s, 0.88 H), 3.99 (s, 0.88 H), 3.94 (s, 0.12 H), 3.40 (d, *J* = 14.5 Hz, 0.88 H), 3.34 (d, *J* = 14.5 Hz, 0.12 H), 2.65−2.56 (m, 0.2 H), 2.50−2.46 (m, 1 H), 2.45−2.34 (m, 5.6 H), 2.33−2.20 (m, 5.2 H), 2.13−2.06 (m, 1 H), 1.55 (s, 2.7 H), 1.44 (s, 2.7 H), 1.40 (s, 0.3 H), 1.35 (s, 0.3 H); ^{13}C NMR (125 MHz, $CDCl_3$) δ (182.5), 182.2, (148.4), 147.4, (144.5), 144.0, (139.0), 138.8, 134.1, (132.5), 130.7, (130.1), (129.8), (129.7), (129.2), 129.1, 128.8, 128.6, (128.5), 127.94, 127.91, 126.3, 124.2, (123.7), (60.6), (60.5), (60.4), 60.23, 60.18, (53.4), (50.5), 50.3, (50.0), (49.5), 49.2, 48.8, 48.6, 47.8, 47.5, 47.0, 46.1, 45.6, (29.7), 21.9, 21.1, 21.0, (minor diastereomer signals in parentheses), some signals account for more than one carbon; IR (thin film, cm^{-1}): 1617 (s); HRMS (ES^+) calcd

for $C_{29}H_{38}N_3OPd$ (M + H^+), 550.2050; found, 550.2025. Anal. Calcd for $C_{29}H_{37}N_3OPd$: C, 63.32; H, 6.78; N, 7.64. Found: C, 63.38; H, 6.52; N, 6.97.

A sample of complex (±)-**4.40** highly enriched in the *cis* diastereomer (dr > 20:1 by ^{1}H NMR) was obtained by precipitation and trituration (benzene) of solids obtained directly from the EtOAc eluent after chromatography. Analytical data for complex *cis*-(±)-**4.40** (dr > 20:1): ^{1}H NMR (500 MHz, $CDCl_3$) δ 7.67 (d, *J* = 8.3 Hz, 2 H), 7.37 (d, *J* = 7.5 Hz, 2 H), 7.32−7.23 (m, 7 H), 7.14−7.09 (m, 3 H), 4.89 (d, *J* = 14.5 Hz, 1 H), 4.16 (s, 1 H), 4.03 (s, 1 H), 3.43 (d, *J* = 14.5 Hz, 1 H), 2.56−2.52 (m, 1 H), 2.45 (s, 3 H), 2.42 (s, 3 H), 2.34−2.29 (m, 5 H), 2.17−2.13 (m, 1 H), 1.60 (s, 3 H), 1.50 (s, 3 H); ^{13}C NMR (125 MHz, $CDCl_3$) δ 182.0, 147.5, 144.2, 139.0, 134.0, 130.8, 129.1, 129.0, 127.9, 126.3, 124.2, 60.2, 50.2, 49.2, 48.9, 48.6, 47.8, 47.0, 21.1, several signals account for more than one carbon.

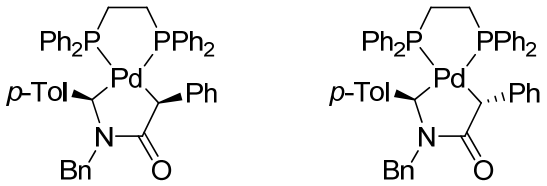

(±)-**4.41**

Amide complex (±)-**4.39** (0.089 g, 0.091 mmol) was treated with *t*-BuOK (0.100 mL, 0.100 mmol) at 45 °C under argon according to the general procedure above. Elution with EtOAc/Hex (1:1) followed by trituration with pentane afforded palladacycle (±)-**4.39** (0.068 g, 90%) as a yellow powder in dr 72:28, *cis*:*trans*.

Alternatively, palladacycle (±)-**4.41** was also synthesized via ligand exchange reaction. Thus, complex (±)-**4.40** (dr 89:11, *cis*:*trans*) (0.396 g, 0.719 mmol) and 1,2-

bis(diphenylphosphino)ethane (0.573 g, 1.44 mmol) were dissolved in dichloromethane (10 mL). The resulting yellow solution was stirred for 3.5 h at rt under argon. Solvents were removed under reduced pressure, and the crude product was purified by flash chromatography over silica, eluting with EtOAc/hexane (1:1) to afford palladacycle (±)-**4.41** (0.534 g, 89%) as a yellow powder (dr 87:13).

Complex (±)-**4.41** was characterized as a mixture of diastereomers in the ratio dr 91:9, *cis*:*trans* (obtained from an analogous but separate experiment in 89% yield) providing the analytical data below: mp = 150−165 °C (dec.); R_f = 0.50 (2:1 EtOAc/Hex); ^{1}H NMR (500 MHz, $CDCl_3$) δ 7.63−7.56 (m, 2.2 H), 7.54−7.45 (m, 5.8 H), 7.42 (td, *J* = 7.6 Hz, 1.6 Hz, 2 H), 7.39−7.16 (m, 7 H), 7.12 (td, *J* = 7.6 Hz, 1.6 Hz, 1.9 H), 7.08 (td, *J* = 7.6 Hz, 1.6 Hz, 1.9 H), 7.02−6.82 (m, 7.8 H), 6.79−6.61 (m, 5.0 H), 6.58−6.44 (m, 0.4 H), 5.12 (dd, *J* = 14.0 Hz, 1.6 Hz, 0.09 H), 5.03 (dd, *J* = 14.4 Hz, 2.0 Hz, 0.91 H), 4.78 (t, *J* = 7.0 Hz, 0.09 H), 4.75 (t, *J* = 7.6 Hz, 0.91 H), 4.53 (t, *J* = 7.0 Hz, 0.09 H), 4.40 (dd, *J* = 8.8 Hz, 6.0 Hz, 0.91 H), 3.61 (d, *J* = 14.2 Hz, 0.91 H), 3.55 (d, *J* = 14.2 Hz, 0.09 H), 2.19 (s, 3H), 2.17−1.85 (m, 3.7 H), 1.78−1.61 (m, 0.3 H); ^{13}C NMR (125 MHz, $CDCl_3$) δ 182.5 (t, $J(^{13}C - ^{31}P)$ = 6.4 Hz), (182.2 (t, $J(^{13}C - ^{31}P)$ = 6.4 Hz)), 148.2 (t, $J(^{13}C - ^{31}P)$ = 3.0 Hz), (146.1 (d, $J(^{13}C - ^{31}P)$ = 7.3 Hz)), 145.4 (d, $J(^{13}C - ^{31}P)$ = 3.0 Hz), (144.6 (d, $J(^{13}C - ^{31}P)$ = 4.5 Hz)), 138.9, (138.7), 134.2 (dd, $J(^{13}C - ^{31}P)$ = 16.9 Hz, 14.0 Hz), 133.5 (d, $J(^{13}C - ^{31}P)$ = 13.8 Hz), 133.2 (d, $J(^{13}C - ^{31}P)$ = 13.8 Hz), 133.0 (d, $J(^{13}C - ^{31}P)$ = 12.8 Hz), 132.8 (d, $J(^{13}C - ^{31}P)$ = 12.8 Hz), 132.46, 132.35 (d, $J(^{13}C - ^{31}P)$ = 1.8 Hz), 132.30 (dd, $J(^{13}C - ^{31}P)$ = 31.2 Hz, 1.8 Hz), 132.31, 132.2, 132.19, (131.9), 131.59 (dd, $J(^{13}C$ −

^{31}P) = 29.3 Hz, 1.8 Hz), (131.4), (131.15), (131.07), (130.71), (130.61), 130.3 (dd, J(^{13}C – ^{31}P) = 10.1 Hz, 1.8 Hz), 129.84, 129.63, (129.55), 129.5 (d, J(^{13}C – ^{31}P) = 12.5 Hz), 129.3 (d, J(^{13}C – ^{31}P) = 15.0 Hz), 129.26, 128.80, 128.70, 128.67, 128.59, (128.50), (128.46), (128.29), 128.24, 128.17, 127.79, 127.38, 127.3, (126.3), 126.16, 126.0 (d, J(^{13}C – ^{31}P) = 2.5 Hz), (125.46), 122.90, (122.31), (64.3), 57.0 (t, J(^{13}C – ^{31}P) = 3.7 Hz), 56.7 (dd, J(^{13}C – ^{31}P) = 70.1 Hz, 2.8 Hz), 56.3 (dd, J(^{13}C – ^{31}P) = 86.6 Hz, 3.7 Hz), 49.1 (d, J(^{13}C – ^{31}P) = 3.7 Hz), 29.2 (td, J(^{13}C – ^{31}P) = 24.7 Hz, 17.4 Hz), (27.6 (d, J(^{13}C – ^{31}P) = 16.5 Hz)), (27.4 (d, J(^{13}C – ^{31}P) = 16.5 Hz)), (27.1 (d, J(^{13}C – ^{31}P) = 16.5 Hz)), (26.9 (d, J(^{13}C – ^{31}P) = 16.5 Hz)), (20.9), 20.8, (signals for the minor diastereomer are in parentheses), some signals account for more than one carbon;^{31}P NMR (162 MHz, $CDCl_3$) δ (39.5 (br s, 0.05 P)), (35.9 (br s, 0.05 P)), 34.8 (br s, 0.45 P), 32.7 (br s, 0.45 P), (signals for the minor diastereomer in parentheses); IR (thin film, cm^{-1}): 1607 (s); HRMS (ES$^+$) calcd for $C_{49}H_{46}NOP_2Pd$ (M + H$^+$), 832.2089; found, 832.2108. Anal. Calcd for $C_{49}H_{45}NOP_2Pd$: C, 70.71; H, 5.45; N, 1.68. Found: C, 70.86; H, 5.34; N, 1.64.

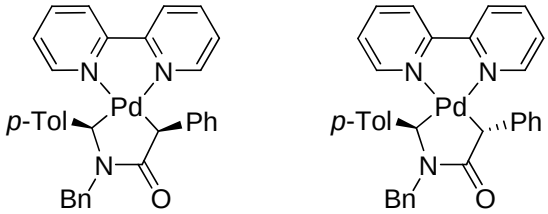

(±)-**4.42**

Complex (±)-**4.38** (0.144 g, 0.182 mmol) was treated with KO^{t}Bu (0.200 mL, 0.200 mmol) at 45°C in accordance with the general procedure above. Chromatography (20 : 1 CH_2Cl_2 : MeOH) followed by trituration with pentane afforded **4.42** (0.092 g,

85%) as a bright orange powder in dr 63 : 37 *cis* : *trans*: mp = 122 – 125°C (dec.); R*f* = 0.25 (19 : 1 DCM/MeOH); ^{1}H NMR (500 MHz, $CDCl_3$) δ 8.65 (d, *J* = 5.5 Hz, 0.3 H), 8.63 (d, *J* = 4.5 Hz, 0.5 H), 7.93 – 7.75 (m, 5.5 H), 7.57 (d, *J* = 7.0 Hz, 0.7 H), 7.37 – 7.35 (m, 3 H), 7.33 – 7.11 (m, 10 H), 7.05 – 6.98 (m, 2 H), 5.09 (d, *J* = 14.5 Hz, 0.37 H), 5.05 (d, *J* = 15.0 Hz, 0.63 H), 4.70 (s, 0.63 H), 4.65 (s, 0.63 H), 4.64 (s, 0.37 H), 4.62 (s, 0.37 H), 3.56 (d, *J* = 15.0 Hz, 0.63 H), 3.54 (d, *J* = 14.5 Hz, 0.37 H), 2.26 (s, 1.9 H), 2.23 (s, 1.1 H); ^{13}C NMR (125 MHz, $CDCl_3$) δ (182.5), 181.9, 154.2, (154.1), (154.0), 150.0, 149.1, (148.7), (147.7), 146.6, (144.5), 144.1, 139.0, 138.7, 138.0, 137.8, (137.7), 134.0, 131.2, 130.0, 128.8, (126.9), 128.5, 128.2, 128.1, (127.9), 127.7, (127.4), 126.4, 125.5, 125.4, (125.2), 124.6, (123.9), 121.7, 121.6, (121.4), 50.7, (50.5), (49.6), 49.0, 48.0, (34.0), (22.2), 21.0, (signals for the minor diastereomer are in parenthesis), some signals account for more than one carbon; IR (thin film, cm^{-1}): 1616 (s); HRMS (ES^+) calcd for $C_{33}H_{30}N_3OPd$ ($M + H^+$), 590.1423; found, 590.1426.

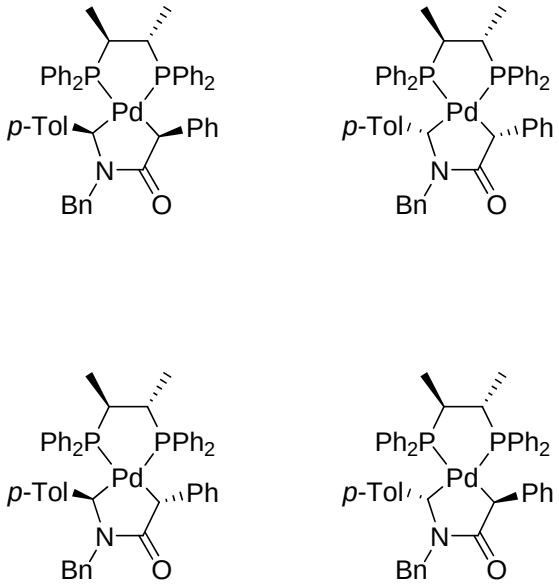

4.46a – 4.46d

Amide complex **4.45** (dr 1:1) (0.155 g, 0.154 mmol) was treated with *t*-BuOK (0.170 mL, 0.170 mmol) at 45 °C according to the general procedures described above. Elution with EtOAc/Hex (1:1) followed by trituration with pentane afforded complex **4.46a**−**d** (0.120 g, 91%) as a yellow powder, dr **4.46a**:**4.46b**:**4.46c**:**4.46d** = 5.9:7.3:2:1, "*cis*:*trans*", 81:19.

Alternatively, palladacycle **4.46** was also synthesized via a ligand exchange reaction. Thus, complex (±)-**4.40** (dr 91:9, *cis*:*trans*) (0.082 g, 0.149 mmol) and (*S*,*S*)-CHIRAPHOS (0.095 g, 0.223 mmol) were dissolved in dichloromethane (2 mL). The yellow solution was stirred for 3.5 h at rt under argon. Solvents were removed under reduced pressure, and the crude product was purified by flash chromatography over silica, eluting with EtOAc/hexanes (1:1) to afford palladacycle **4.46** (0.107 g, 83%) (dr 91:9 "*cis* : *trans"*, **4.46a**:**4.46b**:**4.46c**:**4.46d** = 4.5:4.5:0.5:0.5,) as a yellow powder after trituration with pentane. Analytical data for this sample of complex

4.46a:**4.46b**:**4.46c**:**4.46d**: mp = 90−135 °C (dec.); R_f = 0.52 (2:1 EA/Hex); ^{1}H NMR (500 MHz, $CDCl_3$) δ 7.64 (td, *J* = 8.2 Hz, 1.6 Hz, 1.9 H), 7.60−7.39 (m, 7.5 H), 7.38−7.09 (m, 11 H), 7.09−6.91 (m, 4.5 H), 6.86−6.55 (m, 8 H), 6.51 (d, *J* = 7.3 Hz, 1 H), 6.19 (d, *J* = 7.9 Hz, 0.1 H), 5.10 (dd, *J* = 14.0 Hz, 2.2 Hz, 0.05 H), 4.97 (d, *J* = 2.2 Hz, 0.22 H), 4.96 (d, *J* = 1.9 Hz, 0.23 H), 4.93 (d, *J* = 2.2 Hz, 0.22 H), 4.92 (d, *J* = 2.2 Hz, 0.23 H), 4.58 (t, *J* = 6.3 Hz, 0.05 H), 4.54 (dd, *J* = 8.1 Hz, 6.7 Hz, 0.45 H), 4.42 (dd, *J* = 8.8 Hz, 6.0 Hz, 0.05 H), 4.32 (dd, *J* = 9.5 Hz, 4.0 Hz, 0.45 H), 4.28 (t, *J* = 8.0 Hz, 0.45 H), 4.17 (dd, *J* = 9.8 Hz, 4.0 Hz, 0.03 H), 4.08 (t, *J* = 6.9 Hz, 0.22 H), 3.86 (t, *J* = 7.6 Hz, 0.45 H), 3.57 (d, *J* = 14.2 Hz, 0.45 H), 3.53 (s, 0.05 H), 3.49 (d, *J* = 14.5 H, 0.45 H), 3.44 (d, *J* = 14.2 Hz, 0.05 H), 2.28 (s, 0.1 H), 2.25−2.18 (m, 1 H), 2.17−2.09 (m, 1.3 H), 2.08−2.02 (m, 0.5 H), 1.68−1.46 (m, 1.0 H), 1.45−1.25 (m, 1.0 H), 1.03−0.93 (m, 3 H), 0.92−0.86 (m, 1 H), 0.84−0.75 (m, 0.4 H), 0.72 (dd, *J* = 10.0 Hz, 7.0 Hz, 1.3 H), 0.69−0.64 (m, 0.3 H); ^{13}C NMR (125 MHz, $CDCl_3$) δ 182.9 (t, $J(^{13}C - ^{31}P)$ = 7.0 Hz), (182.6 (t, $J(^{13}C - ^{31}P)$ = 6.4 Hz)), 182.1 (t, $J(^{13}C - ^{31}P)$ = 7.0 Hz), (182.0 (t, $J(^{13}C - ^{31}P)$ = 6.4 Hz)), 148.6 (t, $J(^{13}C - ^{31}P)$ = 2.8 Hz), (148.3), 147.0 (t, $J(^{13}C - ^{31}P)$ = 1.8 Hz), (146.0 (d, $J(^{13}C - ^{31}P)$ = 5.5 Hz)), 145.7 (d, $J(^{13}C - ^{31}P)$ = 2.8 Hz), 145.2 (d, $J(^{13}C - ^{31}P)$ = 4.6 Hz), (143.9 (d, $J(^{13}C - ^{31}P)$ = 7.3 Hz)), (143.3 (d, $J(^{13}C - ^{31}P)$ = 6.4 Hz)), (138.9), 138.8, (138.4), (136.96 (d, $J(^{13}C - ^{31}P)$ = 15.6 Hz)), 136.92 (d, $J(^{13}C - ^{31}P)$ = 14.7 Hz), 136.7 (d, $J(^{13}C - ^{31}P)$ = 14.7 Hz), (135.7 (d, $J(^{13}C - ^{31}P)$ = 13.8 Hz)), (135.4 (d, $J(^{13}C - ^{31}P)$ = 13.2 Hz)), 134.9 (t, $J(^{13}C - ^{31}P)$ = 12.5 Hz), (133.9 (d, $J(^{13}C - ^{31}P)$ = 8.0 Hz)), (133.7 (d, $J(^{13}C - ^{31}P)$ = 8.4 Hz), 133.2 (d, $J(^{13}C - ^{31}P)$ = 12.3 Hz), 132.2 (d, $J(^{13}C - ^{31}P)$ = 16.8 Hz), 132.16, (132.1), 132.04,

(132.01), 131.94 (d, $J(^{13}C - ^{31}P)$ = 3.6 Hz), 131.86 (d, $J(^{13}C - ^{31}P)$ = 2.9 Hz), (131.4 (d, $J(^{13}C - ^{31}P)$ = 2.8 Hz)), (131.3 (d, $J(^{13}C - ^{31}P)$ = 2.8 Hz)), 131.0, 130.93, 130.86, 130.80, 130.7 (dd, $J(^{13}C - ^{31}P)$ = 4.6 Hz, 1.8 Hz), 130.6 (d, $J(^{13}C - ^{31}P)$ = 2.8 Hz), 130.5, 130.4 (d, $J(^{13}C - ^{31}P)$ = 1.8 Hz), 130.3, 130.1 (d, $J(^{13}C - ^{31}P)$ = 4.6 Hz), (130.0 (d, $J(^{13}C - ^{31}P)$ = 1.8 Hz)), 129.8 (d, $J(^{13}C - ^{31}P)$ = 4.6 Hz), 129.7 (d, $J(^{13}C - ^{31}P)$ = 2.8 Hz), 129.6, 129.5, 129.44, 129.36, 129.2, 129.1 (d, $J(^{13}C - ^{31}P)$ = 1.2 Hz), 129.0 (d, $J(^{13}C - ^{31}P)$ = 3.7 Hz), (128.93), 128.89, 128.87, 128.8, 128.63, 128.58, 128.5, 128.4, (128.3), 128.25, 128.20, 128.18, 128.14, 128.11, (127.84), (127.82), 127.76, 127.7 (d, $J(^{13}C - ^{31}P)$ = 3.7 Hz), 127.6 (d, $J(^{13}C - ^{31}P)$ = 10.0 Hz), 127.4, (127.1), 126.7, (126.6), (126.5 (d, $J(^{13}C - ^{31}P)$ = 2.8 Hz)), (126.4), 126.2 (d, $J(^{13}C - ^{31}P)$ = 3.0 Hz), 126.05, 126.01 (d, $J(^{13}C - ^{31}P)$ = 3.5 Hz), 125.8, (125.7 (d, $J(^{13}C - ^{31}P)$ = 2.8 Hz)), 125.6 (d, $J(^{13}C - ^{31}P)$ = 2.4 Hz), 125.5, (125.33), 125.28, 64.3, 59.0 (dd, $J(^{13}C - ^{31}P)$ = 38.0 Hz, 2.8 Hz), 58.4 (dd, $J(^{13}C - ^{31}P)$ = 28.4 Hz, 1.8 Hz), 57.8 (dd, $J(^{13}C - ^{31}P)$ = 52.2 Hz, 2.8 Hz), (57.4 (dd, $J(^{13}C - ^{31}P)$ = 7.3 Hz, 2.8 Hz)), 57.1 (dd, $J(^{13}C - ^{31}P)$ = 40.0 Hz, 1.8 Hz), 56.9 (d, $J(^{13}C - ^{31}P)$ = 2.8 Hz), (56.0 (d, $J(^{13}C - ^{31}P)$ = 2.8 Hz)), (49.4 (d, $J(^{13}C - ^{31}P)$ = 2.8 Hz)), 49.1 (d, $J(^{13}C - ^{31}P)$ = 3.7 Hz), 49.0 (d, $J(^{13}C - ^{31}P)$ = 2.8 Hz), (48.9 d, $J(^{13}C - ^{31}P)$ = 3.7 Hz)), 41.8 (d, $J(^{13}C - ^{31}P)$ = 2.8 Hz), 41.71 (dd, $J(^{13}C - ^{31}P)$ = 45.8 Hz, 14.7 Hz), 41.66 (d, $J(^{13}C - ^{31}P)$ = 3.7 Hz), 37.0 (d, $J(^{13}C - ^{31}P)$ = 22.0 Hz, 17.4 Hz), 35.7 (dd, $J(^{13}C - ^{31}P)$ = 23.3 Hz, 18.8 Hz), 34.02, (33.98), 30.5, 22.3, 20.98, (20.94), 20.85 (20.80), 20.7, 19.0, 15.9 (dd, $J(^{13}C - ^{31}P)$ = 15.6, 5.5 Hz), 15.2 (dd, $J(^{13}C - ^{31}P)$ = 15.6, 5.5 Hz), 14.31, 14.26, 14.23, 14.18, 14.12, 14.06, 14.00, (13.39), (13.34), (13.27), (13.20), (13.08), (13.04), (signals for

the minor diastereomers are in parentheses), several signals account for more than one carbon; ^{31}P NMR (162 MHz, $CDCl_3$) δ (46.3 (br s, 0.12 P)), 45.1 (br s, 0.38 P), 42.8 (br s, 0.55 P (major + minor), (41.7 (br s, 0.063 P)), (39.7 (br s, 0.067 P)), 38.8 (br s, 0.44 P), 36.0 (br s, 0.38 P), (signals for the minor diastereomers in parentheses); IR (thin film, cm^{-1}): 1607 (br); HRMS (ES^+) calcd for $C_{51}H_{50}NOP_2Pd$ ($M + H^+$), 860.2402; found, 860.2382. Anal. Calcd for $C_{51}H_{49}NOP_2Pd$: C, 71.20; H, 5.74; N, 1.63. Found: C, 71.01; H, 5.59; N, 1.58.

Description of the experimental procedures for the experiments reported in Table 4.4

General Procedure: To a solution of cationic palladium complex (0.1 M) in THF at a given temperature was added a solution of base (*t*-BuOK 1.0 M in THF, KHMDS 0.5 M in toluene, LDA 2.0 M in heptane/THF/ethylbenzene), and the reaction mixture was stirred for the designated time(s) and temperatures under argon. The suspension was diluted with dichloromethane, and the solvents were removed under reduced pressure. The oily residue was dissolved in dichloromethane and filtered through celite to remove any insoluble materials. Solvents were removed under reduced pressure, and the crude product was purified by flash chromatography over silica eluting with ethyl acetate (EtOAc) and hexane mixtures or with EtOAc to afford the corresponding palladacycles as yellow or orange solids.

Entry 1, Table 4.4: Amide complex (±)-**4.37** (0.540 g, 0.7710 mmol) was treated with *t*-BuOK (0.85 mL, 0.85 mmol) at 45 °C for 30 min according to the general procedure described above. Elution with EtOAc/Hex (1:1) and EtOAc followed by

trituration with pentane afforded palladacycle (±)-**4.40** (0.3471 g, 82%) (dr 88 : 12, *cis* : *trans*) as a light orange powder.

Entry 2, Table 4.4: Amide complex (±)-**4.37** (0.127 g, 0.181 mmol) was treated with *t*-BuOK (0.20 mL, 0.20 mmol) at rt for 5 h according to the general procedure described above. Elution with EtOAc/Hex (1:1) and EtOAc followed by trituration with pentane afforded palladacycle (±)-**4.40** (0.067 g, 67%) (dr 94 : 6, *cis* : *trans*) as a light orange powder.

Entry 3, Table 4.4: Amide complex (±)-**4.37** (0.070 g, 0.101 mmol) was treated with KHMDS (0.20 mL, 0.10 mmol) at rt for 5 h according to the general procedure described above. Elution with EtOAc/Hex (1:1) and EtOAc followed by trituration with pentane afforded palladacycle (±)-**4.40** (0.020 g, 35%) (dr 95 : 5, *cis* : *trans*) as a light orange powder.

Entry 4, Table 4.4: Amide complex (±)-**4.37** (0.070 g, 0.100 mmol) was treated with LDA (50 μL, 0.10 mmol) at -78°C (1 h) to rt (4 h) according to the general procedure described above. Elution with EtOAc/Hex (1:1) and EtOAc followed by trituration with pentane afforded palladacycle (±)-**4.40** (0.015 g, 25%) (dr 88 : 12, *cis* : *trans*) as a light orange powder.

Entry 5, Table 4.4: Amide complex (±)-**4.39** (0.089 g, 0.091 mmol) was treated with *t*-BuOK (0.100 mL, 0.100 mmol) at 45 °C for 30 min. under argon according to the general procedure above. Elution with EtOAc/Hex (1 : 1) followed by trituration with pentane afforded palladacycle (±)-**4.41** (0.068 g, 90%) (dr 72 : 28, *cis* : *trans*) as a yellow powder.

Entry 6, Table 4.4: Amide complex (±)-**4.39** (0.090 g, 0.091 mmol) was treated with *t*-BuOK (0.10 mL, 0.10 mmol) at rt for 5 h under argon according to the general procedure above. Elution with EtOAc/Hex (1 : 1) followed by trituration with pentane afforded palladacycle (±)-**4.41** (0.068 g, 89%) (dr 74 : 26, *cis* : *trans*) as a yellow powder.

Entry 7, Table 4.4: Amide complex (±)-**4.39** (0.098 g, 0.100 mmol) was treated with KHMDS (0.20 mL, 0.10 mmol) at rt for 5 h according to the general procedure described above. Elution with EtOAc/Hex (1 : 1) followed by trituration with pentane afforded complex (±)-**4.41** (0.072 g, 86%) (dr 76 : 24, *cis* : *trans*) as a yellow powder.

Entry 8, Table 4.4: Amide complex (±)-**4.39** (0.098 g, 0.100 mmol) was treated with LDA (50 μL, 0.100 mmol) from -78°C (1 h) to rt (4 h) under argon according to the general procedure above. Elution with EtOAc/Hex (1 : 1) followed by trituration with pentane afforded palladacycle (±)-**4.41** (0.072 g, 86%) (dr 77 : 23, *cis* : *trans*) as a yellow powder.

Entry 9, Table 4.4: Amide complex (±)-**4.38** (0.404 g, 0.546 mmol) was treated with *t*-BuOK (0.60 mL, 0.60 mmol) at 45 °C for 30 min. according to the general procedure described above. Elution with DCM/MeOH (20 : 1) followed by trituration with pentane afforded palladacycle (±)-**4.42** (0.277 g, 86%) (dr 42 : 58, *cis* : *trans*) as an orange powder.

Entry 10, Table 4.4: Amide complex (±)-**4.38** (0.135 g, 0.182 mmol) was treated with *t*-BuOK (0.2 mL, 0.2 mmol) at rt for 5 h according to the general procedure described above. Elution with DCM/MeOH (20 : 1) and followed by trituration with

pentane afforded complex (±)-**4.42** (0.106 g, 83%) (dr 75 : 25, *cis* : *trans*) as an orange powder.

Entry 11, Table 4.4: Amide complex (±)-**4.38** (0.074 g, 0.100 mmol) was treated with KHMDS (0.2 mL, 0.1 mmol) at rt for 5 h according to the general procedure described above. Elution with DCM/MeOH (20 : 1) and followed by trituration with pentane afforded complex (±)-**4.42** (0.072 g, 71%) (dr 57 : 43, *cis* : *trans*) as an orange powder.

Entry 12, Table 4.4: Amide complex (±)-**4.38** (0.074 g, 0.100 mmol) was treated with LDA (50 μL, 0.10 mmol) at -78°C (1 h) to rt (4 h) according to the general procedure described above. Elution with DCM/MeOH (20 : 1) and followed by trituration with pentane afforded complex (±)-**4.42** (0.038 g, 64%) (dr 83 : 17, *cis* : *trans*) as an orange powder.

Description of the experimental procedures for the experiments reported in Table 4.5

Entry 1, Table 4.5: A solution of palladacycle (±)-**4.40** (0.078 g, 0.141 mmol, dr 88 : 12, *cis* : *trans*) in 2 mL THF was heated to 45°C for 3 h. The solution was then filtered through celite and the celite washed with DCM until colorless. The solvents were removed under reduced pressure, and the reside triturated with pentane to afford palladacycle (±)-**4.40** (0.072 g, 92%) (dr 88 : 12, *cis* : *trans*) as a light orange powder.

Entry 2, Table 4.5: A solution of palladacycle (±)-**4.41** (0.063 g, 0.076 mmol, dr 91 : 9, *cis* : *trans*) in 2 mL THF was heated to 45°C for 3 h. The solution was then filtered through celite and the celite washed with DCM until colorless. The solvents were

removed under reduced pressure, and the reside triturated with pentane to afford palladacycle (±)-**4.41** (0.057 g, 90%) (dr 83 : 17, *cis* : *trans*) as a light orange powder.

Entry 3, Table 4.5: A solution of palladacycle (±)-**4.42** (0.040 g, 0.067 mmol, dr 63 : 37, *cis* : *trans*) in 1.5 mL THF was heated to 45°C for 3 h. The solvents were removed under reduced pressure, and the reside triturated with pentane to afford palladacycle (±)-**4.42** (0.038 g, 96%) (dr 50 : 50, *cis* : *trans*) as an orange powder.

Description of the experimental procedures for the experiments reported in Table 4.6

Entry 1, Table 4.6: To a solution of palladacycle (±)-**4.40** (0.051 g, 0.092 mmol) with dr 90 : 10 in THF (2.5 mL) was added a 1 M solution of potassium *tert*-butoxide (9 μL, 0.090 mmol) at room temperature. The reaction was allowed to stir at room temperature for 1 h. The crude reaction mixture was loaded on the top of a short plug of silica. Elution with ethyl acetate followed by removal of solvents under reduced pressure and trituration with hexanes afforded recovered (±)-**4.40** (0.042 g, 83% recovery yield) with a dr of 94 : 6.

Entry 2, Table 4.6: To a solution of palladacycle (±)-**4.40** (0.051 g, 0.092 mmol) with dr 90 : 10 in THF (2.5 mL) was added a 1 M solution of potassium *tert*-butoxide (46 μL, 0.046 mmol) at room temperature. The reaction was allowed to stir at room temperature for 1 h. The crude reaction mixture was loaded on the top of a short plug of silica. Elution with ethyl acetate followed by removal of solvents under reduced pressure and trituration with hexanes afforded recovered (±)-**4.40** (0.029 g, 58% recovery yield) with a dr of 93 : 7.

Entry 3, Table 4.6: To a solution of palladacycle (±)-**4.40** (0.051 g, 0.092 mmol) with dr 90 : 10 in THF (2.5 mL) was added a 1 M solution of potassium *tert*-butoxide 0.1 mL, 0.1 mmol) at room temperature. The reaction was allowed to stir at room temperature for 5 min. The crude reaction mixture was loaded on the top of a short plug of silica. Elution with ethyl acetate followed by removal of solvents under reduced pressure and trituration with hexanes afforded recovered (±)-**4.40** (0.042 g, 83% recovery yield) with a dr of 88 : 12.

Entry 4, Table 4.6: To a solution of palladacycle (±)-**4.40** (0.051 g, 0.092 mmol) with dr 90 : 10 in THF (2.5 mL) was added a 1 M solution of potassium *tert*-butoxide (0.1 mL, 0.1 mmol) at room temperature. The reaction was allowed to stir at room temperature for 30 min. The crude reaction mixture was loaded on the top of a short plug of silica. Elution with ethyl acetate followed by removal of solvents under reduced pressure and trituration with hexanes afforded recovered (±)-**4.40** (0.042 g, 82% recovery yield) with a dr of 78 : 22.

Entry 5, Table 4.6: To a solution of palladacycle (±)-**4.41** (0.076 g, 0.092 mmol) with dr 87 : 13 in THF (2.5 mL) was added a 1 M solution of potassium *tert*-butoxide (0.1 mL, 0.1 mmol) at room temperature. The reaction was allowed to stir at room temperature for 1 h. The crude reaction mixture was loaded on the top of a short plug of silica. Elution with ethyl acetate followed by removal of solvents under reduced pressure and trituration with hexanes afforded recovered (±)-**4.41** (0.069 g, 91% recovery yield) with a dr of 42 : 58.

Entry 6, Table 4.6: To a solution of palladacycle (±)-**4.41** (0.076 g, 0.092 mmol) with dr 87 : 13 in THF (2.5 mL) was added a 1 M solution of potassium *tert*-butoxide (0.1 mL, 0.1 mmol) at room temperature. The reaction was allowed to stir at room temperature for 1 h. The crude reaction mixture was loaded on the top of a short plug of silica. Elution with ethyl acetate followed by removal of solvents under reduced pressure and trituration with hexanes afforded recovered (±)-**4.41** (0.070 g, 92% recovery yield) with a dr of 42 : 58.

Entry 7, Table 4.6: To a solution of palladacycle (±)-**4.42** (0.054 g, 0.092 mmol) in THF with dr 42 : 58 (2.5 mL) was added a 1 M solution of potassium *tert*-butoxide (0.1 mL, 0.1 mmol) at room temperature. The reaction was allowed to stir at room temperature for 1 h. The crude reaction mixture was loaded on the top of a short plug of silica. Elution with ethyl acetate followed by removal of solvents under reduced pressure and trituration with hexanes afforded recovered (±)-**4.42** (0.052 g, 96% recovery yield) with a dr of 22 : 78.

Entry 8, Table 4.6: To a solution of palladacycle (±)-**4.42** (0.053 g, 0.092 mmol) with dr 42 : 58 in THF (2.5 mL) was added a 1 M solution of potassium *tert*-butoxide (0.1 mL, 0.1 mmol) at room temperature. The reaction was allowed to stir at room temperature for 3 h. The crude reaction mixture was loaded on the top of a short plug of silica. Elution with ethyl acetate followed by removal of solvents under reduced pressure and trituration with hexanes afforded recovered (±)-**4.42** (0.049 g, 92% recovery yield) with a dr of 23 : 77.

Description of the experimental procedures for the reactions of complex 4.46 reported in Scheme 4.22

To a solution of palladacycle **4.46** with dr 81 : 19, "*cis* : *trans"* (0.092 mmol) in THF (2.5 mL) at rt under argon was added a 1 M solution of potassium *tert*-butoxide (0.1 mL). The reaction mixture was stirred for 3.5 h. The crude reaction mixture was loaded on the top of a short plug of silica. Elution with ethyl acetate followed by removal of solvents under reduced pressure and trituration with hexanes afforded the recovered complex **4.46** in the indicated yields and diastereomeric ratios dr 57 : 43, "*cis* : *trans"*. The ratios of diastereomers in the recovered complex **4.46** (**4.46a** : **4.46b** : **4.46c** : **4.46d** = 1.1 : 1.6 : 1. : 1) were established by integration of ^{31}P NMR spectra.

Description of experiment reported in Scheme 4.18 and Figures 4.6 and 4.7

Complex (±)-**4.41** (0.020 g, 0.024 mmol) with dr 68 :32 was dissolved in THF-d_8 (0.5 mL) inside an NMR tube. ^{1}H (400 MHz, THF-d_8) and ^{31}P NMR (162 MHz, THF-d_8) were recorded before addition of base. Ten minutes after the addition of potassium *tert*-butoxide (1.0 M in THF, 26μL, 0.026 mmol), the ^{1}H NMR (400 MHz, THF-d_8) and ^{31}P NMR (162 MHz, THF-d_8) spectrum indicated a change in the diastereomeric ratio, reaching the ratio (dr 41 : 59 *cis* : *trans*) within one hour.

Description of experiment reported in Figure 4.15

Complex (±)-**4.40** (0.008 g, 0.015 mmol) and (*S*,*S*)-CHIRAPHOS (0.003 g, 0.006 mmol) were dissolved in dichloromethane (0.5 mL). The solution was allowed to stir

for 3.5 h at rt under argon, and the solvent was removed under reduced pressure to afford the crude product, which was analyzed by ^{1}H NMR (400 MHz).

Description of experiments reported in Figure 4.16

40 mol% (*S*,*S*)-CHIRAPHOS

Complex (±)-**4.37** (0.101 g, 0.144 mmol) and (*S*,*S*)-CHIRAPHOS) (0.025 g, 0.057 mmol) were dissolved in dichloromethane (3 mL). The solution was allowed to stir for 3.5 h at rt under argon, the solvent was removed under reduced pressure to afford the crude product, which was analyzed by ^{1}H NMR (400 MHz).

20 mol% (*S*,*S*)-CHIRAPHOS

Complex (±)-**4.37** (0.094 g, 0.134 mmol) and (*S*,*S*)-CHIRAPHOS) (0.012 g, 0.027 mmol) were dissolved in dichloromethane (3 mL). The solution was allowed to stir for 3.5 h at rt under argon, the solvent was removed under reduced pressure to afford the crude product, which was analyzed by ^{1}H NMR (400 MHz).

10 mol% (*S*,*S*)-CHIRAPHOS

Complex (±)-**4.37** (0.144 g, 0.206 mmol) and (*S*,*S*)-CHIRAPHOS) (0.009 g, 0.021 mmol) were dissolved in dichloromethane (4 mL). The solution was allowed to stir for 3.5 h at rt under argon, the solvent was removed under reduced pressure to afford the crude product, which was analyzed by ^{1}H NMR (400 MHz).

Description of experiments reported in Figure 4.17

Reaction of complex (±)-**4.37** with (*S*,*S*)-BDPP

Complex (±)-**4.37** (0.014 g, 0.020 mmol) and (*S*,*S*)-BDPP (0.010 g, 0.022 mmol) were dissolved in 0.5 mL of CD_2Cl_2 and transferred into an NMR tube. A ^{1}H NMR

(400 MHz, CD_2Cl_2) spectrum indicating a complete conversion was recorded after 3 hours.

Reaction of complex (±)-**4.37** with (*S*,*S*)-DIOP

Complex (±)-**4.37** (0.014 g, 0.020 mmol) and (*S*,*S*)-DIOP (0.024 g, 0.040 mmol) were dissolved in 0.5 mL of CD_2Cl_2 and transferred into an NMR tube. A ^{1}H NMR (400 MHz, CD_2Cl_2) spectrum indicating a complete conversion was recorded after 3 hours.

Reaction of complex (±)-**4.37** with (*S*)-BINAP

Complex (±)-**4.37** (0.014 g, 0.020 mmol) and (*S*)-BINAP (0.025 g, 0.040 mmol) were dissolved in 0.5 mL of CD_2Cl_2 and transferred into an NMR tube. A ^{1}H NMR (400 MHz, CD_2Cl_2) spectrum indicating incomplete conversion was recorded after 24 hours.

Description of experiments reported in Figures 4.18 and 4.19

Reaction of complex (±)-**4.40** with (*S*,*S*)-BDPP

Complex (±)-**4.40** (0.017 g, 0.031 mmol, dr *cis* : *trans* 85 : 15) and (*S*,*S*)-BDPP (0.027 g, 0.061 mmol) were dissolved in 0.5 mL of CD_2Cl_2 and transferred into an NMR tube. A ^{1}H NMR (400 MHz, CD_2Cl_2) spectrum indicating complete conversion was recorded after 3 hours. The ^{31}P NMR (162 MHz, CD_2Cl_2) spectrum did not give useful data for the differentiation of diastereomers.

Reaction of complex (±)-**4.40** with (*S*,*S*)-BDPP

Complex (±)-**4.40** (0.017 g, 0.031 mmol, dr *cis* : *trans* 85 : 15) and (*S*,*S*)-DIOP (0.031 g, 0.062 mmol) were dissolved in 0.5 mL of CD_2Cl_2 and transferred into an NMR tube. A ^{1}H NMR (400 MHz, CD_2Cl_2) spectrum indicating complete conversion was

recorded after 3 hours. The ^{31}P NMR (162 MHz, CD_2Cl_2) spectrum did not give useful data for the differentiation of diastereomers.

Reaction of complex (±)-**4.40** with (*S*)-BINAP

Complex (±)-**4.40** (0.018 g, 0.033 mmol, dr *cis* : *trans* 85 : 15) and (*S*)-BINAP (0.041 g, 0.067 mmol) were dissolved in 0.5 mL of CD_2Cl_2 and transferred into an NMR tube. A ^{1}H NMR (500 MHz, CD_2Cl_2) spectrum indicating complete conversion was recorded after 7 hours. The ^{31}P NMR (162 MHz, CD_2Cl_2) spectrum did not give useful data for the differentiation of diastereomers.

Bibliography

1. Trost, B. M., When is a Proton Not a Proton? *Chem. Eur. J.* **1998**, *4*, 2405 - 2412.

2. Long, N. J.; Williams, C. K., Metal Alkynyl σ Complexes: Synthesis and Materials. *Angew. Chem., Int. Ed.* **2003**, *42*, 2586 - 2617.

3. Wong, W.-Y., Mercury Alkynyls as Versatile Templates for New Organometallic Materials and Polymers. *Coord. Chem. Rev.* **2007**, *251*, 2400 - 2427.

4. Rosi, N. L.; Eckert, J.; Eddaoudi, M.; Vodak, D. T.; Kim, J.; O'Keeffe, M.; Yaghi, O. M., Hydrogen Storage in Microporous Metal-Organic Frameworks. *Science* **2003**, *300*, 1127 - 1130.

5. Tietze, L. F.; Ila, H.; Bell, H. P., Enantioselective Palladium-Catalyzed Transformations. *Chem. Rev.* **2004**, *104*, 3453 - 3516.

6. Beller, M.; Bolm, C., *Transition Metals for Organic Synthesis: Building Blocks and Fine Chemicals*. Wiley-VCH: Weinheim, 2004; Vol. 1 and 2.

7. Dyker, G., *Handbook of C-H Transformations: Applications in Organic Synthesis*. Wiley-VCH: Weinheim, 2005; Vol. 1 and 2.

8. Negishi, E., *Organopalladium Chemistry for Organic Synthesis*. Wiley-Interscience: New York, 2002; Vol. 1 and 2.

9. Heck, R. F., Arylation, Methylation, and Carboxyalkylation of Olefins by Group VIII Metal Derivatives. *J. Am. Chem. Soc.* **1968**, *90*, 5518 - 5526.

10. Tsuji, J. M., M.; Kiji, J., Reaction of Olefin-Palladium Chloride Complex with Carbon Monoxide. *Tetrahedron Lett.* **1963**, *16*, 1061 - 1063.

11. Trost, B. M.; Van Vranken, D. L., Asymmetric Transition Metal-Catalyzed Allylic Alkylations. *Chem. Rev.* **1996**, *96*, 395 - 422.

12. Trost, B. M.; Crawley, M. L., Asymmetric Transition-Metal-Catalyzed Allylic Alkylations: Applications in Total Synthesis. *Chem. Rev.* **2003**, *103*, 2921 - 2943.

13. Miyaura, N.; Suzuki, A., Palladium-Catalyzed Cross-Coupling Reactions of Organoboron Compounds. *Chem. Rev.* **1995**, *95*, 2457 - 2483.

14. Roglans, A.; Pla-Quintana, A.; Moreno-Manas, M., Diazonium Salts as Substrates in Palladium-Catalyzed Cross-Coupling Reactions. *Chem. Rev. (Washington, DC, U. S.)* **2006**, *106*, 4622-4643.

15. Zeni, G.; Larock, R. C., Synthesis of Heterocycles Via Palladium-Catalyzed Oxidative Addition. *Chem. Rev.* **2006**, *106*, 4644 - 4680.

16. Chinchilla, R.; Najera, C., The Sonogashira Reaction: A Booming Methodology in Synthetic Organic Chemistry. *Chem. Rev.* **2007**, *107*, 874 - 922.

17. de Meijere, A.; Diederich, F., *Metal-Catalyzed Cross-Coupling Reactions*. Wiley-VCH: Weinheim, 2004; Vol. 1 and 2.

18. Goossen, L. J.; Rodriguez, N.; Linder, C., Decarboxylative Biaryl Synthesis from Aromatic Carboxylates and Aryl Triflates. *J. Am. Chem. Soc.* **2008**, *130*, 15248 - 15249.

19. Goossen, L. J.; Rodriguez, N.; Melzer, B.; Linder, C.; Deng, G.; Levy, L. M., Biaryl Synthesis Via Pd-Catalyzed Decarboxylative Coupling of Aromatic Carboxylates with Aryl Halides. *J. Am. Chem. Soc.* **2007**, *129*, 4824 - 4833.

20. Rayabarapu, D. K.; Tunge, J. A., Catalytic Decarboxylative sp-sp^3 Coupling. *J. Am. Chem. Soc.* **2005**, *127*, 13510 - 13511.

21. Waetzig, S. R.; Rayabharapu, D. K.; Weaver, J. D.; Tunge, J. A., A Versatile Hexadiene Synthesis by Decarboxylative sp^3-sp^3 Coupling/Cope Rearrangement. *Angew. Chem., Int. Ed.* **2006**, *45*, 4977 - 4980.

22. Waetzig, S. R.; Tunge, J. A., Palladium-Catalyzed Decarboxylative sp^3-sp^3 coupling of Nitrobenzene Acetic Esters. *J. Am. Chem. Soc.* **2007**, *129*, 14860 - 14861.

23. Mohr, J. T.; Behenna, D. C.; Harned, A. M.; Stoltz, B. M., Deracemization of Quaternary Stereocenters by Pd-Catalyzed Enantioconvergent Decarboxylative Allylation of Racemic β-Keto Esters. *Angew. Chem., Int. Ed.* **2005**, *44*, 6924 - 6927.

24. Trost, B. M.; Dietsch, T. J., New Synthetic Reactions. Asymmetric Induction in Allylic Alkylations. *J. Am. Chem. Soc.* **1973**, *95*, 8200 - 8201.

25. Trost, B. M.; Fullerton, T. J., New Synthetic Reactions. Allylic Alkylation. *J. Am. Chem. Soc.* **1973**, *95*, 292 - 294.

26. Spencer, J.; Pfeffer, M., The Fate of the Stereogenic Center Linked to Palladium Upon Reaction With an Alkyne. *Tetrahedron: Asymmetry* **1995**, *6*, 419 - 426.

27. Bock, P. L.; Boschetto, D. J.; Rasmussen, J. R.; Demers, J. P.; Whitesides, G. M., Stereochemistry of Reactions at Carbon-Transition metal σ bonds. π-Cyclopentadienyldicarbonyliron Erythro-and Threo-3,3-dimethylbutyl-1,2-d_2. *J. Am. Chem. Soc.* **1974**, *96*, 2814 - 2825.

28. Hashmi, A. S. K.; Naumann, F.; Bolte, M., Asymmetric Synthesis of Palladacycles by Regioselective Oxidative Cyclization of C_2-Symmetrical, Chiral Alkenes and Determination of the Configuration of All Stereocenters. *Organometallics* **1998**, *17*, 2385 - 2387.

29. Hoffmann, H. M. R.; Otte, A. R.; Wilde, A.; Menzer, S.; Williams, D. J., Isolation and X-Ray Crystal Structure of a Palladacyclobutane: Insight into the Mechanism of Cyclopropanation. *Angew. Chem., Int. Ed. Engl.* **1995**, *34*, 100 - 102.

30. Seyferth, D., $[(C_2H_4)PtCl_3]^-$, the Anion of Zeise's Salt, $K[(C_2H_4)PtCl_3]\cdot H_2O$. *Organometallics* **2001**, *20*, 2 - 6.

31. Grignard, V., Mixed Organomagnesium Combinations and Their Application in Acid, Alcohol, and Hydrocarbon Synthesis. *Ann. Chim. Phys.* **1901**, *24*, 433 - 490.

32. Schlenk, W.; Holtz, J., The Simplest Organo-Metallic Alkali Compounds. *Ber. Dtsch. Chem. Ges.* **1917**, *50*, 262 - 274.

33. Gilman, H.; Parker, H. H., Reaction Between Organomagnesium Halides and Cupric Chloride. *J. Am. Chem. Soc.* **1924**, *46*, 2823 - 2827.

34. Kharasch, M. S.; Kleiger, S. C.; Martin, J. A.; Mayo, F. R., Factors Determining the Course and Mechanisms of Grignard Reactions. I. Preliminary Study: the Effects of Metallic Compounds on Some Grignard-Carbonyl Interactions. *J. Am. Chem. Soc.* **1941**, *63*, 2305 - 2307.

35. Kharasch, M. S.; Tawney, P. O., Factors Determining the Course and Mechanisms of Grignard Reactions. II. The Effect of Metallic Compounds on the

Reaction Between Isophorone and Methylmagnesium Bromide. *J. Am. Chem. Soc.* **1941**, *63*, 2308 - 2315.

36. House, H. O.; Respess, W. L.; Whitesides, G. M., The Chemistry of Carbanions. XII. The Role of Copper in the Conjugate Addition of Organometallic Reagents. *J. Org. Chem.* **1966**, *31*, 3128 - 3141.

37. Corey, E. J.; Posner, G. H., Selective Formation of Carbon-Carbon Bonds Between Unlike Groups Using Organocopper Reagents. *J. Am. Chem. Soc.* **1967**, *89*, 3911 - 3912.

38. Kealy, T. J.; Pauson, P. L., A New Type of Organo-Iron Compound. *Nature* **1951**, *168*, 1039 - 1040.

39. Miller, S. A.; Tebboth, J. A.; Tremaine, J. F., Dicyclopentadienyliron. *J. Chem. Soc.* **1952**, 632 - 635.

40. Wilkinson, G.; Rosenblum, M.; Whiting, M. C.; Woodward, R. B., The Structure of Iron Biscyclopentadienyl. *J. Am. Chem. Soc.* **1952**, *74*, 2125 - 2126.

41. Woodward, R. B.; Rosenblum, M.; Whiting, M. C., A new aromatic system. *J. Am. Chem. Soc.* **1952**, *74*, 3458-3459.

42. Fischer, E. O.; Pfab, W., Cyclopentadiene-metallic Complex, a New Type of Organo-metallic Compound. *Z. Naturforsch.* **1952**, *7b*, 377 - 389.

43. Dunitz, J. D.; Orgel, L. E.; Rich, A., The Crystal Structure of Ferrocene. *Acta Crystallogr.* **1956**, *9*, 373 - 375.

44. Kuhn, T. S., Historical Structure of Scientific Discovery. *Science* **1962**, *136*, 760 - 764.

45. Smidt, J.; Hafner, W.; Jira, R.; Sieber, R.; Sedlmeier, J.; Sabel, A., Palladium Chloride-Catalyzed Oxidation of Olefins. *Angew. Chem.* **1962**, *74*, 93 - 102.

46. Stern, E. W.; Spector, M. L., Reactions of Olefin-Palladium(II) Chloride Complexes with Nucleophiles: A New Vinylation. *Proc. Chem. Soc., London* **1961**, 370.

47. Moiseev, I. I.; Vargaftik, M. N.; Syrkin, Y. K., Mechanism of the Reaction of Palladium Salts with Olefins in Hydroxyl-Containing Solvents. *Dokl. Akad. Nauk SSSR* **1960**, *133*, 377 - 380.

48. Tsuji, J.; Morikawa, M.; Kiji, J., Organic Syntheses by Means of Noble Metal Compounds. VII. Reactions of Olefin-Palladium Chloride Complexes with Carbon Monoxide. *J. Am. Chem. Soc.* **1964**, *86*, 4851 - 4853.

49. Tsuji, J.; Hosaka, S., Organic Syntheses by Means of Noble Metal Compounds. XIII. Carbonylation of Butadiene- and Isoprene-Palladium Chloride Complexes. *J. Am. Chem. Soc.* **1965**, *87*, 4075 - 4079.

50. Tsuji, J.; Kiji, J.; Hosaka, S., Organic syntheses by means of noble metal compounds. V. Reaction of butadiene-palladium chloride complex with carbon monoxide. *Tetrahedron Lett.* **1964**, 605-608.

51. Tsuji, J.; Susuki, T., Organic Syntheses by Means of Noble Metal Compounds. XVI. Carbonylation of Allene-Palladium Chloride Complexes. *Tetrahedron Lett.* **1965**, 3027 - 3031.

52. Susuki, T.; Tsuji, J., Organic Syntheses by Means of Noble Metal Compounds. XXXVII. Carbonylation of Allene-Palladium Chloride Complexes. *Bull. Chem. Soc. Jpn.* **1968**, *41*, 1954 - 1958.

53. Tsuji, J.; Hosaka, S.; Kiji, J.; Susuki, T., Organic Synthesis with Noble Metal Compounds. XIV. The Carbonylation of Cyclooctadienes. *Bull. Chem. Soc. Jpn.* **1966**, *39*, 141 - 145.

54. Tsuji, J.; Imamura, S., Organic Synthesis by Means of Noble Metal Compounds. XXVIII. Synthesis of a New Type of π-Allylic Palladium Complexes from α, β and β , γ - Unsaturated Esters and Their Carbonylation. *Bull. Chem. Soc. Jpn.* **1967**, *40*, 197 - 201.

55. Kajimoto, T.; Takahashi, H.; Tsuji, J., Organic Syntheses by Means of Noble Metal Compounds. XLI. Reaction of Isocyanide with π-Allylpalladium Chloride. *J. Organomet. Chem.* **1970**, *23*, 275 - 280.

56. Yamamoto, Y.; Yamazaki, H., A Convenient Synthesis of 3-Imino-2-Phenylindazolines. *Synthesis* **1976**, 750 - 751.

57. Thompson, J. M.; Heck, R. F., Carbonylation Reactions of *ortho*-Palladation Products of α-Arylnitrogen Derivatives. *J. Org. Chem.* **1975**, *40*, 2667 - 2674.

58. Heck, R. F., 2-(Phenylazo)phenyl complexes of the transition metals. *J. Am. Chem. Soc.* **1968**, *90*, 313-317.

59. Cope, A. C.; Siekman, R. W., Formation of Covalent Bonds from Platinum or Palladium to Carbon by Direct Substitution. *J. Am. Chem. Soc.* **1965**, *87*, 3272 - 3273.

60. Larock, R. C.; Harrison, L. W., Mercury in Organic Chemistry. 26. Synthesis of Heterocycles Via Intramolecular Solvomercuration of Aryl Acetylenes. *J. Am. Chem. Soc.* **1984**, *106*, 4218 - 4227.

61. Larock, R. C.; Riefling, B.; Fellows, C. A., Mercury in Organic Chemistry. 12. Synthesis of β-Chloro-$\Delta^{\alpha,\beta}$-butenolides via Mercuration-Carbonylation of Propargylic Alcohols. *J. Org. Chem.* **1978**, *43*, 131 - 137.

62. Larock, R. C.; Varaprath, S.; Lau, H. H.; Fellows, C. A., Synthesis of Isocoumarins via Thallation-Olefination of Benzoic Acids. *J. Am. Chem. Soc.* **1984**, *106*, 5274 - 5284.

63. Tsuji, J.; Takahashi, H., Organic syntheses by means of noble metal compounds. XII. Reaction of the cyclooctadiene-palladium chloride complex with ethyl malonate. *J. Am. Chem. Soc.* **1965**, *87*, 3275-3276.

64. Tsuji, J.; Takahashi, H.; Morikawa, M., Organic Syntheses by Means of Noble Metal Compounds. XVII. Reaction of π-Allylpalladium Chloride with Nucleophiles. *Tetrahedron Lett.* **1965**, 4387 - 4388.

65. Trost, B. M.; Weber, L., New Synthetic Reactions. Stereochemistry of Allylic Alkylation. *J. Am. Chem. Soc.* **1975**, *97*, 1611 - 1612.

66. Trost, B. M.; Strege, P. E., Regio- and stereoselectivity of allylic alkylation. *J. Am. Chem. Soc.* **1975**, *97*, 2534-2535.

67. Trost, B. M.; Verhoeven, T. R., New Synthetic Reactions. Catalytic vs. Stoichiometric Allylic Alkylation. Stereocontrolled Approach to Steroid Side Chain. *J. Am. Chem. Soc.* **1976**, *98*, 630 - 632.

68. Trost, B. M.; Verhoeven, T. R., Stereocontrolled Approach to Steroid Side Chain via Organopalladium Chemistry. Partial Synthesis of 5α-Cholestanone. *J. Am. Chem. Soc.* **1978**, *100*, 3435 - 3443.

69. Parra-Hake, M.; Rettig, M. F.; Wing, R. M., Stereochemistry of Palladium Migration on Coordinated Cyclooctenyl. Molecular Structure and Dechloropalladation of Tetrakis(μ-chloro)bis[1,3-η^6-(α-chloroethyl)cyclooctenyl]-tripalladium(II). *Organometallics* **1983**, *2*, 1013 - 1017.

70. Kurosawa, H.; Urabe, A.; Miki, K.; Kasai, N., Reactions of η^1-Allyl Complexes of Palladium(II) with Electrophiles. Molecular Structure of a [2 + 3] Cycloadduct of (η^1-Allyl)palladium with Maleic Anhydride. *Organometallics* **1986**, *5*, 2002 - 2008.

71. Barczak, N. T.; Grote, R. E.; Jarvo, E. R., Catalytic Umpolung Allylation of Aldehydes by π-Allylpalladium Complexes Containing Bidentate N-Heterocyclic Carbene Ligands. *Organometallics* **2007**, *26*, 4863 - 4865.

72. Hopkins, C. D.; Malinakova, H. C., Synthesis of Homoallylic Alcohols via Palladium-Catalyzed Three-Component Coupling of an Arylboronic Acid with Allenes and Aldehydes. *Org. Lett.* **2004**, *6*, 2221 - 2224.

73. Heck, R. F., Mechanism of Arylation and Carbomethoxylation of Olefins with Organopalladium Compounds. *J. Am. Chem. Soc.* **1969**, *91*, 6707 - 6714.

74. Horino, H.; Inoue, N., Ortho Vinylation of Aromatic Amides via Cyclopalladation Complexes. *J. Org. Chem.* **1981**, *46*, 4416 - 4422.

75. Holton, R. A.; Kjonaas, R. A., Carbopalladation-Depalladation of Allylic Amines and Sulfides. *J. Am. Chem. Soc.* **1977**, *99*, 4177 - 4179.

76. Bergstrom, D. E.; Ruth, J. L., Synthesis of C-5 Substituted Pyrimidine Nucleosides via Organopalladium Intermediates. *J. Am. Chem. Soc.* **1976**, *98*, 1587 - 1589.

77. Wu, G.; Rheingold, A. L.; Heck, R. F., Alkyne Reactions with Cyclopalladated Complexes. *Organometallics* **1986**, *5*, 1922 - 1924.

78. Wu, G.; Rheingold, A. L.; Heck, R. F., Cinnolinium Salt Synthesis from Cyclopalladated Azobenzene Complexes and Alkynes. *Organometallics* **1987**, *6*, 2386 - 2391.

79. Ball, N. D.; Sanford, M. S., Synthesis and Reactivity of a Mono-σ-Aryl Palladium(IV) Fluoride Complex. *J. Am. Chem. Soc.* **2009**, *131*, 3796 - 3797.

80. Desai, L. V.; Sanford, M. S., Construction of Tetrahydrofurans by Pd(II)/Pd(IV)-Catalyzed Aminooxygenation of Alkenes. *Angew. Chem., Int. Ed.* **2007**, *46*, 5737 - 5740.

81. Kalyani, D.; Deprez, N. R.; Desai, L. V.; Sanford, M. S., Oxidative C-H Activation/C-C Bond Forming Reactions: Synthetic Scope and Mechanistic Insights. *J. Am. Chem. Soc.* **2005**, *127*, 7330 - 7331.

82. Dick, A. R.; Hull, K. L.; Sanford, M. S., A Highly Selective Catalytic Method for the Oxidative Functionalization of C-H Bonds. *J. Am. Chem. Soc.* **2004**, *126*, 2300 - 2301.

83. Furuya, T.; Ritter, T., Carbon-Fluorine Reductive Elimination from a High-valent Palladium Fluoride. *J. Am. Chem. Soc.* **2008**, *130*, 10060 - 10061.

84. Byers, P. K.; Canty, A. J.; Skelton, B. W.; White, A. H., Oxidative Addition of Iodomethane to [PdMe2(bpy)] and the X-Ray Structure of the Organopalladium(IV) Product fac-[PdMe3(bpy)I] (bpy = 2,2'-bipyridyl). *J. Chem. Soc., Chem. Commun.* **1986**, 1722 - 1724.

85. Holton, R. A.; Natalie, K. J., Jr., A New Regiospecific Synthesis of Aryl Ketones from Palladocycles. *Tetrahedron Lett.* **1981**, *22*, 267 - 270.

86. Markies, B. A.; Canty, A. J.; Janssen, M. D.; Spek, A. L.; Boersma, J.; Van Koten, G., Selectivity in Reductive Elimination from Dialkyl(aryl)palladium(IV) Complexes, and the Observation of Benzyl Halide Transfer from Palladium(IV) to Palladium(II). The X-Ray Structure of Methyl(phenyl)(2,2'-bipyridyl)palladium(II). *Recl. Trav. Chim. Pays-Bas* **1991**, *110*, 477 - 479.

87. Canty, A. J.; Watson, A. A.; Skelton, B. W.; White, A. H., Studies of Oxidative Addition-Reductive Elimination Reactions, and the Crystal Structure of the Palladium(IV) Complex Me2(*p*-$BrC_6H_4CH_2$)Pd(phen)Br. *J. Organomet. Chem.* **1989**, *367*, C25 - C28.

88. Canty, A. J.; Traill, P. R.; Skelton, B. W.; White, A. H., Synthesis of Halo, Pseudohalo, and Carboxylatopalladium(IV) Complexes, by Halogen Exchange. Crystal Structure of Azido(2,2'-bipyridyl)benzylpalladium(II), Formed on Reductive Elimination of Ethane from $Pd(N_3)Me_2(CH_2Ph)$(bpy). *J. Organomet. Chem.* **1992**, *433*, 213 - 222.

89. Markies, B. A.; Canty, A. J.; Boersma, J.; van Koten, G., Phenylpalladium(IV) Chemistry: Selectivity in Reductive Elimination from Palladium(IV) Complexes and Alkyl Halide Transfer from Palladium(IV) to Palladium(II). *Organometallics* **1994**, *13*, 2053 - 2058.

90. Canty, A. J.; Rodemann, T.; Skelton, B. W.; White, A. H., Access to Alkynylpalladium(IV) and -Platinum(IV) Species, Including Triorgano(diphosphine)metal(IV) Complexes and the Structural Study of an Alkynyl(pincer)platinum(IV) Complex, $Pt(O_2CAr_F)I(CCSiMe_3)(NCN)$ (Ar_F = 4-$CF_3C_6H_4$, NCN = [2,6-(dimethylaminomethyl)phenyl-N,C,N]$^-$). *Organometallics* **2006**, *25*, 3996 - 4001.

91. Uson, R.; Fornies, J.; Navarro, R., Dichlorobis(pentafluorophenyl)(chelate) Complexes of Palladium(IV). *J. Organomet. Chem.* **1975**, *96*, 307 - 312.

92. Merrifield, R. B., Solid Phase Peptide Synthesis. I. The Synthesis of a Tetrapeptide. *J. Am. Chem. Soc.* **1963**, *85*, 2149 - 2154.

93. Merrifield, R. B., Solid Phase Peptide Synthesis. IV. The Synthesis of Methionyl-lysyl-bradykinin. *J. Org. Chem.* **1964**, *29*, 3100 - 3102.

94. Merrifield, R. B., Solid-Phase Peptide Synthesis. III. An Improved Synthesis of Bradykinin. *Biochemistry* **1964**, *3*, 1385 - 1389.

95. Merrifield, R. B., Solid Phase Peptide Synthesis. II. Synthesis of Bradykinin. *J. Am. Chem. Soc.* **1964**, *86*, 304 - 305.

96. Gravert, D. J.; Janda, K. D., Organic Synthesis on Soluble Polymer Supports: Liquid-Phase Methodologies. *Chem. Rev.* **1997**, *97*, 489 - 509.

97. Hodge, P., Polymer-Supported Organic Reactions: What Takes Place in the Beads? *Chem. Soc. Rev.* **1997**, *26*, 417 - 424.

98. Bergbreiter, D. E., Using Soluble Polymers to Recover Catalysts and Ligands. *Chem. Rev.* **2002**, *102*, 3345 - 3383.

99. Dickerson, T. J.; Reed, N. N.; Janda, K. D., Soluble Polymers as Scaffolds for Recoverable Catalysts and Reagents. *Chem. Rev. (Washington, DC, U. S.)* **2002**, *102*, 3325 - 3343.

100. McNamara, C. A.; Dixon, M. J.; Bradley, M., Recoverable Catalysts and Reagents Using Recyclable Polystyrene-Based Supports. *Chem. Rev.* **2002**, *102*, 3275 - 3299.

101. Guino, M.; Hii, K. K., Applications of Phosphine-Functionalized Polymers in Organic Synthesis. *Chem. Soc. Rev.* **2007**, *36*, 608 - 617.

102. Lebl, M., Parallel Personal Comments on "Classical" Papers in Combinatorial Chemistry. *J. Comb. Chem.* **1999**, *1*, 3 - 24.

103. Uozumi, Y.; Danjo, H.; Hayashi, T., Palladium-Catalyzed Asymmetric Allylic Substitution in Aqueous Media Using Amphiphilic Resin-Supported MOP Ligands. *Tetrahedron Lett.* **1998**, *39*, 8303 - 8306.

104. Nozaki, K.; Itoi, Y.; Shibahara, F.; Shirakawa, E.; Ohta, T.; Takaya, H.; Hiyama, T., Asymmetric Hydroformylation of Olefins in a Highly Cross-Linked Polymer Matrix. *J. Am. Chem. Soc.* **1998**, *120*, 4051 - 4052.

105. Gilbertson, S. R.; Chen, G.; McLoughlin, M., Versatile Building Block for the Synthesis of Phosphine-Containing Peptides: The Sulfide of Diphenylphosphinoserine. *J. Am. Chem. Soc.* **1994**, *116*, 4481 - 4482.

106. Gilbertson, S. R.; Wang, X.; Hoge, G. S.; Klug, C. A.; Schaefer, J., Synthesis of Phosphine-Rhodium Complexes Attached to a Standard Peptide Synthesis Resin. *Organometallics* **1996**, *15*, 4678 - 4680.

107. Graden, H.; Olsson, T.; Kann, N., Carbon-Carbon and Carbon-Heteroatom Bond Formation on Solid Phase Using Cationic Iron Carbonyl Complexes. *Org. Lett.* **2005**, *7*, 3565 - 3567.

108. Rigby, J. H.; Kondratenko, M. A., A Facile and Highly Efficient Route to a Traceless π-Arene Chromium Linker. Applications to Synthetic and Combinatorial Chemistry. *Org. Lett.* **2001**, *3*, 3683 - 3686.

109. Rigby, J. H.; Kondratenko, M. A., Solid-Phase C-C and C-O Bond Forming Reactions Using 'Traceless' π-Arene-Chromium Linkers. *Bioorg. Med. Chem. Lett.* **2002**, *12*, 1829 - 1831.

110. Barluenga, J.; de Prado, A.; Santamaria, J.; Tomas, M., Polymer-Bound Fischer Tungsten Carbene Complexes: Synthesis and Reactivity. *Organometallics* **2005**, *24*, 3614 - 3617.

111. Malinakova, H. C., Chiral Nonracemic Late-Transition-Metal Organometallics With a Metal-Bonded Stereogenic Carbon Atom: Development of New Tools for Asymmetric Organic Synthesis. *Chem. Eur. J.* **2004**, *10*, 2636 - 2646.

112. Milstein, D.; Stille, J. K., Mechanism of Reductive Elimination. Reaction of Alkylpalladium(II) Complexes with Tetraorganotin, Organolithium, and Grignard Reagents. Evidence for Palladium(IV) Intermediacy. *J. Am. Chem. Soc.* **1979**, *101*, 4981 - 4991.

113. Milstein, D.; Stille, J. K., Palladium-Catalyzed Coupling of Tetraorganotin Compounds with Aryl and Benzyl Halides. Synthetic Utility and Mechanism. *J. Am. Chem. Soc.* **1979**, *101*, 4992 - 4998.

114. Byers, P. K.; Canty, A. J.; Crespo, M.; Puddephatt, R. J.; Scott, J. D., Reactivity and Mechanism in Oxidative Addition to Palladium(II) and Reductive Elimination from Palladium(IV) and an Estimate of the Palladium-Methyl Bond Energy. *Organometallics* **1988**, *7*, 1363 - 1367.

115. Liebeskind, L. S.; Welker, M. E.; Fengl, R. W., Transformations of Chiral Iron Complexes Used in Organic Synthesis. Reactions of η^5-$CpFe(PPh_3)(CO)COCH_3$ and Related Species Leading to a Mild, Stereospecific Synthesis of β-Lactams. *J. Am. Chem. Soc.* **1986**, *108*, 6328 - 6343.

116. Hansson, S.; Miller, J. F.; Liebeskind, L. S., Synthesis and Reactions of Enantiomerically Pure Molybdenum π-Complexes of 2*H*-Pyran. A General Approach to the Enantiospecific Synthesis of *cis*-2,5-Disubstituted-5,6-Dihydro-2*H*-pyrans and *cis*-2,6-Disubstituted Tetrahydropyrans. *J. Am. Chem. Soc.* **1990**, *112*, 9660 - 9661.

117. Ward, Y. D.; Villanueva, L. A.; Allred, G. D.; Liebeskind, L. S., Stereocontrolled Oxidative Addition of Zerovalent Molybdenum to Enantiomerically

Pure Allylic Acetates with Either Inversion or Retention at the Stereogenic Center. *J. Am. Chem. Soc.* **1996**, *118*, 897 - 898.

118. Liebeskind, L. S.; Bombrun, A., Synthesis and structural characterization of (η^4-Cyclopentadienone)(η^5-Cyclopentadienyl)Dicarbonylmolybdenum Hexafluorophosphate. A Template for the Stereospecific Construction of *cis*-4,5-Disubstituted-2-Cyclopentenones. *J. Am. Chem. Soc.* **1991**, *113*, 8736 - 8744.

119. McCallum, J. S.; Sterbenz, J. T.; Liebeskind, L. S., Efficient synthesis of (η^5-Cyclopentadienyl)(η^3-Allyl)$Mo(CO)_2$ Molybdenum Complexes from Allylic Diphenylphosphinates. *Organometallics* **1993**, *12*, 927 - 932.

120. Yu, R. H.; McCallum, J. S.; Liebeskind, L. S., Stereospecific Functionalization of (π-Allyl)Molybdenum Complexes Derived from Cyclopentenone.Toward the Stereocontrolled Construction of Substituted 2-Cyclopentenones. *Organometallics* **1994**, *13*, 1476 - 1486.

121. Ward, Y. D.; Villanueva, L. A.; Allred, G. D.; Payne, S. C.; Semones, M. A.; Liebeskind, L. S., Synthesis, Characterization, and Configurational Lability of (η^3-Allyl)Dicarbonyl[hydrotris(1-pyrazolyl)borato]Molybdenum Complexes Bearing Substituents at the Termini: Thermodynamic Preference for the Anti Stereoisomer. *Organometallics* **1995**, *14*, 4132 - 4156.

122. Ward, Y. D.; Villanueva, L. A.; Allred, G. D.; Liebeskind, L. S., Preparation of Dicarbonyl[hydrotris(1-pyrazolyl)borato](η3-Allyl)Molybdenum Complexes Bearing Electron-Donating Substituents (1-((tert-Butyldimethylsilyl)oxy), 1-Alkoxy,

and 1-Acetoxy) via the Nucleophilic Addition of $Mo(CO)_3(DMF)_3$ to Enals and Enones. *Organometallics* **1996**, *15*, 4201 - 4210.

123. Yin, J.; Liebeskind, L. S., Enantiocontrolled [5 + 2] Cycloaddition to η^3-Pyranylmolybdenum π-Complexes. Synthesis of Substituted Oxabicyclo[3.2.1]Octenes of High Enantiopurity. *J. Am. Chem. Soc.* **1999**, *121*, 5811 - 5812.

124. Malinakova, H. C.; Liebeskind, L. S., Enantiocontrolled Synthesis of Highly Functionalized Tropanes via [5+2] Cycloaddition to η^3-Pyridinylmolybdenum π-Complexes. *Org. Lett.* **2000**, *2*, 3909 - 3911.

125. Arrayas, R. G.; Liebeskind, L. S., Chiral Scaffolds for Enantiocontrolled Synthesis: Enantio- and Regiocontrolled [4 + 2] Cycloaddition to 3-Alkenyl-η^3-Pyranylmolybdenum Complexes. *J. Am. Chem. Soc.* **2001**, *123*, 6185 - 6186.

126. Shu, C.; Alcudia, A.; Yin, J.; Liebeskind, L. S., Enantiocontrolled Synthesis of 2,3,6-Trisubstituted Piperidines Using (η^3-Dihydropyridinyl)Molybdenum Complexes as Chiral Scaffolds. Total Synthesis of (-)-Indolizidine 209B. *J. Am. Chem. Soc.* **2001**, *123*, 12477 - 12487.

127. Gomez Arrayas, R.; Liebeskind, L. S., η^3-Pyranyl and η^3-Pyridinyl Molybdenum π-Complexes as Chiral Scaffolds for the Enantioselective Construction of Substituted Oxa- and Aza[3.3.1]bicyclics: First Enantio- and Regiocontrolled [5+3] Cycloaddition Reactions. *J. Am. Chem. Soc.* **2003**, *125*, 9026 - 9027.

128. Shu, C.; Liebeskind, L. S., Enantiocontrolled Synthesis of 2,6-Disubstituted Piperidines by Desymmetrization of *meso*-*η*-(3,4,5)-Dihydropyridinylmolybdenum

Complexes. Application to the Total Synthesis of (-)-Dihydropinidine and (-)-Andrachcinidine. *J. Am. Chem. Soc.* **2003**, *125*, 2878 - 2879.

129. Zhang, Y.; Liebeskind, L. S., Synthesis of Substituted Oxa- and Aza[3.2.1] and [4.3.1]Bicyclics via an Unprecedented Molybdenum-Mediated 1,5-"Michael-Type" Reaction. *J. Am. Chem. Soc.* **2005**, *127*, 11258 - 11259.

130. Zhang, Y.; Liebeskind, L. S., Organometallic Enantiomeric Scaffolding: Organometallic Chirons. Total Synthesis of (-)-Bao Gong Teng A by a Molybdenum-Mediated [5+2] Cycloaddition. *J. Am. Chem. Soc.* **2006**, *128*, 465 - 472.

131. Lu, G.; Malinakova, H. C., Mechanism of Stereoinduction in Asymmetric Synthesis of Highly Functionalized 1,2-Dihydroquinolines and 2H-1-Benzopyrans via Nonracemic Palladacycles with a Metal-Bonded Stereogenic Carbon. *J. Org. Chem.* **2004**, *69*, 4701-4715.

132. Coombs, T. C.; Zhang, Y.; Garnier-Amblard, E. C.; Liebeskind, L. S., Organometallic Enantiomeric Scaffolding. Sequential Semipinacol/1,5-"Michael-like" Reactions as a Strategic Approach to Bridgehead-Quaternary Center Aza[3.3.1]Bicyclics: Application to the Total Synthesis of (-)-Adaline. *J. Am. Chem. Soc.* **2009**, *131*, 876 - 877.

133. Norton, J. R., Organometallic Elimination Mechanisms: Studies on Osmium Alkyls and Hydrides. *Acc. Chem. Res.* **1979**, *12*, 139 - 145.

134. Gillie, A.; Stille, J. K., Mechanisms of 1,1-Reductive Elimination from Palladium. *J. Am. Chem. Soc.* **1980**, *102*, 4933 - 4941.

135. Loar, M. K.; Stille, J. K., Mechanisms of 1,1-Reductive Elimination from Palladium: Coupling of Styrylmethylpalladium Complexes. *J. Am. Chem. Soc.* **1981**, *103*, 4174 - 4181.

136. Moravskiy, A.; Stille, J. K., Mechanisms of 1,1-Reductive Elimination from Palladium: Elimination of Ethane from Dimethylpalladium(II) and Trimethylpalladium(IV). *J. Am. Chem. Soc.* **1981**, *103*, 4182 - 4186.

137. Tatsumi, K.; Hoffmann, R.; Yamamoto, A.; Stille, J. K., Reductive Elimination of d_8-Organotransition Metal Complexes. *Bull. Chem. Soc. Jpn.* **1981**, *54*, 1857 - 1867.

138. Kellenberger, B.; Young, S. J.; Stille, J. K., Intramolecular Reductive Elimination of Methane from a Dinuclear Palladium Complex Containing Methyl and Hydride on Adjacent Palladium Centers. *J. Am. Chem. Soc.* **1985**, *107*, 6105 - 6107.

139. Dick, A. R.; Kampf, J. W.; Sanford, M. S., Unusually Stable Palladium(IV) Complexes: Detailed Mechanistic Investigation of C-O Bond-Forming Reductive Elimination. *J. Am. Chem. Soc.* **2005**, *127*, 12790 - 12791.

140. Delgado, M.; Janda, K. D., Polymeric Supports for Solid Phase Organic Synthesis. *Curr. Org. Chem.* **2002**, *6*, 1031 - 1043.

141. Graden, H.; Kann, N., Solid Phase Synthesis Using Organometallic Reagents. *Curr. Org. Chem.* **2005**, *9*, 733 - 763.

142. Sarin, V. K.; Kent, S. B. H.; Merrifield, R. B., Properties of Swollen Polymer Networks. Solvation and Swelling of Peptide-Containing Resins in Solid-Phase Peptide Synthesis. *J. Am. Chem. Soc.* **1980**, *102*, 5463 - 5470.

143. Walsh, D. P.; Pang, C.; Parikh, P. B.; Kim, Y.-S.; Chang, Y.-T., Comparative Resin Kinetics Using *In Situ* Fluorescence Measurements. *J. Comb. Chem.* **2002**, *4*, 204 - 208.

144. Li, W.; Yan, B., Effects of Polymer Supports on the Kinetics of Solid-Phase Organic Reactions: A Comparison of Polystyrene- and TentaGel-Based Resins. *J. Org. Chem.* **1998**, *63*, 4092 - 4097.

145. Vaino, A. R.; Janda, K. D., Solid-Phase Organic Synthesis: A Critical Understanding of the Resin. *J. Comb. Chem.* **2000**, *2*, 579 - 596.

146. Zhang, M.; Moore, J. D.; Flynn, D. L.; Hanson, P. R., Development of High-Load, Soluble Oligomeric Sulfonate Esters via ROM Polymerization: Application to the Benzylation of Amines. *Org. Lett.* **2004**, *6*, 2657 - 2660.

147. Zhang, M.; Vedantham, P.; Flynn, D. L.; Hanson, P. R., High-Load, Soluble Oligomeric Carbodiimide: Synthesis and Application in Coupling Reactions. *J. Org. Chem.* **2004**, *69*, 8340 - 8344.

148. Zhang, M.; Flynn, D. L.; Hanson, P. R., Oligomeric Benzylsulfonium Salts: Facile Benzylation via High-Load ROMP Reagents. *J. Org. Chem.* **2007**, *72*, 3194 - 3198.

149. Rolfe, A.; Probst, D. A.; Volp, K. A.; Omar, I.; Flynn, D. L.; Hanson, P. R., High-Load, Oligomeric Dichlorotriazine: A Versatile ROMP-Derived Reagent and Scavenger. *J. Org. Chem.* **2008**, *73*, 8785 - 8790.

150. Stoianova, D. S.; Yao, L.; Rolfe, A.; Samarakoon, T.; Hanson, P. R., High-load, Oligomeric Monoamine Hydrochloride: Facile Generation via ROM

Polymerization and Application as an Electrophile Scavenger. *Tetrahedron Lett.* **2008**, *49*, 4553-4555.

151. Barrett, A. G. M.; Hopkins, B. T.; Koebberling, J., ROMPgel Reagents in Parallel Synthesis. *Chem. Rev.* **2002**, *102*, 3301 - 3323.

152. Barrett, A. G. M.; Bibal, B.; Hopkins, B. T.; Koebberling, J.; Love, A. C.; Tedeschi, L., Facile and purification free synthesis of peptides utilizing ROMPgel- and ROMPsphere-supported coupling reagents. *Tetrahedron* **2005**, *61*, 12033-12041.

153. Vaino, A. R.; Goodin, D. B.; Janda, K. D., Investigating Resins for Solid Phase Organic Synthesis: The Relationship Between Swelling and Microenvironment As Probed by EPR and Fluorescence Spectroscopy. *J. Comb. Chem.* **2000**, *2*, 330 - 336.

154. Brittain, D. E. A.; Gray, B. L.; Schreiber, S. L., From Solution-Phase to Solid-Phase Enyne Metathesis: Crossover in the Relative Performance of Two Commonly Used Ruthenium Pre-catalysts. *Chem. Eur. J.* **2005**, *11*, 5086 - 5093.

155. Testero, S. A.; Mata, E. G., Prospect of Metal-Catalyzed C-C Forming Cross-Coupling Reactions in Modern Solid-Phase Organic Synthesis. *J. Comb. Chem.* **2008**, *10*, 487 - 497.

156. Villar, H.; Frings, M.; Bolm, C., Ring Closing Enyne Metathesis: A Powerful Tool for the Synthesis of Heterocycles. *Chem. Soc. Rev.* **2007**, *36*, 55 - 66.

157. Yan, B.; Sun, Q., Crucial Factors Regulating Site Interactions in Resin Supports Determined by Single Bead IR. *J. Org. Chem.* **1998**, *63*, 55 - 58.

158. Grubbs, R.; Lau, C. P.; Cukier, R.; Brubaker, C., Jr., Polymer Attached Metallocenes. Evidence for Site Isolation. *J. Am. Chem. Soc.* **1977**, *99*, 4517 - 4518.

159. Dahan, A.; Portnoy, M., Dendritic Effect in Polymer-Supported Catalysis of the Intramolecular Pauson-Khand Reaction. *Chem. Commun.* **2002**, 2700 - 2701.

160. Barrett, A. G. M.; de Miguel, Y. R., Synthesis and Characterization of a New Polymer Support for a Metallocene Catalyst. *Tetrahedron* **2002**, *58*, 3785 - 3792.

161. Portscheller, J. L.; Malinakova, H. C., Synthesis of 2*H*-1-Benzopyrans via Palladacycles with a Metal-Bonded Stereogenic Carbon. *Org. Lett.* **2002**, *4*, 3679 - 3681.

162. Portscheller, J. L.; Lilley, S. E.; Malinakova, H. C., Ligand-Controlled Asymmetric Induction at a Transition Metal-Bonded α-Carbon in Ester and Amide Enolates. Diastereoselective Formation of Oxapalladacycles Applied to the Synthesis of a Chiral Non-Racemic 2*H*-1-Benzopyran. *Organometallics* **2003**, *22*, 2961 - 2971.

163. Lu, G.; Portscheller, J. L.; Malinakova, H. C., Palladacycles with a Metal-Bonded sp^3-Hybridized Carbon as Intermediates in the Synthesis of 2,2,3,4-Tetrasubstituted 2*H*-1-Benzopyrans and 1,2-Dihydroquinolines. Effects of Auxiliary Ligands and Substitution at a Palladium-Bonded Tertiary Carbon. *Organometallics* **2005**, *24*, 945 - 961.

164. Wallner, F. K.; Elofsson, M., NMR Tube Filter Reactor for Solid-Phase Synthesis and Gel-Phase 19F NMR Spectroscopy. *J. Comb. Chem.* **2006**, *8*, 150 - 152.

165. Danjo, H.; Tanaka, D.; Hayashi, T.; Uozumi, Y., Allylic Substitution in Water Catalyzed by Amphiphilic Resin-Supported Palladium-Phosphine Complexes. *Tetrahedron* **1999**, *55*, 14341 - 14352.

166. Masson, G.; Housseman, C.; Zhu, J., The Enantioselective Morita-Baylis-Hillman Reaction and Its Aza Counterpart. *Angew. Chem., Int. Ed.* **2007**, *46*, 4614 - 4628.

167. Uson, R.; Fornies, J.; Espinet, P.; Martinez, F.; Tomas, M., Reactivity of Tetra-*n*-Butylammonium Di-μ-Chlorobis[bis(pentafluorophenyl)palladate(II)]. A general Method for the Synthesis of *cis* Isomers of Neutral and Anionic Palladium(II) Complexes. *J. Chem. Soc., Dalton Trans.* **1981**, 463 - 465.

168. Aiet-Mohand, S.; Henin, F.; Muzart, J., Palladium-Catalyzed Oxidations: Inhibition of a Pd-H Elimination by Coordination of a Remote Carbon-Carbon Double Bond. *Organometallics* **2001**, *20*, 1683 - 1686.

169. Greaves, E. O.; Lock, C. J. L.; Maitlis, P. M., Metal-Acetylene Complexes. II. Acetylene Complexes of Nickel, Palladium, and Platinum. *Can. J. Chem.* **1968**, *46*, 3879 - 3891.

170. Coghlan, M. J.; Kym, P. R.; Elmore, S. W.; Wang, A. X.; Luly, J. R.; Wilcox, D.; Stashko, M.; Lin, C.-W.; Miner, J.; Tyree, C.; Nakane, M.; Jacobson, P.; Lane, B. C., Synthesis and Characterization of Non-Steroidal Ligands for the Glucocorticoid Receptor: Selective Quinoline Derivatives with Prednisolone-equivalent Functional Activity. *J. Med. Chem.* **2001**, *44*, 2879 - 2885.

171. Elmore, S. W.; Coghlan, M. J.; Anderson, D. D.; Pratt, J. K.; Green, B. E.; Wang, A. X.; Stashko, M. A.; Lin, C. W.; Tyree, C. M.; Miner, J. N.; Jacobson, P. B.; Wilcox, D. M.; Lane, B. C., Nonsteroidal Selective Glucocorticoid Modulators: the Effect of C-5 Alkyl Substitution on the Transcriptional Activation/Repression Profile of 2,5-Dihydro-10-Methoxy-2,2,4-Trimethyl-1*H*-[1]Benzopyrano[3,4-f]Quinolines. *J. Med. Chem.* **2001**, *44*, 4481 - 4491.

172. Leeson, P. D.; Carling, R. W.; Moore, K. W.; Moseley, A. M.; Smith, J. D.; Stevenson, G.; Chan, T.; Baker, R.; Foster, A. C.; et al., 4-Amido-2-Carboxytetrahydroquinolines. Structure-activity Relationships for Antagonism at the Glycine Site of the NMDA Receptor. *J. Med. Chem.* **1992**, *35*, 1954 - 1968.

173. Evans, P. A.; Robinson, J. E.; Moffett, K. K., Regioselective and Enantiospecific Rhodium-Catalyzed Allylic Amination with N-(Arylsulfonyl)anilines. *Org. Lett.* **2001**, *3*, 3269 - 3271.

174. Takamura, M.; Funabashi, K.; Kanai, M.; Shibasaki, M., Asymmetric Reissert-type Reaction Promoted by Bifunctional Catalyst. *J. Am. Chem. Soc.* **2000**, *122*, 6327 - 6328.

175. Takamura, M.; Funabashi, K.; Kanai, M.; Shibasaki, M., Catalytic Enantioselective Reissert-type Reaction: Development and Application to the Synthesis of a Potent NMDA Receptor Antagonist (-)-L-689,560 Using a Solid-Supported Catalyst. *J. Am. Chem. Soc.* **2001**, *123*, 6801 - 6808.

176. Ma, C.; Liu, X.; Li, X.; Flippen-Anderson, J.; Yu, S.; Cook, J. M., Efficient Asymmetric Synthesis of Biologically Important Tryptophan Analogues via a

Palladium-Mediated Heteroannulation Reaction. *J. Org. Chem.* **2001**, *66*, 4525 - 4542.

177. Kofink, C. C.; Blank, B.; Pagano, S.; Goetz, N.; Knochel, P., Iron-catalyzed Aryl-Aryl Cross-Coupling Reaction Tolerating Amides and Unprotected Quinolinones. *Chem. Commun.* **2007**, 1954 - 1956.

178. Corey, E. J.; Fuchs, P. L., Synthetic Method for Conversion of Formyl Groups into Ethynyl Groups. *Tetrahedron Lett.* **1972**, 3769 - 3772.

179. Crimmins, M. T.; Jung, D. K.; Gray, J. L., Synthetic Studies on the Ginkgolides: Total Synthesis of (±)-Bilobalide. *J. Am. Chem. Soc.* **1993**, *115*, 3146 - 3155.

180. Guo, R.; Portscheller, J. L.; Day, V. W.; Malinakova, H. C., An Allylpalladium(IV) Intermediate in the Synthesis of Highly Substituted Benzoxepines and Benzopyrans via Reactions of Stable Pallada(II)cycles with Allyl Bromides. *Organometallics* **2007**, *26*, 3874 - 3883.

181. Dghaym, R. D.; Dhawan, R.; Arndtsen, B. A., The Use of Carbon Monoxide and Imines as Peptide Derivative Synthons: A Facile Palladium-Catalyzed Synthesis of α-Amino Acid Derived Imidazolines. *Angew. Chem., Int. Ed.* **2001**, *40*, 3228 - 3230.

182. Davis, J. L.; Dhawan, R.; Arndtsen, B. A., Imines in Stille-type Cross-Coupling Reactions: A Multicomponent Synthesis of α-Substituted Amides. *Angew. Chem., Int. Ed.* **2004**, *43*, 590 - 594.

183. Maryanoff, B. E.; Zhang, H.-C.; Cohen, J. H.; Turchi, I. J.; Maryanoff, C. A., Cyclizations of N-acyliminium Ions. *Chem. Rev.* **2004**, *104*, 1431 - 1628.

184. Culkin, D. A.; Hartwig, J. F., Carbon-Carbon Bond-Forming Reductive Elimination from Arylpalladium Complexes Containing Functionalized Alkyl Groups. Influence of Ligand Steric and Electronic Properties on Structure, Stability, and Reactivity. *Organometallics* **2004**, *23*, 3398 - 3416.

185. Saito, B.; Fu Gregory, C., Alkyl-Alkyl Suzuki Cross-Couplings of Unactivated Secondary Alkyl Halides at Room Temperature. *J. Am. Chem. Soc.* **2007**, *129*, 9602 - 9603.

186. Ishiyama, T.; Abe, S.; Miyaura, N.; Suzuki, A., Palladium-Catalyzed Alkyl-Alkyl Cross-Coupling Reaction of 9-Alkyl-9-BBN Derivatives with Iodoalkanes Possessing β-hydrogens. *Chem. Lett.* **1992**, 691 - 694.

187. Silverstein, R. M.; Webster, F. X.; Kiemle, D. J., *Spectrometric Identification of Organic Compounds*. 7th ed.; John Wiley and Sons, Inc.: Hoboken, N.J., 2005.

188. Gawley, R. E.; Aubé, J., *Principles of Asymmetric Synthesis*. 1st ed.; Pergamon: Oxford, 1996.

189. Hershberger, J. C.; Day, V. W.; Malinakova, H. C., Diastereoinduction in the Synthesis of Pallada(II)pyrrolidinones: Palladacycles with Two Pd-bonded Stereogenic Carbons. *Organometallics* **2009**, *28*, 810 - 818.

190. Pauling, L. N., *The Nature of the Chemial Bond*. 3rd ed.; Ithaca, N.Y., 1960.

191. Pfaltz, A.; Drury, W. J., III, Design of chiral ligands for asymmetric catalysis: from C_2-symmetric P,P- and N,N-ligands to Sterically and Electronically Nonsymmetrical P,N-ligands. *Proc. Natl. Acad. Sci. U. S. A.* **2004**, *101*, 5723 - 5726.

192. Anslyn, E. V.; Dougherty, D. A., *Modern Physical Organic Chemistry*. University Science Books: Sausalito, 2006.

193. Bordwell, F. G., Equilibrium Acidities in Dimethyl Sulfoxide Solution. *Acc. Chem. Res.* **1988**, *21*, 456 - 463.

194. Trepka, R. D.; Belisle, J. W.; Harrington, J. K., Acidites and Partition Coefficients of Fluoromethanesulfonamides. *J. Org. Chem.* **1974**, *39*, 1094 - 1098.

195. Barrow, K. D.; Spotswood, T. M., Stereochemistry and Proton Magnetic Resonance Spectra of β-lactams. *Tetrahedron Lett.* **1965**, 3325 - 3335.

196. Diversi, P.; Ingrosso, G.; Lucherini, A.; Lumini, T.; Marchetti, F.; Adovasio, V.; Nardelli, M., Synthesis and Thermal Decomposition of Palladacyclopentane Derivatives of the Type [Pd($CH_2CHRCHRCH_2$)L2] (R = H or Me). X-Ray Crystal Structure of (2,2'-bipyridyl)(butane-1,4-diyl)Palladium(II). *J. Chem. Soc., Dalton Trans.* **1988**, 133 - 140.

197. Diversi, P.; Fasce, D.; Santini, R., Neopentyl Complexes of Palladium. *J. Organomet. Chem.* **1984**, *269*, 285 - 293.

198. Diversi, P.; Ingrosso, G.; Lucherini, A.; Murtas, S., Synthesis and Chemistry of Some Palladacyclopentanes. *J. Chem. Soc., Dalton Trans.* **1980**, 1633 - 1637.

199. Zhao, L.; Li, C.-J., Highly Efficient Three-component Synthesis of β-lactams from N-methylhydroxylamine, Aldehydes, and Phenylacetylene. *Chem. Asian J.* **2006**, *1*, 203 - 209.

200. Fuchigami, T.; Narizuka, S.; Konno, A., Electrolytic Partial Fluorination of Organic Compounds. 4. Regioselective Anodic Monofluorination of 4-Thiazolidinones and its Application to the Synthesis of Monofluoro β-lactams. *J. Org. Chem.* **1992**, *57*, 3755 - 3757.

201. Johnson, M. R.; Fazio, M. J.; Ward, D. L.; Sousa, L. R., Synthesis of β-lactams by the Photochemical Extrusion of Sulfur Dioxide from 1,1-Dioxo-4-Thiazolidinones. *J. Org. Chem.* **1983**, *48*, 494 - 499.

202. Dahan, A.; Portnoy, M., Remarkable Dendritic Effect in the Polymer-Supported Catalysis of the Heck Arylation of Olefins. *Org. Lett.* **2003**, *5*, 1197-1200.

203. Santini, R.; Griffith, M. C.; Qi, M., A Measure of Solvent Effects on Swelling of Resins for Solid Phase Organic Synthesis. *Tetrahedron Lett.* **1998**, *39*, 8951 - 8954.

204. Sturino, C. F.; O'Neill, G.; Lachance, N.; Boyd, M.; Berthelette, C.; Labelle, M.; Li, L.; Roy, B.; Scheigetz, J.; Tsou, N.; Aubin, Y.; Bateman, K. P.; Chauret, N.; Day, S. H.; Levesque, J.-F.; Seto, C.; Silva, J. H.; Trimble, L. A.; Carriere, M.-C.; Denis, D.; Greig, G.; Kargman, S.; Lamontagne, S.; Mathieu, M.-C.; Sawyer, N.; Slipetz, D.; Abraham, W. M.; Jones, T.; McAuliffe, M.; Piechuta, H.; Nicoll-Griffith, D. A.; Wang, Z.; Zamboni, R.; Young, R. N.; Metters, K. M., Discovery of a Potent and Selective Prostaglandin D_2 Receptor Antagonist, [(3*R*)-4-(4-Chlorobenzyl)-7-

fluoro-5-(methylsulfonyl)-1,2,3,4-tetrahydrocyclopenta[b]indol-3-yl]-acetic Acid (MK-0524). *J. Med. Chem.* **2007**, *50*, 794 - 806.

205. Xiao, W.-J.; Alper, H., Regioselective Carbonylative Heteroannulation of *o*-Iodothiophenols with Allenes and Carbon Monoxide Catalyzed by a Palladium Complex: A Novel and Efficient Access to Thiochroman-4-one Derivatives. *J. Org. Chem.* **1999**, *64*, 9646 - 9652.

206. Ingham, C. F.; Massy-Westropp, R. A.; Reynolds, G. D., Synthesis of Freelingyne. *Aust. J. Chem.* **1974**, *27*, 1477 - 1489.

207. He, W.; Herrick, I. R.; Atesin, T. A.; Caruana, P. A.; Kellenberger, C. A.; Frontier, A. J., Polarizing the Nazarov Cyclization: The Impact of Dienone Substitution Pattern on Reactivity and Selectivity. *J. Am. Chem. Soc.* **2008**, *130*, 1003 - 1011.

208. Hari, Y.; Date, K.; Aoyama, T., Facile One-pot Synthesis of Functionalized Acetylenes from Aryl and Heteroaryl Aldehydes Using Lithium Trimethylsilyldiazomethane. *Heterocycles* **2007**, *74*, 545 - 552.

209. Vasilyev, A. V.; Walspurger, S.; Chassaing, S.; Pale, P.; Sommer, J., One-step Addition of Sulfonic Acids to Acetylene Derivatives: An Alternative and Stereoselective Approach to Vinyl Triflates and Fluorosulfonates. *Eur. J. Org. Chem.* **2007**, 5740 - 5748.

210. Lecercle, D.; Mothes, C.; Taran, F., Straightforward synthesis of 2-Aryl-1-Alkynylphosphonates and Arylpropiolates. *Synth. Commun.* **2007**, *37*, 1301 - 1311.

211. Xie, C.; Liu, L.; Zhang, Y.; Xu, P., Copper-Catalyzed Alkyne-Aryne and Alkyne-Alkene-Aryne Coupling Reactions. *Org. Lett.* **2008**, *10*, 2393 - 2396.

Appendix

Selected NMR spectra and X-Ray Crystallographic Data

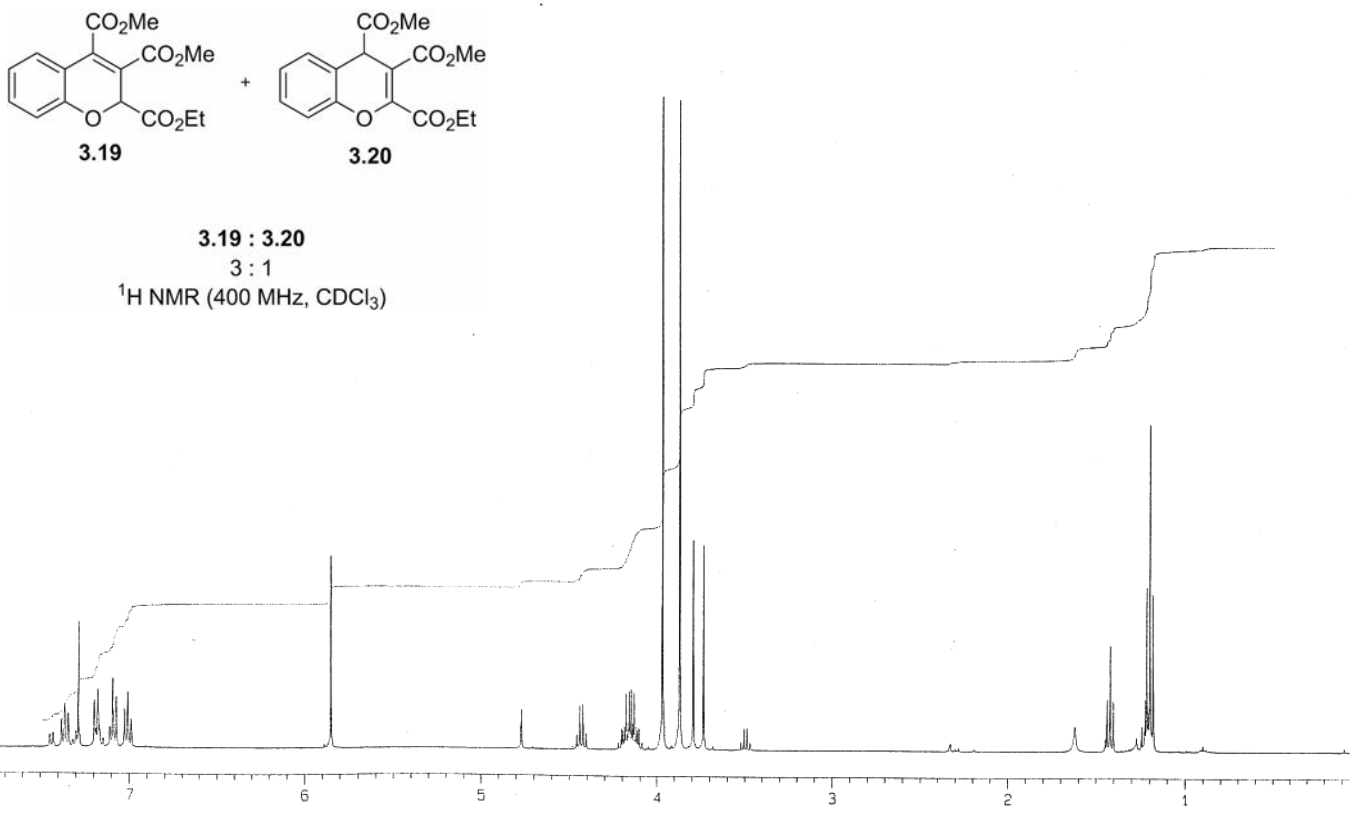
CO2Me
CO2Me
CO2Et
O
3.19
+
CO2Me
CO2Me
CO2Et
O
3.20
3.19 : 3.20
3 : 1
1H NMR (400 MHz, CDCl3)
ppm
7
6
5
4
3
2
1

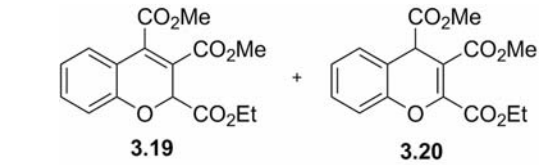

3.19 : 3.20
3 : 1
^{13}C NMR (100 MHz, $CDCl_3$)

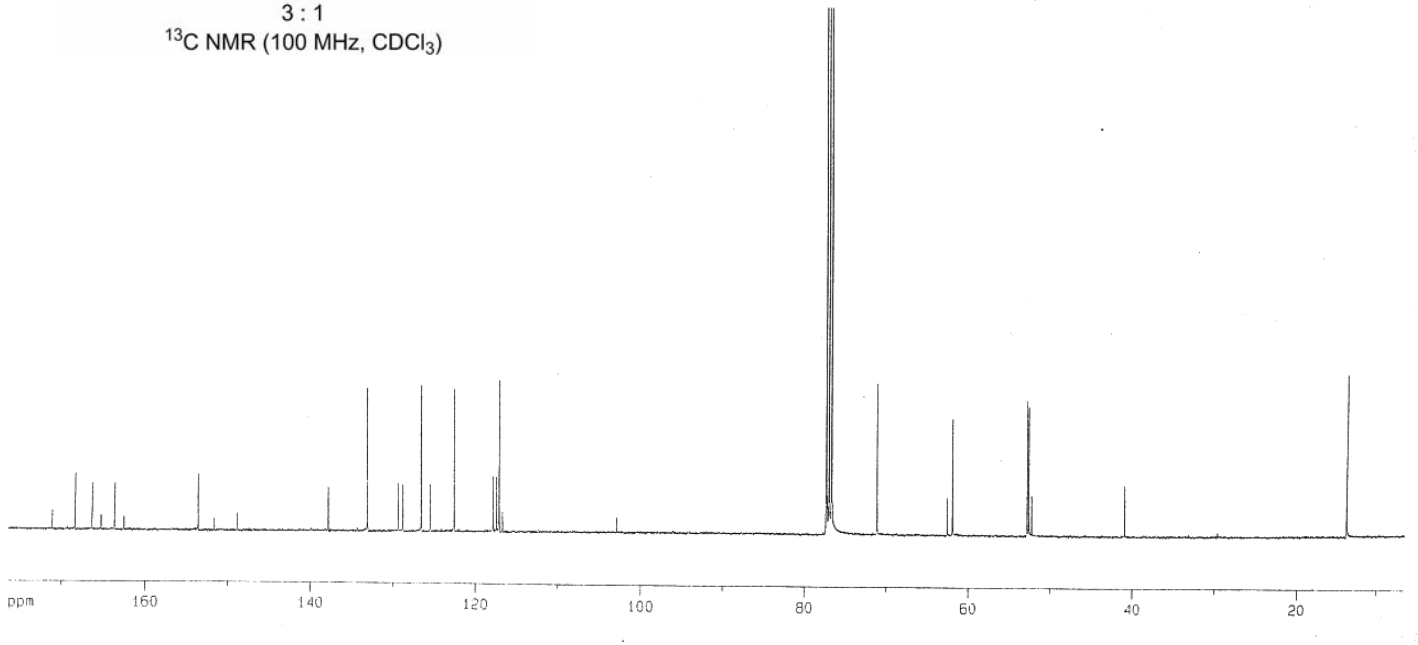

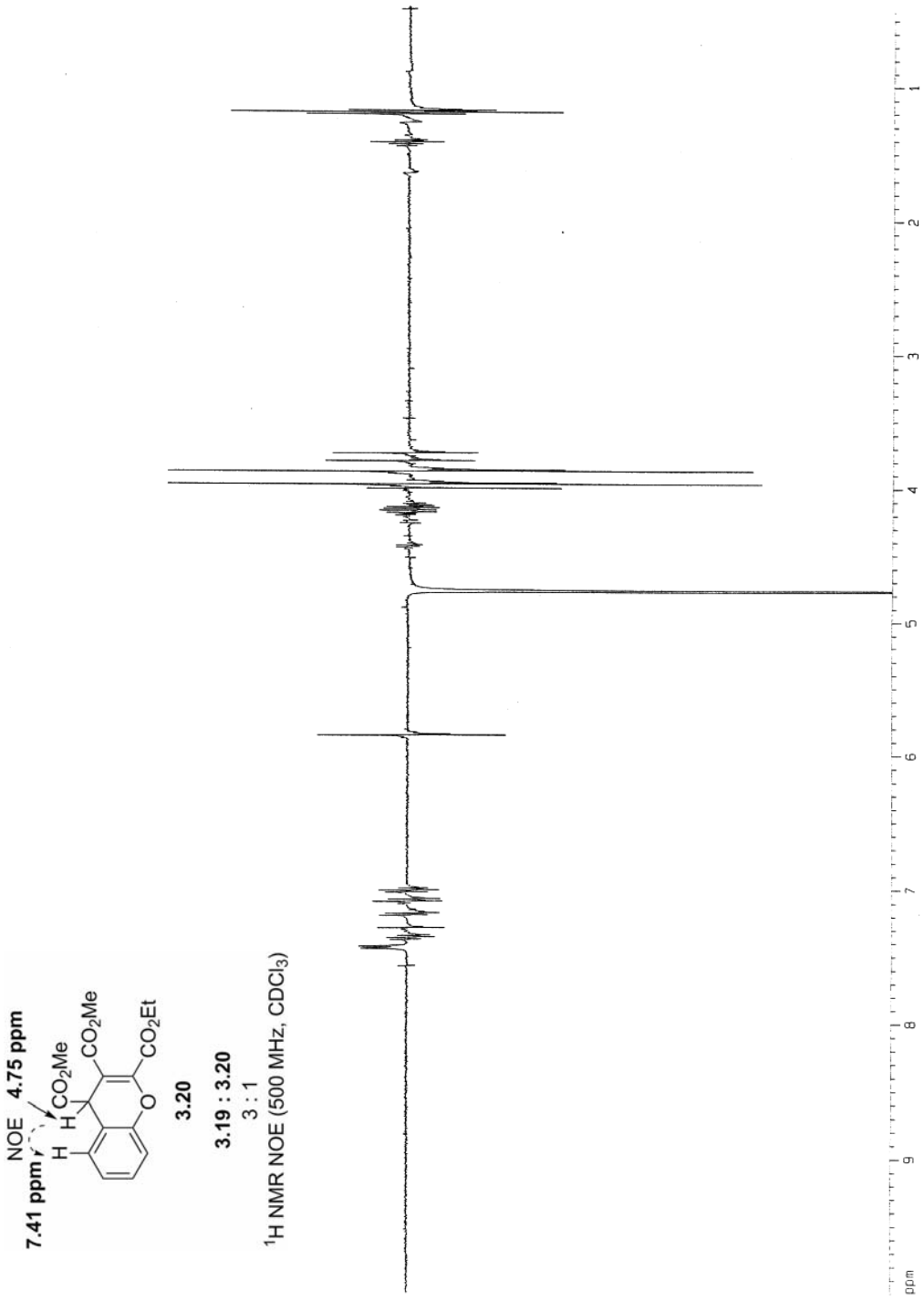
NOE 4.75 ppm
7.41 ppm
CO2Me
CO2Me
CO2Et
O
H
H
3.20
3.19 : 3.20
3 : 1
1H NMR NOE (500 MHz, CDCl3)
ppm

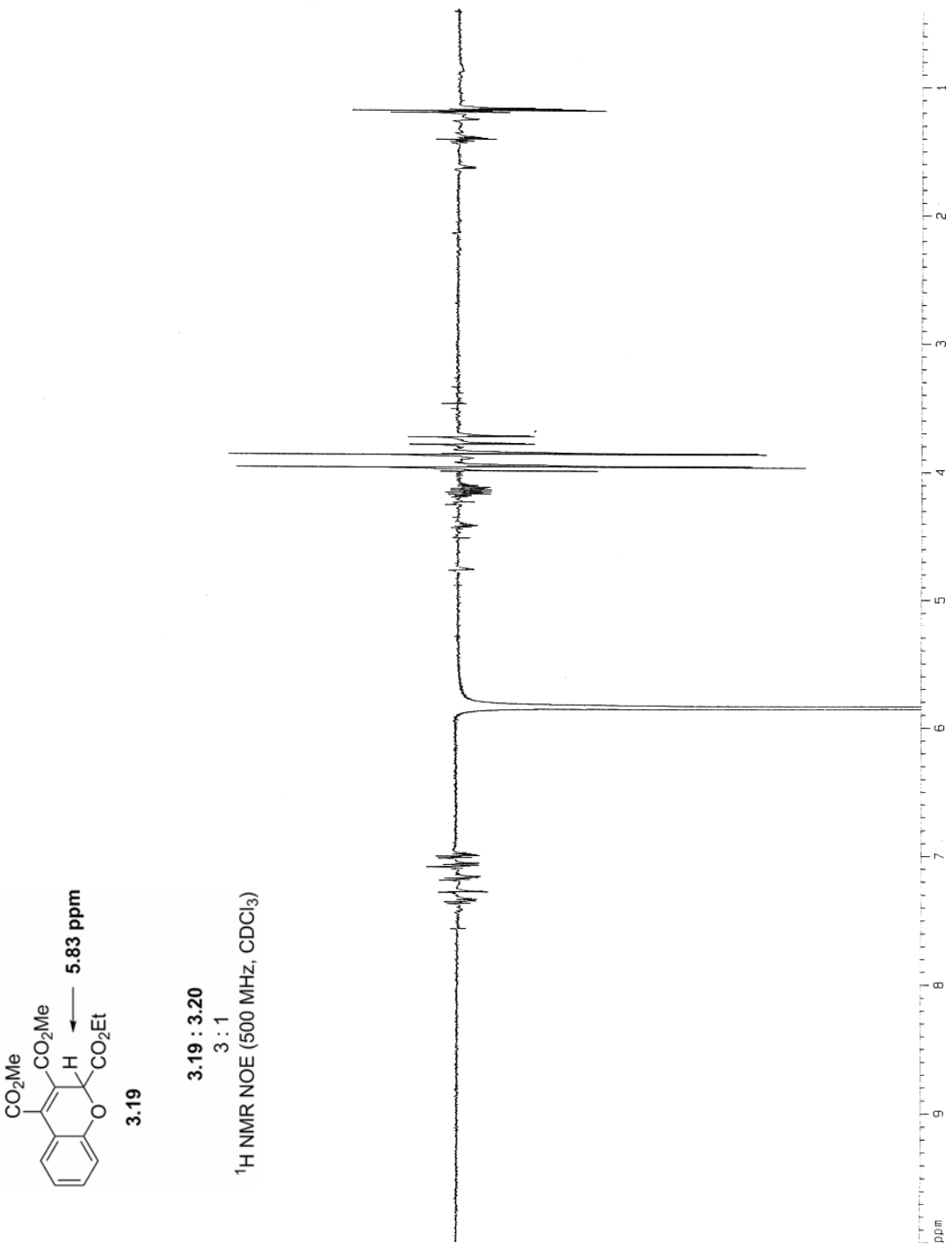
CO2Me
CO2Me
H
CO2Et
O
5.83 ppm
3.19
3.19 : 3.20
3 : 1
1H NMR NOE (500 MHz, CDCl3)
ppm

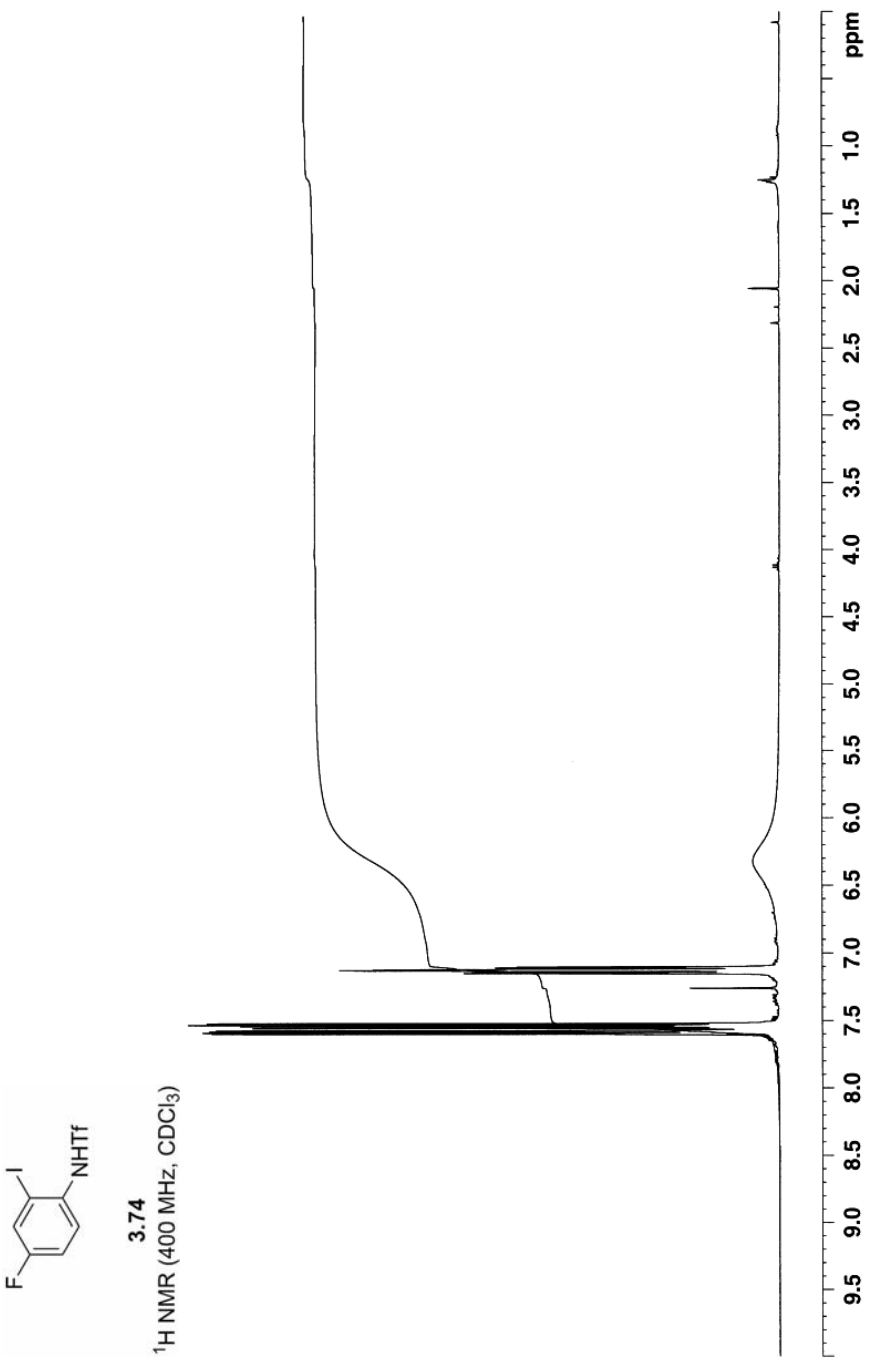
I
NHTf
F
3.74
^{1}H NMR (400 MHz, $CDCl_3$)
9.5
9.0
8.5
8.0
7.5
7.0
6.5
6.0
5.5
5.0
4.5
4.0
3.5
3.0
2.5
2.0
1.5
1.0
ppm

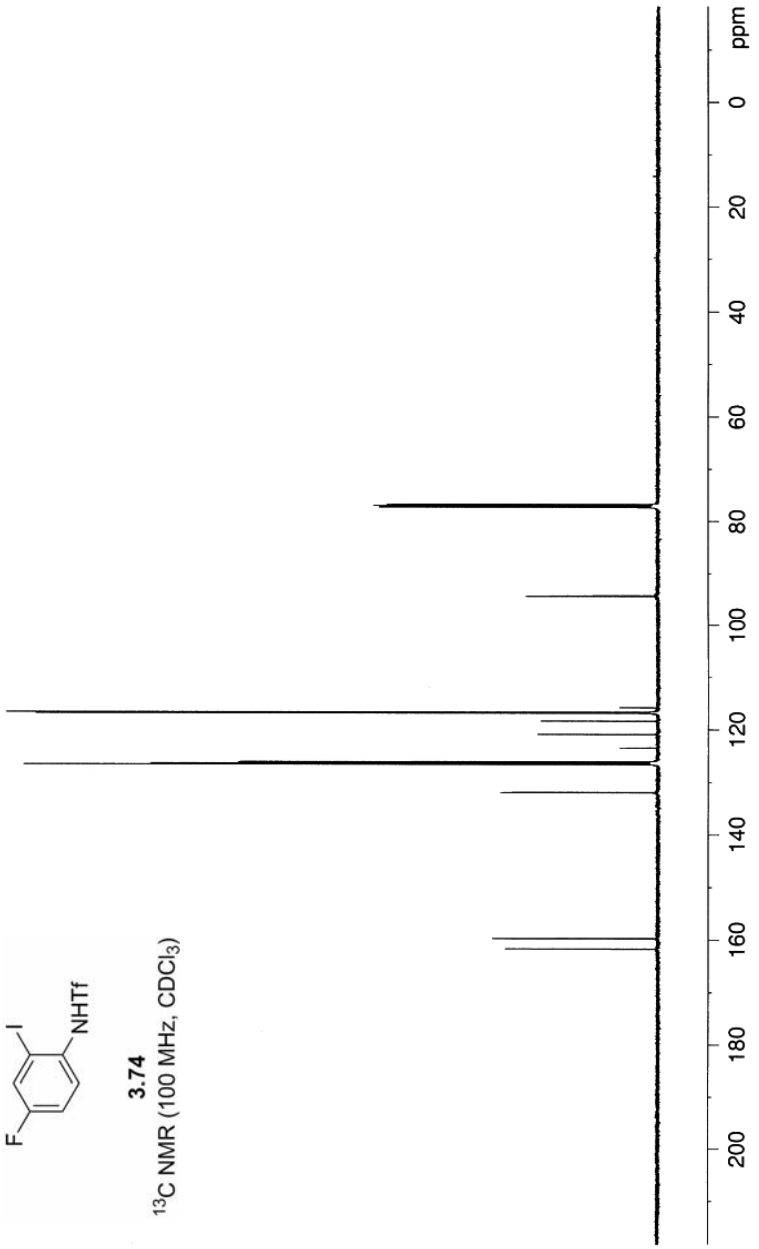
I
NHTf
F
3.74
^{13}C NMR (100 MHz, $CDCl_3$)
200
180
160
140
120
100
80
60
40
20
0
ppm

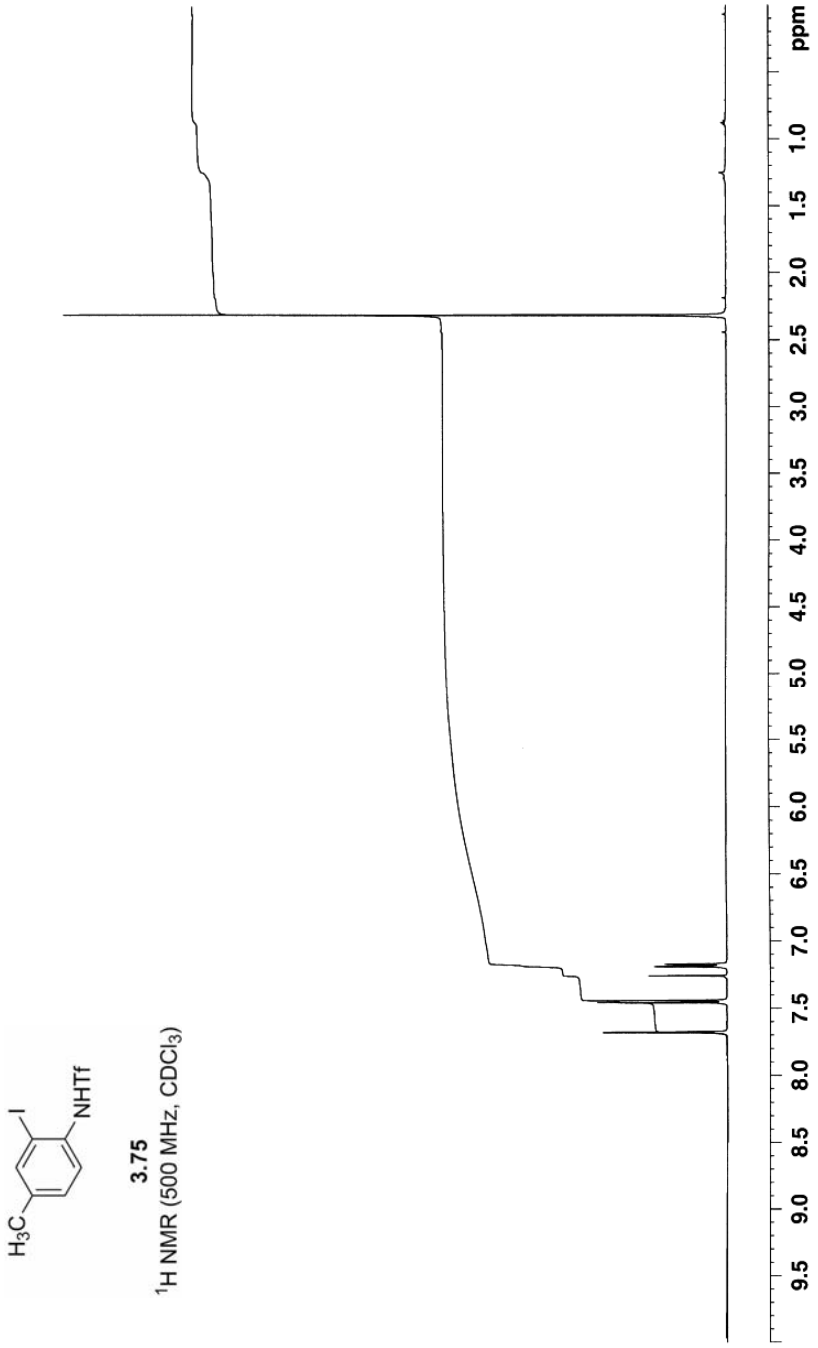
I
NHTf
H3C
3.75
1H NMR (500 MHz, CDCl3)
9.5 9.0 8.5 8.0 7.5 7.0 6.5 6.0 5.5 5.0 4.5 4.0 3.5 3.0 2.5 2.0 1.5 1.0
ppm

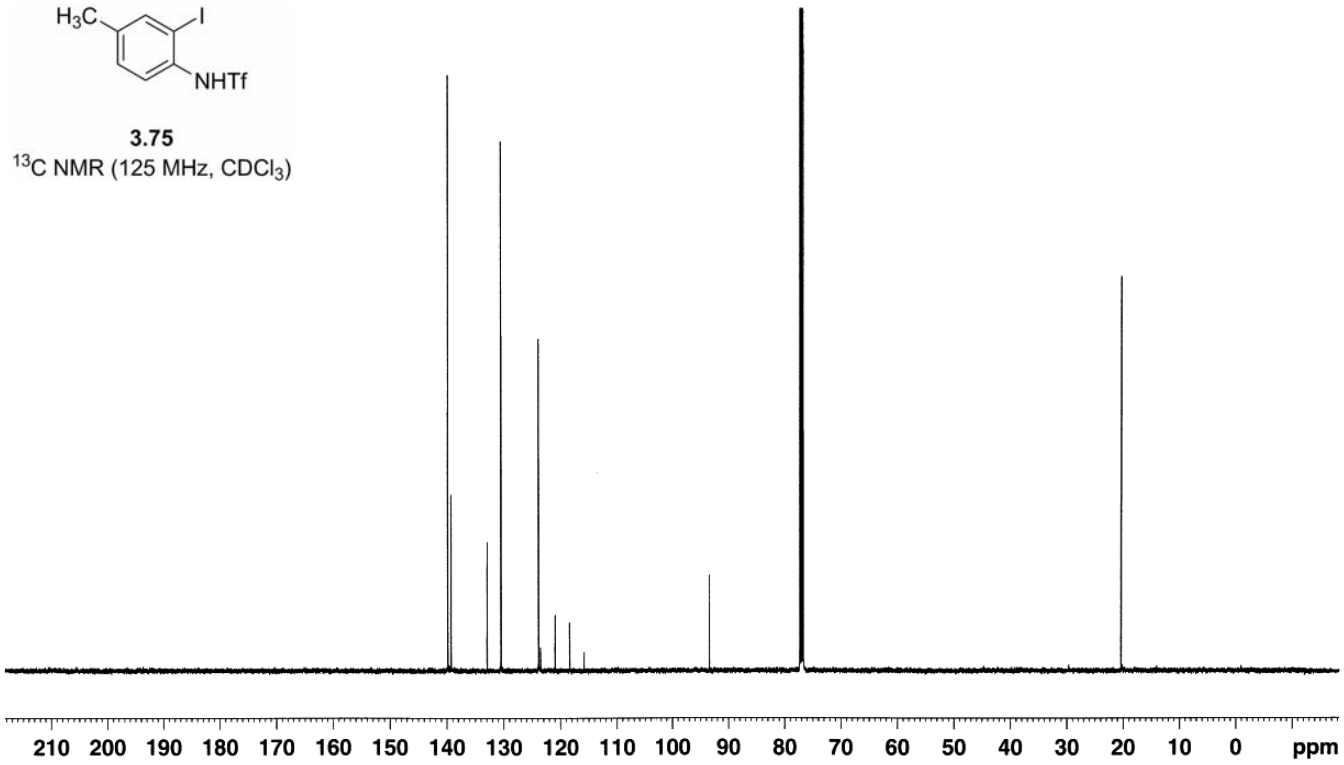
H3C
I
NHTf
3.75
13C NMR (125 MHz, CDCl3)
210 200 190 180 170 160 150 140 130 120 110 100 90 80 70 60 50 40 30 20 10 0 ppm

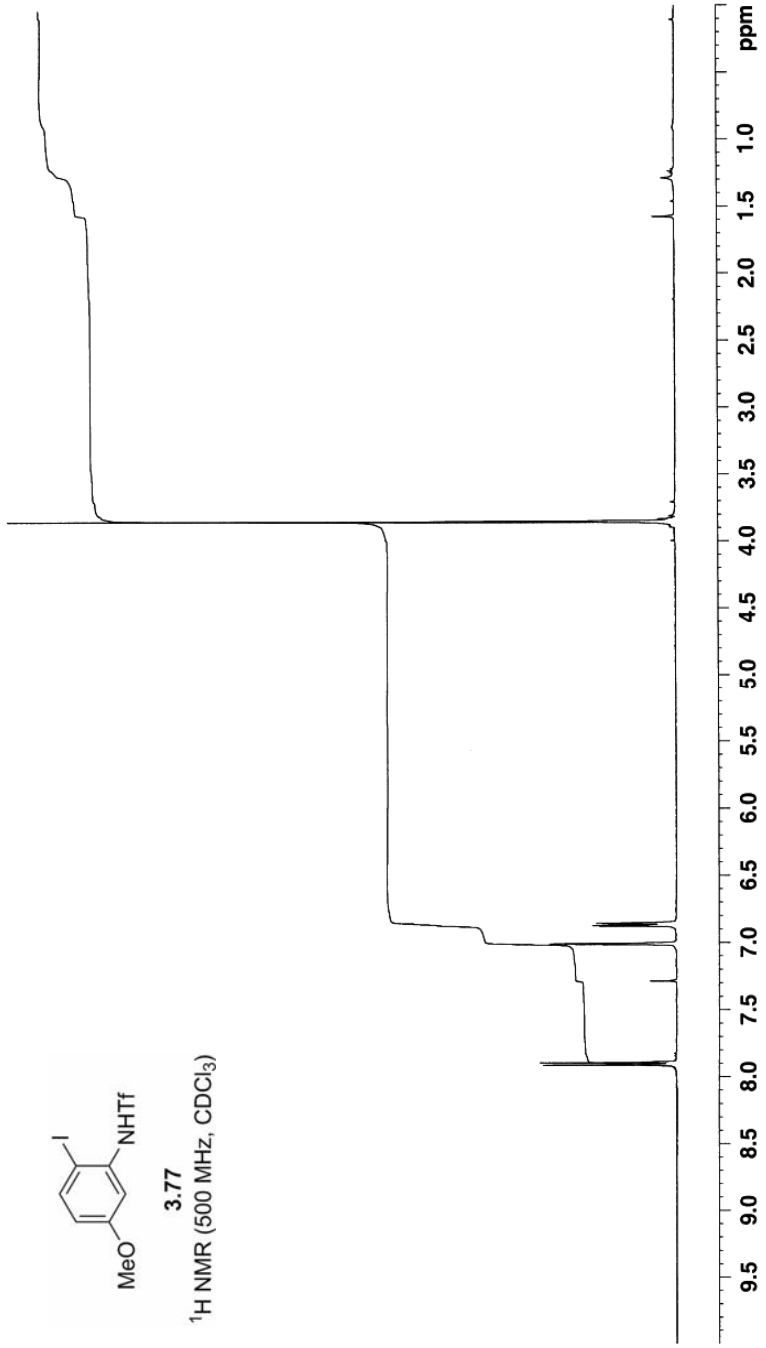
I
NHTf
MeO
3.77
^{1}H NMR (500 MHz, $CDCl_3$)
9.5 9.0 8.5 8.0 7.5 7.0 6.5 6.0 5.5 5.0 4.5 4.0 3.5 3.0 2.5 2.0 1.5 1.0
ppm

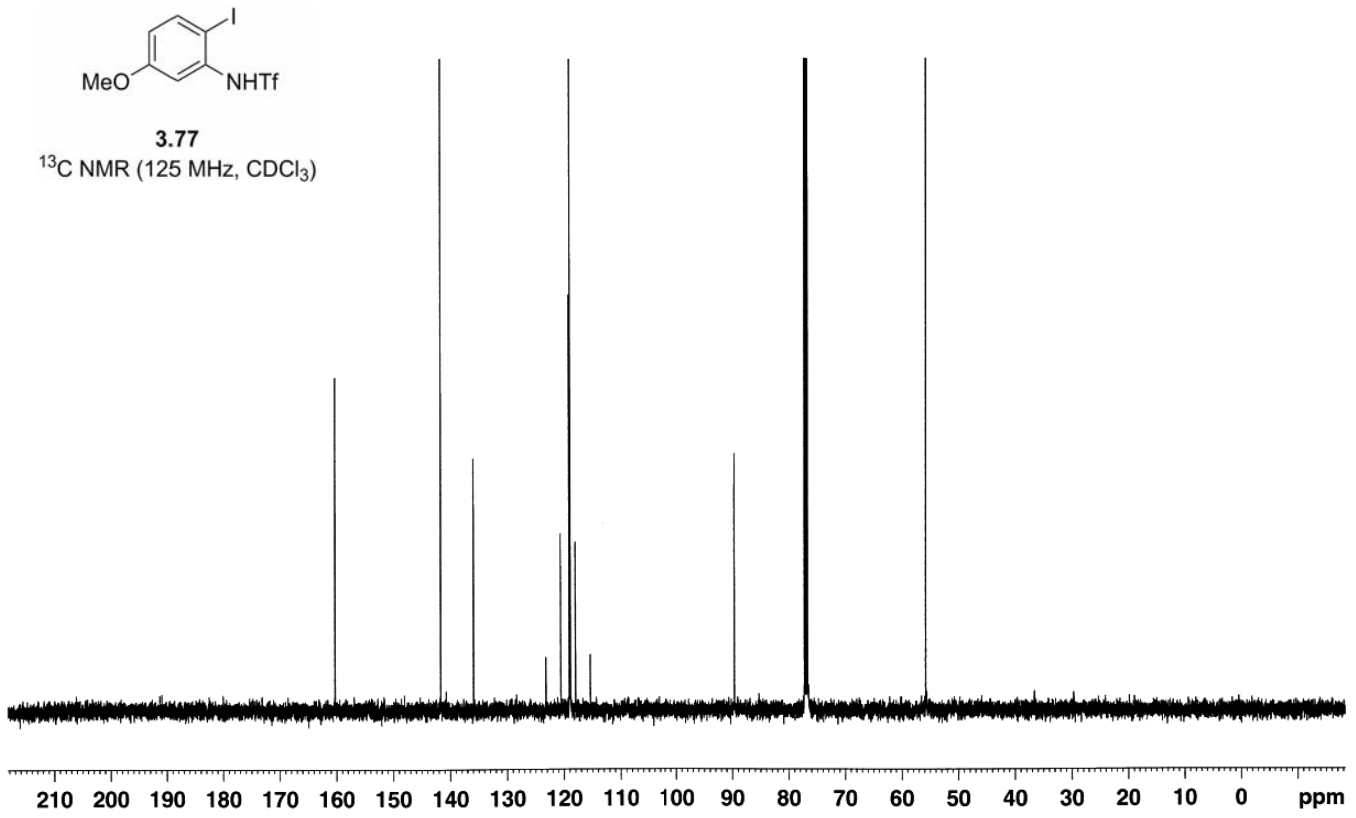
I
MeO
NHTf
3.77
13C NMR (125 MHz, CDCl3)
210 200 190 180 170 160 150 140 130 120 110 100 90 80 70 60 50 40 30 20 10 0 ppm

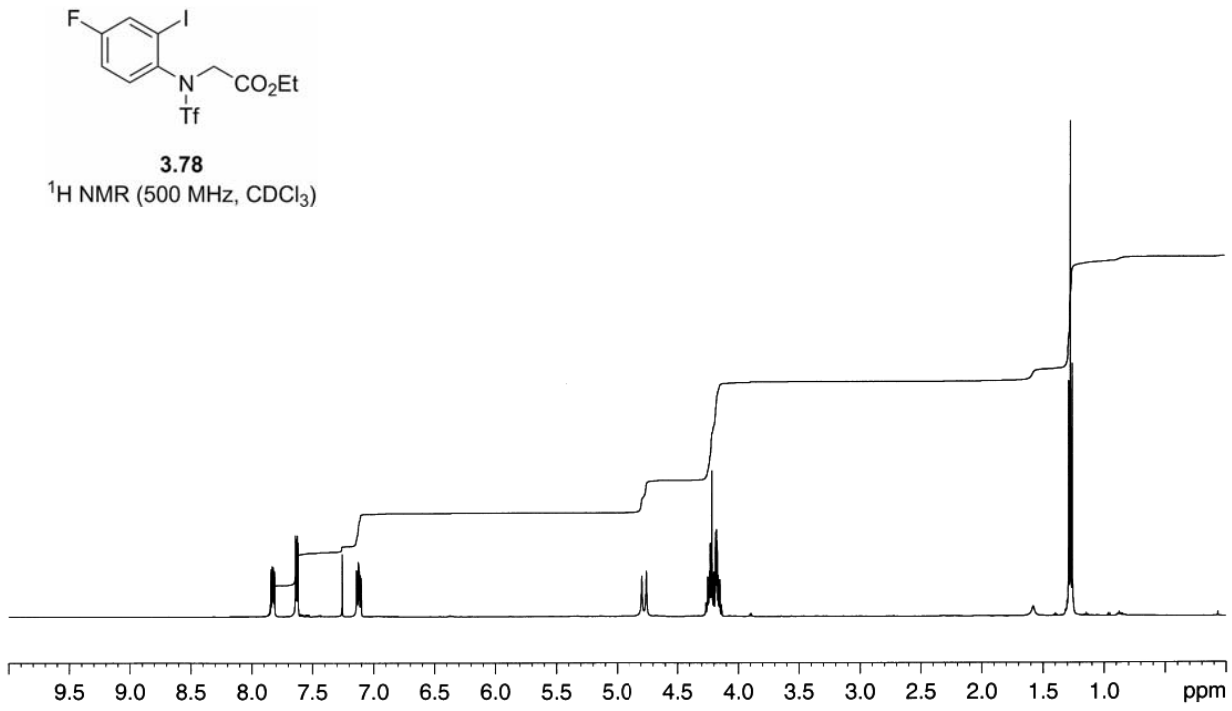
F
I
N
CO2Et
Tf
3.78
1H NMR (500 MHz, CDCl3)
9.5
9.0
8.5
8.0
7.5
7.0
6.5
6.0
5.5
5.0
4.5
4.0
3.5
3.0
2.5
2.0
1.5
1.0
ppm

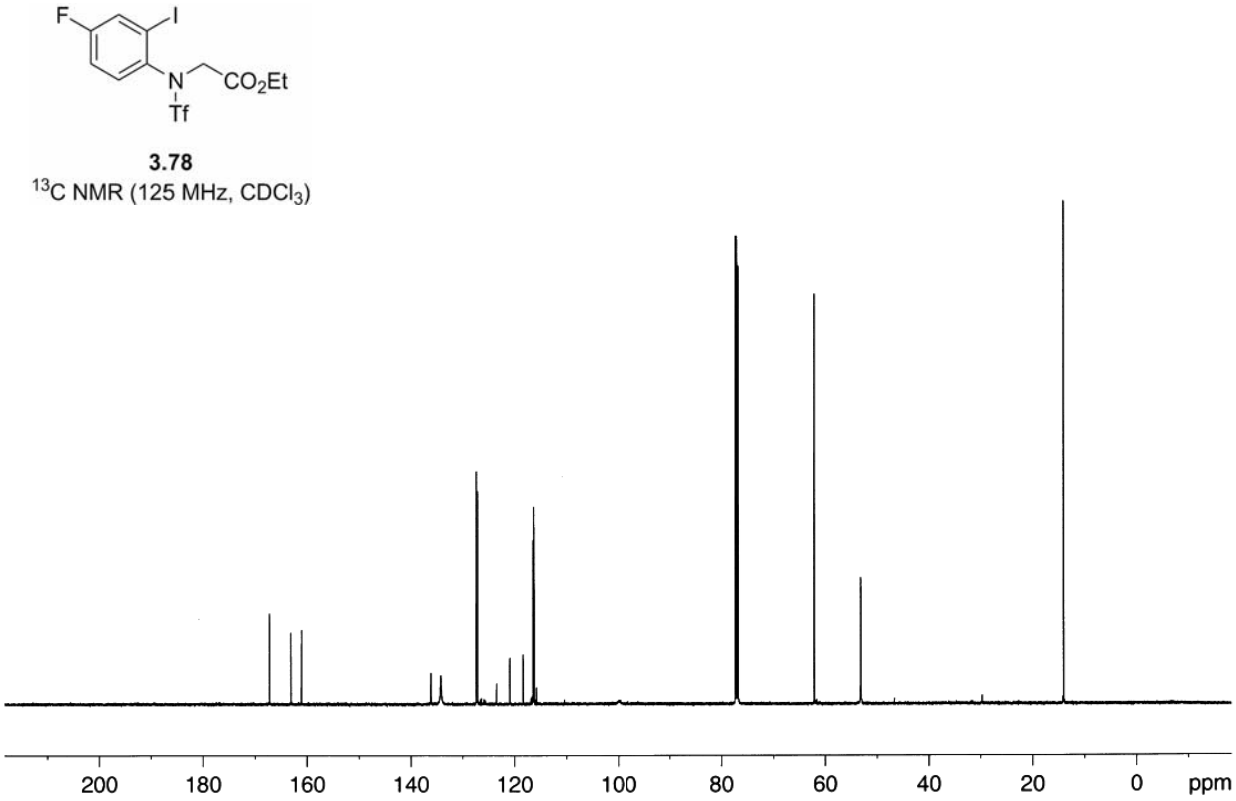
F
I
N
CO2Et
Tf
3.78
13C NMR (125 MHz, CDCl3)
200
180
160
140
120
100
80
60
40
20
0
ppm

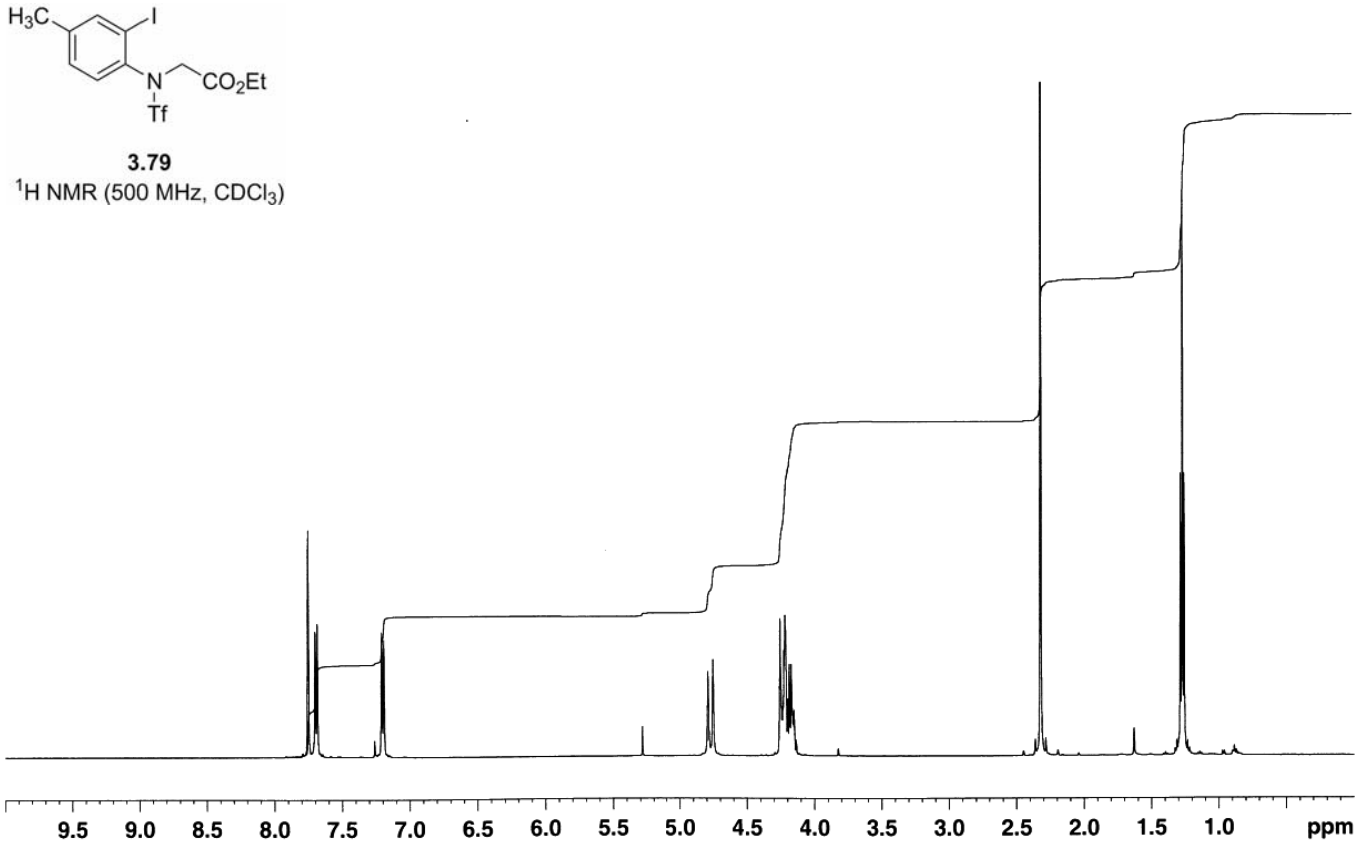
H3C
I
N
CO2Et
Tf
3.79
1H NMR (500 MHz, CDCl3)
9.5
9.0
8.5
8.0
7.5
7.0
6.5
6.0
5.5
5.0
4.5
4.0
3.5
3.0
2.5
2.0
1.5
1.0
ppm

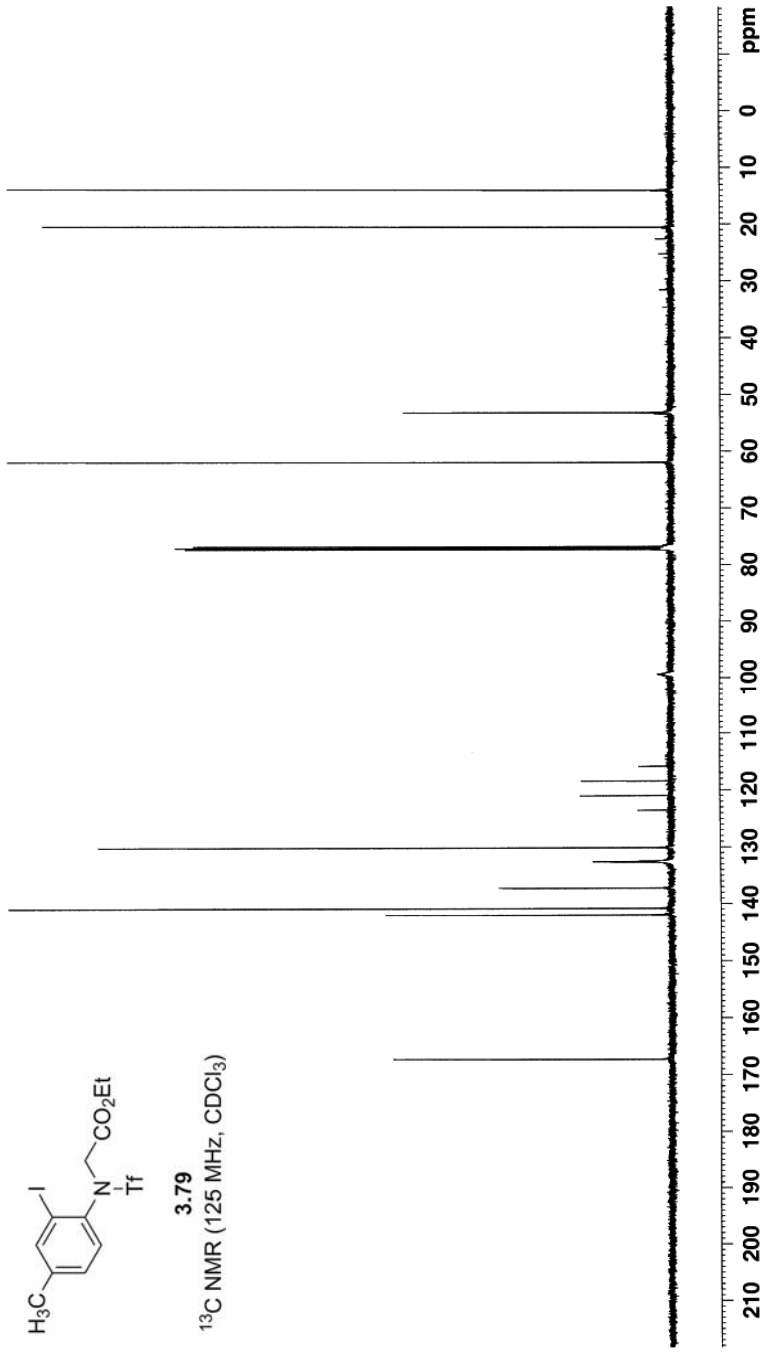
I
CO2Et
N
Tf
H3C
3.79
13C NMR (125 MHz, CDCl3)
210 200 190 180 170 160 150 140 130 120 110 100 90 80 70 60 50 40 30 20 10 0 ppm

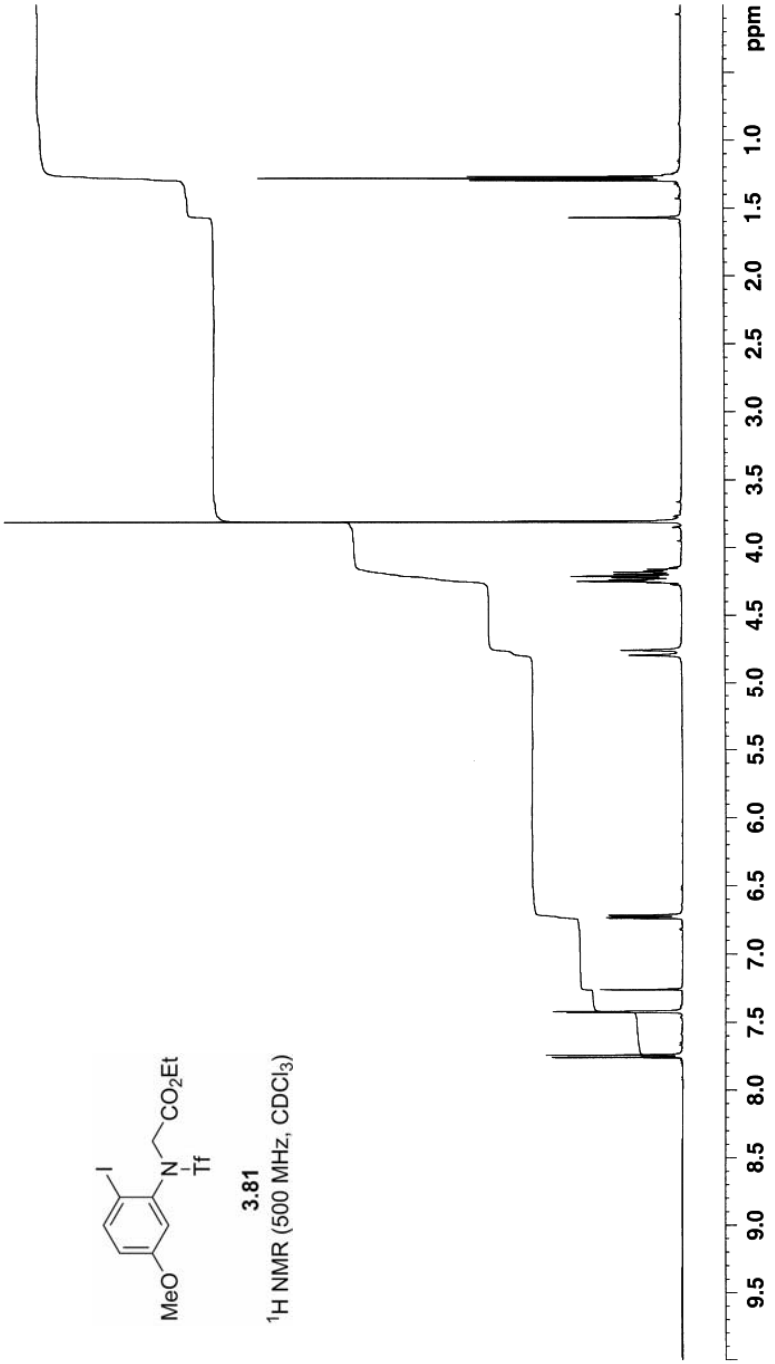
I
MeO
N
Tf
CO2Et
3.81
1H NMR (500 MHz, CDCl3)
9.5 9.0 8.5 8.0 7.5 7.0 6.5 6.0 5.5 5.0 4.5 4.0 3.5 3.0 2.5 2.0 1.5 1.0
ppm

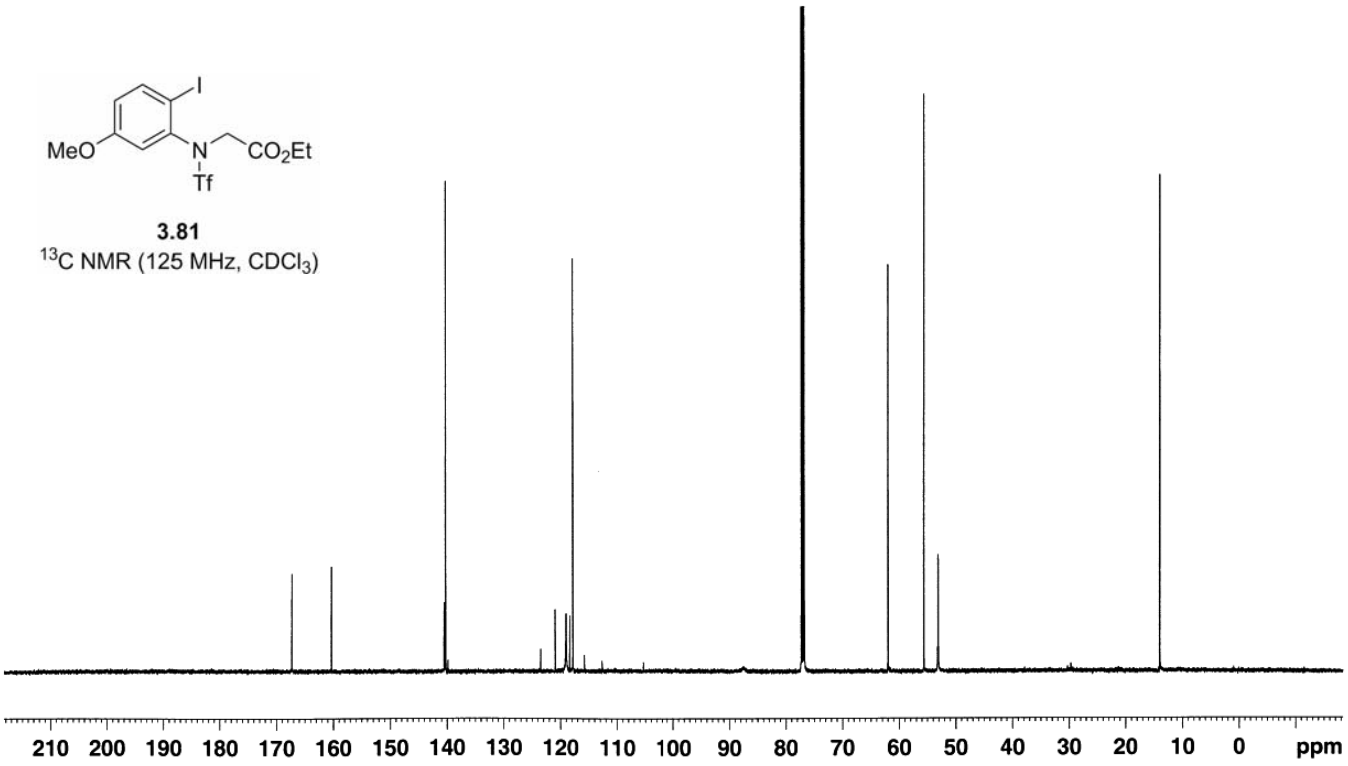
I
MeO
N
CO2Et
Tf
3.81
13C NMR (125 MHz, CDCl3)
210 200 190 180 170 160 150 140 130 120 110 100 90 80 70 60 50 40 30 20 10 0 ppm

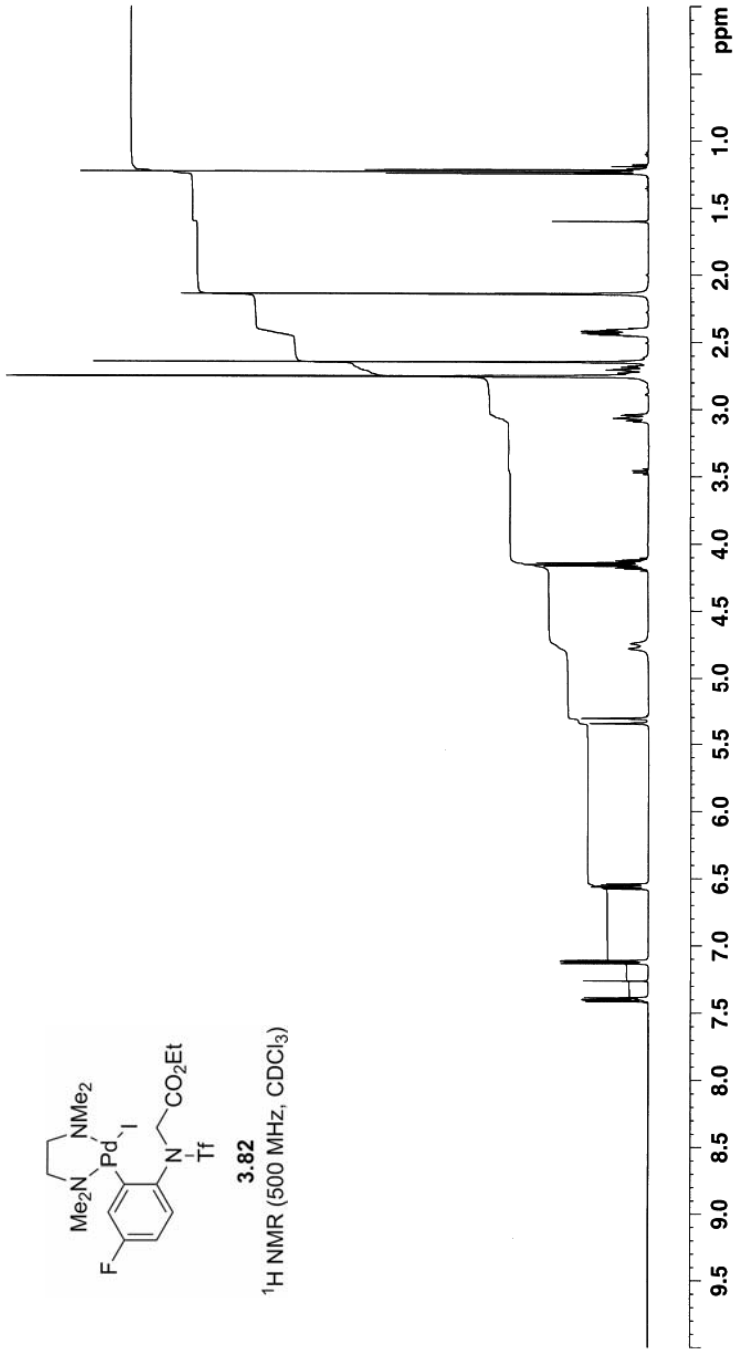
Me2N
NMe2
Pd
I
F
N
Tf
CO2Et
3.82
1H NMR (500 MHz, CDCl3)
9.5 9.0 8.5 8.0 7.5 7.0 6.5 6.0 5.5 5.0 4.5 4.0 3.5 3.0 2.5 2.0 1.5 1.0
ppm

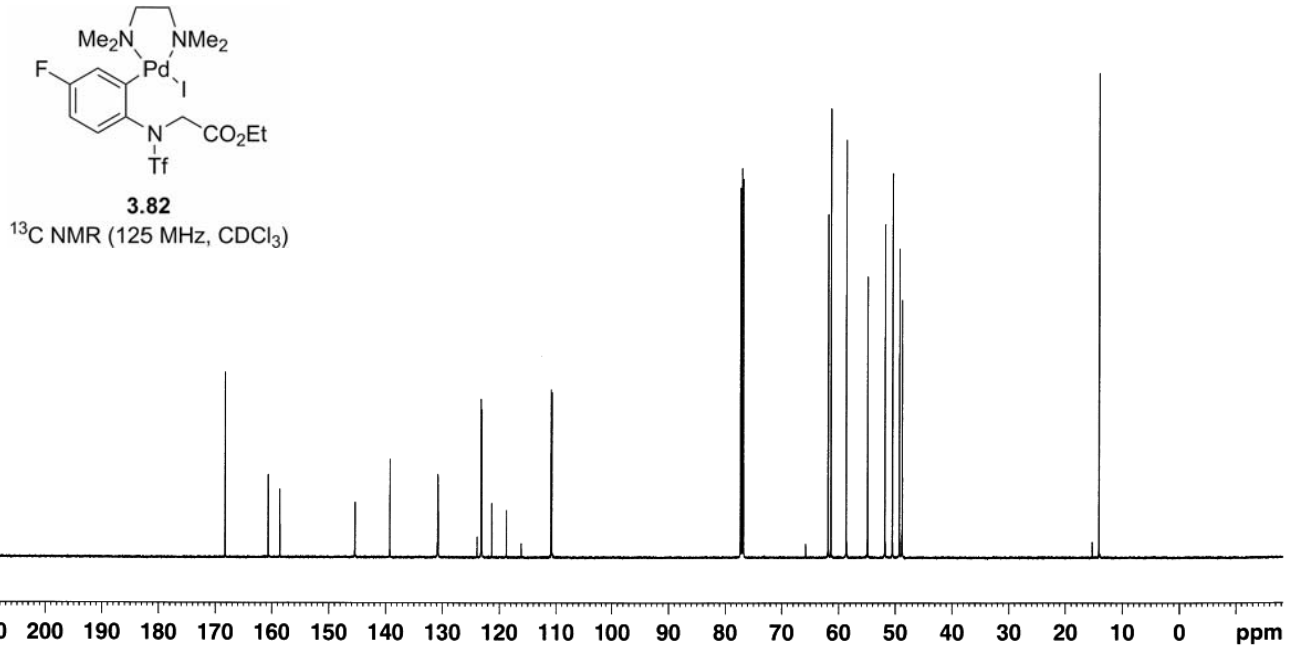
Me2N
NMe2
Pd
I
F
N
CO2Et
Tf
3.82
13C NMR (125 MHz, CDCl3)
210 200 190 180 170 160 150 140 130 120 110 100 90 80 70 60 50 40 30 20 10 0 ppm

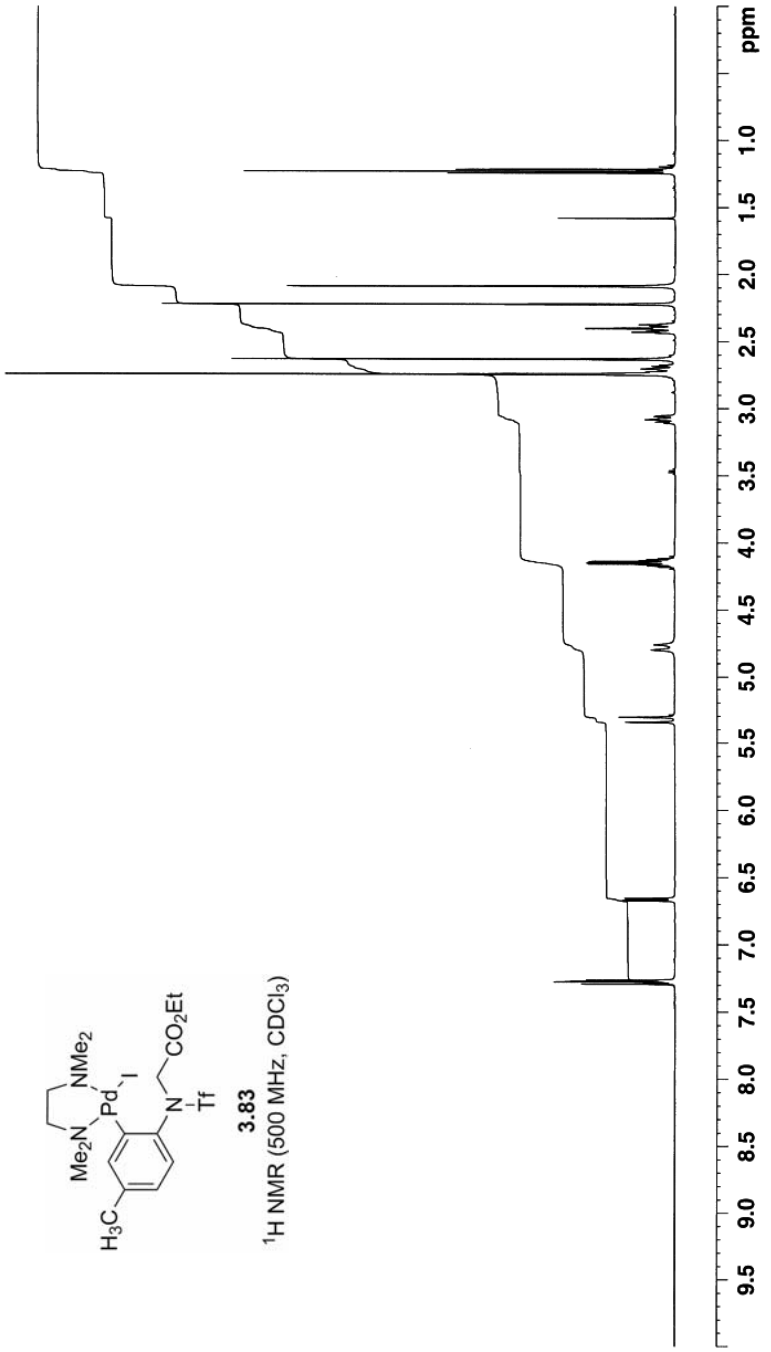
Me2N
NMe2
Pd
I
N
Tf
CO2Et
H3C
3.83
1H NMR (500 MHz, CDCl3)
9.5
9.0
8.5
8.0
7.5
7.0
6.5
6.0
5.5
5.0
4.5
4.0
3.5
3.0
2.5
2.0
1.5
1.0
ppm

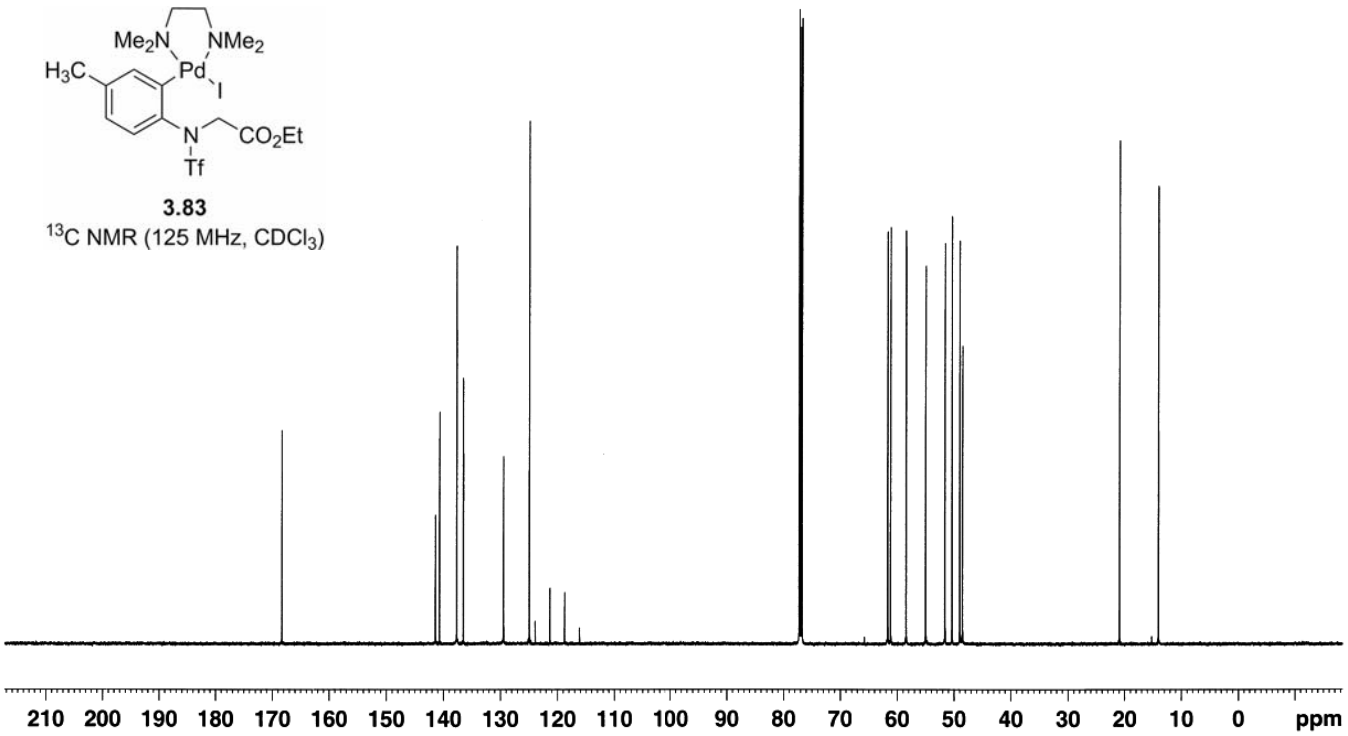
Me2N
NMe2
H3C
Pd
I
N
CO2Et
Tf
3.83
13C NMR (125 MHz, CDCl3)
210 200 190 180 170 160 150 140 130 120 110 100 90 80 70 60 50 40 30 20 10 0 ppm

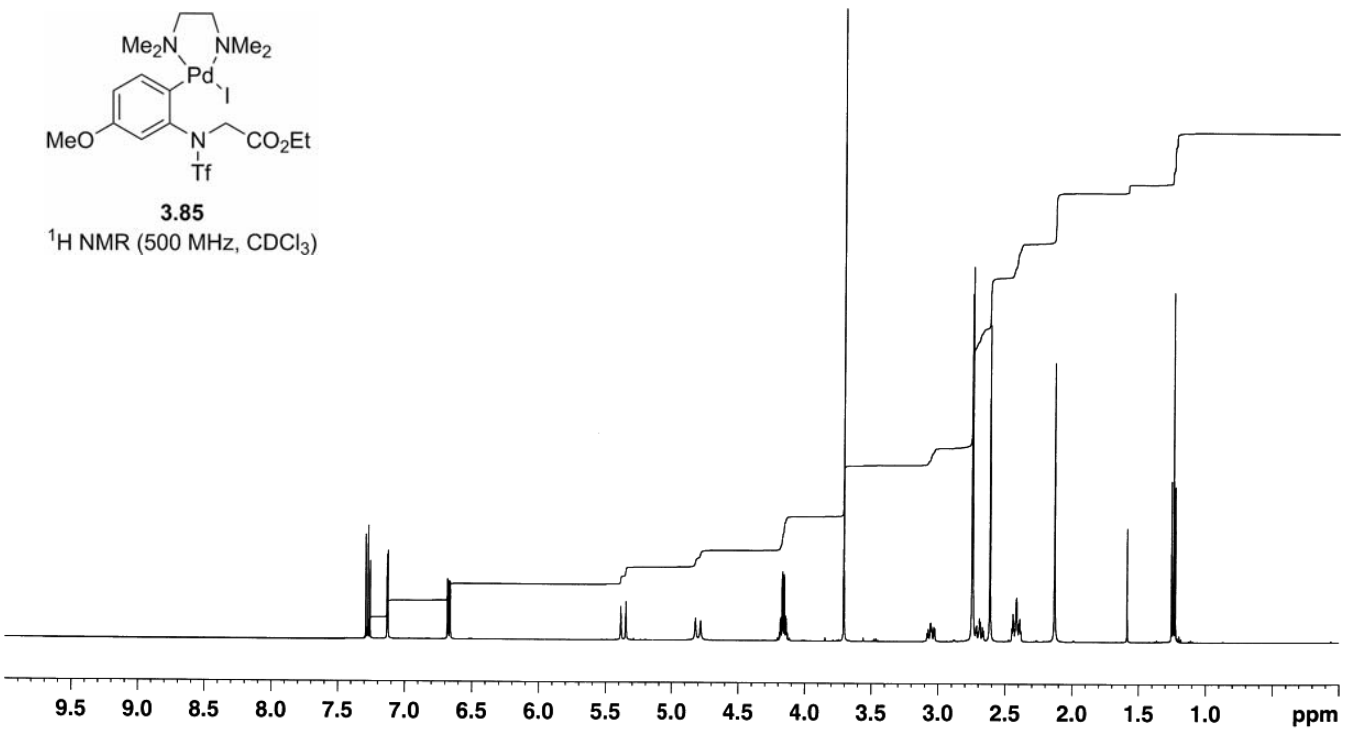
Me2N
NMe2
Pd
I
MeO
N
CO2Et
Tf
3.85
1H NMR (500 MHz, CDCl3)
9.5
9.0
8.5
8.0
7.5
7.0
6.5
6.0
5.5
5.0
4.5
4.0
3.5
3.0
2.5
2.0
1.5
1.0
ppm

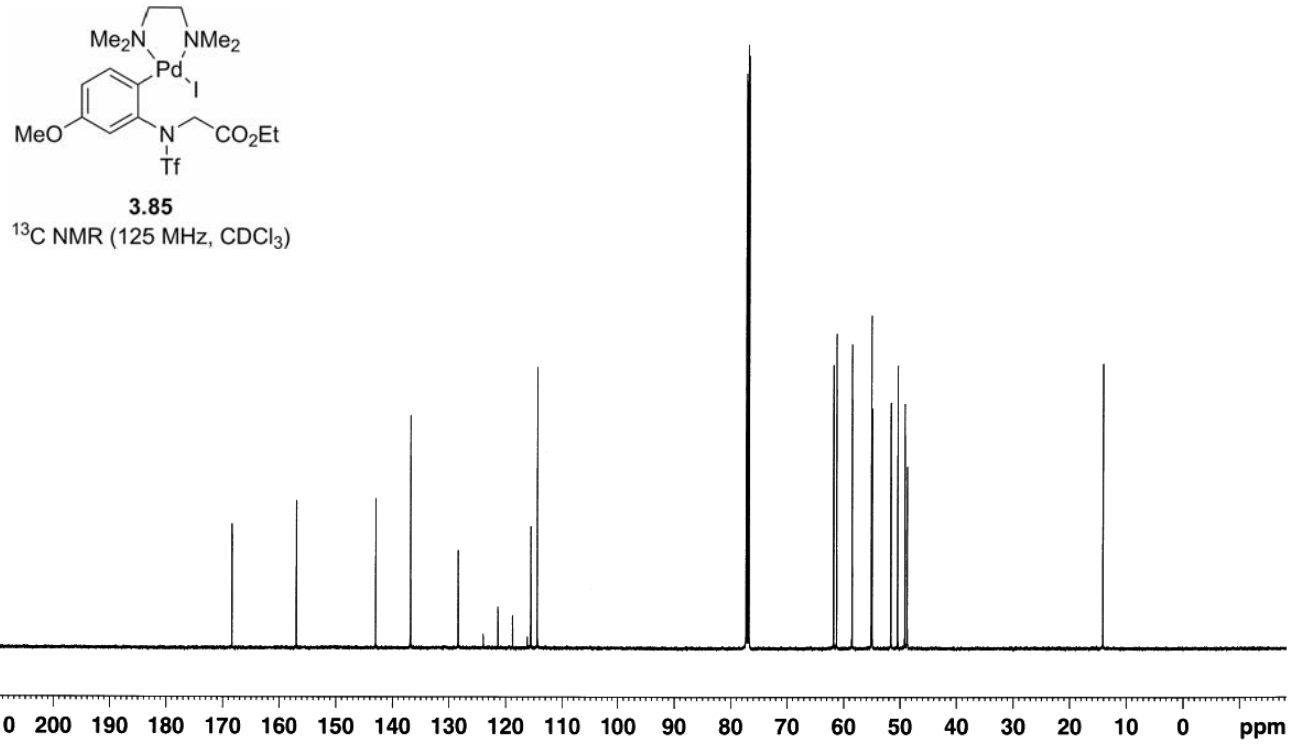
Me2N
NMe2
Pd
I
MeO
N
CO2Et
Tf
3.85
13C NMR (125 MHz, CDCl3)
210 200 190 180 170 160 150 140 130 120 110 100 90 80 70 60 50 40 30 20 10 0 ppm

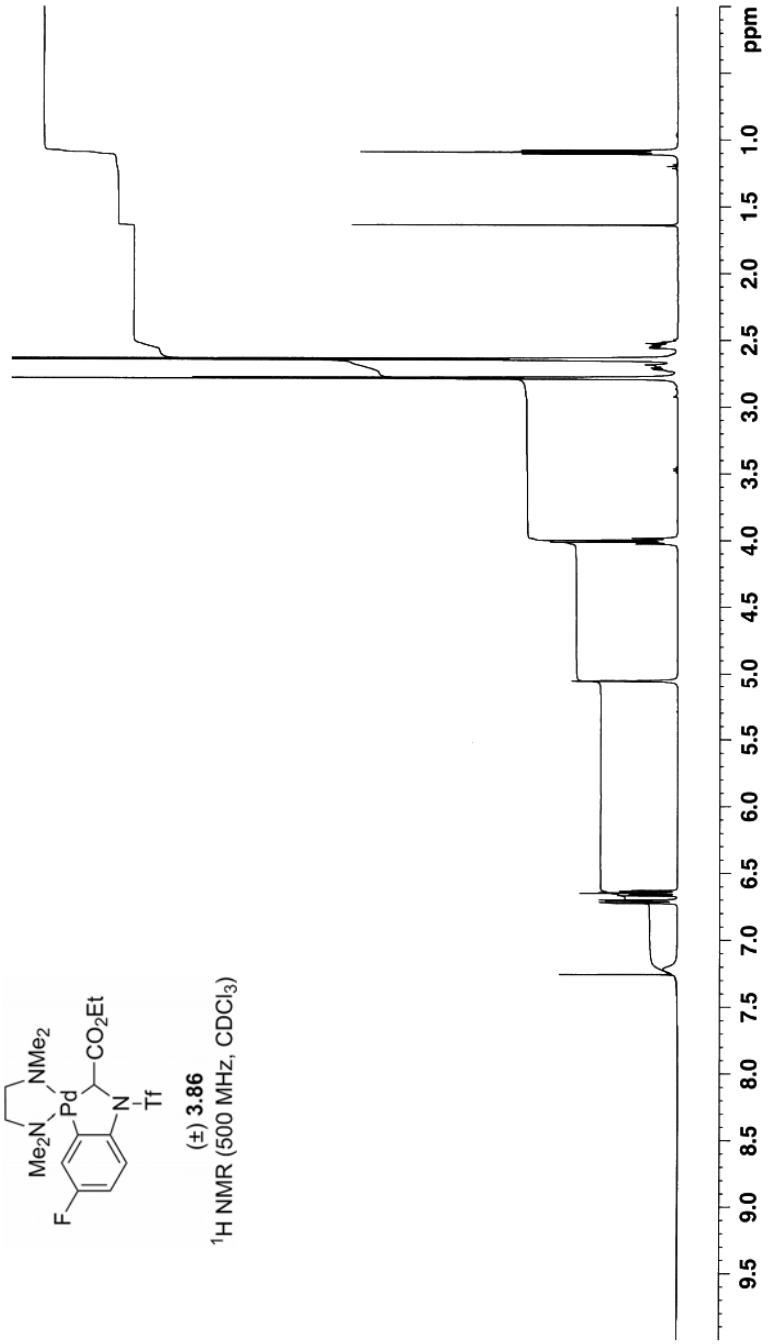
NMe2
Pd
CO2Et
Me2N
N
Tf
F
(±) 3.86
1H NMR (500 MHz, CDCl3)
9.5
9.0
8.5
8.0
7.5
7.0
6.5
6.0
5.5
5.0
4.5
4.0
3.5
3.0
2.5
2.0
1.5
1.0
ppm

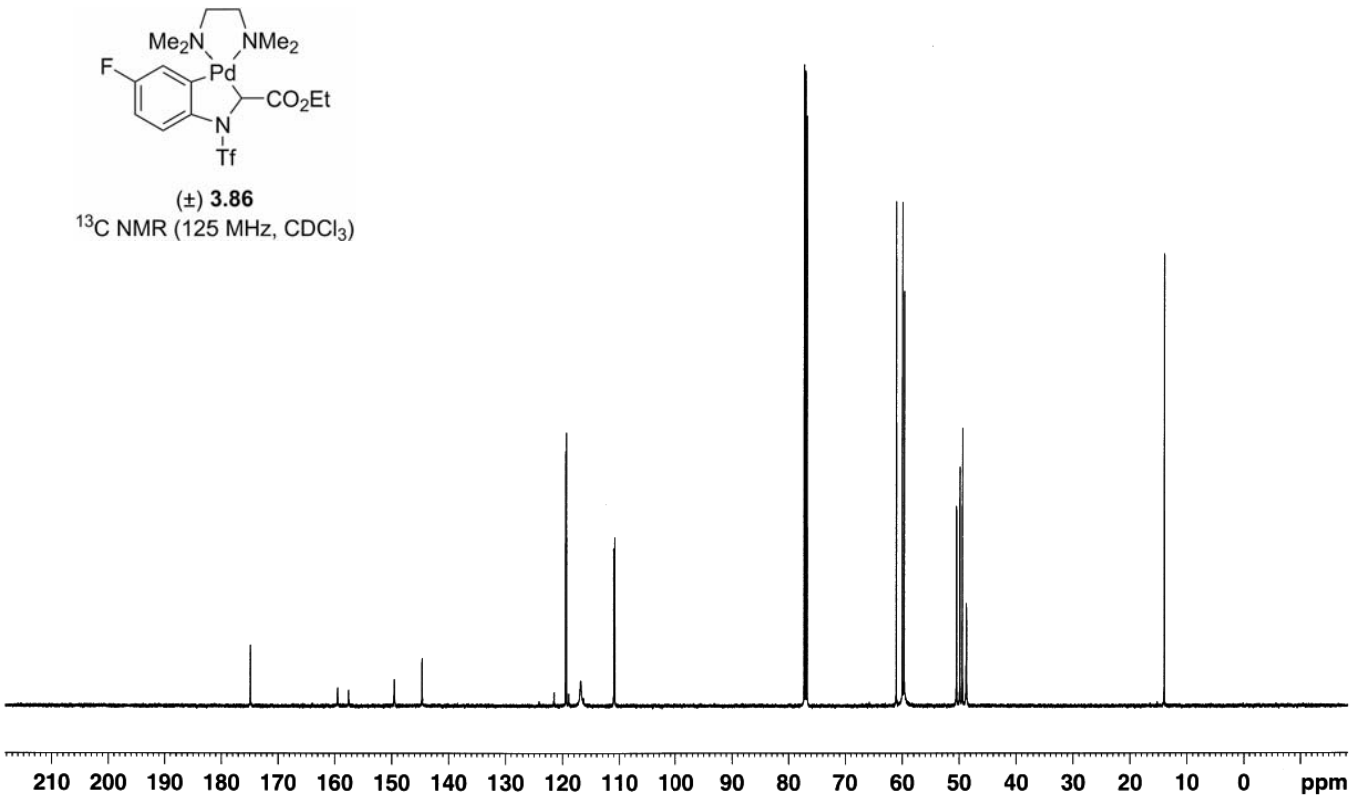
Me2N
NMe2
F
Pd
CO2Et
N
Tf
(±) 3.86
13C NMR (125 MHz, CDCl3)
210 200 190 180 170 160 150 140 130 120 110 100 90 80 70 60 50 40 30 20 10 0 ppm

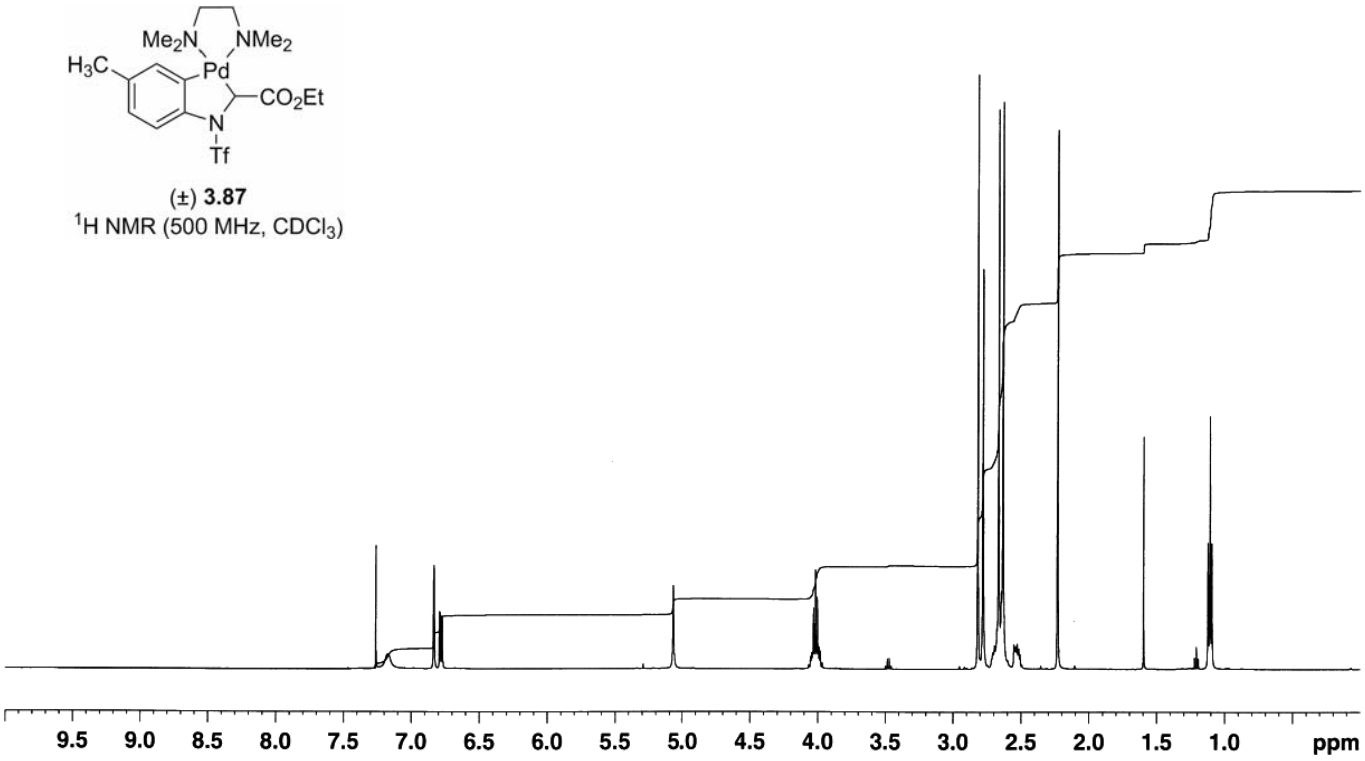
Me2N
NMe2
H3C
Pd
CO2Et
N
Tf
(±) 3.87
1H NMR (500 MHz, CDCl3)
9.5
9.0
8.5
8.0
7.5
7.0
6.5
6.0
5.5
5.0
4.5
4.0
3.5
3.0
2.5
2.0
1.5
1.0
ppm

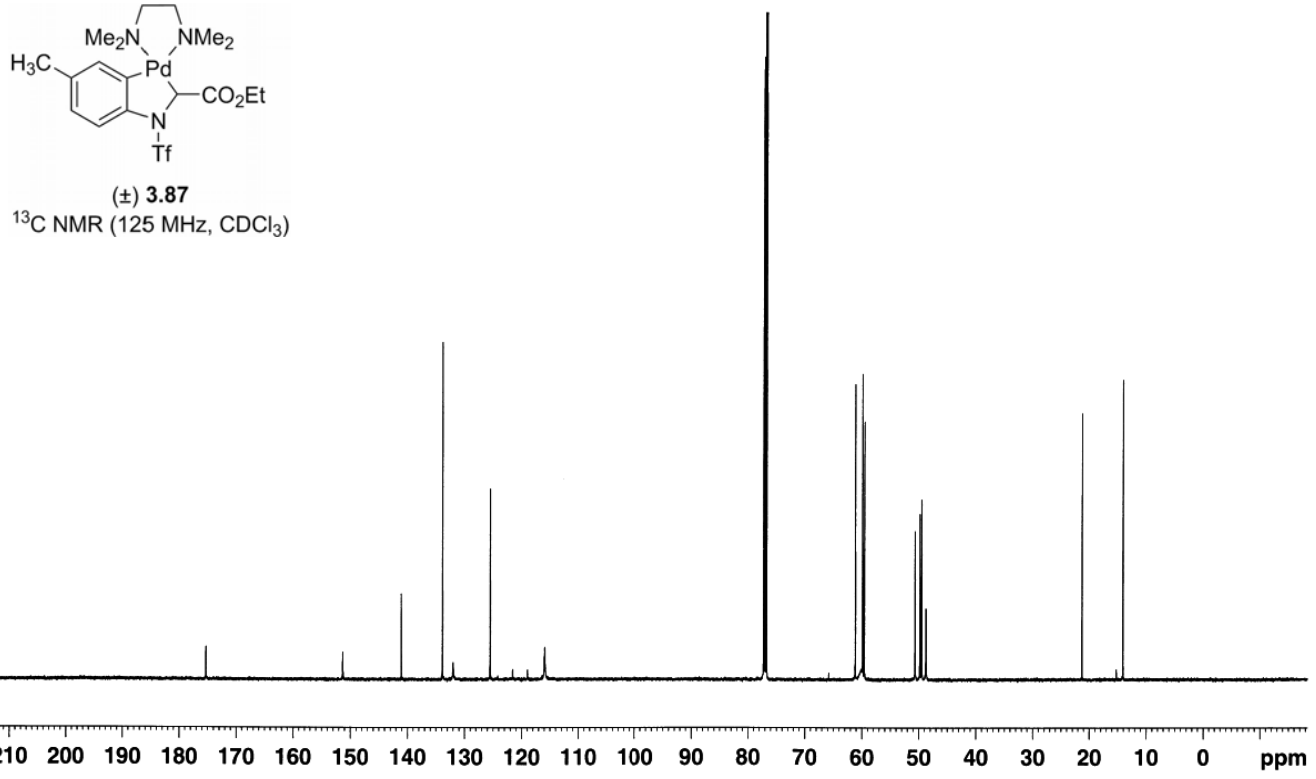
Me2N
NMe2
H3C
Pd
CO2Et
N
Tf
(±) 3.87
13C NMR (125 MHz, CDCl3)
210 200 190 180 170 160 150 140 130 120 110 100 90 80 70 60 50 40 30 20 10 0 ppm

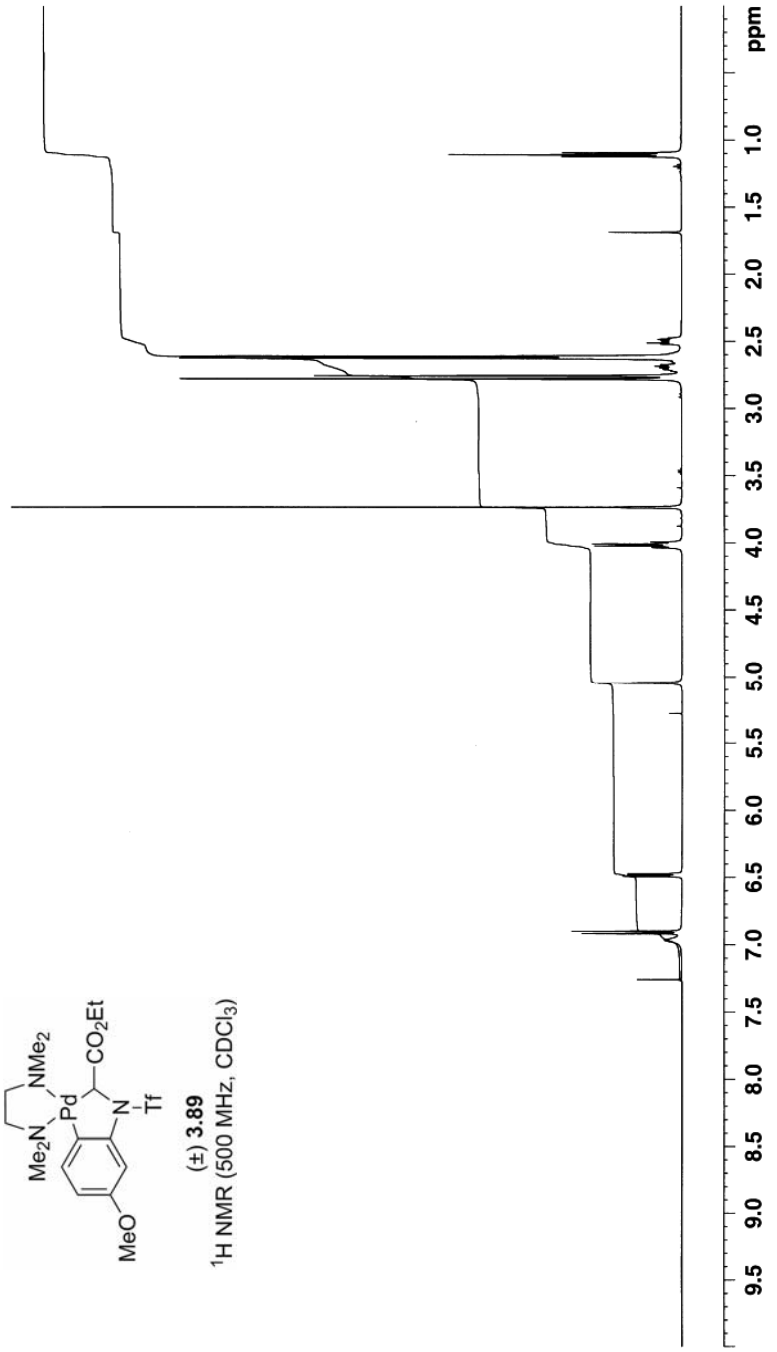
Me2N
NMe2
Pd
CO2Et
N
Tf
MeO
(±) 3.89
1H NMR (500 MHz, CDCl3)
9.5
9.0
8.5
8.0
7.5
7.0
6.5
6.0
5.5
5.0
4.5
4.0
3.5
3.0
2.5
2.0
1.5
1.0
ppm

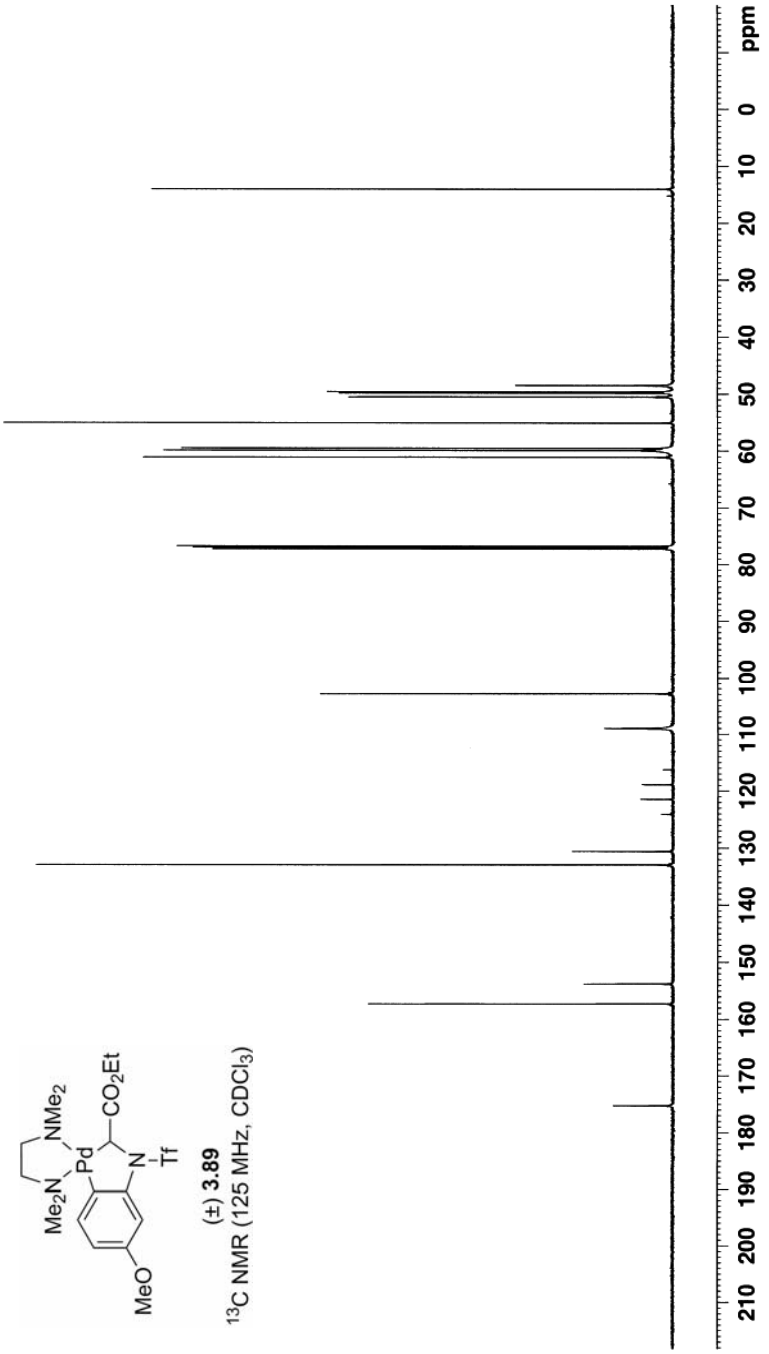
Me2N
NMe2
Pd
CO2Et
N
Tf
MeO
(±) 3.89
13C NMR (125 MHz, CDCl3)
210 200 190 180 170 160 150 140 130 120 110 100 90 80 70 60 50 40 30 20 10 0 ppm

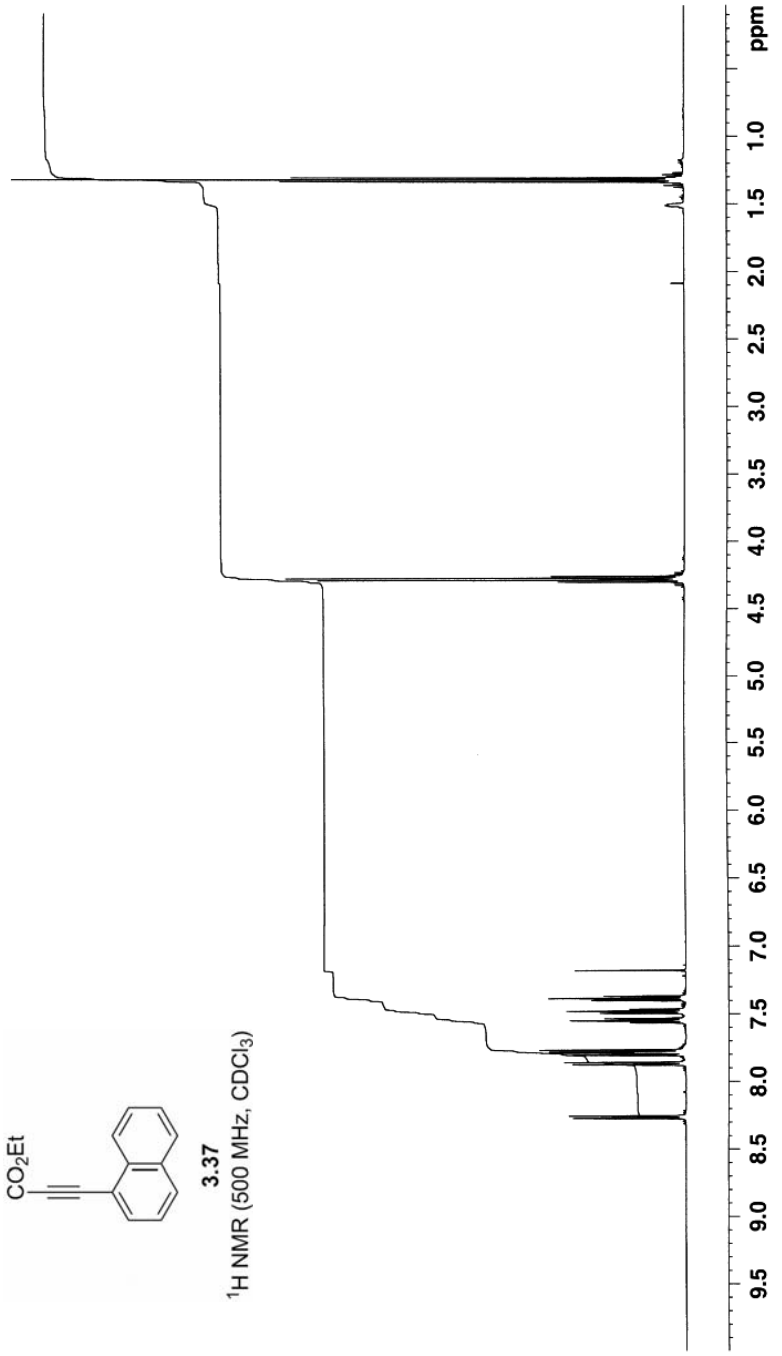
CO2Et
3.37
1H NMR (500 MHz, CDCl3)
ppm
9.5
9.0
8.5
8.0
7.5
7.0
6.5
6.0
5.5
5.0
4.5
4.0
3.5
3.0
2.5
2.0
1.5
1.0

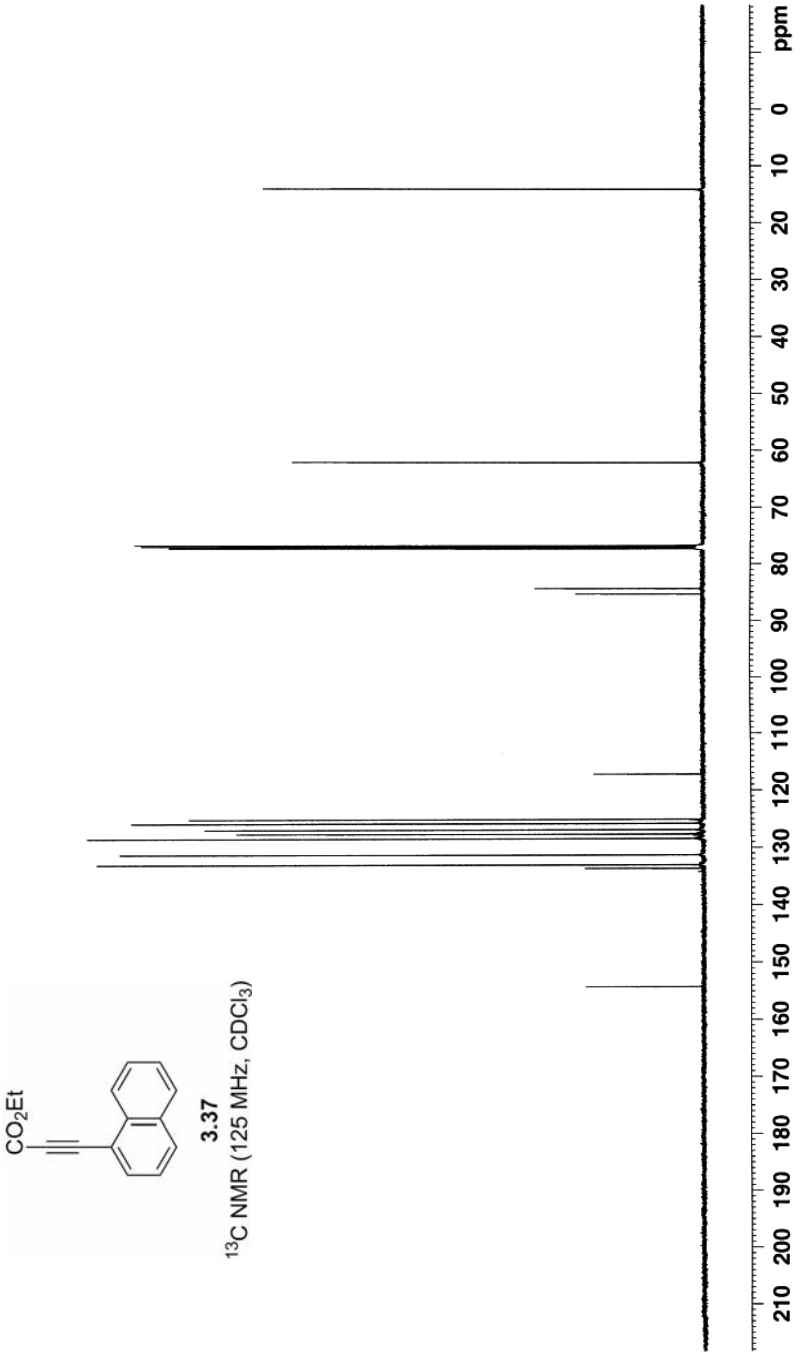
CO2Et
3.37
13C NMR (125 MHz, CDCl3)
210 200 190 180 170 160 150 140 130 120 110 100 90 80 70 60 50 40 30 20 10 0 ppm

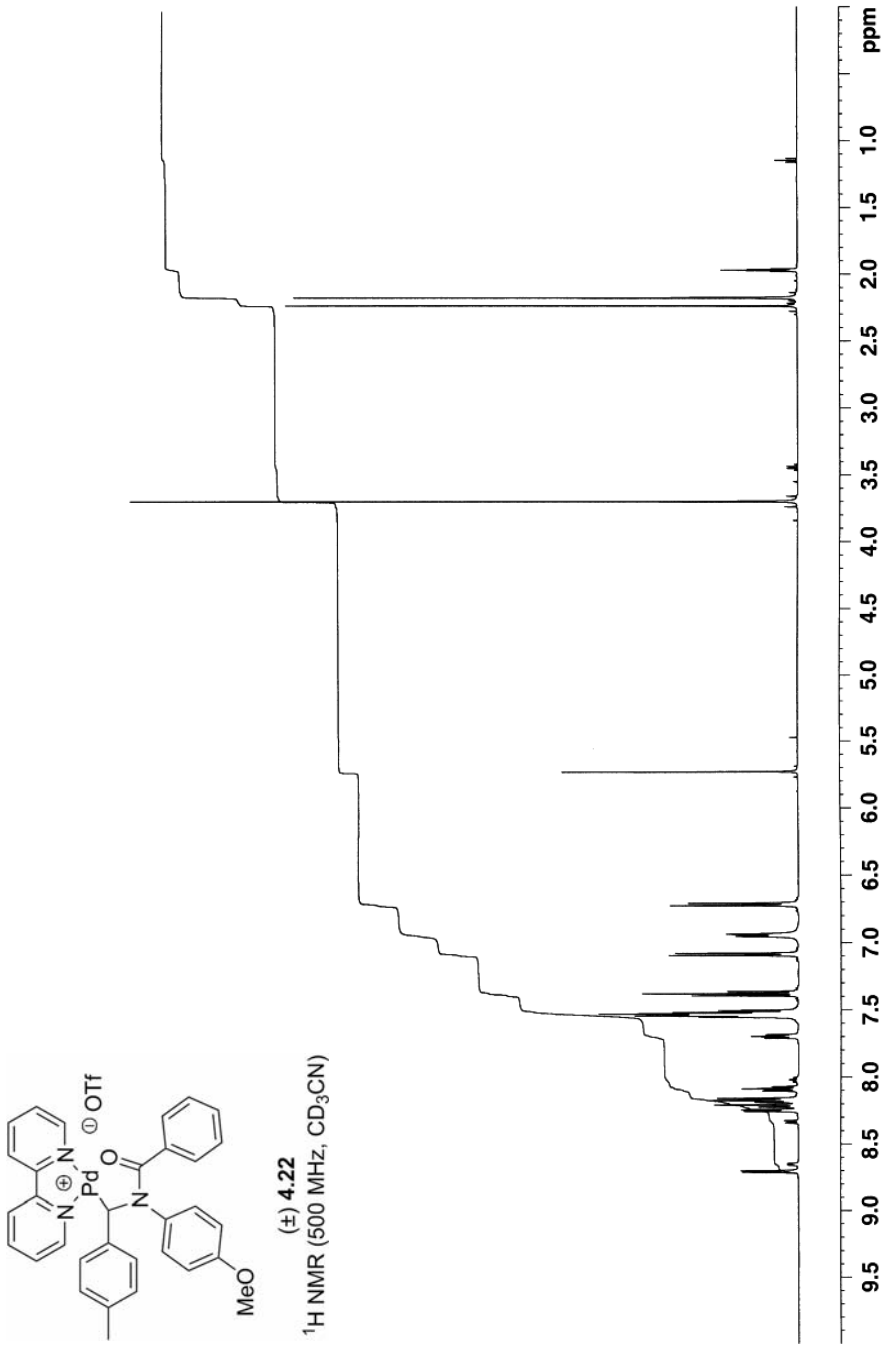
OTf
Pd
O
N
MeO
(±) 4.22
^{1}H NMR (500 MHz, CD_3CN)
9.5 9.0 8.5 8.0 7.5 7.0 6.5 6.0 5.5 5.0 4.5 4.0 3.5 3.0 2.5 2.0 1.5 1.0 ppm

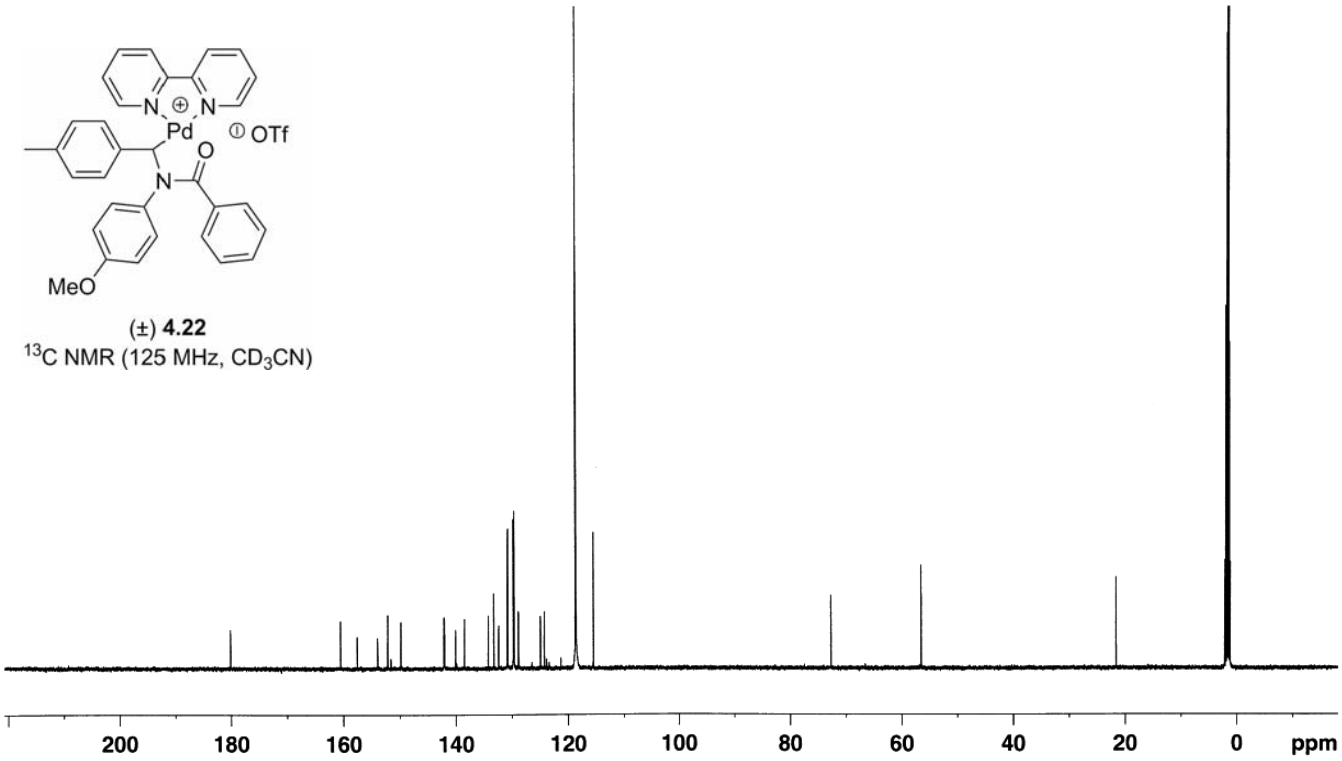

(±) **4.22**
^{13}C NMR (125 MHz, CD_3CN)

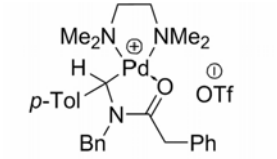

(±) **4.37**
^{1}H NMR (500 MHz, $CDCl_3$)

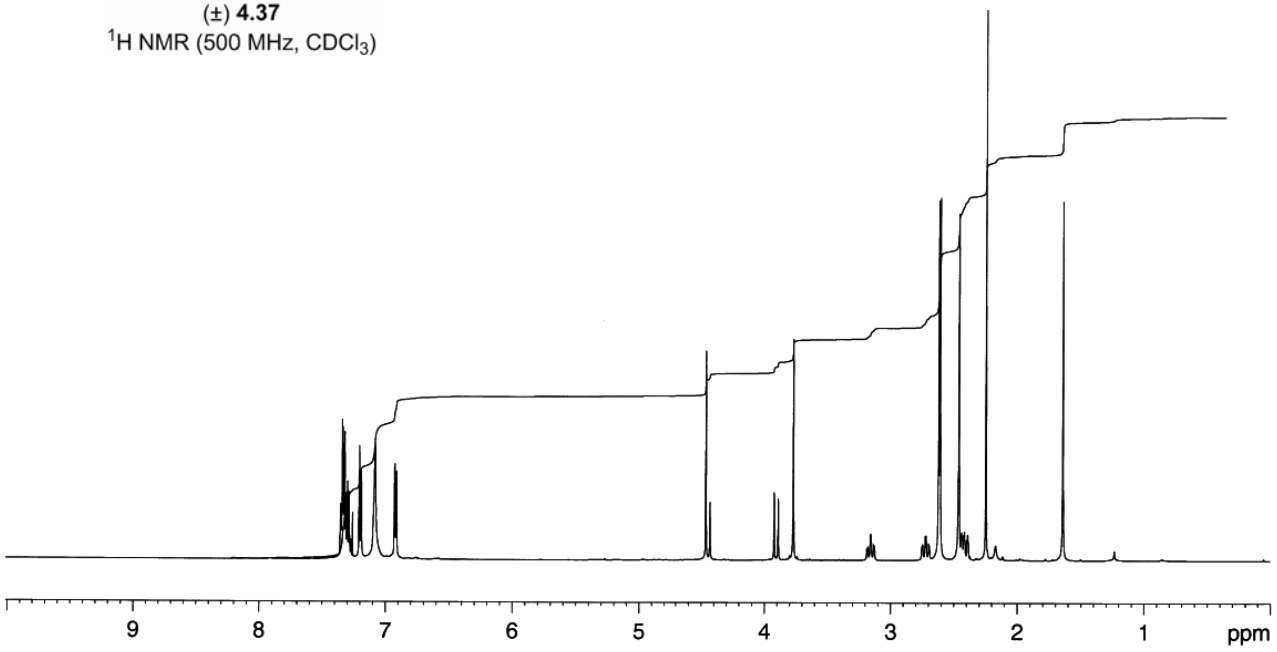

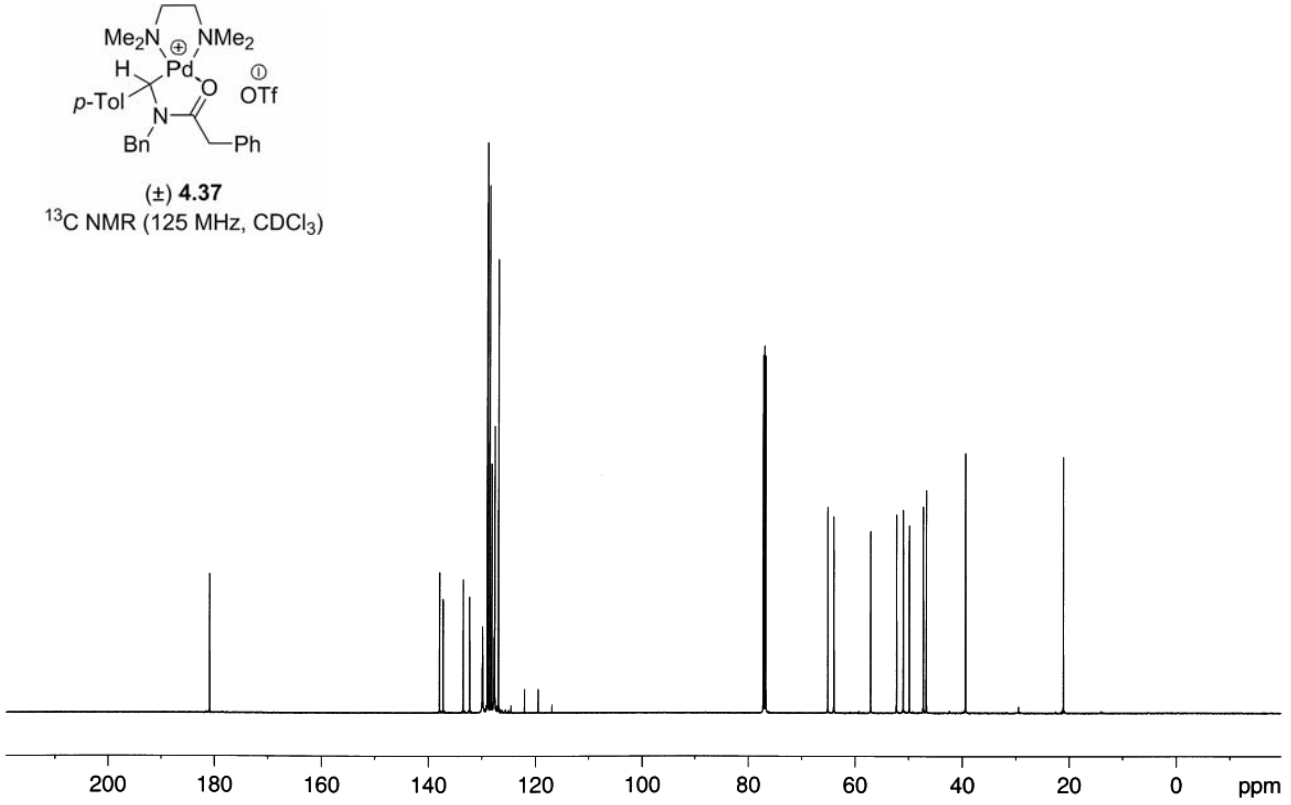
Me2N
NMe2
H
Pd
O
OTf
p-Tol
N
Bn
Ph
(±) 4.37
13C NMR (125 MHz, CDCl3)
200
180
160
140
120
100
80
60
40
20
0
ppm

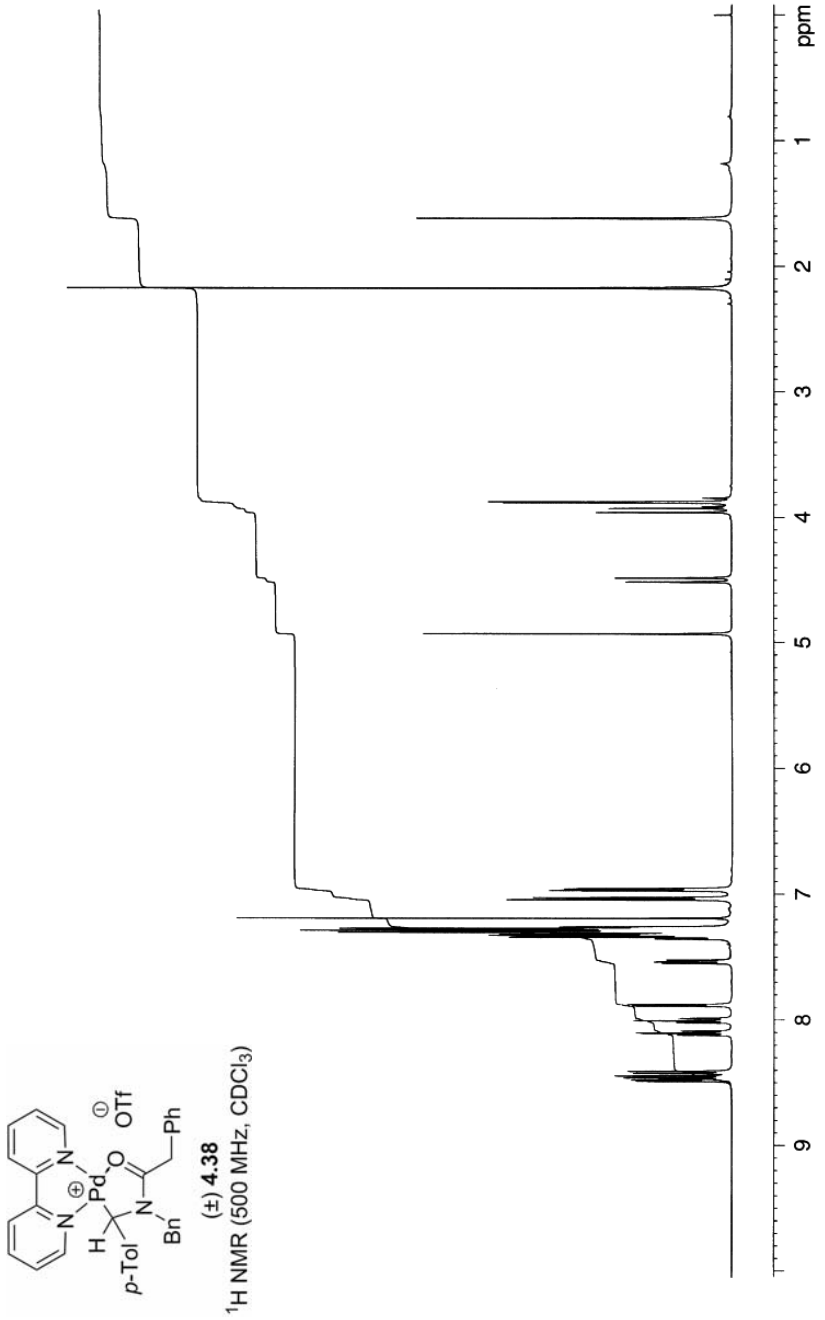
(±) 4.38
^{1}H NMR (500 MHz, CDCl$_3$)
ppm

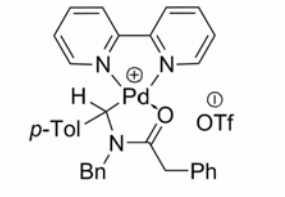

(±) **4.38**

^{13}C NMR (125 MHz, $CDCl_3$)

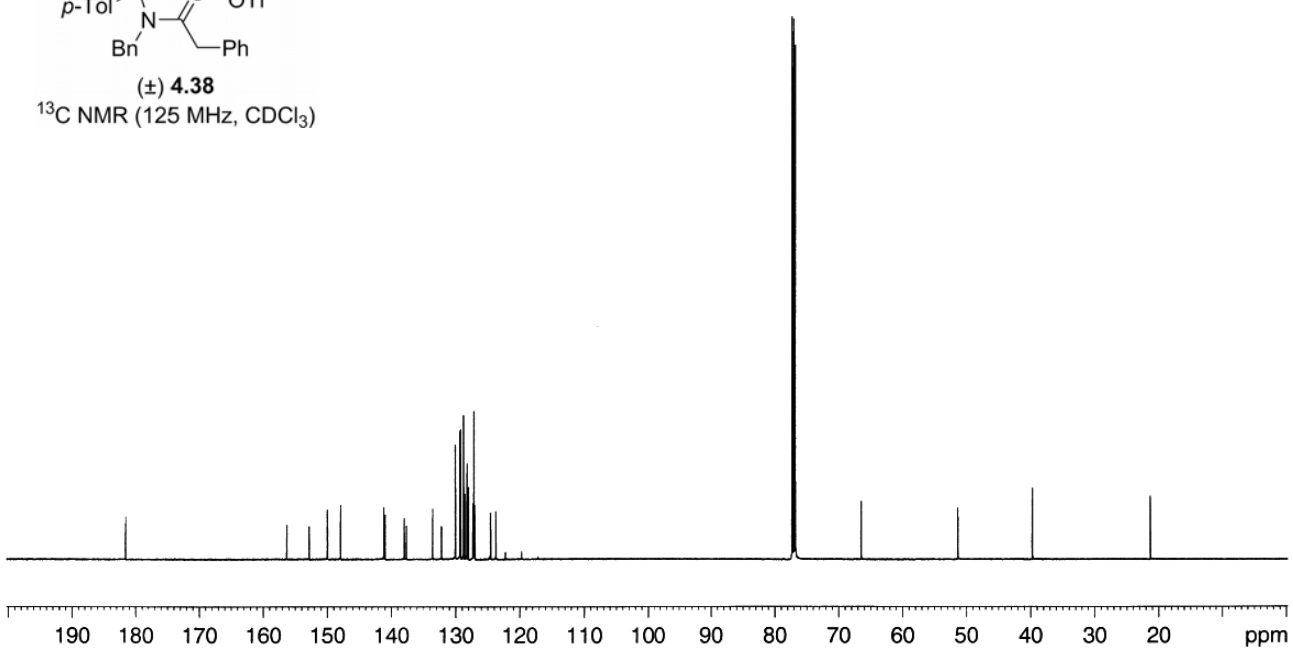

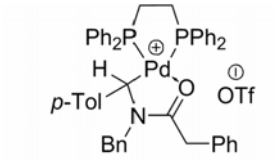

(±) **4.39**
^{1}H NMR (500 MHz, $CDCl_3$)

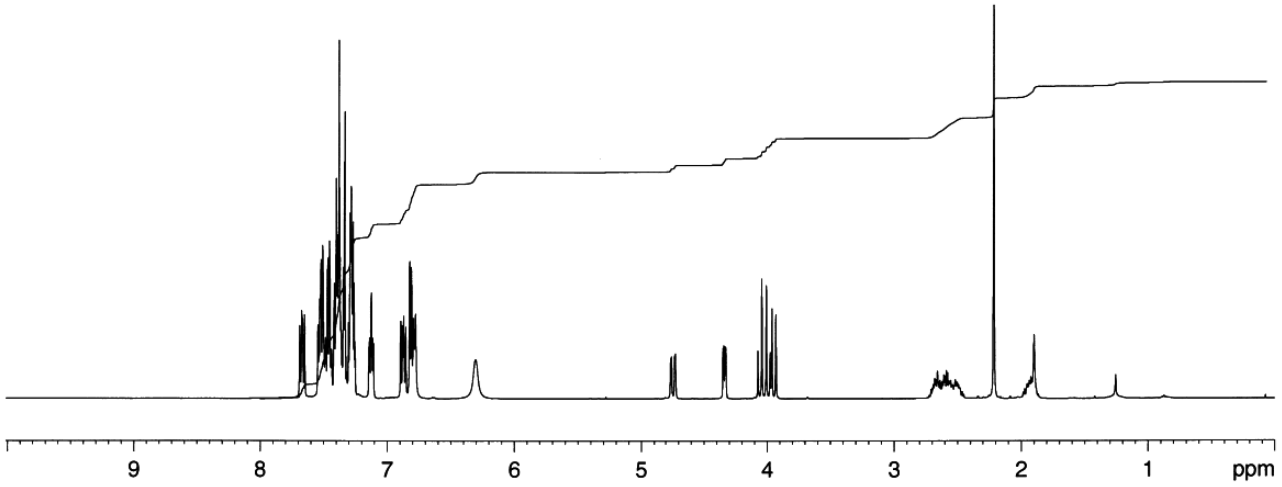

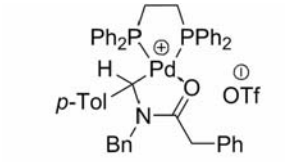

(±) **4.39**
^{13}C NMR (125 MHz, $CDCl_3$)

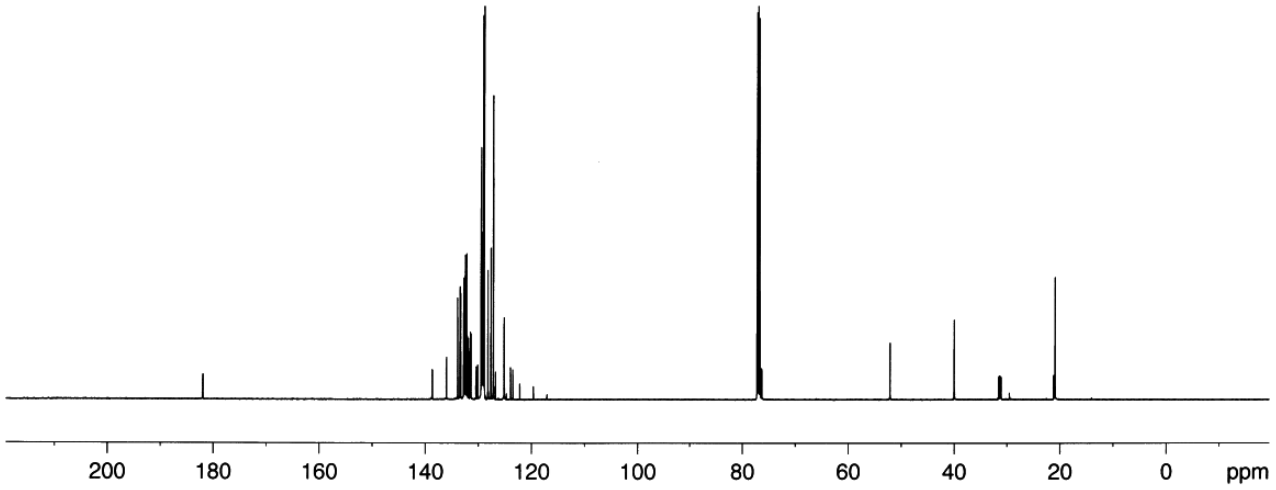

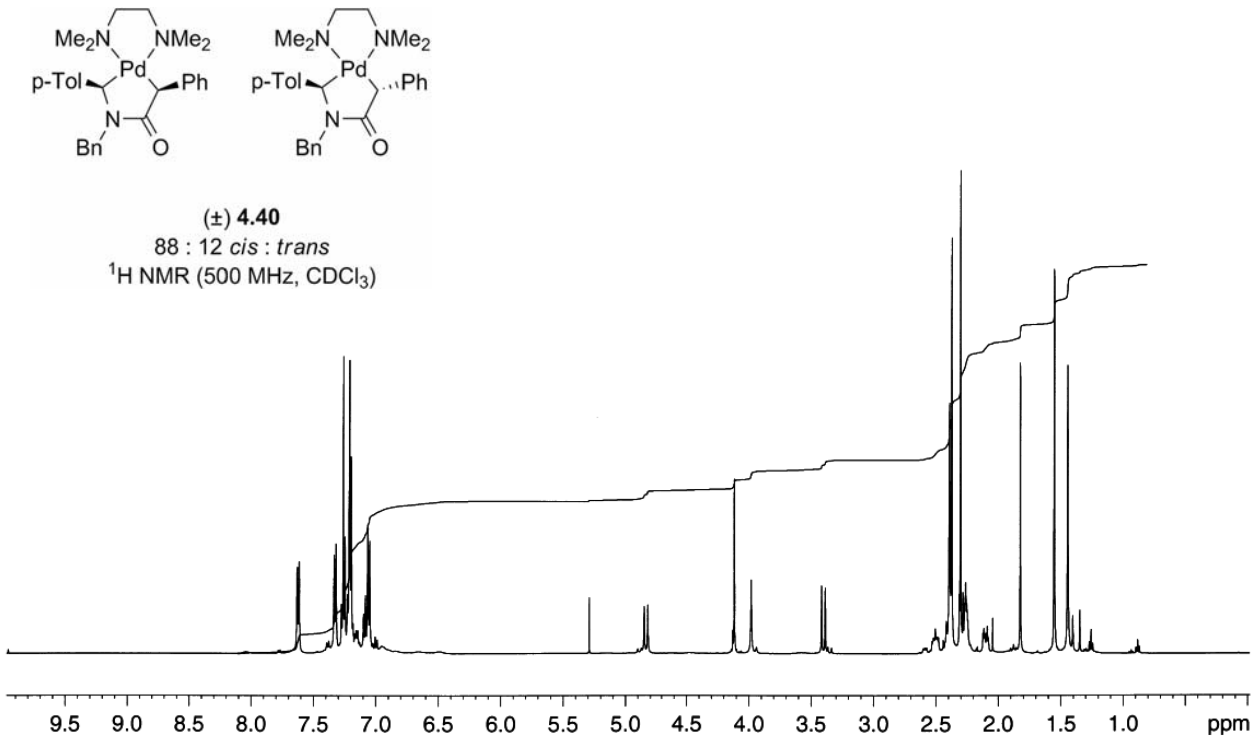
Me2N
NMe2
Pd
p-Tol
Ph
N
Bn
O
(±) 4.40
88 : 12 cis : trans
1H NMR (500 MHz, CDCl3)
9.5
9.0
8.5
8.0
7.5
7.0
6.5
6.0
5.5
5.0
4.5
4.0
3.5
3.0
2.5
2.0
1.5
1.0
ppm

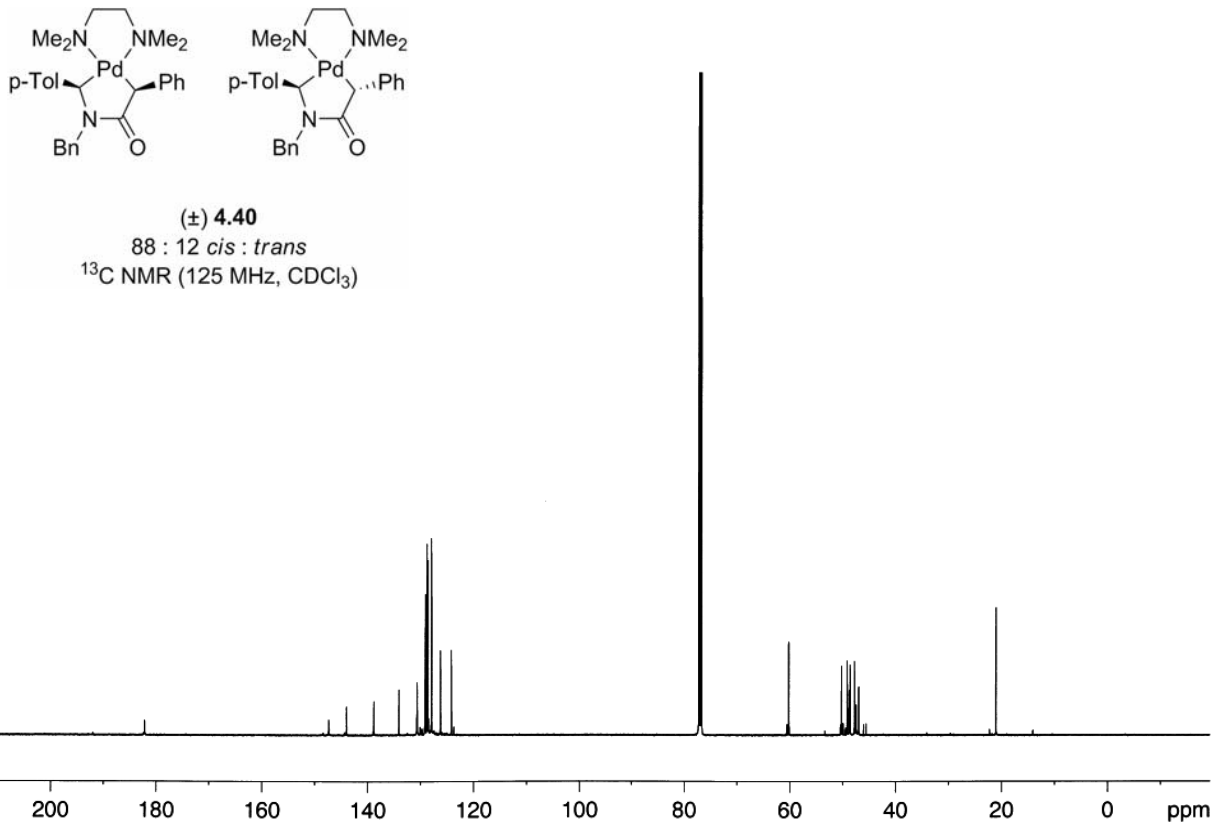
Me2N
NMe2
Pd
p-Tol
Ph
N
Bn
O
(±) 4.40
88 : 12 cis : trans
13C NMR (125 MHz, CDCl3)
200
180
160
140
120
100
80
60
40
20
0
ppm

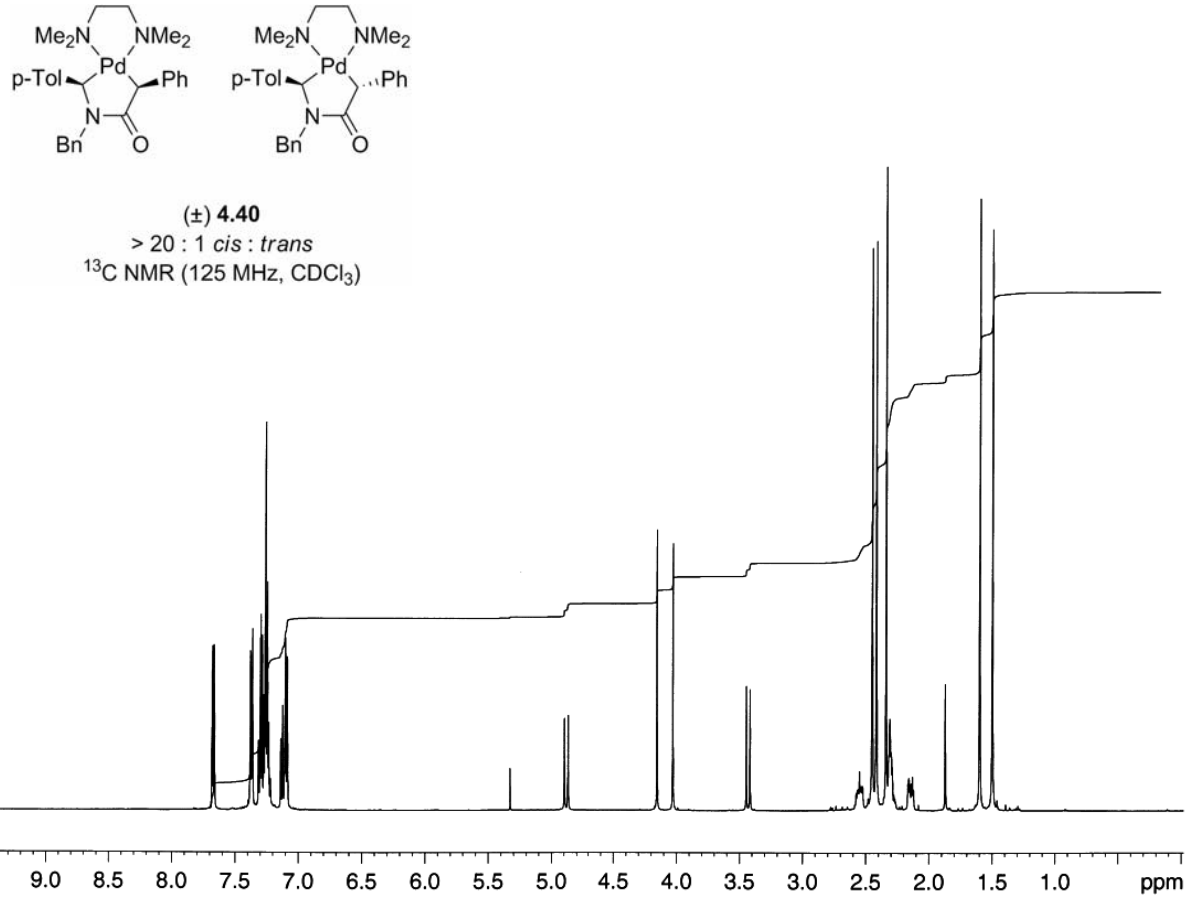
Me2N
NMe2
Pd
p-Tol
Ph
N
Bn
O
(±) 4.40
> 20 : 1 cis : trans
13C NMR (125 MHz, CDCl3)
9.5
9.0
8.5
8.0
7.5
7.0
6.5
6.0
5.5
5.0
4.5
4.0
3.5
3.0
2.5
2.0
1.5
1.0
ppm

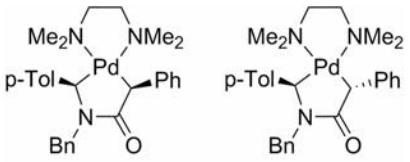

(±) **4.40**
> 20 : 1 *cis* : *trans*
^{13}C NMR (125 MHz, $CDCl_3$)

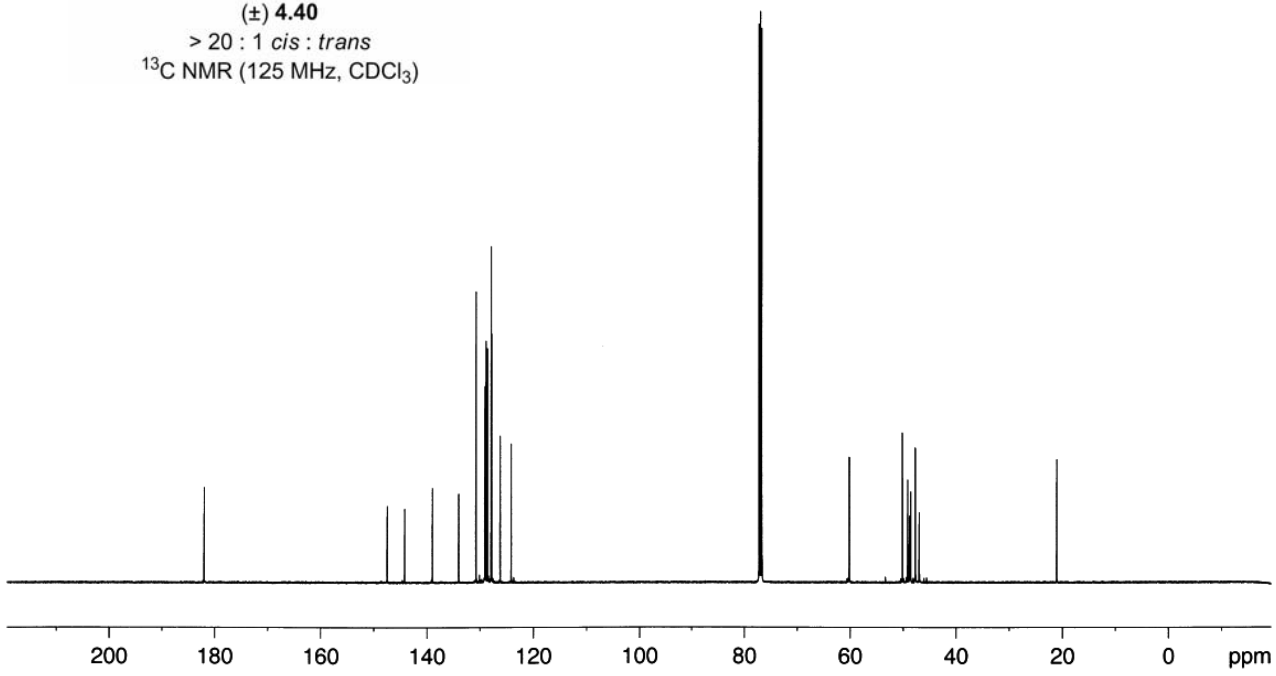

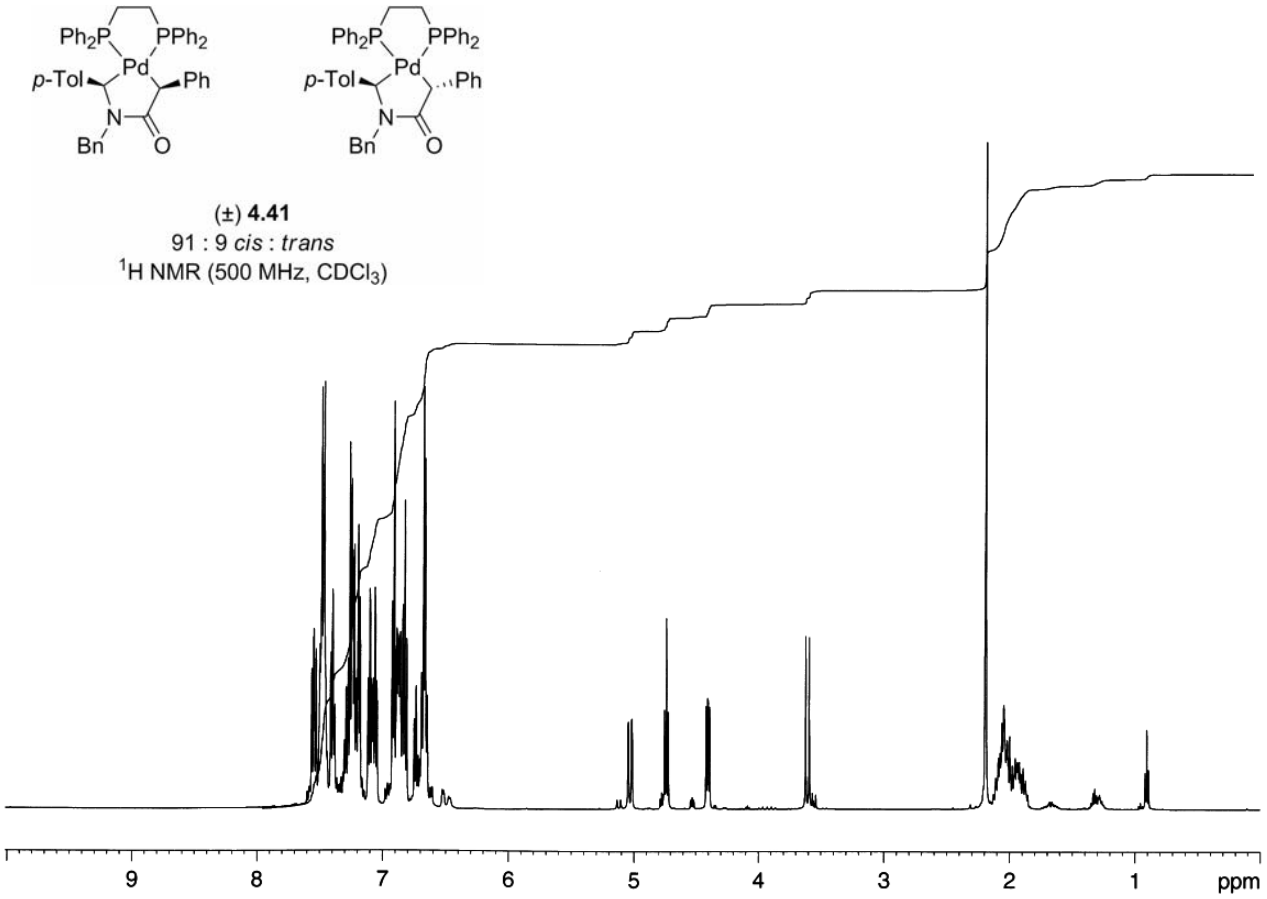
Ph2P
PPh2
Pd
p-Tol
Ph
N
Bn
O
(±) 4.41
91 : 9 cis : trans
1H NMR (500 MHz, CDCl3)
9
8
7
6
5
4
3
2
1
ppm

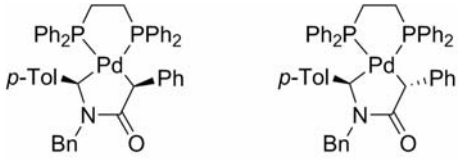

(±) **4.41**
91 : 9 *cis* : *trans*
^{13}C NMR (125 MHz, $CDCl_3$)

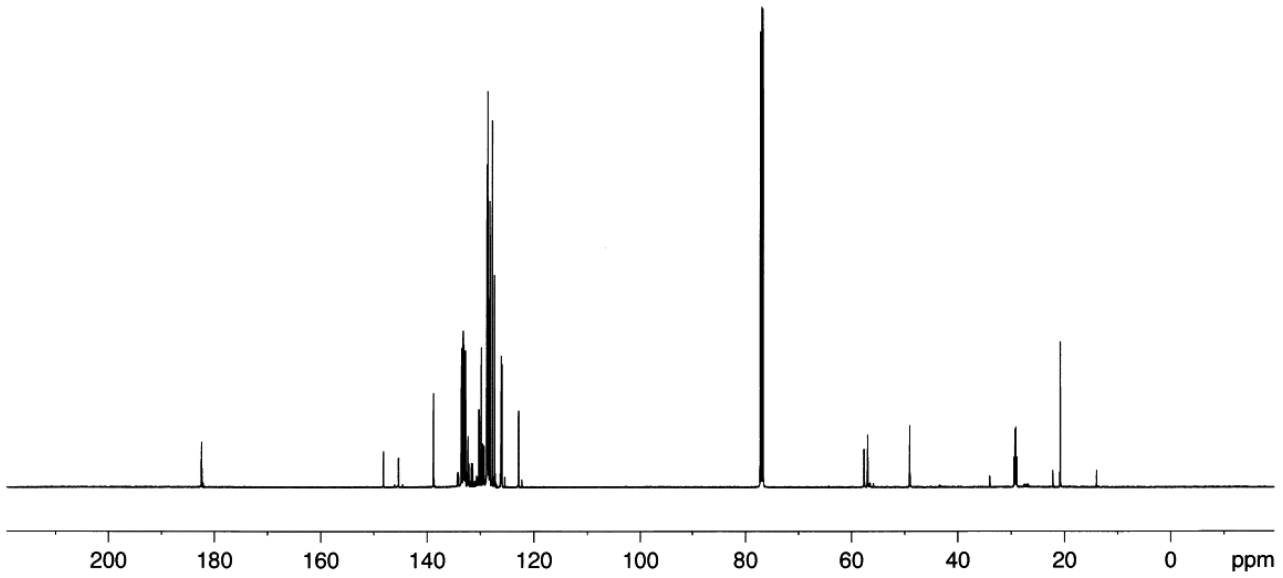

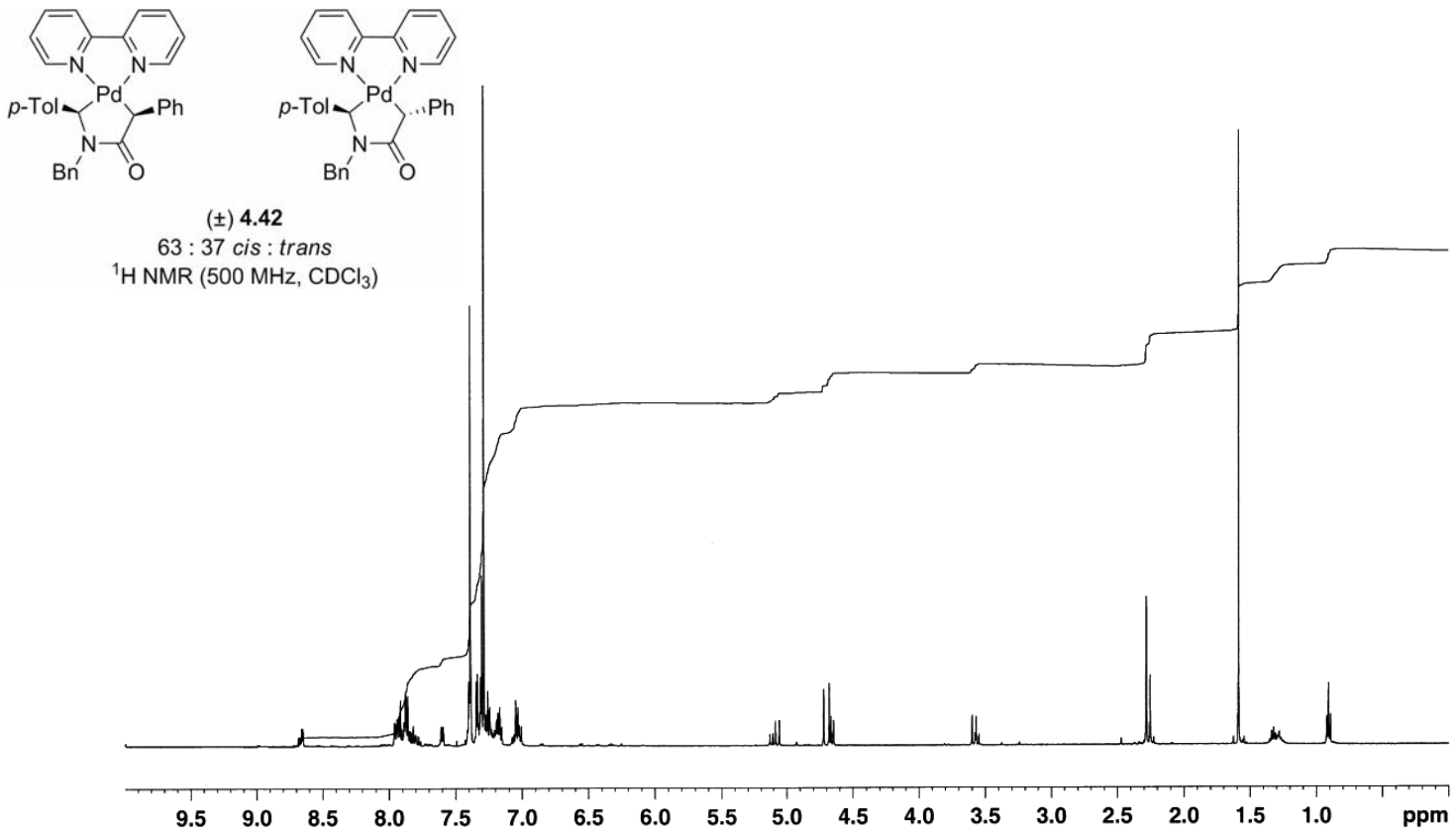
p-Tol
Pd
Ph
N
Bn
O
(±) 4.42
63 : 37 cis : trans
1H NMR (500 MHz, CDCl3)
9.5
9.0
8.5
8.0
7.5
7.0
6.5
6.0
5.5
5.0
4.5
4.0
3.5
3.0
2.5
2.0
1.5
1.0
ppm

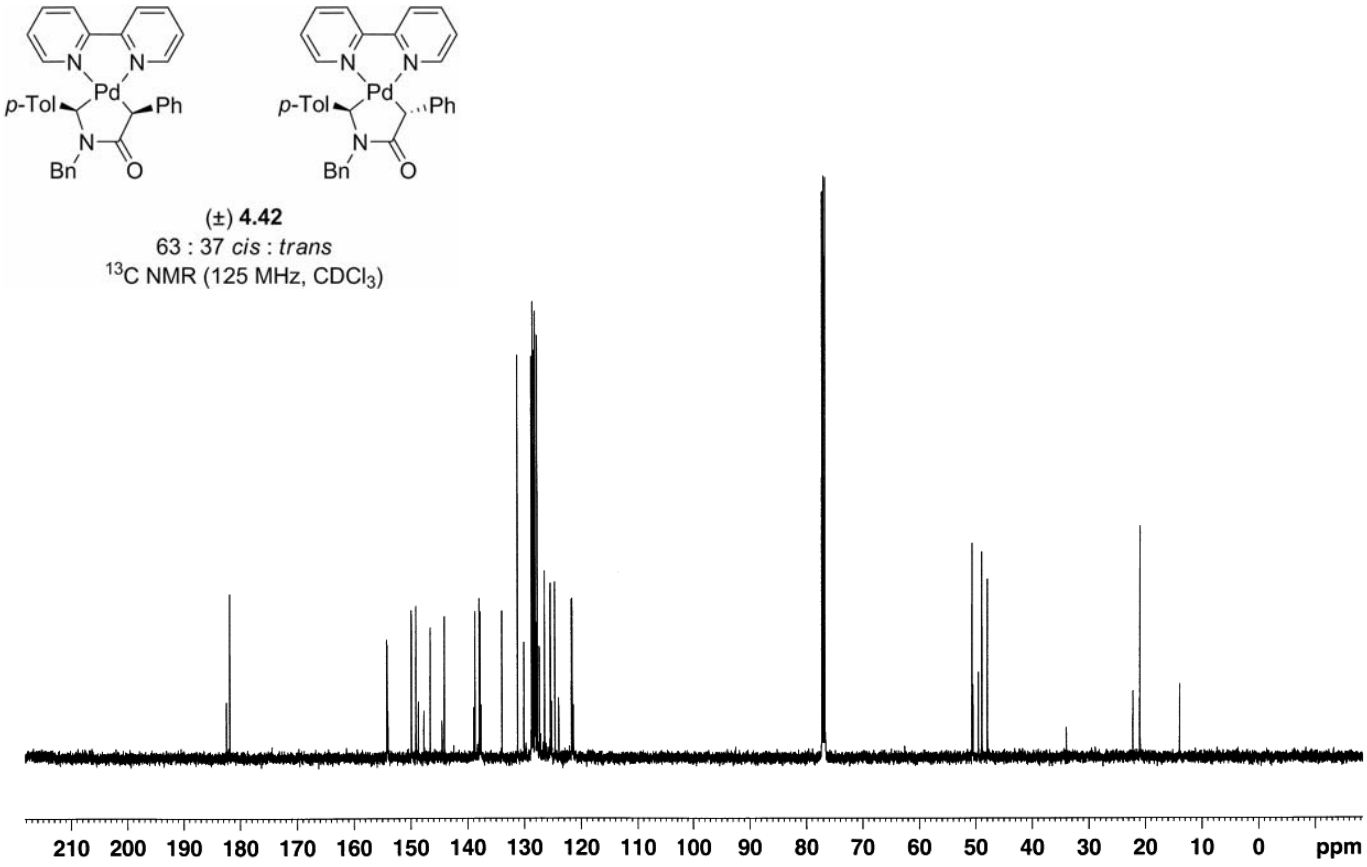
p-Tol
Ph
Pd
N
Bn
O
(±) 4.42
63 : 37 cis : trans
13C NMR (125 MHz, CDCl3)
210 200 190 180 170 160 150 140 130 120 110 100 90 80 70 60 50 40 30 20 10 0 ppm

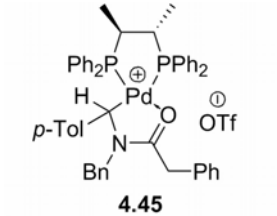

4.45

^{1}H NMR (500 MHz, $CDCl_3$)

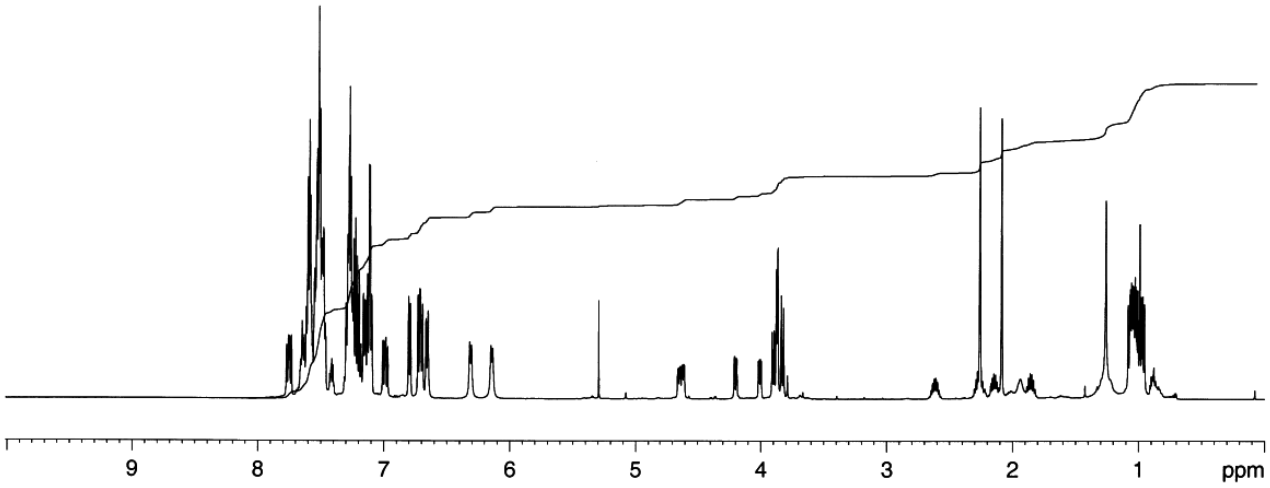

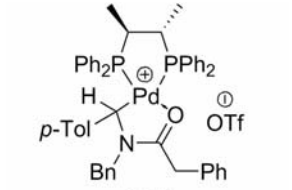

4.45

^{13}C NMR (125 MHz, $CDCl_3$)

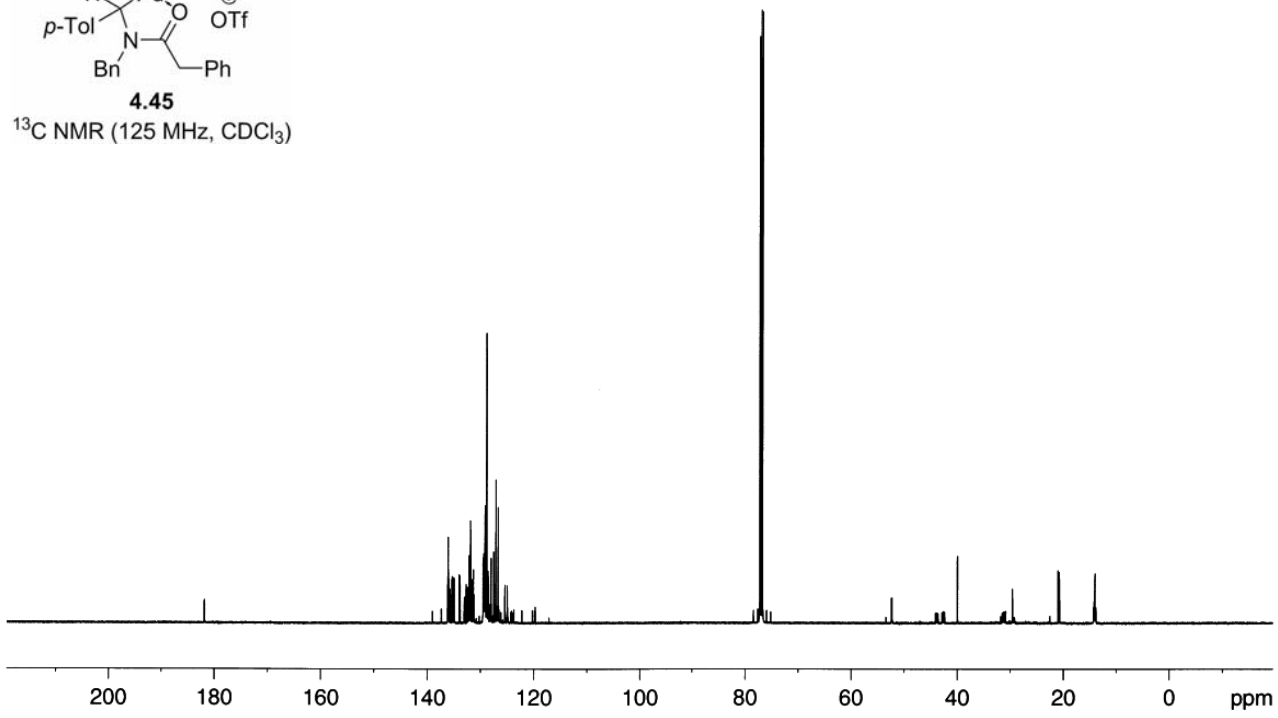

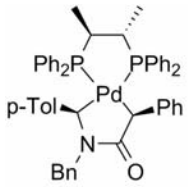

4.46a

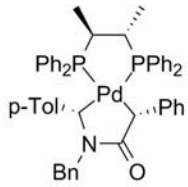

4.46b

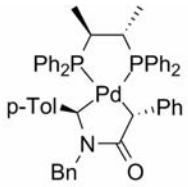

4.46c

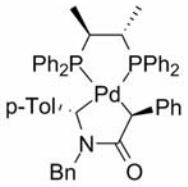

4.46d

4.46
4.46a : **4.46b** : **4.46c** : **4.46d**
45 : 45 : 5 : 5
91 : 9 "*cis* : *trans*"
^{1}H NMR (500 MHz, $CDCl_3$)

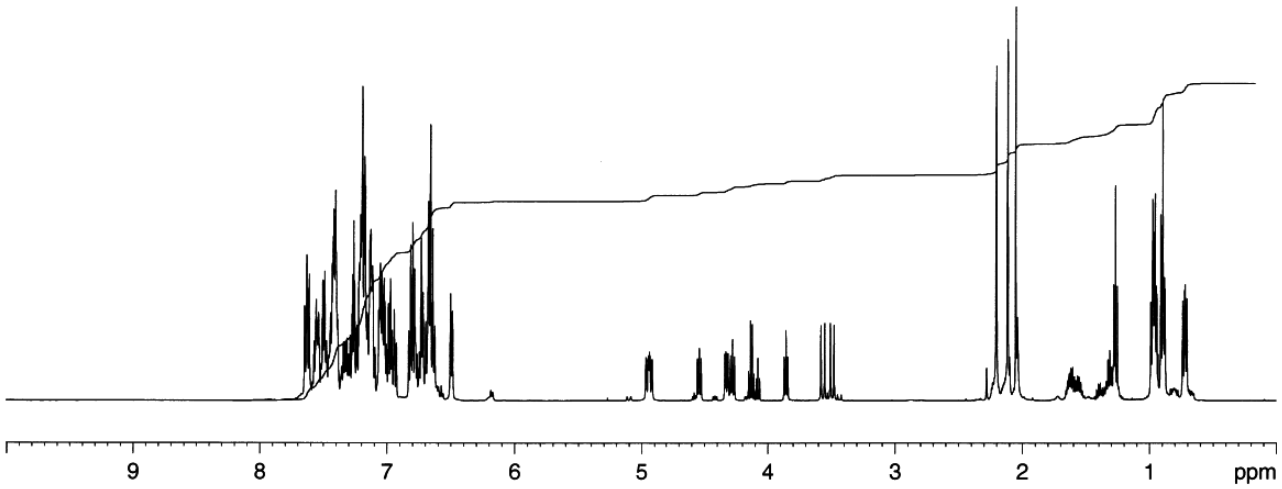

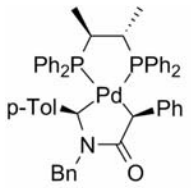

4.46a

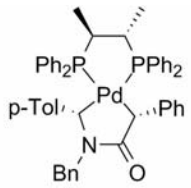

4.46b

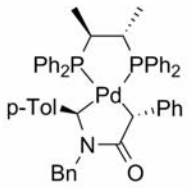

4.46c

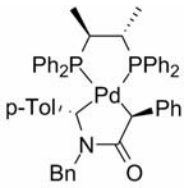

4.46d

4.46

4.46a : **4.46b** : **4.46c** : **4.46d**

45 : 45 : 5 : 5

91 : 9 "*cis* : *trans*"

^{13}C NMR (125 MHz, $CDCl_3$)

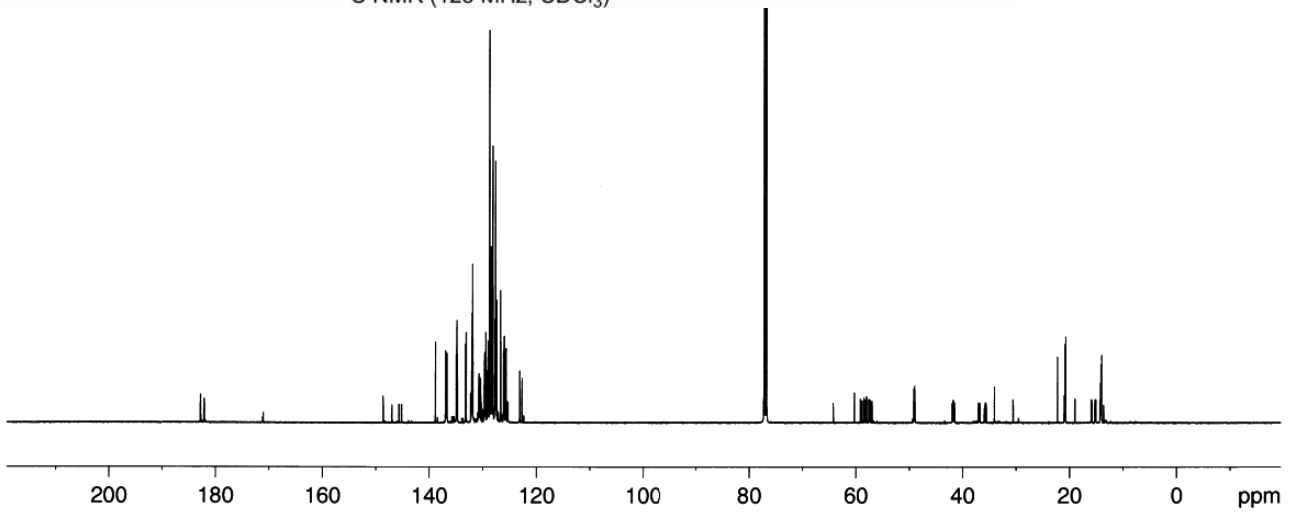

Crystal Structure Report

for

trans-(±)-**4.40**

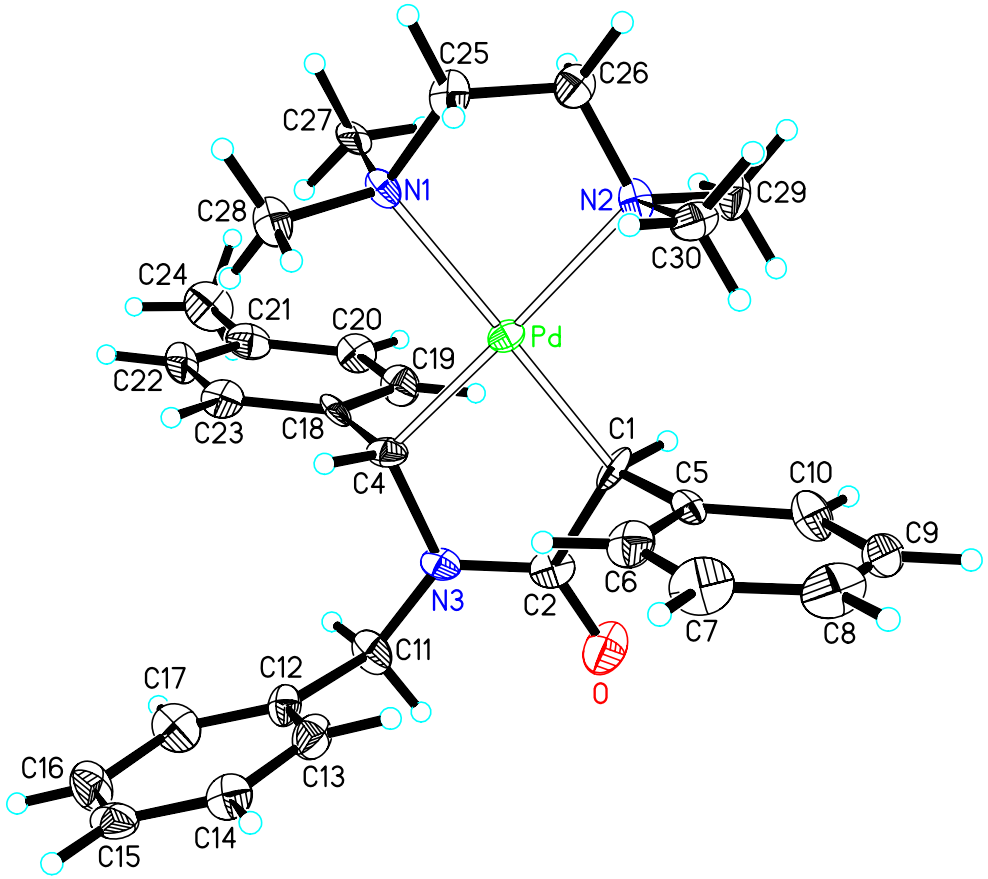
C25
C26
C27
N1
N2
C29
C28
C30
C24
C21
C20
Pd
C22
C19
C23
C18
C1
C4
C5
C10
C9
N3
C2
C6
C7
C8
C11
C12
O
C17
C16
C13
C14
C15

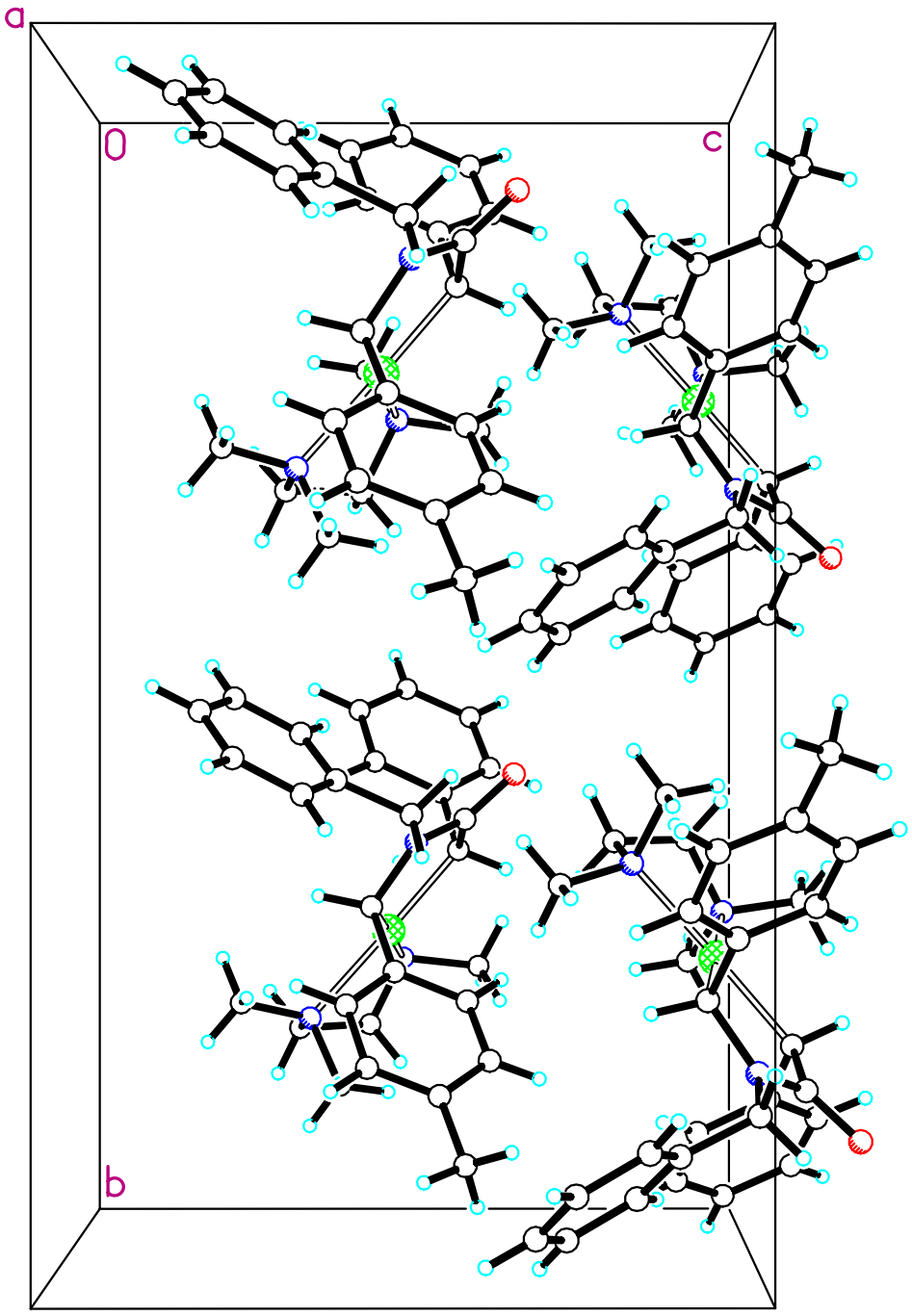
a
0
c
b

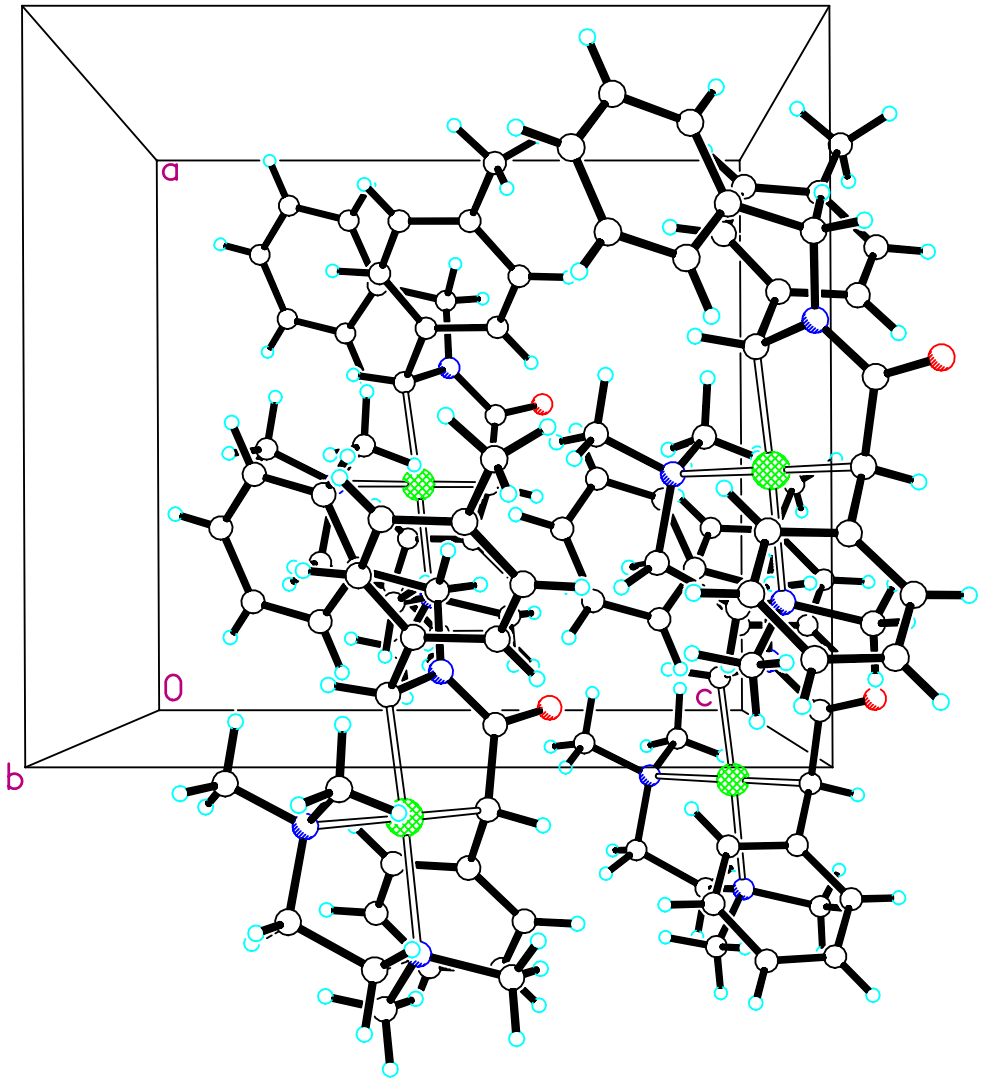
a
0
b
c

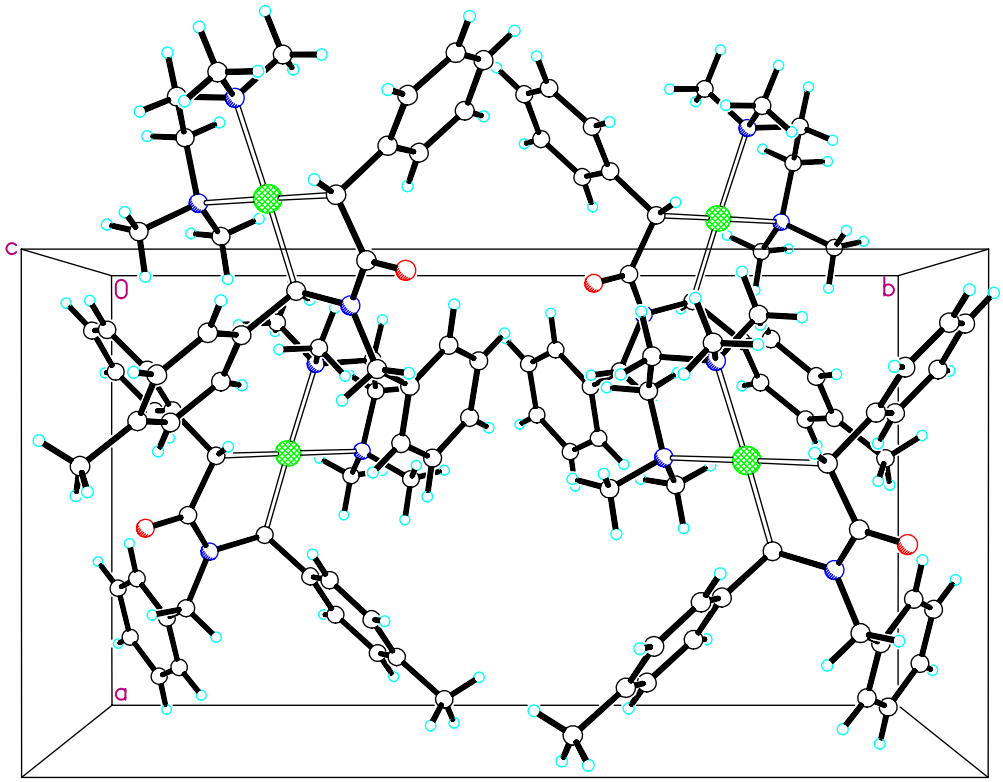
c
0
b
a

Comments

The asymmetric unit contains one [(trans-$C_{23}H_{21}NO$)Pd($N_2C_6H_{16}$)] molecule. The crystal used for data collection was a 2-domain twin with the major domain accounting for 92% of the sample volume and the minor domain accounting for 8% of the volume. All displacement ellipsoids are drawn at the 50% probability level.

Experimental Description

Crystals of [(trans-$C_{23}H_{21}NO$)Pd($N_2C_6H_{16}$)] are, at 100(2) K, monoclinic, space group Cc – C_s^4 (No. 9) (1) with **a** = 11.021(1) Å, **b** = 20.163(2) Å, **c** = 11.690(1) Å, β = 90.247(2)°, V = 2597.6(5) $Å^3$ and Z = 4 molecules {d_{calcd} = 1.406 g/cm^3; μ_a(MoKα) = 0.740 mm^{-1}}. A full hemisphere of diffracted intensities (1850 30-second frames with a ω scan width of 0.30°) was measured for a 2-domain specimen using graphite-monochromated MoKα radiation (λ= 0.71073 Å) on a Bruker SMART APEX CCD Single Crystal Diffraction System (2). X-rays were provided by a fine-focus sealed x-ray tube operated at 50kV and 35A. Lattice constants were determined with the Bruker SAINT software package using peak centers for 6609 reflections. A total of 11027 integrated reflection intensities having 2θ((MoKα)< 52.00° were produced using the Bruker program SAINT(3); 5053 of these were unique and gave R_{int} = 0.037 with a coverage which was 100.0% complete. The data were corrected empirically for variable absorption effects using equivalent reflections; the relative transmission factors ranged from 0.886 to 1.000. The Bruker software package SHELXTL was used to solve the structure using "direct methods" techniques. All stages of weighted full-matrix least-squares refinement

were conducted using F_o^2 data with the SHELXTL Version 6.10 software package(4).

All five methyl groups were incorporated into the structural model as rigid groups (using idealized sp^3-hybridized geometry and a C-H bond length of 0.98 Å) which were allowed to rotate about their N-C or C-C bonds during least-squares refinement cycles. The remaining hydrogen atoms were included into the structural model as idealized atoms (assuming sp^2- or sp^3-hybridization of the carbon atoms and C-H bond lengths of 0.95 – 1.00 Å). The isotropic thermal parameters of all hydrogen atoms were fixed at values 1.2 (nonmethyl) or 1.5 (methyl) times the equivalent isotropic thermal parameter of the carbon atom to which they are covalently bonded.

The final structural model incorporated anisotropic thermal parameters for all nonhydrogen atoms and isotropic thermal parameters for all hydrogen atoms. It also took into account the fact that the crystal used for data collection was a 93/7 racemic twin. Mild restraints had to be imposed on the anisotropic thermal parameters for two carbon atoms [C(2) and C(27)]. A total of 313 parameters were refined using 14 restraints, 5053 data and weights of $w = 1/ [\sigma^2(F^2) + (0.0307 P)^2 + 16.938 P]$, where $P = [F_o^2 + 2F_c^2] / 3$. Final agreement factors at convergence are: R_1(unweighted, based on F) = 0.057 for 4660 independent absorption-corrected "observed" reflections having $2\theta(MoK\alpha) < 52.00°$ and $I > 2\sigma(I)$; R_1(unweighted, based on F) = 0.063 and wR_2(weighted, based on F^2) = 0.121 for all 5053 independent absorption-corrected reflections having $2\theta(MoK\alpha) < 52.00°$. The largest shift/s.u. was 0.000 in the final refinement cycle. The top 6 peaks (1.61 to 0.90 $e^-/Å^3$) in the final difference

map were within 0.97 Å of the Pd atom. There were no other peaks above 0.47$e^-/Å^3$ in the final difference Fourier which had a minimum electron density of -0.71 $e^-/Å^3$.

Acknowledgment

This X-Ray analysis was performed by Victor W. Day

References

(1) International Tables for Crystallography, Vol A, 4th ed., Kluwer: Boston (1996).

(2) Data Collection: SMART Software Reference Manual (1998). Bruker-AXS, 5465 E. Cheryl Parkway, Madison, WI 53711-5373 USA.

(3) Data Reduction: SAINT Software Reference Manual (1998). Bruker-AXS, 6300 Enterprise Dr., Madison, WI 53719-1173, USA.

(4) G. M. Sheldrick (2000). SHELXTL Version 6.10 Reference Manual. Bruker-AXS, 5465 E. Cheryl Parkway, Madison, WI 53711-5373 USA.

Table 1. Crystal data and structure refinement for [(trans-$C_{23}H_{21}NO$)Pd($N_2C_6H_{16}$)].

Empirical formula	$C_{29}H_{37}N_3OPd$	
Formula weight	550.02	
Temperature	100(2) K	
Wavelength	0.71073 Å	
Crystal system	Monoclinic	
Space group	Cc – C_s^4 (No. 9)	
Unit cell dimensions	**a** = 11.021(1) Å	**α** = 90.000°
	b = 20.163(2) Å	**β** = 90.247(2)°

	c = 11.690(1) Å **γ** = 90.000°
Volume	2597.6(5) $Å^3$
Z	4
Density (calculated)	1.406 Mg/m^3
Absorption coefficient	0.740 mm^{-1}
F(000)	1144
Crystal size	0.25 x 0.10 x 0.05 mm^3
Theta range for data collection	2.11° to 26.00°
Index ranges	$-13 \leq h \leq 13$, $-24 \leq k \leq 24$, $-14 \leq l \leq 14$
Reflections collected	11027
Independent reflections	5053 [R_{int} = 0.037]
Completeness to theta = 26.00°	100.0 %
Absorption correction	Semi-empirical from equivalents
Max. and min. transmission	1.000 and 0.886
Refinement method	Full-matrix least-squares on F^2
Data / restraints / parameters	5053 / 14 / 313
Goodness-of-fit on F^2	1.248
Final R indices [I>2sigma(I)]	R_1 = 0.057, wR_2 = 0.119
R indices (all data)	R_1 = 0.063, wR_2 = 0.121
Absolute structure parameter	0.0(1)
Largest diff. peak and hole	1.61 and -0.71 $e^-/Å^3$

$R_1 = \Sigma \, ||F_o| - |F_c|| \, / \, \Sigma \, |F_o|$

$wR_2 = \{ \, \Sigma \, [w(F_o^2 - F_c^2)^2] \, / \, \Sigma \, [w(F_o^2)^2] \, \}^{1/2}$

Table 2. Atomic coordinates (x 10^4) and equivalent isotropic displacement parameters (Å^2 x 10^3) for [(trans-$C_{23}H_{21}NO$)Pd($N_2C_6H_{16}$)]. U(eq) is defined as one third of the trace of the orthogonalized U_{ij} tensor.

	x	y	z	U(eq)
Pd	4012(1)	2476(1)	4566(1)	16(1)
O	5486(5)	989(3)	6576(5)	35(1)
N(1)	3994(6)	3293(3)	3300(5)	16(1)
N(2)	2111(6)	2808(3)	4766(5)	16(1)
N(3)	6070(6)	1597(3)	5044(6)	17(1)
C(1)	4034(8)	1718(4)	5692(7)	20(2)
C(2)	5261(7)	1406(4)	5801(6)	19(2)
C(4)	5763(7)	2191(4)	4334(7)	18(2)
C(5)	3090(6)	1200(3)	5409(6)	14(1)
C(6)	3110(7)	905(4)	4323(6)	26(2)
C(7)	2270(8)	425(4)	4046(7)	34(2)
C(8)	1404(8)	224(4)	4817(7)	35(2)
C(9)	1417(8)	498(5)	5875(9)	31(2)
C(10)	2248(6)	979(4)	6201(6)	26(2)
C(11)	7269(7)	1322(4)	4986(6)	23(2)

C(12)	7588(6)	1009(3)	3840(6)	19(1)
C(13)	6782(7)	605(4)	3267(7)	26(2)
C(14)	7079(7)	288(4)	2259(6)	23(2)
C(15)	8222(7)	393(4)	1805(6)	26(2)
C(16)	9033(7)	795(4)	2346(7)	31(2)
C(17)	8712(7)	1116(4)	3370(7)	30(2)
C(18)	6622(7)	2743(4)	4710(6)	15(2)
C(19)	6607(7)	3012(4)	5840(6)	25(2)
C(20)	7388(6)	3502(4)	6185(6)	23(2)
C(21)	8248(6)	3762(4)	5426(7)	26(2)
C(22)	8290(6)	3512(4)	4332(6)	21(2)
C(23)	7503(6)	3005(3)	3992(6)	20(1)
C(24)	9083(7)	4312(4)	5818(8)	36(2)
C(25)	2684(7)	3452(4)	3082(6)	21(2)
C(26)	2018(8)	3452(4)	4216(7)	22(2)
C(27)	4586(6)	3889(4)	3796(6)	17(2)
C(28)	4574(6)	3123(4)	2220(6)	24(2)
C(29)	1796(7)	2900(4)	6015(6)	26(2)
C(30)	1219(7)	2334(4)	4278(8)	23(2)

Table 3. Bond lengths [Å] for [(trans-$C_{23}H_{21}NO$)Pd($N_2C_6H_{16}$)]

Pd-C(1)	2.016(7)	C(8)-C(9)	1.355(13)
Pd-C(4)	2.032(8)	C(9)-C(10)	1.387(12)
Pd-N(2)	2.213(7)	C(11)-C(12)	1.524(9)
Pd-N(1)	2.215(6)	C(12)-C(17)	1.375(10)
O-C(2)	1.261(9)	C(12)-C(13)	1.377(11)
N(1)-C(28)	1.458(9)	C(13)-C(14)	1.381(11)
N(1)-C(27)	1.484(9)	C(14)-C(15)	1.385(10)
N(1)-C(25)	1.500(10)	C(15)-C(16)	1.360(11)
N(2)-C(26)	1.454(10)	C(16)-C(17)	1.407(11)
N(2)-C(30)	1.483(10)	C(18)-C(23)	1.391(10)
N(2)-C(29)	1.513(9)	C(18)-C(19)	1.428(10)
N(3)-C(2)	1.316(10)	C(19)-C(20)	1.370(11)
N(3)-C(11)	1.434(9)	C(20)-C(21)	1.403(10)
N(3)-C(4)	1.496(9)	C(21)-C(22)	1.376(10)
C(1)-C(2)	1.497(11)	C(21)-C(24)	1.510(10)
C(1)-C(5)	1.510(10)	C(22)-C(23)	1.397(10)
C(4)-C(18)	1.525(11)	C(25)-C(26)	1.518(11)
C(5)-C(10)	1.387(10)		
C(5)-C(6)	1.403(10)		
C(6)-C(7)	1.377(11)		
C(7)-C(8)	1.375(12)		

Table 4. Bond angles [°] for [(trans-$C_{23}H_{21}NO$)Pd($N_2C_6H_{16}$)].

C(1)-Pd-C(4)	82.2(3)
C(1)-Pd-N(2)	99.7(3)
C(4)-Pd-N(2)	178.0(3)
C(1)-Pd-N(1)	178.8(3)
C(4)-Pd-N(1)	97.3(3)
N(2)-Pd-N(1)	80.8(2)
C(28)-N(1)-C(27)	109.6(6)
C(28)-N(1)-C(25)	109.2(5)
C(27)-N(1)-C(25)	108.3(5)
C(28)-N(1)-Pd	113.7(5)
C(27)-N(1)-Pd	109.8(4)
C(25)-N(1)-Pd	106.1(4)
C(26)-N(2)-C(30)	111.1(6)
C(26)-N(2)-C(29)	107.5(6)
C(30)-N(2)-C(29)	107.2(6)
C(26)-N(2)-Pd	106.8(5)
C(30)-N(2)-Pd	113.1(5)
C(29)-N(2)-Pd	111.1(5)
C(2)-N(3)-C(11)	123.1(6)
C(2)-N(3)-C(4)	117.1(6)

C(11)-N(3)-C(4)	119.3(6)
C(2)-C(1)-C(5)	110.4(6)
C(2)-C(1)-Pd	112.5(5)
C(5)-C(1)-Pd	112.0(5)
O-C(2)-N(3)	123.1(7)
O-C(2)-C(1)	121.1(7)
N(3)-C(2)-C(1)	115.7(6)
N(3)-C(4)-C(18)	106.6(6)
N(3)-C(4)-Pd	111.4(5)
C(18)-C(4)-Pd	110.1(5)
C(10)-C(5)-C(6)	118.7(7)
C(10)-C(5)-C(1)	122.6(7)
C(6)-C(5)-C(1)	118.6(7)
C(7)-C(6)-C(5)	119.9(7)
C(8)-C(7)-C(6)	121.4(7)
C(9)-C(8)-C(7)	118.2(8)
C(8)-C(9)-C(10)	122.7(8)
C(5)-C(10)-C(9)	119.0(7)
N(3)-C(11)-C(12)	114.7(6)
C(17)-C(12)-C(13)	118.6(7)
C(17)-C(12)-C(11)	119.9(6)
C(13)-C(12)-C(11)	121.4(7)

C(12)-C(13)-C(14)	122.2(7)
C(13)-C(14)-C(15)	118.4(7)
C(16)-C(15)-C(14)	120.6(7)
C(15)-C(16)-C(17)	120.2(7)
C(12)-C(17)-C(16)	119.9(7)
C(23)-C(18)-C(19)	115.2(7)
C(23)-C(18)-C(4)	122.5(7)
C(19)-C(18)-C(4)	122.3(7)
C(20)-C(19)-C(18)	122.4(7)
C(19)-C(20)-C(21)	120.6(7)
C(22)-C(21)-C(20)	118.4(7)
C(22)-C(21)-C(24)	121.9(7)
C(20)-C(21)-C(24)	119.6(7)
C(21)-C(22)-C(23)	120.7(7)
C(18)-C(23)-C(22)	122.7(7)
N(1)-C(25)-C(26)	108.7(6)
N(2)-C(26)-C(25)	110.6(7)

Table 5. Anisotropic displacement parameters ($Å^2$ x 10^3) for [(trans-$C_{23}H_{21}NO$)Pd($N_2C_6H_{16}$)]. The anisotropic displacement factor exponent takes the form: $-2\pi^2[h^2 a^{*2}U_{11} + ... + 2 h k a^* b^* U_{12}]$

	U_{11}	U_{22}	U_{33}	U_{23}	U_{13}	U_{12}
Pd	18(1)	15(1)	14(1)	2(1)	-4(1)	0(1)
O	23(3)	45(3)	36(3)	18(3)	-9(2)	-5(2)
N(1)	15(3)	23(3)	10(3)	-6(2)	-1(3)	2(2)
N(2)	11(3)	29(3)	9(3)	-2(3)	-5(3)	-2(3)
N(3)	15(3)	21(3)	16(3)	0(3)	-6(3)	5(3)
C(1)	30(5)	22(4)	8(3)	10(3)	-3(3)	-6(3)
C(2)	17(3)	24(3)	15(3)	0(2)	-15(3)	-1(3)
C(4)	20(4)	17(4)	18(4)	1(3)	-5(3)	6(3)
C(5)	7(3)	21(3)	15(3)	0(3)	-5(3)	3(3)
C(6)	31(4)	30(4)	17(3)	3(3)	-4(3)	2(3)
C(7)	42(5)	35(4)	24(4)	-8(3)	-14(4)	-3(4)
C(8)	31(4)	30(4)	42(5)	-1(4)	-19(4)	-8(4)
C(9)	16(4)	27(5)	50(6)	10(4)	3(4)	0(3)
C(10)	18(4)	37(4)	23(4)	-4(3)	0(3)	0(3)
C(11)	27(4)	33(4)	9(3)	-6(3)	-1(3)	5(3)
C(12)	17(3)	26(4)	13(3)	3(3)	-1(3)	-1(3)
C(13)	15(4)	30(5)	32(4)	10(4)	0(3)	-1(3)

C(14)	28(4)	27(4)	14(3)	0(3)	-6(3)	0(3)
C(15)	36(4)	23(4)	18(4)	3(3)	-3(3)	11(3)
C(16)	15(4)	41(5)	38(5)	3(4)	4(3)	3(3)
C(17)	27(4)	38(4)	25(4)	-3(3)	-6(3)	3(4)
C(18)	9(4)	26(4)	12(4)	-1(3)	0(3)	8(3)
C(19)	28(4)	31(4)	15(3)	-2(3)	0(3)	4(3)
C(20)	23(4)	38(4)	9(3)	2(3)	-9(3)	7(3)
C(21)	16(3)	27(4)	33(4)	-2(3)	-9(3)	2(3)
C(22)	8(3)	34(4)	21(4)	2(3)	-3(3)	-2(3)
C(23)	20(3)	27(4)	13(3)	-1(3)	-11(3)	2(3)
C(24)	24(4)	43(5)	40(5)	-8(4)	-11(4)	-7(4)
C(25)	21(4)	34(4)	7(3)	0(3)	-8(3)	-4(3)
C(26)	18(4)	25(4)	23(4)	3(3)	-5(3)	-5(3)
C(27)	5(3)	25(3)	19(3)	1(2)	-4(2)	3(2)
C(28)	18(3)	38(4)	17(3)	-1(3)	-1(3)	0(3)
C(29)	26(4)	36(4)	18(4)	5(3)	4(3)	-4(3)
C(30)	20(4)	18(4)	30(5)	4(3)	-8(3)	-2(3)

Table 6. Hydrogen coordinates (x 10^4) and isotropic displacement parameters ($Å^2$ x 10^3) for [(trans-$C_{23}H_{21}NO$)Pd($N_2C_6H_{16}$)].

	x	y	z	U(eq)
H(1)	3824	1906	6458	24
H(4)	5899	2088	3508	22
H(6)	3703	1035	3780	31
H(7)	2288	228	3308	40
H(8)	813	-98	4612	42
H(9)	833	354	6417	37
H(10)	2241	1155	6955	31
H(11A)	7355	982	5591	28
H(11B)	7862	1678	5153	28
H(13)	5995	542	3576	31
H(14)	6513	5	1886	27
H(15)	8442	182	1110	31
H(16)	9818	859	2032	37
H(17)	9272	1406	3735	36
H(19)	6034	2845	6372	30
H(20)	7347	3667	6945	28
H(22)	8859	3685	3803	25
H(23)	7573	2832	3239	24

H(24A)	9661	4416	5209	53
H(24B)	9527	4168	6503	53
H(24C)	8603	4707	5997	53
H(25S)	2324	3117	2563	25
H(25B)	2612	3892	2714	25
H(26A)	2369	3796	4724	27
H(26B)	1152	3562	4085	27
H(27A)	4415	4275	3311	25
H(27B)	5464	3818	3839	25
H(27C)	4268	3968	4566	25
H(28A)	4478	3491	1680	36
H(28B)	4195	2723	1902	36
H(28C)	5440	3040	2353	36
H(29A)	974	3081	6077	40
H(29B)	2375	3208	6369	40
H(29C)	1835	2471	6408	40
H(30A)	398	2514	4364	34
H(30B)	1278	1910	4684	34
H(30C)	1390	2266	3465	34

Table 7. Torsion angles [°] for [(trans-$C_{23}H_{21}NO$)Pd($N_2C_6H_{16}$)].

C(1)-Pd-N(1)-C(28)	-21(18)
C(4)-Pd-N(1)-C(28)	44.1(5)
N(2)-Pd-N(1)-C(28)	-135.6(5)
C(1)-Pd-N(1)-C(27)	-144(17)
C(4)-Pd-N(1)-C(27)	-79.0(5)
N(2)-Pd-N(1)-C(27)	101.3(5)
C(1)-Pd-N(1)-C(25)	99(17)
C(4)-Pd-N(1)-C(25)	164.1(4)
N(2)-Pd-N(1)-C(25)	-15.5(4)
C(1)-Pd-N(2)-C(26)	166.6(5)
C(4)-Pd-N(2)-C(26)	-25(10)
N(1)-Pd-N(2)-C(26)	-14.5(5)
C(1)-Pd-N(2)-C(30)	-70.9(6)
C(4)-Pd-N(2)-C(30)	97(10)
N(1)-Pd-N(2)-C(30)	108.0(5)
C(1)-Pd-N(2)-C(29)	49.7(5)
C(4)-Pd-N(2)-C(29)	-142(10)
N(1)-Pd-N(2)-C(29)	-131.4(5)
C(4)-Pd-C(1)-C(2)	3.6(6)
N(2)-Pd-C(1)-C(2)	-176.8(5)
N(1)-Pd-C(1)-C(2)	69(17)

C(4)-Pd-C(1)-C(5)	-121.5(6)
N(2)-Pd-C(1)-C(5)	58.1(6)
N(1)-Pd-C(1)-C(5)	-56(18)
C(11)-N(3)-C(2)-O	3.5(11)
C(4)-N(3)-C(2)-O	-167.6(7)
C(11)-N(3)-C(2)-C(1)	-176.6(7)
C(4)-N(3)-C(2)-C(1)	12.2(9)
C(5)-C(1)-C(2)-O	-64.0(9)
Pd-C(1)-C(2)-O	170.0(6)
C(5)-C(1)-C(2)-N(3)	116.1(7)
Pd-C(1)-C(2)-N(3)	-9.8(8)
C(2)-N(3)-C(4)-C(18)	111.4(7)
C(11)-N(3)-C(4)-C(18)	-60.1(8)
C(2)-N(3)-C(4)-Pd	-8.8(8)
C(11)-N(3)-C(4)-Pd	179.7(5)
C(1)-Pd-C(4)-N(3)	2.2(5)
N(2)-Pd-C(4)-N(3)	-166(10)
N(1)-Pd-C(4)-N(3)	-176.6(5)
C(1)-Pd-C(4)-C(18)	-115.8(6)
N(2)-Pd-C(4)-C(18)	76(10)
N(1)-Pd-C(4)-C(18)	65.3(6)
C(2)-C(1)-C(5)-C(10)	106.7(8)

Pd-C(1)-C(5)-C(10)	-127.1(6)
C(2)-C(1)-C(5)-C(6)	-69.6(8)
Pd-C(1)-C(5)-C(6)	56.6(8)
C(10)-C(5)-C(6)-C(7)	2.7(11)
C(1)-C(5)-C(6)-C(7)	179.2(7)
C(5)-C(6)-C(7)-C(8)	-0.2(12)
C(6)-C(7)-C(8)-C(9)	-1.8(13)
C(7)-C(8)-C(9)-C(10)	1.4(14)
C(6)-C(5)-C(10)-C(9)	-3.2(11)
C(1)-C(5)-C(10)-C(9)	-179.5(7)
C(8)-C(9)-C(10)-C(5)	1.1(13)
C(2)-N(3)-C(11)-C(12)	121.9(7)
C(4)-N(3)-C(11)-C(12)	-67.2(9)
N(3)-C(11)-C(12)-C(17)	137.7(7)
N(3)-C(11)-C(12)-C(13)	-43.8(10)
C(17)-C(12)-C(13)-C(14)	2.1(12)
C(11)-C(12)-C(13)-C(14)	-176.4(7)
C(12)-C(13)-C(14)-C(15)	-1.1(11)
C(13)-C(14)-C(15)-C(16)	0.5(11)
C(14)-C(15)-C(16)-C(17)	-0.8(11)
C(13)-C(12)-C(17)-C(16)	-2.3(11)
C(11)-C(12)-C(17)-C(16)	176.2(7)

C(15)-C(16)-C(17)-C(12)	1.7(12)
N(3)-C(4)-C(18)-C(23)	114.0(8)
Pd-C(4)-C(18)-C(23)	-125.0(7)
N(3)-C(4)-C(18)-C(19)	-63.8(9)
Pd-C(4)-C(18)-C(19)	57.2(9)
C(23)-C(18)-C(19)-C(20)	1.2(11)
C(4)-C(18)-C(19)-C(20)	179.2(7)
C(18)-C(19)-C(20)-C(21)	0.0(11)
C(19)-C(20)-C(21)-C(22)	-0.3(11)
C(19)-C(20)-C(21)-C(24)	178.8(7)
C(20)-C(21)-C(22)-C(23)	-0.7(10)
C(24)-C(21)-C(22)-C(23)	-179.8(7)
C(19)-C(18)-C(23)-C(22)	-2.3(11)
C(4)-C(18)-C(23)-C(22)	179.8(7)
C(21)-C(22)-C(23)-C(18)	2.1(11)
C(28)-N(1)-C(25)-C(26)	165.5(6)
C(27)-N(1)-C(25)-C(26)	-75.3(7)
Pd-N(1)-C(25)-C(26)	42.6(6)
C(30)-N(2)-C(26)-C(25)	-80.8(8)
C(29)-N(2)-C(26)-C(25)	162.3(6)
Pd-N(2)-C(26)-C(25)	42.9(7)
N(1)-C(25)-C(26)-N(2)	-59.8(8)

Crystal Structure Report

for

cis-(±)-**4.40**

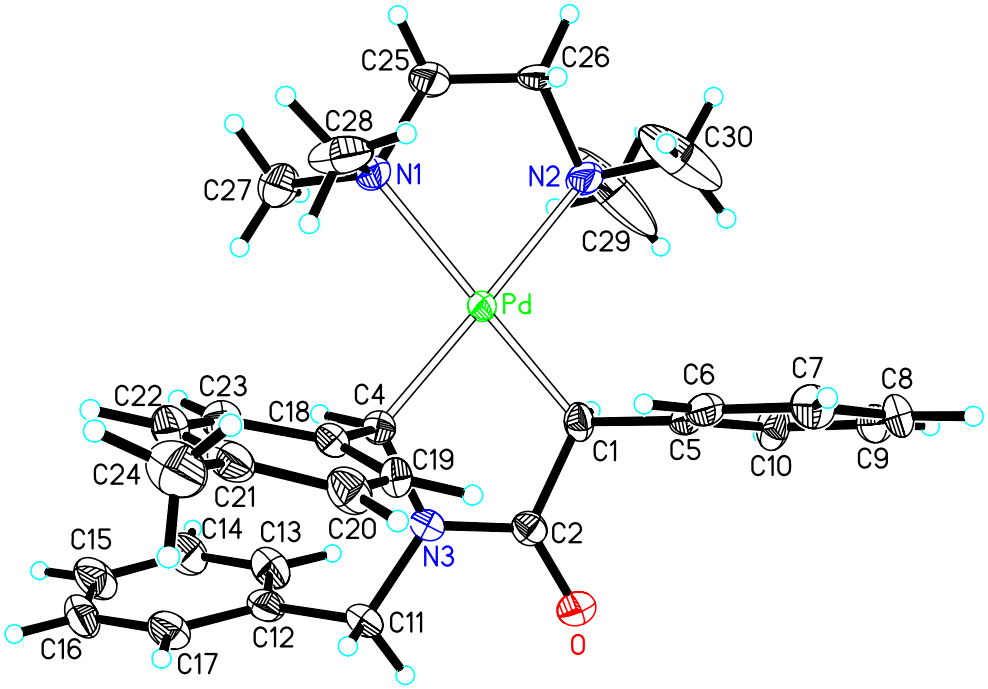
C25
C26
C28
C30
N1
N2
C27
C29
Pd
C22
C23
C18
C4
C6
C7
C8
C1
C5
C10
C9
C24
C21
C19
C20
C14
C13
C15
N3
C2
C16
C17
C12
C11
O

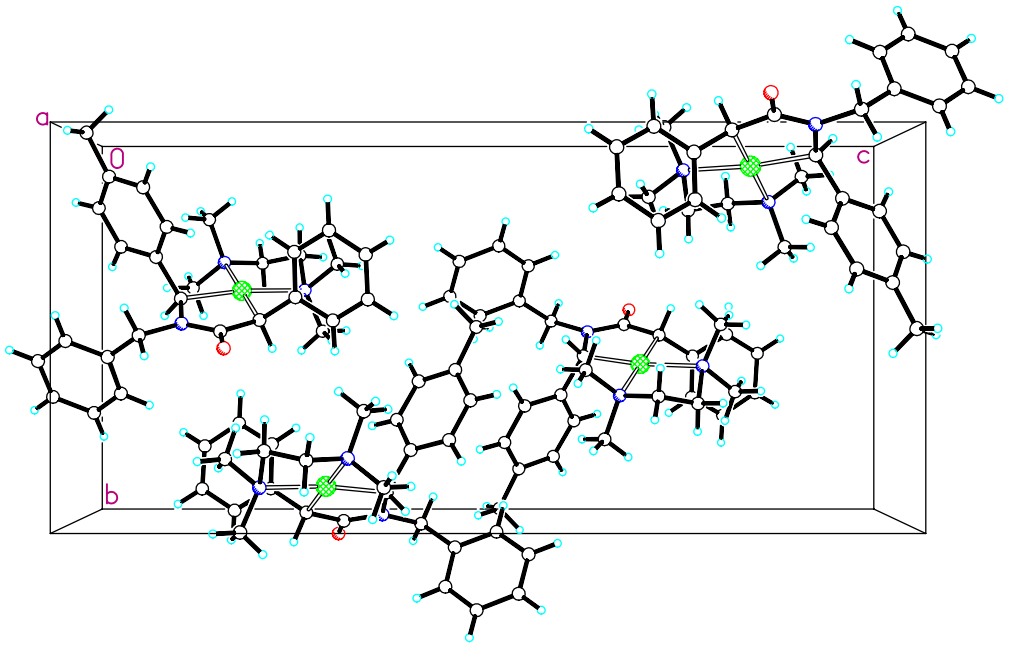
a
0
c
b

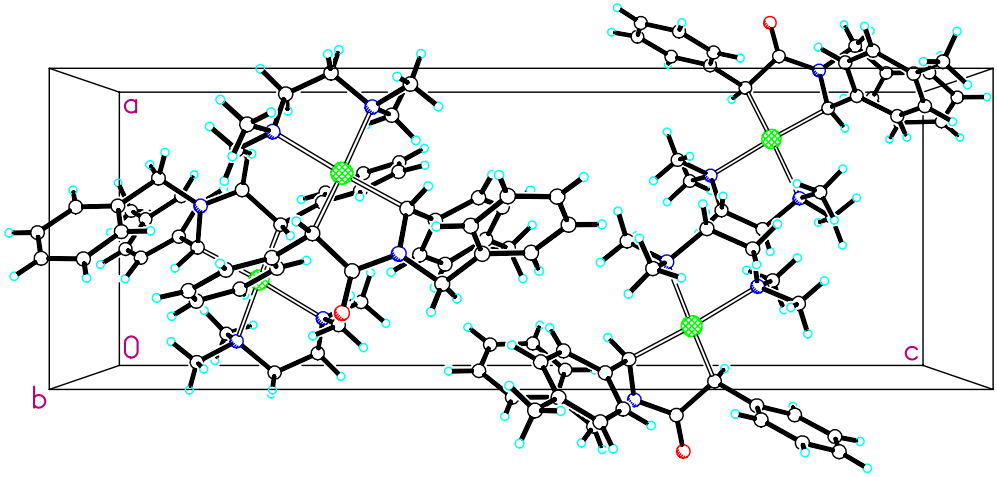
a
0
b
c

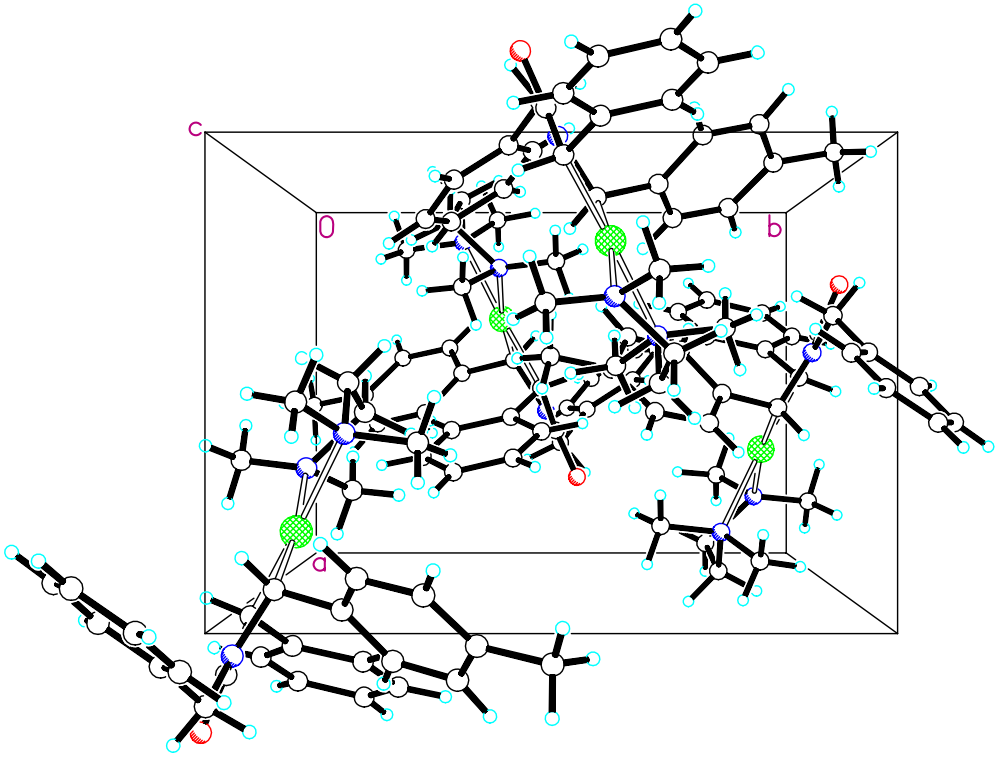
c
0
b
a

Comments

The asymmetric unit contains one [(cis-$C_{23}H_{21}NO$)Pd($N_2C_6H_{16}$)] molecule. The crystal used for data collection was a 52/48 racemic twin. All displacement ellipsoids are drawn at the 50% probability level.

Experimental Description

Yellow crystals of [(cis-$C_{23}H_{21}NO$)Pd($N_2C_6H_{16}$)] are, at 100(2) K, orthorhombic, space group $P2_12_12_1$ – D_2^4 (No. 19) with **a** = 8.6209(7) Å, **b** = 11.898(1) Å, **c** = 25.296(2) Å, V = 2594.7(4) $Å^3$ and Z = 4 molecules {d_{calcd} = 1.408 g/cm^3; μ_a(MoKα) = 0.741 mm^{-1}}. A full hemisphere of diffracted intensities (1850 10-second frames with a ω scan width of 0.30°) was measured for a 2-domain specimen using graphite-monochromated MoKα radiation (λ= 0.71073 Å) on a Bruker SMART APEX CCD Single Crystal Diffraction System (2). X-rays were provided by a fine-focus sealed x-ray tube operated at 50kV and 30mA. Lattice constants were determined with the Bruker SAINT software package using peak centers for 8698 reflections. A total of 31796 integrated reflection intensities having 2θ((MoKα)< 61.08° were produced using the Bruker program SAINT(3); 7897 of these were unique and gave R_{int} = 0.067 with a coverage which was 99.6% complete. The data were corrected empirically for variable absorption effects using equivalent reflections; the relative transmission factors ranged from 0.752 to 1.000. The Bruker software package SHELXTL was used to solve the structure using "direct methods" techniques. All stages of weighted full-matrix least-squares refinement were conducted using F_o^2 data with the SHELXTL Version 6.10 software package(4).

All five methyl groups were incorporated into the structural model as rigid groups (using idealized sp^3-hybridized geometry and a C-H bond length of 0.98 Å) which were allowed to rotate about their N-C or C-C bonds during least-squares refinement cycles. The remaining hydrogen atoms were included into the structural model as idealized atoms (assuming sp^2- or sp^3-hybridization of the carbon atoms and C-H bond lengths of 0.95 – 1.00 Å). The isotropic thermal parameters of all hydrogen atoms were fixed at values 1.2 (nonmethyl) or 1.5 (methyl) times the equivalent isotropic thermal parameter of the carbon atom to which they are covalently bonded.

The final structural model incorporated anisotropic thermal parameters for all nonhydrogen atoms and isotropic thermal parameters for all hydrogen atoms. A total of 323 parameters were refined using no restraints, 7897 data and weights of $w = 1/[\sigma^2(F^2) + (0.0442\ P)^2]$, where $P = [F_o^2 + 2F_c^2] / 3$. Final agreement factors at convergence are: R_1(unweighted, based on F) = 0.048 for 7406 independent absorption-corrected "observed" reflections having $2\theta(MoK\alpha) < 61.08°$ and $I > 2\sigma(I)$; R_1(unweighted, based on F) = 0.053 and wR_2(weighted, based on F^2) = 0.099 for all 7897 independent absorption-corrected reflections having $2\theta(MoK\alpha) < 61.08°$. The largest shift/s.u. was 0.000 in the final refinement cycle. The final difference map had maxima and minima of 1.51 and

-1.38 $e^-/Å^3$, respectively.

Acknowledgment

This X-Ray analysis was performed by Victor W. Day

References

(1) International Tables for Crystallography, Vol A, 4th ed., Kluwer: Boston (1996).

(2) Data Collection: SMART Software Reference Manual (1998). Bruker-AXS, 5465 E. Cheryl Parkway, Madison, WI 53711-5373 USA.

(3) Data Reduction: SAINT Software Reference Manual (1998). Bruker-AXS, 6300 Enterprise Dr., Madison, WI 53719-1173, USA.

(4) G. M. Sheldrick (2000). SHELXTL Version 6.10 Reference Manual. Bruker-AXS, 5465 E. Cheryl Parkway, Madison, WI 53711-5373 USA.

Table 1. Crystal data and structure refinement for [(cis-$C_{23}H_{21}NO$)Pd($N_2C_6H_{16}$)].

Empirical formula	$C_{29}H_{37}N_3OPd$	
Formula weight	550.02	
Temperature	100(2) K	
Wavelength	0.71073 Å	
Crystal system	Orthorhombic	
Space group	$P2_12_12_1 - D_2^4$ (No. 19)	
Unit cell dimensions	**a** = 8.6209(7) Å	**α** = 90.000°
	b = 11.898(1) Å	**β** = 90.000°
	c = 25.296(2) Å	**γ** = 90.000°
Volume	2594.7(4) $Å^3$	
Z	4	

Density (calculated)	1.408 Mg/m^3
Absorption coefficient	0.741 mm^{-1}
F(000)	1144
Crystal size	0.22 x 0.19 x 0.10 mm^3
Theta range for data collection	2.50° to 30.54°
Index ranges	$-12 \leq h \leq 12$, $-16 \leq k \leq 17$, $-35 \leq l \leq 35$
Reflections collected	31796
Independent reflections	7897 [$R_{int} = 0.067$]
Completeness to theta = 30.54°	99.6 %
Absorption correction	Semi-empirical from equivalents
Max. and min. transmission	1.000 and 0.752
Refinement method	Full-matrix least-squares on F^2
Data / restraints / parameters	7897 / 0 / 323
Goodness-of-fit on F^2	1.099
Final R indices [I>2sigma(I)]	$R_1 = 0.048$, $wR_2 = 0.098$
R indices (all data)	$R_1 = 0.053$, $wR_2 = 0.099$
Absolute structure parameter	0.0(10)
Largest diff. peak and hole	1.51 and -1.38 $e^-/Å^3$

$R_1 = \Sigma \, ||F_o| - |F_c|| \, / \, \Sigma \, |F_o|$

$wR_2 = \{ \, \Sigma \, [w(F_o^2 - F_c^2)^2] \, / \, \Sigma \, [w(F_o^2)^2] \, \}^{1/2}$

Table 2. Atomic coordinates (x 10^4) and equivalent isotropic displacement parameters ($Å^2$ x 10^3) for [(cis-$C_{23}H_{21}NO$)Pd($N_2C_6H_{16}$)]. U(eq) is defined as one third of the trace of the orthogonalized U_{ij} tensor.

	x	y	z	U(eq)
Pd	3241(1)	4020(1)	1932(1)	18(1)
O	7598(3)	5512(2)	1882(1)	30(1)
N(1)	1087(4)	3220(3)	1628(1)	24(1)
N(2)	1918(4)	3985(4)	2680(1)	35(1)
N(3)	5782(4)	4890(3)	1300(1)	22(1)
C(1)	5143(4)	4799(3)	2219(1)	21(1)
C(2)	6316(4)	5091(3)	1789(1)	21(1)
C(4)	4362(4)	4233(3)	1225(1)	21(1)
C(5)	5912(4)	4213(3)	2679(1)	21(1)
C(6)	6266(4)	3061(3)	2676(2)	24(1)
C(7)	6958(4)	2535(3)	3109(2)	29(1)
C(8)	7322(5)	3154(4)	3553(2)	33(1)
C(9)	6955(5)	4279(4)	3571(2)	33(1)
C(10)	6283(4)	4813(3)	3140(1)	28(1)
C(11)	6709(5)	5190(3)	834(1)	26(1)
C(12)	5767(4)	5750(3)	409(1)	25(1)
C(13)	4908(5)	6706(3)	520(2)	32(1)

C(14)	4019(5)	7233(4)	138(2)	33(1)
C(15)	4031(5)	6812(4)	-369(2)	36(1)
C(16)	4874(5)	5867(4)	-495(2)	35(1)
C(17)	5738(5)	5338(3)	-104(2)	29(1)
C(18)	4728(4)	3158(3)	939(1)	21(1)
C(19)	5849(4)	2410(3)	1124(1)	25(1)
C(20)	6170(5)	1408(3)	858(2)	29(1)
C(21)	5348(5)	1095(4)	401(2)	29(1)
C(22)	4281(5)	1865(4)	212(2)	31(1)
C(23)	3991(4)	2872(3)	469(2)	27(1)
C(24)	5655(6)	-20(4)	145(2)	41(1)
C(25)	-8(5)	3221(4)	2077(2)	35(1)
C(25')	-8(5)	3221(4)	2077(2)	35(1)
C(26)	655(9)	3022(8)	2582(3)	33(2)
C(26')	262(8)	4079(9)	2476(3)	26(2)
C(27)	405(5)	3900(5)	1197(2)	47(1)
C(28)	1280(5)	2062(4)	1443(2)	44(1)
C(29)	1753(11)	5091(5)	2899(2)	110(4)
C(30)	2458(8)	3293(5)	3104(3)	82(2)

Table 3. Bond lengths [Å] for [(cis-$C_{23}H_{21}NO$)Pd($N_2C_6H_{16}$)].

Pd-C(1)	2.020(4)	C(6)-C(7)	1.396(5)
Pd-C(4)	2.048(3)	C(7)-C(8)	1.379(6)
Pd-N(2)	2.209(3)	C(8)-C(9)	1.375(6)
Pd-N(1)	2.223(3)	C(9)-C(10)	1.388(5)
O-C(2)	1.237(4)	C(11)-C(12)	1.503(5)
N(1)-C(28)	1.464(5)	C(12)-C(13)	1.386(5)
N(1)-C(25)	1.478(5)	C(12)-C(17)	1.387(5)
N(1)-C(27)	1.479(5)	C(13)-C(14)	1.384(6)
N(2)-C(30)	1.431(7)	C(14)-C(15)	1.376(6)
N(2)-C(29)	1.436(7)	C(15)-C(16)	1.377(6)
N(2)-C(26')	1.522(8)	C(16)-C(17)	1.387(6)
N(2)-C(26)	1.600(8)	C(18)-C(23)	1.390(5)
N(3)-C(2)	1.341(4)	C(18)-C(19)	1.394(5)
N(3)-C(4)	1.464(5)	C(19)-C(20)	1.398(5)
N(3)-C(11)	1.469(4)	C(20)-C(21)	1.405(6)
C(1)-C(5)	1.508(5)	C(21)-C(22)	1.383(6)
C(1)-C(2)	1.525(5)	C(21)-C(24)	1.500(6)
C(4)-C(18)	1.504(5)	C(22)-C(23)	1.385(5)
C(5)-C(6)	1.405(5)	C(25)-C(26)	1.417(9)
C(5)-C(10)	1.405(5)		

Table 4. Bond angles [°] for [(cis-$C_{23}H_{21}NO$)Pd($N_2C_6H_{16}$)].

C(1)-Pd-C(4)	82.8(1)	C(2)-N(3)-C(4)	120.1(3)
C(1)-Pd-N(2)	96.9(1)	C(2)-N(3)-C(11)	120.7(3)
C(4)-Pd-N(2)	173.4(2)	C(4)-N(3)-C(11)	118.7(3)
C(1)-Pd-N(1)	177.6(1)	C(5)-C(1)-C(2)	111.3(3)
C(4)-Pd-N(1)	98.4(1)	C(5)-C(1)-Pd	115.0(2)
N(2)-Pd-N(1)	81.8(1)	C(2)-C(1)-Pd	112.7(2)
C(28)-N(1)-C(25)	108.6(3)	O-C(2)-N(3)	123.7(3)
C(28)-N(1)-C(27)	109.0(4)	O-C(2)-C(1)	123.3(3)
C(25)-N(1)-C(27)	108.2(3)	N(3)-C(2)-C(1)	113.0(3)
C(28)-N(1)-Pd	114.7(3)	N(3)-C(4)-C(18)	109.9(3)
C(25)-N(1)-Pd	105.5(2)	N(3)-C(4)-Pd	110.3(2)
C(27)-N(1)-Pd	110.7(3)	C(18)-C(4)-Pd	114.4(2)
C(30)-N(2)-C(29)	105.6(5)	C(6)-C(5)-C(10)	116.7(3)
C(30)-N(2)-C(26')	127.0(5)	C(6)-C(5)-C(1)	122.9(3)
C(29)-N(2)-C(26')	88.3(6)	C(10)-C(5)-C(1)	120.4(3)
C(30)-N(2)-C(26)	85.7(5)	C(7)-C(6)-C(5)	121.8(4)
C(29)-N(2)-C(26)	130.5(5)	C(8)-C(7)-C(6)	119.8(3)
C(26')-N(2)-C(26)	50.3(5)	C(9)-C(8)-C(7)	119.6(4)
C(30)-N(2)-Pd	119.1(3)	C(8)-C(9)-C(10)	121.0(4)
C(29)-N(2)-Pd	111.4(3)	C(9)-C(10)-C(5)	121.0(4)
C(26')-N(2)-Pd	101.1(3)	N(3)-C(11)-C(12)	112.8(3)
C(26)-N(2)-Pd	103.4(3)	C(13)-C(12)-C(17)	118.0(4)

C(13)-C(12)-C(11)	120.5(3)	C(18)-C(19)-C(20)	121.4(4)
C(17)-C(12)-C(11)	121.5(3)	C(19)-C(20)-C(21)	121.5(4)
C(14)-C(13)-C(12)	121.8(4)	C(22)-C(21)-C(20)	116.3(4)
C(15)-C(14)-C(13)	118.7(4)	C(22)-C(21)-C(24)	123.7(4)
C(14)-C(15)-C(16)	121.1(4)	C(20)-C(21)-C(24)	120.0(4)
C(15)-C(16)-C(17)	119.3(4)	C(21)-C(22)-C(23)	122.1(4)
C(12)-C(17)-C(16)	121.0(4)	C(22)-C(23)-C(18)	122.0(4)
C(23)-C(18)-C(19)	116.6(3)	C(26)-C(25)-N(1)	115.7(4)
C(23)-C(18)-C(4)	121.6(3)	C(25)-C(26)-N(2)	107.1(6)
C(19)-C(18)-C(4)	121.8(3)		

Table 5. Anisotropic displacement parameters ($Å^2$ x 10^3) for [(cis-$C_{23}H_{21}NO$)Pd($N_2C_6H_{16}$)].The anisotropic displacement factor exponent takes the form: $-2\pi^2[h^2 a^{*2}U_{11} + ... + 2 h k a^* b^* U_{12}]$

	U_{11}	$U2_2$	U_{33}	U_{23}	U_{13}	U_{12}
Pd	15(1)	25(1)	13(1)	-1(1)	1(1)	1(1)
O	23(1)	40(1)	27(1)	-1(1)	0(1)	-8(1)
N(1)	16(1)	35(2)	21(2)	-3(1)	0(1)	-1(1)
N(2)	17(1)	66(2)	21(1)	-10(2)	4(1)	-9(2)
N(3)	20(2)	27(2)	19(1)	2(1)	3(1)	-3(1)
C(1)	23(2)	26(2)	15(2)	-3(1)	-1(1)	6(1)
C(2)	21(2)	20(2)	21(2)	0(1)	2(1)	2(1)
C(4)	18(2)	28(2)	18(2)	-1(1)	1(1)	2(1)
C(5)	13(2)	30(2)	18(2)	-3(1)	1(1)	-2(1)
C(6)	17(2)	32(2)	23(2)	-3(2)	1(1)	-4(1)
C(7)	28(2)	21(2)	36(2)	15(2)	0(2)	8(1)
C(8)	32(2)	52(3)	16(2)	9(2)	-3(2)	-5(2)
C(9)	29(2)	50(3)	18(2)	-6(2)	0(2)	-11(2)
C(10)	29(2)	37(2)	18(2)	-12(2)	-4(1)	8(2)
C(11)	24(2)	34(2)	19(2)	3(1)	6(2)	-2(2)
C(12)	22(2)	30(2)	23(2)	7(1)	4(1)	-1(1)
C(13)	38(2)	32(2)	24(2)	-1(2)	5(2)	0(2)
C(14)	40(2)	31(2)	29(2)	6(2)	4(2)	2(2)

C(15)	38(2)	44(3)	27(2)	17(2)	5(2)	8(2)
C(16)	36(2)	51(3)	18(2)	6(2)	2(2)	3(2)
C(17)	28(2)	33(2)	27(2)	1(2)	7(2)	4(2)
C(18)	20(2)	26(2)	16(2)	-1(1)	3(1)	-1(1)
C(19)	24(2)	35(2)	17(2)	5(2)	-4(1)	-4(2)
C(20)	34(2)	28(2)	25(2)	6(2)	3(2)	5(2)
C(21)	31(2)	33(2)	25(2)	-3(2)	9(2)	-3(2)
C(22)	32(2)	41(2)	19(2)	-6(2)	3(2)	-8(2)
C(23)	20(2)	36(2)	25(2)	-2(2)	1(2)	0(2)
C(24)	51(3)	33(2)	41(2)	-6(2)	10(2)	-6(2)
C(25)	22(2)	56(3)	25(2)	-4(2)	7(2)	-7(2)
C(25')	22(2)	56(3)	25(2)	-4(2)	7(2)	-7(2)
C(26)	19(4)	52(5)	30(4)	-3(4)	10(3)	-14(4)
C(26')	12(3)	49(5)	16(3)	0(4)	1(2)	-3(4)
C(27)	26(2)	78(4)	37(2)	21(3)	-11(2)	-3(3)
C(28)	30(2)	40(2)	61(3)	-18(2)	15(2)	-13(2)
C(29)	206(9)	62(4)	63(4)	24(3)	93(5)	65(5)
C(30)	100(5)	65(4)	80(4)	43(4)	62(4)	43(3)

Table 6. Hydrogen coordinates (x 10^4) and isotropic displacement parameters ($Å^2$ x 10^3) for [(cis-$C_{23}H_{21}NO$)Pd($N_2C_6H_{16}$)].

	x	y	z	U(eq)
H(1)	4770	5536	2361	25
H(4)	3661	4682	991	25
H(6)	6029	2628	2371	28
H(7)	7178	1753	3098	34
H(8)	7823	2806	3845	40
H(9)	7164	4696	3883	39
H(10)	6072	5595	3157	34
H(11A)	7189	4501	688	31
H(11B)	7556	5702	943	31
H(13)	4930	7007	867	38
H(14)	3412	7874	224	40
H(15)	3447	7180	-636	44
H(16)	4864	5579	-845	42
H(17)	6318	4684	-190	35
H(19)	6405	2586	1437	30
H(20)	6961	927	988	34
H(22)	3729	1698	-103	37
H(23)	3267	3383	319	33
H(24A)	4869	-163	-127	62

H(24B)	5610	-615	413	62
H(24C)	6686	-13	-18	62
H(25A)	-542	3957	2086	42
H(25B)	-806	2639	2012	42
H(25C)	-1071	3318	1937	42
H(25D)	37	2476	2251	42
H(26A)	1152	2272	2591	40
H(26B)	-155	3050	2859	40
H(26C)	-476	3981	2772	31
H(26D)	94	4833	2321	31
H(27A)	-586	3568	1088	71
H(27B)	1117	3913	895	71
H(27C)	231	4669	1323	71
H(28A)	304	1796	1289	65
H(28B)	1566	1580	1742	65
H(28C)	2100	2035	1175	65
H(29A)	983	5075	3184	165
H(29B)	1411	5612	2623	165
H(29C)	2753	5342	3041	165
H(30A)	1717	3326	3397	123
H(30B)	3472	3564	3224	123
H(30C)	2555	2515	2981	123

Table 7. Torsion angles [°] for [(cis-$C_{23}H_{21}NO$)Pd($N_2C_6H_{16}$)].

C(1)-Pd-N(1)-C(28)	-169(3)
C(4)-Pd-N(1)-C(28)	72.1(3)
N(2)-Pd-N(1)-C(28)	-114.6(3)
C(1)-Pd-N(1)-C(25)	-50(3)
C(4)-Pd-N(1)-C(25)	-168.5(3)
N(2)-Pd-N(1)-C(25)	4.9(3)
C(1)-Pd-N(1)-C(27)	67(3)
C(4)-Pd-N(1)-C(27)	-51.7(3)
N(2)-Pd-N(1)-C(27)	121.7(3)
C(1)-Pd-N(2)-C(30)	-67.8(4)
C(4)-Pd-N(2)-C(30)	-154.1(11)
N(1)-Pd-N(2)-C(30)	114.2(4)
C(1)-Pd-N(2)-C(29)	55.5(5)
C(4)-Pd-N(2)-C(29)	-30.8(13)
N(1)-Pd-N(2)-C(29)	-122.5(5)
C(1)-Pd-N(2)-C(26')	148.1(5)
C(4)-Pd-N(2)-C(26')	61.8(13)
N(1)-Pd-N(2)-C(26')	-30.0(5)
C(1)-Pd-N(2)-C(26)	-160.4(4)
C(4)-Pd-N(2)-C(26)	113.4(12)
N(1)-Pd-N(2)-C(26)	21.6(4)

C(4)-Pd-C(1)-C(5)	-129.8(3)
N(2)-Pd-C(1)-C(5)	56.9(3)
N(1)-Pd-C(1)-C(5)	111(3)
C(4)-Pd-C(1)-C(2)	-0.8(2)
N(2)-Pd-C(1)-C(2)	-174.2(2)
N(1)-Pd-C(1)-C(2)	-120(3)
C(4)-N(3)-C(2)-O	170.5(3)
C(11)-N(3)-C(2)-O	-1.2(5)
C(4)-N(3)-C(2)-C(1)	-12.4(5)
C(11)-N(3)-C(2)-C(1)	175.9(3)
C(5)-C(1)-C(2)-O	-44.9(5)
Pd-C(1)-C(2)-O	-175.8(3)
C(5)-C(1)-C(2)-N(3)	138.0(3)
Pd-C(1)-C(2)-N(3)	7.1(4)
C(2)-N(3)-C(4)-C(18)	-115.6(4)
C(11)-N(3)-C(4)-C(18)	56.2(4)
C(2)-N(3)-C(4)-Pd	11.5(4)
C(11)-N(3)-C(4)-Pd	-176.6(2)
C(1)-Pd-C(4)-N(3)	-5.1(2)
N(2)-Pd-C(4)-N(3)	82.0(11)
N(1)-Pd-C(4)-N(3)	172.9(2)
C(1)-Pd-C(4)-C(18)	119.6(3)

N(2)-Pd-C(4)-C(18)	-153.3(10)
N(1)-Pd-C(4)-C(18)	-62.5(3)
C(2)-C(1)-C(5)-C(6)	-80.9(4)
Pd-C(1)-C(5)-C(6)	48.7(4)
C(2)-C(1)-C(5)-C(10)	100.2(4)
Pd-C(1)-C(5)-C(10)	-130.1(3)
C(10)-C(5)-C(6)-C(7)	-0.2(5)
C(1)-C(5)-C(6)-C(7)	-179.1(3)
C(5)-C(6)-C(7)-C(8)	-0.5(6)
C(6)-C(7)-C(8)-C(9)	2.0(6)
C(7)-C(8)-C(9)-C(10)	-2.8(6)
C(8)-C(9)-C(10)-C(5)	2.1(6)
C(6)-C(5)-C(10)-C(9)	-0.6(5)
C(1)-C(5)-C(10)-C(9)	178.3(3)
C(2)-N(3)-C(11)-C(12)	-135.8(3)
C(4)-N(3)-C(11)-C(12)	52.3(4)
N(3)-C(11)-C(12)-C(13)	55.4(5)
N(3)-C(11)-C(12)-C(17)	-125.1(4)
C(17)-C(12)-C(13)-C(14)	1.1(6)
C(11)-C(12)-C(13)-C(14)	-179.4(4)
C(12)-C(13)-C(14)-C(15)	-1.9(6)
C(13)-C(14)-C(15)-C(16)	1.7(7)

C(14)-C(15)-C(16)-C(17)	-0.7(7)
C(13)-C(12)-C(17)-C(16)	0.0(6)
C(11)-C(12)-C(17)-C(16)	-179.5(4)
C(15)-C(16)-C(17)-C(12)	-0.2(6)
N(3)-C(4)-C(18)-C(23)	-123.7(4)
Pd-C(4)-C(18)-C(23)	111.5(3)
N(3)-C(4)-C(18)-C(19)	54.7(4)
Pd-C(4)-C(18)-C(19)	-70.1(4)
C(23)-C(18)-C(19)-C(20)	-2.1(5)
C(4)-C(18)-C(19)-C(20)	179.4(3)
C(18)-C(19)-C(20)-C(21)	-1.8(6)
C(19)-C(20)-C(21)-C(22)	4.0(6)
C(19)-C(20)-C(21)-C(24)	-176.1(4)
C(20)-C(21)-C(22)-C(23)	-2.3(6)
C(24)-C(21)-C(22)-C(23)	177.8(4)
C(21)-C(22)-C(23)-C(18)	-1.6(6)
C(19)-C(18)-C(23)-C(22)	3.8(5)
C(4)-C(18)-C(23)-C(22)	-177.7(3)
C(28)-N(1)-C(25)-C(26)	86.4(6)
C(27)-N(1)-C(25)-C(26)	-155.5(6)
Pd-N(1)-C(25)-C(26)	-37.1(6)
N(1)-C(25)-C(26)-N(2)	59.0(7)

C(30)-N(2)-C(26)-C(25)	-165.9(5)
C(29)-N(2)-C(26)-C(25)	87.2(7)
C(26')-N(2)-C(26)-C(25)	46.4(5)
Pd-N(2)-C(26)-C(25)	-47.0(6)

Crystal Structure Report

for

cis-(±)-**4.41**

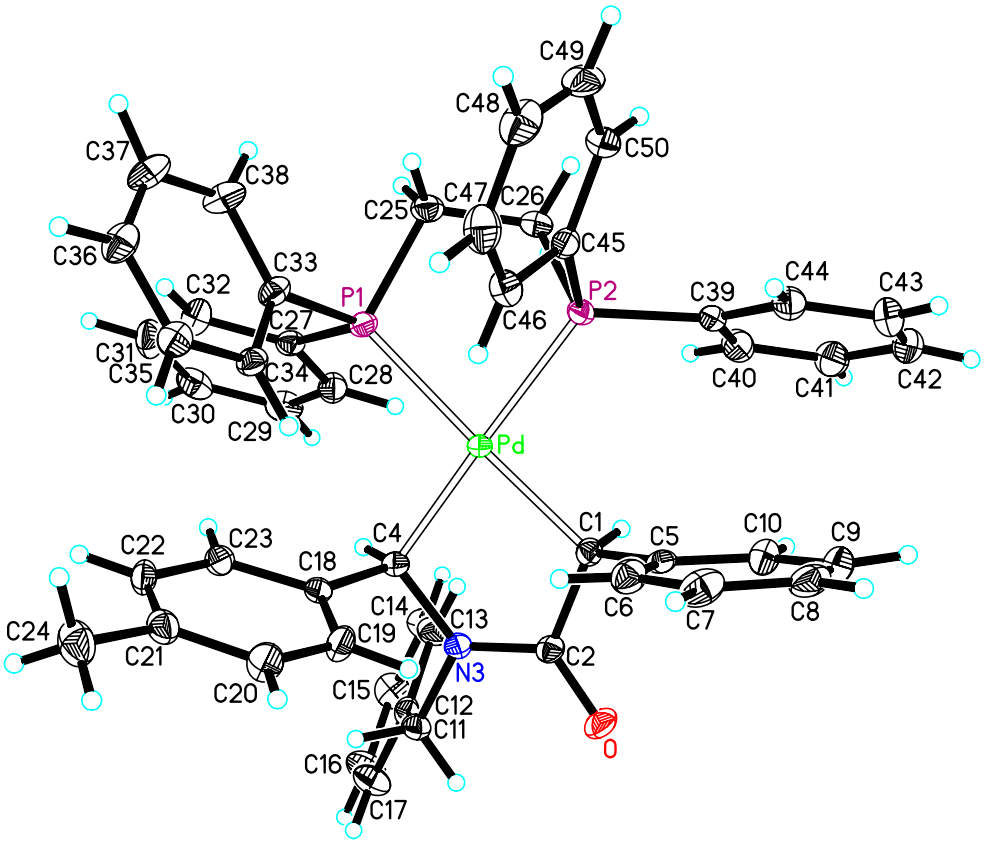
C49
C48
C50
C37
C38
C25
C47
C26
C45
C36
C33
C32
P1
P2
C39
C44
C43
C27
C46
C31
C35
C34
C28
C40
C41
C42
C30
C29
Pd
C4
C1
C22
C23
C18
C5
C10
C9
C6
C7
C8
C14
C13
C24
C19
C21
N3
C2
C20
C15
C12
C11
O
C16
C17

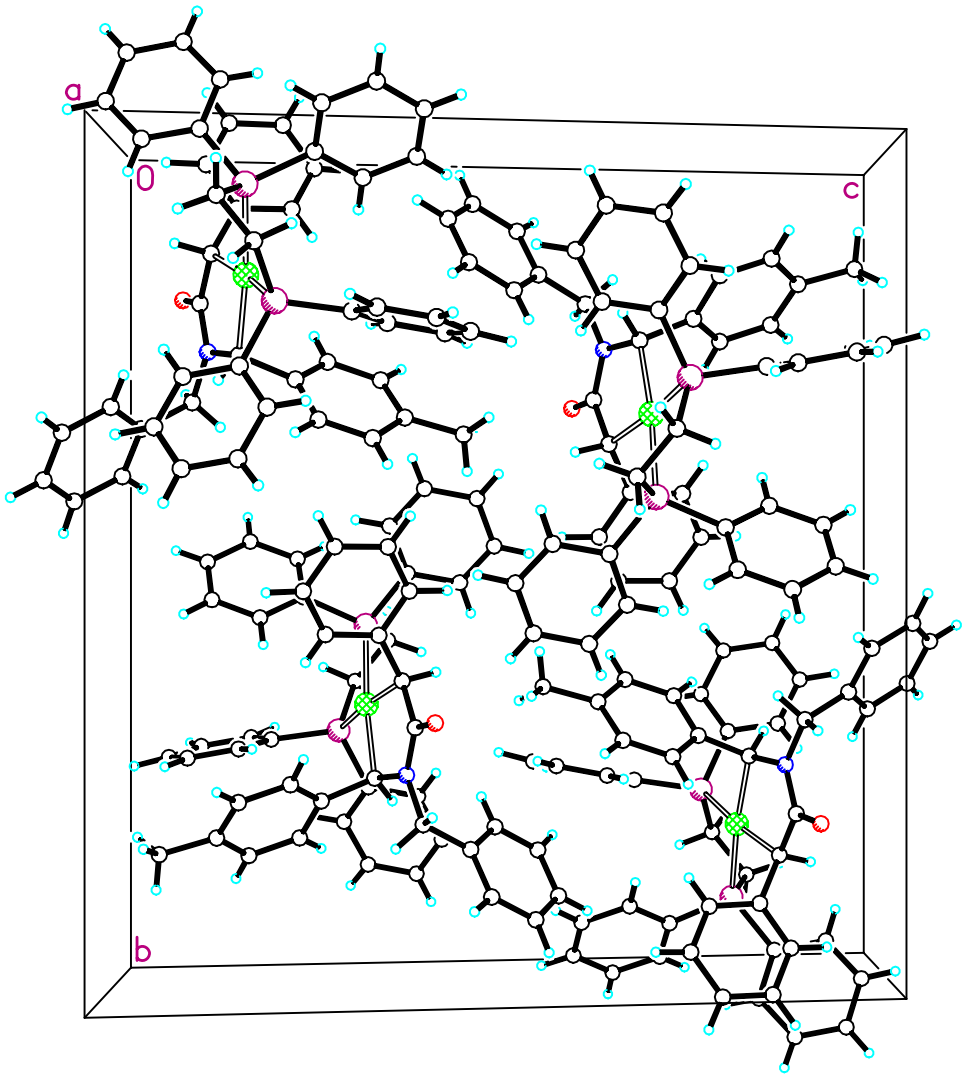
a
0
c
b

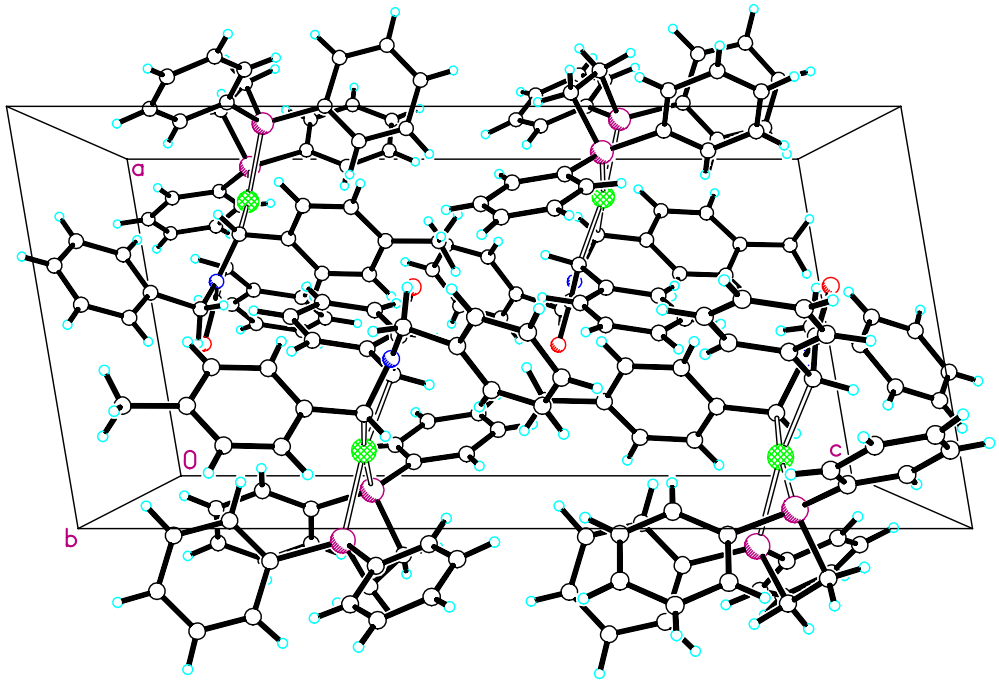
a
0
b
c

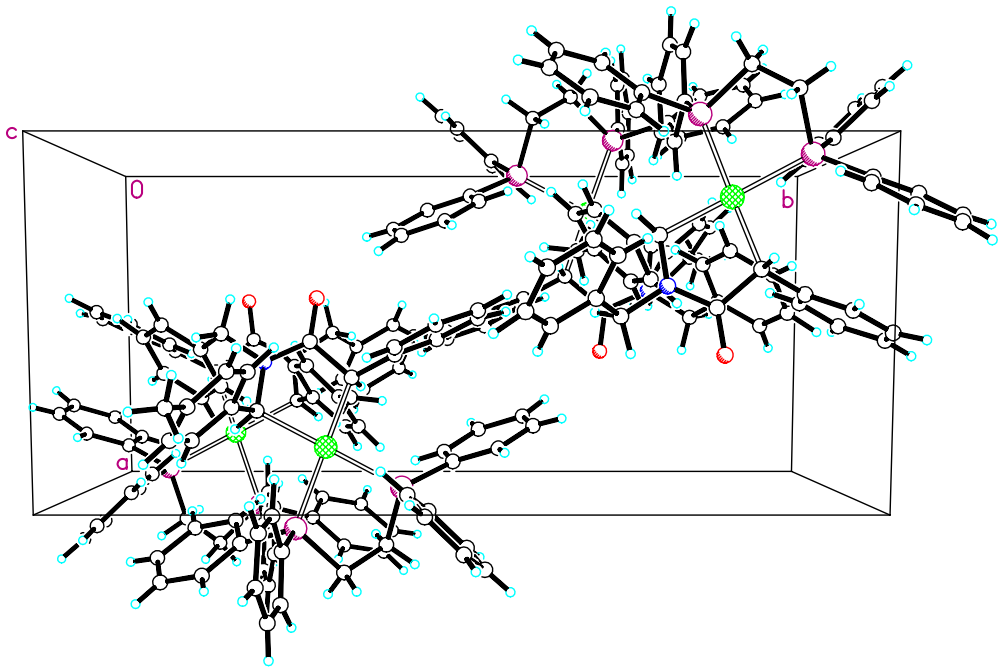
c
0
b
a

Comments

The asymmetric unit contains one [cis-$C_{23}H_{21}NO$]Pd[$(C_6H_5)_2PCH_2CH_2P(C_6H_5)_2$] molecule. All displacement ellipsoids are drawn at the 50% probability level.

Experimental Description

Pale yellow crystals of [cis-$C_{23}H_{21}NO$]Pd[$(C_6H_5)_2PCH_2CH_2P(C_6H_5)_2$] are, at 100(2) K, monoclinic, space group $P2_1/c - C_{2h}^5$ (No. 14) (1) with **a** = 9.4625(4) Å, **b** = 21.0456(9) Å, **c** = 19.7459(8) Å, β = 99.638(1)°, V = 3876.8(3) Å^3 and Z = 4 molecules {d_{calcd} = 1.426 g/cm^3; μ_a(MoKα) = 0.601 mm^{-1}}. A full hemisphere of diffracted intensities (1850 10-second frames with a ω scan width of 0.30°) was measured for a single-domain specimen using graphite-monochromated MoKα radiation (λ= 0.71073 Å) on a Bruker SMART APEX CCD Single Crystal Diffraction System (2). X-rays were provided by a fine-focus sealed x-ray tube operated at 50kV and 30mA. Lattice constants were determined with the Bruker SAINT software package using peak centers for 6831 reflections. A total of 48863 integrated reflection intensities having 2θ((MoKα)< 61.06° were produced using the Bruker program SAINT(3); 11852 of these were unique and gave R_{int} = 0.053 with a coverage which was 99.8% complete. The data were corrected empirically (4) for variable absorption effects using equivalent reflections; the relative transmission factors ranged from 0.910 to 1.000. The Bruker software package SHELXTL was used to solve the structure using "direct methods" techniques. All stages of weighted full-matrix least-squares refinement were conducted using F_o^2 data with the SHELXTL Version 6.10 software package(5).

The final structural model incorporated anisotropic thermal parameters for all nonhydrogen atoms and isotropic thermal parameters for all hydrogen atoms. All

hydrogen atoms were located in a difference Fourier and included in the structural model as independent isotropic atoms whose parameters were allowed to vary in least-squares refinement cycles. A total of 667 parameters were refined using no restraints, 11852 data and weights of $w = 1/ [\sigma^2(F^2) + (0.0338\ P)^2 + 1.4061\ P]$, where $P = [F_o^2 + 2F_c^2] / 3$. Final agreement factors at convergence are: R_1(unweighted, based on F) = 0.038 for 9729 independent absorption-corrected "observed" reflections having $2\theta(MoK\alpha) < 61.06°$ and $I > 2\sigma(I)$; R_1(unweighted, based on F) = 0.052 and wR_2(weighted, based on F^2) = 0.082 for all 11852 independent absorption-corrected reflections having $2\theta(MoK\alpha) < 61.06°$. The largest shift/s.u. was 0.001 in the final refinement cycle. The final difference map had maxima and minima of 0.67 and -0.44 $e^-/Å^3$, respectively.

Acknowledgment

This X-Ray analysis was performed by Victor W. Day.

References

(1) International Tables for Crystallography, Vol A, 4th ed., Kluwer: Boston (1996).

(2) Data Collection: SMART Software Reference Manual (1998). Bruker-AXS, 5465 E. Cheryl Parkway, Madison, WI 53711-5373 USA.

(3) Data Reduction: SAINT Software Reference Manual (1998). Bruker-AXS, 6300 Enterprise Dr., Madison, WI 53719-1173, USA.

(4) G. M. Sheldrick (2002). SADABS. Program for Empirical Absorption Correction of Area Detector Data. University of Göttingen, Germany.

(5) G. M. Sheldrick (2000). SHELXTL Version 6.10 Reference Manual. Bruker-AXS, 5465

E. Cheryl Parkway, Madison, WI 53711-5373 USA.

Table 1. Crystal data and structure refinement for [cis-$C_{23}H_{21}NO$]Pd[$(C_6H_5)_2PCH_2CH_2P(C_6H_5)_2$].

Empirical formula	$C_{49}H_{45}NOP_2Pd$	
Formula weight	832.20	
Temperature	100(2) K	
Wavelength	0.71073 Å	
Crystal system	Monoclinic	
Space group	$P2_1/c - C_{2h}^5$ (No. 14)	
Unit cell dimensions	**a** = 9.4625(4) Å	α = 90.000°
	b = 21.0456(9) Å	β = 99.638(1)°.
	c = 19.7459(8) Å	γ = 90.000°
Volume	3876.8(3) $Å^3$	
Z	4	
Density (calculated)	1.426 Mg/m^3	
Absorption coefficient	0.601 mm^{-1}	
F(000)	1720	
Crystal size	0.16 x 0.12 x 0.08 mm^3	
Theta range for data collection	2.39° to 30.53°	
Index ranges	$-13 \le h \le 13$, $-30 \le k \le 30$, $-28 \le l \le 28$	
Reflections collected	48863	

Independent reflections	11852 [R_{int} = 0.053]
Completeness to theta = 30.53°	99.8 %
Absorption correction	Semi-empirical from equivalents
Max. and min. transmission	1.000 and 0.910
Refinement method	Full-matrix least-squares on F^2
Data / restraints / parameters	11852 / 0 / 667
Goodness-of-fit on F^2	1.033
Final R indices [I>2sigma(I)]	R_1 = 0.038, wR_2 = 0.078
R indices (all data)	R_1 = 0.052, wR_2 = 0.082
Largest diff. peak and hole	0.67 and -0.44 $e^-/Å^3$

$R_1 = \Sigma \, ||F_o| - |F_c|| \, / \, \Sigma \, |F_o|$

$wR_2 = \{ \, \Sigma \, [w(F_o^2 - F_c^2)^2] \, / \, \Sigma \, [w(F_o^2)^2] \, \}^{1/2}$

Table 2. Atomic coordinates (x 10^4) and equivalent isotropic displacement parameters ($Å^2$ x 10^3) for [cis-$C_{23}H_{21}NO$]Pd[$(C_6H_5)_2PCH_2CH_2P(C_6H_5)_2$]. U(eq) is defined as one third of the trace of the orthogonalized U_{ij} tensor.

	x	y	z	U(eq)
Pd	1501(1)	6732(1)	3161(1)	12(1)
P(1)	-801(1)	7100(1)	2737(1)	15(1)
P(2)	335(1)	5763(1)	3128(1)	14(1)
O	5795(2)	6876(1)	4118(1)	24(1)
C(1)	3484(2)	6414(1)	3666(1)	15(1)
C(2)	4527(2)	6957(1)	3849(1)	15(1)
N(3)	3939(2)	7539(1)	3726(1)	16(1)
C(4)	2542(2)	7613(1)	3289(1)	14(1)
C(5)	4158(2)	5854(1)	3375(1)	16(1)
C(6)	4383(2)	5841(1)	2695(1)	21(1)
C(7)	5024(2)	5323(1)	2431(1)	27(1)
C(8)	5424(2)	4796(1)	2839(1)	28(1)
C(9)	5204(2)	4798(1)	3511(1)	30(1)
C(10)	4595(2)	5323(1)	3775(1)	24(1)
C(11)	4756(2)	8107(1)	3954(1)	18(1)
C(12)	4287(2)	8431(1)	4562(1)	18(1)
C(13)	3176(2)	8201(1)	4877(1)	22(1)

C(14)	2802(3)	8506(1)	5444(1)	26(1)
C(15)	3530(3)	9040(1)	5712(1)	27(1)
C(16)	4640(3)	9273(1)	5409(1)	31(1)
C(17)	5010(3)	8974(1)	4837(1)	25(1)
C(18)	2689(2)	7877(1)	2598(1)	15(1)
C(19)	3701(2)	7645(1)	2227(1)	20(1)
C(20)	3739(2)	7851(1)	1564(1)	24(1)
C(21)	2785(2)	8305(1)	1246(1)	21(1)
C(22)	1823(2)	8562(1)	1627(1)	21(1)
C(23)	1769(2)	8356(1)	2289(1)	18(1)
C(24)	2803(3)	8495(1)	513(1)	30(1)
C(25)	-2116(2)	6500(1)	2933(1)	20(1)
C(26)	-1385(2)	5971(1)	3397(1)	17(1)
C(27)	-1309(2)	7836(1)	3131(1)	16(1)
C(28)	-737(2)	7942(1)	3816(1)	20(1)
C(29)	-1009(2)	8503(1)	4139(1)	25(1)
C(30)	-1848(2)	8968(1)	3782(1)	25(1)
C(31)	-2443(3)	8866(1)	3104(1)	27(1)
C(32)	-2179(2)	8302(1)	2778(1)	23(1)
C(33)	-1304(2)	7219(1)	1813(1)	18(1)
C(34)	-245(2)	7310(1)	1413(1)	17(1)
C(35)	-608(2)	7427(1)	716(1)	21(1)

C(36)	-2034(2)	7451(1)	401(1)	23(1)
C(37)	-3091(2)	7339(1)	792(1)	26(1)
C(38)	-2744(2)	7223(1)	1489(1)	24(1)
C(39)	1025(2)	5115(1)	3697(1)	16(1)
C(40)	1252(2)	5231(1)	4403(1)	23(1)
C(41)	1880(2)	4778(1)	4863(1)	26(1)
C(42)	2292(2)	4197(1)	4634(1)	26(1)
C(43)	2057(3)	4074(1)	3937(1)	27(1)
C(44)	1433(2)	4530(1)	3468(1)	22(1)
C(45)	-227(2)	5415(1)	2281(1)	16(1)
C(46)	302(2)	5667(1)	1717(1)	21(1)
C(47)	-212(3)	5445(1)	1060(1)	27(1)
C(48)	-1239(3)	4974(1)	957(1)	29(1)
C(49)	-1758(2)	4715(1)	1513(1)	26(1)
C(50)	-1259(2)	4936(1)	2169(1)	20(1)

Table 3. Bond lengths [Å] for [cis-$C_{23}H_{21}NO$]Pd[$(C_6H_5)_2PCH_2CH_2P(C_6H_5)_2$].

Pd-C(1)	2.082(2)
Pd-C(4)	2.096(2)
Pd-P(1)	2.331(1)
Pd-P(2)	2.313(1)
P(1)-C(33)	1.825(2)
P(1)-C(27)	1.834(2)
P(1)-C(25)	1.859(2)
P(2)-C(39)	1.818(2)
P(2)-C(45)	1.823(2)
P(2)-C(26)	1.847(2)
O-C(2)	1.240(2)
C(1)-C(5)	1.499(3)
C(1)-C(2)	1.513(3)
C(1)-H(1)	0.96(2)
C(2)-N(3)	1.351(2)
N(3)-C(11)	1.454(2)
N(3)-C(4)	1.461(2)
C(4)-C(18)	1.502(3)
C(4)-H(4)	0.97(2)
C(5)-C(10)	1.392(3)
C(5)-C(6)	1.395(3)

C(6)-C(7)	1.391(3)
C(6)-H(6)	0.89(2)
C(7)-C(8)	1.386(3)
C(7)-H(7)	0.95(3)
C(8)-C(9)	1.376(4)
C(8)-H(8)	0.97(3)
C(9)-C(10)	1.388(3)
C(9)-H(9)	0.95(3)
C(10)-H(10)	0.99(3)
C(11)-C(12)	1.511(3)
C(11)-H(11A)	0.92(2)
C(11)-H(11B)	0.97(2)
C(12)-C(17)	1.393(3)
C(12)-C(13)	1.394(3)
C(13)-C(14)	1.388(3)
C(13)-H(13)	0.90(3)
C(14)-C(15)	1.376(3)
C(14)-H(14)	0.90(3)
C(15)-C(16)	1.383(3)
C(15)-H(15)	0.93(2)
C(16)-C(17)	1.389(3)
C(16)-H(16)	0.97(2)

C(17)-H(17)	0.88(3)
C(18)-C(19)	1.388(3)
C(18)-C(23)	1.402(3)
C(19)-C(20)	1.386(3)
C(19)-H(19)	0.96(3)
C(20)-C(21)	1.389(3)
C(20)-H(20)	0.89(3)
C(21)-C(22)	1.384(3)
C(21)-C(24)	1.505(3)
C(22)-C(23)	1.387(3)
C(22)-H(22)	0.92(2)
C(23)-H(23)	0.95(3)
C(24)-H(24A)	0.97(3)
C(24)-H(24B)	0.91(3)
C(24)-H(24C)	0.96(3)
C(25)-C(26)	1.531(3)
C(25)-H(25A)	0.94(2)
C(25)-H(25B)	1.00(2)
C(26)-H(26A)	0.94(2)
C(26)-H(26B)	0.95(2)
C(27)-C(28)	1.388(3)
C(27)-C(32)	1.390(3)

C(28)-C(29)	1.386(3)
C(28)-H(28)	0.95(2)
C(29)-C(30)	1.379(3)
C(29)-H(29)	0.97(3)
C(30)-C(31)	1.379(3)
C(30)-H(30)	0.90(3)
C(31)-C(32)	1.394(3)
C(31)-H(31)	0.91(3)
C(32)-H(32)	0.92(3)
C(33)-C(34)	1.389(3)
C(33)-C(38)	1.405(3)
C(34)-C(35)	1.384(3)
C(34)-H(34)	0.96(2)
C(35)-C(36)	1.388(3)
C(35)-H(35)	0.98(3)
C(36)-C(37)	1.381(3)
C(36)-H(36)	0.97(3)
C(37)-C(38)	1.382(3)
C(37)-H(37)	0.96(3)
C(38)-H(38)	0.99(2)
C(39)-C(44)	1.388(3)
C(39)-C(40)	1.395(3)

C(40)-C(41)	1.382(3)
C(40)-H(40)	0.91(3)
C(41)-C(42)	1.383(3)
C(41)-H(41)	0.92(2)
C(42)-C(43)	1.381(3)
C(42)-H(42)	0.92(2)
C(43)-C(44)	1.395(3)
C(43)-H(43)	0.87(3)
C(44)-H(44)	0.90(3)
C(45)-C(50)	1.395(3)
C(45)-C(46)	1.400(3)
C(46)-C(47)	1.387(3)
C(46)-H(46)	0.92(2)
C(47)-C(48)	1.379(3)
C(47)-H(47)	0.92(2)
C(48)-C(49)	1.387(3)
C(48)-H(48)	0.94(2)
C(49)-C(50)	1.382(3)
C(49)-H(49)	0.87(3)
C(50)-H(50)	0.89(2)

Table 4. Bond angles [°] for [cis-$C_{23}H_{21}NO$]Pd[$(C_6H_5)_2PCH_2CH_2P(C_6H_5)_2$].

C(1)-Pd-C(4)	81.87(7)
C(1)-Pd-P(2)	96.78(5)
C(4)-Pd-P(2)	174.62(5)
C(1)-Pd-P(1)	172.59(6)
C(4)-Pd-P(1)	98.08(5)
P(2)-Pd-P(1)	82.58(2)
C(33)-P(1)-C(27)	105.41(9)
C(33)-P(1)-C(25)	103.29(10)
C(27)-P(1)-C(25)	104.69(9)
C(33)-P(1)-Pd	118.45(7)
C(27)-P(1)-Pd	115.10(7)
C(25)-P(1)-Pd	108.47(7)
C(39)-P(2)-C(45)	106.56(9)
C(39)-P(2)-C(26)	104.07(9)
C(45)-P(2)-C(26)	102.87(9)
C(39)-P(2)-Pd	121.59(6)
C(45)-P(2)-Pd	116.39(7)
C(26)-P(2)-Pd	102.84(7)
C(5)-C(1)-C(2)	112.50(16)
C(5)-C(1)-Pd	118.45(13)
C(2)-C(1)-Pd	111.83(13)

C(5)-C(1)-H(1)	111.4(15)
C(2)-C(1)-H(1)	102.5(15)
Pd-C(1)-H(1)	98.0(15)
O-C(2)-N(3)	122.69(18)
O-C(2)-C(1)	123.05(18)
N(3)-C(2)-C(1)	114.18(16)
C(2)-N(3)-C(11)	120.64(16)
C(2)-N(3)-C(4)	120.48(16)
C(11)-N(3)-C(4)	118.45(16)
N(3)-C(4)-C(18)	111.31(15)
N(3)-C(4)-Pd	109.72(12)
C(18)-C(4)-Pd	109.40(12)
N(3)-C(4)-H(4)	107.7(13)
C(18)-C(4)-H(4)	108.3(13)
Pd-C(4)-H(4)	110.4(13)
C(10)-C(5)-C(6)	116.80(19)
C(10)-C(5)-C(1)	121.31(19)
C(6)-C(5)-C(1)	121.89(18)
C(7)-C(6)-C(5)	121.6(2)
C(7)-C(6)-H(6)	120.9(15)
C(5)-C(6)-H(6)	117.5(15)
C(8)-C(7)-C(6)	120.2(2)

C(8)-C(7)-H(7)	121.0(15)
C(6)-C(7)-H(7)	118.8(15)
C(9)-C(8)-C(7)	119.2(2)
C(9)-C(8)-H(8)	121.8(16)
C(7)-C(8)-H(8)	119.0(16)
C(8)-C(9)-C(10)	120.3(2)
C(8)-C(9)-H(9)	121.8(16)
C(10)-C(9)-H(9)	117.8(16)
C(9)-C(10)-C(5)	121.9(2)
C(9)-C(10)-H(10)	119.6(15)
C(5)-C(10)-H(10)	118.5(15)
N(3)-C(11)-C(12)	113.93(17)
N(3)-C(11)-H(11A)	109.0(14)
C(12)-C(11)-H(11A)	107.2(14)
N(3)-C(11)-H(11B)	108.9(14)
C(12)-C(11)-H(11B)	108.2(14)
H(11A)-C(11)-H(11B)	109.5(19)
C(17)-C(12)-C(13)	118.0(2)
C(17)-C(12)-C(11)	119.26(19)
C(13)-C(12)-C(11)	122.77(18)
C(14)-C(13)-C(12)	120.8(2)
C(14)-C(13)-H(13)	122.5(17)

C(12)-C(13)-H(13)	116.7(16)
C(15)-C(14)-C(13)	120.6(2)
C(15)-C(14)-H(14)	120.0(18)
C(13)-C(14)-H(14)	119.4(18)
C(14)-C(15)-C(16)	119.4(2)
C(14)-C(15)-H(15)	120.3(15)
C(16)-C(15)-H(15)	120.4(15)
C(15)-C(16)-C(17)	120.3(2)
C(15)-C(16)-H(16)	123.5(14)
C(17)-C(16)-H(16)	116.2(15)
C(16)-C(17)-C(12)	120.9(2)
C(16)-C(17)-H(17)	123.3(18)
C(12)-C(17)-H(17)	115.8(18)
C(19)-C(18)-C(23)	117.18(18)
C(19)-C(18)-C(4)	121.71(17)
C(23)-C(18)-C(4)	121.06(18)
C(20)-C(19)-C(18)	121.12(19)
C(20)-C(19)-H(19)	117.6(15)
C(18)-C(19)-H(19)	121.3(15)
C(19)-C(20)-C(21)	121.7(2)
C(19)-C(20)-H(20)	122.7(18)
C(21)-C(20)-H(20)	115.6(18)

C(22)-C(21)-C(20)	117.32(19)
C(22)-C(21)-C(24)	122.2(2)
C(20)-C(21)-C(24)	120.4(2)
C(21)-C(22)-C(23)	121.44(19)
C(21)-C(22)-H(22)	119.6(15)
C(23)-C(22)-H(22)	118.9(15)
C(22)-C(23)-C(18)	121.10(19)
C(22)-C(23)-H(23)	122.8(16)
C(18)-C(23)-H(23)	116.0(16)
C(21)-C(24)-H(24A)	112.9(16)
C(21)-C(24)-H(24B)	109.9(17)
H(24A)-C(24)-H(24B)	106(2)
C(21)-C(24)-H(24C)	113.7(17)
H(24A)-C(24)-H(24C)	108(2)
H(24B)-C(24)-H(24C)	106(2)
C(26)-C(25)-P(1)	111.54(14)
C(26)-C(25)-H(25A)	111.0(15)
P(1)-C(25)-H(25A)	107.2(14)
C(26)-C(25)-H(25B)	110.8(14)
P(1)-C(25)-H(25B)	106.1(14)
H(25A)-C(25)-H(25B)	110(2)
C(25)-C(26)-P(2)	109.42(14)

C(25)-C(26)-H(26A)	111.7(14)
P(2)-C(26)-H(26A)	109.1(14)
C(25)-C(26)-H(26B)	110.1(14)
P(2)-C(26)-H(26B)	105.6(14)
H(26A)-C(26)-H(26B)	110.7(19)
C(28)-C(27)-C(32)	118.50(19)
C(28)-C(27)-P(1)	117.53(15)
C(32)-C(27)-P(1)	123.92(16)
C(29)-C(28)-C(27)	120.9(2)
C(29)-C(28)-H(28)	119.0(14)
C(27)-C(28)-H(28)	120.1(14)
C(30)-C(29)-C(28)	120.3(2)
C(30)-C(29)-H(29)	119.2(17)
C(28)-C(29)-H(29)	120.4(17)
C(29)-C(30)-C(31)	119.5(2)
C(29)-C(30)-H(30)	121.2(17)
C(31)-C(30)-H(30)	119.3(16)
C(30)-C(31)-C(32)	120.4(2)
C(30)-C(31)-H(31)	122.3(17)
C(32)-C(31)-H(31)	117.2(17)
C(27)-C(32)-C(31)	120.4(2)
C(27)-C(32)-H(32)	118.7(16)

C(31)-C(32)-H(32)	120.9(16)
C(34)-C(33)-C(38)	118.54(19)
C(34)-C(33)-P(1)	119.70(15)
C(38)-C(33)-P(1)	121.76(16)
C(35)-C(34)-C(33)	120.47(19)
C(35)-C(34)-H(34)	120.2(12)
C(33)-C(34)-H(34)	119.4(12)
C(34)-C(35)-C(36)	120.8(2)
C(34)-C(35)-H(35)	118.3(15)
C(36)-C(35)-H(35)	120.8(15)
C(37)-C(36)-C(35)	119.0(2)
C(37)-C(36)-H(36)	119.8(16)
C(35)-C(36)-H(36)	121.2(16)
C(36)-C(37)-C(38)	120.8(2)
C(36)-C(37)-H(37)	122.5(16)
C(38)-C(37)-H(37)	116.6(16)
C(37)-C(38)-C(33)	120.3(2)
C(37)-C(38)-H(38)	123.8(14)
C(33)-C(38)-H(38)	115.7(14)
C(44)-C(39)-C(40)	118.45(19)
C(44)-C(39)-P(2)	123.67(16)
C(40)-C(39)-P(2)	117.71(15)

C(41)-C(40)-C(39)	120.9(2)
C(41)-C(40)-H(40)	121.3(16)
C(39)-C(40)-H(40)	117.7(16)
C(40)-C(41)-C(42)	120.6(2)
C(40)-C(41)-H(41)	119.2(15)
C(42)-C(41)-H(41)	120.2(15)
C(43)-C(42)-C(41)	119.0(2)
C(43)-C(42)-H(42)	117.9(14)
C(41)-C(42)-H(42)	122.9(14)
C(42)-C(43)-C(44)	120.9(2)
C(42)-C(43)-H(43)	120.5(17)
C(44)-C(43)-H(43)	118.6(17)
C(39)-C(44)-C(43)	120.2(2)
C(39)-C(44)-H(44)	119.7(16)
C(43)-C(44)-H(44)	119.9(16)
C(50)-C(45)-C(46)	118.75(19)
C(50)-C(45)-P(2)	121.71(16)
C(46)-C(45)-P(2)	119.35(15)
C(47)-C(46)-C(45)	120.0(2)
C(47)-C(46)-H(46)	120.5(14)
C(45)-C(46)-H(46)	119.4(14)
C(48)-C(47)-C(46)	120.5(2)

C(48)-C(47)-H(47)	121.8(15)
C(46)-C(47)-H(47)	117.7(15)
C(47)-C(48)-C(49)	120.0(2)
C(47)-C(48)-H(48)	121.4(15)
C(49)-C(48)-H(48)	118.6(15)
C(50)-C(49)-C(48)	119.9(2)
C(50)-C(49)-H(49)	119.1(17)
C(48)-C(49)-H(49)	120.9(17)
C(49)-C(50)-C(45)	120.8(2)
C(49)-C(50)-H(50)	120.3(15)
C(45)-C(50)-H(50)	118.9(15)

Table 5. Anisotropic displacement parameters ($Å^2 x\ 10^3$) for [cis-$C_{23}H_{21}NO$]Pd[$(C_6H_5)_2PCH_2CH_2P$- $(C_6H_5)_2$]. The anisotropic displacement factor exponent takes the form: $-2\pi^2[\ h^2\ a^{*2}U_{11} + ...\ + 2\ h\ k\ a^*\ b^*\ U_{12}\ ]$

	U_{11}	U_{22}	U_{33}	U_{23}	U_{13}	U_{12}
Pd	11(1)	12(1)	13(1)	0(1)	1(1)	-1(1)
P(1)	12(1)	15(1)	17(1)	-1(1)	1(1)	0(1)
P(2)	14(1)	13(1)	15(1)	0(1)	2(1)	-2(1)
O	16(1)	22(1)	30(1)	-2(1)	-8(1)	1(1)
C(1)	15(1)	14(1)	14(1)	1(1)	0(1)	0(1)

C(2)	15(1)	18(1)	12(1)	-1(1)	-1(1)	-1(1)
N(3)	14(1)	15(1)	16(1)	1(1)	-2(1)	-2(1)
C(4)	13(1)	14(1)	16(1)	0(1)	1(1)	-1(1)
C(5)	10(1)	16(1)	23(1)	-2(1)	0(1)	-1(1)
C(6)	20(1)	22(1)	22(1)	-3(1)	1(1)	1(1)
C(7)	21(1)	33(1)	26(1)	-11(1)	0(1)	2(1)
C(8)	15(1)	22(1)	45(2)	-12(1)	2(1)	2(1)
C(9)	21(1)	19(1)	48(2)	4(1)	4(1)	4(1)
C(10)	21(1)	22(1)	29(1)	4(1)	3(1)	4(1)
C(11)	16(1)	17(1)	19(1)	1(1)	0(1)	-4(1)
C(12)	18(1)	15(1)	18(1)	2(1)	-2(1)	1(1)
C(13)	24(1)	22(1)	20(1)	-1(1)	-2(1)	-8(1)
C(14)	26(1)	33(1)	18(1)	1(1)	4(1)	-7(1)
C(15)	34(1)	29(1)	19(1)	-5(1)	5(1)	-2(1)
C(16)	38(1)	23(1)	32(1)	-9(1)	9(1)	-11(1)
C(17)	28(1)	21(1)	28(1)	-5(1)	9(1)	-8(1)
C(18)	14(1)	12(1)	16(1)	-1(1)	0(1)	-3(1)
C(19)	18(1)	23(1)	20(1)	5(1)	3(1)	6(1)
C(20)	23(1)	30(1)	21(1)	4(1)	8(1)	4(1)
C(21)	24(1)	19(1)	18(1)	2(1)	0(1)	-4(1)
C(22)	23(1)	14(1)	24(1)	4(1)	-5(1)	1(1)
C(23)	18(1)	13(1)	23(1)	-1(1)	1(1)	0(1)

C(24)	39(2)	29(1)	20(1)	5(1)	1(1)	-3(1)
C(25)	14(1)	19(1)	26(1)	-2(1)	4(1)	-1(1)
C(26)	16(1)	19(1)	18(1)	-2(1)	4(1)	-4(1)
C(27)	13(1)	18(1)	18(1)	0(1)	4(1)	-1(1)
C(28)	20(1)	20(1)	21(1)	2(1)	4(1)	1(1)
C(29)	25(1)	27(1)	22(1)	-6(1)	6(1)	-4(1)
C(30)	26(1)	17(1)	35(1)	-5(1)	15(1)	-2(1)
C(31)	28(1)	22(1)	33(1)	7(1)	10(1)	9(1)
C(32)	24(1)	25(1)	20(1)	2(1)	2(1)	6(1)
C(33)	15(1)	19(1)	17(1)	-3(1)	-2(1)	2(1)
C(34)	15(1)	16(1)	19(1)	-2(1)	-1(1)	0(1)
C(35)	21(1)	20(1)	20(1)	-2(1)	2(1)	1(1)
C(36)	25(1)	25(1)	16(1)	-5(1)	-2(1)	5(1)
C(37)	19(1)	36(1)	20(1)	-7(1)	-5(1)	4(1)
C(38)	15(1)	37(1)	21(1)	-4(1)	1(1)	0(1)
C(39)	14(1)	15(1)	19(1)	3(1)	0(1)	-3(1)
C(40)	25(1)	21(1)	22(1)	1(1)	2(1)	-3(1)
C(41)	28(1)	28(1)	19(1)	5(1)	0(1)	-3(1)
C(42)	24(1)	26(1)	26(1)	9(1)	-3(1)	-1(1)
C(43)	29(1)	18(1)	34(1)	2(1)	3(1)	3(1)
C(44)	23(1)	20(1)	22(1)	-1(1)	0(1)	-1(1)
C(45)	16(1)	15(1)	17(1)	-1(1)	-1(1)	2(1)

C(46)	23(1)	18(1)	22(1)	1(1)	5(1)	1(1)
C(47)	37(1)	26(1)	19(1)	3(1)	5(1)	4(1)
C(48)	33(1)	31(1)	19(1)	-7(1)	-3(1)	7(1)
C(49)	22(1)	24(1)	28(1)	-9(1)	-5(1)	-4(1)
C(50)	19(1)	18(1)	22(1)	-2(1)	1(1)	-3(1)

Table 6. Hydrogen coordinates (x 10^4) and isotropic displacement parameters ($Å^2$ x 10^3) for [cis-$C_{23}H_{21}NO$]Pd[$(C_6H_5)_2PCH_2CH_2P(C_6H_5)_2$].

	x	y	z	U(eq)
H(1)	3210(30)	6313(12)	4100(13)	29(7)
H(4)	1990(20)	7910(11)	3512(11)	15(5)
H(6)	4100(20)	6177(11)	2433(12)	17(6)
H(7)	5180(30)	5339(12)	1969(13)	29(7)
H(8)	5860(30)	4436(13)	2644(14)	38(7)
H(9)	5400(30)	4435(13)	3797(13)	35(7)
H(10)	4440(30)	5319(12)	4261(13)	30(7)
H(11A)	4650(20)	8398(10)	3600(11)	12(5)
H(11B)	5760(30)	7994(11)	4079(12)	21(6)
H(13)	2730(30)	7847(13)	4696(13)	31(7)
H(14)	2080(30)	8348(13)	5641(14)	39(8)
H(15)	3280(30)	9240(12)	6095(13)	24(6)
H(16)	5210(30)	9640(12)	5577(12)	27(7)

H(17)	5690(30)	9113(13)	4620(14)	36(7)
H(19)	4380(30)	7328(12)	2415(13)	28(7)
H(20)	4370(30)	7708(13)	1316(14)	38(8)
H(22)	1180(30)	8867(11)	1433(12)	23(6)
H(23)	1100(30)	8513(12)	2552(13)	30(7)
H(24A)	2020(30)	8311(12)	194(14)	32(7)
H(24B)	2700(30)	8925(14)	467(13)	35(7)
H(24C)	3680(30)	8395(13)	357(14)	37(8)
H(25A)	-2800(30)	6717(11)	3147(12)	22(6)
H(25B)	-2580(20)	6325(11)	2483(12)	23(6)
H(26A)	-1960(20)	5605(11)	3378(11)	17(6)
H(26B)	-1140(30)	6119(11)	3855(13)	24(6)
H(28)	-130(30)	7632(11)	4068(12)	24(6)
H(29)	-570(30)	8581(13)	4611(15)	40(8)
H(30)	-2010(30)	9340(12)	3981(13)	29(7)
H(31)	-3020(30)	9158(13)	2851(14)	38(8)
H(32)	-2540(30)	8237(12)	2322(14)	31(7)
H(34)	750(20)	7290(9)	1625(10)	6(5)
H(35)	160(30)	7511(12)	454(13)	32(7)
H(36)	-2300(30)	7565(13)	-80(14)	39(8)
H(37)	-4090(30)	7316(13)	596(14)	38(8)
H(38)	-3460(30)	7110(11)	1786(12)	24(6)

H(40)	970(30)	5613(12)	4548(13)	29(7)
H(41)	2040(20)	4871(11)	5328(12)	20(6)
H(42)	2780(20)	3899(10)	4921(11)	15(6)
H(43)	2280(30)	3708(12)	3783(13)	27(7)
H(44)	1350(30)	4456(12)	3016(13)	28(7)
H(46)	950(20)	5995(11)	1783(11)	18(6)
H(47)	160(30)	5621(11)	702(13)	24(6)
H(48)	-1620(30)	4832(12)	515(13)	26(6)
H(49)	-2380(30)	4403(13)	1457(13)	31(7)
H(50)	-1590(20)	4775(11)	2525(12)	17(6)

Table 7. Torsion angles [°] for [cis-$C_{23}H_{21}NO$]Pd[$(C_6H_5)_2PCH_2CH_2P(C_6H_5)_2$].

C(1)-Pd-P(1)-C(33)	177.2(4)
C(4)-Pd-P(1)-C(33)	88.1(1)
P(2)-Pd-P(1)-C(33)	-97.3(1)
C(1)-Pd-P(1)-C(27)	51.2(4)
C(4)-Pd-P(1)-C(27)	-37.9(1)
P(2)-Pd-P(1)-C(27)	136.7(1)
C(1)-Pd-P(1)-C(25)	-65.7(4)
C(4)-Pd-P(1)-C(25)	-154.8(1)
P(2)-Pd-P(1)-C(25)	19.9(1)
C(1)-Pd-P(2)-C(39)	18.9(1)

C(4)-Pd-P(2)-C(39)	-56.2(6)
P(1)-Pd-P(2)-C(39)	-153.6(1)
C(1)-Pd-P(2)-C(45)	-113.8(1)
C(4)-Pd-P(2)-C(45)	171.1(6)
P(1)-Pd-P(2)-C(45)	73.6(1)
C(1)-Pd-P(2)-C(26)	134.6(1)
C(4)-Pd-P(2)-C(26)	59.5(6)
P(1)-Pd-P(2)-C(26)	-37.97(7)
C(4)-Pd-C(1)-C(5)	-132.5(2)
P(2)-Pd-C(1)-C(5)	52.8(2)
P(1)-Pd-C(1)-C(5)	137.4(3)
C(4)-Pd-C(1)-C(2)	0.8(1)
P(2)-Pd-C(1)-C(2)	-173.9(1)
P(1)-Pd-C(1)-C(2)	-89.3(4)
C(5)-C(1)-C(2)-O	-39.8(3)
Pd-C(1)-C(2)-O	-175.9(2)
C(5)-C(1)-C(2)-N(3)	143.3(2)
Pd-C(1)-C(2)-N(3)	7.2(2)
O-C(2)-N(3)-C(11)	-4.6(3)
C(1)-C(2)-N(3)-C(11)	172.3(2)
O-C(2)-N(3)-C(4)	167.7(2)
C(1)-C(2)-N(3)-C(4)	-15.3(3)

C(2)-N(3)-C(4)-C(18)	-105.7(2)
C(11)-N(3)-C(4)-C(18)	66.8(2)
C(2)-N(3)-C(4)-Pd	15.5(2)
C(11)-N(3)-C(4)-Pd	-172.0(1)
C(1)-Pd-C(4)-N(3)	-7.9(1)
P(2)-Pd-C(4)-N(3)	67.9(6)
P(1)-Pd-C(4)-N(3)	164.6(1)
C(1)-Pd-C(4)-C(18)	114.5(1)
P(2)-Pd-C(4)-C(18)	-169.7(5)
P(1)-Pd-C(4)-C(18)	-73.0(1)
C(2)-C(1)-C(5)-C(10)	101.1(2)
Pd-C(1)-C(5)-C(10)	-125.9(2)
C(2)-C(1)-C(5)-C(6)	-78.7(2)
Pd-C(1)-C(5)-C(6)	54.4(2)
C(10)-C(5)-C(6)-C(7)	-0.5(3)
C(1)-C(5)-C(6)-C(7)	179.3(2)
C(5)-C(6)-C(7)-C(8)	1.7(3)
C(6)-C(7)-C(8)-C(9)	-1.3(3)
C(7)-C(8)-C(9)-C(10)	-0.3(3)
C(8)-C(9)-C(10)-C(5)	1.5(4)
C(6)-C(5)-C(10)-C(9)	-1.1(3)
C(1)-C(5)-C(10)-C(9)	179.2(2)

C(2)-N(3)-C(11)-C(12)	-106.7(2)
C(4)-N(3)-C(11)-C(12)	80.8(2)
N(3)-C(11)-C(12)-C(17)	178.6(2)
N(3)-C(11)-C(12)-C(13)	0.3(3)
C(17)-C(12)-C(13)-C(14)	0.2(3)
C(11)-C(12)-C(13)-C(14)	178.6(2)
C(12)-C(13)-C(14)-C(15)	-0.5(4)
C(13)-C(14)-C(15)-C(16)	0.2(4)
C(14)-C(15)-C(16)-C(17)	0.4(4)
C(15)-C(16)-C(17)-C(12)	-0.8(4)
C(13)-C(12)-C(17)-C(16)	0.4(3)
C(11)-C(12)-C(17)-C(16)	-178.0(2)
N(3)-C(4)-C(18)-C(19)	45.7(2)
Pd-C(4)-C(18)-C(19)	-75.7(2)
N(3)-C(4)-C(18)-C(23)	-136.7(2)
Pd-C(4)-C(18)-C(23)	101.9(2)
C(23)-C(18)-C(19)-C(20)	-3.8(3)
C(4)-C(18)-C(19)-C(20)	173.9(2)
C(18)-C(19)-C(20)-C(21)	1.0(3)
C(19)-C(20)-C(21)-C(22)	2.3(3)
C(19)-C(20)-C(21)-C(24)	-176.9(2)
C(20)-C(21)-C(22)-C(23)	-2.8(3)

C(24)-C(21)-C(22)-C(23)	176.4(2)
C(21)-C(22)-C(23)-C(18)	0.0(3)
C(19)-C(18)-C(23)-C(22)	3.3(3)
C(4)-C(18)-C(23)-C(22)	-174.4(2)
C(33)-P(1)-C(25)-C(26)	134.1(2)
C(27)-P(1)-C(25)-C(26)	-115.8(2)
Pd-P(1)-C(25)-C(26)	7.5(2)
P(1)-C(25)-C(26)-P(2)	-39.8(2)
C(39)-P(2)-C(26)-C(25)	-177.7(1)
C(45)-P(2)-C(26)-C(25)	-66.7(2)
Pd-P(2)-C(26)-C(25)	54.7(1)
C(33)-P(1)-C(27)-C(28)	-164.5(2)
C(25)-P(1)-C(27)-C(28)	86.9(2)
Pd-P(1)-C(27)-C(28)	-32.0(2)
C(33)-P(1)-C(27)-C(32)	12.8(2)
C(25)-P(1)-C(27)-C(32)	-95.8(2)
Pd-P(1)-C(27)-C(32)	145.3(2)
C(32)-C(27)-C(28)-C(29)	-0.9(3)
P(1)-C(27)-C(28)-C(29)	176.5(2)
C(27)-C(28)-C(29)-C(30)	-0.5(3)
C(28)-C(29)-C(30)-C(31)	1.5(3)
C(29)-C(30)-C(31)-C(32)	-1.1(3)

C(28)-C(27)-C(32)-C(31)	1.3(3)
P(1)-C(27)-C(32)-C(31)	-176.0(2)
C(30)-C(31)-C(32)-C(27)	-0.3(3)
C(27)-P(1)-C(33)-C(34)	108.0(2)
C(25)-P(1)-C(33)-C(34)	-142.4(2)
Pd-P(1)-C(33)-C(34)	-22.5(2)
C(27)-P(1)-C(33)-C(38)	-71.9(2)
C(25)-P(1)-C(33)-C(38)	37.7(2)
Pd-P(1)-C(33)-C(38)	157.6(2)
C(38)-C(33)-C(34)-C(35)	2.6(3)
P(1)-C(33)-C(34)-C(35)	-177.3(2)
C(33)-C(34)-C(35)-C(36)	-0.6(3)
C(34)-C(35)-C(36)-C(37)	-1.6(3)
C(35)-C(36)-C(37)-C(38)	1.9(3)
C(36)-C(37)-C(38)-C(33)	0.1(4)
C(34)-C(33)-C(38)-C(37)	-2.3(3)
P(1)-C(33)-C(38)-C(37)	177.5(2)
C(45)-P(2)-C(39)-C(44)	17.8(2)
C(26)-P(2)-C(39)-C(44)	126.1(2)
Pd-P(2)-C(39)-C(44)	-118.9(2)
C(45)-P(2)-C(39)-C(40)	-167.1(2)
C(26)-P(2)-C(39)-C(40)	-58.8(2)

Pd-P(2)-C(39)-C(40)	56.3(2)
C(44)-C(39)-C(40)-C(41)	0.6(3)
P(2)-C(39)-C(40)-C(41)	-174.8(2)
C(39)-C(40)-C(41)-C(42)	-0.4(3)
C(40)-C(41)-C(42)-C(43)	-0.3(3)
C(41)-C(42)-C(43)-C(44)	0.8(4)
C(40)-C(39)-C(44)-C(43)	-0.1(3)
P(2)-C(39)-C(44)-C(43)	175.0(2)
C(42)-C(43)-C(44)-C(39)	-0.6(3)
C(39)-P(2)-C(45)-C(50)	58.6(2)
C(26)-P(2)-C(45)-C(50)	-50.5(2)
Pd-P(2)-C(45)-C(50)	-162.1(1)
C(39)-P(2)-C(45)-C(46)	-126.5(2)
C(26)-P(2)-C(45)-C(46)	124.4(2)
Pd-P(2)-C(45)-C(46)	12.8(2)
C(50)-C(45)-C(46)-C(47)	0.9(3)
P(2)-C(45)-C(46)-C(47)	-174.2(2)
C(45)-C(46)-C(47)-C(48)	-0.5(3)
C(46)-C(47)-C(48)-C(49)	-0.4(4)
C(47)-C(48)-C(49)-C(50)	0.9(3)
C(48)-C(49)-C(50)-C(45)	-0.5(3)
C(46)-C(45)-C(50)-C(49)	-0.4(3)

P(2)-C(45)-C(50)-C(49)	174.6(2)

Crystal Structure Report

for

cis-(±)-**4.42**

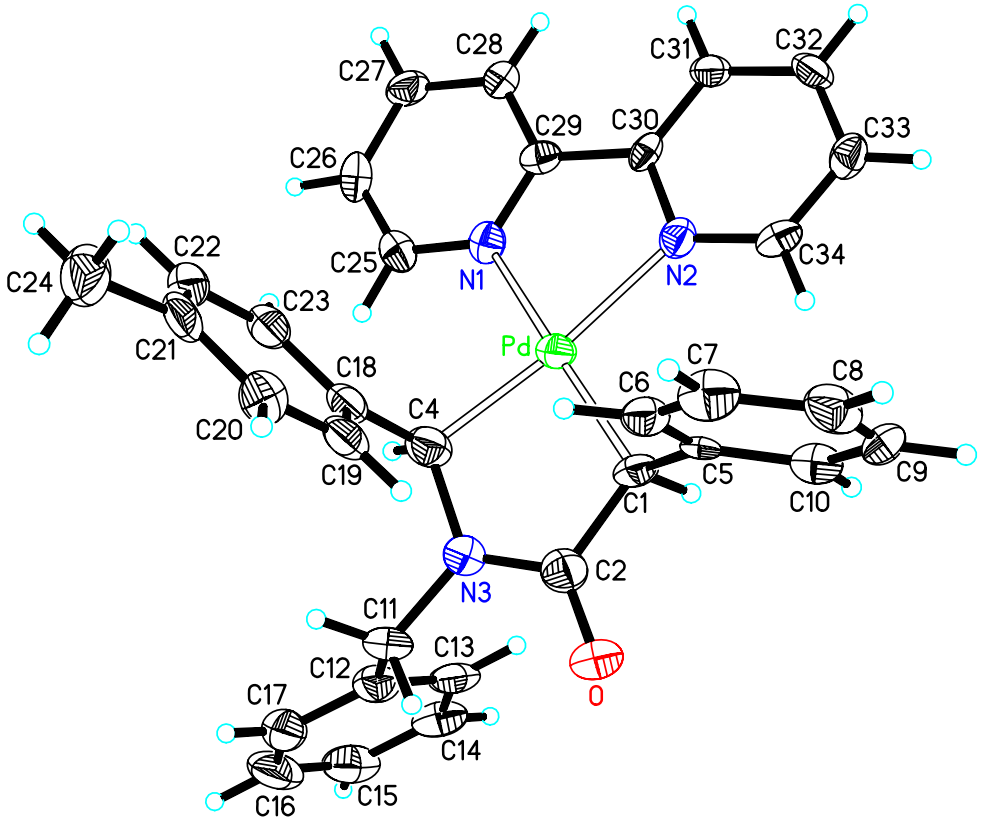
C28
C31
C32
C27
C29
C30
C33
C26
C25
N1
N2
C34
C22
C24
C23
C21
Pd
C7
C8
C18
C6
C4
C20
C5
C9
C19
C1
C10
N3
C2
C11
C13
C12
O
C17
C14
C16
C15

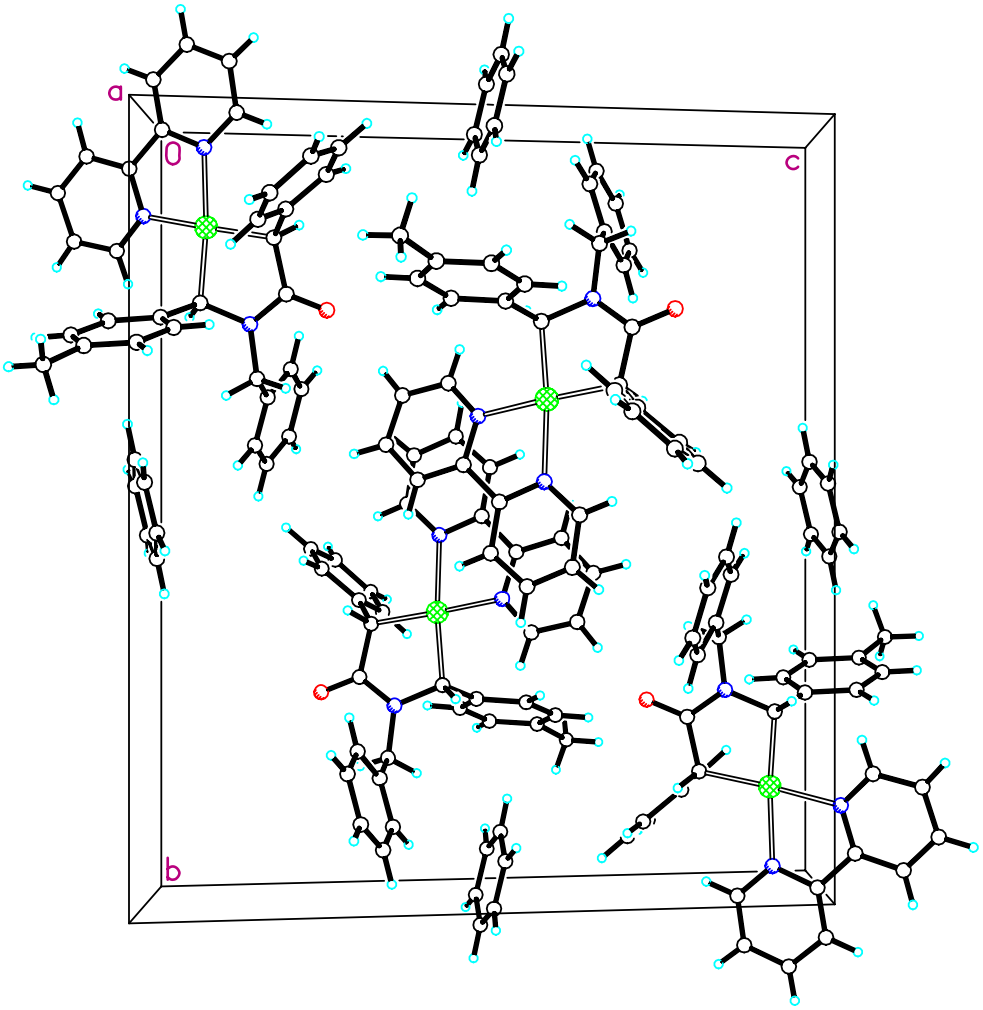
a
0
c
b

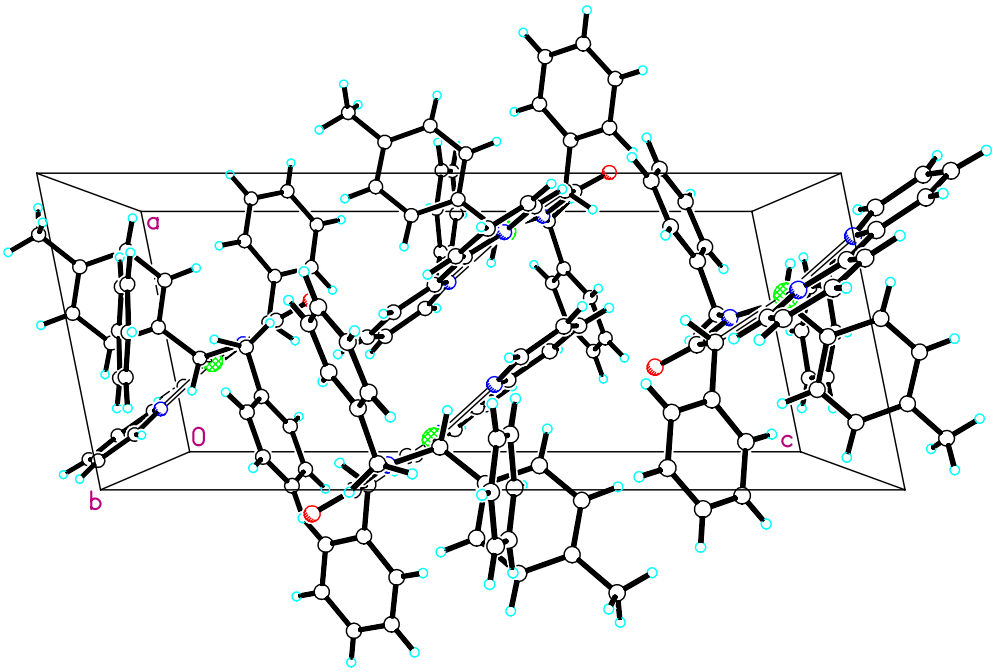
a
0
b
c

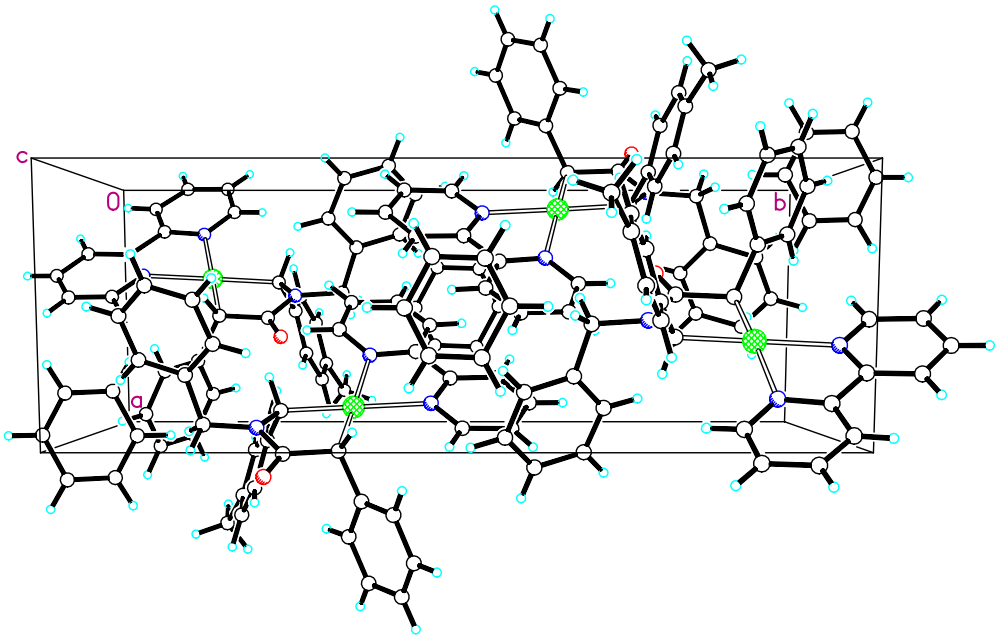
c
0
b
a

Comments

The asymmetric unit contains one [(*cis*-$C_{23}H_{21}NO$)Pd($N_2C_{10}H_8$)] molecule and one-half of a benzene solvent molecule of crystallization. This benzene solvent molecule of crystallization utilizes a crystallographic inversion center. All displacement ellipsoids are drawn at the 50% probability level.

Experimental Description

Small yellow crystals of [(*cis*-$C_{23}H_{21}NO$)Pd($N_2C_{10}H_8$)] • 0.50 C_6H_6 are, at 100(2) K, monoclinic, space group $P2_1/n$ [an alternate setting of $P2_1/c - C_{2h}^5$ (No. 14)] (1) with **a** = 7.4268(5) Å, **b** = 20.773(1) Å, **c** = 18.483(1) Å, β = 101.422(2)°, V = 2795.1(3) $Å^3$ and Z = 4 formula units {d_{calcd} = 1.495 g/cm^3; μ_a(MoKα) = 0.699 mm^{-1}}. A full hemisphere of diffracted intensities (1850 40-second frames with a ω scan width of 0.30°) was measured for a single-domain specimen using graphite-monochromated MoKα radiation (λ= 0.71073 Å) on a Bruker SMART APEX CCD Single Crystal Diffraction System (2). X-rays were provided by a fine-focus sealed x-ray tube operated at 50kV and 35mA. Lattice constants were determined with the Bruker SAINT software package using peak centers for 1934 reflections. A total of 23847 integrated reflection intensities having 2θ((MoKα)< 50.00° were produced using the Bruker program SAINT(3); 4917 of these were unique and gave R_{int} = 0.097 with a coverage which was 100.0% complete. The data were corrected empirically for variable absorption effects using equivalent reflections; the relative transmission factors ranged from 0.890 to 1.000. The Bruker software package SHELXTL was used to solve the structure using "direct methods" techniques. All stages of weighted full-matrix least-squares refinement were conducted using F_o^2 data with the SHELXTL Version 6.10 software

package(4).

The single methyl group was incorporated into the structural model as a rigid group (using idealized sp^3-hybridized geometry and a C-H bond length of 0.98 Å) with a "staggered" orientation. The remaining hydrogen atoms were included into the structural model as idealized atoms (assuming sp^2- or sp^3-hybridization of the carbon atoms and C-H bond lengths of 0.95 – 1.00 Å). The isotropic thermal parameters of all hydrogen atoms were fixed at values 1.2 (nonmethyl) or 1.5 (methyl) times the equivalent isotropic thermal parameter of the carbon atom to which they are covalently bonded.

The final structural model incorporated anisotropic thermal parameters for all nonhydrogen atoms and isotropic thermal parameters for all hydrogen atoms. A total of 370 parameters were refined using no restraints, 4917 data and weights of $w = 1/[\sigma^2(F^2) + (0.0510)^2]$, where $P = [F_o^2 + 2F_c^2] / 3$. Final agreement factors at convergence are: R_1(unweighted, based on F) = 0.065 for 3472 independent absorption-corrected "observed" reflections having $2\theta(MoK\alpha) < 50.00°$ and $I > 2\sigma(I)$; R_1(unweighted, based on F) = 0.103 and wR_2(weighted, based on F^2) = 0.139 for all 4917 independent absorption-corrected reflections having $2\theta(MoK\alpha) < 50.00°$. The largest shift/s.u. was 0.000 in the final refinement cycle. The final difference map had maxima and minima of 1.28 and -1.30 $e^-/Å^3$, respectively.

Acknowledgment

This X-Ray analysis was performed by Victor W. Day.

References

(1) International Tables for Crystallography, Vol A, 4th ed., Kluwer: Boston (1996).

(2) Data Collection: SMART Software Reference Manual (1998). Bruker-AXS, 5465 E. Cheryl Parkway, Madison, WI 53711-5373 USA.

(3) Data Reduction: SAINT Software Reference Manual (1998). Bruker-AXS, 6300 Enterprise Dr., Madison, WI 53719-1173, USA.

(4) G. M. Sheldrick (2000). SHELXTL Version 6.10 Reference Manual. Bruker-AXS, 5465 E. Cheryl Parkway, Madison, WI 53711-5373 USA.

Table 1. Crystal data and structure refinement for [(*cis*-$C_{23}H_{21}NO$)Pd($N_2C_{10}H_8$)] • 0.50 C_6H_6.

Empirical formula	$C_{36}H_{32}N_3OPd$	
Formula weight	629.05	
Temperature	100(2) K	
Wavelength	0.71073 Å	
Crystal system	Monoclinic	
Space group	$P2_1/n$ [an alternate setting of $P2_1/c - C_{2h}^5$ (No. 14)]	
Unit cell dimensions	**a** = 7.4268(5) Å	α = 90.000°
	b = 20.773(1) Å	β = 101.422(2)°
	c = 18.483(1) Å	γ = 90.000°
Volume	2795.1(3) Å^3	
Z	4	
Density (calculated)	1.495 Mg/m^3	
Absorption coefficient	0.699 mm^{-1}	
F(000)	1292	
Crystal size	0.10 x 0.05 x 0.02 mm^3	
Theta range for data collection	2.25° to 25.00°	
Index ranges	$-8 \le h \le 8$, $-24 \le k \le 24$, $-21 \le l \le 21$	
Reflections collected	23847	

Independent reflections	4917 [R_{int} = 0.097]
Completeness to theta = 25.00°	100.0 %
Absorption correction	Multi-scan
Max. and min. transmission	1.000 and 0.890
Refinement method	Full-matrix least-squares on F^2
Data / restraints / parameters	4917 / 0 / 370
Goodness-of-fit on F^2	1.072
Final R indices [I>2sigma(I)]	R_1 = 0.065, wR_2 = 0.127
R indices (all data)	R_1 = 0.103, wR_2 = 0.139
Largest diff. peak and hole	1.28 and -1.30 $e^-/Å^3$

$R_1 = \Sigma \, ||F_o| - |F_c|| \, / \, \Sigma \, |F_o|$

$wR_2 = \{ \, \Sigma \, [w(F_o^2 - F_c^2)^2] \, / \, \Sigma \, [w(F_o^2)^2] \, \}^{1/2}$

Table 2. Atomic coordinates (x 10^4) and equivalent isotropic displacement parameters ($Å^2$ x 10^3) for [(*cis*-$C_{23}H_{21}NO$)Pd($N_2C_{10}H_8$)] • 0.50 C_6H_6. U(eq) is defined as one third of the trace of the orthogonalized U_{ij} tensor.

	x	y	z	U(eq)
Pd	3810(1)	1378(1)	813(1)	26(1)
O	6215(7)	2479(2)	2625(3)	42(1)
N(1)	1872(7)	1183(3)	-180(3)	26(1)
N(2)	3670(8)	345(2)	777(3)	27(1)
C(1)	5361(10)	1545(3)	1841(4)	30(2)
C(2)	5447(10)	2262(3)	2023(4)	33(2)
N(3)	4527(8)	2633(3)	1472(3)	32(1)
C(4)	3955(10)	2354(3)	733(4)	34(2)
C(5)	7233(9)	1243(3)	2063(3)	24(2)
C(6)	8643(9)	1425(3)	1714(4)	32(2)
C(7)	10373(10)	1159(4)	1930(4)	39(2)
C(8)	10736(10)	716(3)	2505(4)	40(2)
C(9)	9382(10)	551(3)	2860(4)	32(2)
C(10)	7628(10)	814(3)	2648(4)	33(2)
C(11)	4400(10)	3328(3)	1571(4)	37(2)
C(12)	2531(10)	3540(3)	1668(4)	35(2)
C(13)	1361(10)	3150(4)	1978(4)	36(2)

C(14)	-265(11)	3390(4)	2096(4)	43(2)
C(15)	-793(11)	4021(4)	1894(4)	46(2)
C(16)	333(12)	4398(4)	1586(5)	49(2)
C(17)	1980(11)	4164(4)	1463(4)	39(2)
C(18)	5175(10)	2571(3)	215(4)	29(2)
C(19)	6989(10)	2737(3)	479(4)	33(2)
C(20)	8137(10)	2949(3)	15(4)	34(2)
C(21)	7494(12)	2984(3)	-744(4)	42(2)
C(22)	5705(11)	2819(3)	-1021(4)	36(2)
C(23)	4550(10)	2611(3)	-556(4)	34(2)
C(24)	8716(12)	3242(4)	-1227(4)	53(2)
C(25)	882(9)	1614(3)	-616(4)	29(2)
C(26)	-181(10)	1468(3)	-1299(4)	36(2)
C(27)	-208(9)	831(3)	-1541(4)	32(2)
C(28)	715(10)	377(3)	-1068(4)	32(2)
C(29)	1740(9)	564(3)	-392(4)	26(2)
C(30)	2745(8)	92(3)	132(3)	21(2)
C(31)	2718(9)	-556(3)	4(4)	26(2)
C(32)	3672(9)	-971(3)	528(4)	31(2)
C(33)	4599(9)	-725(3)	1175(4)	30(2)
C(34)	4570(9)	-72(3)	1281(4)	29(2)
C(1S)	6650(20)	4665(6)	57(6)	98(4)

C(2S)	5030(20)	4374(4)	-155(5)	80(4)
C(3S)	3280(20)	4703(6)	-230(5)	104(4)

Table 3. Bond lengths [Å] for [(*cis*-$C_{23}H_{21}NO$)Pd($N_2C_{10}H_8$)] • 0.50 C_6H_6.

Pd-C(1)	2.047(6)	C(7)-C(8)	1.391(10)
Pd-C(4)	2.037(7)	C(8)-C(9)	1.350(10)
Pd-N(1)	2.135(5)	C(9)-C(10)	1.396(9)
Pd-N(2)	2.149(5)	C(11)-C(12)	1.501(10)
O-C(2)	1.231(8)	C(12)-C(17)	1.388(10)
N(1)-C(25)	1.326(8)	C(12)-C(13)	1.392(10)
N(1)-C(29)	1.342(8)	C(13)-C(14)	1.363(10)
N(2)-C(34)	1.348(8)	C(14)-C(15)	1.399(11)
N(2)-C(30)	1.359(8)	C(15)-C(16)	1.351(11)
C(1)-C(5)	1.506(9)	C(16)-C(17)	1.376(10)
C(1)-C(2)	1.526(9)	C(18)-C(19)	1.382(9)
C(2)-N(3)	1.350(9)	C(18)-C(23)	1.411(9)
N(3)-C(11)	1.462(8)	C(19)-C(20)	1.395(10)
N(3)-C(4)	1.466(8)	C(20)-C(21)	1.392(10)
C(4)-C(18)	1.511(9)	C(21)-C(22)	1.369(10)
C(5)-C(6)	1.386(9)	C(21)-C(24)	1.493(10)
C(5)-C(10)	1.388(9)	C(22)-C(23)	1.397(10)
C(6)-C(7)	1.383(10)	C(25)-C(26)	1.383(9)

C(26)-C(27)	1.395(9)	C(32)-C(33)	1.355(9)
C(27)-C(28)	1.373(9)	C(33)-C(34)	1.372(9)
C(28)-C(29)	1.384(9)	C(1S)-C(2S)	1.337(16)
C(29)-C(30)	1.474(9)	C(1S)-C(3S)#1	1.352(14)
C(30)-C(31)	1.366(9)	C(2S)-C(3S)	1.447(16)
C(31)-C(32)	1.384(9)	C(3S)-C(1S)#1	1.352(14)

Symmetry transformations used to generate equivalent atoms: #1: -x+1, -y+1, -z.

Table 4. Bond angles [°] for [(*cis*-$C_{23}H_{21}NO$)Pd($N_2C_{10}H_8$)] • 0.50 C_6H_6.

C(4)-Pd-C(1)	82.6(3)	C(5)-C(1)-Pd	120.1(4)
C(4)-Pd-N(1)	99.3(2)	C(2)-C(1)-Pd	111.1(5)
C(1)-Pd-N(1)	171.8(3)	O-C(2)-N(3)	123.3(7)
C(4)-Pd-N(2)	174.0(2)	O-C(2)-C(1)	123.2(6)
C(1)-Pd-N(2)	102.3(2)	N(3)-C(2)-C(1)	113.5(6)
N(1)-Pd-N(2)	76.3(2)	C(2)-N(3)-C(11)	120.3(6)
C(25)-N(1)-C(29)	118.0(6)	C(2)-N(3)-C(4)	119.2(6)
C(25)-N(1)-Pd	126.4(5)	C(11)-N(3)-C(4)	119.6(5)
C(29)-N(1)-Pd	115.5(4)	N(3)-C(4)-C(18)	111.8(6)
C(34)-N(2)-C(30)	117.0(6)	N(3)-C(4)-Pd	109.6(4)
C(34)-N(2)-Pd	127.3(5)	C(18)-C(4)-Pd	113.0(5)
C(30)-N(2)-Pd	115.2(4)	C(6)-C(5)-C(10)	118.4(6)
C(5)-C(1)-C(2)	110.5(5)	C(6)-C(5)-C(1)	120.1(6)

C(10)-C(5)-C(1)	121.3(6)	C(20)-C(21)-C(24)	119.6(8)
C(7)-C(6)-C(5)	120.1(7)	C(21)-C(22)-C(23)	121.1(7)
C(6)-C(7)-C(8)	120.9(7)	C(22)-C(23)-C(18)	121.4(7)
C(9)-C(8)-C(7)	119.3(7)	N(1)-C(25)-C(26)	123.6(6)
C(8)-C(9)-C(10)	120.5(7)	C(25)-C(26)-C(27)	118.1(6)
C(5)-C(10)-C(9)	120.8(7)	C(28)-C(27)-C(26)	118.3(6)
N(3)-C(11)-C(12)	112.9(6)	C(27)-C(28)-C(29)	119.8(6)
C(17)-C(12)-C(13)	118.8(7)	N(1)-C(29)-C(28)	121.9(6)
C(17)-C(12)-C(11)	118.1(7)	N(1)-C(29)-C(30)	116.6(6)
C(13)-C(12)-C(11)	123.1(7)	C(28)-C(29)-C(30)	121.5(6)
C(14)-C(13)-C(12)	119.8(7)	N(2)-C(30)-C(31)	121.4(6)
C(13)-C(14)-C(15)	120.7(8)	N(2)-C(30)-C(29)	114.9(6)
C(16)-C(15)-C(14)	119.5(8)	C(31)-C(30)-C(29)	123.6(6)
C(15)-C(16)-C(17)	120.6(8)	C(30)-C(31)-C(32)	120.3(6)
C(16)-C(17)-C(12)	120.6(8)	C(33)-C(32)-C(31)	118.9(6)
C(19)-C(18)-C(23)	116.3(7)	C(32)-C(33)-C(34)	118.7(6)
C(19)-C(18)-C(4)	121.1(6)	N(2)-C(34)-C(33)	123.7(6)
C(23)-C(18)-C(4)	122.6(6)	C(2S)-C(1S)-C(3S)#1	119.7(14)
C(18)-C(19)-C(20)	122.3(7)	C(1S)-C(2S)-C(3S)	123.6(11)
C(21)-C(20)-C(19)	120.4(7)	C(1S)#1-C(3S)-C(2S)	116.6(14)
C(22)-C(21)-C(20)	118.5(7)		
C(22)-C(21)-C(24)	121.8(8)		

Symmetry transformations used to generate equivalent atoms: #1: -x+1, -y+1, -z.

Table 5. Anisotropic displacement parameters ($Å^2 x\ 10^3$) for [(*cis*-$C_{23}H_{21}NO)Pd(N_2C_{10}H_8)] \bullet 0.50\ C_6H_6$. The anisotropic displacement factor exponent takes the form: $-2\pi^2[\ h^2\ a^{*2}U_{11} + ... + 2\ h\ k\ a^*\ b^*\ U_{12}\ ]$

	U_{11}	U_{22}	U_{33}	U_{23}	U_{13}	U_{12}
Pd	29(1)	24(1)	24(1)	-4(1)	5(1)	2(1)
O	54(4)	40(3)	28(3)	-9(2)	4(3)	-1(3)
N(1)	23(3)	29(3)	26(3)	3(3)	4(3)	-3(2)
N(2)	29(3)	28(3)	23(3)	3(3)	7(2)	0(3)
C(1)	38(4)	31(4)	19(4)	-8(3)	-1(3)	0(3)
C(2)	34(4)	33(4)	35(4)	-2(4)	14(4)	4(3)
N(3)	42(4)	26(3)	29(3)	-2(3)	9(3)	-1(3)
C(4)	37(4)	27(4)	35(4)	-5(3)	0(3)	0(3)
C(5)	38(4)	15(4)	18(3)	-10(3)	3(3)	0(3)
C(6)	42(4)	28(4)	27(4)	-6(3)	7(3)	-5(4)
C(7)	33(5)	46(5)	41(5)	-8(4)	12(4)	-6(4)
C(8)	34(5)	35(4)	45(5)	-9(4)	-5(4)	8(3)
C(9)	40(5)	33(4)	18(4)	-3(3)	-6(3)	0(3)
C(10)	34(4)	32(4)	34(4)	-9(3)	9(3)	-4(3)

C(11)	51(5)	29(4)	31(4)	-12(3)	8(4)	-1(4)
C(12)	39(4)	33(4)	29(4)	-8(4)	-1(3)	-1(4)
C(13)	41(5)	40(4)	26(4)	-16(3)	1(3)	5(4)
C(14)	43(5)	53(5)	32(4)	-17(4)	3(4)	-7(4)
C(15)	41(5)	49(5)	43(5)	-18(4)	-2(4)	12(4)
C(16)	60(6)	32(5)	53(6)	-16(4)	5(5)	10(4)
C(17)	49(5)	33(4)	33(4)	-2(4)	1(4)	5(4)
C(18)	35(4)	17(3)	34(4)	-2(3)	6(3)	0(3)
C(19)	39(5)	18(4)	40(4)	-3(3)	1(4)	4(3)
C(20)	28(4)	33(4)	40(5)	3(4)	3(3)	4(3)
C(21)	66(6)	17(4)	50(5)	8(4)	30(5)	13(4)
C(22)	51(5)	26(4)	29(4)	3(3)	2(4)	8(4)
C(23)	42(5)	23(4)	37(4)	0(3)	5(4)	2(3)
C(24)	73(6)	45(5)	50(5)	15(4)	30(5)	23(4)
C(25)	30(4)	23(4)	36(4)	3(3)	8(3)	0(3)
C(26)	41(4)	33(5)	33(4)	14(4)	8(3)	0(4)
C(27)	39(4)	35(4)	21(4)	-7(3)	2(3)	-7(3)
C(28)	46(5)	27(4)	23(4)	1(3)	10(3)	0(3)
C(29)	28(4)	30(4)	23(4)	-4(3)	9(3)	0(3)
C(30)	17(4)	32(4)	15(3)	5(3)	5(3)	4(3)
C(31)	33(4)	24(4)	23(4)	-6(3)	9(3)	-2(3)
C(32)	42(5)	16(4)	37(4)	-3(3)	16(4)	2(3)

C(33)	34(4)	32(4)	25(4)	6(3)	7(3)	-6(3)
C(34)	29(4)	38(4)	19(4)	-6(3)	3(3)	-4(3)
C(1S)	181(15)	55(8)	50(7)	5(6)	4(8)	15(9)
C(2S)	173(13)	28(5)	37(6)	-1(4)	12(7)	24(7)
C(3S)	193(14)	83(9)	40(6)	19(6)	34(8)	44(10)

Table 6. Hydrogen coordinates (x 10^4) and isotropic displacement parameters (Å^2 x 10^3) for [(*cis*-$C_{23}H_{21}NO$)Pd($N_2C_{10}H_8$)] • 0.50 C_6H_6.

	x	y	z	U(eq)
H(1)	4630	1354	2188	36
H(4)	2686	2514	528	41
H(6)	8420	1732	1326	39
H(7)	11326	1280	1682	47
H(8)	11925	531	2646	47
H(9)	9624	254	3258	38
H(10)	6692	699	2908	39
H(11A)	4702	3549	1136	44
H(11B)	5320	3460	2009	44
H(13)	1695	2717	2108	44
H(14)	-1049	3125	2317	52
H(15)	-1934	4184	1973	55

H(16)	-15	4829	1452	59
H(17)	2747	4431	1237	47
H(19)	7470	2705	994	40
H(20)	9366	3071	219	41
H(22)	5241	2847	-1537	43
H(23)	3319	2495	-763	41
H(24A)	8036	3263	-1738	80
H(24B)	9782	2958	-1200	80
H(24C)	9134	3674	-1060	80
H(25)	903	2048	-451	35
H(26)	-872	1791	-1594	43
H(27)	-848	714	-2020	39
H(28)	650	-65	-1205	38
H(31)	2040	-722	-448	32
H(32)	3678	-1421	437	37
H(33)	5256	-999	1546	36
H(34)	5222	96	1736	35
H(1S)	7759	4428	84	117
H(2S)	5018	3926	-261	96
H(3S)	2151	4485	-394	125

Table 7. Torsion angles [°] for [(*cis*-$C_{23}H_{21}NO$)Pd($N_2C_{10}H_8$)] • 0.50 C_6H_6.

C(4)-Pd-N(1)-C(25)	-10.3(6)
C(1)-Pd-N(1)-C(25)	92.7(18)
N(2)-Pd-N(1)-C(25)	174.0(6)
C(4)-Pd-N(1)-C(29)	166.0(5)
C(1)-Pd-N(1)-C(29)	-91.0(17)
N(2)-Pd-N(1)-C(29)	-9.7(4)
C(4)-Pd-N(2)-C(34)	137(2)
C(1)-Pd-N(2)-C(34)	-6.7(6)
N(1)-Pd-N(2)-C(34)	-178.4(6)
C(4)-Pd-N(2)-C(30)	-34(3)
C(1)-Pd-N(2)-C(30)	-178.0(5)
N(1)-Pd-N(2)-C(30)	10.3(4)
C(4)-Pd-C(1)-C(5)	-120.8(6)
N(1)-Pd-C(1)-C(5)	135.0(15)
N(2)-Pd-C(1)-C(5)	55.6(6)
C(4)-Pd-C(1)-C(2)	10.4(5)
N(1)-Pd-C(1)-C(2)	-93.8(17)
N(2)-Pd-C(1)-C(2)	-173.2(5)
C(5)-C(1)-C(2)-O	-48.1(9)
Pd-C(1)-C(2)-O	175.9(6)
C(5)-C(1)-C(2)-N(3)	134.8(6)

Pd-C(1)-C(2)-N(3)	-1.2(8)
O-C(2)-N(3)-C(11)	-0.1(11)
C(1)-C(2)-N(3)-C(11)	177.0(6)
O-C(2)-N(3)-C(4)	168.6(7)
C(1)-C(2)-N(3)-C(4)	-14.2(9)
C(2)-N(3)-C(4)-C(18)	-103.5(7)
C(11)-N(3)-C(4)-C(18)	65.3(8)
C(2)-N(3)-C(4)-Pd	22.5(8)
C(11)-N(3)-C(4)-Pd	-168.6(5)
C(1)-Pd-C(4)-N(3)	-16.9(5)
N(1)-Pd-C(4)-N(3)	155.0(5)
N(2)-Pd-C(4)-N(3)	-161(2)
C(1)-Pd-C(4)-C(18)	108.5(5)
N(1)-Pd-C(4)-C(18)	-79.6(5)
N(2)-Pd-C(4)-C(18)	-36(3)
C(2)-C(1)-C(5)-C(6)	-65.1(8)
Pd-C(1)-C(5)-C(6)	66.4(7)
C(2)-C(1)-C(5)-C(10)	110.5(7)
Pd-C(1)-C(5)-C(10)	-118.0(6)
C(10)-C(5)-C(6)-C(7)	2.8(9)
C(1)-C(5)-C(6)-C(7)	178.4(6)
C(5)-C(6)-C(7)-C(8)	-1.1(10)

C(6)-C(7)-C(8)-C(9)	-0.8(11)
C(7)-C(8)-C(9)-C(10)	0.9(10)
C(6)-C(5)-C(10)-C(9)	-2.7(10)
C(1)-C(5)-C(10)-C(9)	-178.3(6)
C(8)-C(9)-C(10)-C(5)	0.9(10)
C(2)-N(3)-C(11)-C(12)	-106.2(7)
C(4)-N(3)-C(11)-C(12)	85.1(8)
N(3)-C(11)-C(12)-C(17)	-153.5(6)
N(3)-C(11)-C(12)-C(13)	28.9(9)
C(17)-C(12)-C(13)-C(14)	-2.0(10)
C(11)-C(12)-C(13)-C(14)	175.5(6)
C(12)-C(13)-C(14)-C(15)	1.4(10)
C(13)-C(14)-C(15)-C(16)	-0.6(11)
C(14)-C(15)-C(16)-C(17)	0.6(12)
C(15)-C(16)-C(17)-C(12)	-1.3(12)
C(13)-C(12)-C(17)-C(16)	2.0(11)
C(11)-C(12)-C(17)-C(16)	-175.7(7)
N(3)-C(4)-C(18)-C(19)	28.1(9)
Pd-C(4)-C(18)-C(19)	-96.0(6)
N(3)-C(4)-C(18)-C(23)	-152.4(6)
Pd-C(4)-C(18)-C(23)	83.5(7)
C(23)-C(18)-C(19)-C(20)	1.6(10)

C(4)-C(18)-C(19)-C(20)	-178.9(6)
C(18)-C(19)-C(20)-C(21)	-1.9(10)
C(19)-C(20)-C(21)-C(22)	1.5(10)
C(19)-C(20)-C(21)-C(24)	177.1(6)
C(20)-C(21)-C(22)-C(23)	-1.0(10)
C(24)-C(21)-C(22)-C(23)	-176.5(6)
C(21)-C(22)-C(23)-C(18)	0.8(10)
C(19)-C(18)-C(23)-C(22)	-1.0(10)
C(4)-C(18)-C(23)-C(22)	179.4(6)
C(29)-N(1)-C(25)-C(26)	-4.5(10)
Pd-N(1)-C(25)-C(26)	171.7(5)
N(1)-C(25)-C(26)-C(27)	-0.1(10)
C(25)-C(26)-C(27)-C(28)	4.5(10)
C(26)-C(27)-C(28)-C(29)	-4.4(10)
C(25)-N(1)-C(29)-C(28)	4.7(9)
Pd-N(1)-C(29)-C(28)	-171.9(5)
C(25)-N(1)-C(29)-C(30)	-175.4(6)
Pd-N(1)-C(29)-C(30)	8.0(7)
C(27)-C(28)-C(29)-N(1)	-0.3(10)
C(27)-C(28)-C(29)-C(30)	179.8(6)
C(34)-N(2)-C(30)-C(31)	0.6(9)
Pd-N(2)-C(30)-C(31)	172.9(5)

C(34)-N(2)-C(30)-C(29)	178.3(6)
Pd-N(2)-C(30)-C(29)	-9.4(7)
N(1)-C(29)-C(30)-N(2)	1.0(8)
C(28)-C(29)-C(30)-N(2)	-179.1(6)
N(1)-C(29)-C(30)-C(31)	178.6(6)
C(28)-C(29)-C(30)-C(31)	-1.5(10)
N(2)-C(30)-C(31)-C(32)	-1.4(10)
C(29)-C(30)-C(31)-C(32)	-178.8(6)
C(30)-C(31)-C(32)-C(33)	1.3(10)
C(31)-C(32)-C(33)-C(34)	-0.6(10)
C(30)-N(2)-C(34)-C(33)	0.1(10)
Pd-N(2)-C(34)-C(33)	-171.1(5)
C(32)-C(33)-C(34)-N(2)	-0.1(10)
C(3S)#1-C(1S)-C(2S)-C(3S)	1.7(18)
C(1S)-C(2S)-C(3S)-C(1S)#1	-1.6(18)

Symmetry transformations used to generate equivalent atoms: #1: -x+1, -y+1, -z.